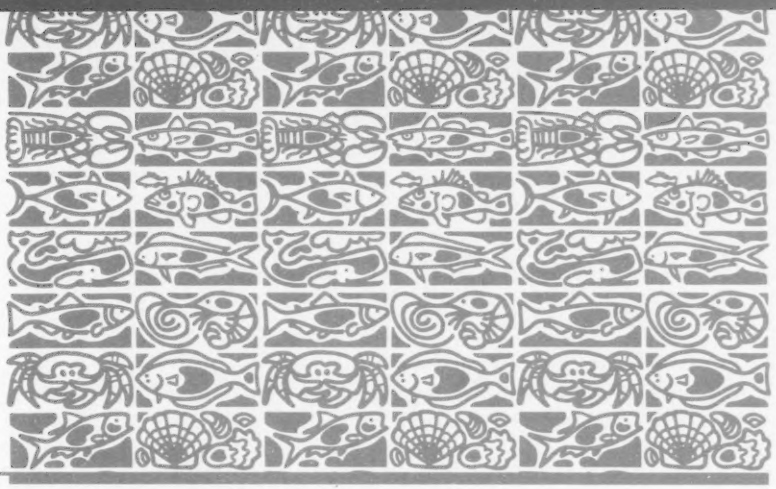

U.S. Department
of Commerce

Volume 100
Number 4
October 2002

Fishery Bulletin

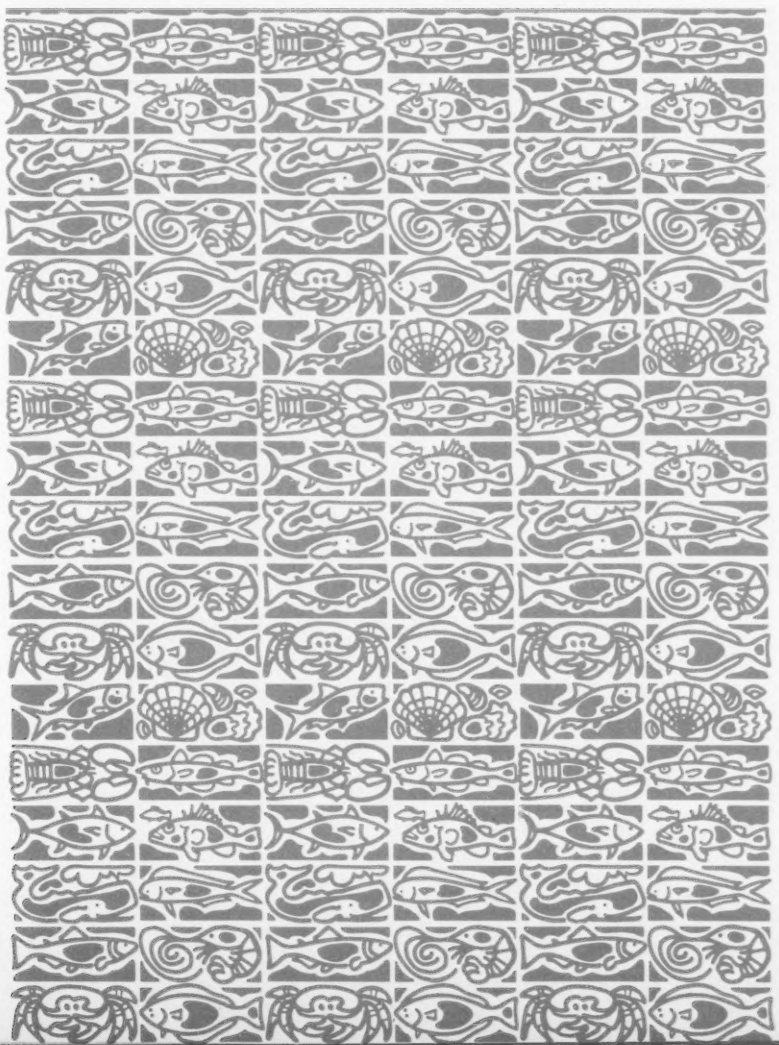

U.S. Department of Commerce
Donald L. Evans
Secretary

National Oceanic and Atmospheric Administration
Vice Admiral
Conrad C. Lautenbacher Jr., USN (ret.)
Under Secretary for Oceans and Atmosphere

National Marine Fisheries Service
William T. Hogarth
Assistant Administrator for Fisheries

The *Fishery Bulletin* (ISSN 0090-0656) is published quarterly by the Scientific Publications Office, National Marine Fisheries Service, NOAA, 7600 Sand Point Way NE, BIN C15700, Seattle, WA 98115-0070. Periodicals postage is paid at Seattle, WA, and at additional mailing offices. POSTMASTER: Send address changes for subscriptions to Fishery Bulletin, Superintendent of Documents, Attn.: Chief, Mail List Branch, Mail Stop SSOM, Washington, DC 20402-9373.

Although the contents of this publication have not been copyrighted and may be reprinted entirely, reference to source is appreciated.

The Secretary of Commerce has determined that the publication of this periodical is necessary according to law for the transaction of public business of this Department. Use of funds for printing of this periodical has been approved by the Director of the Office of Management and Budget.

For sale by the Superintendent of Documents, U.S. Government Printing Office, Washington, DC 20402. Subscription price per year: $45.00 domestic and $56.25 foreign. Cost per single issue: $28.00 domestic and $35.00 foreign. **See back for order form.**

Fishery Bulletin

Scientific Editor
Dr. John V. Merriner

Editorial Assistant
Sarah Shoffler

Center for Coastal Fisheries and Habitat Research, NOS
101 Pivers Island Road
Beaufort, NC 28516

Managing Editor
Sharyn Matriotti
National Marine Fisheries Service
Scientific Publications Office
7600 Sand Point Way NE, BIN C15700
Seattle, Washington 98115-0070

Editorial Committee

Dr. Harlyn O. Halvorson	University of Massachusetts, Boston
Dr. Ronald W. Hardy	University of Idaho, Hagerman
Dr. Richard D. Methot	National Marine Fisheries Service
Dr. Theodore W. Pietsch	University of Washington, Seattle
Dr. Joseph E. Powers	National Marine Fisheries Service
Dr. Harald Rosenthal	Universität Kiel, Germany
Dr. Fredric M. Serchuk	National Marine Fisheries Service

***Fishery Bulletin* web site: fishbull.noaa.gov**

The *Fishery Bulletin* carries original research reports and technical notes on investigations in fishery science, engineering, and economics. It began as the Bulletin of the United States Fish Commission in 1881; it became the Bulletin of the Bureau of Fisheries in 1904 and the *Fishery Bulletin* of the Fish and Wildlife Service in 1941. Separates were issued as documents through volume 46; the last document was No. 1103. Beginning with volume 47 in 1931 and continuing through volume 62 in 1963, each separate appeared as a numbered bulletin. A new system began in 1963 with volume 63 in which papers are bound together in a single issue of the bulletin. Beginning with volume 70, number 1, January 1972, the *Fishery Bulletin* became a periodical, issued quarterly. In this form, it is available by subscription from the Superintendent of Documents, U.S. Government Printing Office, Washington, DC 20402. It is also available free in limited numbers to libraries, research institutions, State and Federal agencies, and in exchange for other scientific publications.

U.S. Department of Commerce
Seattle, Washington

Volume 100
Number 4
October 2002

Fishery Bulletin

Contents

Articles

651–661 **Bostrom, Meredith A., Bruce B. Collette, Brian E. Luckhurst, Kimberly S. Reece, and John E. Graves**
Hybridization between two serranids, the coney (*Cephalopholis fulva*) and the creole-fish (*Paranthias furcifer*), at Bermuda

662–673 **Carter, Sarah K., and Glenn R. VanBlaricom**
Effects of experimental harvest on red sea urchins (*Strongylocentrotus franciscanus*) in northern Washington

674–682 **Conrath, Christina L., James Gelsleichter, and John A. Musick**
Age and growth of the smooth dogfish (*Mustelus canis*) in the northwest Atlantic Ocean

683–689 **Gaertner, Daniel, Frédéric Ménard, Carol Develter, and Javier Ariz**
Bycatch of billfishes by the European tuna purse-seine fishery in the Atlantic Ocean

690–710 **Griffiths, Marc H.**
Life history of South African snoek, *Thyrsites atun* (Pisces: Gempylidae): a pelagic predator of the Benguela ecosystem

711–719 **Hannah, Robert W, Steven J. Parker, and Erica L. Fruh**
Length and age at maturity of female petrale sole (*Eopsetta jordani*) determined from samples collected prior to spawning aggregation

720–726 **Hjellvik, Vidar, Olav Rune Godø, and Dag Tjøstheim**
The measurement error in marine survey catches: the bottom trawl case

727–738 **Jensen, Christopher F., Lisa J. Natanson, Harold L. Pratt Jr., Nancy Kohler, and Steven E. Campana**
The reproductive biology of the porbeage shark (*Lamna nasus*) in the western North Atlantic Ocean

The conclusions and opinions expressed in *Fishery Bulletin* are solely those of the authors and do not represent the official position of the National Marine Fisheries Service (NOAA) or any other agency or institution.

The National Marine Fisheries Service (NMFS) does not approve, recommend, or endorse any proprietary product or proprietary material mentioned in this publication. No reference shall be made to NMFS, or to this publication furnished by NMFS, in any advertising or sales promotion which would indicate or imply that NMFS approves, recommends, or endorses any proprietary product or proprietary material mentioned herein, or which has as its purpose an intent to cause directly or indirectly the advertised product to be used or purchased because of this NMFS publication.

739–751 **Nasby-Lucas, Nicole M., Bob W. Embley, Mark A. Hixon, Susan G. Merle, Brian N. Tissot, and Dawn J. Wright**
Integration of submersible transect data and high-resolution multibeam sonar imagery for a habitat-based groundfish assessment of Heceta Bank, Oregon

752–764 **Olsen, Jeffrey B., Susan E. Merkouris, and James E. Seeb**
An examination of spatial and temporal genetic variation in walleye pollock (*Theragra chalcogramma*) using allozyme, mitochondrial DNA, and microsatellite data

765–788 **Schaefer, Kurt M., and Daniel W. Fuller**
Movements, behavior, and habitat selection of bigeye tuna (*Thunnus obesus*) in the eastern equatorial Pacific, ascertained through archival tags

789–799 **Schirripa, Michael J.**
An evaluation of back-calculation methodology using simulated otolith data

800–821 **Stobutzki, Ilona C., Margaret J. Miller, Don S. Heales, and David T. Brewer**
Sustainability of elasmobranchs caught as bycatch in a tropical prawn (shrimp) trawl fishery

822–835 **Sun, Chi-Lu, Sheng-Ping Wang, and Su-Zan Yeh**
Age and growth of the swordfish (*Xiphias gladius* L.) in the waters around Taiwan determined from anal-fin rays

836–855 **Williams, Erik H., and Stephen Ralston**
Distribution and co-occurrence of rockfishes (family: Sebastidae) over trawlable shelf and slope habitats of California and southern Oregon

Notes

856–860 **Latour, Robert J., John M. Hoenig, and Kenneth H. Pollock**
Properties of the residuals from two tag-recovery models

861–864 **McFarlane, Gordon A., Jacquelynne R. King, and Mark W. Saunders**
Preliminary study on the use of neural arches in the age determination of bluntnose sixgill sharks (*Hexanchus griseus*)

865–875 **Mollet, Henry F., Antonio D. Testi, Leonard J. V. Compagno, and Malcolm P. Francis**
Re-identification of a lamnid shark embryo

876–880 **Work, Thierry M., and George H. Balazs**
Necropsy findings in sea turtles taken as bycatch in the North Pacific longline fishery

881–882 *Acknowledgment of reviewers*

883–892 *Index*

893 *Subscription form*

Hybridization between two serranids, the coney (*Cephalopholis fulva*) and the creole-fish (*Paranthias furcifer*), at Bermuda*

Meredith A. Bostrom
Department of Fisheries Science
Virginia Institute of Marine Science
College of William and Mary
Gloucester Point Virginia 23062-1346
Present address: Division of Endocrinology and Molecular Medicine
University of Kentucky
Lexington, Kentucky 40536-0001

Bruce B. Collette
National Systematics Laboratory
National Marine Fisheries Service, NOAA
National Museum of Natural History
Washington D.C. 20560-0153

Brian E. Luckhurst
Division of Fisheries
Department of Agriculture and Fisheries
Crawl CR BX, Bermuda

Kimberly S. Reece
John E. Graves
Department of Fisheries Science
Virginia Institute of Marine Science
College of William and Mary
Gloucester Point, Virginia 23062-1346
E-mail address (for J. E. Graves, contact author): graves@vims.edu

Abstract—Intergeneric hybridization between the epinepheline serranids *Cephalopholis fulva* and *Paranthias furcifer* in waters off Bermuda was investigated by using morphological and molecular characters. Putative hybrids, as well as members of each presumed parent species, were analyzed for 44 morphological characters and screened for genetic variation at 16 nuclear allozyme loci, two nuclear (n)DNA loci, and three mitochondrial (mt)DNA gene regions. Four of 16 allozyme loci, creatine kinase (*CK-B**), fumarase (*FH**), isocitrate dehydrogenase (*ICDH-S**), and lactate dehydrogenase (*LDH-B**), were unique in *C. fulva* and *P. furcifer*. Restriction fragments of two nuclear DNA intron regions, an actin gene intron and the second intron in the S7 ribosomal protein gene, also exhibited consistent differences between the two presumed parent species. Restriction fragments of three mtDNA regions—ND4, ATPase 6, and 12S/16S ribosomal RNA—were analyzed to identify maternal parentage of putative hybrids. Both morphological data and nuclear genetic data were found to be consistent with the hypothesis that the putative hybrids were the result of interbreeding between *C. fulva* and *P. furcifer*. Mean values of 38 morphological characters were different between presumed parent species, and putative hybrids were intermediate to presumed parent species for 33 of these characters. A principal component analysis of the morphological and meristic data was also consistent with hybridization between *C. fulva* and *P. furcifer*. Thirteen of 15 putative hybrids were heterozygous at all diagnostic nuclear loci, consistent with F_1 hybrids. Two putative hybrids were identified as post-F_1 hybrids based on homozygosity at one nuclear locus each. Mitochondrial DNA analysis showed that the maternal parent of all putative hybrid individuals was *C. fulva*. A survey of nuclear and mitochondrial loci of 57 *C. fulva* and 37 *P. furcifer* from Bermuda revealed no evidence of introgression between the parent species mediated by hybridization.

Manuscript accepted 25 March 2002.
Fish. Bull. 100(4):651–661 (2002).

Poey (1860, 1875) described the genus *Menephorus* for two species, *M. dubius* Poey, 1860 and *M. punctiferus* Poey, 1875, each based on a single specimen of grouper that appeared to be intermediate in morphology between the coney, *Cephalopholis fulva* and the creole-fish, *Paranthias furcifer*. Smith (1966) analyzed Poey's specimens for 45 meristic and morphometric characters and found the specimens to be intermediate to *P. furcifer* and *C. fulva* for 40 of these characters—results consistent with intergeneric hybridization. Smith (1966) also noted that *P. furcifer* may be more closely related to the epinepheline serranids (such as *C. fulva*) than previously thought. Interest in this possible case of intergeneric hybridization was renewed in 1993 when Bermudian ichthyology student James Parris Jr. asked one of the authors if he would be interested in a specimen his father caught that "had the head of a coney and the tail of a barber (creole-fish)." Since that time several other putative hybrids have been caught off Bermuda (Smith-Vaniz et al., 1999), and we have initiated a program to collect putative hybrids from local fishermen to further investigate this phenomenon.

The presumed parents of the putative hybrids are members of different serranid genera that have strikingly different morphologies, occupy different ecological niches, and have different behaviors (Heemstra and Randall, 1993; Smith, 1966). The major distinguishing features of *P. furcifer* are its forked

* Contribution 2469 of the Virginia Institute of Marine Science, College of William and Mary, Gloucester Point, VA 23062-1346.

Figure 1

Photograph of the creole-fish (top), *Paranthias furcifer*, the coney (bottom), *Cephalopholis fulva*, and the putative hybrid (middle), Bermuda. (Courtesy of Jan Cordes.)

caudal fin and the size and shape of its mouth (Fig. 1). *Paranthias furcifer* is dark red in color; darker dorsally, lightening ventrally (Heemstra and Randall, 1993). There is an orange spot at the upper end of the base of the pectoral fin and three white spots dorsal to the lateral line. Bermuda is the northern limit of the distribution of *P. furcifer* in the western Atlantic and the species occurs throughout the Bahamas and Antilles and along the American coast from the Gulf of Mexico south to Brazil (Smith, 1971; Smith-Vaniz et al., 1999).

In contrast, *C. fulva* is usually scarlet in color and covered with light blue-green spots, each surrounded by a black ring (Heemstra and Randall, 1993). There are two black spots on the edge of the lower jaw as well as on top of the caudal peduncle. *Cephalopholis fulva* has rounded caudal, anal, and dorsal fins, similar to fins of other epinepheline serranids (Heemstra and Randall, 1993) (Fig. 1). In the northwestern Atlantic, *C. fulva* has a distribution similar to that of *P. furcifer*; it occurs as far north as Bermuda, throughout the Bahamas, Antilles, and along the east coast of the Americas from South Carolina to Brazil (Heemstra and Randall, 1993; Smith, 1971; Smith-Vaniz et al., 1999).

Morphologically, the putative hybrids are almost exactly intermediate to the parent species (Fig. 1). In his 1966 review, Smith noted that the hybrids have some characters unique to *C. fulva* and *P. furcifer*. For example, the putative hybrid individuals have both a moderately forked tail and blue spots surrounded by a black ring. *Paranthias furcifer* is the only Atlantic grouper with a forked tail suggesting that it is one of the putative parents and *C. fulva* is the only Atlantic grouper that has blue spots with a black ring. Presence of both traits together in a single individual strongly suggests interbreeding between the two species. The geographic extent of the putative hybrid is not well known; however specimens exist from Cuba and Bermuda (Smith-Vaniz et al., 1999), and it has been reported from Jamaica (Thompson and Munro, 1978).

Hybridization has traditionally been detected by using morphological characters, but increasingly, genetic analyses have also been used for this purpose. Allozyme electrophoresis provides a rapid and cost-effective method to

assess hybridization (Campton, 1987). Through the analysis of multiple loci it is possible to identify F_1 and post-F_1 hybrids, as well as to detect the introgression of alleles between species by hybrid backcrossing. It became evident however, that analysis of nuclear DNA loci is necessary in studies of hybridization as a means to overcome some of the sampling restrictions of allozyme analysis and to provide a survey of biparentally inherited genes (Verspoor and Hammar, 1991). Mitochondrial DNA (mtDNA) has also been used extensively in studies of hybridization. Because mtDNA is maternally inherited in fishes, analysis of the molecule allows one to identify the maternal parent of F_1 hybrids, as well as the sexual preferences of F_1 hybrids and their offspring (Dowling et al., 1996).

The key to using molecular markers to identify hybridization is to find multiple independent nuclear loci and a mitochondrial gene region that have unique alleles in each putative parent species (Dowling et al., 1996). An F_1 hybrid would be heterozygous at all nuclear loci and have a mitochondrial haplotype identical to one parent species (Campton, 1987; Dowling et al., 1989). A backcrossed individual would be heterozygous at some diagnostic nuclear loci and homozygous at others. Therefore the power of demonstrating an F_1 hybrid, as opposed to a backcross or pure parent individual, increases with the number of nuclear loci examined.

In this study, genetic information from four diagnostic allozyme loci, two diagnostic nuclear DNA loci, and three diagnostic mtDNA gene regions, was used to assess hybridization and introgression between *Cephalopholis fulva* and *Paranthias furcifer* in Bermuda waters.

Materials and methods

A total of 51 *Cephalopholis fulva* (Linnaeus, 1758), three *C. cruentata* (Lacepède, 1802), and 37 *Paranthias furcifer* (Valenciennes, 1828) were collected from Bermuda with baited handlines or rotenone solution. In addition, six *C. fulva* and two *C. cruentata* were sampled from Navassa Island. Fifteen putative hybrids were captured by Bermudian fishermen using handlines or lobster traps. *Cephalopholis cruentata* was in-cluded in the study as a possible parent species of the putative hybrid and three *Epinephelus guttatus* (Linnaeus, 1758) specimens from Lee Stocking Island, Bahamas, were used in the preliminary mitochondrial DNA study.

Specimens were frozen upon capture and stored at –20°C or –80°C and transported to the laboratory for analysis. For mitochondrial and nuclear DNA analysis, muscle tissues were removed and placed in storage buffer (0.25M EDTA, 20% DMSO and saturated with NaCl). For allozyme analysis, 1.5-cm^3 pieces of liver and muscle tissue were separately homogenized in 250 µL of chilled (4°C) grinding buffer (0.1 M Tris, 0.9 mM EDTA, and 0.05 mM $NADP^+$, pH 7.2). Samples were centrifuged for 3 min at 16,000 ×g and stored at –80°C or analyzed immediately.

Genomic DNA was isolated from a 1.0-cm^3 piece of muscle tissue by using the phenol/chloroform protocol of Winnepenninckx et al. (1993) with the following modifications. CTAB (hexadecyltrimethylammonium bromide) was not added to the extraction and phenol was added immediately following incubation of the tissue at 37°C. DNA was precipitated by the addition of 0.04 volume of 5M NaCl and 1.0 volume of isopropanol. DNA was resuspended in 150 µL of sterile 0.1X TE (Tris-EDTA) and stored at –20°C.

Table 1

National Museum of Natural History (USNM) and Virginia Institute of Marine Science (VIMS) catalogue numbers for specimens used in the morphological analysis.

Species	Collection	Specimen	Standard length (mm)
C. fulva	USNM	88717	232
	USNM	53134	217
	USNM	53134	176
	USNM	133689	171
	VIMS	10413	222
	VIMS	10414	213
	VIMS	10415	210
	VIMS	10416	170
	VIMS	10417	146
	USNM	320539	240
P. furcifer	VIMS	10410	274
	VIMS	10411	259
	VIMS	10412	274
	USNM	107108	218
	USNM	358541	237
	USNM	33255	207
	USNM	12540	185
	USNM	65605-8244	201
	USNM	65605-8246	176
	USNM	65605-8246	129
Putative hybrid	VIMS	10403	190
	VIMS	10402	199
	VIMS	10401	222
	VIMS	10404	237
	VIMS	10405	210
	VIMS	10406	195
	VIMS	10407	172
	VIMS	10408	114
	VIMS	10409	181
	USNM	1240011	230

Morphological analyses

Specimens of *C. fulva* and *P. furcifer* used in the morphological analysis were obtained from and measured at the National Museum of Natural History (Table 1). Ten putative hybrids were suitable for morphological analysis. The remaining five samples were not properly preserved and morphological analysis was not possible. Hybrid specimens as well as a small number of the *C. fulva* and *P. furcifer* were frozen. Specimens obtained from the National Museum of Natural History were fixed in for-

malin. Morphometric and meristic characters were examined as described in Smith (1971) by using dial calipers and a meter stick. The morphometric data were analyzed by using a sheared principal component analysis with a covariance matrix to confine the effect of size to the first principal component (Humphries et al., 1981; Bookstein et al., 1985; Stauffer et al., 1997). The meristic data were analyzed by using a principal component analysis with a correlation matrix.

Allozyme analysis

Horizontal starch gel electrophoresis followed the protocols described in Murphy et al. (1996). Gels (12%w/v; Starch Art Corp., Smithville, TX) were run on one of three buffer systems: Tris-citrate II buffer (TC II) (30 mAmps for 14 hours), lithium hydroxide buffer (LIOH) (25 mAmps for 14 hours), or Tris borate-EDTA buffer (EBT) (30 mAmps for 14 hours). Histochemical staining followed the protocols of Murphy et al. (1996), and locus nomenclature and allelic designations followed Shaklee et al. (1990).

A preliminary survey of 16 loci in 15 individuals each of *C. fulva* and *P. furcifer* (Table 2) was performed to identify those loci for which the alleles were consistently different among the presumed parent species, *C. fulva* and *P. furcifer*. All parent individuals and putative hybrids were then surveyed for all loci that demonstrated differences between the species.

Nuclear DNA analysis

An actin gene intron and the second intron in the S7 ribosomal protein gene (Chow and Hazama, 1998) were investigated by using restriction fragment length polymorphism (RFLP) analysis. Amplification primers and reaction conditions are listed in Table 3. The regions were amplified by using the PCR reagent system (GIBCO/BRL Life Technologies®, Bethesda, MD) and a 25-µL reaction cocktail (1X PCR buffer with $MgCl_2$, 0.2 mM dNTP, 0.5 µM primer, 2.5 U of *Taq* DNA polymerase, and 25–50 ng genomic DNA template). Some PCR reactions were performed with Platinum® *Taq* high fidelity (GIBCO/BRL Life Technologies®) with a 25-µL reaction cocktail (1X high fidelity buffer, 2 mM $MgSO_4$, 0.2 mM dNTP, 0.2 µM primer, and 2.5 U of Platinum® *Taq* DNA polymerase high fidelity). In other cases, 1 µL dimethyl sulfoxide (DMSO, Fisher Scientific BP231-1, Pittsburgh, PA) was added to the reaction to increase sensitivity.

The amplification products from two individuals of each species for both loci were digested with a panel of restriction enzymes to identify those that exhibited differences between the putative parent species. All samples were subsequently digested with those enzymes that demonstrated differences in the pilot study (Table 3). Digestion reactions (1.5-µL 10X buffer, 3 U restriction enzyme, and 4-µL PCR product) were incubated 2 to 18 hours at 37°C. Digestion products were separated on 2.5% agarose gels (1.25% Ultrapure Agarose, GIBCO/BRL Life Technology (R) + 1.25% NuSieve GTG (R) agarose, FMC Biochemical, Rockland, ME), stained with ethidium bromide and visualized under UV light.

Table 2

Allozyme analysis: information includes loci, buffer systems, and tissues.

Locus	Buffer	Tissue
Alcohol dehydrogenase (*ADH-1** 1.1.1.1)	EBT	liver
Creatine kinase (*CK-B** 2.7.3.2)	LIOH	liver
Creatine kinase (*CK-C**2.7.3.2)	LIOH	liver
Esterase, (*EST-1** 3.1.1.1)	EBT	liver
Esterase, (*EST-2** 3.1.1.1)	EBT	liver
Fumarase, (*FH** 4.2.1.2)	TCII	liver
Glucosephosphate isomerase (*GPI-A** 1.1.1.49)	EBT	liver
Isocitrate dehydrogenase (*ICDH-S** 1.1.1.42)	TCII	liver
Lactate dehydrogenase (*LDH-A** 1.1.1.27)	TCII	muscle
Lactate dehydrogenase (*LDH-B** 1.1.1.27)	TCII	liver
Malate dehydrogenase (*MDH-A** 1.1.1.37)	EBT	muscle
Malate dehydrogenase (*MDH-B** 1.1.1.37)	EBT	muscle
Peptidase-B (*PEP-1** 3.4.11)	LIOH	liver
Peptidase-S (*PEP-2** 3.4.11)	LIOH	liver
Peptidase-C (*PEP-3** 3.4.11)	LIOH	liver
Xanthine dehydrogenase (*XDH** 1.1.1.204)	EBT	liver

MtDNA analysis

The following regions of the mitochondrial genome were surveyed in the three putative parent species and hybrids; the adenosine 5′-triphosphatase subunit 6 (ATPase 6) gene, the 12S/16S ribosomal RNA gene region, and the nicotinamide dehydrogenase subunit 4 (ND4) gene. Amplification primers and reaction conditions are listed in Table 3. Amplified products of two individuals of each putative parent species were screened with restriction enzymes to identify potential differences between *C. fulva* and *P. furcifer* (Table 3). All individuals were screened at the three regions with those enzymes that revealed differences in the preliminary study. Restriction digestion reactions were performed and visualized as described for nuclear DNA. For each individual, the haplotype designations of each region were combined in sequence creating a composite haplotype.

Molecular data analysis

Nei's (1978) unbiased genetic distance was calculated from the allozyme data by using the computer program BIOSYS2 (Swofford and Selander, 1989). Mean nucleotide

Table 3

PCR primers and conditions used in the RFLP analysis of mtDNA and nuclear intron regions. The forward primer is on top, the reverse is on the bottom.

Region	Primer sequence	PCR conditions	Citation	Enzymes
12S/16S	12SA-L: 5′ AAA CTG GGA TTA GAT ACC CCA CTA T 3′ 16SA-H: 5′ ATG TTT TTG ATA AAC AGG CG 3′	94°C for 1 min., 45°C for 1 min., 65°C for 3 min.	Palumbi et al., 1991	*Ban* II, *Rsa* I
ATPase 6	H8969: 5′ GGG GNC GRA TRA ANA GRC T 3′ L8331: 5′ TAA GCR NYA GCC TTT TAA G 3′	95°C for 1 min., 45°C for 1min., 65°C for 3 min.	Quattro[1]	*Dde* I
ND4	ARG-BL: 5′ CAA GAC CCT TGA TTT CGG CTC A 3′ LEU: 5′ CCA GAG TTT CAG GCT CCT AAG ACC A 3′	95°C for 1 min., 45°C for 1 min., 65°C for 3 min.	Bielawski and Gold, 1996	*Bst*O I, *Hpa* II, *Mbo* I, *Rsa* I
S7 ribosomal	S7RPEX2F: 5′ AGC GCC AAA ATA GTG AAG CC 3′ S7RPEX2R: 5′ GCC TTC AGG TCA GAG TTC AT 3′	95°C for 30 sec., 60°C for 1 min., 72°C for 2 min.	Chow and Hazama, 1998	*Alu* I, *Dra* I
Actin intron	F3: 5′ ATG CCT CTG GTC GTA CCA CTG G 3′ R1: 5′ CAG GTC CTTACG GAT GTC G 3′	94°C for 1 min., 48°C for 1 min., 65°C for 3 min.	Cordes, 2000	*Hinf* I

[1] Quattro, J. 1999. Personal commun. Department of Biology, Univ. South Carolina, Columbia, SC 29208.

sequence divergence was calculated for the mitochondrial DNA RFLP results by using the equation of Nei and Li (1979) for fragment data with weighting based on Nei and Tajima (1983) as performed by the computer program REAP (McElroy et al., 1992). Genetic distance was not calculated for the nuclear DNA loci owing to an absence of shared restriction fragments between *C. fulva* and *P. furcifer*.

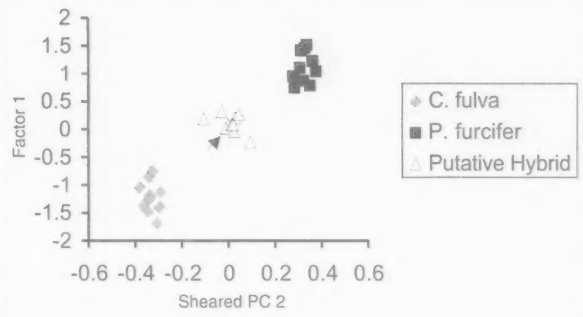

Figure 2

Graph of principal component 2 for the morphological data and factor 1 for the meristic data for ten *Cephalopholis fulva*, ten *Paranthias furcifer*, and ten putative hybrids. The arrow indicates putative hybrid H7, an individual identified as a backcross to *C. fulva*, according to the genetic data.

Results

Morphological analysis

Of 44 counts and measurements analyzed, mean values of 38 were different between *C. fulva* and *P. furcifer*, and the putative hybrids were intermediate in morphology to presumed parents for 33 of these characters (Table 4). The mean value for the putative hybrids exceeded the values of either presumed parent species for four characters (caudal peduncle scales, interorbital width, anal base length, and pectoral length) and was lower than either presumed parent species for two characters (orbit length and depressed dorsal length). In the principal component analysis, the first component accounted for 66% of the variation in the data and the second accounted for 23%. Suborbital width, caudal peduncle length, caudal peduncle to upper fin rays and caudal penduncle to lower fin rays were the characters with the highest loadings. In the meristic data, the first principal component accounted for 62% of the variation. Dorsal rays, gill rakers, and transverse scale rows had the highest loadings. A plot of the second principal component from the morphological analysis (variation in shape) and the first factor of the correlation matrix of the meristic data shows a discrete difference between the putative parents (Fig. 2). Hybrid individuals were shown to be intermediate between the putative parent species.

Allozyme analysis

Sixteen allozyme loci were surveyed in 15 *C. fulva* and 15 *P. furcifer* to identify those that had different alleles in

Table 4

Ranges of counts and measurements for ten *Paranthias furcifer*, ten *Cephalopholis fulva*, and ten putative hybrids. Measurements are given in millimeters. Raw measurements were divided by the standard length and multiplied by 1000. Means are given in parentheses, L.L. = lateral line, and the measurement for one hybrid discarded because of a broken third dorsal spine (*).

Measurement	*C. fulva*	Putative hybrids	*P. furcifer*
dorsal rays	IX, 15–16 (16)	IX, 17–18 (17)	IX, 18–19 (19)
anal soft rays	8–10 (9)	9–10 (9)	9–11 (10)
pectoral rays	32–35 (34)	35–37 (36)	36–39 (38)
gill rakers	22–28 (25)	24–35 (31)	32–39 (36)
scales above the L.L.	6–8 (8)	10–12 (11)	10–14 (12)
scales below the L.L.	22–27 (25)	26–30 (28)	26–32 (30)
transverse scale rows	64–84 (71)	75–91 (84)	85–96 (91)
caudal peduncle scales	40–49 (46)	44–52 (47)	43–48 (46)
head length	374–427 (402)	320–353 (335)	259–301 (280)
head width	173–227 (200)	150–189 (164)	130–162 (142)
head depth	248–288 (266)	212–250 (233)	183–241 (212)
snout length	86–122 (107)	79–111 (94)	53–79 (67)
suborbital width	44–52 (47)	29–35 (32)	20–24 (22)
interorbital width	64–78 (71)	73–89 (82)	76–89 (80)
orbit length (diameter)	62–76 (68)	56–67 (62)	52–89 (65)
postorbital head length	217–243 (232)	173–210 (192)	146–171 (159)
maxillary length	166–194 (182)	120–163 (141)	96–115 (104)
lower jaw length	176–200 (186)	117–149 (138)	98–114 (105)
snout to angle of preopercle	257–306 (282)	213–246 (229)	176–200 (188)
maxillary width	42–56 (48)	30–45 (41)	28–38 (34)
tip of lower jaw to gular notch	119–181 (145)	90–174 (123)	69–121 (89)
body width	154–223 (178)	155–181 (165)	138–162 (150)
body depth	325–385 (357)	302–361 (332)	282–354 (316)
caudal peduncle depth	128–139 (134)	118–145 (129)	102–122 (111)
tip of snout to dorsal origin	386–422 (407)	334–373 (354)	321–361 (329)
tip of snout to pectoral base	287–415 (371)	293–340 (319)	265–293 (277)
tip of lower jaw to pelvic base	398–449 (420)	359–420 (382)	321–384 (351)
dorsal base length	523–549 (538)	532–561 (543)	543–613 (583)
depressed dorsal length	609–663 (629)	574–643 (609)	603–658 (635)
anal base length	166–187 (174)	171–192 (182)	165–204 (180)
depressed anal length	268–320 (294)	248–273 (261)	232–278 (253)
end of dorsal to caudal base	129–150 (141)	148–165 (157)	145–175 (162)
length of caudal peduncle	166–198 (178)	194–217 (203)	174–241 (219)
pectoral length	257–292 (274)	253–295 (279)	249–290 (274)
pelvic length	186–211 (197)	143–192 (180)	150–187 (173)
dorsal spine I length	54–66 (62)	43–70 (61)	40–64 (53)
dorsal spine III length	103–138 (123)	90–119 (106)*	86–117 (105)
dorsal spine IX length	97–150 (127)	104–123 (111)	76–105 (94)
anal spine I length	52–72 (62)	35–66 (53)	36–48 (43)
anal spine II length	95–121 (106)	91–112 (101)	78–98 (86)
anal spine III length	78–118 (108)	97–121 (106)	74–101 (87)
caudal base to tip of upper rays	197–246 (216)	228–304 (280)	321–373 (347)
caudal base to tip of middle rays	204–248 (222)	164–192 (175)	122–143 (128)
caudal base to tip of lower rays	197–242 (217)	278–318 (294)	308–346 (322)

the two species (Table 2). At four loci (*CK-B**, *FH**, *LDH-B**, and *ICDH-S**) *C. fulva* and *P. furcifer* had different alleles. Forty *C. fulva*, *28 P. furcifer*, one *C. cruentata*, and ten putative hybrids were subsequently screened at the four diagnostic allozyme loci (Table 5). Eight of ten putative hybrids were heterozygous at all four diagnostic loci. One putative hybrid was heterozygous at all loci except the *LDH-B** locus, for which it displayed two alleles characteristic of *P. furcifer*, and another individual was heterozygous at all diagnostic loci, except the *FH** locus

Table 5

Allozyme genotypes of *Cephalopholis fulva*, *Paranthias furcifer*, *C. cruentata*, and putative hybrid individuals at four diagnostic loci, *CK-B**, *FH**, *ICDH-S**, and *LDH-B**. *n* = number of fish in a sample.

	n	*CK-B**	*FH**	*ICDH-S**	*LDH-B**
C. fulva	40	*100/100	*90/90	*95/95	*100/100
P. furcifer	28	*50/50	*100/100	*100/100	*75/75
C. cruentata	1	*100/100	*90/90	*105/105	*75/75
Putative hybrids	8	*50/100	*90/100	*100/95	*75/100
	1	*50/100	*90/100	*100/95	*75/75
	1	*50/100	*90/90	*100/95	*75/100

Table 6

RFLP genotypes for the nuclear intron and mtDNA loci. Some bands (†) were inferred so that fragments would sum to the total (uncut) size of the amplified gene region.

Locus	Enzyme	Allele	Approximate size (bp)
actin intron	Hin*f* I	A	400, 50†
		B	450
S7 intron	*Dra* I	A	575, 550, 75†
		D	1200
		E	575, 525, 75†, 25†
ATPase 6	*Dde* I	A	600, 50†
		B	360, 150, 90, 50†
		C	650
12S/16S	*Rsa* I	A	600, 500, 300, 200
		B	600, 300, 250, 250, 200
		C	450, 375, 300, 275, 100, 100†
	Ban II	A	1600
		B	1100, 500
ND4	*Bst*O I	A	1250, 625, 25†
		B	1250, 450, 200
		C	1450, 450
	Hpa II	A	1400, 500
		C	1900
		D	1000, 900
	Mbo I	A	700, 500, 400, 300
		B	550, 500, 400, 300, 150
		C	525, 400, 300, 275, 250, 80, 70
	Rsa I	A	1025, 500, 375
		B	610, 500, 400, 390
		C	500, 400, 350, 300, 300, 50†
		D	900, 425, 325, 250

for which it displayed two alleles diagnostic of *C. fulva*. *Cephalopholis cruentata* was distinguished from *C. fulva* and *P. furcifer* at the *ICDH-S** locus and was eliminated as a potential parent species.

Table 7

Genotypes of *Cephalopholis fulva*, *Paranthias furcifer*, *C. cruentata*, and putative hybrids for the short actin intron and the second intron in the S7 ribosomal protein region. *n* = number of fish in a sample.

	Actin intron		S7 intron	
Species	*n*	*Hinf* I	*n*	*Dra* I
Cephalopholis fulva	57	A/A	50	A/A
			3	E/E
			4	A/E
Paranthias furcifer	37	B/B	37	D/D
C. cruentata	5	B/B	5	D/D
Putative hybrid	15	A/B	14	A/D
			1	E/D

Nuclear intron regions

An actin intron approximately 450 base pairs in length was amplified. The region was surveyed with 14 restriction enzymes, of which *Hinf* I showed a genetic difference between species. After digestion with *Hinf* I, all *C. fulva* demonstrated allele A, and all *P. furcifer* diplayed allele B (Tables 6 and 7). All fifteen putative hybrids were heterozygous for both alleles.

The second intron region of the S7 ribosomal protein, which was approximately 1200 base pairs in length, was screened with thirty-five enzymes. Two enzymes, *Dra* I and *Alu* I, demonstrated differences between *P. furcifer* and *C. fulva*. *Paranthias furcifer* and *C. cruentata* both exhibited allele D after digestion with *Dra* I (Tables 6 and 7). *Cephalopholis fulva* was variable at this locus—fifty individuals were homozygous for allele A, three homozygous for allele E, and four heterozygous for alleles A and E. All fifteen putative hybrids were heterozygous at this locus with one of the *C. fulva* alleles (A or E), and the *P. furcifer* allele (D). Digestion of the second intron in the S7 region by *Alu* I produced a large number of small fragments that were not easily interpreted and the data were not used

to identify hybridization between *C. fulva* and *P. furcifer*. With this enzyme, however, *C. cruentata* had a unique allele and was thus eliminated as a putative parent for the hybrid individuals.

Mitochondrial DNA

Allelic differences between *C. fulva* and *P. furcifer* were found in all three mitochondrial gene regions. The ATPase 6 region was screened with six enzymes, one of which, *Dde* I, showed differences between *C. fulva*, *P. furcifer*, and *C. cruentata* (Tables 3 and 6). The 12S/16S region was screened with seven enzymes. Two of these, *Ban* II and *Rsa* I, demonstrated differences between *C. fulva*, *P. furcifer*, and *C. cruentata*. The ND4 region was screened with nine restriction enzymes, four of which (*Bst*O I, *Hpa* II, *Mbo* I, and *Rsa* I) showed differences between the species; mtDNA composite haplotypes were unique to each species (Table 8). All 15 putative hybrids in the study had a composite haplotype matching the common haplotype of *C. fulva*, indicating that it was the maternal parent for all hybrid individuals. Three *Epinephelus guttatus* specimens were screened at the ND4 and ATPase 6 regions and showed a unique composite haplotype; therefore this species was not included in the study as a putative parent species.

Discussion

Morphological analysis

In most cases, F_1 hybrids should be morphologically intermediate to the parent species and have low variation within characters among themselves. Backcross individuals, because of random sorting of chromosomes, should have higher variation within intermediate characters and could fall anywhere in the morphological range of the pure parent species (Anderson, 1949). In a principal component analysis plot, a backcross hybrid's score would be expected to be closer to the parent species to which the hybrid backcrossed, whereas an F_1 hybrid's characters would be expected to be in the center, closer to an average of the scores of the parent species.

A plot of the second principal component of the morphological analysis and the first factor of the meristic analysis (Fig. 2) shows that *C. fulva* and *P. furcifer* are well segregated according to morphological characters. The putative hybrid individuals were clustered in between the parent species. The post-F_1 hybrid detected by using genetic analyses, indicated by an arrow in Figure 2, clustered with the putative F_1 hybrid individuals.

Table 8

Composite haplotypes of *Cephalopholis fulva*, *Paranthias furcifer*, and *C. cruentata* for the mitochondrial DNA data. Haplotypes are given for the following sequences of mtDNA loci and enzymes: 1) ATPase 6—*Dde* I; 2) ND4—*Bst*O I, *Hpa* II, *Mbo* I, *Rsa* I; and 3) 12S/16S—*Rsa* I, *Ban* II. *n* = number of fish in a sample.

Species	*n*	Composite haplotype
Cephalopholis fulva	56	AAABBAA
	1	AAABCAA
Paranthias furcifer	36	BBCADBB
	1	BBDADBB
C. cruentata	5	CCDCACB
Putative hybrids	15	AAABBAA

Genetic analyses

Results of the allozyme analysis also supported hybridization between *C. fulva* and *P. furcifer* in Bermuda. The putative hybrids were heterozygous at four distinguishing loci, with the exception of two individuals that were homozygous at one diagnostic locus each. One individual was homozygous at the *LDH-B** locus for the **75* allele. All twenty-eight *P. furcifer* were homozygous for this same allele, indicating hybrid backcrossing to *P. furcifer*. Another hybrid individual was homozygous at the *FH** locus for the **90* allele. The 40 *C. fulva* sampled in this study were homozygous for this allele, suggesting hybrid backcrossing to *C. fulva*. This hybrid individual was among those included in the morphological study and, as shown in the principal component plot (Fig. 2), was morphologically the most similar to *C. fulva*. It was not possible to distinguish F_2 hybrids and backcross hybrid individuals and henceforth the two individuals described above are referred to as post-F_1 hybrids. Because all members of the presumed parent samples were homozygous at all loci for diagnostic alleles, there was no evidence of introgression between *C. fulva* and *P. furcifer*.

The nuclear intron data were consistent with the allozyme data and supported the hypothesis of hybridization between *C. fulva* and *P. furcifer*. Because all hybrid individuals were heterozygous, post-F_1 hybridization was not evident at these loci. Alleles present at both nuclear DNA loci were unique between parent species and there was no indication of introgression between these species.

The mtDNA data clearly showed that *C. fulva* was the maternal parent for all putative hybrids, including the two post-F_1 hybrids. This finding suggests a strong gender bias in hybridization. All *C. fulva* had composite haplotypes quite distinct from those of *P. furcifer*, and there was no evidence of mtDNA introgression between the two parent species.

Overall, the genetic and morphological analyses suggest that all but two of the 15 putative hybrids were F_1 individuals representing first generation hybridization between a female *C. fulva* and a male *P. furcifer* (Table 9). The occurrence of two post-F_1 hybrids indicates that F_1 hybrids are fertile, and the genotypes of the two post-F_1 hybrids demonstrate that F_1 hybrids can backcross with either parent species.

Hybridization in Bermuda

Hybridization between *C. fulva* and *P. furcifer* is known from only certain localities in the tropical Atlantic, despite

Table 9

Classification of all putative hybrid individuals as F_1 and post-F_1 individuals based on morphological and genetic data.

Sample ID	Classification	Data
H1	post-F_1	allozyme, mtDNA, nDNA
H2	F_1	mtDNA, nDNA
H3	F_1	mtDNA, nDNA
H4	F_1	mtDNA, nDNA
H5	F_1	mtDNA, nDNA
H6	F_1	mtDNA, nDNA
H7	post-F_1	morphology, allozyme, mtDNA, nDNA
H8	F_1	morphology, allozyme, mtDNA, nDNA
H9	F_1	morphology, allozyme, mtDNA, nDNA
H10	F_1	morphology, allozyme, mtDNA, nDNA
H11	F_1	morphology, allozyme, mtDNA, nDNA
H12	F_1	morphology, allozyme, mtDNA, nDNA
H13	F_1	morphology, allozyme, mtDNA, nDNA
H14	F_1	morphology, allozyme, mtDNA, nDNA
H15	F_1	morphology, allozyme, mtDNA, nDNA
USNM 124001	F_1	morphology

broad overlap in the geographical ranges of the two species. Bermuda exists at the northern range of *C. fulva* and *P. furcifer*, and the two species have restricted spawning times. *Cephalopholis fulva* and *P. furcifer* both spawn in Bermuda from May to early August (Smith, 1958, as cited in Thompson and Munro, 1978), and spawning individuals of the two species have been sampled in the same location (Burnett-Herkes, 1975; B. Luckhurst, personal observ.). Similarly, two hybrids have been reported from Jamaica where the parent species also have overlapping spawning times (Thompson and Munro, 1978).

Hybridization between *C. fulva* and *P. furcifer* could be the result of directed interspecific interactions, or the chance meeting of gametes spawned at the same time in the same general location. However, because all 13 F_1 hybrids were the result of *C. fulva* eggs fertilized with *P. furcifer* sperm, it appears that there is a gender bias in hybridization. Possible hybridization scenarios include differences in sex ratio between *C. fulva* and *P. furcifer*, a biochemical block on fertilization of *P. furcifer* eggs by *C. fulva* sperm, or "sneaker" *P. furcifer* males in *C. fulva* spawning groups.

Based on the number of individuals collected in Bermuda over the last two years, hybridization between *C. fulva* and *P. furcifer* seems to be relatively rare. Although the reproductive status of the hybrids is unknown, the occurrence of two fertile female F_1 hybrids (one of which was ripe), a spent male F_1 hybrid, and the presence of post-F_1 hybrids, it can be concluded that some F_1 hybrids are capable of producing viable offspring. However, reproduction of F_1 hybrids does not appear to be very extensive. Within the limits of the samples analyzed there was no evidence of introgression of alleles between parent species.

Intergeneric hybridization

Intergeneric hybridization in animals seems to be relatively rare. It is believed that the ability to hybridize is an indication of evolutionary relatedness and that divergent taxa should have lost the ability to interbreed through the evolution of reproductive isolating barriers (Sibley, 1957). However, there are several examples of intergeneric hybridization in fishes, most notably in the cyprinids (Hubbs, 1955; Smith, 1973; Aspinwall et al., 1993; Stauffer et al., 1997).

Intergeneric hybridization between two such ecologically different species as *C. fulva* and *P. furcifer* has also been noted in the lutjanids. Poey (1860) described an intergeneric hybrid between *Lutjanus synagris* and *Ocyurus chrysurus*. Both Loftus (1992) and Domeier and Clarke (1992) presented reviews of this case of hybridization and Loftus (1992) theorized that the species were capable of interbreeding on the basis of overlap of spawning time and habitat. Both Loftus (1992) and Domeier and Clarke (1992) surmised that *O. chrysurus* should not constitute its own genus but be included within the genus *Lutjanus*, owing to its ability to hybridize with a member of that genus. Further support for this revision was provided by Chow and Walsh (1992), who reported a high genetic similarity between *O. chrysurus* and several *Lutjanus* species of the western North Atlantic. They suggested that the species appeared to be misplaced due to its unique morphological features.

A parallel situation exists with the epinepheline serrands because the genetic distance data suggest that *P. furcifer* does not belong in a separate genus from *Cephalopholis*. Recently, Craig et al. (2001) used mitochondrial DNA sequencing to demonstrate a close phylogenetic relationship

between the genera *Paranthias* and *Cephalopholis*. They also cited several morphological and ontogenetic similarities between the two genera. In the present study, an analysis of 16 allozyme loci produced a Nei's (1978) unbiased genetic distance of 0.356 between *P. furcifer* and *C. fulva*, which is within the range reported between *Ocyurus chrysurus* and species of *Lutjanus* (Chow and Walsh, 1992). The mitochondrial DNA sequence divergence data indicated that *P. furcifer* is closer to, or at least no farther from, *C. fulva* (0.036) than is *C. cruentata* (0.042) and that the congeners are most distant, (0.052). Both values are within the range reported between other congeneric serranids (Graves et al., 1990).

Taxonomic revision of *P. furcifer* is not recommended at this time; however, the incidence of hybridization and the small genetic distance between *C. fulva* and *P. furcifer* suggest that a full-scale phylogenetic analysis of the subfamily is warranted. Such a study would have to include more species of *Cephalopholis*, other members of the subfamily Epinephelinae, and *P. colonus*, the eastern Pacific geminate species of *P. furcifer*.

Acknowledgments

Special thanks are extended to J. Parris Jr., J. Parris Sr., W. McCallan, J. Payne, A. Marshall, K. Gregory, L. Hollis, D. Young, L. Outerbridge, and M. Battersbee for donating captured hybrid specimens. T. Trott kindly assisted with field dissections in Bermuda, J. R. McDowell provided expert guidance with molecular techniques, and J. Stauffer Jr. is credited with the analysis of morphological data. J. Quattro and J. Cordes provided primer sequences. Financial assistance to MAB was generously provided by a scholarship from the International Women's Fishing Association. A draft of this manuscript was reviewed by T. A. Munroe and B. W. Bowen.

Literature cited

Anderson, E.
1949. Introgressive hybridization, 109 p. J. Wiley, New York, NY.

Aspinwall, N., D. Carpenter, and J. Bramble.
1993. The ecology of hybrids between the peamouth, *Mylocheilus caurinus*, and the redside shiner, *Richardsonius balteatus*, at Stave Lake, British Columbia, Canada. Can. J. Zool. 71:83–90.

Bielawski, J. P., and J. R. Gold.
1996. Unequal synonymous substitution rates within and between two protein-coding mitochondrial genes. Molec. Biol. Evol. 13:889–892.

Bookstein, F. L., B. Chernoff, R. L. Elder, J. M. Humphries, G. R. Smith, and R. E. Strauss.
1985. Morphometrics in evolutionary biology, 177 p. Academy of Natural Sciences of Philadelphia, Special Publication 15, Philadelphia, PA.

Burnett-Herkes, J.
1975. Contribution to the biology of the red hind, *Epinephelus guttatus*, a commercially important serranid fish from the tropical western Atlantic. Ph. D. diss., 154 p. Univ. Miami, Coral Gables, FL.

Campton, D. E.
1987. Natural hybridization and introgression in fishes: methods of detection and genetic interpretations. *In* Population genetics and fishery management (N. Ryman. and F. Utter, eds.), p. 161–192. Univ. Washington Press, Seattle, WA.

Chow, S., and K. Hazama.
1998. Universal PCR primers for S7 ribosomal protein gene introns in fish. Mol. Ecol. 7:1255–1256.

Chow, S., and P. J. Walsh.
1992. Biochemical and morphometric analyses for phylogenetic relationships between seven snapper species (subfamily Lutjaninae) of the western Atlantic. Bull. Mar. Sci. 50(3):508–519.

Cordes, J. F. A.
2000. Application of genetic markers to provide species identification and define stock structure: analyses of selected marine fishes of the mid-Atlantic bight. Ph.D. diss., 142 p. College of William and Mary, Gloucester Point, VA.

Craig, M. T., D. J. Pondella II, J. P. C. Franck, J. C. Hafner.
2001. On the status of the serranid fish genus *Epinephelus*: evidence for paraphyly based upon 16S rDNA sequence. Molec. Phylo. Evol. 19(1):121–130.

Domeier, M. L., and M. E. Clarke.
1992. A laboratory produced hybrid between *Lutjanus synagris* and *Ocyurus chrysurus* and a probable hybrid between *L. griseus* and *O. chrysurus* (Perciformes: Lutjanidae). Bull. Mar. Sci. 50(3):501–507.

Dowling, T. E., C. Moritz, J. D. Palmer, and L. H. Rieseberg.
1996. Nucleic acids III: analysis of fragments and restriction sites. *In* Molecular systematics (D. M. Hillis, C. Moritz, and B. K. Mable, eds.), p. 249–320. Sinauer Assoc. Inc., Sunderland, MA.

Dowling, T. E., G. R. Smith, and W. M. Brown.
1989. Reproductive isolation and introgression between *Notropis cornutus* and *Notropis chrysocephalus* (family Cyprinidae): comparison of morphology, allozymes, and mitochondrial DNA. Evolution 43(3):620–634.

Graves, J. E., M. J. Curtis, P. A. Oeth, and R. S. Waples.
1990. Biochemical genetics of southern California basses of the genus *Paralabrax*: specific identification of fresh and ethanol-preserved individual eggs and early larvae. Fish. Bull. 88:59–66.

Heemstra, P. C., and J. E. Randall.
1993. FAO species catalogue, vol. 16. Groupers of the world (family Serranidae, subfamily Epinephelinae). FAO Fish. Synop. 125, vol. 16, 382 p. FAO, Rome.

Hubbs, C. L.
1955. Hybridization between fish species in nature. Syst. Zool. 4:1–20.

Humphries, J. M., F. L. Bookstein, B. Chernoff, G. R. Smith, R. L. Elder, and S. G. Poss.
1981. Multivariate discrimination by shape in relation to size. Syst. Zool. 30:291–308.

Loftus, W. F.
1992. *Lutjanus ambiguus* (Poey), a natural intergeneric hybrid of *Ocyurus chrysurus* (Bloch) and *Lutjanus synagris* (Linnaeus). Bull. Mar. Sci. 50(3):489–500.

McElroy, D., P. Morgan, E. Bermingham, and I. Kornfield.
1992. REAP—the restriction enzyme analysis package. J. Heredity 83:157–158.

Murphy, R. W., J. W. Sites, D. G. Buth, and C. H. Haufler.
1996. Proteins: isozyme electrophoresis. *In* Molecular systematics (D. M. Hillis, C. Moritz, and B. K. Mable, eds.), p. 51–120. Sinauer Assoc. Inc., Sunderland, MA.

Nei, M.
1978. Estimation of average heterozygosity and genetic

distance from a small number of individuals. Genetics 23:341–369.

Nei, M.,and W.-H. Li.
1979. Mathematical model for studying genetic variation in terms of restriction endonucleases. Proc. Natl. Acad. Sci. 76:5269–5273.

Nei, M., and F. Tajima.
1983. Maximum likelihood estimation of the number of nucleotide substitutions from restriction site data. Genetics 105:207–217.

Palumbi, S. R., A. Martin, S. Romano, W. O. McMillan, L. Stice, and G. Grabowski.
1991. The simple fool's guide to PCR ver. 2.0, 47 p. [Available from the Dept. of Zoology and Kewalo Marine Laboratory, Univ. Hawaii, Hawaii, HI.]

Poey, F.
1860. Memorias sobre la historia natural de la Isla de Cuba. La Habana 2:97–336.
1875. Enumeratio piscium cubensium. An. Soc. Esp. Hist. Nat. Madrid 4:75–112.

Shaklee, J. B., F. W. Allendorf, D. C. Morizot, and G. S. Whitt.
1990. Gene nomenclature for protein-coding loci in fish. Trans. Am. Fish. Soc. 119:2–15.

Sibley, C. G.
1957. The evolutionary and taxonomic significance of sexual dimorphism and hybridization in birds. The Condor 59:166–191.

Smith, C. L.
1958. The groupers of Bermuda. *In* Bermuda Fisheries Research Program Final Report (J. E. Bardach, ed.), p. 37–59. Bermuda Trade Board, Hamilton, Bermuda.
1966. *Menephorus* Poey, a serranid genus based on two hybrids of *Cephalopholis fulva* and *Paranthias furcifer*, with comments on the systematic placement of *Paranthias*. Am. Mus. Nov. 2276:1–11.
1971. A revision of the American groupers: *Epinephelus* and allied genera. Bull. Am. Mus. Nat. Hist. 146:71–225.

Smith, G. R.
1973. Analysis of several hybrid cyprinid fishes from western North America. Copeia 1973:395–410.

Smith-Vaniz, W. F., B. B. Collette, and B. E. Luckhurst.
1999. Fishes of Bermuda: history, zoogeography, annotated checklist, and identification keys. ASIH (American Society of Ichthyologists and Herpatologists) Special Publ. 4, 424 p.

Stauffer, J. R. Jr., C. H. Hocutt, and R. L. Mayden.
1997. *Pararhinichthys*, a new monotypic genus of minnows (Teleostsi: Cyprinidae) of hybrid origin from eastern North America. Ichthyl. Explor. Freshwaters 7(4):327–336.

Swofford, D. L., and R. B. Selander.
1989. BIOSYS-2. A computer program for the analysis of allelic variation in population genetics and biochemical systematics, release 1.7. Illinois Natural History Survey, Champaign, Illinois.

Thompson, R., and J. L. Munro.
1978. Aspects of the biology and ecology of Caribbean reef fishes: Serranidae (hinds and groupers). J. Fish Biol. 12: 115–146.

Verspoor, E., and J. Hammar.
1991. Introgressive hybridization in fishes: the biochemical evidence. J. Fish Biol. 39 (suppl. A):309–334.

Winnepenninckx, B., T. Backeljau, and R. De Wachter.
1993. Extraction of high molecular weight DNA from molluscs. Trends Genet. 9 (12):407.

Effects of experimental harvest on red sea urchins (*Strongylocentrotus franciscanus*) in northern Washington

Sarah K. Carter
Glenn R. VanBlaricom
Washington Cooperative Fish and Wildlife Research Unit
School of Aquatic and Fishery Sciences
Box 355020
University of Washington
Seattle, Washington 98195-5020
Present address (for S. K. Carter): Wisconsin Department of Natural Resources
Bureau of Endangered Resources
101 South Webster St.
Madison, Wisconsin 53707-7921
E-mail address (for S. K. Carter): cartesk@dnr.state.wi.us

Abstract—Commercial harvest of red sea urchins began in Washington state in 1971. Harvests peaked in the late 1980s and have since declined substantially in Washington and other areas of the U.S. west coast. We studied effects of experimental harvest on red sea urchins in San Juan Channel (SJC), a marine reserve in northern Washington. We recorded changes in density and size distribution of sea urchin populations resulting from three levels of experimental harvest: 1) annual size-selective harvest (simulating current commercial urchin harvest regulations), 2) monthly complete (non–size-selective) harvest, and 3) no harvest (control) sites. We also examined recolonization rates of harvested sites. The red sea urchin population in SJC is composed of an accumulation of large, old individuals. Juvenile urchins represent less than 1% of the population. Lower and upper size limits for commercial harvest protect 5% and 45% of the population, respectively. Complete harvest reduced sea urchin densities by 95%. Annual size-selective harvest significantly decreased sea urchin densities by 67% in the first year and by 47% in the second year. Two years of size-selective harvest significantly altered the size distribution of urchins, decreasing the density of legal-size urchins. Recolonization of harvested sites varied seasonally and occurred primarily through immigration of adults. Selective harvest sites were recolonized to 51% and 38% of original densities, respectively, six months after the first and second annual harvests. Yields declined substantially in the second year of size-selective harvest because of the fishing down of the population and because of low recolonization rates of harvested sites. We recommend that managers consider the potential efficacy of marine harvest refuges and reevaluate the existing upper and lower size limits for commercial harvest to improve long-term management of the sea urchin fishery in Washington.

Manuscript accepted 28 March 2002.
Fish. Bull. 100:662–673 (2002).

Red sea urchins (*Strongylocentrotus franciscanus*) are the most commonly harvested species of sea urchin on the west coast of North America. Sea urchin harvest in this region occurs primarily in California, Washington, and British Columbia. The commercial sea urchin fishery in Washington began in 1971, and landings were low through the early 1980s (Fig. 1). Landings increased dramatically in the late 1980s, peaking at over 4000 metric tons (t) in 1988. Landings have since declined. Approximately 387 t of sea urchins were harvested in 2000, valued at $699,052 (Ulrich[1]). Red sea urchins currently constitute approximately 60% of landings—the remainder being green sea urchins (*S. droebachiensis*, Ulrich[1]).

The Washington sea urchin fishery currently is managed by using harvest quotas, size limits, license restrictions, limited entry, and mandatory log books (Lai and Bradbury, 1998). Season length is not limited, but harvest occurs primarily during the winter when roe quality is highest (Bradbury[2]). A rotational harvest strategy was practiced from 1977 until 1995, in which each harvest district (Fig. 2) was harvested once every third year. In 1995 a U.S. federal court ruling on shellfishery management in Washington's coastal marine waters (Shellfish Subproceedings of United States vs. State of Washington, 873 F. suppl. 1422, 1994, known commonly as the "Rafeedie Decision") allotted one half of all harvestable shellfish to native tribes. As a result, rotational harvest was discontinued and replaced by annual harvest to ensure that all tribes had equal access to their usual and accustomed fishing areas each year.

Sea urchin harvests declined substantially in the early 1990s along parts of the west coast (Fig. 1). Quotas and season lengths were reduced in Washington because of overharvesting concerns (Bradbury[2]). Quotas were not reduced in California, and catches declined substantially (Kalvass and Hendrix, 1997). Sea urchin densities in some harvested areas in northern California are less than one quarter of those in nearby reserve areas (Kalvass and Hendrix, 1997). In Washington, densities and the proportion of legal-size sea urchins in the population have declined (Pfister and Bradbury, 1996). Harvesters may be maintaining catch per unit of effort at high levels by exploiting new populations, thereby masking stock declines (Pfister and Bradbury, 1996).

Experimental harvests may indicate potential effects of commercial harvest

[1] Ulrich, M. 2001. Personal commun. Washington State Department of Fish and Wildlife, 600 Capitol Way North, Olympia, WA 98501.

[2] Bradbury, A. 2000. Personal commun. Washington State Department of Fish and Wildlife, Point Whitney Shellfish Laboratory, 1000 Point Whitney Road, Brinnon, WA 98320.

Table 1

Depth and area of study sites in San Juan Channel, Washington. Site numbers are those shown in Figure 2. Initial sea urchin densities are from sampling in permanently marked circular sampling areas in early March 1997.

Site	Abbreviation	Treatment	Depth (m)	Area (m^2)	Initial sea urchin density (no./m^2)
1. Mid San Juan Island	Mid SJI	complete harvest	6.6	428	1.15
2. South McConnell Island	South McConnell	complete harvest	10.4	405	1.13
3. O'Neal Island	O'Neal	complete harvest	5.8	430	1.36
4. Point Caution, San Juan Island	Point Caution	selective harvest	7.5	422	1.95
5. Upper San Juan Island	Upper SJI	selective harvest	9.1	421	1.27
6. North McConnell Island	North McConnell	selective harvest	9.1	415	0.37
7. Yellow Island	Yellow	control	6.9	404	2.05
8. Point George, Shaw Island	Point George	control	7.5	406	1.96
9. Shady Cove, San Juan Island	Shady Cove	control	10.2	447	0.94

on sea urchin populations in Washington. We examined changes in density and size distribution of red sea urchin populations resulting from two levels of experimental harvest. Our study site was San Juan Channel (SJC), one of two areas in Washington where commercial sea urchin harvest has been prohibited since the 1970s (Fig. 2). We compared density and size distribution data for sea urchins from experimentally harvested sites in SJC with similar data collected from 1) nearby control sites, and 2) 19 sites in the Strait of Juan de Fuca (SJDF), an area commercially harvested since the early 1970s. We also examined recolonization of harvested sites through recruitment and immigration. We discuss implications of our results for management of sea urchin harvest effort and the potential use of marine harvest refuges in enhancing Washington's sea urchin fishery.

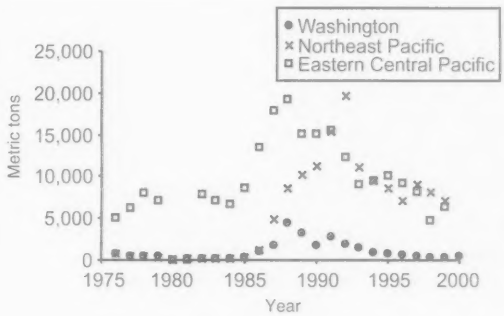

Figure 1

Annual harvest of red sea urchins (*Strongylocentrotus* spp.) in Washington state and in the larger Northeast Pacific and eastern Central Pacific areas of the west coast of the United States. Northeast Pacific includes the area north of 40°30′N (approximately Oregon-California border). Eastern Central Pacific includes the area south of 40°30′N. (Sources: Hoines, 1994, 1998; FAO, 1980, 1981, 1992, 2001; Bradbury.[2])

Methods

We established nine study sites in SJC from November 1996 to March 1997 (Fig. 2). Sites were 6–10 m in depth and approximately 10 m × 40 m, with the long axis of each site running parallel to the shoreline along the depth contour (Table 1). Eight permanently marked circular sampling areas (each 7.07 m^2) were located along the midline of each site along the depth contour. Site selection was based on high red sea urchin density (≥1.5/m^2 in preliminary surveys), substrate (primarily large cobble or bedrock) and safety considerations.

We applied one of three harvest treatments to each site. "Selective harvest" consisted of annual removal of all legal-size sea urchins (102–140 mm test diameter) each winter (March of 1997 and 1998). Selective harvest simulated the annual commercial harvest of a bed of sea urchins in the San Juan Islands (Pfister and Bradbury, 1996). "Complete harvest" consisted of removal of all sea urchins present in March 1997, and at monthly intervals thereafter through September 1998. The complete harvest treatment did not represent any current management strategy for commercial harvest. Rather, the complete harvest treatment represented one extreme (the control treatment being the second) against which effects of selective harvest may be compared. Sea urchin densities were not manipulated in the "control" treatment. Because of logistical constraints, control sites were located in smaller preserve areas within SJC where harvest of all invertebrates and fish is prohibited. Harvest treatments were randomly assigned to the remaining six sites. All sea urchins harvested were measured at the surface and released at other locations in SJC well away from the study sites.

In SJC, we sampled at large (sites) and small (circular areas within sites) spatial scales. Small-scale sampling was more frequent, allowing detection of potential short-

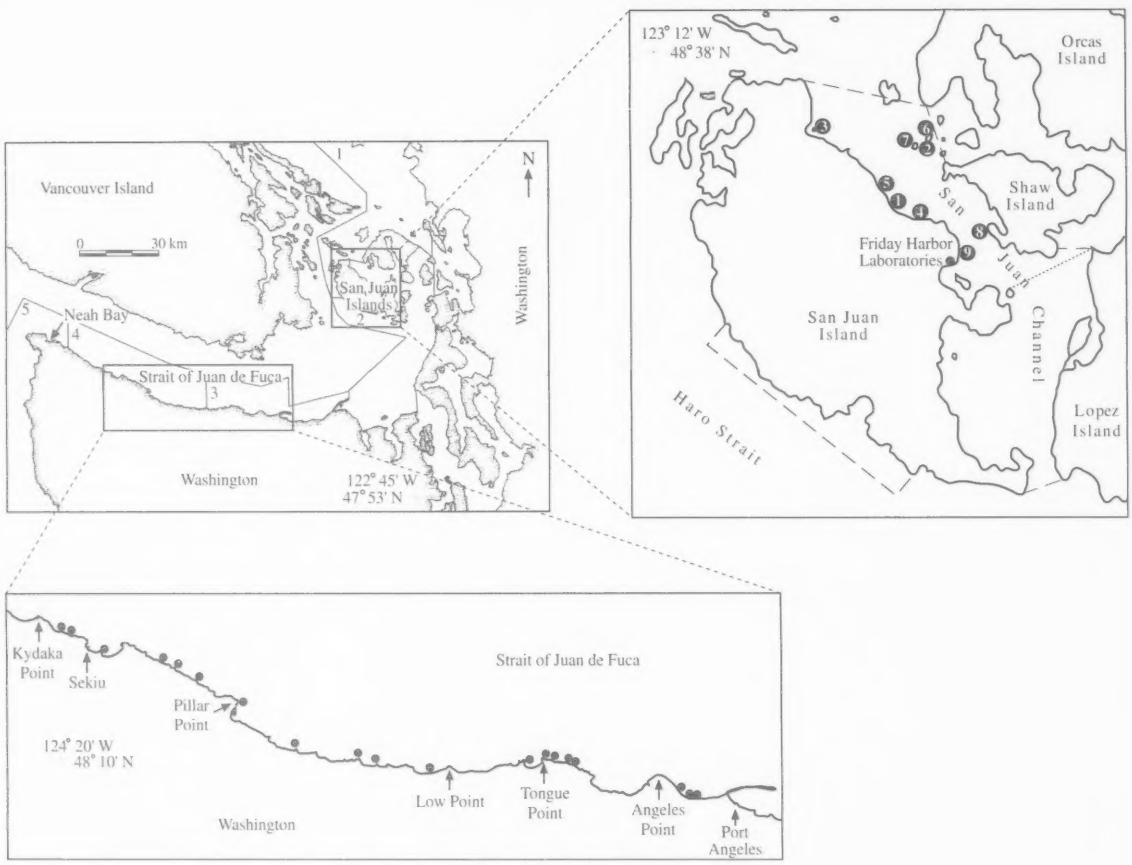

Figure 2

(**Upper left**) The commercial harvesting districts for sea urchins in Washington (after Lai and Bradbury, 1998). Harvest district numbers are shown in the upper left corner of each district. (**Right**) Enlargement of San Juan Channel, showing locations of study sites. Sites 1–3 are complete harvest sites, sites 4–6 are selective harvest sites, and sites 7–9 are control sites. Dashed lines represent the boundary of the areas on the west coast of San Juan Island and in San Juan Channel closed to commercial sea urchin harvest through fall 1998. The dotted line represents the modified southern boundary of the reserve area in San Juan Channel established in fall 1998. (**Lower left**) Enlargement of the Strait of Juan de Fuca sampling area. Black circles indicate locations of randomly chosen sampling sites.

term effects of harvest; whereas large-scale sampling better indicated how treatments affected the entire bed of sea urchins. We identify the scale of sampling (sites vs. circular areas within sites) for all results.

Size distribution

In SJC, we measured all sea urchins removed during the initial harvest of complete and selective harvest sites in March 1997, and all sea urchins removed during the second annual harvest of selective harvest sites in March 1998. In September of 1997 and 1998, we measured a minimum of 100 sea urchins *in situ* in all sites in randomly chosen 5 m × 5 m quadrats. We also measured sea urchins in the circular areas within sampling sites *in situ* in all sites five times per year: early March, mid March, April, June, and September. The sampling periods represented preharvest and 5, 30, 90, and 180 days after harvesting in each year for the selective harvest treatment.

Nineteen randomly chosen sites in the western SJDF were sampled in August and September 1997 (Fig. 2). All sites were 7–8 m below mean lower low water. At each site, we measured sea urchins *in situ* on 1–3 transects parallel to shore, each ≥30 m^2.

Lower and upper size limits for commercial sea urchin harvest are 102 and 140 mm test diameter in SJC, and 83 and 114 mm in SJDF (Pfister and Bradbury, 1996). Sea urchin measurements in SJC and SJDF were recorded to the nearest 5 mm (e.g. 130 mm=test diameters 130–134 mm), except during the initial sampling periods (March–June 1997), when sea urchins measured *in situ* only were recorded to the nearest 10 mm (e.g. 130 mm=test diameters

130–139 mm). Because of the measurement increment used, we could only estimate proportions of under-, legal-, and over-size sea urchins in SJC and SJDF. Asterisks (*) indicate estimated size classes. Estimated size classes are as follows: SJC—under*-size: 0–95 mm, legal*-size: 100–135 mm, and over*-size: 140–175 mm; SJDF—under*-size: 0–80 mm, legal*-size: 85–110 mm, and over*-size: 115–175 mm. Sea urchins less than 50 mm are less than two years old and were classified as juveniles (see Pfister and Bradbury, 1996).

Harvest and recolonization

Recolonization was determined for three periods: summer 1997 (March 1997 [postharvest]–September 1997), winter 1997 (September 1997–March 1998 [preharvest]), and summer 1998 (March 1998 [postharvest]–September 1998). In complete harvest sites, monthly recolonization for each time period was calculated as the sum of the number of sea urchins removed each month from each site during the time period divided by the number of months in the time period. A few sea urchins that divers did not harvest in March 1997 because they could not safely be removed from the substrate were excluded from the calculation of recolonization for the first time period. Size of recolonizers was based on sea urchins harvested from May 1997 to September 1998. In selective harvest sites where sea urchins were removed only once each year, we calculated monthly recolonization for each time period as the difference between the number of sea urchins counted in each site at the beginning and end of the time period, divided by the number of months in the time period.

At the end of the study (September 1998), divers sampled destructively for juvenile sea urchins in one 0.80-m^2 wedge within each circular area within a sampling site. Prior to this time, divers may not have seen very small sea urchins concealed underneath rocks or large sea urchins because sampling was not destructive to avoid disturbing other experiments. We include results on both red and green juvenile sea urchins sampled because of the very low number of red sea urchins sampled and to provide an indication of the microhabitats inhabited by juvenile sea urchins in general in SJC.

Data analysis

Size-frequency data were grouped into discrete size classes and compared by using chi-square analysis. Sea urchin data collected at each site were correlated over time. Therefore, we used a paired t-test to analyze the effect of harvest on the total number of sea urchins in sites and on the density of sea urchins in each size class. Similarly, we analyzed sea urchin densities in permanent circular areas over time by using repeated measures analysis of variance. In the analysis, site was treated as a random factor and was nested within treatment, which was treated as a fixed factor. Densities of juvenile sea urchins in September 1998 were analyzed by using analysis of variance. Sea urchin densities were log-transformed to improve the variance structure for analysis (Zar, 1984). Mean values generally are followed by one standard deviation in the text. The level of significance for all tests was $\alpha = 0.05$.

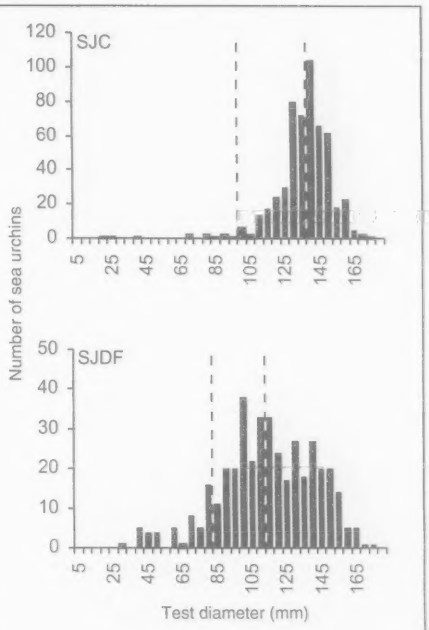

Figure 3

Size-frequency distribution of red sea urchins sampled in the three control sites combined in San Juan Channel (SJC) in September 1997 (n=537) and in the western Strait of Juan de Fuca (SJDF) in August 1997 (n=405). Dashed lines indicate minimum and maximum size limits for commercial harvest in each location.

Results

Size distribution of sea urchins in SJC and SJDF

Size distributions of red sea urchins in SJC were strongly skewed to the right and had a modal size of 140 mm (range 20–175 mm, Fig. 3). 4.8% (±3.1%) of sea urchins in circular areas in all sites in early March were <100 mm (under*-size), 50.0% (±13.0%) were 100–139 mm (legal*-size), and 45.2% (±12.5%) were ≥140 mm (over*-size). Juveniles represented 0.3% (±0.4%) of the population.

The modal size of red sea urchins in SJDF was 100 mm (range 30–175 mm, Fig. 3). 12.1% of the red sea urchin population was under*-size, 35.6% was legal*-size, and 52.4% was over*-size. Juveniles represented 2.5% of the population.

Effect of harvest on size distribution

Sea urchins harvested in the initial size-selective harvest in 1997 were 90–160 mm in diameter (mode 135 mm,

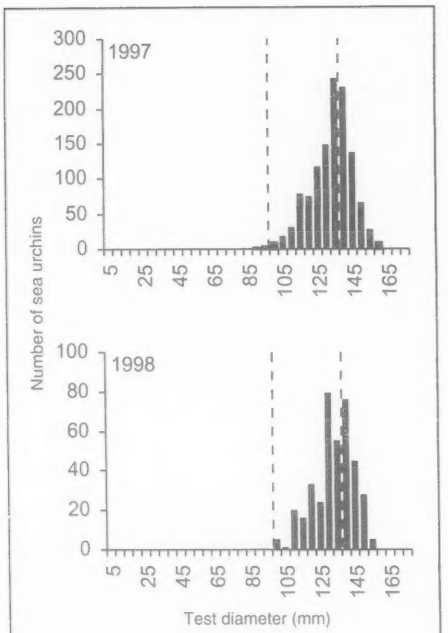

Figure 4

Size distribution of red sea urchins harvested from the three selective harvest sites combined in San Juan Channel (SJC) in March 1997 (n=1194) and March 1998 (n=387). Dashed lines indicate minimum and maximum size limits for commercial harvest in SJC.

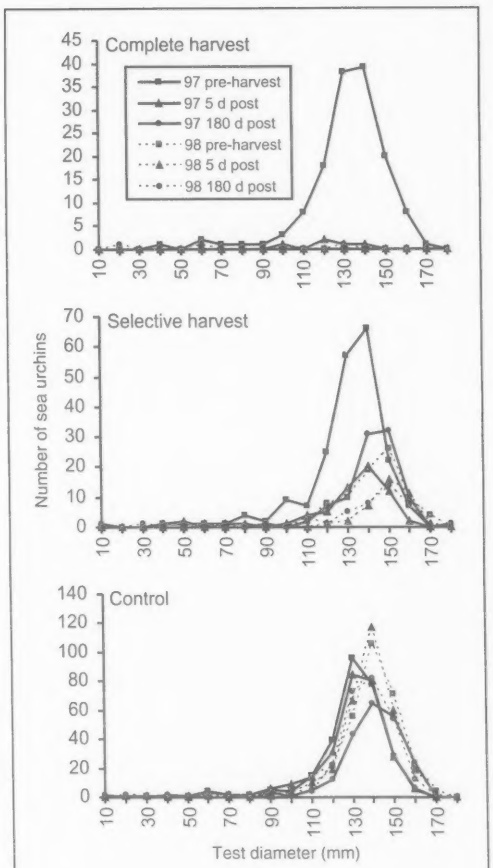

Figure 5

Size distribution of red sea urchins in the complete harvest, selective harvest, and control treatments in San Juan Channel (SJC) in early March (before harvest), mid-March (five days after harvest), and September (180 days after harvest) of 1997 and 1998. Solid lines represent sampling periods in 1997, and dashed lines represent sampling periods in 1998. Cumulative sample sizes for the three sites within each treatment and for all sampling periods illustrated are n = 149, 518, and 1627 for the complete harvest, selective harvest, and control treatments, respectively. Samples are from urchins measured *in situ* in sampling circles. One site (mid SJI) was excluded from the 1997 early March sampling period for the complete harvest treatment.

Fig. 4). The harvest consisted of 0.5% (±0.4%) under*-size sea urchins, 59.5% (±6.6%) legal*-size sea urchins, and 39.9% (±9.2%) over*-size sea urchins. Sea urchins harvested in the second annual size-selective harvest in 1998 were 100–155 mm in diameter (mode 130 mm). The composition of the harvest was similar: 0.0% (±0.0%), 57.1% (±18.7%), and 42.9% (±18.7%) of sea urchins were under*-, legal*-, and over*-size, respectively.

The initial size-selective harvest did not significantly alter the size distribution of the population (P=0.18, Fig. 5) but did significantly reduce the density of legal*-size sea urchins (P=0.05, Table 2). The cumulative effect of two annual size-selective harvests on the size distribution of the population was highly significant (P<0.0001, Fig. 5) and significantly reduced the density of legal*-size sea urchins (P=0.03, Table 2). The modal size of sea urchins in selective harvest sites increased to 150 mm after the second annual harvest (Fig. 5). Six months after the second annual harvest, the size distribution of the population remained significantly different from the original (1997 preharvest) size distribution (P=0.0001). Size distributions of sea urchins in selective harvest sites did not differ between fall 1997 and fall 1998 according to large-scale sampling (P=0.06), averaging 5.8%, 34.3%, and 60.0% for under*-, legal*-, and over*-size sea urchins, respectively (n=756). Size distributions of sea urchins in control sites, based on small-scale sampling, were similar throughout the study (Fig. 5) and did not differ between fall 1997 and fall 1998 according to large-scale sampling (P=0.10).

Table 2

Changes in the density (no./m^2) of under*-, legal*- and over*-size sea urchins as a result of selective harvests in March of 1997 and 1998. Values are averages (±SD) of the three selective harvest sites and are based on sea urchins sampled in permanent circular sampling areas within each site. See text for explanation of size categories.

	1997			1998		
	Preharvest	5 days after harvest	180 days after harvest	Preharvest	5 days after harvest	180 days after harvest
Under*-size	0.06 (±0.06)	0.03 (±0.04)	0.01 (±0.02)	0.00 (±0.00)	0.01 (±0.01)	0.01 (±0.01)
Legal*-size	0.62 (±0.37)	0.14 (±0.10)	0.18 (±0.24)	0.14 (±0.18)	0.04 (±0.06)	0.07 (±0.05)
Over*-size	0.52 (±0.39)	0.20 (±0.13)	0.37 (±0.18)	0.32 (±0.06)	0.19 (±0.08)	0.15 (±0.10)

Table 3

Total number of sea urchins (±SD) in San Juan Channel study sites over time. Harvests occurred in early March of 1997 and 1998. "Postharvest" data were collected immediately after the harvest by divers performing the harvest. SJI = San Juan Island.

	1997			1998		
Site	Preharvest	Postharvest	180 days after harvest	Preharvest	Postharvest	180 days after harvest
Complete harvest						
O'Neal Island	511	19				
Mid SJI	639	40				
South McConnell	641	37				
Average	597 (±74)	32 (±11)				
Selective harvest						
North McConnell	261	100	173	181	113	147
Upper SJI	560	206	229	207	92	139
Point Caution	907	228	421	430	226	290
Average	576 (±323)	178 (±68)	274 (±130)	273 (±137)	144 (±72)	192 (±85)
Control						
Yellow Island			547			646
Point George			823			859
Shady Cove			347			266
Average			572 (±239)			590 (±300)

Effect of harvest on density

Sea urchin densities in the SJC sites initially averaged 1.35/m^2 (±0.55, Table 1). Differences in initial sea urchin density between sites were marginally significant (P=0.05) because of the low density of sea urchins at North McConnell. Because of the difference in initial density, we expressed changes from preharvest to postharvest densities in SJC sites as percentages of the original population.

Initial harvest in March 1997 decreased the number of sea urchins in complete harvest sites by 94.7% (range: 93.7–96.3%) and in selective harvest sites by 66.6% (range: 61.7–74.9%, Table 3). Reharvest of selective harvest sites in March 1998 reduced sea urchin numbers 46.9% (range: 37.6–55.6%). All decreases were significant ($P \leq 0.04$). Yields from selective harvest sites averaged 0.95 sea urchins/m^2 in 1997, and 0.31 sea urchins/m^2 in 1998. The number of sea urchins in control sites did not differ between 1997 and 1998 (P=0.77, average 1.41/m^2).

Small-scale sampling also demonstrated significant changes in sea urchin density as a result of the experimental harvest treatments (Table 4). Initial harvest reduced sea urchin densities by 97.6% and 69.5% in complete and selective harvest sites, respectively. Mid-March (5 days after harvest) densities averaged 0.03/m^2 (±0.07/m^2) and 0.37/m^2 (±0.45/m^2) in complete and selective harvest sites, respectively. Sea urchin densities in complete harvest sites remained low for the duration of the study (<0.04/m^2). Sea urchin densities in selective harvest sites increased slight-

Table 4

Summary of repeated measure analysis of variance results for red sea urchin density. In cases where the degrees of freedom for the tests of significance for the within-subjects effects were adjusted by the Huynh-Feldt epsilon, the unadjusted degrees of freedom are given in parentheses. Asterisks in column five indicate factors significant at the 0.05 level. Power was estimated by using graphs in Zar (1984). (—) indicates that power was very low for the effect but could not be computed exactly (Sokal and Rohlf, 1995).

Source	Degrees of freedom	Mean square	*F*-ratio	*P*-value	Observed power
Within-subjects effects					
Year	1	0.24	1.88	0.22	<0.20
Year × treatment	2	0.11	0.88	0.46	—
Year × site (treatment)	6	0.13			
Season	3.56 (4)	0.28	14.34	* 0.000	>0.99
Season × treatment	7.11 (8)	0.055	2.78	* 0.033	0.44
Season × site (treatment)	21.34 (24)	0.020			
Year × season	3.72 (4)	0.12	9.42	* 0.000	0.98
Year × season × treatment	7.45 (8)	0.070	5.32	* 0.001	0.86
Year × season × site (treatment)	22.34 (24)	0.013			
Between-subjects effects					
Intercept	1	22.11	214.92	0.000	1.00
Treatment	2	6.79	14.99	* 0.005	0.95
Site (treatment)	6	0.45			

Table 5

Monthly recolonization (no. of sea urchins/site) for complete and selective harvest sites from April 1997 through September 1998. The summer and winter time periods are April–September and October–March, respectively. SJI = San Juan Island.

Treatment	Site	Summer 1997	Winter 1997	Summer 1998
Complete harvest	O'Neal Island	22.7	11.7	16.0
	Mid SJI	29.5	13.8	34.2
	South McConnell	16.3	4.7	6.3
	Average	22.8	10.1	18.8
Selective harvest	North McConnell	12.2	1.3	5.7
	Upper SJI	3.8	3.7	7.8
	Point Caution	32.2	1.5	10.7
	Average	16.1	0.3	8.1

ly in the summer following each harvest (see next section). Sea urchin densities in control sites changed little over time, averaging 1.61/m^2 (±1.4/m^2) over the study period.

Recolonization of harvested sites

Recolonization of complete harvest sites averaged 17.2 sea urchins per month (range: 0–68), or 0.04/m^2·month. The average size of sea urchins recolonizing complete harvest sites was 129 mm (±19 mm, range: 35–175 mm, n=824). Recolonization of complete harvest sites was higher during the summer of each year than during the winter and decreased slightly but not significantly over time (P=0.31, Table 5).

Recolonization of selective harvest sites was lower than observed in complete harvest sites (average 7.9 sea urchins/month or 0.02/m^2·month, Table 5). Recolonization was highest during summer 1997, followed by summer 1998. There was no net recolonization during winter 1997. Sites were recolonized to 51.2% of original densities by September 1997 (range: 40.9–66.3%, Table 3). In September 1998, after two annual harvests, sites averaged 37.7% of original densities (range: 24.8–56.3%).

Juvenile recruitment

Juvenile sea urchins were rare in all SJC study sites in March 1997 (0.4% (±0.6%) of sea urchins sampled in

Table 6

Modal size and proportion of juveniles in red sea urchin populations along the west coast of North America.

Location	Modal size (mm)	% of juveniles	Source
Southeast Alaska, shallow habitats	100–120	~35% <60 mm	Carney, 1991
Southeast Alaska, deep habitats	140–160	~8% <60 mm	Carney, 1991
Vancouver Island, BC	100–120	<5% <30 mm, ~50% <100 mm	Watson, 1993
Vancouver Island, BC	100–150*	~7% <50 mm*	Breen et al., 1978
Vancouver Island, BC	80–150*	0–11% <50 mm*	Breen et al., 1976
Strait of Georgia, BC	100–139*	9.5% <50 mm*	Sloan et al., 1987
San Juan Channel, Washington	140–144	0.3% <50 mm, 4.8% < 100 mm	This study
Strait of Juan de Fuca, Washington	100–104	2.5% <50 mm, 24.7% <100 mm	This study
Northern California	~107	~8–12% <50 mm	Rogers-Bennett et al., 1995; Smith et al., 1998
San Nicolas Island, Southern California	100–120	~7% < 50 mm	Cowen, 1983
Southern California	25 and 110	39% < 30 mm	Tegner and Dayton, 1981

* Commercially harvested populations.

circular areas). Over the entire study period, juvenile red sea urchin densities in circular areas averaged 0.005/m^2 in control sites (0.6% of the population), 0.001/m^2 in selective harvest sites (0.9% of the population), and 0.0006/m^2 in complete harvest sites. Sampling at the larger spatial scale revealed similar results. Juvenile sea urchin density averaged 0.002/m^2 in control sites in September of both 1997 and 1998. Juvenile sea urchin density averaged 0.001/m^2 and 0.005/m^2 in selective harvest sites in September of 1997 and 1998, respectively.

Invasive sampling in September 1998 confirmed that juvenile sea urchins were rare in SJC sites during the study. One juvenile (13 mm) red sea urchin and 45 juvenile (2–12 mm) green sea urchins were found in a search of 6.4 m^2 of substrate in each site (57.6 m^2 total). Density of juvenile green sea urchins sampled did not differ between treatments (P=0.79; average 0.79/m^2 [±0.86]). Only 4.3% of the juvenile green sea urchins were associated with (found within 8 cm of) an adult red sea urchin. 26.7% of juvenile green sea urchins were found in cryptic microhabitats (algal holdfasts), and the remainder were found on algal blades or on top of cobble, boulders, or bedrock.

Discussion

Size distribution of sea urchins in SJC and SJDF

The modal size of sea urchins in SJC is larger than observed in most other locations on the west coast (Table 6). The size distribution of red sea urchins in SJC sites is strongly skewed toward large individuals. The slow growth rate of sea urchins in Washington (Lai and Bradbury, 1998), combined with the fact that SJC was, at the time of our study, a reserve area that has never been subject to significant harvest, indicates that the sea urchin population in SJC is composed primarily of older individuals. Fewer juveniles are present in SJC and SJDF than in most other areas on the west coast (Table 6). Large recruitment events appear to be rare for red sea urchins in SJC, evidenced by the lack of peaks in the size distribution at small test diameters.

Effect of harvest on size distribution

The first annual size-selective harvest only slightly affected the size distribution of sea urchins in SJC. The cumulative effect of two annual size-selective harvests was significant, however, significantly reducing the density of legal*-size sea urchins in the population and increasing the modal size of the population. Commercial fisheries elsewhere along the west coast have also affected the size distribution of sea urchin populations. Three commercial harvests in the San Juan Islands (outside the SJC reserve) over a nine-year period decreased the proportion of legal-size sea urchins by about 73% (Pfister and Bradbury, 1996). In southern California, two years of harvest reduced the proportion of legal-size sea urchins in shallow waters by 15% (Tegner and Dayton, 1981). In northern California, the modal size of sea urchins in unharvested reserve sites was 108 mm, whereas the modal size of sea urchins in nearby heavily harvested sites with a 76-mm minimum size limit was 73 mm (Smith et al., 1998). On the east coast of Vancouver Island, however, the modal size of sea urchins remained above the legal size limit after 3+ years of significant harvest (Sloan et al., 1987).

The modal size of the sea urchin population and the upper size limit for legal harvest coincided in SJC. Small errors in the measurement of sea urchins by divers led to an incomplete harvest of legal-size sea urchins and inadvertent "poaching" of many over-size sea urchins (41% of the catch, likely a slight overestimate because sea urchins

140 mm in diameter were incorrectly classified as over-size). Both actions would tend to minimize effects of our experimental size-selective harvest. Commercial harvesters take a much smaller proportion of over-size sea urchins (11.2% of catch) and harvest a higher proportion of legal-size sea urchins (Pfister and Bradbury, 1996). Thus commercial harvest should produce larger differences in size distribution than observed in our study.

Effect of harvest on sea urchin density

Commercial harvest in nonreserve habitats of the San Juan Islands for over two decades has significantly decreased sea urchin densities (Pfister and Bradbury, 1996). Both harvest treatments in our study reduced sea urchin densities dramatically and immediately, as expected. The accumulation of older larger individuals in the SJC population led to high yields in selective harvest sites in 1997. Yields in selective harvest sites declined by more than two thirds in 1998 owing to the fishing down of the population (Hilborn and Walters, 1992), low immigration of legal-size sea urchins, and the presence of few under-size sea urchins in the population with a potential of growing to legal size.

Recolonization of harvested sites

Recolonization of harvested sites occurred primarily by immigration of adult red sea urchins. Recolonization began within one month of harvest and continued for the next 18 months. In northern California sites at 11 m in depth, red sea urchins also immigrated into harvested sites within a short time period (Rogers-Bennett et al., 1998). Complete and selective harvest sites in California were recolonized to 32% and 86% of their original densities, respectively, within nine days. These recolonization rates are much higher than those observed in SJC, possibly because of high sea urchin movement (up to 10 m/h, Rogers-Bennett et al., 1995, 1998) and smaller study plots (64 m^2 per site) in the northern California location. Sea urchins move less (~1 m/day) in areas with abundant food, such as in SJC, than in areas with little food (Mattison et al., 1977; Carney, 1991).

Seasonally high recolonization rates observed each spring in both harvest treatments may be related to feeding activity. Spring and summer are seasons when sea urchins feed more frequently (Vadas, 1968) and densities of algae preferred by sea urchins in SJC (e.g. *Laminaria*, *Nereocystis*, *Alaria*, and *Costaria*; Vadas, 1968, 1977) are highest (Carter, 1999). Both factors may have stimulated movement of sea urchins from deeper waters (with lower algal densities) into our sites.

On a monthly basis, selective harvest sites were recolonized at about half the rate at which complete harvest sites were recolonized. Sea urchins recolonizing complete harvest sites were removed monthly, whereas those recolonizing selective harvest sites were not. The presence of sea urchins, however, did not inhibit immigration in another study (Watson, 1993). Differences in sea urchin densities in adjacent habitats or food availability may have contributed to the observed differences in recolonization rates both within and between treatments.

Recolonization of selective harvest sites was insufficient to maintain sea urchin populations at the densities and size distributions observed prior to harvest under an annual harvest scenario. A site in Washington was recolonized to preharvest density and size distribution after 2.5 years (Bradbury, 1991). Recolonization of SJC sites varied substantially in the first year following harvest (range 1–202 sea urchins per site). One year, after harvest, sites varied between 37% and 69% of their original densities. Such variability in recolonization between sites may be common and should be considered when estimating recolonization rates for commercially harvested areas.

Recolonization rates observed in this study should be considered maximum estimates for recolonization of commercially harvested areas. SJC study sites were small, and sea urchins were relatively abundant adjacent to sites. Commercial fishermen harvest entire beds of sea urchins before moving on to the next bed and prefer to harvest at shallow depths (Pfister and Bradbury, 1996; Kalvass and Hendrix, 1997; Bradbury[2]). Thus sea urchins in adjoining habitats at the same depth would likely be harvested, and only sea urchins inhabiting deeper waters would be available for recolonization.

Juvenile recruitment

The unimodal size distribution of red sea urchins and the rarity of juvenile red sea urchins in SJC suggest variable and infrequent red sea urchin recruitment in northern Washington. In central California, red sea urchin recruitment was also rare; no major recruitment events occurred during a ten-year period (Pearse and Hines, 1987). Size structures of other sea urchin populations north of Point Conception also suggest low red sea urchin recruitment (Table 6).

Commercial harvest may negatively affect juvenile recruitment in several ways. Commercial harvest decreases sea urchin densities in northern Washington (Pfister and Bradbury, 1996; our study), potentially decreasing fertilization rates and larval supply (Levitan et al., 1992). A reduction in adult sea urchin density might also negatively affect juveniles in benthic habitats because adult sea urchins may provide associated juveniles with protection from predators (Duggins, 1981; Breen et al., 1985) and provide an increased food source (Tegner and Dayton, 1977, but see Andrew and Choat, 1985). In southern and northern California, 81% and 73%, respectively, of juvenile red sea urchins were found under the spine canopy of adults (Tegner and Dayton, 1977; Rogers-Bennett et al., 1995). In southern California, juvenile sea urchins were less abundant in harvested sites than in control sites (Tegner and Dayton, 1977). In northern California, juvenile red sea urchins were rare or absent in completely harvested sites but were present in similar numbers in selectively harvested and control sites (Rogers-Bennett et al., 1998). In British Columbia, 69% of juvenile red sea urchins were associated with adults (Breen et al., 1985). Adults may be less important to juveniles in SJC than in other west coast areas because few (4.3%) juvenile green

sea urchins were found to be associated with adult red sea urchins (our study), juvenile abundance did not differ by harvest treatment (our study), refuge habitats (cobble, crevices, kelp holdfasts) are abundant, and fast moving sea urchin predators (e.g. fish, lobster) are rare or absent (Breen et al., 1985; Sloan et al., 1987).

Management implications

The current harvest strategy in Washington, applied to sea urchin beds in SJC, results in low yields in the second year of harvest owing to the fishing down of the population and slow recolonization of harvested areas. Annual commercial harvest of a single location is probably not economically viable. Commercial harvests in Washington and other areas of the west coast are well below levels observed in the late 1980s, and biomass estimates are not available to evaluate the status of stocks in Washington (Bradbury[2]). In such circumstances, options for managing the fishery to conserve, and possibly increase, stocks over the long term include artificially enhancing stocks, redirecting or reducing harvest, and establishing marine harvest refuges (Tegner, 1989; Quinn et al., 1993; Rogers-Bennett et al., 1995). Stock enhancement efforts often confer limited success (e.g. Tegner, 1989) and may negatively impact behavioral and genetic diversity of wild populations (Rogers-Bennett, 1997).

Sea urchin harvest in Washington is currently controlled by using harvest quotas, limited entry, and size limits; seasonal closures and rotational harvests were also employed until relatively recently (Pfister and Bradbury, 1996; Lai and Bradbury, 1998). Washington also has two marine harvest refuges (Fig. 2). Both rotational harvests and marine harvest refuges increase the probability of long-term survivorship of populations, particularly when recruitment is low and variable, as it appears to be in SJC (Botsford et al., 1993; Quinn et al., 1993; Pfister and Bradbury, 1996). Rotational harvests were discontinued in Washington in 1995, and the size of one of the two marine harvest refuges was reduced substantially in 1998 (Fig. 2). Additional marine harvest refuges in Washington might be established in areas difficult for harvesters to access (e.g. areas hazardous to navigation and far from port) with little decrease in the actual size of harvested areas (Starr, 1998). Critical to the effectiveness of marine harvest refuges in enhancing recruitment and fishery yields outside of refuge areas is the ability of larvae produced in refuges to recruit to areas outside of the refuge (Carr and Reed, 1992). The extended period that sea urchin larvae spend in the plankton (9–19 weeks, Strathmann, 1978) and the short residence time of water in SJC (Thomson, 1981; Hickey et al., 1991) suggest that larval dispersal from this and other refuge areas to areas outside of the refuge is highly likely, probably occurring on a scale of tens to hundreds of kilometers. Research on sea urchin recruitment patterns (including larval dispersal, settlement, and juvenile survival) in this region is needed to assess the potential for marine harvest refuges in Washington to contribute to recruitment of fished stocks in Washington.

The current size limits in SJC protect a substantially smaller proportion of the population than in SJDF (50% vs. 63%, respectively). Because there are very few small sea urchins in SJC, the lower size limit protects less than 5% of the population. The upper size limit, established to protect larger "broodstock," currently protects 45% of the population. Size limits in Washington were originally established to protect the lower and upper 20% of the population and to allow some individuals to grow through the legal-size "window" under a three-year rotational harvest policy (Pfister and Bradbury, 1996). Considering the small number of juveniles in the population and the return to an annual harvest in 1995, the existing size limits should be reevaluated for their efficacy at protecting local stocks in the context of other harvest control techniques.

Acknowledgments

This work was conducted as part of the requirements for a Master of Science degree for S. K. Carter in the School of Fisheries (now the School of Aquatic and Fishery Sciences) at the University of Washington. David Duggins, Terrie Klinger, Chris Foote, and Ken Chew provided helpful suggestions and guidance on many aspects of the project. Brian Allen cheerfully provided many hours of expert assistance with diving work. Sam Sublett, Martin Grassley, and many others also assisted with data collection. Dennis Willows and the staff and faculty at Friday Harbor Laboratories provided logistical support and use of the facilities and equipment. David Duggins and Terrie Klinger provided helpful comments on earlier versions of the manuscript. Funding for the project was provided by the U.S. Geological Survey-Biological Resources Division, the Washington Department of Fish and Wildlife, the North Pacific Universities Marine Mammal Research Consortium, the Washington Cooperative Fish and Wildlife Research Unit, the H. Mason Keeler Endowment for Excellence, the Egtvedt Endowment Scholarship, the John N. Cobb Scholarship, and the School of Fisheries, University of Washington. We offer sincere thanks to all.

Literature cited

Andrew, N. L., and J. H. Choat.
1985. Habitat related differences in the survivorship and growth of juvenile sea urchins. Mar. Ecol. Prog. Ser. 27: 155–161.

Botsford, L. W., J. F. Quinn, S. R. Wing and J. G. Brittnacher.
1993. Rotating spatial harvest of a benthic invertebrate, the red sea urchin, *Strongylocentrotus franciscanus*. *In* Proceedings of the international symposium on management strategies for exploited fish populations, p. 409–428. Alaska Sea Grant College Program AK-SC-93-02.

Bradbury, A.
1991. Management and stock assessment of the red sea urchin (*Strongylocentrotus franciscanus*) in Washington state: periodic rotation of the fishing grounds. J. Shellfish Res. 10(1):233.

Breen, P. A., B. E. Adkins, and D. C. Miller.
1978. Recovery rate in three exploited sea urchin popula-

tions from 1972 to 1977. Fish. Mar. Serv. Manuscr. Rep. 1446:1–27.

Breen, P. A., W. Carolsfeld, and K. L. Yamanaka.
1985. Social behaviour of juvenile red sea urchins, *Strongylocentrotus franciscanus* (Agassiz). J. Exp. Mar. Biol. Ecol. 92:45–61.

Breen, P. A., D. C. Miller and B. E. Adkins.
1976. An examination of harvested sea urchin populations in the Tofino area. Fish. Res. Board Can. Manuscr. Rep. Ser. 1401:1–23.

Carney, D.
1991. A comparison of densities, size distribution, gonad and total-gut indices, and relative movements, of red sea urchins (*Strongylocentrotus franciscanus*), in two depth regimes. M.S. thesis, 37 p. Univ. California, Santa Cruz, CA.

Carr, M. H., and D. C. Reed.
1992. Conceptual issues relevant to marine harvest refuges: examples from temperate reef fishes. Can. J. Fish. Aquat. Sci. 50:2019–2028.

Carter, S. K.
1999. Ecosystem effects of simulated sea otter predation and commercial sea urchin harvest on nearshore benthic communities in northern Washington. M.S. thesis, 302 p. Univ. Washington, Seattle, WA,

Cowen, R. K.
1983. The effect of sheephead (*Semicossyphus pulcher*) predation on red sea urchin (*Strongylocentrotus franciscanus*) populations: an experimental analysis. Oecologia 58:249–255.

Duggins, D. O.
1981. Interspecific facilitation in a guild of benthic marine herbivores. Oecologia 48:157–163.

FAO (Food and Agriculture Organization of the United Nations).
1980. Yearbook of fishery statistics, catches and landings. 1979. Vol. 48. FAO Fish. Ser. 13, 384 p. FAO, Rome.
1981. Yearbook of fishery statistics, catches and landings. 1978. Vol. 50. FAO Fish. Ser. 16, 386 p. FAO, Rome.
1992. FAO yearbook, fishery statistics, catches and landings. 1990. Vol. 70. FAO Fish. Ser. 38, 646 p. FAO, Rome.
2001. FAO yearbook, fishery statistics, capture production. 1999. Vol. 88/1. FAO Fish. Ser. 57, 752 p. FAO, Rome.

Hickey, B. M., R. E. Thomson, H. Yih, and P. H. LeBlond.
1991. Velocity and temperature fluctuations in a buoyancy-driven current off Vancouver Island. J. Geophys. Res. 96(C6):10507–10538.

Hilborn, R., and C .J. Walters.
1992. Quantitative fisheries stock assessment: choice, dynamics and uncertainty, 570 p. Chapman and Hall, New York, NY.

Hoines, L.
1994. 1991 fisheries statistical report, 80 p. Washington State Department of Fish and Wildlife, Olympia, WA.
1998. 1995 fisheries statistical report, 80 p. Washington State Department of Fish and Wildlife, Olympia, WA.

Kalvass, P. E., and J. M. Hendrix.
1997. The California red sea urchin, *Strongylocentrotus franciscanus*, fishery: catch, effort, and management trends. Mar. Fish. Rev. 59(2):1–17.

Lai, H. L., and A. Bradbury.
1998. A modified catch-at-size analysis model for a red sea urchin (*Strongylocentrotus franciscanus*) population. *In* Proceedings of the North Pacific symposium on invertebrate stock assessment and management (G. S. Jamieson and A. Campbell, eds.), p. 85–96. Can. Spec. Publ. Fish. Aquat. Sci. 125.

Levitan, D. R., M. A. Sewell and F. S. Chia.
1992. How distribution and abundance influence fertilization success in the sea urchin *Strongylocentrotus franciscanus*. Ecology 73:248–254.

Mattison, J. E., J. D. Trent, A. L. Shanks, T. B. Akin, and J. S. Pearse.
1977. Movement and feeding activity of red sea urchins (*Strongylocentrotus franciscanus*) adjacent to a kelp forest. Mar. Biol. 39:25–30.

Pearse, J. S., and A. H. Hines.
1987. Long-term population dynamics of sea urchins in a central California kelp forest: rare recruitment and rapid decline. Mar. Ecol. Prog. Ser. 39:275–283.

Pfister, C. A., and A. Bradbury.
1996. Harvesting red sea urchins: recent effects and future predictions. Ecol. Appl. 6:298–310.

Quinn, J. F., S. R. Wing, and L. W. Botsford.
1993. Harvest refugia in marine invertebrate fisheries: models and applications to the red sea urchin, *Strongylocentrotus franciscanus*. Am. Zool. 33:537–550.

Rogers-Bennett, L.
1997. Marine protected areas and the red sea urchin fishery. *In* California and the world ocean '97, proceedings of the conference; March 24–27, 1997, p. 412–423. American Society of Civil Engineers, San Diego, CA.

Rogers-Bennett, L., W. A. Bennett, H. C. Fastenau, and C. M. Dewees.
1995. Spatial variation in red sea urchin reproduction and morphology: implications for harvest refugia. Ecol. Appl. 5:1171–1180.

Rogers-Bennett, L., H. C. Fastenau, and C. M. Dewees.
1998. Recovery of red sea urchin beds following experimental harvest. *In* Echinoderms: San Francisco, Proceedings of the ninth international echinoderm conference, San Francisco, CA, August 5–9, 1996 (R. Mooi and M. Telford, eds.), p. 805–809. A.A. Balkema, Rotterdam, and Brookfield, VE.

Sloan, N. A., C. P. Lauridsen, and R. M. Harbo.
1987. Recruitment characteristics of the commercially harvested red sea urchin *Strongylocentrotus franciscanus* in southern British Columbia, Canada. Fish. Res. 5:55–69.

Smith, B. D., L. W. Botsford and S. R. Wing.
1998. Estimation of growth and mortality parameters from size frequency distributions lacking age patterns: the red sea urchin (*Strongylocentrotus franciscanus*) as an example. Can. J. Fish. Aquat. Sci. 55:1236–1247.

Sokal, R. R., and F. J. Rohlf.
1995. Biometry: the principles and practice of statistics in biological research, 887 p. W.H. Freeman and Company, New York, NY.

Starr, R. M.
1998. Design principles for rockfish reserves on the U.S. west coast. *In* Marine harvest refugia for west coast rockfish: a workshop (M. Yoklavich, ed.), p. 50–63. U.S. Dep. Commer., NOAA-TM-NMFS-SWFSC 255.

Strathmann, R.
1978. Length of pelagic period in echinoderms with feeding larvae from the northeast Pacific. J. Exp. Mar. Biol. Ecol. 34:23–27.

Tegner, M. J.
1989. The feasibility of enhancing red sea urchin, *Strongylocentrotus franciscanus*, stocks in California: an analysis of the options. Mar. Fish. Rev. 51(2):1–22.

Tegner, M. J., and P. K. Dayton.
1977. Sea urchin recruitment patterns and implications of commercial fishing. Science 196:324–326.

1981. Population structure, recruitment and mortality of two sea urchins (*Strongylocentrotus franciscanus* and *S. purpuratus*) in a kelp forest. Mar. Ecol. Prog. Ser. 5: 255–268.

Thomson, R. E.
1981. Oceanography of the British Columbia coast. Can. Spec. Publ. Fish. Aquat. Sci. 56, 291 p.

Vadas, R. L.
1968. The ecology of *Agarum* and the kelp bed community. Ph.D. diss., 280 p. Univ. Washington, Seattle, WA.

1977. Preferential feeding: an optimization strategy in sea urchins. Ecol. Monogr. 47:337–371.

Watson, J. C.
1993. The effects of sea otter (*Enhydra lutris*) foraging on shallow rocky communities off northwestern Vancouver Island, British Columbia. Ph.D. diss., 169 p. Univ. California, Santa Cruz, CA.

Zar, J. H.
1984. Biostatistical analysis, second edition, 718 p. Prentice Hall, Englewood Cliffs, NJ.

Age and growth of the smooth dogfish (*Mustelus canis*) in the northwest Atlantic Ocean

Christina L. Conrath
Virginia Institute of Marine Science
College of William and Mary
1208 Greate Road
Gloucester Point, Virginia 23062
E-mail address: conrath@vims.edu

James Gelsleichter
Mote Marine Laboratory
1600 Ken Thompson Parkway
Sarasota, Florida 34236

John A. Musick
Virginia Institute of Marine Science
College of William and Mary
1208 Greate Road
Gloucester Point, Virginia 23062

Abstract—The northwest Atlantic population of smooth dogfish (*Mustelus canis*) ranges from Cape Cod, Massachusetts, to South Carolina. Although *M. canis* is seasonally abundant in this region, very little is known about important aspects of its biology, such as growth and reproductive rates. In the early 1990s, commercial fishery landings of smooth dogfish dramatically increased on the east coast of the United States. This study investigated growth rates of the east coast *M. canis* population through analysis of growth patterns in vertebral centra. Marginal increment analysis, estimates of precision, and patterns in seasonal growth supported the use of vertebrae to age these sharks. Growth bands in vertebral samples were used to estimate ages for 894 smooth dogfish. Age-length data were used to determine von Bertalanffy growth parameters for this population: K = 0.292/yr, L_∞ = 123.57 cm, and t_0 = −1.94 years for females, and K = 0.440/yr, L_∞ = 105.17 cm, and t_0 = −1.52 years for males. Males matured at two or three years of age and females matured between four and seven years of age. The oldest age estimate for male and female samples was ten and sixteen years, respectively.

Manuscript accepted 14 June 2002.
Fish. Bull. 100:674–682 (2002).

The smooth dogfish, *Mustelus canis*, is a small shark species found throughout the western Atlantic Ocean from Massachusetts to Florida, and in the northern Gulf of Mexico, including Cuba, Jamaica, Barbados, Bermuda, Bahamas, and southern Brazil to northern Argentina. Smooth dogfish are demersal and typically are found in inshore continental shelf and slope waters (Compagno, 1984). Several discrete populations of smooth dogfish likely exist, separated by large geographic areas; and there appears to be little intermigration between the different populations (Bigelow and Schroeder, 1948). The northwest Atlantic population of smooth dogfish ranges from Cape Cod, Massachusetts, to South Carolina and migrates seasonally in response to changing water temperatures (Bigelow and Schroeder, 1948; Castro, 1983).

Recently, commercial harvest of smooth dogfish has increased on the east coast of the United States. Annual landings were under 80,000 pounds before 1990, over 300,000 pounds in 1990, and increased to around 1 million pounds from 1998 to 2000. In one year (1995) landings exceeded 2.5 million pounds (Fig. 1) (NMFS, 2002). Smooth dogfish have been landed in significant amounts (i.e. over 50 metric tons) in Massachusetts, New Jersey, Maryland, Virginia, and North Carolina (NMFS, 2002).

Sharks are often highly susceptible to overfishing because of life history traits that include slow growth, large adult size, late reproduction, and the production of a few large well-formed young (Hoenig and Gruber, 1990). Because of these characteristics, shark fisheries tend to decline drastically after a short time and take long periods to recover (Holden, 1974). The determination of how increased exploitation will affect a shark population, like that of *M. canis* in the northwest Atlantic Ocean, requires information on the growth and reproductive rates of the species targeted by the fishery. The purpose of this study was to determine the growth rates of smooth dogfish from the northwest Atlantic Ocean by using age estimates derived from vertebral growth-band counts.

Materials and methods

Smooth dogfish were collected from NMFS groundfish and longline surveys, Virginia Institute of Marine Science (VIMS) longline surveys, Grice Marine Laboratory longline surveys, the Massachusetts state trawl survey, and by the Massachusetts Division of Marine Fish-

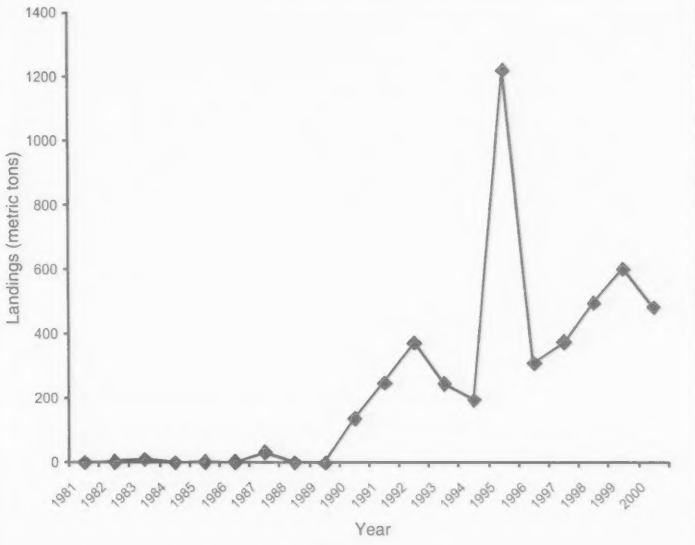

Figure 1

Reported smooth dogfish landings from National Marine Fisheries Service commercial catch statistics for the Atlantic and Gulf states, from 1981 to 2000.

eries (MDMF). Total length (TL), precaudal length (PCL), and male clasper length (CL) were measured, and sex was recorded at the time of collection. A section of the vertebral column containing eight to twelve vertebrae was removed from directly under the first dorsal fin and stored frozen. Reproductive samples were taken from smooth dogfish at this time and maturity state was assessed from these samples.

Vertebral samples were cleaned, soaked in 70% ETOH for 24 hours, and air-dried for 24 hours. Dried vertebrae were sagitally sectioned through the focus with an Isomet rotary diamond saw (Buehler, Lake Bluff, IL). Afterwards, vertebral sections were affixed to microscope slides with mounting medium and polished with wet fine-grit sand paper to a thickness of about 0.5 mm. The vertebrae were viewed under a binocular dissecting microscope with transmitted light.

Vertebral radius was measured from the focus of the vertebra along the axis of the corpus calcarium to the edge of the vertebra (Fig. 2). Total length (TL) was plotted against vertebral radius (VR) to determine if the growth of the vertebra was proportional to somatic growth of the animal and whether the structure was appropriate for estimating growth rate of the animal.

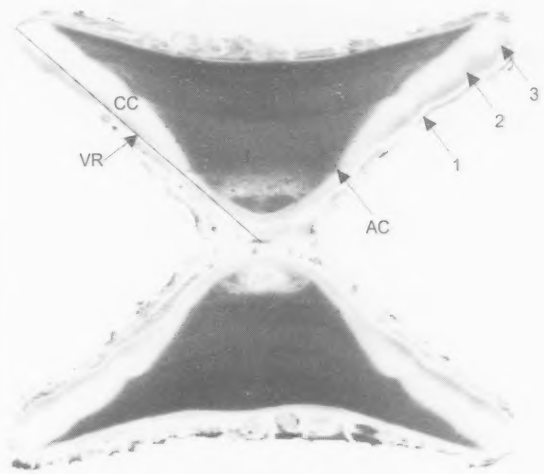

Figure 2

An age-3+ *Mustelus canis* vertebra, VR = vertebral radius, AC = angle change denoting birthmark, 1, 2, 3 = age 1, 2, and 3 growth bands, CC = corpus calcareum, and I = intermedialia.

Growth patterns of the vertebrae consisted of wide translucent bands separated by narrow opaque bands that extended from the intermedialia to the corpus calcareum (Fig. 2). An angle change—the result of a change in growth rates at this time—was present in the intermedialia approximately 2 mm from the focus of each vertebra and was considered to be a birthmark. Age was estimated by enumerating the narrow opaque bands, which were considered to form annually owing to a slowing or stopping of

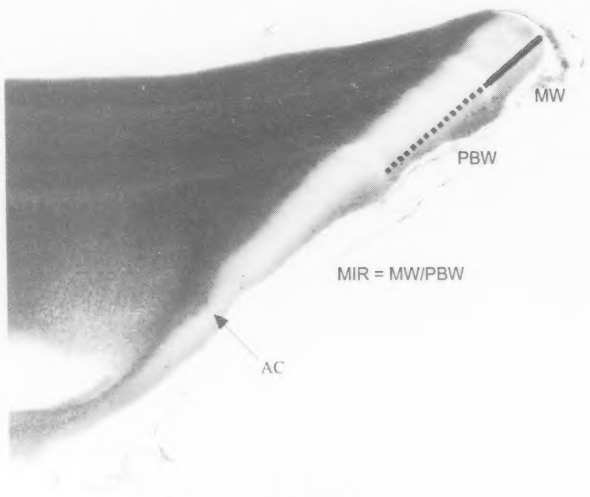

Figure 3

An age-2+ *Mustelus canis* vertebra showing the calculation of the marginal increment ratio, MW = margin width, PBW = previous band width, MIR = marginal increment ratio, AC = angle change.

growth during the winter months. This study followed the criteria found in Casey et al. (1985), who defined an "annulus" as a mark that appears as an opaque band in the intermedialia and continues as an opaque band into the corpus calcareum.

A random sample of twenty vertebrae from each of ten 10-cm size classes (33–132 cm TL) was read independently by two readers, and a chi-square test was used to test for systematic differences between the ages. The number of observations above the main diagonal of a contingency table of reader one's and reader two's ages was compared with the number of observations below the main diagonal to determine if this ratio was significantly different from 1:1. The percent agreement (PA), i.e. the percentage of vertebrae in each length group that were assigned the same ages by both readers, was determined to test for precision between the two readers.

Marginal increment analysis verified the annual nature of the narrow opaque growth bands. The distance from the last opaque band to the edge of the margin was measured and divided by the width of the last growth band on the vertebra to determine the marginal increment ratio (MIR, Fig. 3). The margin width was divided by the distance to the angle change or birthmark for age-1 animals. For age-0 animals, the distance from the angle change to the edge of the vertebrae was measured and divided by the distance from the focus to the angle change. The mean MIR for each month was plotted for juvenile-size animals to determine if there was a yearly pattern in margin width.

The length-at-age data were used to generate a von Bertalanffy growth curve for males and females by using the computer program SigmaPlot (SPSS Inc., 2000) and the Marquardt-Levenberg algorithm to estimate curve-fitting parameters (Press et al., 1986; Marquardt, 1963; Nash, 1979; Shrager, 1970, 1972).

To determine if there was a period of the year when smooth dogfish were growing at a faster rate, the mean total length of age-0 and age-1 smooth dogfish was plotted for each month. For this procedure, we used data from several years and we assumed that every year class followed the same general growth pattern during the first two years of life. The mean monthly length of age-0 animals determined for the 1997 and 1998 cohorts was also calculated. Because we did not collect free-swimming age-0 *M. canis* during May, the largest estimate of birth length (40 cm) was used to minimize the possibility of creating an artificially large growth increment during the summer months.

Results

Vertebrae were collected from 918 smooth dogfish ranging in size from 33 to 132 cm TL. The relationship between TL and VR for males and females was not significantly different (ANCOVA, $P<0.05$); therefore the data for both sexes were combined. The statistically significant relationship ($P<0.001$) between TL and VR was positive and curvilinear (Fig. 4):

$$TL = -0.477(VR)^2 + 17.06\,(VR) + 0.807$$
$$[n=833,\ r^2=0.97,\ P<0.001].$$

Of the original 918 vertebral samples, 894 animals were aged and vertebrae from 24 animals were found to be un-

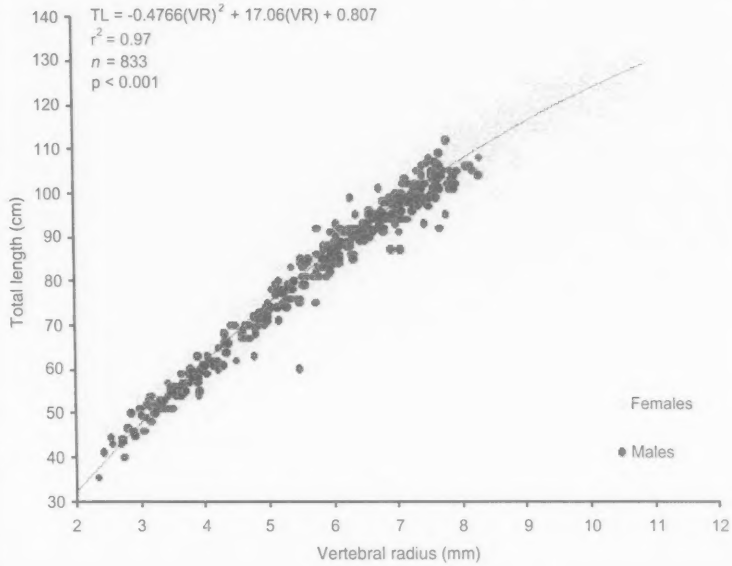

Figure 4

Relationship between vertebral radius (VR) and total length (TL) for *Mustelus canis*.

Table 1

Contingency table of reader one's ages versus reader two's ages, the bold numbers are along the main diagonal (where reader one's age = reader two's age).

		Reader one															
		0	1	2	3	4	5	6	7	8	9	10	11	12	13	14	15
Reader two	0	**53**															
	1		**19**	2													
	2		1	**19**	1												
	3				**19**												
	4				3	**2**	1										
	5					2	**6**	1									
	6						2	**11**	2								
	7								**14**								
	8									**4**							
	9									1	**2**						
	10									1	1	**1**					
	11										1	2	**2**	1			
	12											1	1	**2**			
	13											2	1		**2**		
	14														**0**	1	
	15															**0**	

readable. To test for precision, a second reader read vertebrae from a total of 185 animals (twenty from each 10-cm size group, except for the 33–42 cm size group [*n*=9]) and four vertebrae were found to be unreadable. A contingency table of reader one's versus reader two's ages was made and a chi-square test resulted in a $\chi^2 = 3.19$, which was less than the critical value of $\chi^2_{0.05,1} = 3.84$; thus the hypothesis of symmetry was not rejected (Table 1). The overall percent

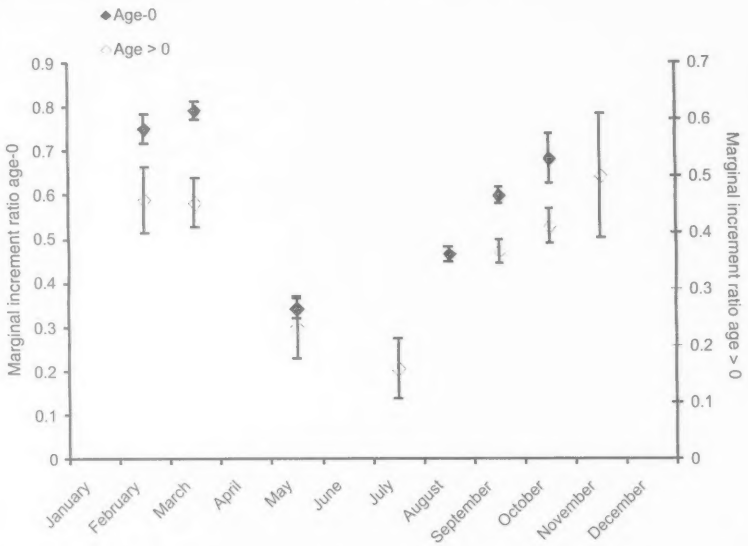

Figure 5

Monthly average marginal increment ratio for male (TL<86 cm) and female (T<102 cm) smooth dogfish (error bars are standard error).

Table 2

Percent agreement (PA) between reader one's ages and reader two's ages for each 10-cm size group.

Size group	Total vertebrae read	No. of vertebrae aged in agreement	No. of vertebrae aged in agreement ±1 year	PA	PA ±1 year
33–42 cm	9	9	9	100	100
43–52 cm	20	20	20	100	100
53–62 cm	20	20	20	100	100
63–72 cm	20	20	20	100	100
73–82 cm	19	16	19	84.21	100
83–92 cm	20	18	20	90	100
93–102 cm	20	15	20	75	100
103–112 cm	19	15	18	78.95	94.74
113–122 cm	19	13	18	68.42	94.74
123–132 cm	19	11	15	57.89	78.95
Total	185	157	179	84.86	96.76

agreement between the two readers was over 84% and the percent agreement within one year was over 96% (Table 2). Agreement within one year was high (over 90%) for all size groups except the largest, where it dropped to 79%.

The largest marginal increments were observed in vertebrae from animals collected in March (Fig. 5). A large drop in marginal width appears to occur in May indicating that band formation most likely occurs during April. The marginal analysis was only conclusive for juvenile-size animals (males less than 86 cm TL, females less than 102 cm TL). By the time these animals become mature, their growth has slowed dramatically and the difference between margin widths becomes very small, making it difficult to elucidate monthly changes in margin width.

Von Bertalanffy growth parameters were calculated separately for males and females because of the approxi-

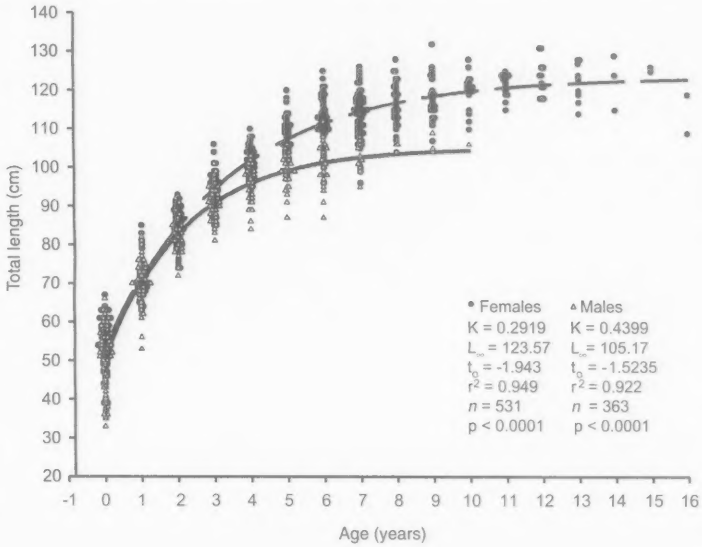

Figure 6
Von Bertalanffy growth function parameters for male and female *Mustelus canis*.

mately 20-cm size difference in both maximum length and length at maturity for males and females. Female growth parameters (Fig. 6) were L_∞ = 123.57 cm, K = 0.2919/yr, and t_0 = −1.9432 years (Table 3). The largest female was 132 cm TL, and 50% of females were found to mature at 102 cm TL and at four to five years of age (Conrath and Musick, 2002). The oldest estimated age for a female smooth dogfish in the study was 16 years and age of the largest female was estimated at nine years old. Male growth parameters (Fig. 6) were L_∞ = 105.17 cm, K = 0.4399/yr, and t_0 = −1.5235 years (Table 3). The largest male in the study was 112 cm TL, and 50% of males were found to mature at 85 cm TL and two to three years of age (Conrath and Musick, 2002). The oldest estimated age for a male smooth dogfish in the study was 10 years, and age of the largest male was estimated at six years old.

The plot of seasonal growth of age-0 and age-1 smooth dogfish indicated a plateau in growth between the months of October and February or March, suggesting slow growth during this period (Fig. 7). There was also a plateau in growth between October and February for both the 1997 and the 1998 cohorts. The mean TL of the 1997 cohort in September 1997 was 51.62 cm (n=31, SE=0.552) and the mean TL of the 1998 cohort in September 1998 was 53.39 cm (n=23, SE=0.579), whereas the mean TL of the 1997 cohort in February 1998 was 57.89 cm (n=18, SE=0.836) and the mean TL of the 1998 cohort in February 1999 was 57.29 cm (n=14, SE=1.605). Assuming a birth length of 40 cm, age-0 animals grew approximately 12–14 cm between May and September and only 4–7 cm between September and February.

Table 3
Von Bertalanffy growth parameters for *Mustelus canis*. SE = standard error.

Parameter	Male	Female
L_∞	105.17	123.56
L_∞ SE	1.0402	0.7353
K	0.4399	0.2919
K SE	0.0226	.0089
t_0	−1.5235	−1.9432
t_0 SE	0.0740	.0641
r^2	0.922	0.949
n	363	531
P	<0.0001	<0.0001

Discussion

Precision estimates, marginal increment analysis, and seasonal growth patterns justify the use of vertebrae as an aging tool for the North Atlantic population of smooth dogfish. The agreement within one year between two readers was high for all size groups (>90%) with the exception of the largest size class (123–132 cm). At this length it becomes very difficult to interpret the margin of the vertebrae and to distinguish between real growth bands and growth checks. Therefore, the maximum age may be

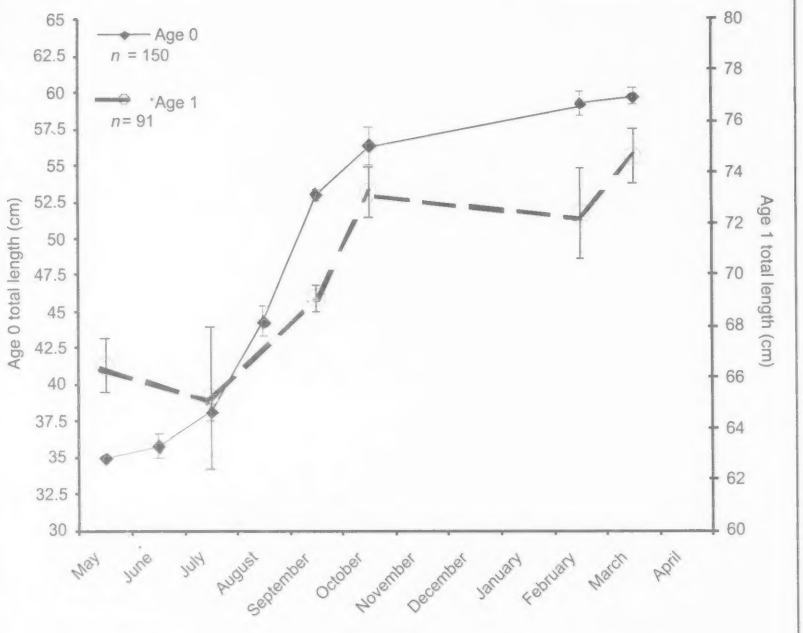

Figure 7

Seasonal growth for smooth dogfish, *M. canis*. Solid line and dashed line show mean size by month of age-0 and age-1 animals (error bars are standard error), respectively.

slightly older or younger than the reported maximum of 16 years for females and 10 years for males.

The marginal increment analysis included only animals of length less than or equal to the length of 50% maturity; therefore the annular nature of the growth bands was verified for these length groups only. Although the marginal widths of the largest animals in the population were too small to discern seasonal differences in these widths, we assumed that these animals follow the same patterns of growth throughout their lifespan.

Estimates of seasonal growth indicated that animals in this population experience a plateau in growth during the winter months between October and February or March, at least for the first two years of life. Their major period of growth is during the summer, between March and October. This finding supports the well established conclusion that an opaque band is deposited annually at the time of slowing or cessation of growth during the winter months. Resuming a faster growth rate after February or March supports the conclusion that a growth band becomes visible in the months of April or May.

Moss (1972) constructed von Bertalanffy growth curves for smooth dogfish by relating tooth width to body length. He estimated that smooth dogfish mature after about one year and reach their maximum size in seven to eight years. He acknowledged that his estimated growth curve did not account for variation in tooth replacement rate and seasonal differences in body growth rate. Francis (1981) estimated von Bertalanffy growth rates by extrapolation from embryonic growth rates using Holden's (1974) method, but this method has subsequently been discredited for application to sharks by Pratt and Casey (1990).

Rountree and Able (1996) used length-frequency analysis to determine growth rates in young of the year (YOY) smooth dogfish in a New Jersey estuary. YOY animals born in May at 29–38 cm TL reached 55–70 cm TL by October of the same year. We found a slightly slower growth rate: age-0 animals in October 1999 ranged from 53–60 cm with a mean size of 56.3 cm (n=6, SE=1.31). We found smooth dogfish grew to a mean of 66.5 cm TL in their first year (size range 61–69 cm, mean size of estimated age-1 May captures, n=13, SE=0.924). The majority of smooth dogfish used in this study were collected in Virginia and North Carolina; therefore geographical differences in growth or differences in growth between years may have contributed to the small discrepancy between our results and those of Rountree and Able.

Values of K reported from various *Mustelus* species (Table 4) ranged from 0.1 for male *Mustelus lenticulatus* from Pegasus Bay, New Zealand, to 0.695 for male *Mustelus manazo*, and from 0.049 for female *Mustelus antarcticus* to 0.42 for female *Mustelus lenticulatus* from Hauraki Gulf, New Zealand (Tanaka and Mizue, 1979; Yudin and Cailliet, 1990; Francis and Francis, 1992; Moulton et al.,

Table 4

Age and growth parameters for *Mustelus* species.

Species	Sex	K	L_∞	t_0	Age at maturity (yr)	Reference
M. californicus	M+F	0.168	154.4	−1.271	1–4	Yudin and Cailliet (1990)
M. henlei	M+F	0.244	97.7	−1.296	1–4	Yudin and Cailliet (1990)
M. manazo	M	0.695	71.4	−0.734	2–3	Tanaka and Mizue (1979)
	F	0.379	88.6	−1.113	2–3	Tanaka and Mizue (1979)
M. manazo	M	0.120	124.1	−2.59		Yamaguchi et al. (1996)
	F	0.113	134.1	−2.55		Yamaguchi et al. (1996)
M. lenticulatus (Pegasus Bay)	M	0.10			5	Francis and Francis (1992)
	F	0.40				
M. lenticulatus (Harakai Gulf)	M	0.16			3.7	Francis and Francis (1992)
	F	0.42			4.7	
M. antarcticus	M	0.160	155.9	−1.94		Moulton et al. (1992)
	F	0.094	233.6	−2.05		
M. mustelus	M	0.12	1451	−2.14	6–9	Goosen and Smale (1997)
	F	0.06	2049	−3.55	12–15	
M. canis	M	0.440	105.17	−1.524	3	Present study, Conrath and Musick (2002)
	F	0.292	123.57	−1.943	4–5	

1992; Yamaguchi et al., 1996; Goosen and Smale, 1997). Smooth dogfish growth coefficients are at the high end of this range (K=0.4399 for males and K=0.2919 for females). Mean asymptotic length of *M. canis* is at the midrange of reported L_∞ values for *Mustelus* species, which range from L_∞ = 71.4, and 88.6 cm for male and female *M. manazo* (Tanaka and Mizue, 1979) to L_∞=155.9 and 233.6 cm for male and female *M. antarcticus* (Moulton et al., 1992). As in nearly all accounts of age and growth for *Mustelis* species, male and female growth in our study was virtually identical in the first few years, and males have a higher growth coefficient (K) than females due to a plateau in growth at a much smaller size (Table 4). However, Francis and Francis (1992) found that female *M. lenticulatus* grow faster than males but still reach a larger maximum length. Their estimates were based on length-frequency data and they acknowledged that the lack of large females may have affected their estimates of von Bertalanffy growth coefficients.

Our growth coefficients for male and female smooth dogfish were comparably high for a shark population; previously reported K values ranged from 0.038 for dusky sharks, *Carcharhinus obscurus* (Natanson et al., 1993) to 1.337 for male Australian sharpnose sharks, *Rhizoprionodon taylori* (Simpfendorfer, 1993). Smooth dogfish grow very quickly for a shark species and mature at a relatively young age. These characteristics may make the northwest Atlantic population more productive and possibly more resilient to exploitation than many other shark populations.

Acknowledgments

This project was supported by Wallop-Breaux funds administered by the Virginia Marine Resources Commission. We thank the following individuals, organizations, and vessel crews for their assistance in obtaining samples for this project: J. Galbraith, H. McBride, V. Nordahl, N. Shepherd, A. Howe, J. Loefer, G. Skomal, B. Falterman, R. Kraus, D. Grubbs, K. Goldman, J. Romine, D. Ward, the National Marine Fisheries Service Northeast Fisheries Science Center survey crew, Massachusetts State Fisheries survey crew, scientists at Grice Marine Laboratory and the Massachusetts Division of Marine Fisheries, and the crews of the RV *Albatross IV*, RV *Gloria Michelle*, and the RV *Bay Eagle*.

Literature cited

Bigelow, H. B., and W. C. Schroeder.
1948. Sharks. *In* Fishes of the western North Atlantic, part 1: lancelets, cyclostomes, and sharks (A. E. Parr and Y. H. Olsen, eds.), p. 244–254. Sears Found. Mar. Res. Memoir 1 Yale Univ, New Haven, CT.

Casey, J. G., H. L. Pratt, and C. E. Stillwell.
1985. Age and growth of the sandbar shark (*Carcharhinus plumbeus*) from the western North Atlantic. Can. J. Fish. Aquat. Sci. 42:963–975.

Castro, J. I.
1983. The sharks of North American waters, 180 p. Texas A&M Univ. Press, College Station, TX.

Compagno, L. J. V.
1984. Sharks of the world. An annotated and illustrated catalogue of shark species known to date. FAO Species Catalogue, vol 4, part 2. FAO Fish. Synop., p. 404–406. FAO, Rome.

Conrath, C. L., and J. A. Musick.
2002. Reproductive biology of the smooth dogfish, *Mustelus canis*, in the northwest Atlantic Ocean. Environ. Biol. Fishes 64:367–377.

Francis, M. P.
1981. Von Bertalanffy growth rates in species of *Mustelus* (Elasmobranchii: Triakidae). Copeia 1981:189–192.

Francis, M. P., and R. I. C. C. Francis.
1992. Growth rate estimates for New Zealand rig (*Mustelus lenticulatus*). Aust. J. Mar. Freshwater Res. 43:1157–1176.

Goosen, A. J. J., and M. J. Smale.
1997. A preliminary study of age and growth of the smoothhound shark *Mustelus mustelus* (Triakidae). S. Afr. J. Mar. Sci. 18:85–91.

Hoenig, J. M., and S. H. Gruber.
1990. Life history patterns in the elasmobranchs: implications for fisheries management. *In* Elasmobranchs as living resources: advances in biology, ecology, systematics, and status of the fisheries (H. L. Pratt Jr., S. H. Gruber, and T. Taniuchi, eds.), p. 1–16. U.S. Dep. Commer., NOAA Tech. Rep. NMFS 90.

Holden, M. J.
1974. Problems in the rational exploitation of elasmobranch populations and some suggested solutions. *In* Sea fisheries research (F. R. Harden Jones, ed.), p. 117–137. J. Wiley and Sons, New York, NY.

Marquardt, D. W.
1963. An algorithm for least squares estimation of parameters. J. Soc. Industrial and Applied Mathematics 11: 431–441.

Moss, S. A.
1972. Tooth replacement and body growth rates in the smooth dogfish, *Mustelus canis* (Mitchill). Copeia 1972: 808–811.

Moulton, P. L., T. I. Walker, and S. R. Saddlier.
1992. Age and growth studies of gummy shark, *Mustelus antarcticus* Gunther, and school shark, *Galeorhinus galeus* (Linnaeus), from southern Australian waters. Aust. J. Mar. Freshwater Res. 43:1241–1267.

Nash, J. C.
1979. Compact mumerical methods for computers: linear algebra and function minimization, 292 p. John Wiley & Sons, Inc., New York, NY.

Natanson, L. J., J. G. Casey, and N. E. Kohler.
1993. Age and growth estimates for the dusky shark, *Carcharhinus obscurus*, in the western North Atlantic Ocean. Fish. Bull. 93:116–126.

National Marine Fisheries Service.
2002. Commercial fishery statistics. Internet. August 28, 2001. [Available from http://www.st.nmfs.gov/st1/commercial/landings/annual_landings.html. Search terms: species: shark, smooth dogfish and shark, dogfish; from: 1980 to 2000; state area: Atlantic and Gulf by state. Access date: 2 June, 2002.]

Pratt, H. L., Jr., and J. G. Casey.
1990. Shark reproductive strategies as a limiting factor in directed fisheries, with a review of Holden's method of estimating growth parameters. *In* Elasmobranchs as living resources: advances in biology, ecology, systematics and status of the fisheries (H. L. Pratt Jr., S. H. Gruber, and T. Taniuchi, eds.), p. 97–109. U.S. Dep. Commer., NOAA Tech. Rep. NMFS 90.

Press, W. H., B. P. Flannery, S. A. Teukolsky, and W. T. Vetterling.
1986. Numerical recipes. Cambridge Univ. Press, Cambridge.

Rountree, R. A., and K. W. Able.
1996. Seasonal abundance, growth, and foraging habits of juvenile smooth dogfish, *Mustelus canis*, in a New Jersey estuary. Fish. Bull. 94:522–534.

Shrager, R. I.
1970. Regression with linear constraints: an extension of the magnified diagonal method. J. Assoc. Computing Machinery 17:446–452.
1972. Quadratic programming for N. Communications of the ACM 15:41–45.

SPSS, Inc.
2000. SigmaPlot 2000 user's quide, 435 p. SPSS, Inc., Chicago, IL.

Simpfendorfer, C. A.
1993. Age and growth of the Australian sharpnose shark, *Rhizoprionodon taylori*, from north Queensland, Australia. Environ. Biol. Fishes 36:233–241.

Tanaka, S., and K. Mizue.
1979. Age and growth of Japanese dogfish *Mustelus manazo* Bleeker in the East China Sea. Bull. Jpn. Soc. Sci. Fish. 45:43–50.

Yamaguchi, A., T. Taniuchi, and M. Shimizu.
1996. Age and growth of the starspotted dogfish, *Mustelus manazo*, from Tokyo Bay, Japan. Fish. Sci. 62:919–922.

Yudin, K. G., and G. M. Cailliet.
1990. Age and growth of the gray smoothhound, *Mustelus californicus*, and the brown smoothhound, *Mustelus henlei*, sharks from central California. Copeia 1990:191–204.

Bycatch of billfishes by the European tuna purse-seine fishery in the Atlantic Ocean

Daniel Gaertner
Frédéric Ménard
Carol Develter
IRD (UR 109) Centre de Recherche Halieutique Méditerranéenne et Tropicale
B.P. 171
34203 Sète cedex, France
E-mail address (for D. Gaertner): gaertner@ird.fr

Javier Ariz
Alicia Delgado de Molina
IEO, Centro Oceanografico Canarias
Apdo 1373
Santa Cruz de Tenerife
Islas Canarias, Spain

Abstract—Billfishes are a component of offshore ecosystems; thus it is important to quantify the impact of the tuna fishery on these species in the world's ocean. The aim of this study was to assess the bycatch of billfishes generated by the tropical tuna purse-seine fishery in the eastern Atlantic Ocean. Information on bycatch was collected by observers at sea during the European Union Bigeye Program. With a total of 62 observers' trips, conducted on Spanish and French vessels between June 1997 and May 1999, this project is the biggest observer program ever carried out in the European tuna purse-seine fishery. This study showed that billfish bycatch by the purse seiners is very low (less than 0.021% of the total tuna catches and less than 10% of the total billfish catches currently reported). A Monte Carlo simulation was performed to account for some uncertainties in the fishing strategies of purse seiners operating in this ocean. One of the findings of this study indicated that the temporary moratorium on fishing with FADs (fish aggregating devices), adopted by the European purse-seine fishery in the eastern Atlantic Ocean, produced a decrease in incidental catches of marlins from 600–700 metric tons (t) to less than 300 t. In contrast, this trend was reversed for sailfishes, for which the bycatch increased from 25 t to 45 t. The difficulty of defining indices that express the conservation status in marine fishes and that gauge key ecosystem parameters and the need to promote an ecosystem approach for large-pelagic-resource management which takes into account biologic and socioeconomic criteria are briefly discussed.

Manuscript accepted 27 May 2002.
Fish. Bull. 100:683–689 (2002).

In the spirit of the code of conduct for responsible fisheries it is important to quantify discards and bycatches taken by the main fishing fleets in the world's ocean. Despite recommendations made by different fishery agencies, such as the tuna commissions, this information is rarely reported by skippers in their commercial logbooks. Thus the level of catches of billfishes taken incidentally by the tropical tuna purse-seine fishery is not well-known. In contrast to the recreational fishery, or to some specific small-scale fisheries, billfishes are not targeted by the purse-seine fishery but they can be taken incidentally during the setting operation. In the eastern Atlantic Ocean, parts of bycatch, including billfishes, are kept and are sold in the local African fish market (Romany et al., 2000).

The purpose of this study was to estimate the amount of billfish taken as bycatch by fishing modes (i.e. by FAD [fish aggregating devices] sets, school sets [sets without the use of FADs], and seamount sets) and as bycatch by the Spanish and the French purse seiners in the eastern Atlantic Ocean. Because bycatch information is not recorded in commercial purse seiner logbooks, observations collected by scientific observers aboard purse seiners appeared to be a useful way to assess the amount of bycatch taken by this fleet. Although the European Union Bigeye Program focused on the study of the increase in catch of bigeye tuna (*Thunnus obesus*) by the European tuna-purse seiners in the Atlantic Ocean (Ariz and Gaertner, 1999), information on bycatch was also collected by observers on these purse seiners. We used this data set to estimate the bycatch of billfish in the European purse-seine fishery. These estimates will contribute to the calculation of the total bycatch of billfishes taken in the Atlantic Ocean.

Materials and methods

Data

A total of 62 observer trips (44 for the Spanish fleet and 18 for the French fleet) were conducted opportunistically between June 1997 and May 1999, except from November 1998 through January 1999, a period when there was a moratorium on the use of FADs in fishing operations. In spite of this limitation, this project was the largest observer program ever carried out in the European tuna purse-seine fishery (a total of 2706 fishing days, with 1884 observed sets). The catch of commercial tunas reached 34,693 t, whereas discards (composed mainly of small tuna species or of juveniles of commercial tuna species) were estimated at about 737 t and total bycatch (billfishes,

Table 1

Probabilities of setting with a specific fishing mode k (observed values for a standard year with moratorium and averaged values for a standard year without moratorium; see explanations in the text) and observed conditional probabilities that a specific group of billfish s is associated with this fishing mode. These values were used to perform the Monte Carlo simulation. School sets were made without FADs.

Fishing mode	Number of observed sets	Prob. {fishing mode=k}		Prob. {s present | k}	
		Moratorium	Without moratorium	Marlins	Sailfishes
FAD sets	373	0.2932	0.5500	0.3539	0.0134
School sets	859	0.6753	0.4185	0.0408	0.1036
Seamount sets	40	0.0315	0.0315	0.2500	0.0750

sharks, other fish, etc.) at about 762 t (Ariz and Gaertner, 1999).

Based on the ecological provinces in the oceans established by Longhurst (1998), the eastern tropical Atlantic Ocean (from 25°N to 15°S and from 35°W to the African coasts) was stratified by quarters into two areas:

the Senegalese area (from latitude 12°N to 25°N),
the remaining areas, termed "equatorial" areas.

Owing to time constraints during the set (and bearing in mind that this program was directed at bigeye tuna), it was very difficult for the observer to accomplish some additional bycatch tasks. Consequently, in some circumstances the billfish species may not have been correctly identified. For this reason we established two groups; the blue marlin (*Makaira nigricans*) and the white marlin (*Tetrapterus albidus*) in one group and the sailfishes (*Istiophorus albicans*) and the longbill spearfish (*T. pfluegeri*) in the second group. The weight ranges of billfishes captured as incidental catch by the purse seiners were approximately 130–150 kg for blue marlin, 10–20 kg for sailfish and 45–70 kg for nonidentified marlins (there were no weight estimates for white marlin and longbill spearfish because of their low numbers in the bycatch).

On the basis of a study made on tuna size classes by set type in this fishery (Pallares and Petit, 1998), the sets made on whales and on whale sharks (*Rhiniodon typus*) were classified as school sets (i.e. sets made without FADs) and as FAD sets, respectively. In contrast, it must be stressed that seamounts constitute a specific environment for small size classes of tuna species. In the Atlantic Ocean 2000–3000 t of tunas can be taken yearly on some seamounts (Fonteneau, 1991). Because large pelagic species can be concentrated on seamounts (e.g. sphyrnids, Klimley et al., 1988), we distinguished the sets made on seamounts from the usual tuna fishing modes (i.e. school sets and FAD sets).

Methods

For the two groups of billfishes (i.e. sailfishes and marlins) the total bycatch taken by the European tuna purse-seine fishery in the eastern Atlantic Ocean was estimated for a period of 12 months. The period between October 1997 and September 1998 was considered the best representative standard year for the observer program because it included the best coverage in terms of tuna catches (approximately 17% of the total tuna catch is taken by the European purse seiners from October 1997 to September 1998). Assuming that billfish bycatch was proportional to the tuna catch, the observed bycatch for each billfish group was raised to the total European purse-seine catch with the use of a raising factor RF_{sijk} as in the following equation:

$$TBC_s = \sum_k \sum_j \sum_i RF_{sijk} BC_{sijk},$$

where TBC_s = total bycatch for the group s during a standard year;
RF_{sijk} = total purse seine tuna catch_{ijk}/observed aboard purse seine tuna catch_{ijk};
BC_{sijk} = bycatch for the group s, in area i, quarter j, and fishing mode k;
and i = 1, 2; j = 1, 2, 3, 4; k = school set, FAD set, set on seamount.

Sources of uncertainty in the calculation of the billfish bycatch are caused by 1) changes in fishing strategies adopted by the fishermen over the year, e.g. the probability of choosing the fishing mode k and 2) some features of the bycatch species, e.g. the conditional probability for a given group of billfish s to be present in a set of type k, as well as the probability of obtaining x tons of group s in the set (Table 1). To account for some of these uncertainties our approach differed from that of Perkins and Edwards (1996), who used a modified negative binomial distribution to model bycatch per set. We used computer-intensive methods, such as a Monte Carlo simulation, to estimate the total bycatch generated by the European tuna purse-seine fishery. Monte Carlo methods of simulation introduce a large number of random inputs into a model while recording the range of outputs (Gaertner et al., 1996; Shelton et al., 1997).

In the present analysis, the model mimics the fishing operations made by the purse seiners over a standard

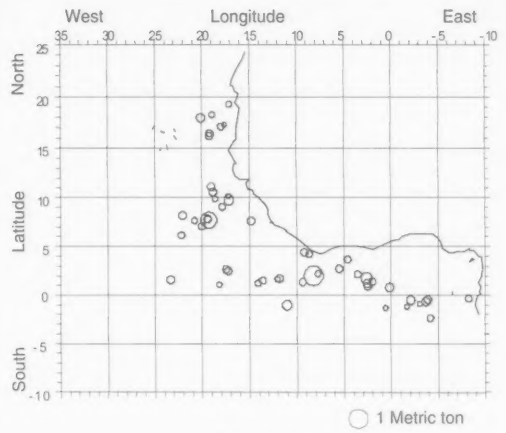

Figure 1

Spatial distribution of the bycatch (t) per school set for the marlin group from the observers' trips during the European Union bigeye tuna program.

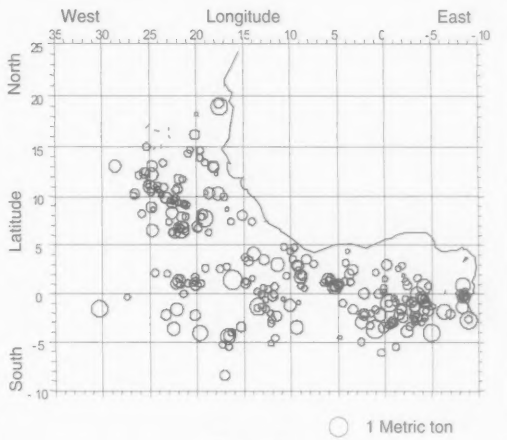

Figure 2

Spatial distribution of the bycatch (t) per FAD set for the marlin group from the observers' trips during the European Union bigeye tuna program.

year. That means that we take into account the probability of setting on the fishing mode k, and the conditional probability that group s is present in this type of set. For each group s, the simulated input (i.e. the bycatch generated by one set) is drawn from the observed distribution of the bycatch by set for the fishing mode k. Note that the calculation of the total bycatch is based on the proportion of total sets (including those made on trips without observers at sea) recorded in commercial logbooks in each strata by fishing mode. That means that the observed bycatch in each set was previously raised by the corresponding raising factor: RF_{ijk}. A single set is then generated by randomly selecting inputs from the distributions of bycatch per set. This is repeated 1272 times (the total number of sets reported by observers aboard) to give the total bycatch of group s during the standard year. 500 Monte Carlo simulations were generated to determine the amount of variation expected in the yearly bycatch estimates. Confidence limits for total bycatch by group were performed by the percentile method.

However, the results obtained in our study may have been affected by the moratorium on fishing with FADs adopted by the French and the Spanish tuna purse-seine companies in the eastern Atlantic Ocean. This temporary ban was adopted over a large area from the African coast to 20°W and from 5°N to 4°S, between 1 November and 31 January in 1997–98 and in 1998–99, respectively. With this consideration in mind, the Monte Carlo simulation was performed a second time to simulate a standard year without a moratorium. We assumed that the probability of setting on FADs (estimated at 0.293 during a year with a moratorium) increases to 0.55 during the years without a moratorium (estimated from commercial logbooks). Consequently, the second Monte Carlo simulation was conducted with the following probabilities: 0.55 (for FAD sets), 0.419 (school sets) and 0.031 (for seamount sets, assuming that the percentage of sets made on seamounts was not affected by a ban on fishing on logs, Table 1).

Table 2

Estimated bycatches of billfishes (t) and observed commercial tuna catches (t) taken by fishing modes by the European purse seiners in the eastern Atlantic Ocean for a standard year (October 1997–September 1998). School sets were made without FADs.

Fishing mode	Marlins	Sailfish	Tuna catches
FAD sets	200.8	7.6	49,214
School sets	42.8	34.7	88,456
Seamount sets	1.5	0.1	1,285
Total	245.1	42.4	138,955

Results

Table 2 shows the estimated bycatch of billfishes taken by each fishing mode during a standard year. The results indicate that 245 t marlin and 42 t sailfishes were taken as bycatch by the European purse seiners in the eastern Atlantic Ocean. Figures 1 and 2 depict the spatial distribution by fishing modes of the marlin bycatch in the eastern Atlantic for all data collected during the observer program. Figure 2 shows that marlin bycatch in FAD sets were spread across a large area in the eastern Atlantic Ocean. When compared to FAD sets, the occurrence of marlins bycatch in school sets was lower, specifically in central

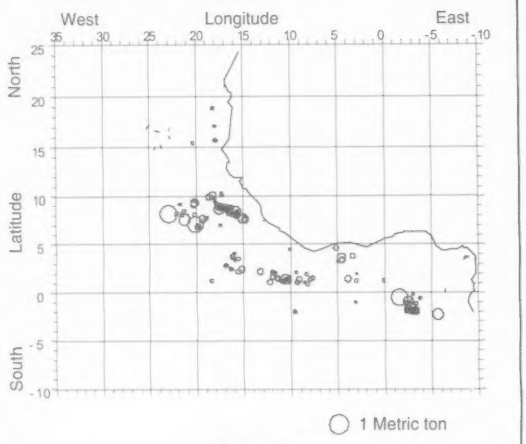

Figure 3

Spatial distribution of the bycatch (t) per school set for the sailfish group from the observers' trips during the European Union bigeye tuna program.

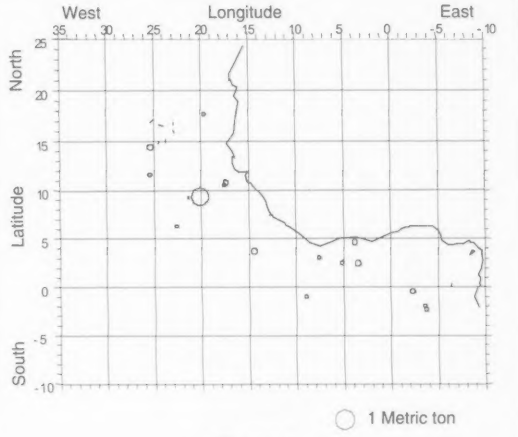

Figure 4

Spatial distribution of the bycatch (t) per FAD set for the sailfish group from the observers' trips during the European Union bigeye tuna program.

Table 3

Results of the Monte Carlo simulation for a standard year with and without a moratorium on FAD sets. Monte Carlo estimates are the average bycatch (t) taken by the European purse seiners in the eastern Atlantic Ocean and the confidence intervals (CI, in tons). "The ratio of billfish to tuna" is the ratio of billfish bycatch to tuna catch (in tons), and corresponding confidence intervals.

	Marlins		Sailfishes	
Group case	Moratorium	Without moratatorium	Moratorium	Without moratorium
Monte Carlo estimates (t)	238.79	396.38	37.52	14.86
Lower CI 0.025	192.86	338.25	23.22	2.89
Upper CI 0.975	283.51	450.54	53.91	33.38
Ratio of billfish to tuna	1.718E-03	2.853E-03	2.700E-04	1.069E-04
Lower CI 0.025	1.388E-03	2.434E-03	1.671E-04	2.076E-05
Upper CI 0.975	2.040E-03	3.242E-03	3.879E-04	2.402E-04

tropical areas. If we compare the spatial distribution of the sailfishes with the spatial distribution of the marlin, we find that the bycatch of sailfishes was associated more with school sets than with FAD sets (Figs. 3 and 4). However, the "sampling scheme" adopted for assessing these incidental catches was constrained by the purse seiners' fishing-effort distribution. Consequently, because purse seiners move seasonally from one area to another, there is a lack of information about the presence of billfishes when the fishing area is temporarily abandoned.

In both runs of the Monte Carlo simulation we used the same conditional probability about the presence of each billfish group by fishing mode (Table 1), as well as for the observed distribution of the bycatch per set by fishing mode. Results indicated that the bycatch of marlins decreased during the moratorium from 396 t to 289 t (Table 3 and Fig. 5). This result is a consequence of the larger association of marlins with floating objects than with school sets. In looking at Table 1, we can see that the occurrence of marlin was around 35% for FAD fishing operations compared to only 4% for school sets. Marlin were also present in 25% of the seamount sets but, from the small number of sets made on seamounts, we could not determined any apparent effect on the total bycatch for this group. Sailfishes were more commonly observed in school sets than in FAD sets (Table 1). Thus it appeared that the bycatch of sailfish increased from about 15 t to 38 t with a moratorium on FADs, as summarized in Table 3 and Figure 5.

Table 4

Estimates of the total bycatch (t) taken by the entire purse-seine fishery in the eastern Atlantic Ocean based on the results of the Monte Carlo simulation applied to the European purse seiners. Because of the moratorium on FAD sets, a decrease of the percentage of FAD sets was assumed for the last three years.

		Marlins			Sailfishes		
Year	Total tuna catch (t)	Estimated bycatch (t)	Lower CI 0.025	Upper CI 0.975	Estimated bycatch (t)	Lower CI 0.025	Upper CI 0.975
1990	211,882	604.50	515.72	686.92	22.65	4.40	50.89
1991	246,110	702.15	599.03	797.89	26.31	5.11	59.12
1992	204,040	582.13	496.63	661.50	21.81	4.24	49.01
1993	249,086	710.64	606.28	807.54	26.63	5.17	59.83
1994	225,646	643.77	549.22	731.54	24.12	4.68	54.20
1995	218,735	624.05	532.40	709.14	23.38	4.54	52.54
1996	194,173	553.98	472.62	629.51	20.76	4.03	46.64
1997	168,826	290.04	234.33	344.41	45.58	28.21	65.49
1998	172,478	296.32	239.40	351.86	46.57	28.82	66.90
1999	157,933	271.33	219.21	322.18	42.64	26.39	61.26

Introducing some elements of uncertainty in the inputs highlighted the large variability of the bycatch estimates (see the values obtained for the lower and upper CI [confidence intervals]; Table 4.). However, even including uncertainty in the inputs, these values remained very low compared with bycatches reported from other fisheries. Based on these results, the total bycatch of billfishes taken by the entire purse-seine fleet operating in the eastern Atlantic was tentatively estimated. This calculation is supported by the facts that 1) the European fleet is the main component of the purse-seine fishery operating in this part of the ocean and 2) it is reasonable to assume that other fleets of purse seiners adopted the same fishing strategies as the European fleet. With this approach, the ratio of the billfish bycatch per tons of tunas (obtained from the European fleet; Table 3) was raised to the total tuna catch taken by the entire purse-seine fishery (Table 4). To account for the change in fishing strategies caused by the ban on FAD fishing operations, we performed new billfish ratio estimates for the years 1997, 1998, and 1999. These results give an indication of the bycatch of billfishes in the eastern Atlantic purse-seine fishery (Table 4).

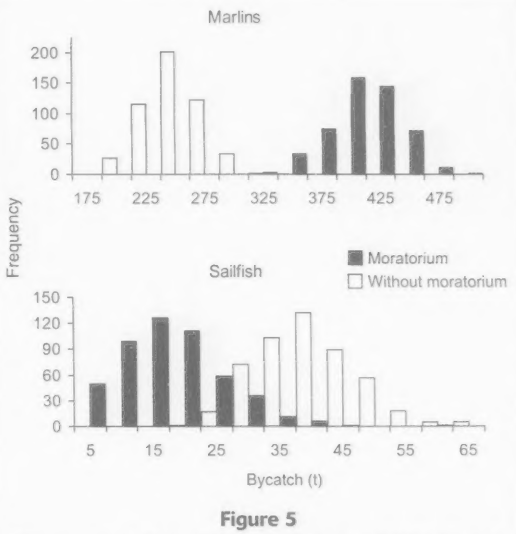

Figure 5

Histograms of Monte-Carlo-generated total billfish bycatch (marlin group in the upper histogram and sailfish group in the lower histogram) taken by the European Union tuna purse-seine fishery, taking into account whether a moratorium on FAD fishing was applied or not, in the eastern Atlantic Ocean.

Discussion

The ecosystem approach to assessing and managing large coastal marine ecosystems has been developing since the early nineties (Sherman and Duda, 1999). To date, with the exception of the central Pacific Ocean (Kitchell et al., 1999), this approach generally has not been used for monitoring large pelagic fisheries in offshore waters. Our study, in presenting data on bycatch of billfishes taken by the tuna purse-seine fishery, helps to extend this approach to the monitoring of the eastern Atlantic epipelagic ecosystem.

A purse-seine fishery cannot be assessed purely in terms of the tuna catch. In the eastern Atlantic Ocean, it can be assumed that the large catches of tunas taken by the purse seiners (around 200,000 t per year in the last decade, Table 4) affect the abundance of billfishes 1) directly, by generating bycatch and 2) indirectly, by increasing or decreasing

the abundance of predators or competitors, thereby changing the ratio of predators to prey in the trophic chain.

That the bycatch of Istiophoridae represents less than 0.021% of the total tuna catch and less than 10% of the total catches of billfishes currently reported for the eastern Atlantic Ocean (assumed to fluctuate around 7000–8000 t per year) suggests that the direct impact of the purse-seine fishery on these stocks is weak. By comparison, previous research has shown that the discards of small tunas and the total bycatch (billfishes, sharks, other fishes, etc.) generated by this fishery were close to 2% and 1.9%, respectively (Ariz and Gaertner, 1999). Compared with the longline fishery, the European tuna purse-seine fishery generates less bycatch of billfishes than the longline fisheries targeting tuna (Matsumoto and Miyabe, 2000; Gonzalez Ania et al., 2001), swordfish (Mejuto et al., 2000), or both species (Cramer, 2000; Marcano et al., 2000).

One of the more general implications of our findings concerns the impact of the ban of FADs by the purse-seine fishery on the bycatch of Istiophoridae. Our analysis suggests that this moratorium led to a decrease in incidental catch of marlin from 600–700 t to less than 300 t. In contrast, this trend was reversed for sailfishes, but the corresponding bycatch increased only from 25 t to 45 t. Because in the present study we did not take into account different probabilities (see Table 1) for each strata, it could be argued that the Monte Carlo simulations lead to only a partial exploration of the uncertainty in the calculation of the total billfish bycatch. However, it would be interesting to consider this source of uncertainty in the future. Consequently, the potential for possible regulations at different spatial and temporal scales needs further exploration.

Large bycatches of billfishes could affect the food web of the epipelagic ecosystem inhabited by other apex predators. However, the "zero bycatch solution" propounded by some environmentalist groups could accelerate the change in biomass ratios between the different trophic levels of the ecosystem. In a critique of the conventional risk factors (e.g. biological reference points) used to define the risk of extinction in marine fishes, Musick (1999) introduced other interesting criteria, such as rarity of a species, the small distribution range of a species, endemic species, and specialized habitat requirements. As can be seen in Figures 1–4, the range of spatial distribution of the billfishes is very large. It could be argued that billfishes are relatively widespread but occupy very specific habitats within their range, and as a consequence, habitat loss could be examined as a risk factor. However there is no clear evidence to support this hypothesis for billfishes.

The difficulty of objectively measuring an ecological risk when it concerns unexploited components of the ecosystem must be stressed because of the vagueness of this concept (Antoine et al., 1998). As a consequence, estimating the ecological risk is reduced to the analysis of the impact of a fishing practice on a limited number of symbolic species (e.g. dolphins, sea turtles; Hall, 1996). Nevertheless, there is no reason to believe that these charismatic species play a larger role in the food web of the epipelagic ecosystem than other targeted or nontargeted species. As shown by Kitchell et al, (1999), there was no clear conclusion on the ecological role of apex predators (including billfishes) in foods webs of the central North Pacific. Furthermore, if a decision is made to reduce the ecological impact of the bycatch in a given fishery, management actions cannot be focused only on providing full protection for a single species (Hall, 1996). Although everybody understands what "ecosystem overfishing" means, Murawski (2000) highlighted the lack of consensus for defining this concept and suggested the need for objective metrics that gauge properties associated with the main features of the ecosystem (e.g. production, diversity, and variability).

In addition, decision makers need to evaluate management options that are both scientifically credible and economically practical regarding the use of the ecosystems. Because billfishes are sold on the local African fish market (Romany et al., 2000), the effects of the fishing on the ecological processes, as well as on human activities, must be evaluated. Although in the past the regulatory process did not account for sharing of gains nor the social costs associated with fishing practices (Antoine et al., 1998), evidence suggests that the ecosystem approach for managing marine resources should also include these socioeconomic considerations in a multicriteria analysis (Chesson et al, 1999, Sherman and Duda, 1999).

Conclusion

This study examined the bycatch taken by the European tuna purse-seine fishery in the eastern Atlantic Ocean. Results obtained from this fleet have been extrapolated to the entire purse-seine fleet operating in the same areas of this ocean. The main conclusion of this paper is that the direct impact of the purse-seine fishery on the billfish component of the epipelagic ecosystem is weak. Results of this study provide additional information on the effect of the moratorium on FAD fishing. Although some caution is required at this stage, due to limitations of the spatial and temporal sampling coverage, it was found that the ban on FAD fishing operations led to a substantial decrease in marlin bycatch.

The present state of knowledge allows us to reach only preliminary conclusions. However, it should be borne in mind that inadequate data can lead to the formation of misguided policies. It is clear that detailed information on bycatch is needed to counter the arguments of those who propose total bans on some fishing practices. Consequently tuna commissions must continue to pay attention to the collection of bycatch statistics and must encourage fishermen to report incidental catches in their logbooks, at least by large taxa (e.g. billfishes, sharks, etc.). In order to use accurate information for management purposes, we recommend that data from regularly conducted observer programs be used as part of any future research.

Acknowledgments

This research was funded in part by the European Commission (DG XIV) research project n° 96/028: "A study of the causes of the increase in the catches of bigeye tuna

by the European purse-seiner tuna fleets in the Atlantic Ocean." This study would not have been possible without the help of the Spanish and French tuna companies and the skippers and crews who accepted observers aboard.

Literature cited

Antoine, L., O. Guyader, and M. Goujon.
1998. Un changement de technique de pêche est-il compatible avec une pêche responsable? L'exemple de la pêche au germon (*Thunnus alalunga*) au filet dérivant en Atlantique Nord. *In* ICCAT tuna symposium (J. S. Beckett, ed.), p. 651–660. ICCAT (International Commission for the Conservation of Atlantic Tunas) Coll. Vol. Sci. Papers 50(2).

Ariz, J., and D. Gaertner.
1999. A study of the causes of the increase in the catches of bigeye tuna by the European purse seiner tuna fleets in the Atlantic Ocean, 70 p. + appendices. Program n° 96/028, European Union, DG XIV, Bruxelles, (Belgium).

Chesson, J., H. Clayton, and B. Whitworth.
1999. Evaluation of fisheries-management systems with respect to sustainable development. ICES J. Mar. Sci. 56: 980–984.

Cramer, J.
2000. Pelagic longline bycatch. ICCAT Coll. Vol. Sci. Pap. 51:1895–1930.

Fonteneau, A.
1991. Monts sous-marins et thons dans l'Atlantique tropical est. Aquat. Living Resour. 4:13–25.

Gaertner, D., M. Pagavino, and J. Marcano.
1996. Utilisation de modèles linéaires généralisés pour évaluer les stratégies de pêche thonière à la senne en présence d'espèces associées dans l'Atlantique Ouest. Aquat. Living Resour. 9:305–323.

Gonzalez Ania, L. V., C. A. Brown, and E. Cortes.
2001. Standardized catch rates for yellowfin tuna (*Thunnus albacares*) in the 1992–1999 Gulf of Mexico longline fishery based upon observer program from Mexico and the United States. ICCAT Coll. Vol. Sci. Pap. 52:222–237.

Hall, M. A.
1996. On bycatches. Rev. Fish. Biol. Fish. 6:319–352.

Kitchell, J. K., C. H. Boggs, Xi. Le, and C. J. Walters.
1999. Keystone predators in the Central Pacific. *In* Ecosystem approaches for fisheries management, p. 665–683. Univ. Alaska Sea Grant, Fairbanks AK.

Klimley, A. P., S. B. Butler, D. R. Nelson, and A. T. Stull.
1988. Diel movements of scalloped hammerhead sharks, *Sphyrna lewini* Griffith and Smith, to and from a seamont in the Gulf of California. J. Fish Biol. 33:751–761.

Longhurst, A.
1998. Ecological geography of the sea, 398 p. Academic Press, San Diego, CA.

Marcano, L., F. Arocha, J. Marcano, and A. Larez.
2000. Actividades desarolladas en el programa expandido de ICCAT para peces de pico en Venezuela. Periodo : 1998–99. ICCAT Coll. Vol. Sci. Pap. 51:981–993.

Matsumoto, T., and N. Miyabe.
2000. Report of 1999 observer program for Japanese tuna longline fishery in the Atlantic Ocean. ICCAT Coll. Vol. Sci. Pap. 51:729–750.

Mejuto, J, B. Garcia-Cortes, and J. M. De La Serna.
2000. Estimaciones cientificas preliminares de desembarcos de peces de pico capturados en el O. Atlantico y Mar Mediterraneo por la flota española de palangre de superficie de pez espada, durante el periodo 1988–1998. ICCAT Coll. Vol. Sci. Pap. 51:976–980.

Murawski, S. A.
2000. Definitions of overfishing from an ecosystem perspective. ICES J. Mar. Sci. 57:649–658.

Musick, J. A.
1999. Criteria to define extinction risk in marine fishes. The American Fisheries Society initiative. Fishery 24 (12):6–14

Pallares, P., and C. Petit.
1998. Tropical tunas: new sampling and data processing strategy for estimating the composition of catches by species and size. ICCAT Coll. Vol. Sci. Pap. 48:230–246.

Perkins, P. C., and E. F. Edwards.
1996. A mixture model for estimating discarded bycatch from data with many zero observations: tuna discards in the eastern tropical Pacific Ocean. Fish. Bull. 94:330–340.

Romany, B., F. Ménard, P. Dewals, D. Gaertner, and N. N'Goran.
2000. Le "faux-poisson" d'Abidjan et la pêche sous DCP dérivants dans l'Atlantique tropical Est: circuit de commercialisation et rôle socio-économique. *In* Pêche thonière et dispositifs de concentration de poisons (J. Y. Le Gall, P. Cayré, and M. Taquet, eds.), p. 634–652. IFREMER (Institut Français de recherche pour l'exploitation de la mer) Actes de Colloques 28.

Shelton, P. A., W. G. Warren, G. B. Stenson, and J. W. Lawson.
1997. Quantifying some of the major sources of uncertainty associated with estimates of harp seal prey consumption. Part II: Uncertainty in consumption. Estimates associated with population size, residency, energy requirement and diet. J. Northwest Atl. Fish. Soc. 22:303–315.

Sherman, K., and A. M. Duda.
1999. An ecosystem approach to global assessment and management of costal waters. Mar Ecol. Prog. Ser. 190:271–287.

Life history of South African snoek, *Thyrsites atun* (Pisces: Gempylidae): a pelagic predator of the Benguela ecosystem

Marc H. Griffiths
Department of Environmental Affairs and Tourism
Branch Marine and Coastal Management
Private Bag X2
Roggebaai 8012
Cape Town, South Africa
E-mail address: mgriffit@sfri.wcape.gov.za

Abstract—Snoek (*Thyrsites atun*) is a valuable commercial species and an important predator of small pelagic fishes in the Benguela ecosystem. The South African population attains 50% sexual maturity at a fork length of ca.73.0 cm (3 years). Spawning occurs offshore during winter–spring, along the shelf break (150–400 m) of the western Agulhas Bank and the South African west coast. Prevailing currents transport eggs and larvae to a primary nursery ground north of Cape Columbine and to a secondary nursery area to the east of Danger Point; both shallower than 150 m. Juveniles remain on the nursery grounds until maturity, growing to between 33 and 44 cm in the first year (3.25 cm/month). Onshore–offshore distribution (between 5- and 150-m isobaths) of juveniles is determined largely by prey availability and includes a seasonal inshore migration in autumn in response to clupeoid recruitment. Adults are found throughout the distribution range of the species, and although they move offshore to spawn—there is some southward dispersion as the spawning season progresses—longshore movement is apparently random and without a seasonal basis. Relative condition of both sexes declined dramatically with the onset of spawning. Mesenteric fat loss was, however, higher in females, despite a greater rate of prey consumption. Spatial differences in sex ratios and indices of prey consumption suggest that females on the west coast move inshore to feed between spawning events, but that those found farther south along the western Agulhas Bank remain on the spawning ground throughout the spawning season. This regional difference in female behavior is attributed to higher offshore abundance of clupeid prey on the western Agulhas Bank, as determined from both diet and rates of prey consumption.

Manuscript accepted 27 May 2002.
Fish. Bull. 100:690–710 (2002).

Snoek (*Thyrsites atun*) is a medium-size, pelagic predator (max. size 9 kg; Nepgen, 1979a) inhabiting the coastal waters of the temperate Southern Hemisphere; it is found from the surface to the seabed, to depths of 550 m (Kailola et al., 1993). Occurring off southern Africa, Australia, New Zealand, the east and west coasts of southern South America, Tristan da Cunha, and the islands of Amsterdam and St. Paul (Nakamura and Parin, 1993), snoek have successfully colonized environments as diverse as oceanic island, west coast upwelling, and subtropical convergence ecosystems. It is an important food fish throughout much of its distribution, supporting moderate fisheries (<1000 metric tons [t]/yr) off southern Australia, Chile, and Tristan de Chuna, and substantial fisheries (>10,000 t/yr) off New Zealand and Southern Africa (Andrew et al., 1995; FAO, 1997).

Southern African snoek have been recorded from northern Angola to Algoa Bay on the South African east coast but are mostly found between the Cunene River and Cape Agulhas, i.e. in the Benguela ecosystem. *Thyrsites atun* has been an important commercial species in this system since the early 1800s, caught initially with hand lines but also trawled after 1960 (Crawford, 1995). Total catch peaked at about 81,000 t in 1978 but dropped substantially with the exclusion of foreign trawlers from the Namibian fishing grounds in 1991 (FAO, 1978, 1981, 1990, 1997). Current annual-catch ranges between 14,437 and 22,920 t (1991–95), and 93% of it is made in South African waters (FAO, 1995). *Thyrsites atun* is far the most important species caught by the South African commercial line fishery[1] (comprising 39% of the 1986–97 catch [National Marine Linefish System[2]]); it is also targeted by recreational anglers, for which catch statistics are not available. Around 40% of the South African catch (1990–96) is made by commercial handline fishermen and 60% by trawlers (Demersal Commercial Data Base[3]). However, the commercial line-catch may be under-reported by as much as 75% (Sauer et al., 1997); therefore the total catch could be substantially larger. In addition to its fishery significance, *T. atun* is a major predator of anchovy (*Engraulis japonicus*) and sardine (*Sardinops sagax*) in the southern Benguela ecosystem (Wickens et al., 1992) and has been implicated in top down effects on both prey and consequently zooplankton populations (Verheye et al., 1998).

Life-history information is fundamental to identifying and assessing fish stocks, as well as to formulating management strategies for their sustainable use. Whereas snoek stocks off Australia (Blackburn and Gartner, 1954; Blackburn, 1957; Grant et al., 1978) and New Zealand (Mehl, 1971;

[1] The South African commercial linefishery consists of about 2500 vessels (5.5–15 m long) that operate on the continental shelf using handline or rod-and-reel.

[2] National Marine Linefish System. 2000. Unpubl. data. Linefish Section, Marine and Coastal Management, Private Bag X2 Roggebaai 8012, Cape Town, South Africa.

[3] Demersal Commercial Data Base. 2000. Unpubl. data. Demersal Section, Marine and Coastal Management, Private Bag X2 Roggebaai 8012, Cape Town, South Africa.

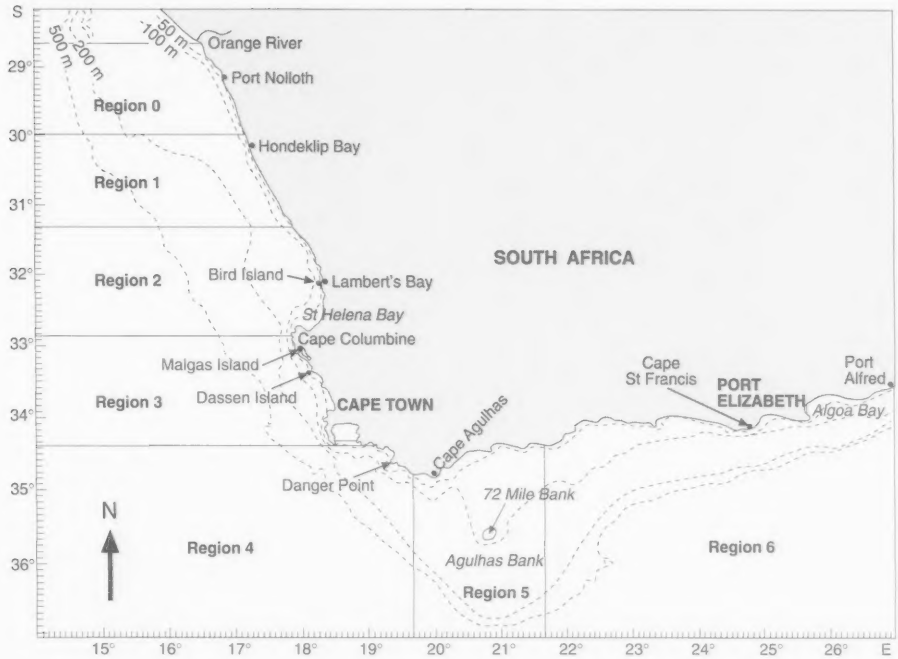

Figure 1

Map of the seven regions in which snoek (*Thyrsites atun*) were sampled, and the localities mentioned in the text. Snoek caught by hook and line were, with the exception of the 72-mile bank (region 5), taken within 15 km of the coastline, whereas those that were trawled were caught farther from the shore at water depths between 150 and 600 m.

Hurst, 1988; Hurst and Bagley, 1987; 1989) have been extensively studied, knowledge of the life history of the Benguela snoek is surprisingly fragmented, in spite of its socioeconomic and ecological importance and long history of exploitation. An extensive seasonal migration between the northern and southern regions of the Benguela system has been postulated (Davies, 1954; Crawford and De Villiers, 1985; Crawford et al., 1987); however, this migration was based largely on anecdotal reports of line catches and remains to be confirmed. Preliminary observations of gonad maturity (Davies, 1954; Nepgen, 1979a) and trends in the abundance of eggs and larvae (Olivar and Fortuño, 1991; Olivar and Shelton, 1993) suggest that spawning occurs in winter and spring, but the spawning season has not been accurately described. Three previous studies on the diet of snoek in South African waters (Nepgen, 1979b, 1982; Dudley, 1987) excluded juveniles (<75 cm fork length) because nursery grounds were not sampled, and inadequate sample sizes precluded meaningful comparisons of snoek offshore and closer to the coast, and spatial comparisons of offshore diet.

The objective of this study was to provide information on the life history of South African *T. atun*, including season and localities of spawning, condition, nursery areas, juvenile growth, size-at-maturity, diet, and patterns of juvenile and adult distribution.

Materials and methods

The South African coastline between the Orange River and Cape St Francis was divided into seven sampling regions (Fig. 1). Biological (September 1994–January 1998) and length-frequency (January 1985–December 1997) data were collected in each region from fish caught by 1) the line fishery, 2) the demersal trawl fishery, and 3) research trawl surveys of pelagic and demersal fish conducted by Marine and Coastal Management. The trawl fishery operates farther offshore than the line fishery; consequently all fish sampled deeper than 150 m were trawl caught, whereas the bulk of those from shallower depths were caught by hook and line (except for a small number caught by trawl during research cruises).

Demersal biomass surveys (DBS), based on the swept-area method, are designed to provide annual indices of biomass for the resources exploited by the South African hake-directed trawl fishery, and methods have been fully described by Badenhorst and Smale (1991). DBSs are subdivided into two areas: the Namibian border to Cape Agulhas (west coast), and Cape Agulhas to Port Alfred (south coast). In each survey, area was divided into four depth zones (0–50 m, 51–100 m, 101–200 m, and 200–500 m) which, in turn, were subdivided into blocks of 5 × 5 nautical miles. The blocks trawled each survey were

determined semirandomly according to the ratio of blocks per stratum. Bobbins were not used, so that trawling was limited to nonreef substrata. A 180-foot German trawl was used with 25-mm mesh (bar) liner attached to the bag. Trawl duration was limited to 30 minutes; results of shorter trawls (caused by technical reasons or to hitting reef) were standardized to that time. Winter and summer cruises were undertaken on the west coast between July 1985 and January 1991; and autumn and winter–spring cruises on the south coast between September 1987 and April 1996.

Pelagic biomass surveys (PBS) are hydroacoustic surveys designed to estimate annual spawner biomass and recruitment strength of small, pelagic clupeoids—*E. japonicus*, *S. sagax*, and round herring, *Etrumeus whiteheadi* (see Hampton, 1992, for details). Acoustic targets are identified by directed trawling with an Engels 308 midwater trawl fitted with a codend liner of 8-mm mesh. Small *T. atun* (<30 cm) shoal with the pelagic species while larger individuals feed on them. As a result snoek are regularly caught by trawl on PBSs, albeit in small numbers (<30 per trawl). These surveys provide qualitative data on the distribution of juvenile snoek. A total of 80 PBSs, including more than 1500 midwater trawls, were completed between 1985 and 1997. Although the survey area varied considerably, with the extremes being Lüderitz (26°39′S; 15°09′E) in southern Namibia and Cape St Lucia (28°31′S; 32°25′E) in northern KwaZulu-Natal, regions 0–5 of the present study were consistently covered.

Migration of *T. atun* was studied by using spatial and temporal variation in magnitude and size composition of catches. Owners of commercial line boats and trawlers are required to submit daily catch returns to Marine and Coastal Management (MCM). The monthly catches of snoek reported by the trawl and line fisheries in each of the seven regions (1986–97) were expressed as percentages of the respective annual totals. Mean monthly handline catch per unit of effort (kg/boat/day) and trawl CPUE (kg/hour) by 50-m depth zones were calculated for each region. Catch rates recorded during fishery-independent DBSs were mapped separately for summer and winter cruises and presented as mean numbers of snoek per 30-min trawl, per grid block.

Fish sampled for biological purposes were measured to the nearest 1 mm (fork length), weighed, to the nearest gram (fish <500 g), or the nearest 10 g (fish >500 g), cut open, and sex was determined. Gonads were removed, assigned a macroscopic index of maturity (see Table 1), and weighed to the nearest 0.1 g. Random samples (n=5–30) of each macroscopic ovarian stage were fixed in Bouins solution for 48 hours and then stored in 70% ethanol for microscopic verification. They were routinely embedded in paraffin wax, sectioned to 3–7 µm, and stained with haemotoxylin and eosin. Stomach contents were analyzed fresh, and prey items were identified to the lowest possible taxon and weighed (wet) to the nearest 0.1 g. Bait was recognized easily and discarded.

The size at 50% maturity (L_{50}) for males and females was estimated by PROBIT analysis (SPSS, 1992) of the fractions of mature fish (gonad stage 3+) per 5-cm length class (midpoint), sampled during the breeding season. Upper and lower 95% confidence limits were calculated by the software package by using maximum-likelihood estimation.

Seasonal patterns of reproduction were established by calculating gonadosomatic indices (GSIs) and the monthly percent frequency of each maturity stage, for fish >L_{50}:

$$GSI = gonad\ weight / \left(\begin{bmatrix} fish\ weight - \\ gonad\ weight + \\ stomach\ content\ weight \end{bmatrix} \right) \times 100.$$

The extent of the spawning area was determined by computing the percent frequency of each maturity stage for females (>L_{50}) that were sampled in each region during peak spawning (June–October). Snoek spawn on the trawl grounds (see below); thus spawning grounds were further delineated by mapping commercial trawl CPUE (standardized by using general linear modelling to account for vessel size) during June–October (1986–97) with a 20 × 20 mile grid system. Commercial trawl CPUE was also used to establish the depth distribution of snoek on the trawl grounds, and hence the depth of the spawning area. Sex ratios were tested statistically for significant deviations from equality with chi-square tests.

Nursery areas were delineated by comparing the length-frequency distributions of snoek caught in each region 1) during pelagic and demersal biomass surveys, 2) by the line fishery, and iii) by Cape gannets, *Morus capensis*. Because trawling activities during PBSs were aimed at small pelagic clupeoids, it was not possible to use CPUE data from these cruises to analyze spatial patterns in juvenile snoek abundance. However, gannets from Lambert's Bay and Malgas Island (Fig. 1) have feeding distributions that, although large, are separated at Cape Columbine and do not overlap to any large extent (Berruti, 1987). Previous studies (Crawford et al., 1992; Berruti et al., 1993; Crawford, 1998) have demonstrated that gannet diet adequately reflects temporal and spatial patterns in prey abundance. Relative abundance of early-juvenile snoek north and south of Cape Columbine was therefore estimated by comparing rates of snoek consumption by the two colonies. Stomach contents of gannets at the two colonies have been sampled on a monthly basis since 1978 (see Berruti et al., 1993, for methods). Lengths of snoek prey were obtained from undigested specimens, and snoek consumption by the two colonies was compared annually (1978–97) using the mean mass per stomach containing food and percentage frequency of occurrence (i.e. percentage of stomachs with food that contained snoek).

Dietary importance of snoek prey was assessed by percentage frequency of occurrence (%F), which provides an indication of how often a particular item is selected within a population (Hynes, 1950), and by percentage by mass (%M) (Windell and Bowen, 1978), a measure of the energy contribution of that item (Macdonald and Green, 1983). An index of relative importance (*IRI*) was calculated for each prey category i as the product of $\%M_i$ and $\%F_i$. To facilitate comparisons of prey importance between analyses (e.g. separated spatially, temporally or according to predator size), this was expressed as a percentage (Cortés, 1997):

Table 1

Description of gonad maturity stages of snoek (*Tyrsites atun*) in South African waters. Microscopic descriptions are given only for females.

Stage	Macroscopic appearance	Microscopic appearance
1 Immature and resting	Ovaries appear as clear, pinkish, or translucent orange tubes. Eggs are not visible to the naked eye. Testes thread-like and clear, to ribbon-like and pinkish white in color.	Some ovaries in this stage consist entirely of primary growth oocytes and others contain oocytes to the early cortical alveoli stage. α atresia of unyolked and β atresia of yolked oocytes are also observed.
2 Active	Eggs discernible to the naked eye as yellow granules that do not occupy all available space in ovary. There is very little increase in the diameter of the ovary. Testes are wider, triangular in cross-section, and beige or cream in color. Sperm is present if the gonad is cut and gently squeezed.	Primary growth to early yolked oocytes evident. Those at the end of the spawning season show a high degree of α atresia.
3 Ripe	Ovaries completely opaque and orange to yellow in color. They are larger in diameter and eggs occupy all available space. Testes still larger in cross-section and softer in texture. They become creamier in color due to considerable quantities of sperm.	Primary growth to late yolk-stage oocytes present. Atresia and postovulatory follicles evident in some.
4 Ripe or running	Ovaries considerably larger in diameter, amber in color with a substantial proportion of hydrated eggs. Sperm is freely extruded when pressure is applied to the abdomen of the whole fish.	All stages from primary growth to hydrated oocytes present.
5 Spent	Ovaries are reduced in size, similar in appearance to stage-1 ovaries, and have a few yolked oocytes remaining. These yolked oocytes are generally aspherical and appear to be undergoing resorption. Testes are shrivelled in appearance and mottled beige and cream in color. A little viscous semen may still ooze from the genital pore when pressure is applied to the abdomen.	Primary growth to advanced yolk-stage oocytes present, but a much lower proportion of yolked oocytes than in previous stages; major atresia of yolked oocytes also present.

$$\%IRI_i = 100IRI_i / \sum_{i=1}^{n} IRI_i,$$

where n = the total number of food categories considered at a given taxonomic level.

Numerical percentage contribution (Pillay, 1952) was excluded because *T. atun* has a diverse diet and this method would bias the results towards small crustaceans, e.g. euphausiids and amphipods, which are not individually selected. Inshore samples for dietary analysis were collected from the west coast (regions 1–3) while offshore samples were collected from both the west coast (regions 1–3) and western Agulhas Bank (regions 4 and 5).

Proportion of stomachs containing food and the mean mass of stomach contents (including fish with empty stomachs) were used as indices of the rate of prey consumption for adult (≥75 cm) snoek. Sexual and spatial differences were tested for statistical significance by using chi-square tests (2×2 contingency tables) for frequency data (i.e. numbers with and without food), and a two-way ANOVA with single observations for mean prey mass data.

Monthly relative condition (Kn) was calculated for adult snoek (≥75 cm) as follows:

$$Kn_j = \frac{\sum_{i}^{n} \frac{w_i}{aFL_i^b}}{n_j},$$

where W_I = the gonad and stomach content free weight (g) of the i^{th} individual in the j^{th} month;
FL_i = the fork length (mm) of the i^{th} individual;
a (0.000018) and b (2.80) are constants from the length-weight (gonad and stomach content free) relationship derived from data collected during the present study (all months combined); and
n_j = the number of fish sampled in the j^{th} month.

Snoek accumulate fat as three longitudinal mesenteric deposits along the outer walls of the stomach. Monthly

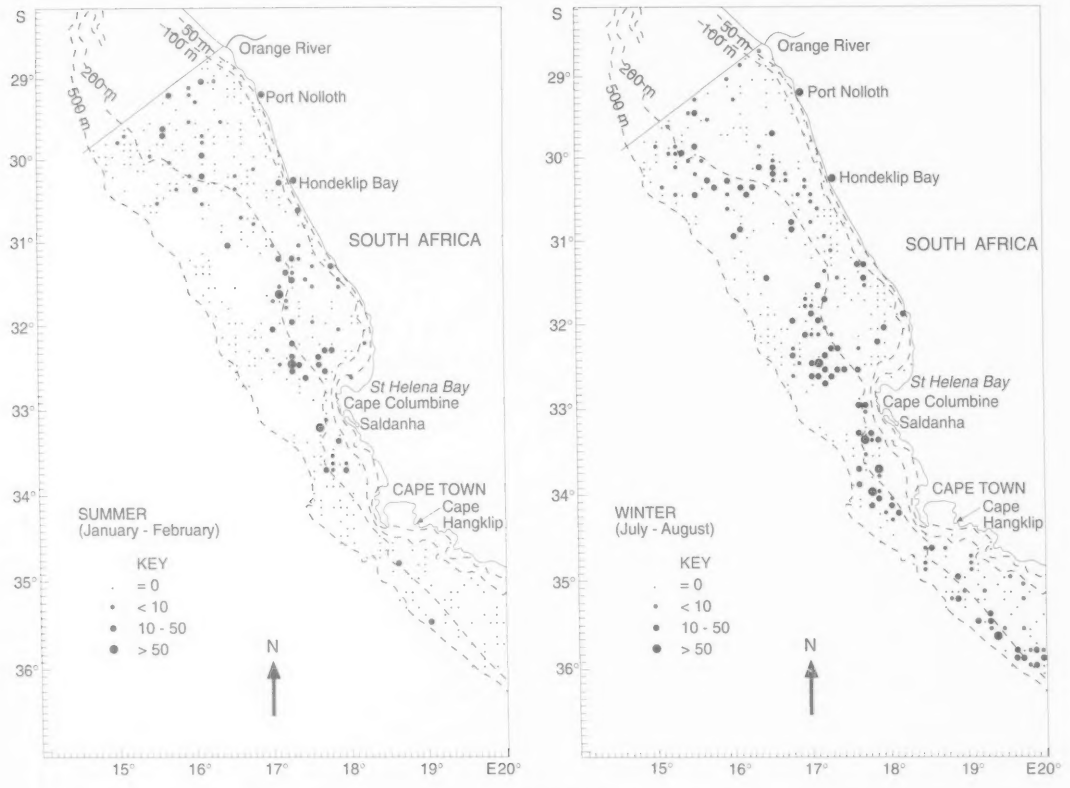

Figure 2A

Mean number of *Thyrsites atun* per trawl per grid block (5 × 5 nmi) by season for (**A**) the west coast (July 1985–Jan 1991; n=18 surveys and 1624 trawls) and (**B**) the south coast (September 1987–April 1996; n=18 surveys and 1554 trawls) demersal biomass surveys off South Africa.

proportions of stomachs with no fat were calculated separately for adult (≥75 cm) males and females.

Results

Migration

Spatial analysis of CPUE from fishery-independent DBSs indicated that *T. atun* are distributed farther offshore and farther southeast in winter and spring than in summer and autumn (Fig. 2). Fishery-dependent data support this pattern; commercial catches from the trawl grounds (i.e. >150 m) were highest from June to October, and those in the southern regions (3–6) lagged behind catches in the north (regions 0–2) by approximately one month (Fig. 3). Analysis of trawl CPUE by depth, area, and season (Fig. 4) further confirmed offshore movement during the spawning period (June–October) and furthermore revealed that *T. atun* were most abundant between bottom depths of 150 m and 350 m while on the trawl grounds. Snoek found on the trawl grounds were generally >65 cm FL (Fig. 5A).

Line-based catch and CPUE in regions 0–2 was distinctly seasonal; most of the catch was made from April to June (Fig. 3) and a slight southwards progression in peak catch and CPUE occurred within this period (Fig. 3). Line-caught snoek from regions 1 and 2 were substantially smaller (50–75 cm) and younger (1–3 years; author, unpubl. data) than those from region 3 (80–95 cm; 3–7 years) (Fig. 5B).

Line-caught snoek in region 3 were mostly >L_{50} (Fig. 5B). Monthly catch and CPUE statistics from this region depicted no trend, indicating that adult snoek are available to line fishermen throughout the year (Fig. 3). Catch rates in region 4 were highest between July and October, which is consistent with the winter–spring south–eastward dispersal of adult snoek evident from trawl data (above). Handline catch and CPUE in regions 5 and 6 were highest during the first half of the year but declined dramatically in winter.

Size at maturity

The ratio of active (stage-2) to ripe (stage-3) ovaries during the spawning season decreased with fish length

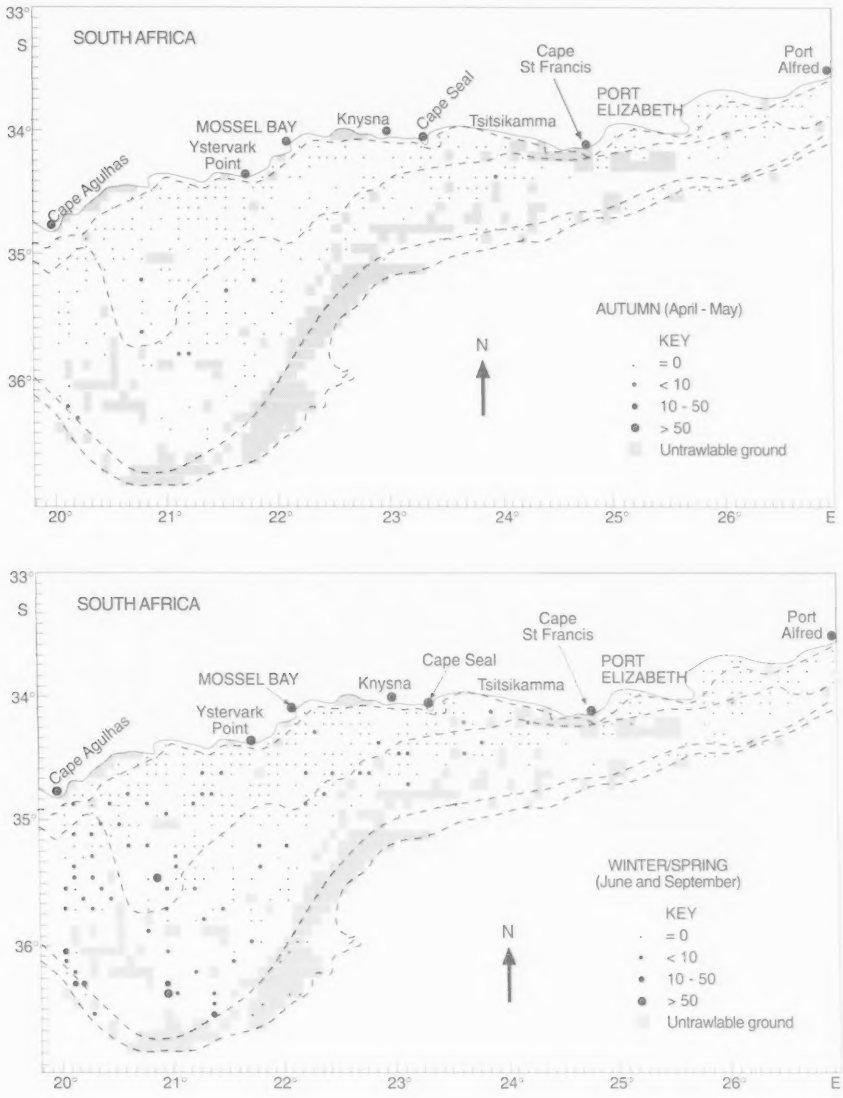

Figure 2B

(Fig. 6A), suggesting (as in other teleosts; Griffiths and Hecht, 1995) that substantial proportions of snoek in the smaller size classes undergo partial gonad development during the season prior to maturity. Because these fish are unlikely to spawn, only specimens with gonads developed to at least stage 3 (ripe) were regarded as mature. Given that snoek spawn offshore (see below) and that almost all fish on the trawl grounds (regardless of size) were mature (Fig. 6B), L_{50} maturity calculations were limited to fish sampled inshore (<150 m)[4]: 72.0 cm for males and 73.4 cm for females (Fig. 7). Upper and lower 95% confidence limits were 69.3 and 74.3 cm for males, and 71.3 and 75.4 cm for females. L_{50} for combined male and female data was 73.0 cm with 95% confidence intervals of 70.0 and 75.2 cm. In all cases the L_{50} values corresponded with an age of 3 years (author, unpubl. data).

[4] In situations where fish migrate to spawn, all fish on the spawning ground are mature. As a result, even if 10% of a particular size class (x–y cm) in the population are mature, the sampling of that 10% once it had migrated onto the spawning grounds would suggest that 100% of that size class are mature. Because mature snoek move back and forth between the spawning and feeding grounds (offshore and inshore) in regions 0–3 during the spawning season, and could readily be distinguished from immature fish, inshore samples were used to determine size at maturity.

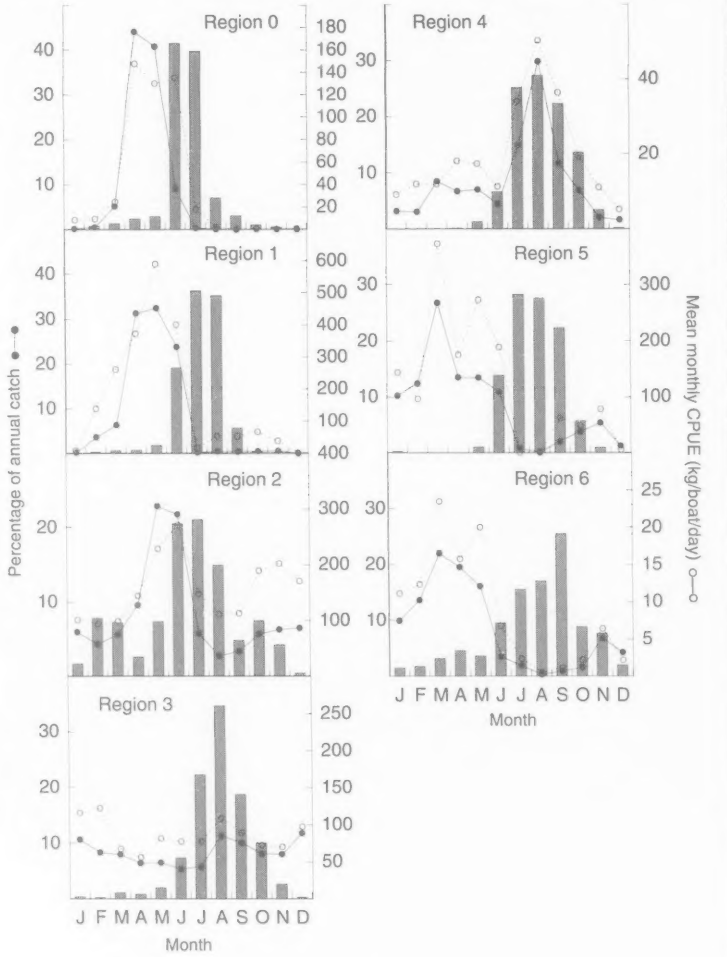

Figure 3

Catches of *Thyrsites atun* made by South African commercial trawlers (bars) and line fishermen (black circles) summed on a monthly basis in each region and expressed as percentages of the total catch for the period 1985–1997. Mean monthly catch per unit of effort (kg/boat/day) of *T. atun* caught by South African commercial line fishermen in each region (open circles) is also given (1985–97). Because the bulk (70 %) of the line catch in region 5 was made on offshore pinnacles (i.e. over a 72-mile bank), the CPUE trend for this region was based on data from this area. The offshore pinnacles (the 72-mile bank being the deepest) are, however, located well inshore of the trawl grounds in that region (see Fig. 1).

Spawning

Gonadosomatic indices (Fig. 8) and gonad maturity indices (Fig. 9) showed that South African snoek spawn from May to November and that peak spawning occurs from June to October (winter–spring). Monthly male GSIs were similar inshore and offshore, but female values were higher offshore during the spawning season. In addition, a substantial proportion (20+%) of offshore females in regions 2 to 5 had hydrated oocytes (stage 4), whereas this gonad stage was rarely observed inshore. Spatial patterns in trawl CPUE from both fishery-independent (Fig. 2) and fishery-dependent (Fig. 10) data collected during winter–spring suggest an extensive spawning ground that encom-

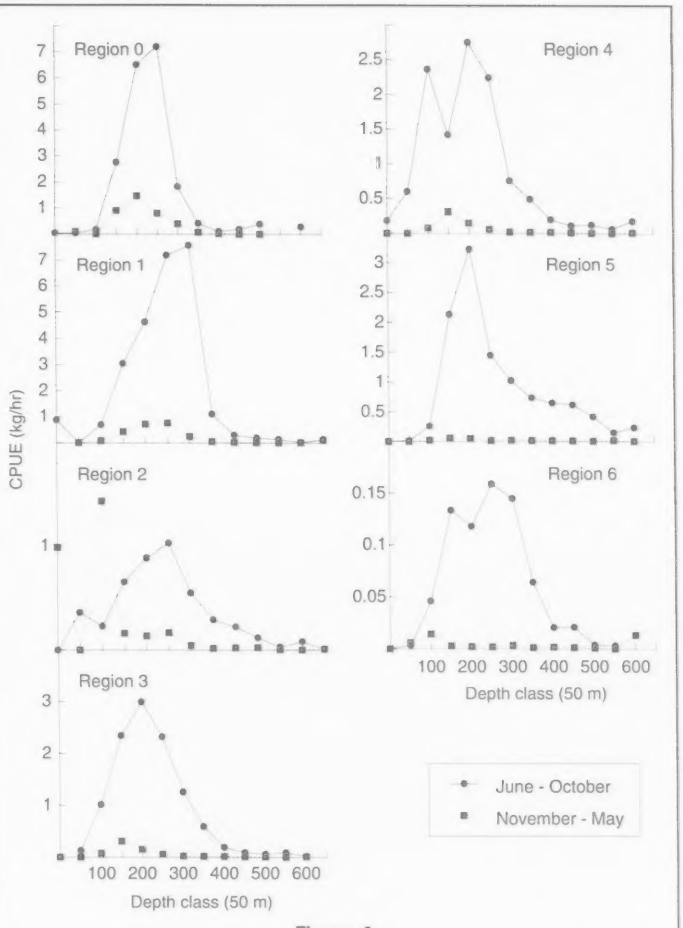

Figure 4

Catch per unit of effort (CPUE; kg/h) per 50-m depth category for *Thyrsites atun* commercially bottom trawled in each of the seven regions during winter–spring and summer–autumn, 1986–97.

passed the western edge of the Agulhas Bank and most of the South African west coast, to a point just north of Hondeklip Bay.

The predominance of ripe (stage-3) females (both inshore and offshore) throughout the protracted spawning season (Fig. 9) is indicative of multiple spawning (Griffiths, 1997). Moreover, the simultaneous occurrence of postovulatory follicles (POFs) with both primary growth and advanced yolked-stage oocytes (Fig. 11) confirmed that snoek are indeterminate, serial spawners.

Sex ratio

Sex ratios in regions 0–3 were skewed towards females inshore and males offshore (Table 2), a pattern most pronounced during the spawning season (winter–spring). Inshore, this pattern was most evident in the adult size class (≥75 cm). Adult sex ratios in regions 0–3 during the spawning season were 2.9F:1M inshore and 1F:2M offshore. Inshore and offshore sex ratios of adult snoek in regions 4 and 5 (Table 2) revealed no clear pattern; although moderately more females were sampled on the trawl grounds of these regions during the spawning season (1.6F:1M), the inshore ratio (1M:1.2F) did not deviated significantly from unity.

Nursery areas

Monthly length-frequency distributions comprised fairly discrete modes in spite of variation in collection method and sampling period and clearly depicted early juvenile growth (Fig. 12). Young-of-the-year snoek first appeared

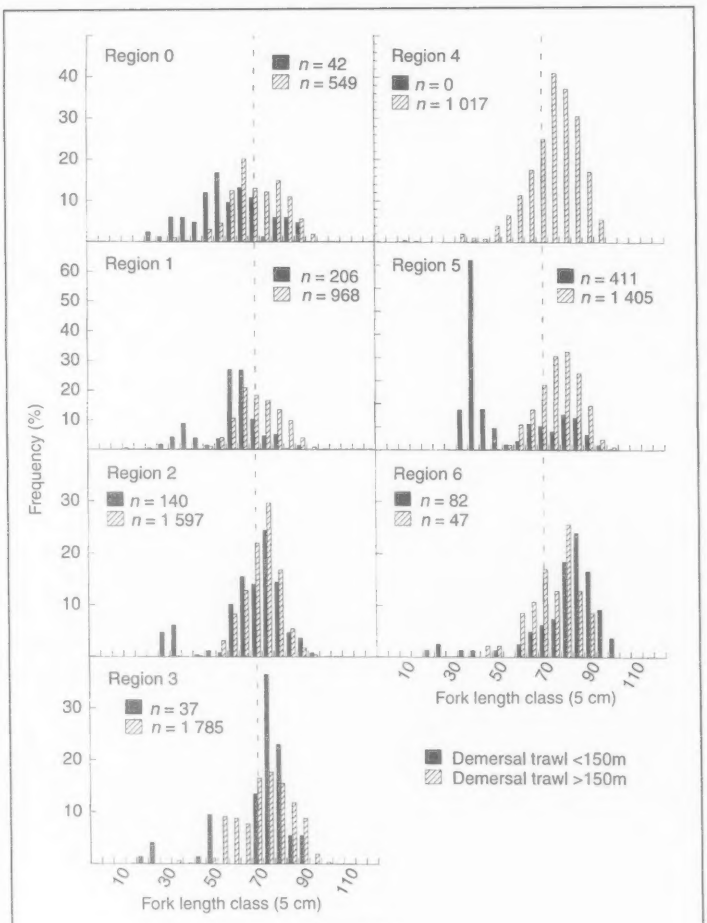

Figure 5A

Fork-length distributions of *Thyrsites atun* caught by (**A**) demersal trawl and (**B**) handline and midwater trawl in each region. Handline and midwater catches were made shorewards of the 150-m isobath and demersal catches were divided into those made deeper and shallower than this depth. The dotted line indicates length at maturity (L_{50}).

in the diets of gannets and in pelagic trawls during spring (Oct–Nov) at lengths 7–12 cm and grew rapidly to 33–44 cm by the spawning season (winter) of the following year (±3.25 cm/month). Early juveniles (<1 year old) were sampled (with fishing gear) in each of the seven regions (Fig. 5) but formed a larger proportion (by mass and frequency of occurrence) of the diet of gannets at Bird Island (Lamberts Bay) than in gannets of Malgas Island (Fig. 13). Snoek smaller than 70 cm comprised a far higher proportion of the handline and pelagic trawl catches of regions 0–2 than those from region 3 (Fig. 5B). Length frequencies of pelagic trawl, demersal trawl (<150 m), and line-caught snoek suggested that juveniles were also found in reasonable numbers to the east of Danger Point in regions 4 and 5. *Thyrsites atun* collected in demersal trawls deeper than 150 m were mostly >65 cm, whereas those from shallower bottom trawls included substantial proportions smaller than this length (Fig. 5A). Juveniles <30 cm, although present in pelagic trawls (Fig. 5B), were notably absent from demersal trawls, including those shallower than 150 m (Fig. 5A).

Diet

Snoek prey on a wide variety of demersal and pelagic organisms, including teleosts, crustaceans, and cephalopods (Tables 3 and 4) and show ontogenetic shifts. The diet of *T. atun* sampled inshore of the 150-m isobath along the west coast (regions 0–3) consisted predominantly of pelagic fishes, and crustaceans comprised a smaller but

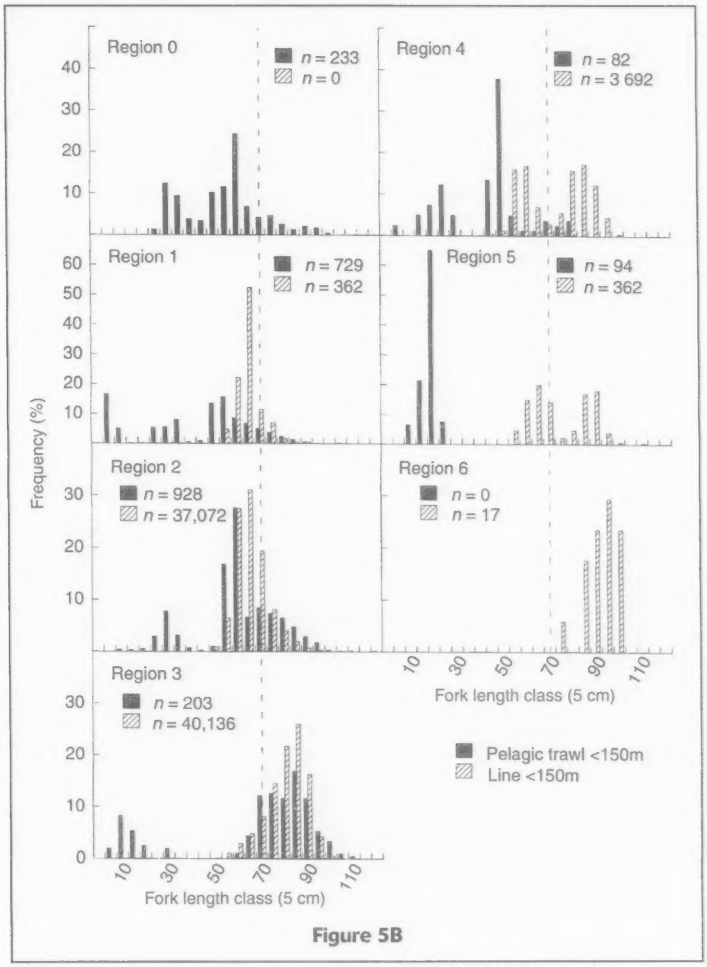

Figure 5B

Table 2

Inshore and offshore sex (M:F) ratios of *Thyrsites atun* during summer–autumn and winter–spring (spawning season) for the period 1994–97. Levels of significance—* ($P<0.05$), ** ($P<0.01$), and *** ($P<0.001$)—were determined by using a chi-square test (Yates' correction factor was applied as df =1).

	Inshore (<150 m)						Offshore (>150m)					
	Summer–Autumn			Winter–Spring			Summer–Autumn			Winter–Spring		
Fork length (cm)	M:F	*n*	χ^2	M:F	*n*	χ^2	M:F	*n*	χ^2	M:F	*n*	χ^2
Regions 0–3												
20–49	1:1	203	0.01	1:1.3	7	0						
50–74	1:1.2	647	4.5*	1:1.1	524	0.6	1.2:1	105	1.0	2.4:1	228	20.3***
>75	1:1.8	523	42.0***	1:2.9	1131	263.0***	1:1.2	134	1.3	2.0:1	704	61.3***
All sizes	1:1.4	1373	30.5***	1:2.0	1662	192.3***	1:1	241	0	2.1:1	933	82.3***
Regions 4–5												
20–49										1.3:1	7	0
50–74	1:1.1	53	0	1:1	24	0		No data		1:1	440	0
>75	1:2.0	6	0.1	1:1.2	46	0.2				1:1.6	586	31.1***
All sizes	1:1.2	59	0.4	1:1.1	70	0.1				1:1.3	1033	18.4***

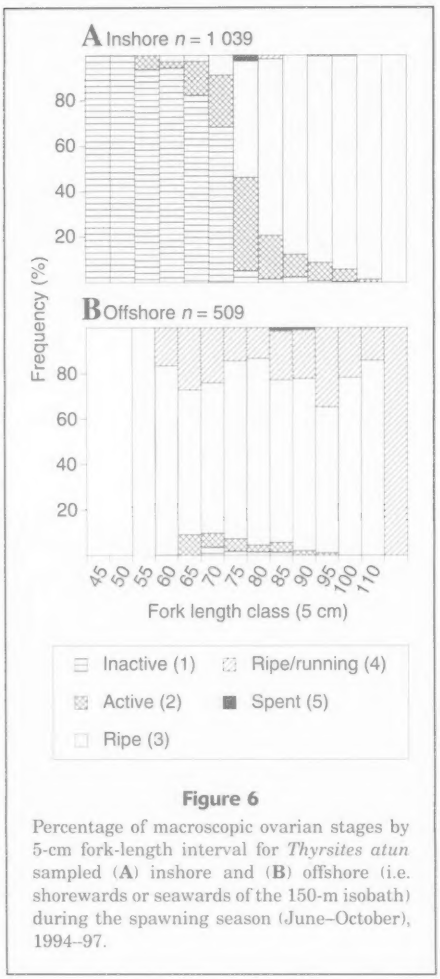

Figure 6

Percentage of macroscopic ovarian stages by 5-cm fork-length interval for *Thyrsites atun* sampled (**A**) inshore and (**B**) offshore (i.e. shorewards or seawards of the 150-m isobath) during the spawning season (June–October), 1994–97.

noteworthy component that declined in importance with growth. In descending order. the most important prey items were as follows: lanternfish *Lampanyctodes hectoris* (IRI=46.5), euphausids *Euphausia leucens* (IRI=23), and the amphipod *Themisto gaudichaudi* (IRI=14.2) for early juveniles (5–24 cm); lanternfish (IRI=34.4), *T. gaudichaudi* (IRI=32.4), anchovies (IRI=2.8), and sardines (IRI=2.4) for juveniles (25–49 cm); anchovy (IRI=38.3), euphausids (IRI=26), and sardine (IRI=11.7) for subadults (50–74 cm); and sardine (IRI=47.4) and anchovy (IRI=38.6) for adults (≥75 cm).

In offshore waters snoek diet consisted almost exclusively of teleosts, including pelagic and demersal taxa. The most important prey items were sardine, round herring, and hake (*Merluccius* spp.) for snoek <75 cm; and hake, sardine and horse-mackerel (*Trachurus trachurus capensis*) for larger specimens. The main difference between the two offshore diets consisted in the greater importance of sardine (IRI=44.4 vs. 17.2 for snoek ≥75 cm) and the

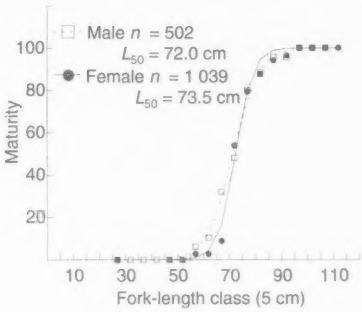

Figure 7

Percentage of mature (gonad stage 3+) *Thyrsites atun* by 5-cm fork-length class sampled during the spawning season (June–October), 1994–97. Symbols represent the observed data and the lines the fitted models. L_{50}= length-at-maturity (cm fork length); n = sample size.

lesser importance of hake (IRI=31.8 vs. 60.8 for snoek ≥75 cm) off the western Agulhas Bank than off the west coast (Table 4). In both areas, large prey species, such as hake and horse mackerel, were more important in the larger (≥75 cm) size class.

Prey consumption

Both indices of prey consumption—proportions of stomachs containing food and mean mass of stomach contents—indicated that within each area and sampling season, adult females consumed more prey than adult males (Table 5); spatial and season trends were also evident. Two-way ANOVA with single observations revealed that differences in the mean mass of stomach contents between sexes (F= 65.9, df=1, $F_{critical}$=10.1) and between areas (F=215.5, df=3, $F_{critical}$=9.3) were both highly significant (P<0.001). Chi-square tests revealed that differences between the proportions of males and females with stomach contents were highly significant inshore on the west coast (WC) and offshore along the western Agulhas Bank (WAB) in winter–spring, but were not significant inshore on the WC in summer–autumn, or offshore on the WC in winter–spring (Table 5). Female mean stomach content mass was lowest (22.1 g) inshore on the WC in summer–autumn and highest (60.1 g) offshore on the WAB in winter–spring (spawning season). Female proportion with stomach contents was also lowest (52.5%) inshore on the WC in summer–autumn but highest (81.2%) in the same area during winter. Differences in female proportions with stomach contents between seasons inshore on the WC (χ^2=99.9, df=1), between inshore and offshore areas of the WC in winter–spring (χ^2=13.0, df=1) and between the offshore WAB and inshore WC during winter–spring (χ^2=26.3, df=1) were highly sig-

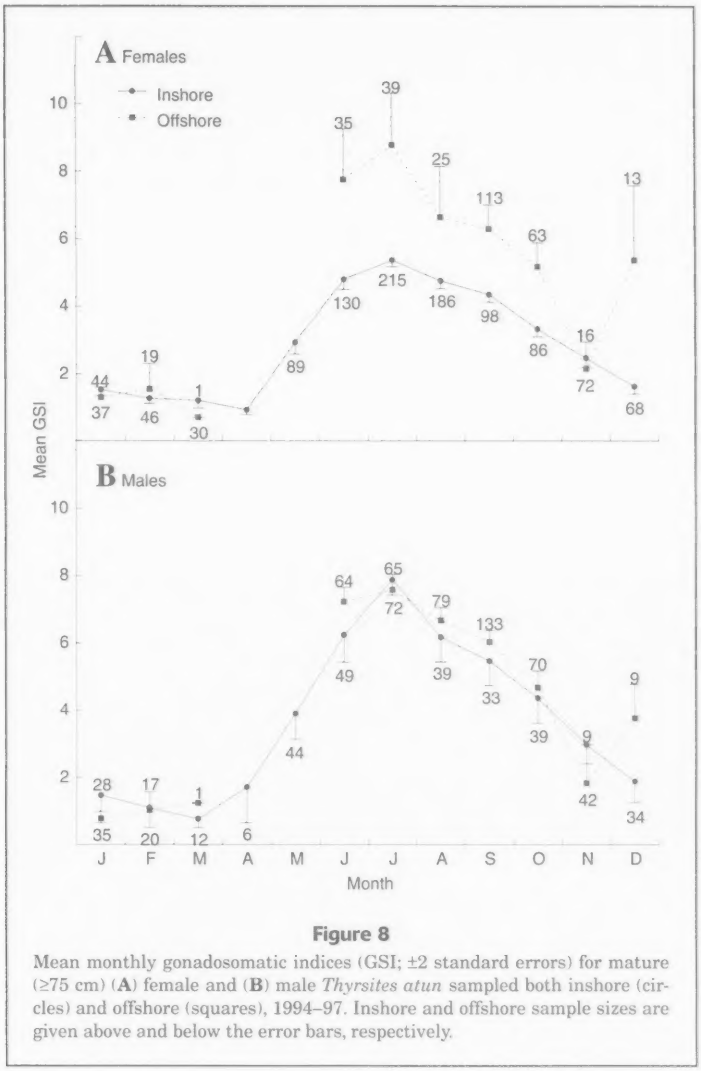

Figure 8

Mean monthly gonadosomatic indices (GSI; ±2 standard errors) for mature (≥75 cm) (**A**) female and (**B**) male *Thyrsites atun* sampled both inshore (circles) and offshore (squares), 1994–97. Inshore and offshore sample sizes are given above and below the error bars, respectively.

nificant ($P<0.01$), but differences between the two offshore areas—WC and WAB—in winter–spring were not. Mean stomach content mass was, nevertheless, substantially higher (60.1 g vs. 44.6 g.) offshore on the WAB than offshore of the WC during winter–spring (Table 5).

Condition

Relative condition (Kn) of adult snoek depicted a clearly seasonal cycle: highest between March and May, declining steeply through June to October (spawning season), increasing again from November through to March (Fig. 14). The proportion of stomachs without any fat was inversely related to Kn (Fig. 14): it was lowest from March to May but increased dramatically during the spawning season. The rate of fat decline was, however, higher in females than males; by September 90% of females and 58% of males had no mesenteric fat reserves.

Discussion

Crawford and De Villiers (1985) postulated that the snoek of the Benguela ecosystem comprise a single stock that undergoes a seasonal longshore migration—moving southwards into South African waters to spawn in winter and returning north, as far as southern Angola, in spring–summer. Although this theory has become widely accepted (Crawford et al., 1987; Crawford, 1995), this study showed that adult snoek are available to South African line fisher-

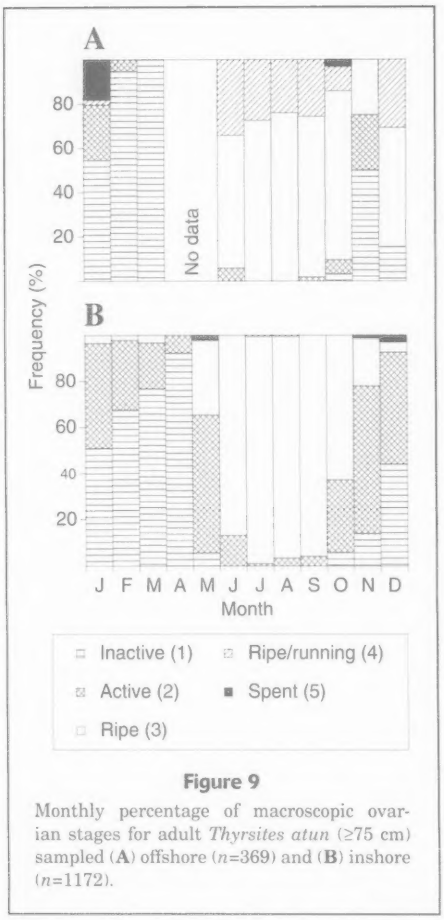

Figure 9

Monthly percentage of macroscopic ovarian stages for adult *Thyrsites atun* (≥75 cm) sampled (**A**) offshore (n=369) and (**B**) inshore (n=1172).

men throughout the year, and that the seasonal availability of adults on the trawl grounds results from an offshore spawning migration rather than southward movement from Namibian waters. Based on these results, *inter alia*, separate nursery areas and egg and larval distributions north and south of the cold upwelling cell (25–27°S) off southern Namibia, Griffiths (in press) concluded that Benguela snoek exist as two subpopulations, and have limited exchange.

The life history of South African *T. atun* is summarized by the conceptual model presented in Figure 15. Movement patterns were inferred largely from spatiotemporal trends in fishery-dependant catch and effort data. Considering that snoek is the most important line fish on the South African western seaboard and that it is a bycatch in the trawl fishery, catch trends are unlikely to have been biased by switches in targeting. Moreover, even though line-fish catches are under-reported (Sauer et al., 1997), they have been demonstrated to accurately reflect seasonal trends in the abundance of migratory species (Griffiths and Hecht, 1995). Given the offshore movement of adult fish during the spawning season and the associated ovarian condition (greater GSIs and the presence of hydrated oocytes), it is concluded that South African snoek spawn offshore between the 150- and 400-m isobaths. Although most of the inshore catch was line-caught, the absence of stage-4 females from trawls made shallower than 150 m during the spawning season (n=46, including 32 ripe [stage-3] specimens) indicates that this observation is not an artifact of gear selectivity. Spatial patterns in trawl CPUE from both fishery-independent (Fig. 2) and fishery-dependent (Fig. 11) data, collected during winter–spring, suggest an extensive spawning ground that encompasses the western edge of the Agulhas Bank and most of the South African west coast, to a point just north of Hondeklip Bay. Presence of snoek eggs and larvae (off South Africa) from the southern tip of the Agulhas Bank to Hondeklip Bay and their great abundance between the 200-m and 600-m isobaths (Olivar and Fortuño, 1991; Olivar and Shelton, 1993) corroborate offshore spawning and an extensive spawning ground. The occurrence of snoek preflexion larvae in region 6 (Wood, 1998) indicates that spawning does occur farther to the east, but the relatively low abundance of adult fish and spawning products suggests it is not an important spawning area.

The sex ratio of adults (≥75 cm) on the west coast (regions 0–3) was skewed towards males on the spawning grounds (2M:1F), and towards females further inshore (2.9F:1M), particularly during the spawning season. Based on the differential loss of intestinal fat, it is evident that the energetic demands of spawning are higher in females than in males. The higher rate of prey consumption by females during winter–spring (i.e. spawning season) than during summer–autumn and the greater prey consumption by females than by males during the spawning season indicate that they are able to enhance their spawning effort with exogenous energy. It is therefore postulated that because snoek are indeterminate serial spawners, females on the west coast move inshore between spawning events, where their principal prey—*Sardinops sajax* and *Engraulis japonicus*—are more abundant.

Females spawning off the western Agulhas Bank do not appear to move inshore to feed between spawning events, according to near equal sex ratios and low inshore catch rates in winter–spring (region 5). Although line catches in region 4 were highest during the spawning season, which at first glance may appear to be contradictory, CPUE was an order of magnitude lower than in region 3 or region 5, indicating relatively low inshore abundance at that time of the year. High female mean stomach content mass (60.1 g) and the significantly higher proportion of females than males with food (shared only with the inshore feeding ground of the WC) suggest that the offshore WAB functions as both spawning and feeding ground during winter–spring. In addition, PBSs have revealed that clupeids—adult sardine and round herring—are more abundant near the shelf edge of the WAB in winter than along the WC (Coetzee[5]), and dietary comparison (this study) showed that clupeids indeed represent a larger component of the offshore diet

[5] Coetzee, J. 2000. Personnal commun. Pelagic Section, Marine & Coastal Management, Private Bag X2, Roggebaai, 8012, Cape Town.

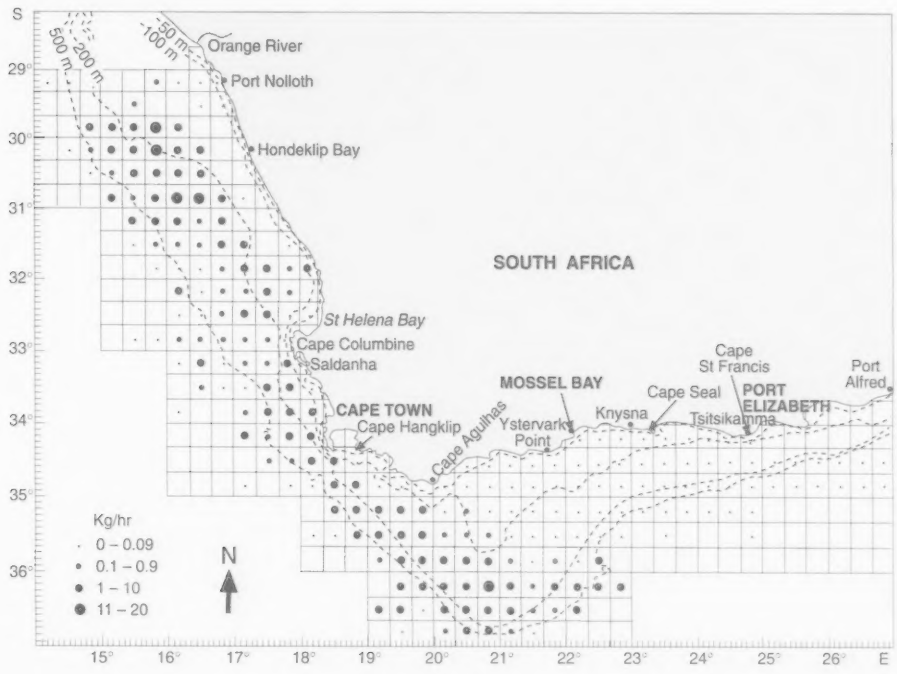

Figure 10

Catch per unit of effort (kg/h) by 20-mile block (1986–97) for *Thyrsites atun* caught by commercial trawls in the southern Benguela system during the spawning season.

of the WAB than offshore along the WC, where hake was dominant. Sex ratios and feeding patterns of adult snoek in the present study were confirmed as persistent biological features of the western Agulhas Bank by experimental trawl surveys on the spawning ground of region 4 during August 1999 and August 2000. The principal prey taxon for 1875 snoek with a sex ratio of 1M:1.2F ($P<0.001$) was Clupeidae (67% by weight); mean stomach content masses were 58.2 g for females and 27.6 g for males.

Even though young-of-the-year snoek were sampled (with fishing gear) in each of the seven regions, they formed a larger proportion (by mass and frequency of occurrence) of the diet of gannets at Bird Island (Lamberts Bay) than in gannets at Malgas Island. Either early juveniles are more abundant north of Cape Columbine than between Cape Columbine and Cape Infanta or they are selected at a higher frequency by gannets in the former area. Higher proportions of snoek smaller than 70 cm in the handline and pelagic-trawl catches of regions 0–2 than in catches from region 3 support the first suggestion, confirming that the area north of Cape Columbine has an important nursery function. Length frequencies of pelagically trawled, demersally trawled (<150 m), and line-caught snoek, nevertheless suggest a second nursery area to the east of Danger Point. But because handline catches in

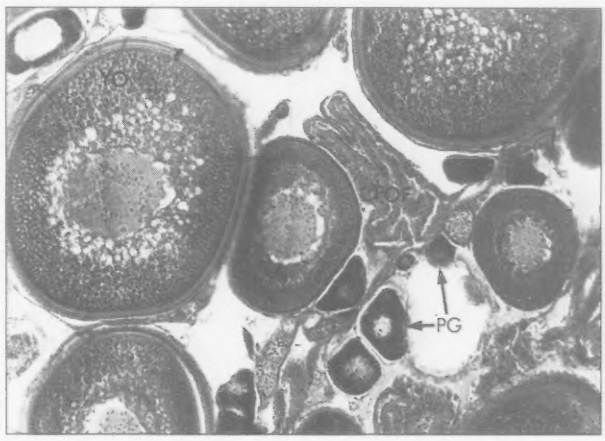

Figure 11

Photomicrograph of transverse section of *Thyrsites atun* ovary stained with haemoxylin and eosin, showing co-occurrence of postovulatory follicles (POF) together with primary growth (PG) and advanced yolk-stage oocytes (YO).

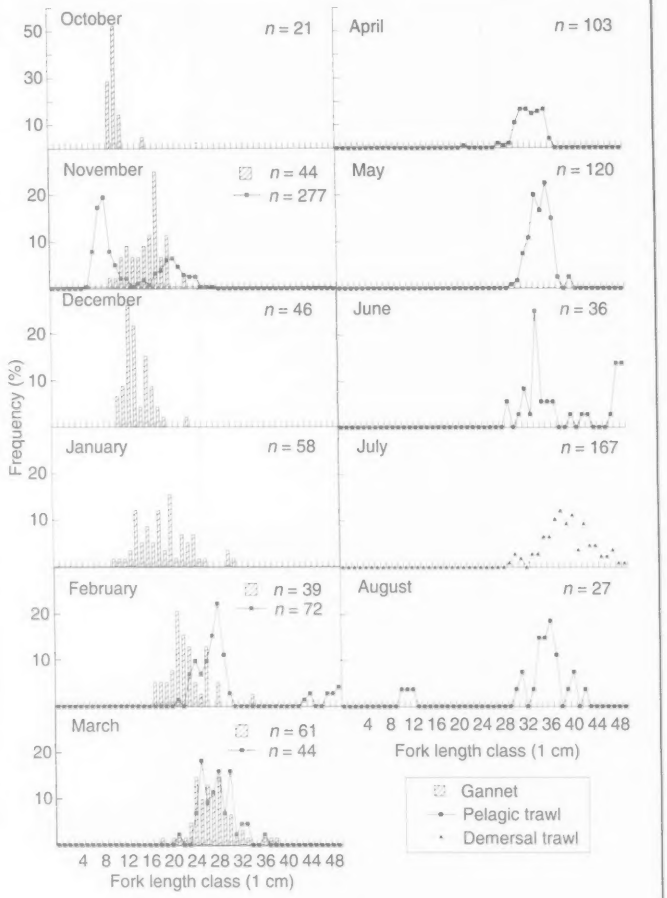

Figure 12

Monthly fork-length distributions of *Thyrsites atun* <50 cm caught by midwater trawls (1985–97), demersal trawls (1985–97), and Cape gannets (1978–97) in the southern Benguela system. *n* = sample size. Dotted line at 25 cm is included as a reference point.

regions 4 and 5 amounted to only 10% of those in regions 1and 2 (1985–97) and given that juvenile snoek made a substantially lower contribution to the diets of gannets foraging in this area, the area north of Cape Columbine is regarded as considerably more important to juvenile snoek. *Thyrsites atun* in demersal trawls made deeper than 150 m were mostly >65 cm, whereas those from shallower bottom trawls included substantial proportions smaller than this length. It is therefore concluded that the primary nursery ground is situated on the west coast, north of Cape Columbine and in water shallower than 150 m; a secondary nursery exists to the east of Danger Point. The absence of specimens <30 cm from demersal trawls, particularly those made shallower than 150 m, and their presence in pelagic trawls, indicates that 0-year-old snoek are largely epipelagic but become pelagic with growth (at ca. 8 months old).

The northward flowing Benguela Current provides a mechanism for transporting epipelagic snoek eggs and larvae (De Jager, 1955; Olivar and Fortuño, 1991) from the spawning ground to the proposed nursery areas. The Benguela current is found offshore (generally between the 150- and 400-m isobaths) and flows along the western edge of the Agulhas Bank and up the South African west coast; rate of flow is fastest (typically 25–80 cm/s) between Cape Point and Cape Columbine, where it develops into a shelf edge jet (Shannon and Nelson, 1996). Although water movement is primarily parallel to the shelf, inshore advection occurs to some degree due south of Danger Point and to a greater extent between Cape Columbine and Hon-

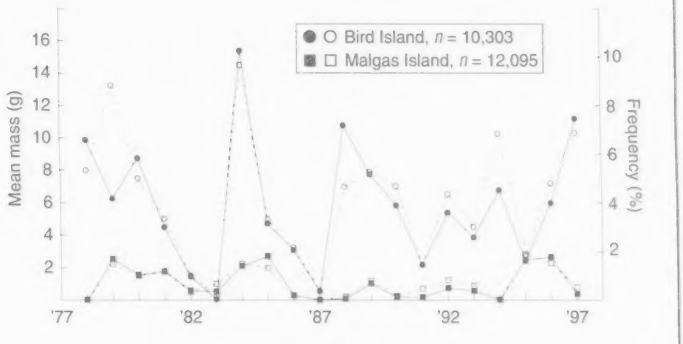

Figure 13

Annual frequency of occurrence (*%F*; dotted line) and mean mass (solid line) of *Thyrsites atun* in the stomachs of Cape gannets from Bird Island (circles) and Malgas Island (squares), 1978–97. *n*=number of gannet stomachs examined.

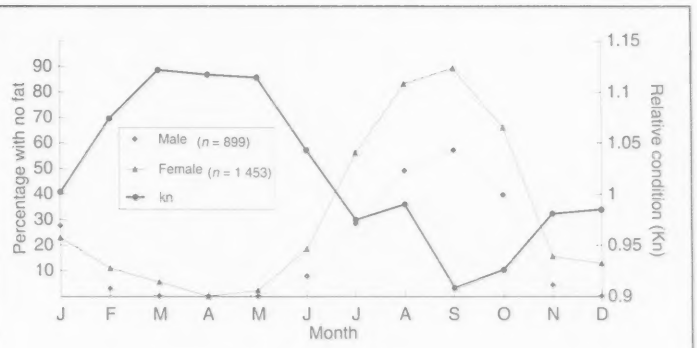

Figure 14

Mean monthly relative condition (Kn) and the proportion of adult *Thyrsites atun* (≥75 cm) without intestinal fat reserves, in the southern Benguela Ecosystem (1994–97).

deklip Bay (Shelton and Hutchings, 1990; Shannon and Nelson, 1996).

Snoek hatch about 2 days (50 hours) after fertilization (De Jager, 1955), are phytoplanktivorous from first feeding (3.5 mm and 3–4 days after hatching) until 8 mm long (standard length), after which they prey largely on the larvae of other fishes (Haigh, 1972). Total abundance of fish larvae in the southern Benguela is highest in spring and summer (Shelton, 1986); snoek larvae spawned during the winter and spring months are therefore assured of an abundant supply of food. Following northward advection in the jet current, young-of-the-year anchovy, round herring, and sardine, which share the northern nursery area with snoek, move shoreward across the shelf, with a concomitant increase in size (Armstrong et al., 1987; Roel and Armstrong 1991; Hampton, 1992; Roel et al., 1994; Barange et al., 1999; Van der Lingen and Merkle, 1999). They arrive at the coast from February through through June at total lengths of 5–11 cm, and, unlike snoek, which are found on the nursery grounds for 2–3 years, immediately begin a southwards migration back onto the Agulhas Bank, where they were originally spawned. Coupled with earlier spawning, rapid growth ensures that 0-year-old snoek are large enough (ca. 35 cm TL) to partake with the older juveniles in this seasonally abundant food source. Substantial increases in line catches during the period of clupeoid recruitment suggest that juvenile snoek follow their prey inshore. Differences in the size and age composition of catches north and south of Cape Columbine, however, indicate that they do not move southwards with them and onto the Agulhas Bank. The large contribution of lanternfish to the diets of snoek <50 cm is attributed to the fact that most of these fish were sampled during the second half of the year, i.e. when juvenile clupeoids (i.e.

Table 3

Stomach contents of snoek (*Thyrsites atun*) sampled inshore of the 150-m isobath along South African west coast (1994–97). *M* = percent mass, *F* = percent frequency of occurrence, *IRI* = percent index of relative prey importance at the species and at a higher (bold) taxonomic level. [P] = pelagic and [D] = demersal species.

Taxon and prey item	5–24 cm FL (n = 11)			25–49 cm FL (n = 212)			50–74 cm FL (n = 540)			>74 cm FL (n = 1,069)		
	M	*F*	*IRI*	*M*	*F*	*IRI*	*M*	*F*	*IRI*	*M*	*F*	*IRI*
Annelida							<0.1	0.2	**<0.1**	0	0	0
Polychaeta							<0.1	0.2	<0.1			
Crustacea	27.7	54.5	**24.7**	19.4	45.5	**12.6**	22.0	39.5	**14.3**	7.4	5.9	0.5
Amphipoda												
Themisto gaudichaudi[P]	20.9	9.1	14.2	17.8	42.0	32.4	1.42	10.9	1.0			
Brachyura												
Megalopa larvae[P]							<0.1	0.2	<0.1			
Euphausiacea												
Euphausia lucens[P]	6.8	45.5	23.0	1.3	3.6	0.2	15.0	27.4	26.0	0.3	1.6	<0.1
Isopoda												
Paridotea ungulata[P]							<0.1	<0.1	<0.1	<0.1	0.1	<0.1
Macrura												
Lobster pueruli[P]							<0.1	0.2	<0.1	<0.1	0.3	<0.1
Pasiphaea spp.[P]							<0.1	0.5	<0.1	0	0	0
Mysidacea[P]				<0.1	0.9	<0.1	0.3	1.0	<0.1	<0.1	0.1	<0.1
Stomatopoda												
Pterygosquilla armata[P]							5.0	10.4	3.3	7.1	4.5	1.1
Unidentified crustaceans				0.3	0.9	<0.1	0.1	0.6	<0.1	<0.1	0.3	<0.1
Mollusca												
Cephalopoda							0.3	2.2	**<0.1**	0.2	1.6	**<0.1**
Inioteuthis							<0.1	0.2	<0.1	0	0	0
Loligo vulgaris reynaudii							0	0	0	<0.1	0.3	<0.1
Lolliguncula mercatoris?							0.2	1.5	<0.1	<0.1	1.1	<0.1
Lycoteuthis?							0	0	0	<0.1	0.1	<0.1
Sepia australis							0.1	0.4	<0.1	<0.1	0.1	<0.1
Todaropsis eblanae							0	0	0	<0.1	0.1	<0.1
Unidentified squid							<0.1	0.2	<0.1	0	0	0
Teleostei	72.3	63.6	**75.3**	80.6	76.0	**87.4**	77.8	66.9	**85.7**	92.4	95.7	**99.5**
Engraulis japonicus[P]				6.1	10.7	2.8	30.9	19.6	38.3	26.9	44.0	38.6
Sardinops sagax[P]				8.9	6.3	2.4	18.9	6.8	11.7	43.1	33.8	47.4
Etrumeus whiteheadi[P]				5.1	1.8	0.4	6.5	3.2	1.3	2.3	3.5	0.3
Lampanyctodes hectoris[P]	68.4	9.1	46.5	37.2	21.4	34.4	0.8	1.9	0.1	0.4	1.3	<0.1
Maurolicus muelleri[P]				1.0	2.7	0.1	0.8	1.5	0.1	<0.1	<0.1	<0.1
Trachurus t. capensis[P]							4.1	2.4	0.6	3.9	6.8	0.9
Scomber japonicus[P]							0	0	0	0.5	0.1	<0.1
Lepidopus caudatus[P]							0.3	0.4	<0.1	0.1	0.5	<0.1
Thyrsites atun[P]							0	0	0	<0.1	0.1	<0.1
Sufflogobius bibartus[P]							1.3	1.0	0.1	0.1	0.2	<0.1
Gonorhynchus gonorhynchus							0	0	0	0.2	1.1	<0.1
Gnathophis capensis							<0.1	0.2	<0.1	0.3	2.9	<0.1
Merluccius spp.[D]				5.0	1.8	0.4	5.7	5.2	1.9	3.1	2.6	0.3
Clinidae[D]							<0.1	0.2	<0.1	<0.1	0.1	<0.1
Emmelichthys nitidusr[D]							0	0	0	0.5	0.1	<0.1
Spondyliosoma emarginatum[D]							0	0	0	0.3	0.2	<0.1
Unidentified Teleostei	4	54.5	16.3	17.4	35.7	28.8	8.5	29.3	15.7	10.7	33.0	11.5

Table 4

Stomach contents of snoek (*Thyrsites atun*) sampled offshore of the 150-m isobath along the west coast (regions 1–3) and the western Agulhas Bank (regions 4 and 5) (1994–97). *M* = percent mass, *F* = percent frequency of occurrence, *IRI* = percent index of relative prey importance at the species and at a higher (bold) taxonomic levels. [P] = pelagic and [D] = demersal species.

	West coast						Western Agulhas Bank					
	50–74 cm FL (n = 147)			≥75 cm FL (n = 447)			50 – 74 cm FL (n =336)			≥75 cm FL (n = 367)		
Taxon and prey item	*M*	*F*	*IRI*	*M*	*F*	*IRI*	*M*	*F*	*IRI*	*M*	*F*	*IRI*
Annelida				<0.1	<0.1	**<0.1**						
Polychaeta				<0.1	<0.1	<0.1						
Crustacea	1.3	4.8	**0.1**	1.5	6.9	**0.1**						
Amphipoda												
Themisto gaudichaudi[P]				0.1	0.2	<0.1						
Brachyura												
Parapagurus dimorphus[D]	0.1	0.7	<0.1	0.1	0.4	<0.1						
Euphausiacea												
Euphausia lucens[P]	1.1	3.4	0.2	1.3	5.3	0.4						
Macrura												
Funchalia?[P]	<0.1	0.7	<0.1	<0.1	0.7	<0.1						
Stomatopoda												
Pterygosquilla armata[P]				0.1	0.4	<0.1						
Mollusca												
Cephalopoda				1.4	2.7	**<0.1**				1.7	1.9	**<0.1**
Lycoteuthis?				0.1	0.2	<0.1						
Sepia australis				0.1	0.4	<0.1						
Todaropsis eblanae				1.2	1.8	0.1				1.7	1.4	0.1
Unidentified squid				<0.1	0.2	<0.1				<0.1	0.5	<0.1
Teleostei	98.7	97.3	**99.9**	97.1	96.4	**99.8**	100	100	**100**	98.3	99.4	**99.9**
Engraulis japonicus[P]	0.1	0.7	<0.1	<0.1	0.2	<0.1	0.2	0.6	<0.1	0.1	0.3	<0.1
Sardinops sagax[P]	25.7	23.8	36.3	17.0	19.2	17.2	61.4	45.2	79.4	25.6	28.3	44.4
Etrumeus whiteheadi[P]	18.5	13.6	14.9	4.9	5.4	1.4	19.6	22.9	12.9	6.3	11.2	4.3
Lampanyctodes hectoris[P]	4.5	12.2	3.2	6.0	18.1	5.7				1.0	4.1	0.3
Maurolicus muelleri[P]	2.5	7.5	1.1	1.4	13.0	1.0	0.4	5.4	0.1	0.2	3.5	<0.1
Trachurus t. capensis[P]				13.2	12.8	8.8	1.4	0.6	<0.1	14.2	10.1	8.8
Scomber japonicus[P]	5.3	0.7	0.2							3.0	1.6	0.1
Lepidopus caudatus[P]	2.6	2.7	0.4	1.2	0.9	0.1				9.3	6.0	3.4
Thyrsites atun[P]										0.8	0.3	<0.1
Gonorhynchus gonorhynchus[D]							2.6	2.7	0.2	4.7	6.8	2.0
Emmelichthys nitidus[D]										<0.1	0.3	<0.1
Diaphus hudsoni[P]				<0.1	0.2	<0.1				<0.1	0.3	<0.1
Scomberesox saurus[P]							1.9	0.9	0.1	0.2	0.3	<0.1
Merluccius spp.[D] [1]	31.4	15.0	27.8	47.6	24.4	60.8	4.4	3.3	0.4	28.0	18.5	31.8
Caelorinchus simorhynchus[D]				0.1	0.7	<0.1						
Sebastes capensis[D]	0.5	0.7	<0.1	0.4	0.4	<0.1				0.2	0.5	<0.1
Zeus capensis[D]				0.7	0.2	<0.1						
Paracallionymus costatus[D]	0.6	0.7	<0.1	1.8	3.6	0.3				1.5	1.6	0.2
Unidentified Teleostei	6.9	37.4	15.2	2.8	24.8	3.7	8.1	30.4	7.0	3.2	23.4	4.6

[1] Two species of hake occur in South African waters—*M. paradoxus* and *M. capensis*–but owing to difficulty differentiating partially digested specimens, they were not analyzed separately.

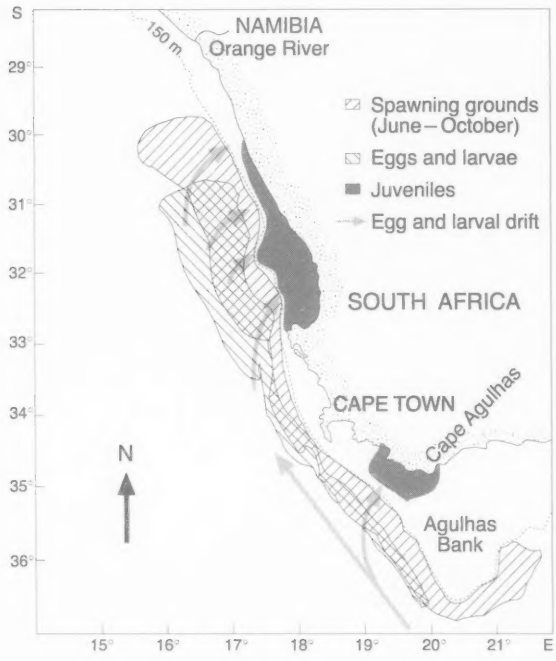

Figure 15

Conceptual model depicting the life history of *Thyrsites atun* in the southern Benguela ecosystem, including spawning grounds, distribution and transport of eggs and larvae, and the nursery areas.

Table 5

Proportions (%) of stomachs with food, and the mean mass of stomach contents for adult (>75 cm) male (M) and female (F) *T. atun* sampled on the South African west coast (WC; regions 1–3) and western Agulhas Bank (WAB; regions 4 and 5). χ^2 values were based on the frequencies of males and females with and without stomach contents (2×2 contingency tables) in each area (Yates' correction factor was applied as df =1). Significance levels are given by * (P<0.05), ** (P<0.01), and *** (P<0.001).

Area	Sex	n	%	χ^2	Mean mass (g)
Summer–autumn					
$WC_{inshore}$	M	197	50.2	0.18	13.3
	F	383	52.5		22.1
Winter–spring					
$WC_{inshore}$	M	130	52.4	6.6**	34.0
	F	729	81.2		43.0
$WC_{Offshore}$	M	374	61.8	2.5	39.0
	F	193	69.0		44.6
$WAB_{Offhore}$	M	212	49.5	15.2**	38.4
	F	336	67		60.1

those small enough to be eaten by young snoek) are least abundant inshore.

Given that the majority of the alternative prey are most abundant at some distance from the coast—euphausids between 10 and 20 km from the coast (Pillar, 1986; Hutchings et al., 1991), lanternfish, and lightfish between the 75- and 300-m isobaths (Hulley and Prosch, 1987), and mantis shrimp in the 20–200 m depth zone (Griffiths and Blaine, 1988)—it is likely that juvenile snoek move farther offshore when anchovy recruits leave the area, i.e. beyond the normal operating range of line fishermen in regions 0–2 (hence the seasonal drop in handline CPUE).

Acknowledgments

The author thanks the Demersal, Pelagic, and Linefish Sections of the Chief Directorate of Marine and Coastal Management, for assisting with the collection of biological material and providing CPUE and length-frequency summaries for research cruises and commercial fisheries; the Sea Bird Section for gannet-diet data; the Reprographics Section for producing the final drafts of the figures; Y. Melo for assistance with histological preparation and interpretation; M. Lapinsky for assistance with the identification of squid beaks; A. Boyd and G. Nelson for helpful discussions on the oceanography of the Benguela region; and Robert Crawford, Pierre Fréon, Larry Hutchings, and three anonymous referees for valuable comments on the manuscript. This research was subsidized by the Marine Living Resources Fund.

Literature cited

Andrew, T. G., T. Hecht, P. C. Heemstra, and J. R. E. Lutjeharms.
1995. Fishes of the Tristan da Cunha group and Gough Island, South Atlantic. Ichthyol. Bull. J. L. B. Smith Inst. Ichthyol. 63, 43 p.

Armstrong, M. J., A. Berruti, and J. Colclough.
1987. Pilchard distribution in South African waters, 1983–1985. S. Afr. J. Mar. Sci. 5:871–886.

Badenhorst, A., and M. J. Smale.
1991. The distribution and abundance of seven commercial trawl fish from the Cape south coast of South Africa, 1986–1990. S. Afr. J. Mar. Sci. 11:377–393.

Barange, M., I. Hampton, and B. A. Roel.
1999. Trends in the abundance and distribution of anchovy and sardine on the South African continental shelf in the 1990s, deduced from acoustic surveys. S. Afr. J. Mar. Sci. 21:367–391

Berruti, A.
1987. The use of Cape gannets in management of the purse-seine fishery of the Western Cape. Ph.D. diss., 340 p. University of Natal, Pietermaritzburg, South Africa.

Berruti, A., L. G. Underhill, P. A. Shelton, C. Moloney, and R. J. M. Crawford.
1993. Seasonal and interannual variation on the diet of two colonies of the Cape gannet (*Morus capensis*) between 1977–78 and 1989. Colonial Waterbirds 16:158–175.

Blackburn, M.
1957. The relation between the food of the Australian barra-

couta, *Thyrsites atun* (Euphrasen) and recent fluctuations in the fisheries. Aust. J. Mar. Freshwater Res. 8:29–54.

Blackburn, M., and P. E. Gartner.
1954. Populations of barracouta *Thyrsites atun* (Euphrasen) in Australian waters. Aust. J. Mar. Freshwater Res. 5:411–468.

Cortés, E.
1997. A critical review of methods of studying fish feeding based on analysis of stomach contents: application to elasmobranch fishes. Can. J. Fish. Aquat. Sci. 54:726–738.

Crawford, R. J. M.
1995. Snoek and chub mackerel. *In* Oceans of life off Southern Africa, 2nd edition (A. I. L. Payne and R. J. M Crawford, eds.), p. 177–187. Vlaeburg, Cape Town.
1998. Responses of African penguins to regime changes of sardine and anchovy in the Benguela system. S. Afr. J. Mar. Sci. 19:355–364.

Crawford, R. J. M., and G. De Villiers.
1985. Snoek and their prey—interrelationships in the Benguela upwelling system. S. Afr. J. Sci. 81:91–97.

Crawford, R. J. M., L. V. Shannon, and D. E. Pollock.
1987. The Benguela ecosystem. Part IV. The major fish and invertebrate resources. Oceanogr. Mar. Biol. Ann. Rev. 25: 353–505.

Crawford, R. J. M., L. G. Underhill, C. Raubenheimer, B. M. Dyer, and J. Martin.
1992. Top predators in the Benguela ecosystem—implications for their trophic position. S. Afr. J. Mar. Sci. 12: 675–687.

Davies, D. H.
1954. The South African pilchard (*Sardinops ocellata*). Development, occurrence and distribution of eggs and larvae, 1950–51. Investl Rep. Div. Fish. S. Afr. 15:1–28.

De Jager, B. v. D.
1955. The South African pilchard (*Sardinops ocellata*). The development of the snoek (*Thyrsites atun*) a fish predator of the pilchard. Investl Rep. Div. Fish. S. Afr. 19:1–11.

Dudley, S. F. J.
1987. Snoek *Thyrsites atun* in South African waters: aspects of its biology, distribution and fishery. M.Sc. thesis, 116 p. Univ. Cape Town, Cape Town, South Africa.

FAO.
1978. Yearbook of fishery statistics (vol. 46). FAO Statistic series 25, 128 p. FAO, Rome.
1981. Yearbook of fishery statistics (vol. 52). FAO Statistic series 45, 156 p. FAO, Rome.
1990. Yearbook of fishery statistics (vol. 70). FAO Statistic series 105, 325 p. FAO, Rome.
1995. Yearbook of fishery statistics (vol. 80). FAO Statistic series 134, 351 p. FAO, Rome.
1997. Yearbook of fishery statistics (vol. 84). FAO Statistic series 147, 343 p. FAO, Rome.

Grant, C .J., T. R. Cowper, and D. D. Reid.
1978. Age and growth of snoek, *Leionura atun* (Euphrasen), in south-eastern Australian waters. Aust. J. Mar. Freshwater Res. 29:435–444.

Griffiths, C. L., and M. J. Blaine.
1988. Distribution, population structure and biology of stomatopod crustacea off the west coast of South Africa. S. Afr. J. Mar. Sci. 7:45–50.

Griffiths, M. H.
1997. The life history and stock separation of silver kob, *Argyrosomus inodorus*, in South African waters. Fish. Bull. 95:47–57.
In press. Stock structure of snoek *Thyrsites atun* in the Benguela: a new hypothesis. S. Afr. J. Mar. Sci. 25.

Griffiths, M. H., and T. Hecht.
1995. On the life-history of *Atractoscion aequidens*, a migratory sciaenid off the east coast of southern Africa. J. Fish Biol. 47:962–985.

Haigh, E. H.
1972. Larval development of three species of economically important South African fishes. Ann. S. Afr. Mus. 59:47–70.

Hampton, I.
1992. The role of acoustic surveys in the assessment of pelagic fish resources on the South African continental shelf. S. Afr. J. Mar Sci. 12:1031–1050.

Hulley, P. A., and R. M. Prosch.
1987. Mesopelagic fish derivatives in the southern Benguela upwelling region. S. Afr. J. Mar Sci. 5:597–611.

Hurst, R. J.
1988. The barracouta, *Thyrsites atun*, fishery around New Zealand: historical trends to 1984. New Zealand Fish. Tech. Rep. 5, 43 p.

Hurst, R. J., and N. W. Bagely.
1987. Results of a trawl survey of barracouta and associated finfish near the Chatham Islands, New Zealand, December 1984. New Zealand Fish. Tech. Rep. 3, 44 p.
1989. Movements and possible stock relationships of the New Zealand barracouta, *Thyrsites atun*, from tag returns. New Zealand J. Mar. Freshwater Res. 23:105–111.

Hutchings, L., Pillar, S. C. and H. M. Verheye.
1991. Estimates of standing stock, production and consumption of meso- and macrozooplankton in the Benguela ecosystem. S. Afr. J. Mar. Sci. 11:499–512.

Hynes, H. B. N.
1950. The food of fresh-water sticklebacks (*Gasterosteus aculeatus* and *Pygosteus pungitius*), with a review of methods used in studies of the food of fishes. J. Anim. Ecol. 19: 36–58.

Kailola, P. J., M .J. Williams, P. C. Stewart, R. E Reichelt, A. Mcnee, and C. Grieve.
1993. Australian fisheries resources, 422 p. Bureau of Resource Sciences and the Fisheries Research and Development Corporation, Canberra, Australia.

MacDonald, J. S., and R. H. Green.
1983. Redundancy of variables used to describe the importance of prey species in fish diets. Can. J. Fish. Aquat. Sci. 39:651–659.

Mehl, J. A.
1971. Spawning and length-weight of barracouta (Teleostei: Gempylidae) from eastern Cook Straight. New Zealand J. Mar. Freshwater Res. 5:300–317.

Nakamura, I., and N. V. Parin.
1993. Snake mackerels and cutlassfishes of the world (Families Gempylidae and Trichiuridae). FAO species catalogue 15, 136 p. FAO, Rome.

Nepgen, C. S., de V.
1979a. Trends in the line fishery for snoek *Thyrsites atun* off the south-western Cape, and in size composition, length-weight relationship and condition. Fish. Bull. S. Afr. 12: 35–43.
1979b. The food of the snoek *Thyrsites atun*. Fish. Bull. S. Afr. 11:39–42.
1982. Diet of predatory fish in False Bay and possible effects of pelagic purse-seining on their food supply. Fish. Bull. S. Afr. 16:75–93.

Olivar, M. P., and J. M. Fortuño.
1991. Guide to ichthyoplankton of the southeast Atlantic (Benguela current region). Scientia Marina 55:1–383.

Olivar, M. P., and P. A. Shelton.
1993. Larval fish assemblages of the Benguela current. Bull. Mar. Sci. 53:450–474.
Pillar, S. C.
1986. Temporal and spatial variations in copepod and euphausid biomass offf the southern and south-western coasts of South Africa in 1977/78. S. Afr. J. Mar. Sci. 4: 219–229.
Pillay, T. V. R.
1952. A critique for the methods of study of food of fishes. J. Zool. Soc., India 4:185–200.
Roel, B. A., and M. J. Armstrong.
1991. The round herring *Etrumeus whiteheadi*, and abundant, underexploited clupeoid species off the coast of southern Africa. S. Afr. J. Mar. Sci. 11:267–287.
Roel, B. A., J. Hewitson, S. Kerstan, and I. Hampton.
1994. The role of the Agulhas Bank in the life cycle of pelagic fish. S. Afr. J. Sci. 90:185–196.
Sauer, W. H. H., A. J. Penney, C. Erasmus, B. Q. Mann, S. L. Brouwer, S.J. Lamberth, and T. J. Stewart.
1997. An evaluation of attitudes and responses to monitoring and management measures for the South African boat-based linefishery. S. Afr. J. Mar. Sci. 18:147–163.
Shannon, L. V., and G. Nelson.
1996. The Benguela: large scale features and processes and system variability. *In* The South Atlantic, present and past circulation (G. Wefer, W. H. Berger, G. Siedler, and D. J. Webb, eds.), p. 163–210. Springer-Verlag, Berlin.
Shelton, P. A.
1986. Fish spawning strategies in the variable southern Benguela Current region. PhD diss., 327 p. Univ. Cape Town, South Africa.
Shelton, P. A., and L. Hutchings.
1990. Ocean stability and anchovy spawning in the southern Benguela Current region. Fish. Bull. 88:323–338.
SPSS Inc.
1992. SPSS for Windows™: advanced statistics, release 5.0, p. 233–244. SPSS Inc, Chicago, IL.
Van der Lingen, C., and D. Merkle.
1999. Predicting anchovy and sardine recruitment from pelagic pre-recruit surveys. South African shipping news and fishing industry review, Cape Town, South Africa. March/April 1999:24–27.
Verheye, H. M., A. J. Richardson, L. Hutchings, G. Marska, and D. Gianokouras.
1998. Long-term trends in the abundance and community structure of coastal zooplankton in the southern Benguela system, 1951–1996. S. Afr. J. Mar. Sci. 19:317–332.
Wickens, P. A., D. W. Japp, P. Shelton, F. Kriel, P. C. Goosen, B. Rose, C. J. Augustyn, C. A. R. Bross, A. J. Penney, and R. G. Krohn.
1992. Seals and fisheries in South Africa—competition and conflict. S. Afr. J. Mar. Sci. 12:773–789.
Windell, J. T., and S. H. Bowen
1978. Methods for the study of fish diets based on analysis of stomach contents. *In* Methods for assessment of fish production in fresh waters, 3rd edition (T. B. Bagenal, ed.), p. 219–226. London, Blackwell.
Wood, A. D.
1998. A contribution towards the taxonomy of the ichthyoplankton species community and understanding of its dynamics along the south east coast of South Africa. Ph.D. diss., 338 p. Rhodes Univ., Grahamstown, South Africa.

Length and age at maturity of female petrale sole (*Eopsetta jordani*) determined from samples collected prior to spawning aggregation

Robert W. Hannah
Steven J. Parker
Oregon Department of Fish and Wildlife
Marine Resources Program
2040 Marine Science Drive
Newport, Oregon 97365
Email address (for Robert W. Hannah): Bob.Hannah@hmsc.orst.edu

Erica L. Fruh
National Marine Fisheries Service
Northwest Science Center
Fisheries Research and Monitoring Division
2030 Marine Science Drive
Newport, Oregon, 97365

Abstract–The problem of bias in female petrale sole age and length-at-maturity relationships caused by sampling from spawning aggregations was investigated. Samples were collected prior to aggregation, and histological methods were used to determine maturity status. Mature and immature fish were classified by inspecting oocytes for the presence of yolk in September, when substantial divergence in yolked and unyolked oocyte diameters had been observed. Comparison of macroscopic and microscopic assessment of maturity showed that maturity status cannot be determined accurately by using macroscopic inspection during the summer. Female petrale sole from the central Oregon coast were 50% mature at 33 cm and 5 years of age. Comparison of data from our study with data used in recent petrale sole stock assessments showed that both sampling bias and the use of samples from seasons when status cannot be accurately determined have likely caused errors in fitted maturity relationships.

Manuscript accepted 21 March 2002.
Fish. Bull. 100:711–719 (2002).

Petrale sole (*Eopsetta jordani*) have been the target of a valuable commercial trawl fishery off the U.S. West Coast since before World War II (Sampson and Lee[1]). Management and assessment of petrale sole is complicated by the fact that modern fishing activity targets winter deepwater aggregations of spawning fish (Fig. 1). Because most of the available female maturity data are derived from the winter commercial fishery, they are potentially biased with respect to age and length at maturity (e.g. small mature fish are more likely to be sampled than small immature fish). Some summer samples are available for analysis, including those from the National Marine Fisheries Service triennial shelf survey (e.g. Zimmermann et al., 1994). However, in the summer, when mature and immature fish are well mixed, maturity status is not easily determined visually because of the similarity in appearance between ovaries of immature fish and those of fish in the "resting" state (Ketchen and Forrester, 1966).

The age and length at maturity for female fish is an important parameter in many stock assessment models. Clark (1991), Lunsford (1999) and Al-Jufaily (1996) have demonstrated that variation in the age at 50% maturity, especially in relation to the median age of recruitment to the fishery, can have a major influence on the calculation of a target fishing rate. Target fishing rates are currently used by the Pacific Fishery Management Council (PFMC) to manage most groundfish stocks (Clark, 1991; PFMC[2]). An example of a target fishing rate would be $F_{40\%}$, the fishing mortality rate that would reduce spawning stock biomass per recruit to 40% of the unexploited level. The potential influence of errors in estimating the median age of female maturity can perhaps best be illustrated with an example. In Lunsford's (1999) study of maturity of Pacific ocean perch

[1] Sampson, D. B., and Y. W. Lee. 1999. An assessment of the stocks of petrale sole off Washington, Oregon and Northern California in 1998. *In* Pacific Fishery Management Council. 1999. Appendix to the status of the Pacific coast groundfish fishery through 1999 and recommended acceptable catches for 2000: stock assessment and fishery evaluation. Pacific Fishery Management Council, 2130 SW Fifth Avenue, Suite 224, Portland, Oregon, 97201.

[2] Pacific Fishery Management Council. 2000. Status of the Pacific Coast groundfish fishery through 2000 and recommended biological catches for 2001: stock assessment and fishery evaluation. (Document prepared for the council and its advisory entities.) Pacific Fishery Management Council 2130 SW Fifth Avenue, Suite 224, Portland, Oregon 97201.

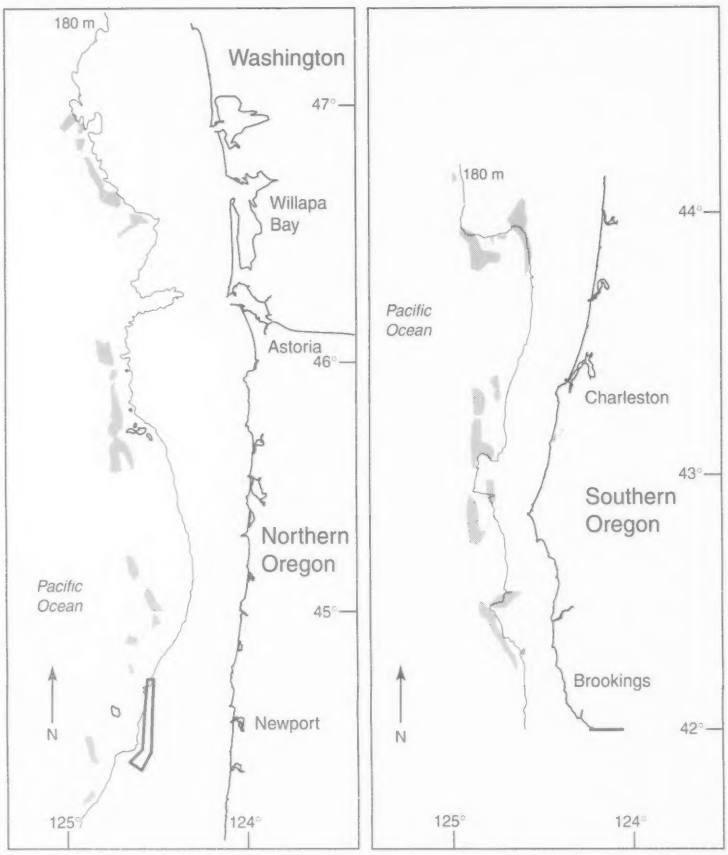

Figure 1

Sampling area for petrale sole (bold-outline polygon) off Newport, Oregon, and areas where winter trawl fishing for petrale sole is concentrated (gray polygons). Also shown is the 180-m depth contour.

(*Sebastes alutus*), a shift in the estimated median age of maturity for female fish from 7.5 to 10.5 years decreased the $F_{40\%}$ value from 0.110 to 0.076, a decrease of 31%. Accordingly, the use of potentially biased maturity data from the winter commercial fishery for petrale sole adds to the uncertainty in stock assessments. The accuracy of maturity information used in recent petrale sole stock assessments is also uncertain because of two additional factors: outmoded data and the blending of samples across space and time (Sampson and Lee.[1]; Turnock et al.[3]). Maturity samples are obtained from various locations and times, and are often combined to produce a general relationship for stock assessment purposes. The combined relationship may poorly account for geographical differences, long-term changes in maturity, or for inadequacies in some samples (e.g. lack of immature fish) (Sampson and Al-Jufaily, 1999) and can result in poorly determined curves that bias and degrade the fit of the combined maturity relationship. The principal objective of our study was to collect maturity data for female petrale sole from the late summer to early fall period and compare them with the maturity data used in recent stock assessments (Sampson and Lee[1]; Turnock et al.[3]). Although sampling in late summer and early fall is probably optimal for assessing female maturity in the petrale sole population, some ovaries may be difficult to classify accurately as mature or immature by macroscopic inspection. A second objective of our study was to evaluate female petrale sole maturity by using microscopic examination of stained thin sections and compare these results with those obtained from simple visual inspection.

The petrale sole maturity data used in recent stock assessments have been obtained from the Oregon Department of Fish and Wildlife's commercial fishery sampling program (Sampson and Lee[1]; Turnock et al.[3]). Potential

[3] Turnock, J., M. Wilkins, M. Saelens, and C. Wood. 1993. Status of West Coast petrale sole in 1993. Appendix G. *In* Status of the Pacific Coast groundfish fishery through 1993 and recommended biological catches for 1994: stock assessment and fishery evaluation. Pacific Fishery Managemenmt Council, 2130 SW Fifth Ave., Suite 224, Portland, OR 97201.

bias in some of these data, arising from spawning aggregation, argues that a different sampling approach might be useful for trying to generate unbiased maturity data from samples of the commercial catch. A third objective of our study was to evaluate problems with available maturity data from fishery samples in light of histological evaluations of maturity stages and to recommend an alternative approach for sampling the commercial catch for age and length at maturity.

Materials and methods

Petrale sole were collected by trawl during August and September 2000 by using a chartered commercial fishing vessel from Newport, Oregon. Sampling was conducted over a very limited geographic range to minimize any spatial variation in the maturity ogive. Individual sampling sites were selected to attempt to sample across the available size range of petrale sole, based on the skipper's experience and expertise. Fish were sorted at-sea according to total length (±0.5 cm), and fifteen fish from each 1-cm size interval were retained for maturity sampling. Upon returning to port, the fish were measured again and sex was determined by dissection. An ovary was removed and assigned a macroscopic maturity stage following the criteria of Hagerman (1952). Only experienced samplers were used to assign macroscopic maturity stages to minimize any errors in visual staging. Otoliths were removed from all female fish for subsequent age determination, and one ovary was preserved for histological examination to determine maturity. Ages were determined by using the break-and-burn technique for sagittal otoliths (Chilton and Beamish, 1982). Consistency of age determination was evaluated by using a blind double reading.

Ovaries were preserved in 10% buffered formalin and later transferred to 70% ethanol for storage. Tissue samples from the midsection of the ovary were then embedded in paraffin, sectioned at 5 µm, and stained with Harris's hematoxylin and eosin *Y*. The samples were examined and classified as mature or immature based on the presence or absence of dark-staining yolk globules (vitellogenin).

The diameter (µm) of the largest spherical nonatretic oocyte in the most advanced oocyte stage from each of five microscope fields was also measured and used to calculate a mean maximum oocyte diameter (MMOD) for each sectioned ovary (West, 1990; Nichol and Pikitch, 1994). MMOD was compared for mature and immature fish. A divergence in MMOD between mature and immature fish was taken as evidence that the presence or absence of dark-staining yolk globules was an accurate indicator of maturity status. Samples from August and September were compared by using this approach. The accuracy of visual examination of ovaries was then evaluated by comparing the maturity status from visual examination with status determined after sectioning, staining, and microscopic examination.

Logistic regression was used to fit sigmoid length-maturity and age-maturity curves. The model fitted had the general form

$$P_{x_1} = e^{(b_0 + b_1 x_1)}/(1 + e^{(b_0 + b_1 x_1)}),$$

where p = the probability that a fish is mature in a given length (cm) or age category x_1; and
b_0 and b_1 are parameters that define the shape and location of the fitted curve.

The predicted length or age at 50% maturity was calculated as

$$L \text{ (or } A)_{50} = -b_0/b_1.$$

Maturity data collected by the Oregon Department of Fish and Wildlife (ODFW) from the 1986–2000 commercial trawl fisheries were also analyzed and compared with the data collected in our study. The most recent petrale sole stock assessment (Sampson and Lee[1]) relied on maturity data used for the 1993 assessment (Turnock et al.[3]), which in turn were derived from combined ODFW port sampling data for the years 1986–91. We fitted a maturity-length relationship to these data for comparison with the maturity data from our study.

We also summarized the ODFW data from 1986–91 and 1992–2000, by month and maturity status, to compare with our data and assess their adequacy for determining length at maturity for female petrale sole. All of these samples were classified by a simple visual evaluation of maturity stage. To examine the effect that a lack of immature fish may have had on estimated maturity curves from these two time periods, we split the data into groups, according to season. Samples from the months of November through February were classified as "fall–winter" samples. These samples represented the seasonal time period when the maturity status of petrale sole was most readily determined visually, but also the time period when samples were most likely to be from spawning aggregations. Samples from April through September were classified as "spring–summer" and represented the seasons in which fish were not aggregated for spawning, but the time when maturity status was most difficult to determine by inspection of the ovaries.

Results

Comparison of visual maturity determinations with results obtained from microscopic evaluation showed that maturity of petrale sole cannot be reliably determined by simple visual inspection in August or September (Tables 1 and 2). For ovaries classified as immature by inspection in August, 16.7% proved to be mature upon microscopic evaluation. Of those classified initially as mature, 6.5% showed no microscopic evidence of vitellogenesis. By September, all of the ovaries classified by inspection as mature, did prove to be vitellogenic. However, 27.9% of those classified as immature, proved to be vitellogenic after viewing the stained sections with a microscope.

MMOD increased markedly in vitellogenic ovaries between August and September, but in nonvitellogenic ovaries the increase was minimal (Fig. 2). The resulting divergence in MMOD and the absence of fish with MMOD

Table 1

Details of petrale sole collected by trawl aboard the FV *Olympic*.

Date	Location	Females	Males	Size range (cm)
8 Aug 2000	4428°N 12434°W	140	103	24–51
23 Aug 2000	4446°N 12432°W	24	46	27–49
26 Sep 2000	4428°N 12435°W	117	123	26–50
Total		281	272	24–51

Table 2

Comparison of macroscopic and microscopic determination of maturity in female petrale sole collected by trawl.

	Macroscopic classification		Microscopic classification	
Sample month	Condition	Number of fish	Number immature (%)	Number mature (%)
August	immature	102	85 (83.3)	17 (16.7)
	mature	62	4 (6.5)	58 (93.5)
September	immature	61	44 (72.1)	17 (27.9)
	mature	56	0 (0.0)	56 (100)
Total		281		

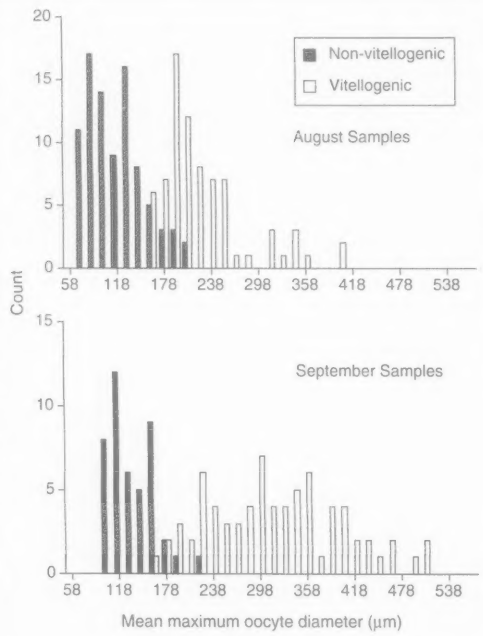

Figure 2

Comparison of mean maximum oocyte diameters (µm, see text) for petrale sole with vitellogenic and nonvitellogenic oocytes, for samples collected in August and September 2000.

around 180 µm suggested that by September, the microscopic classification of ovaries provided an accurate identification of maturity status of individual fish. Immature fish were well represented in the September collections, indicating the fish were still well mixed on the feeding grounds (Table 2). Therefore, the September maturity data generated from microscopic inspection were used to fit age- and length-at-maturity relationships for female petrale sole (Fig. 3). The resulting curves fitted the data well and chi-square tests on the residuals indicated no problems with lack of fit caused by overdispersion (Pearson chi-square of 5.714 [with 20 degrees of freedom] for length, and 0.643 [with 11 degrees of freedom] for age, $P>0.999$). The fitted relationships indicated that female petrale sole off the central Oregon coast were 50% mature at about 33 cm and at about 5 years of age. Complete maturity was obtained at about 40 cm and about 9 years of age (Table 3).

Examination of the monthly samples that, as an aggregate, were used to fit the 1986–91 maturity curve showed that numerous samples were included from the March through August period, especially from the port of Charleston, Oregon (Table 4). The inclusion of these summer samples explains some of the flatness in the fitted maturity curve from Turnock et al.[3] (Fig. 4, L_{50}=30.6, slope=0.29). A maturity curve fitted to these data, but excluding spring and summer samples, was much steeper (Fig. 4, L_{50}=33.56, slope=0.50).

Inspection of the 1986–91 and 1992–2000 maturity data from the winter months, when errors in determining maturity should be minimized (Tables 4 and 5, Fig. 5), showed some evidence of the type of bias that can result from sampling spawning aggregations. First, very few im-

Table 3

Results of logistic regression analysis of histologically determined maturity status of petrale sole versus length (cm) and age (September samples only).

Independent variable		Coefficients	Standard error	Chi-square	*P*-value	L_{50} or A_{50}	95% confidence
Length						33.10 cm	32.13–33.93
	constant	–24.593	4.572	28.936	0.0001		
	length	0.743	0.136	29.759	0.0001		
Age						5.15 yr	4.68–5.54
	constant	–6.358	1.417	20.122	0.0001		
	age	1.234	0.261	22.349	0.0001		

mature fish were sampled, even though the commercial fishery samples showed a similar lower size range to the fish collected in our study (Fig. 6). The lack of immature fish was most evident in the 1986–91 November–February samples from Charleston, Oregon, where 170 fish were sampled for maturity, and only one fish was reported as immature. The 1992–2000 Charleston data also showed low numbers of immature fish. These samples also showed groups of very small fish, and most or all of them were classified as mature (Fig. 5). This kind of bias, where small fish encountered are more likely to be reported as mature than similar-size fish sampled from a well-mixed population, would also act to flatten the resultant maturity curve. The Astoria winter data included more immature fish, and accordingly produced steeper maturity curves. However it was unclear to what degree bias from sampling spawning aggregations may have influenced these curves.

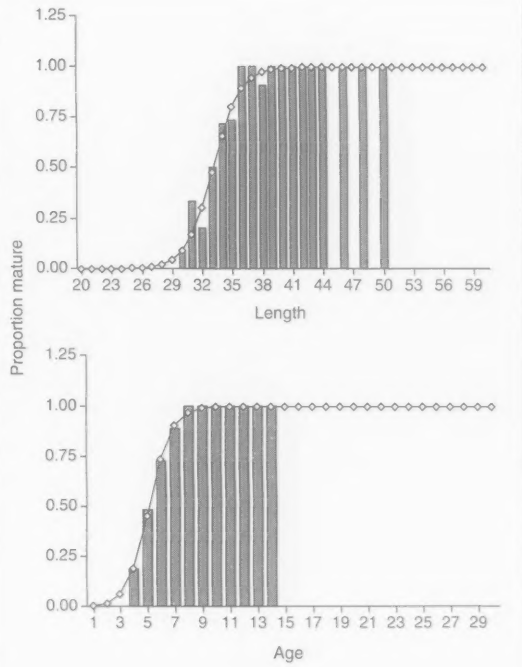

Figure 3

Proportion mature for female petrale sole, by age and length (FL,cm), from September samples. Maturity status was determined by histological examination by using presence and absence of vitellogenesis to determine maturity. Fitted curve is also shown (Table 3).

Discussion

Although it is known that late fall and winter is a better time for visually assessing female maturity status for petrale sole, our data showed clearly that late summer and early fall maturity samples, for which there was a visual determination of maturity, should not be used for estimating maturity in this species. Although our study did not specifically examine ovaries from spring collections, the general timing of ovarian development in this species suggests that this caution can be extended to all late spring and summer samples. Our results are similar to the findings of Ramsay and Witthames (1996), who suggested that visual maturity evaluations of the common sole (*Solea solea*) are generally only reliable during a limited portion of the year.

The maturity data developed in our study (Figs. 3 and 4) suggest a larger size at 50% maturity (33.1 cm vs. 30.7 cm) and a much steeper maturity curve for petrale sole than indicated by the 1986–91 sample data used in the last two petrale sole stock assessments (Turnock et al.[3]). Although the curves appeared to be quite different, the length at 50% maturity increased by only 2.4 cm. The most recent stock assessment model indicates an annual fishing mortality rate, for fully exploited size groups, of 0.285 (Sampson and Lee[1]). Incorporating a revised maturity ogive from our study decreased the equilibrium fishing rate to 0.268, a change of about 6% (Sampson[4]). This modest effect on harvest rate seems odd, given the large apparent difference between the curves in Figure 3. A possible explanation for this discrepancy is that the results depend heav-

[4] Sampson, D. B. 2000. Personal commun. Coastal Oregon Marine Experiment Station and Department of Fisheries and Wildlife, Oregon State University, Hatfield Marine Science Center, Newport, OR 97365.

Table 4

Summary of the numbers of mature and immature petrale sole sampled, from the Oregon bottom trawl fishery, 1986–91.

Port	Month	Immature	Mature	Total
Astoria	November	20	130	150
Astoria	December	0	167	167
Astoria	January	2	135	137
Astoria	February	32	10	42
Winter total		54	442	496
Astoria	March	18	61	79
Astoria	October	7	26	33
Astoria total		79	529	608
Charleston	November	0	37	37
Charleston	December	1	68	69
Charleston	January	0	24	24
Charleston	February	0	40	40
Winter total		1	169	170
Charleston	March	16	64	80
Charleston	April	0	37	37
Charleston	June	14	115	129
Charleston	July	27	123	150
Charleston	August	71	162	233
Charleston	October	2	78	80
Charleston total		131	748	879
Total (all ports)		210	1277	1487

Table 5

Summary of numbers of mature and immature petrale sole sampled by season and port from the Oregon bottom trawl fishery, 1992–2000.

Port	Season	Immature	Mature	Total
Astoria	Winter (Nov–Feb)	19	242	261
	Spring–fall (Mar–Oct)	4	89	93
Charleston	Winter (Nov–Feb)	20	347	367
	Spring–fall (Mar–Oct)	31	179	210
Brookings	Winter (Nov–Feb)	0	56	56
	Spring–fall (Mar–Oct)	0	142	142
Total		84	995	1079

ily on assumptions about fishery selectivity and discard used in the latest assessment model–parameters that are poorly known for most West Coast fish stocks. The modest effect on harvest rate found in our study also does not preclude larger effects for other, later maturing stocks. In the example given earlier from Lunsford's (1999) simulation work with Pacific ocean perch, the drop in target harvest rate was much larger. In that instance, a shift of 3 years in the median age of female maturity resulted in a 31% drop in the target harvest rate. In that example, spawning stock biomass per recruit also fell to 31%, well under the target of $F_{40\%}$.

The maturity data developed in our study differ from those developed by Turnock et al.[3] primarily in the steepness of the maturity curve. It could be argued that the earlier curve is flatter simply because it incorporates data from a wider geographic range. A latitudinal cline in length at 50% maturity, as has been postulated for many flatfish stocks (Ketchen and Forrester, 1966; Castillo, 1995; Brodziak and Mikus, 2000), could cause flattening

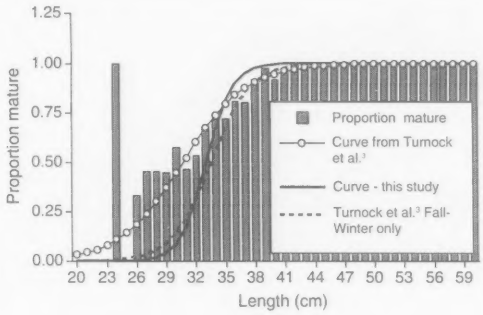

Figure 4

Comparison of fitted petrale sole female maturity curves from September samples (our study) and 1986–91 commercial fishery data used in the last two stock assessments (Turnock et al.[3]). Bars show 1986–91 maturity data used to fit the curve from Turnock et al.[3] Dashed line shows the maturity curve fitted to the 1986–91 samples by using only data from the fall–winter period.

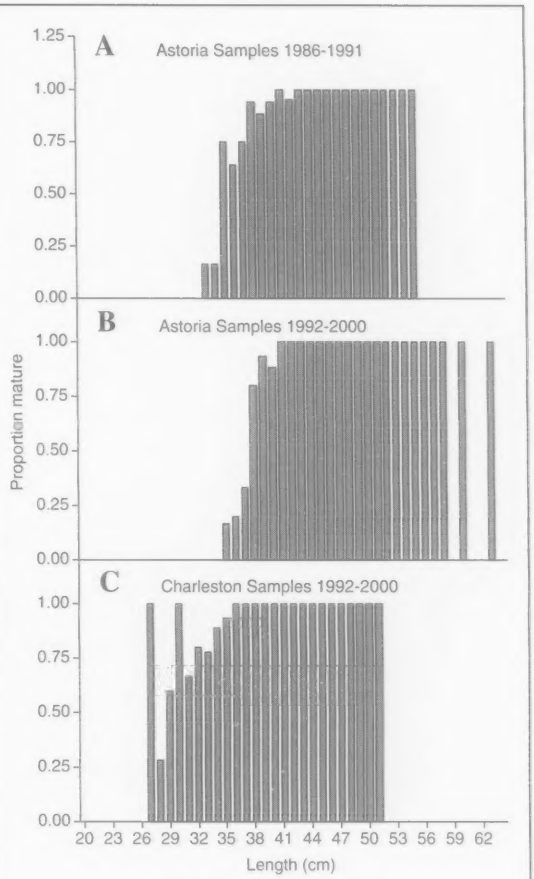

Figure 5

Proportion of female petrale sole identified as mature from November–February samples of trawl landings in Astoria and Charleston, Oregon, 1986–1991 and 1992–2000.

in a combined maturity curve. However, errors in determining maturity status, caused by including samples from time periods when maturity status cannot be accurately assessed visually, would have the same effect. This can be seen in a comparison of the maturity data generated in our study from macroscopic and microscopic evaluations. The macroscopic curve (bars and solid line in Figure 7) is flattened in relation to the curve according to microscopic evaluation (dashed line). The curve is also shifted to the right because, in this case, more large fish were incorrectly classified than small fish. At other times of the year, errors could be more common with smaller fish and the curve would shift the other way. In either case, however, the curve should, in theory, be flatter than the true maturity curve. This flattening of the maturity curve is caused by the way the most likely errors change along a maturity ogive. In small or young fish, which are mostly immature, most of the errors encountered will be immature fish mistakenly considered mature. At larger sizes or older ages, the reverse will be true. Near the inflection point, the two types of errors offset each other and have little impact on the slope because the population is split roughly 50/50 with respect to maturity. These effects, in combination, tend to flatten the resulting curve.

Compared to a length at 50% maturity of 33 cm for the central Oregon coast (our study), the Astoria data from the commercial fishery are consistent with an increase in the length at 50% maturity with latitude, as suggested by Ketchen and Forrester (1966) and Castillo (1995). The methods developed in our study could be applied to petrale sole samples collected over a wider geographic range to shed more light on how length at maturity varies with latitude. Best (1961) reported a length at 50% maturity of 35.5 cm for female petrale sole from California waters, and Harry[5] reported 40.0 cm for the Columbia River area. In comparison with the recent data from Astoria fishery samples (Fig. 5) and from the central Oregon coast (Fig. 3), the data from Harry[5] suggest a very large decrease in the length at 50% maturity for female petrale sole since the 1960s. If this decrease is a biological reponse to exploitation, it could explain how petrale sole stocks have held up quite well under heavy commercial harvest (Sampson and Lee[1]).

The data presented in our study suggest that the collection of maturity data by sampling on spawning aggregations does cause bias in estimates of female age and length at maturity for petrale sole. Use of spring and summer maturity samples in data sets used to estimate age and length at maturity has also caused errors. Our analysis shows that the overall effect on estimates of age and length

[5] Harry, G. Y. 1959. Time of spawning, length at maturity, and fecundity of the English, petrale and Dover soles (*Parophrys vetulus, Eopsetta jordani,* and *Microstomus pacificus*, respectively). Fish. Comm. Oregon, Research Briefs 7(1):5–13.

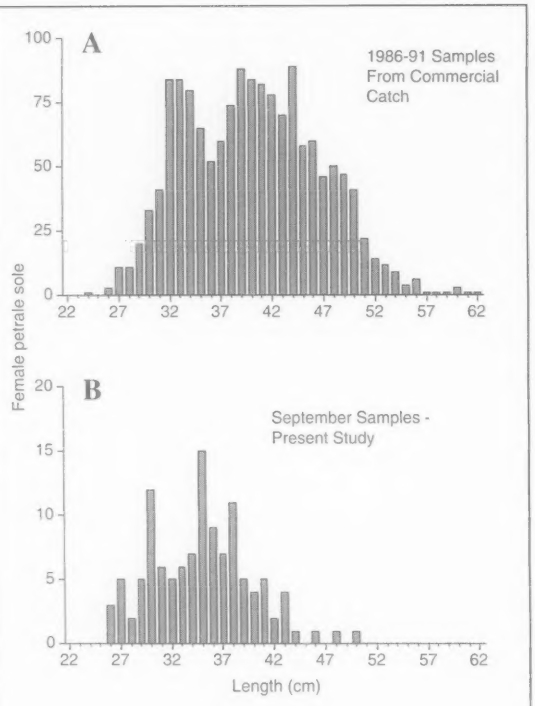

Figure 6

Comparison of female petrale sole length frequency from the 1986–91 commercial fishery samples and the September samples collected in our study. The 1986–91 samples were also used to fit the maturity curve from Turnock et al.[3]

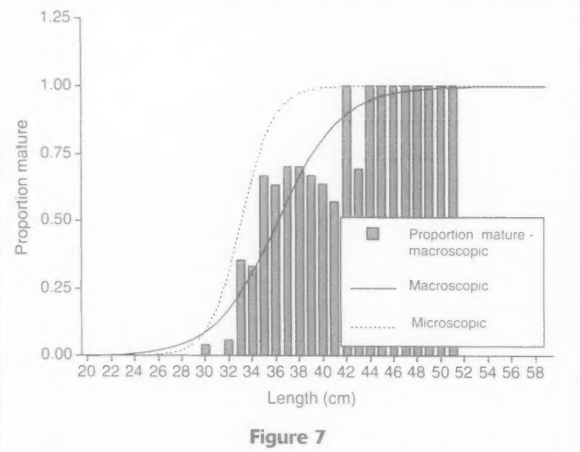

Figure 7

Comparison of maturity curves fitted to the data from our study. Bars show proportion of fish mature by length from the macroscopic evaluations of the August and September samples. The solid line is the fitted curve for those data. The dashed line is the fitted curve from microscopic evaluations of the September samples only.

at 50% maturity has been small. Collection of early fall samples from the commercial catch, followed by histological preparation and classification based on presence or absence of vitellogenin, should yield more accurate maturity information for female petrale sole than winter sampling on spawning aggregations or maturity sampling where only a visual assessment of ovary condition is made.

Acknowledgments

We'd like to thank the skipper and crew of the FV *Olympic*. Staff from ODFW's Marine Program and from the Pacific States Marine Fisheries Commission helped with sample preparation. Jennifer Menkel aged the otoliths and Margo Whipple of Oregon State University prepared the histological sections. Jim Golden and David Sampson provided helpful reviews of the draft manuscript.

Literature cited

Al-Jufaily, and M. S.
1996. Variation in the maturity schedule of english sole and its influence on calculating the F35% target fishing rate. M.S. thesis, 85 p. Oregon State Univ., Corvallis OR.

Best, E. A.
1961. Savings gear studies on Pacific coast flatfish. Bull. Pac. Mar. Fish. Comm. 5:25–47.

Brodziak, J., and R. Mikus.
2000. Variation in life history parameters of Dover sole, *Microstomus pacificus*, off the coasts of Washington, Oregon, and northern California. Fish. Bull. 98:661–673.

Castillo, Gonzalo C.
1995. Latitudinal patterns in reproductive life history traits of northeast Pacific flatfish. *In* Proceedings of the international symposium on north Pacific flatfish. Alaska Sea Grant College Report. AK-SG-95-04, 1995, p. 51–72. Alaska Sea Grant Program, Fairbanks, AK.

Chilton, D. E., and R. J. Beamish.
1982. Age determination methods for fishes studied by the Groundfish Program at the Pacific Biological Station. Can. J. Fish. Aquat. Sci. Spec. Publ. 60:2–18.

Clark, W. G.
1991. Groundfish exploitation rates based on life history parameters. Can. J. Fish. Aquat. Sci. 48:734–750.

Hagerman, F. B.
1952. The biology of the Dover sole. California Dep. Fish and Game, Fish Bull. 85, 48 p.

Ketchen, K. S., and C. R. Forrester.
1966. Population dynamics of the petrale sole. Fish. Res. Board Can. Bull. 153, 195 p.

Lunsford, C. R.
1999. Distribution patterns and reproductive aspects of Pacific ocean perch (*Sebastes alutus*) in the Gulf of Alaska. M.S. thesis, 154 p. Univ. Alaska Fairbanks, AK.

Nichol, D. G., and E. K. Pikitch.
1994. Reproduction of darkblotched rockfish off the Oregon coast. Trans. Am. Fish. Soc. 123:469–481,

Ramsay, K., and P. Witthames.
1996. Using oocyte size to assess seasonal ovarian development in *Solea solea*. J. Sea Res. 36(3/4): 275–283.

Sampson, D. B., and S. M. Al-Jufaily.
1999. Geographic variation in the maturity and growth schedules of English sole along the U.S. west coast. J. Fish Biol. 54:1–17

West, G.
1990. Methods of assessing ovarian development in fishes: a review. Aust. J. Mar. Freshwater Res. 41:199–222.

Zimmermann, M., M. E. Wilkins, R. R. Lauth, and K. L. Weinberg.
1994. The 1992 Pacific west coast bottom trawl survey of groundfish resources: estimates of distribution, abundance and length composition. U.S. Dep. Commer., NOAA Tech. Memo. NMFS-AFSC-42, 110 p. plus appendices.

Abstract–We have formulated a model for analyzing the measurement error in marine survey abundance estimates by using data from parallel surveys (trawl haul or acoustic measurement). The measurement error is defined as the component of the variability that cannot be explained by covariates such as temperature, depth, bottom type, etc. The method presented is general, but we concentrate on bottom trawl catches of cod (*Gadus morhua*). Catches of cod from 10 parallel trawling experiments in the Barents Sea with a total of 130 paired hauls were used to estimate the measurement error in trawl hauls. Based on the experimental data, the measurement error is fairly constant in size on the logarithmic scale and is independent of location, time, and fish density. Compared with the total variability of the winter and autumn surveys in the Barents Sea, the measurement error is small (approximately 2–5%, on the log scale, in terms of variance of catch per towed distance). Thus, the cod catch rate is a fairly precise measure of fish density at a given site at a given time.

Manuscript accepted 20 February 2002.
Fish. Bull. 100:720–726 (2002).

The measurement error in marine survey catches: the bottom trawl case

Vidar Hjellvik
Olav Rune Godø

Institute of Marine Research
Nordnesgt. 33
P.O. Box 1870, Nordnes
N-5817 Bergen, Norway
E-mail address (for V. Hjellvik): vidarh@imr.no

Dag Tjøstheim

Department of Mathematics
University of Bergen,
Johs. Brunsgt 12
N-5008 Bergen, Norway

Surveys are vital for estimating the size and composition of marine populations. In the data collection process, trawl samples or acoustics (or both) are usually employed. It is well known that the resulting estimates are subject to substantial variations, and it is important to quantify and explain, as much as is possible, the variability in terms of relevant explanatory variables or covariates. Typically these variables will depend on the sampling tool used, but for bottom trawl catches important explanatory variables can be depth and location of the haul (Polacheck and Vølstad, 1993), time of the day (Korsbrekke and Nakken, 1999), season, strength of the year classes involved, etc.

Generally, as the number of covariates increases, and the model becomes more complex, the residual variation (or remaining uncertainty) not explained by the model decreases. But no matter how refined the model is, there will always be an unexplained random component that cannot be attributed to any observed variable. This residual variation is caused by the interactions between the fish, the measurement device, and the environment (see e.g. Engås, 1994).

The purpose of this study was to define and quantify this residual source of random variation. This was done by analyzing measurements from parallel tows of multiple vessels, which is the closest one can come to a controlled statistical experiment in this context. The importance of quantifying this type of fluctuation lies in the fact that it is a benchmark uncertainty, which is inherent in the survey process itself, and in this sense it may be termed a measurement error. If the measurement error can be assessed from field data and is consistent over time and space, we improve our understanding and quantification of other causal factors behind the uncertainty associated with survey estimates.

In this study we looked at bottom trawl catches of cod, but we would like to stress that the concepts and techniques developed can in principle be applied to acoustic survey estimates or indeed to any type of measurements collected simultaneously by two or more independent parallel sampling devices. It should be noted that there is a growing related literature on comparative survey analysis. We refer to the review paper by Pelletier (1998) and references therein.

Materials and methods

Parallel trawling experiments

During the annual combined bottom trawl and acoustic survey of demersal fish in the Barents Sea during winter and autumn conducted by the Institute

Table 1

Summary statistics for the parallel trawling experiments; time, vessel, position (latitude, longitude), the number of hauls (n) and the average per cod weight w (in kg) within each group. The vessels involved were *Johan Hjort* (JH), *Anny Kræmer* (LIZY), *G. O. Sars* (GS), *Jan Mayen* (JM), and *Michael Sars* (MS).

Group	Year	Date	Vessels	Lat.	Long.	n	w
1	1991	3–5 Mar	LIZY, JH	71.3	26.2	10	2.01
2	1994	10 Feb	LIZY, JH	71.2	36.0	5	0.81
3	1994	22–23 Feb	LIZY, GS	71.3	26.3	8	1.98
4	1995	22–23 Feb	JM, JH	71.3	25.4	12	1.05
5	1995	23–25 Feb	JH, GS	71.3	25.4	23	0.94
6	1995	15–17 Aug	MS, JH	74.3	17.3	29	0.72
7	1996	17 Feb	JM, GS	70.4	36.5	4	0.03
8	1996	24–25 Feb	JM, GS	71.8	23.8	10	0.19
9	1997	8–10 Feb	JH, GS	71.3	27	17	0.72
10	1997	2–3 Aug	MS, JH	72–73	27–30	12	0.21

of Marine Research, Bergen (IMR), (Jakobsen et al.[1]), parallel trawling experiments were used to compare the efficiency of the participating vessels with gear types as given in Table 1 and Figure 1. During a parallel haul the vessels operated about 500 meters apart and used radio contact to assure proper coordination during hauls. We analyzed ten parallel trawl experiments performed by the IMR during the last decade (Table 1). The data from 1991 are described in Michalsen et al. (1996). Two hauls with unstable bottom contact were excluded from the 1991 data (Michalsen et al., 1996). Similarly, two hauls from 1995 were excluded—one where trawl geometry measurements indicated problems with the doors and another with highly different recorded towed distances (0.7 and 2.2 nautical miles [nmi]). Let $d_{i;j}$ denote the towed distance for haul i and vessel j; i=1, ... , n; j=1,2 where n is the total number of hauls. The average recorded distance is $\bar{d} = (2n)^{-1} \sum_{i=1}^{n} \sum_{j=1}^{2} d_{i;j} = 1.33$ nautical mile (average duration in time is 27 minutes), with $0.8 \le d_{i;j} \le 1.8$ in 98% of the cases. The absolute values $|d_{i;1} - d_{i;2}|$ of the differences in towed distance for the two vessels in the same haul, are 0, 0.1, 0.2, 0.3, 0.4, and 0.6 in 43, 45, 31, 6, 4, and 1 cases, respectively.

The data were subdivided into 10 groups so that the same two vessels performed all hauls within a group, within a period of one to three days, and usually in a small geographical area. Group 10 is an exception where the trawl stations are evenly spread over about 60 nmi both in the east–west and in the north–south directions.

The statistical model

Any study of uncertainty depends on the stochastic model adopted. Two different statistical models may yield quite different uncertainty estimates. A general model for a series of survey measurements $\{y_i, i=1, \dots, n\}$ is given by

$$y_i = f(x_{i1}, \dots, x_{ip}) + \varepsilon_i, \qquad i = 1, \dots, n,$$

where f = a deterministic function, which in general is unknown; and

$x_{i1}, \dots, x_{ip}$ = the ith measurements of p explanatory variables, such as geographical location, depth, or time.

If all of the relevant explanatory variables were included, ε_i would represent the residual uncertainty. In practice, all conceivable explanatory factors will not be observed, and often f is assumed to be linear.

A difficulty in assessing the uncertainty of fish abundance estimates is that we cannot carry out a controlled experiment, where the setting of each experiment is identical. In such an idealized series of experiments the explanatory variables $x_{i1}, \dots, x_{ip}$ would be fixed, and ε would be the only source of random variation so that for a series of N experiments,

$$y_k = f(x_1, \dots, x_p) + \varepsilon_k, \qquad k = 1, \dots, N.$$

The standard error of ε_k could then be estimated directly from the observations $\{y_k\}$ as

$$\hat{\sigma}_\varepsilon = \hat{\sigma}_y = \left\{ \frac{1}{N-1} \sum_{k=1}^{N} (y_k - \bar{y})^2 \right\}^{\frac{1}{2}},$$

and the correctness of the model could be tested by a new series of experiments for a new set of fixed values for the explanatory variables.

The closest we can come to such an idealized experiment is that of parallel trawling described above. The values of the explanatory variables, such as geographical location and depth, will vary somewhat from one vessel to another,

[1] Jakobsen, T., K. Korsbrekke, S. Mehl, and O. Nakken. 1997. Norwegian combined acoustic and bottom trawl surveys for demersal fish in the Barents Sea during winter. ICES CM 1997/Y:17:1–26. Institute of Marine Research, P.O.Box 1870 Nordnes, 5817 Bergen, Norway.

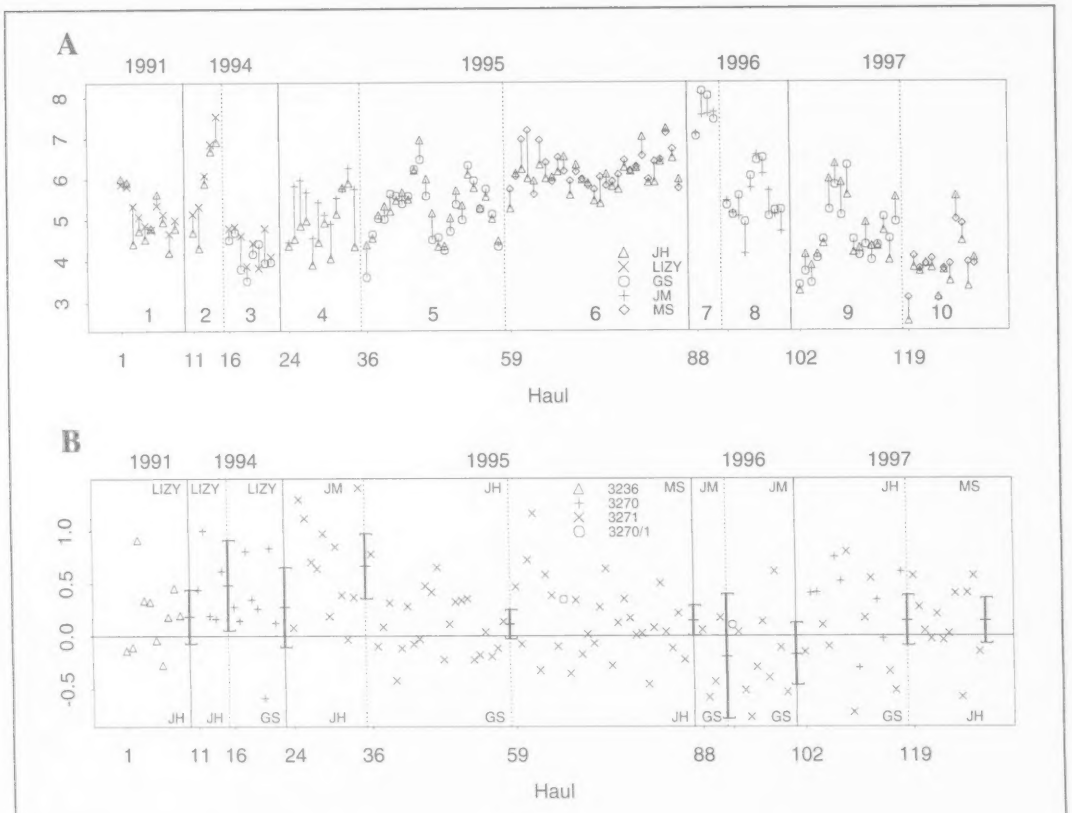

Figure 1

(**A**) Catches $y_{i;j}$ from the parallel trawling experiments in Table 1. The groups are separated by vertical lines and the group numbers corresponding to Table 1 are given at the bottom of the figure. The symbols represent vessels (see Table 1), and the cumulative number of hauls are given at the horizontal axis. (**B**) Corresponding differences $z_i = y_{i;1} - y_{i;2}$. The symbols indicate gear type; 3236: Campelen 1800 shrimp trawl with 35-mm mesh size, 40 m sweeps and rockhopper gear; 3270: same as 3236, but 20-mm mesh size; 3271: same as 3270 but with strapping. 3270/1 indicate that one vessel uses 3270, the other 3271. To the right, 95% confidence intervals for the group means are given. The first and second vessel in each group are given at the top and bottom, respectively, for each group.

but as an approximation they will be considered identical. However, we will allow for an additive individual vessel effect α_j, j=1,2, which permits differences in equipment and efficiency for the two vessels. This leads to the following model for the observations $\{y_{i;j}, i=1, \ldots, n; j=1,2\}$ where j=1, 2 corresponds to the first and second vessel in Table 1:

$$\begin{aligned} y_{i;1} &= f(x_{i1}, \ldots, x_{ip}) + \alpha_1 + \varepsilon_{i;1} \\ y_{1;2} &= f(x_{i1}, \ldots, x_{ip}) + \alpha_2 + \varepsilon_{i;2}. \end{aligned} \tag{1}$$

All the factors affecting jointly tow performance are supposed to be in the function f, and therefore the residuals $\{\varepsilon_{i;j}, i=1, \ldots, n; j=1,2\}$ are assumed to be independent zero-mean identically distributed random variables and $\sigma_\varepsilon = sd(\varepsilon_{i;j})$ is the measurement error.

We can now eliminate f and the explanatory variables by taking differences, i.e.

$$z_i = y_{i;1} - y_{i;2} = \alpha_1 - \alpha_2 + \varepsilon_{i;1} - \varepsilon_{i;2}.$$

The expected difference between the two vessels is then given by

$$E(z_i) = \alpha_1 - \alpha_2$$

and because of the independence of $\varepsilon_{i;1}$ and $\varepsilon_{i;2}$,

$$\sigma_z^2 = \mathrm{var}(z_i) = \mathrm{var}(\varepsilon_{i;1} - \varepsilon_{i;2}) = 2\sigma_\varepsilon^2,$$

and the standard error σ_ε can be estimated as

$$\hat{\sigma}_\varepsilon = \frac{1}{\sqrt{2}}\hat{\sigma}_z = \frac{1}{\sqrt{2}}\left\{\frac{1}{n-1}\sum_{i=1}^{n}(z_i - \bar{z})^2\right\}^{\frac{1}{2}}, \tag{2}$$

whereas $\delta = \alpha_1 - \alpha_2$ is estimated by $\hat{\delta} = \bar{z}$.

It should be noted that in the actual computation of $\hat{\sigma}_\varepsilon$ and $\hat{\delta}$, the data $y_{i;j}$ are log transformed, i.e.

$$y_{i;j} = \log(n_{i;j}/d_{i;j}),\ i = 1, \ldots, n; \qquad j = 1,2, \qquad (3)$$

where $n_{i;j}$ and $d_{i;j}$ denote the catch in numbers and the towed distance, respectively, for vessel j at the ith haul. Log-transformed data are used to reduce the heterogeneity of the variance.

Tests for differences between experimental groups

If our hypothesis, that parallel trawling experiments can be used to quantify a measurement error inherent in the cod catching process itself, is correct, we expect that this error, as estimated by $\hat{\sigma}_\varepsilon$, should be the same for all 10 experimental groups. If the z_i's originate from a Gaussian distribution, the null hypothesis of equal variance can be tested by Bartlett's test (*cf.* all groups tested simultaneously, Bickel and Doksum, 1977, p. 304) and if needed, followed by a series of F-tests where the groups are tested against each other in pairs.

The possible differences in efficiency caused by different vessels or fishing gears (or both) can be tested by an ANOVA test followed by a series of t-tests if the ANOVA test leads to rejection. Again, normally distributed observations are a prerequisite for such tests.

Our first task was therefore to check whether the z_i-data followed a Gaussian distribution. It seemed plausible to assume that observations from different groups followed the same distribution, but possibly with differences in mean and variance. Therefore, when checking for normality, we considered the standardized variables

$$x_i = \frac{z_i - \bar{z}_k}{s_k},$$

where, $k=k(i)$, $k=1, \ldots, 10$, denotes the group that haul i, $i=1, \ldots, n$, belongs to; and $\bar{z}_k$ and s_k are the average and the estimated standard deviation of the z-values in group k, respectively. Deviations from normality of $\{x_i\}$ can be checked visually by inspecting a normal plot, and formally by e.g. the Kolmogorov-Smirnov test (Bickel and Doksum, 1977, ch. 9.6).

Results

The log-catches $\{y_{i;j}\}$ and the corresponding differences $\{z_i\}$ are presented in Figure 1. The catches range from approximately $e^3 \approx 20$ to $e^8 \approx 3000$, but on the log-scale the difference in catch between the vessels does not seem to depend on the size of the catches (see formal test at the end of this section). A normal plot of the standardized observations $\{x_i=(z_i-\bar{z}_k)/s_k\}$ appears linear (Fig. 2) and the Kolmogorov-Smirnov test does not reject the null hypothesis of normality at a 10% level. Testing each group separately (except group 7 where the sample size is too small) yields the same result, i.e. normality is not rejected at a 10% level for any group, thus justifying the use of Bartlett, F- and t-tests. Bartlett's test for testing equality of variances yields a P-value of 0.81. In view of this, it is not really necessary to test the groups in pairs for equality in variance using an F-test, but as a source of additional information we have carried out the tests obtaining the lowest P-value of 0.078 for groups 4 and 5. Thus, based on these data, the hypothesis of a uniform measurement error independent of geographical location, time, depth etc., could not be rejected.

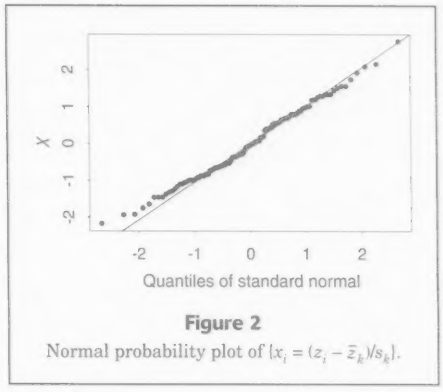

Figure 2
Normal probability plot of $\{x_i = (z_i - \bar{z}_k)/s_k\}$.

To investigate possible differences in efficiency for the participating vessels we did an ANOVA test. We found a P-value less than 10^{-7}, indicating significant differences. This finding was consistent with earlier findings in calibration experiments (Pelletier, 1998). Thus, because $E(Z_i)$ cannot be considered equal for all groups (also the confidence intervals in Fig. 1B), a pooled variance could be used for estimating σ^2_ε. Alternatively, z_i in Equation 2 could be replaced by the variables $z'_i = z_i - \bar{z}_k$, which are adjusted for group means and are identical to the residuals from the ANOVA fit. The resulting estimates with the last approach are $\hat{\sigma}^2_\varepsilon = 0.069$ and $\hat{\sigma}_\varepsilon = 0.263$. The bootstrapped standard errors of $\hat{\sigma}^2_\varepsilon$ and $\hat{\sigma}_\varepsilon$ are 0.0077 and 0.0147, respectively (1000 bootstrap replicates were used). Some caution should be exercised in interpreting these numbers (see e.g. Srivastava and Chan, 1989).

Compared with the total variability of the survey, the measurement error of a single haul is relatively small. For the last 5 years (1996–2000), $\mathrm{var}(y_i)$ for the nonzero catches varied between 1.38 and 2.06 for the winter survey and between 2.53 and 3.92 for the autumn survey. Thus, σ^2_ε is about 2–5% of the total variation. This is the percentage of the variation that we cannot expect to be able to explain by explanatory variables. One should carefully note that these numbers are on the log scale. If antilogs of the catch rate were to be used, the additive model (Eq. 1) would have to be replaced by a multiplicative model, and the relative magnitude of variances would be changed.

The results for length-stratified data are shown in Table 2, as well as the results obtained by measuring the catches by weight instead of by numbers, i.e. by replacing $n_{i;j}$ in (Eq. 3) by, $m_{i;j}$, where $m_{i;j}$ is the weight of the catch in kilograms. Only hauls where both vessels

Table 2

Estimates of σ_ε^2 (with bootstrapped means and standard errors) for catches measured in kg (first column), total number of fish caught (second column), and catch of fish in various length-stratified groups measured in numbers (last four columns). The number of hauls where both vessels caught at least 10 cod is given in the fourth row, the groups excluded due to less than four remaining hauls are given in the fifth row, the average catch of the remaining hauls in the sixth row and *P*-values from Bartlett's test for equal variances, in the seventh row. The means and standard errors were estimated by using 1000 bootstrap replicates.

	kg	Total no. of fish caught	Catch of fish in length stratified groups			
	>0 cm	>0 cm	<30 cm	30–59 cm	≥60 cm	≥30 cm
$\hat{\sigma}_\varepsilon^2$	0.0744	0.0690	0.1124	0.0801	0.0855	0.0643
boot. mean of $\hat{\sigma}_\varepsilon^2$	0.0740	0.0684	0.1113	0.0788	0.0844	0.0637
boot. SE of $\hat{\sigma}_\varepsilon^2$	0.0096	0.0077	0.0140	0.0114	0.0122	0.0083
No. of hauls with at least 10 cod	130	130	113	117	103	118
groups excluded	none	none	2,3	10	2,7,10	10
$\bar{y}$	4.77	5.28	4.61	4.06	3.61	4.52
P-value, Bartlett	0.11	0.81	0.31	0.87	0.60	0.97

collected 10 specimen or more were included, and only groups with at least four such hauls. The null hypothesis of equal variance was not rejected for any of the length groups (*P*-values from Bartlett's test are given in Table 2). It is seen that $\hat{\sigma}_\varepsilon^2$ is highest for small fish, and the bootstrapped standard errors indicate that the difference is statistically significant. Indeed, let $D = \hat{\sigma}^2_{\varepsilon,small} - \hat{\sigma}^2_{\varepsilon,large}$ denote the difference in measurement error between small (<30 cm) and large (≥30 cm) fish. If $\hat{\sigma}^2_{\varepsilon,small}$ and $\hat{\sigma}^2_{\varepsilon,large}$ are independent and normally distributed (their bootstrap distributions are approximately normal) with standard errors as given in Table 2, it follows that $D \sim N(0, 0.0140^2 + 0.0083^2)$ under the null hypothesis of equal measurement errors. The corresponding one-sided *P*-value for the observed D is 0.0016.

The hauls differed in towed distance, with the two most frequently recorded values being 1 and 1.5 nmi which correspond to 20 and 30 minutes tow duration. Stratifying on tow duration (which is recorded more precisely than towed distance), with hauls of less than 25 minutes duration (33%) in group A and the remaining hauls (67%) in group B, and estimating the measurement error for each group separately, we get $\hat{\sigma}^2_\varepsilon$=0.0707 and 0.0656 for group A and B, respectively. Thus, there is no significant difference due to tow duration. For fish less than 30 cm, the corresponding estimates are 0.115 and 0.107 for group A and B, respectively.

No significant relationship was found between the magnitude of the catches and their differences. A regression analysis was performed with the absolute value of the mean-adjusted differences in catch rate, $|z_i'|$, as the dependent variable and the average catch $\bar{y}_i = (y_{i,1} + y_{i,2})/2$ as the independent variable. The regression equation was $|z_i'| = 0.20 + 0.019\bar{y}_i$ and the *P*-value under the null hypothesis of no relationship was 0.31. However, the residuals from the analysis were skewed with a long right-hand tail; therefore a bootstrap test was also done, resulting in an empirical *P*-value of 0.137, and again the null hypothesis of no relationship was not rejected at a 5% level.

Discussion

We have estimated the measurement error (σ_ε^2) of a trawl haul by using data from parallel trawling experiments, including 130 parallel hauls from 10 groups of experiments. No significant differences in σ_ε^2 among the groups were found. Thus, σ_ε^2 seems to be independent of year, time of the year, and geographical position at which the haul was taken. It also seems to be independent of the catch size on a logarithmic scale. The magnitude of σ_ε^2 is small (≈2–5%) compared with the total variability in the survey trawl catches. The results are preliminary in that they are based on a limited set of hauls and more extensive experiments would be of interest to check their consistency. In another investigation, Pelletier (1998) examined the vessel effect between two research vessels. These data could possibly be used to test the general pattern revealed by analyses of data in the current study. Strømme and Iilende (2001) examined a total of 365 paired hauls from intercalibration experiments off Namibia in 1998 and 1999 between the research vessel *Dr. Fridtjof Nansen* and commercial trawlers. These data of Namibian hake (catch in kg/h) were kindly made available to us, and an estimate of $\hat{\sigma}^2_\varepsilon$=0.19 was obtained for the measurement error. The variance of y_i for all the 365 hauls was 2.0; the measurement error for this study on the log scale was about 10% of the survey variance.

Actually σ_ε^2 may be an overestimation of the measurement error because all the explanatory variables are not exactly the same for the two sets of measurements in Equation 1. For example the geographical location is not the same and the fish densities may differ from one vessel to the other because of the distance between them. However, because the towed distance is typically 5–10

times the distance between the vessels, we believe this factor to be of minor importance.

Another problem is the determination of the towed distance. The uncertainty connected with subjective judgments and inaccuracies in the GPS should be included in the measurement error because these factors are also present at a standard survey haul. However, it is not obvious to what extent the differences in the recorded towed distances are due to differences in subjective judgments or to differences in actual towed distances. In our calculations, we used the recorded values from both vessels for $d_{i:j}$. If there is no real difference in the towed distances within a comparison, $\hat{\sigma}_\varepsilon^2$ is expected to decrease by setting $d_{i:1}=d_{i:2}$ for all hauls, thus eliminating one factor of uncertainty. At the other extreme, if the subjective judgments are perfect, and the recorded differences in towed distance are due to real differences, one would expect $\hat{\sigma}_\varepsilon^2$ to increase by setting $d_{i:1}=d_{i:2}$, because an extra error then is added. Actually, by using the values from vessel 2 only and by setting $d_{i:1}=d_{i:2}$ the resulting estimate of σ_ε^2 is $\hat{\sigma}_\varepsilon^2=0.061$, which is a reduction by about 11%. Even though this value is statistically insignificant, it indicates that uncertainty connected to the measurement of towed distance constitutes a part of the measurement error (see also Godø et al., 1990).

In the "Results" section, the null hypothesis of equal efficiency for all the participating vessels was rejected. By joining data from the groups where the same pair of vessels participates, the ability to detect differences in efficiency between the vessels increases through an increased sample size and a smaller number of simultaneous tests (with N tests and a nominal level α, the null hypothesis of equal efficiency is rejected for P-values smaller than the Bonferroni corrected level α/N). For the N=6 tests, we obtained P-values 0.0005 for group 4, 0.009 for groups 1 and 2, 0.011 for groups 6 and 10, 0.034 for groups 5 and 9, 0.107 for groups 7 and 8, and 0.123 for group 3. With a level α=0.05 we have $\alpha/6$=0.0083, and for group 4 the difference is clearly statistically significant. The higher efficiency of *Jan Mayen* (JM) in this group was probably due to her heavier trawl doors. At a 10% level, the vessel *Anny Kræmer* (LIZY) was significantly more efficient than *Johan Hjort* (JH) in groups 1 and 2, and *Michael Sars* (MS) was significantly more efficient than JH in groups 6 and 10. The differences between *G.O. Sars* (GS) and JH (groups 5 and 9), GS and JM (groups 7 and 8) and GS and LIZY (group 3) were not significant. However, excluding group 4, and ignoring statistical significance, the vessels can, in fact, be ranged consistently after increasing efficiency as

$$JM \xrightarrow{(7,8)} GS \xrightarrow{(5,9,3)} JH \xrightarrow{(1,2)/(6,10)} LIZY\ /\ MS. \quad (4)$$

The numbers in parentheses refer to experiment groups, and for each group one vessel to the left, and one to the right of the corresponding arrow, are involved, the one to the right being always the most efficient one.

There also seems to be a significant difference in the measurement error for small and large fish, it being higher for small fish. One explanation may be that the interaction between small fish and the trawl gear is more variable (Godø and Walsh, 1992); another possibility is that small fish operate more in patches than do large fish. If the last assumption is correct, a reduction in $\hat{\sigma}_\varepsilon$ could be expected with increasing tow length. However, for the set of tows considered, we found no significant difference in $\hat{\sigma}_\varepsilon$ due to tow distance.

Consistent with the length dependency of the measurement error is the length dependency of the total variability of the surveys. The average var(y_i) for the winter surveys 1996–2000 for fish ≤31cm and ≥64cm, was 2.49 and 0.98, respectively; whereas for the unstratified data it was 1.66. The corresponding numbers for the autumn surveys 1996–2000 were 3.03, 1.47, and 2.98 for small, large, and unstratified fish, respectively. All numbers are for nonzero catches.

Trawl catches have been considered highly variable (see e.g. Gulland, 1964; Doubleday and Rivard, 1981) and as a result the reliability of trawl survey estimates have been questioned. Abrupt changes in catch size and composition over a short time in a limited area have demonstrated the difficulties in using the information as a relative estimate of density without an understanding of the nature and causes of the variability (Godø, 1994). Unexpected annual changes in survey indices may also be a problem for a reliable evaluation of fish stocks and can be attributed to a variable bias (changes in catchability) among years (Pennington and Godø, 1995). Our analysis demonstrates that for the bottom trawl survey in the Barents Sea, catch rates and composition from the applied survey trawl are repeatable up to a relatively small and constant measurement error and are hence expected to give a reliable picture of the relative fish density at a given site and time. Further, the measurement error of this sampling gear is small compared with the total observed variability. For a particular survey it appears that most of the survey variance is caused by station-to-station differences in catches rather than local conditions at a station. This may be taken as an indication that shorter and more frequent tows may be more efficient for monitoring this cod stock. Moreover, when controlling trawl geometry (Godø and Engås, 1989) and towed distance (Godø et al., 1990), it should be possible to establish explanatory factors to be included in the survey assessment procedure. To the degree that one is able to establish models to determine fish densities at any station, the comparability of density measures throughout the distribution area will improve. The consequences will thus not only be more reliable survey estimates, but we also expect a better understanding of distributional patterns in relation to the physical and biological environment.

Acknowledgments

We are grateful to Atle Totland for help with handling the data and to Michael Pennington for comments on the paper. We are also indebted to the scientific editor and three anonymous referees for a number of useful comments that improved the paper. The work was financially supported by the Norwegian Research Council (127198/120).

Literature cited

Bickel, P. J., and K. A. Doksum.
1977. Mathematical statistics: basic ideas and selected topics. Holden-Day, Oakland, CA, 493 p.

Doubleday, W. G., and D. Rivard.
1981. Bottom trawl surveys. Can. Spec. Publ. Fish. Aquat. Sci. 58:1–273.

Engås, A.
1994. The effects of trawl performance and fish behaviour on the catching efficiency of demersal trawls. *In* Marine fish behaviour related to capture and abundance estimation (A. Fernø and S. Olsen, eds.), p. 45–68. Fishing New Books, Oxford.

Godø, O. R.
1994. Factors affecting reliability of abundance estimates of ground fish from bottom trawl surveys. *In* Marine fish behaviour related to capture and abundance estimation (A. Fernø and S. Olsen, eds.), p. 166–199. Fishing New Books, Oxford.

Godø, O. R., and A. Engås.
1989. Swept area variation with depth and its influence on abundance indices from trawl surveys. J. Northwest Atl. Fish. Sci. 9:133–139.

Godø, O. R., and S. Walsh.
1992. Escapement of fish during trawl sampling—implication of resource assessment. Fish. Res. 13:281–292.

Godø, O. R., M. Pennington, and J. H. Vølstad.
1990. Effect of tow duration on length composition of trawl catches. Fish. Res. 9:165–179.

Gulland, J.A.
1964. Catch per unit effort as a measure of abundance. Rapp. P.-V. Reun. Cons. Int. Explor. Mer 155:8–14.

Korsbrekke, K., and O. Nakken.
1999. Length and species dependent diurnal variation in catch rates in the Norwegian Barents Sea bottom trawl surveys. ICES J. Mar. Sci. 56:284–291.

Michalsen, K., O.R. Godø, and A. Fernø.
1996. Diel variation in the catchability of gadoids and its influence on the reliability of abundance indices. ICES J. Mar. Sci. 53:389–395.

Pelletier, D.
1998. Intercalibration of research survey vessels in fisheries: a review and an application. Can. J. Fish. Aquat. Sci. 55:2672–2690.

Pennington, M., and O. R. Godø.
1995. Measuring the effect of changes in catchability on the variation of marine survey abundance indices. Fish. Res. 23:301–310.

Polacheck, T., and J. H. Vølstad.
1993. Analysis of spatial variability of Georges Bank haddock (*Melanogrammus aeglefinus*) from trawl survey data using a linear regression model with spatial interaction. ICES J. Mar. Sci. 50:1–8.

Srivastava, M. S., and Y. M. Chan.
1989. A comparison of bootstrap method and edgeworth expansion in approximating the distribution of sample variance—one sample and two sample cases. Communication in statistics—simulation 18:339–361.

Strømme, T., and T. Iilende.
2001. Precision in systematic trawl surveys as assessed from replicate sampling by parallel trawling off Namibia. S. Afr. J. Mar. Sci. 23:385–396.

The reproductive biology of the porbeagle shark (*Lamna nasus*) in the western North Atlantic Ocean

Christopher F. Jensen
North Carolina Department of Environment and Natural Resources
Division of Marine Fisheries
P.O. Box 769
Morehead City, North Carolina 28557-0769
E-mail address:Caltimuscd@aol.com

Lisa J. Natanson
Harold L. Pratt Jr.
Nancy E. Kohler
National Marine Fisheries Service, NOAA
28 Tarzwell Dr.
Narragansett, Rhode Island 02882

Steven E. Campana
Marine Fish Division
Bedford Institute of Oceanography
P.O. Box 1006
Dartmouth, Nova Scotia
Canada B2Y 4A2

Abstract–Reproductive organs from 393 male and 382 female porbeagles (*Lamna nasus*), caught in the western North Atlantic Ocean, were examined to determine size at maturity and reproductive cycle. Males ranged in size from 86 to 246 cm fork length (FL) and females ranged from 94 to 288 cm FL. Maturity in males was best described by an inflection in the relationship of clasper length to fork length when combined with clasper calcification. Males matured between 162 and 185 cm FL and 50% were mature at 174 cm FL. In females, all reproductive organ measurements related to body length showed a strong inflection around the size of maturity. Females matured between 210 and 230 cm FL and 50% were mature at 218 cm FL. After a protracted fall mating period (September–November), females give birth to an average of 4.0 young in spring (April–June). As in other lamnids, young are nourished through oophagy. Evidence from this study indicated a one-year reproductive cycle and gestation period lasting 8–9 months.

Manuscript accepted 29 May 2002.
Fish. Bull. 100:727–738 (2002).

The porbeagle (*Lamna nasus*), a pelagic shark in the family Lamnidae, inhabits the cold temperate waters of the North and South Atlantic, South Pacific, and southern Indian Oceans, as well as the subantarctic region of the Southern Ocean (Svetlov, 1978; Compagno, 1984). In the western North (NW) Atlantic Ocean, the porbeagle ranges from the Flemish Cap and the Grand Banks off southern Newfoundland, Canada, to the Gulf of Maine and (rarely) south to New Jersey (Templeman, 1963; Compagno, 1984). The porbeagle is most commonly encountered from the Gulf of Maine to the Grand Banks, where it has been the subject of a commercial fishery since 1961 (O'Boyle et al.[1]; Campana et al[2,3]). Seasonal abundance is related to north–south migrations (Aasen, 1963; Campana et al.[3]; Aasen[4]).

Lamnid sharks are ovoviviparous and nourish their embryos by oophagy (Lohberger, 1910). Early descriptions of porbeagle embryos exhibiting oophagy were documented by Swenander (1907) and Shann (1911, 1923), and more recently by Francis and Stevens (2000). Litter size has been variously reported as one to five pups (Dunlop, 1897; Swenander, 1907; Shann, 1911, 1923; Gauld, 1989; Francis and Stevens, 2000). Birth size has been reported as

[1] O'Boyle, R. N., G. M. Fowler, P. C. F. Hurley, M. A. Showell, W. T. Stobo, and C. Jones. 1996. Observations on porbeagle (*Lamna nasus*) in the north Atlantic. DFO (Department of Fisheries and Oceans) Atl. Fish. Res. Doc. 96/24, 29 p. Marine Fish Division, Bedford Institute of Oceanography, P.O. Box 1006, Dartmouth, Nova Scotia, Canada B2Y 4A2.

[2] Campana, S., L. Marks, W. Joyce, P. Hurley, M. Showell, and D. Kulka. 1999. An analytical assessment of the porbeagle shark (*Lamna nasus*) population in the Northwest Atlantic. CSAC (Canadian Stock Assessment Secretarate) Res. Doc. 99/158, 57 p. Marine Fish Division, Bedford Institute of Oceanography, P.O. Box 1006, Dartmouth, Nova Scotia, Canada B2Y 4A2

[3] Campana, S., W. Joyce, L. Marks, P. Hurley, L. J. Natanson, N. E. Kohler, C.F. Jensen, J. J. Mello, and H. L. Pratt Jr. 2000. The rise and fall (again) of the porbeagle shark population in the Northwest Atlantic. Unpubl. manuscr. Marine Fish Division, Bedford Institute of Oceanography, P.O. Box 1006, Dartmouth, Nova Scotia, Canada B2Y 4A2

[4] Aasen, O. 1961. Some observations on the biology of the porbeagle shark (*Lamna nasus* L.). ICES C.M. Copenhagen 1961, Near Northern Seas Committee 109:1–7.

60–80 cm total length (TL) (54–72 cm fork length [FL]) (Shann, 1923; Compagno 1984, Francis and Stevens, 2000). Bigelow and Schroeder (1948) speculated that females are gravid by 152 cm TL (136 cm FL), whereas Aasen (1963) concluded that females mature between 200 and 250 cm TL (193–240 FL) and males mature between 150 and 200 cm TL (146–193 FL). In a more comprehensive study, Francis and Stevens (2000) found that females mature between 165 and 180 cm FL in the South Pacific.

In this study, we present the results of a comprehensive examination of porbeagle reproduction in the NW Atlantic Ocean. We define the sizes and stages of maturity for both sexes and provide insights into the reproductive cycle, as well as embryo sex ratios and litter sizes. These parameters will be useful for the refinement of fishery management plans for the porbeagle shark in the NW Atlantic Ocean.

Materials and methods

Porbeagles were collected with pelagic longline onboard both U.S. and Canadian commercial fishing vessels and U.S. research vessels fishing in U.S. and Canadian waters from the Gulf of Maine and Georges Bank (northeastern U.S.) to the Grand Banks off southern Newfoundland. Several specimens were obtained at a sport-fishing tournament held on Stellwagen Bank, Massachusetts. Sampling took place between 1979 and 1999, but most of the data were obtained during 1993, 1994, and 1999.

Morphometrics

For each shark, five lengths were measured over the curve of the body to the nearest half centimeter (cm): interdorsal length (posterior dorsal fin base to origin of second dorsal fin; IDL); dorsal length (origin of first dorsal fin to precaudal pit; DL); precaudal length (snout to precaudal pit; PCL); fork length (snout to fork of tail; FL); and total length (snout to a perpendicular line from the tip of the upper caudal fin in a natural position; TL). Total length of embryos were measured along a straight line with the tip of the tail fully extended (TL_s) because of the difficulty in obtaining over-the-body or FL measurements (or both) in embryos less than 6 cm TL. FL and PCL were taken when possible. FL are reported for all sharks in our study; TL values are presented for embryos with calculated or measured FL in parentheses. TL can be converted to FL by using the following regression (Campana et al.[3]):

$$FL = 0.885(TL) + 0.99 \qquad [r^2=0.99, n=361].$$

All other length and weight conversions can be found in Campana et al.[2] Aasen's (1963) TL values were converted to FL by using the approximate formula:

$$FL = 0.947^{*}(AasenTL) + 3.64 \text{ (Campana}^{5}\text{)}.$$

[5] Campana, S.E. 2000. Unpubl. data. Department of Fisheries and Oceans, Bedford Institute of Oceanography, P.O. Box 1006, Dartmouth, Nova Scotia, Canada, B2Y 4A2.

TL_s can be converted to FL for embryos by using the regression

$$FL = 0.832(TL_s) - 0.19 \qquad [r^2=0.99, n=131].$$

Whole weight in kilograms (kg) was taken when possible. Literature values of TL were converted to FL for comparison and the conversions are presented throughout the text in parentheses. The converted values from the literature should be considered good estimates only because of the variation in measurement techniques between studies.

Maturity indicators

A number of measurements, weights, and conditions were taken on reproductive organs in both sexes to develop indices of maturity following Pratt (1979, 1993, 1996). Most specimens were measured fresh; however, some frozen reproductive tracts were also measured. Reproductive tracts were measured on the right side of the specimen. Organ terminology follows Pratt (1979) (Fig. 1, A and B).

For more detail, uteri were divided visually into anterior and posterior segments. The anterior segment is defined as the portion between the origin of the uterus at the isthmus and the point where both uteri join. The posterior segment is the portion from the junction to the posterior constriction of the uterus (Fig. 1B). A length measurement was taken for the anterior uterus, and width was taken midway along this portion of the uterus.

Active ovulation was defined as occurring if 1) ova were entering the ostium or were present inside the upper oviduct, 2) ova and capsules were present in the oviducal gland, 3) encapsulated ova were present in the isthmus, and 4) encapsulated ova were present in the uterus.

Prior mating activity was assessed according to the presence or absence of a vaginal membrane (hymen), determined by passing a probe through the posterior end of the uterus into the cloaca. The presence of vaginal mating scars was used to determine if recent mating had taken place. Scars were identified as either healed or recent. Maturity status of both sexes was assigned to each shark based on all reproductive organ characteristics (Pratt, 1979). The size at 50% maturity was determined by fitting a logistic regression to a plot of percent maturity versus FL.

Embryos were either frozen or preserved in 10% buffered formalin. Litter size and embryo sex were determined in the field or in the laboratory under a dissecting microscope. Embryo growth was related to month. Linear regressions were fitted to the relationship between mean embryo length and month for samples from the NW Atlantic and southwest Pacific Oceans and compared with analysis of covariance (ANCOVA).

Results

Male length at maturity

Reproductive data were obtained from 393 male porbeagle sharks ranging in size from 86 to 246 cm FL, of which

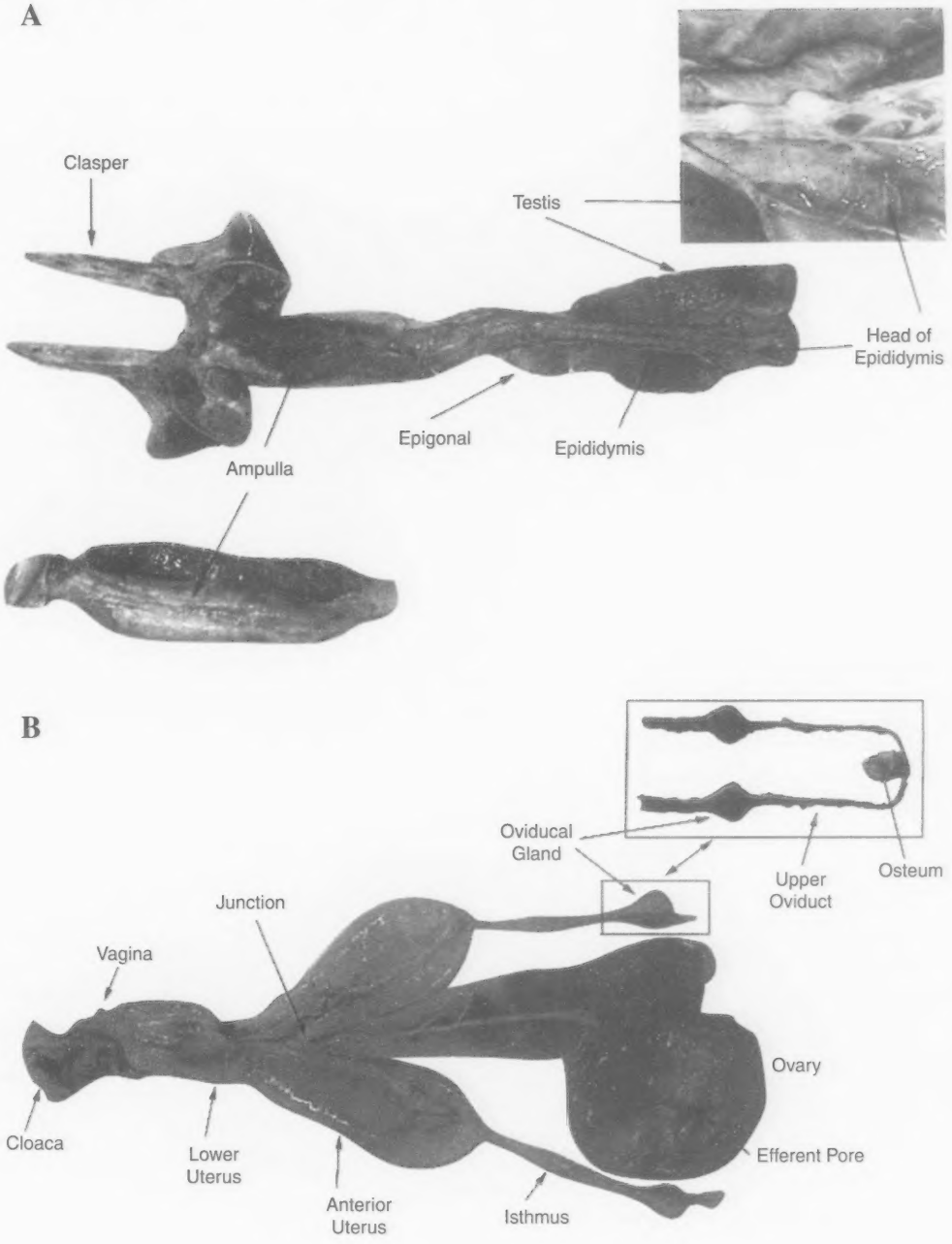

Figure 1

Reproductive systems of the porbeagle shark: (**A**) male reproductive tract with closeup inserts of the head of the epididymis and the ampulla epididymis and (**B**) female reproductive tract with a closeup of the upper oviduct leading into the ostium.

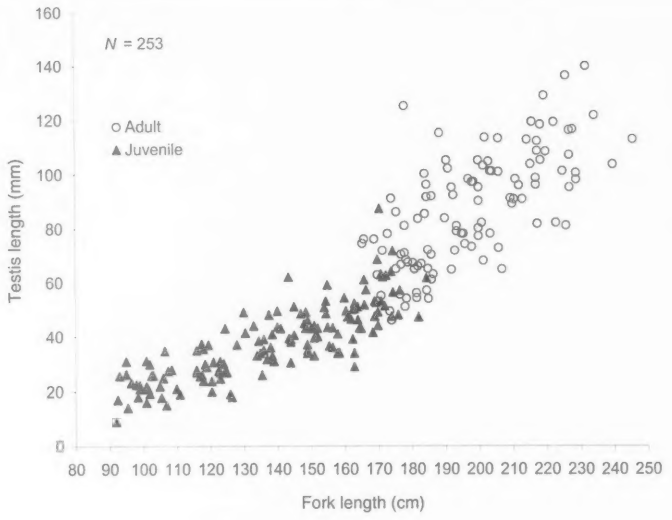

Figure 2
Relationship of right testis length to fork length.

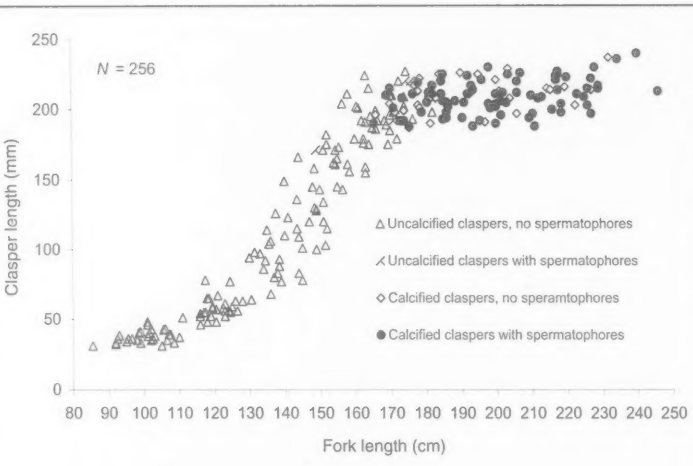

Figure 3
Relationship of right outer clasper length to fork length. Relative amount of clasper calcification and presence or absence of spermatophores are also indicated.

reproductive organs were measured for 267. Development of the siphon sacs, as well as internal male reproductive organs—testes (diameter and length), epididymis, and ampulla epididymis—is gradual in relation to FL (Fig. 2). The development of the claspers, however, shows a distinct inflection (Fig. 3). Claspers begin to elongate when the males approach 120 cm FL, and rapid clasper growth begins at 135 cm FL and slows by about 170 cm FL when they have reached their maximum adult size of 19–24 cm. The largest shark with uncalcified claspers but containing spermatophores in the ampulla epididymis was 176 cm FL, and the smallest shark with calcified claspers, but with no spermatophores, was 166 cm FL. Claspers rotate freely at all sizes in the porbeagle; therefore clasper rotation is not a good measure of maturity. Males of 135 to 184.5 cm FL are in a transitional phase leading to maturity. At this stage, claspers are lengthening and the head of the clasper (rhipidion) is beginning to develop, whereas at 149 cm FL

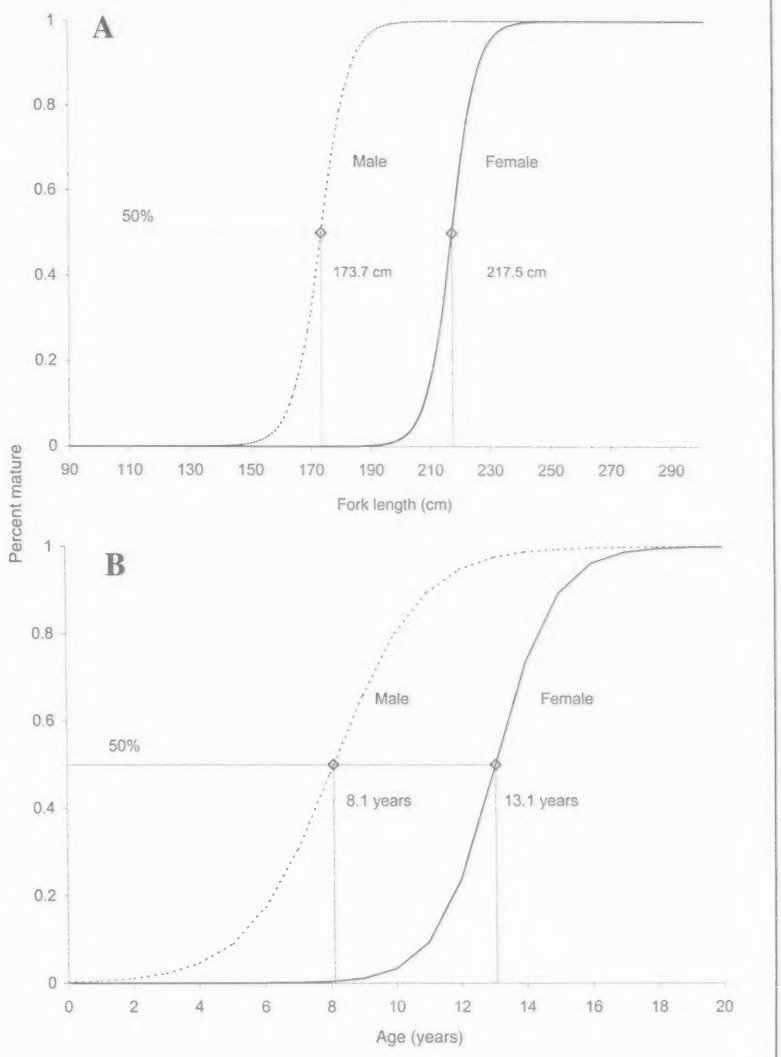

Figure 4

Maturity ogives for male and female porbeagle sharks: (**A**) ogives based on length, (**B**) ogives based on age. Fifty percent maturity is indicated.

and greater, spermatophores appear in the ampulla epididymis. By 162 cm FL fully calcified claspers were observed. Individual variation exists in body length and the order in which these developments take place. All males observed were mature by 185 cm FL based on clasper calcification and the ability of the rhipidion to open. The presence of spermatophores may be used in addition; however, absence of spermatophores can be attributed to season as well as to maturity. Each clasper bears a sharp, conical, calcified spur near the tip which folds out of the distal surface as the rhipidion opens. In adults, the sharp spur tip was either covered by an epidermal membranous sheath, or naked. A naked spur is an indicator of mating activity because mating ruptures the sheath. The FL at which 50% of the male population is mature, based primarily on clasper condition, was estimated as 174 cm FL (Fig. 4A).

Both testis size and the amount of spermatophores in the ampulla epididymis showed distinct fluctuations related to the mating season. From November through mid December, the testis lobes were noticeably reduced in diameter, the testes were smaller, and the epigonal organ had infiltrated the space previously occupied by the

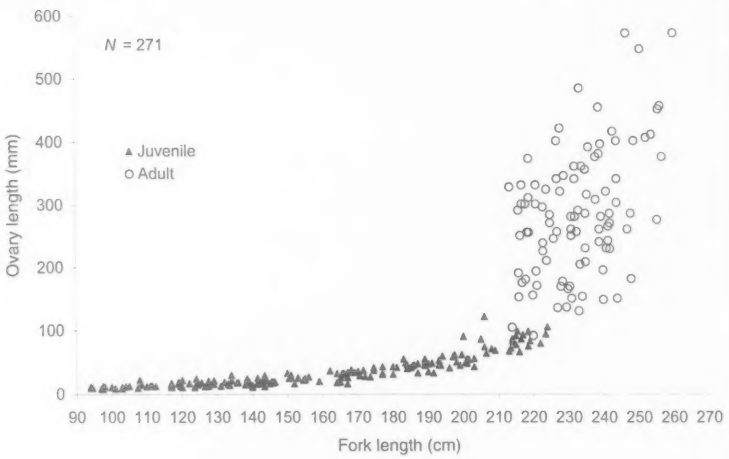

Figure 5

Relationship between ovary length (mm) and fork length (cm) in the porbeagle shark. Juveniles and adults are indicated.

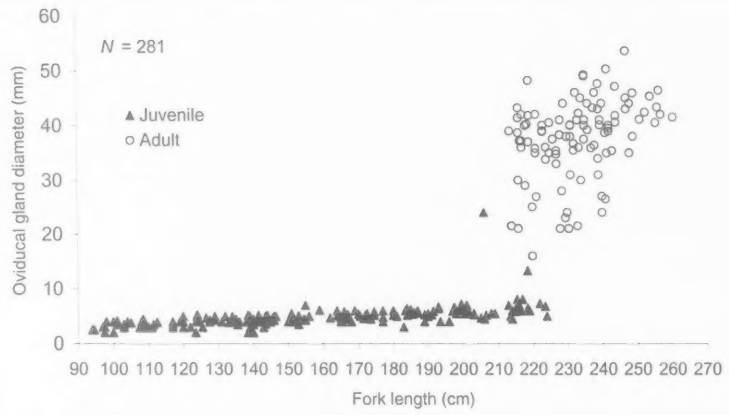

Figure 6

Relationship between oviducal gland diameter (mm) and fork length (cm) in the porbeagle shark. Juveniles and adults are indicated.

testes. Spermatophores in the ampulla epididymides were at their greatest volume in September–December; in February–May relatively few spermatophores were observed, and by June the concentration started to increase.

Female length at maturity

Reproductive data were obtained from 382 female porbeagle sharks ranging in size from 94 to 288 cm FL, of which reproductive organs were measured for 284. The relationship between the measurements of internal reproductive organs (ovary length and width, anterior uterus length and width, and shell gland (oviducal gland) width to FL) showed a sharp increase between 210 and 220 cm FL (Figs. 5 and 6). Oocytes are not visible to the naked eye in juveniles less than about 200 cm FL, and in larger, immature females, small, clear, yolkless oocytes range in size from 0.5 to 3.7 mm in diameter. In mature females, vitellogenic oocytes range from 2.2 to 7.0 mm. The increase in oocyte diameter, as well as the development from clear yolkless oocytes to vitellogenic oocytes, occurs between 210 and 225 cm FL (Fig. 7). Criteria for maturity in female porbeagles include the presence of embryos or fertilized ova in the uteri, and indications of past pregnancy, such

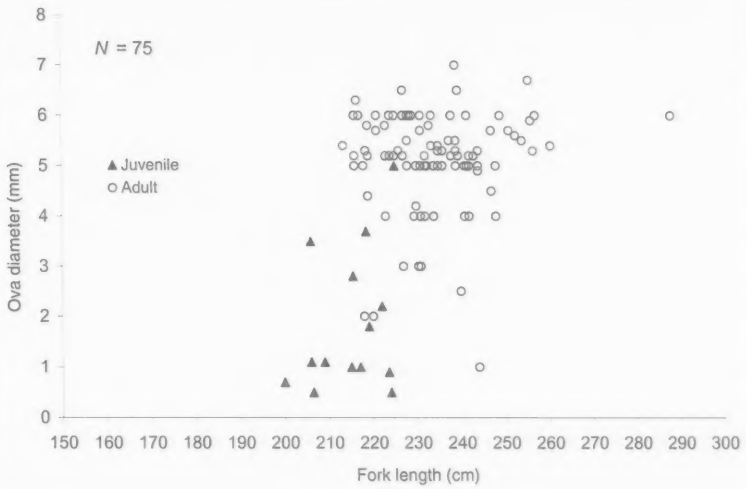

Figure 7

Relationship between maximum **ovum?** diameter (mm) and fork length (cm) for the porbeagle shark.

as flaccid uteri with trophonemata and reduced ovaries containing few maturing or mature oocytes. Juvenile females have small undeveloped ovaries with white to clear oocytes; the uterus appears narrow and constricted, and the oviducal gland is seen as a barely perceptible widening of the oviduct. The juvenile and mature virgin sharks that we examined had a membrane separating the vagina from the cloaca, whereas mature (reproductively active) sharks had no membrane. In nongravid females, maturity is based on the presence of mature oocytes in a developed ovary, an expanded uterus, a well-developed oviducal gland, internal and external mating scars, and the absence of a vaginal membrane. The smallest mature female in our sample was 210 cm FL based on the absence of a vaginal membrane and the condition of the internal reproductive organs, and the largest immature female was 230 cm FL based on the presence of a vaginal membrane and internal organ condition. Fifty percent of the female porbeagle population was mature at 218 cm FL (Fig. 4A).

Mating injuries

Fresh mating scars, containing at least small areas of unhealed dermal lacerations, were observed from late September through mid-December, during which time most adult females appeared to have recently mated or were in the early stages of pregnancy. Scars and cuts were often observed on either or both pectoral fins as single or multiple jaw outlines, and the trailing edge of the fin was often shredded. Tooth scrape marks, puncture wounds, and gouges, some as open, penetrating subdermal lacerations, were observed mainly along the posterior lateral, dorsal, or ventral body surface. None of the wounds appeared to have penetrated the abdominal wall nor were they debilitating. No infected or necrotic tissue was seen in these wounds. Most mature female porbeagles had distinct fresh or healed mating scars.

Internal mating scars were observed on the vaginal walls from late September through mid-December. The scars were generally small, round to ovoid, hematose marks on an otherwise white to light yellow vaginal wall. These were probably caused by the spur that holds the clasper in place during copulation.

Gravid females, embryo growth, and nutrition

Data from 80 litters and 309 embryos were obtained from gravid females sampled from mid-September through April. In addition to embryos, these females had several different types of egg capsules in their oviducal gland, isthmus, and uteri. These were empty capsules, capsules containing one large ovum without a visible embryo (single ovum capsules), capsules with one developing embryo and attached yolk sac, capsules with 22–45 blastodisc-stage ova, and capsules containing 8–100 nonblastodisc-stage ova (nutritive capsules), some appearing atretic and in which individual ova were difficult to detect. The number of capsules present in each uterus ranged from none to 63 (Fig. 8).

The proportion of mature nongravid females with recent mating scars, but no obvious fertilized ova, decreased from September through December, whereas the proportion of gravid females increased (Fig. 9). All mature females examined in December were gravid. During October, several mature females contained either parts of, or entire, spermatophores in the uteri, but no ova capsules, indicating

that mating had taken place but that ova were not yet fertilized. On the basis of the occurrence of early-stage gravid females, the ripe condition of the males, and the presence of recent mating scars, we concluded that most mating occurs from late September through November. Mature males with copious amounts of spermatophores and mature females were captured on the same gear numerous times during the fall.

The right uterus of the one gravid female observed during late September had one single ovum capsule with no visible embryos, along with several blastodisc or nutritive capsules, whereas the contents of other uterus appeared to have been aborted. This was the only recently mated female observed in September. Some gravid females in October and November contained capsules with a single ovum, 6–7 mm diameter, in addition to varying numbers of empty, blastodisc, or nutritive capsules. These single ovum blastodisc capsules (usually two per uteri) were considered to be the annual developing embryos, their single ovum larger than those of the aggregate blastodisc or nutritive capsules. Gravid females examined during October had either single ovum capsules or embryos 0.9–6.8 cm TL_s (0.6–5.3 cm FL), and those seen in November had a decrease in occurrence of single-ovum capsules, and embryos ranged from 1.1 to 37.8 cm TL_s (0.7–31.2 FL). No gravid females with single ovum capsules were seen during December, and embryos ranged from 2.3 to 43.1 cm FL (Fig. 10). Only one nearterm, gravid porbeagle, caught in mid-April, was examined in our study. This shark had three embryos ranging in size from 59 to 72 cm TL_s (50–59 cm FL). The considerable variation in embryo length among litters during early gestation indicates a protracted mating season.

Postpartum females were observed from the first week of May to the first week of June. Our data from these females suggested that parturition extends from early April through early June. The presence of postpartum females in May–June after the September–November mating indicates a gestation period of about 8–9 months.

Although numerous gravid females are present from late September through December on the Scotian shelf and Grand Banks region, mature gravid or nongravid female sharks are seldom seen from January through June in the Canadian fishery. Gravid females were caught between Georges Bank and the Grand Banks (Fig. 11).

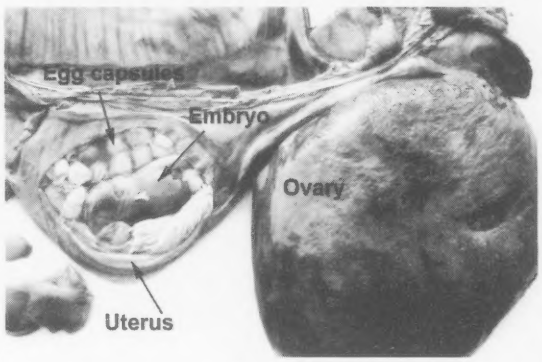

Figure 8

Photograph of an ovary and open uterus of a gravid porbeagle showing a developing embryo amid ova capsules.

Fecundity

Embryos were found to be at the same developmental stage in each female, although embryo size varied as much as 14.6 cm in one litter. Runts were encountered in five females and although clearly developing, were considerably smaller than the coexisting embryos. Fecundity was calculated by using all embryos. The average number of embryos per porbeagle was 4.0 (304 embryos from 76 litters) although litters ranged from 3 to 6. In 66 litters there were two embryos per uterus. The sex ratio of 202 embryos (99 male and 103 female) was not significantly different from one (χ^2=0.08, P>0.1).

In the uteri of six females, fertilized ova were found in the same ova capsule with one to three late developing yolksac embryos. Some of these fertilized ova appeared to be decomposing. These capsules were in the same uteri as a larger, developing litter, but the size of the embryos associated with the capsules (averaging 4–20% of the average size of the developing litter) were smaller than runts (runts averaged 24–43% of the average size of siblings) or the main litter. Because of their small size in relation to the developing litter, and their appearance of decomposition, it was presumed that they were ova that had been fertilized late by remaining sperm and that had probably not continued to develop. However, this is not to rule out the possibility that some of these embryos could have developed into runts or be consumed when littermates initiated feeding on egg capsules. Further research is being conducted on this subject and will be reported at a later date.

Embryonic development and growth

Newly fertilized ova, without visible embryos, were 6–7 mm in diameter. As the embryo developed, their yolk sacs decreased in size, and by the time the embryos were between 4.2 and 9.2 cm TLs (3.3–4.5 cm FL), the yolk sacs were tiny, white, ovoid structures attached to the embryo by a short stalk. Embryos were found in capsules up to 4–4.2 cm TL_s (3.1–3.3 cm FL). The smallest posthatch embryos were 3.2–4.2 cm TL_s (2.5–3.3 cm FL). The abdomens of posthatch embryos between 4.7 and 5.1 cm TL_s (3.7 and 4.0 cm FL) were slightly swollen. Functional embryonic dentition appeared in embryos at 12 cm TL_s (9.8 cm FL). As the embryo continues to grow, the yolk stomach increases in size as a result of *in utero* consumption of ova capsules by the embryo. The stomach becomes grossly distended by the time the embryo reaches 27–43 cm TL_s (23–36 cm FL). The large amounts of yolk material in the stomachs of these embryos was characteristic of oophagy. Frequently, parts of ova capsules, parts of, or whole, ova, and white flocculent material were observed in the clear intrauterine fluid surround-

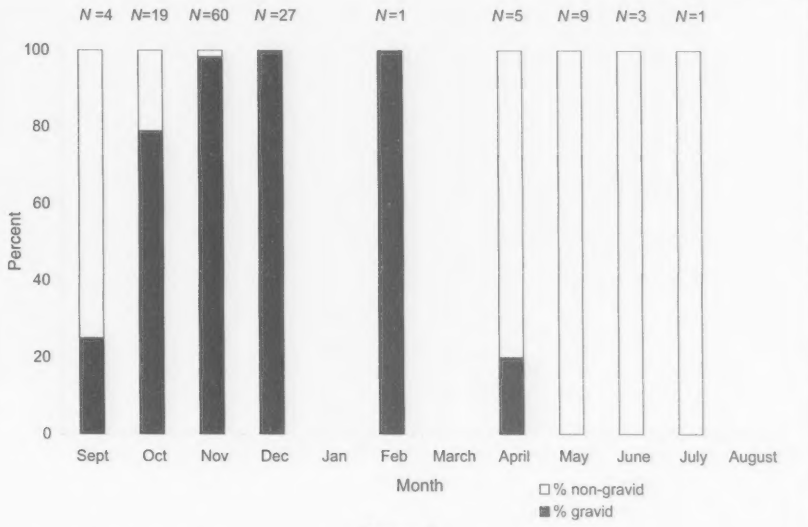

Figure 9

Relationship of gravid to nongravid adult female porbeagle sharks by month from 1979 to 1999.

ing the embryos, suggesting recent embryo feeding. One embryo was seen with a whole, undamaged ova capsule protruding from its mouth. The stomach contents of embryos from several litters did not show parts of other embryos, suggesting that adelphophagy (competitive embryonic cannibalism), found in the sandtiger shark (Gilmore et al., 1983) does not occur in the porbeagle. The existence of developing runts in several litters and consistently two embryos per uterus reinforces these observations. A slight modification to our knowledge of oophagy would be the possible consumption of the late-fertilized ova capsules that had small undeveloped and decomposing embryos along with unfertilized ova, as mentioned previously. Most gravid porbeagles examined during this study were ovulating and, therefore, nourishing their embryos. The times at which ovulation ceases, ovary size decreases, and the large amount of yolk in the stomach is consumed, need further definition.

The mean growth rate of embryos from this study was 11.4 cm per month; however, this is most likely inflated by the lack of larger embryos. Combining data from the present study with previous data from the North Atlantic, which includes later term embryos (Francis and Stevens, 2000), leads to an estimate of 8.15 cm per month. The regression of growth per month for the North Atlantic embryos was significantly different from that of the South Pacific population in intercept (time of year) but not in slope (growth rate) (ANOVA $P>0.10$ slopes, $P<0.1$ intercept) (Fig. 10).

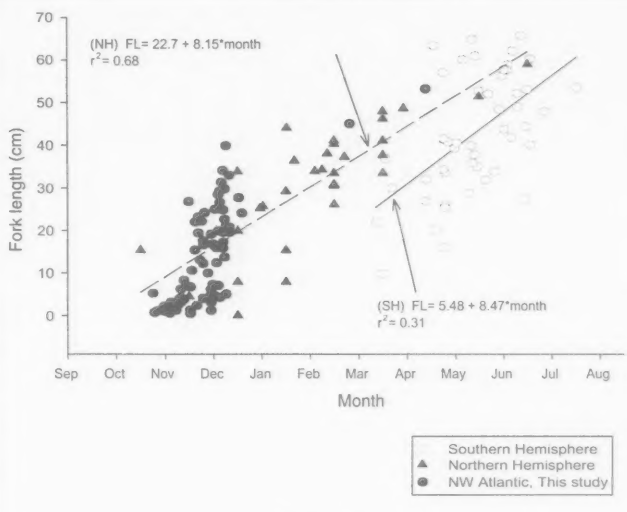

Figure 10

Monthly variation in mean lengths of embryo litters from both hemispheres. Data indicated by open circles and closed triangles are from Francis and Stevens (2000) and Francis,[6] respectively.

Neonates and young of the year

The smallest free-swimming porbeagle examined during this study was 77.5 cm FL (87 cm TL) on 24 May. Other records of free-swimming individuals measured in April–June, ranged from 55 to 79 cm FL (mean=71 cm FL, n=9)

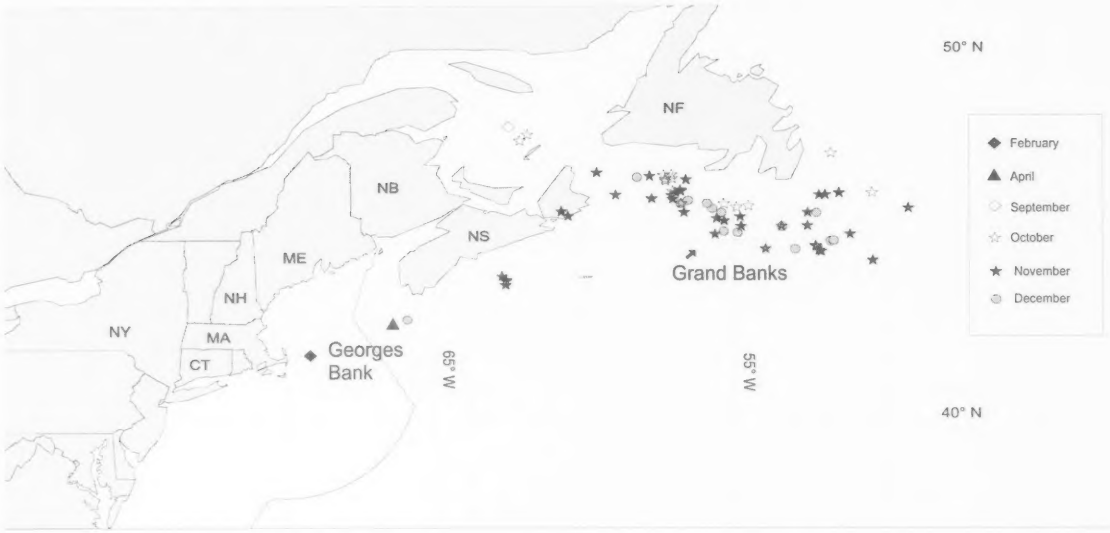

Figure 11

Map of the capture locations of all gravid female porbeagles by month of capture. Approximate locations of Georges Bank and the Grand Banks are indicated.

(Kohler[6]). The largest embryos in our study from one litter in April were 49–60 cm FL (59–72 cm TL).

Discussion

In the NW Atlantic, male porbeagles mature between 166 and 184 cm FL, and 50% maturity was at 174 cm FL, which corresponds to an age of 8 years (Fig. 4B; Natanson et al., 2002). The most accurate means of determining male maturity is clasper length and calcification. Because of the distinct seasonal variability, the presence of seminal products alone, is not a good indicator of maturity. Clasper rotation occurred at all sizes, eliminating it as a maturity indicator. Our estimate of length at maturity substantially refines Aasen's[4] estimate of 150 to 200 cm TL (146–193 cm FL) for this population. Aasen[4] based his estimates on clasper length in relation to dorsal length.

Female NW Atlantic porbeagle sharks mature between 210 and 230 cm FL and 50% maturity was at 218 cm FL, at an age of 13 years (Fig. 4B; Natanson et al., 2002). The sizes of all female reproductive organs measured showed a definitive inflection at maturity in relation to body size and are good indicators of maturity. Aasen[4] estimated female maturity between 2.0 and 2.5 m TL (193–240 cm FL) based on uterus length. Our estimates compare well to the upper part of his range; however our data do not support his lower size at maturity.

The seasonality of spermatophore production, observations of females with fresh mating scars, and observations of males and females on the same longline indicated that porbeagles mate in the fall, primarily between September and November. In an earlier study, sperm in the shell gland of a female, and the presence of a male caught on the same longline set in October, also suggested a fall mating period (Pratt, 1993). Aasen (1963) proposed a fall mating season (September–October) based on an increase in the amount of sperm present in the males "towards the end of August." This period agrees with the suggestion of a long mating season in the SW Pacific porbeagle population (Francis and Stevens, 2000). During this time, females have fresh external mating scars, internal vaginal scars, and spermatophores in the uterus. Gauld (1989) suggested that mating occurs during December–January in the northeast Atlantic on the basis of fresh mating scars on the pectoral fins.

Mating injuries have been documented for many species of sharks. Bite marks on females during mating have been documented in the blue (*Prionace glauca*), nurse (*Ginglymostoma cirratum*), sandtiger, (*Carcharias taurus*), blacknose (*Carcharhinus acronotus*) finetooth (*C. isodon*), blacktip (*C. limbatus*), sandbar (*C. plumbeus*), and Atlantic sharpnose (*Rhizoprionodon terraenovae*) sharks (Stevens, 1974; Gilmore et al., 1983; Schwartz, 1984; Castro, 1993, 1996, 2000). Fresh bite marks may coincide with insemination and ovulation, marking the approximate beginning of the gestation period (Parsons, 1983; Castro, 1996). Matthews (1950) noted lacerations in the vagina of the basking shark (*Cetorhinus maximus*) from the clasper spur. Pratt (1979) also observed abrasions from claspers in the vagina of female blue sharks.

Gravid females typically carry single-ovum capsules from September to November, and developing embryos from October to April. Aasen (1963) reported no gravid porbeagles from July to September 1961, in the NW At-

[6] Kohler, N. K. 2000. Unpubl. data. NMFS Apex Predators Program, 28 Tarzwell Dr., Narragansett, RI 02882.

lantic. Bigelow and Schroeder (1948) described gravid porbeagles in the Gulf of Maine during November, January, and August, although the latter month conflicts with both the present findings and those of Aasen (1963). Aasen (1963) reported that pregnant females carrying large embryos were observed in late May at the Flemish Cap. Templeman (1963) reported three gravid females from the SW Grand Banks during January and February 1953–56. Gauld (1989) reported the presence of gravid females from December to June in the NE Atlantic ocean, whereas Francis and Stevens (2000) reported gravid females from March to July in the SW Pacific Ocean.

Length variability within and between litters has been found in most porbeagle studies (Fig. 10). We found a difference of up to 14.6 cm in the lengths of individuals in one litter. Gauld (1989) found length differences of up to 11 cm within individual litters, and Shann (1923) found a 12–15 cm difference in embryo length within individual litters. Runts were observed in pregnant porbeagles in our study as well as by Francis and Stevens (2000).

As with other lamnids, female porbeagle sharks nurture their young through oophagy. Upon hatching from the single-ovum capsules and after absorption of the external yolk sac, embryos begin orally feeding on yolk-filled nutritive ova capsules. As a result, the internal yolk stomach of the embryos expands to the large size characteristic of lamnid embryos at this stage in their development. Evidence from this study suggests that adelphophagy does not occur in the porbeagle. The ova capsules observed in our study were similar to those found in the sandtiger and other lamnid sharks described by Gubanov (1972), Fujita (1981), Gruber and Compagno (1981), Gilmore et al. (1983), Francis and Stevens (2000), and Mollet et al. (2000).

Embryonic growth was estimated at 8.15 cm per month in our study (Fig. 10). Francis and Stevens (2000) estimated embryonic growth of approximately 7.48 cm per month for embryos in the South Pacific. New data from the South Pacific (Francis[7]) refined this estimate to 8.47 cm per month. Examination of more late-term embryos will further refine this estimate for the NW Atlantic.

Our results indicated a one year reproductive cycle, with gestation lasting 8–9 months. Mating occurs between September and December. Based on the one late-term female and several postpartum females it appears that parturition occurs from early April though June. Aasen (1963) estimated that parturition occurs from late May to early June in the NW Atlantic and suggested about an 8-month gestation period based on the lack of gravid female porbeagles from June to September. All females we examined in December were gravid. Although a nongravid mature portion of the female population could reside elsewhere, we have no data to support this and thus assume that porbeagle females reproduce annually. Parturition time and location and late embryonic development and growth rates need further investigation.

Mean litter size in the NW Atlantic was found to be 4.0—usually two embryos per uteri. Mean litter size from the SW Pacific Ocean was 3.8 from 138 embryos representing 43 litters (Francis and Stevens, 2000). Mean litter size from the NE Atlantic Ocean was 3.7 based on 12 litters examined by Gauld (1989). The sex ratio of the embryos examined in our study was 1:1, which agrees with the findings of Francis and Stevens (2000) for the SW Pacific Ocean. The smallest free-swimming porbeagles in the NMFS historical tagging database range in size from 55 to 79 cm FL (mean 71 cm FL)[7] from April to June; this length range, along with that of the one late-term litter (50–59 cm FL), suggests a birth size similar to Aasen's[4] (1963) prediction of 67 cm FL and to Francis and Steven's (2000) estimate of 58–67 cm FL for the SW Pacific. However, length at birth needs further analysis because few neonates were observed during the parturition period.

Acknowledgments

We thank Clearwater Fine Foods, Karlsen Shipping, the Atlantic Shark Association, and Stephanie Jane, Inc. for providing access to their fishing vessels. We thank Captain Steve James of the Boston Big Game Fishing Club for access to tournament-landed porbeagles from Stellwagan Bank. We also thank Warren Joyce and Andy Kingman for sample collection. Gregg Skomal of the Massachusetts Division of Marine Fisheries coordinated our participation in the porbeagle tournament. Malcolm Francis kindly provided data on embryo growth from the Southern Hemisphere, and corresponding data that he compiled from the Northern Hemisphere, and reviewed an early draft. We also thank Jose Castro for reviewing an early draft.

Literature cited

Aasen, O.
1963. Length and growth of the porbeagle (*Lamna nasus*, Bonnaterre) in the North West Atlantic. Fisk. Skrift. Ser. Havund. 13(6):20–37.

Bigelow, H. B., and W. C. Schroeder.
1948. Fishes of the Western North Atlantic. Part 1. Lancelets, cyclostomes, sharks. Mem. Sears Found. Mar. Res., 576 p.

Castro, J. I.
1993. The biology of the finetooth shark, *Carcharhinus isodon*. Environ. Biol. Fish. 36:219–232.
1996. The biology of the blacktip shark, *Carcharhinus limbatus*, off the Southeastern United States. Bull. Mar. Sci. 59(3):508–522.
2000. The biology of the nurse shark, *Ginglymostoma cirratum*, off the Florida east coast and the Bahama Islands. Environ. Biol. Fish. 58:1–28.

Compagno, L. J. V.
1984. FAO species catalogues. Vol. 4. Sharks of the world. An annotated and illustrated catalogue of the shark species known to date, parts 1 and 2. FAO Fish. Synopsis 125, vol. 4, parts 1 and 2, 655 p. FAO, Rome.

Dunlop, J.
1897. The habits and anatomical structure of the porbeagle shark (*Lamna cornubica*, L, Cuv.). Proceedings and Trans-

[7] Francis, M. 2000. Personal commun. National Institute of Water and Atmospheric Research P.O. Box 14-901, Kilbirnie, Wellington, New Zealand.

actions of the Natural History Society of Glasgow 4:136–137.

Francis, M. P., and J. D. Stevens.
2000. Reproduction, embryonic development, and growth of the porbeagle shark, *Lamna nasus*, in the southwest Pacific Ocean. Fish Bull. 98:41–63.

Fujita, K.
1981. Oviphageous embryos of the pseudocarchariid shark, *Pseudocarcharias kamoharai*, from the central Pacific. Jap. J. Ichthyol. 28:37–44.

Gauld, J. A.
1989. Records of porbeagles landed in Scotland, with observations on the biology, distribution and exploitation of the species. Scot. Fish. Res. Rep. 45, 15 p.

Gilmore, R. G., J. W. Dodrill, and P. A. Linley.
1983. Reproductive and embryonic development of the sandtiger shark, *Odontaspis taurus* (Rafinesque). Fish. Bull. 81(2):201–225.

Gruber, S. H., and L. J. V. Compagno.
1981. Taxonomic status and biology of the bigeye thresher, *Alopias superciliosus*. Fish. Bull. 79(4):617–640.

Gubanov, Y. P.
1972. On the biology of the thresher shark, *Alopias vulpinus* (Bonnaterre), in the northwest Indian Ocean. J. Ichthyol. 12(4):591–600.

Lohberger, J.
1910. Über zwei riesige Embryonen von *Lamna*. Abhand. Math.-Phys. Klasse König Bayer. Akad. Wissen. München suppl. Bd. 4 no. 2 Abhandlung, 45 p.

Matthews, L. H.
1950. Reproduction of the basking shark, *Cetorhinus maximus* (Gunnerus). Phil. Trans. R. Soc. Lond., Ser. B., Biol. Sci. 234:247–316.

Mollet, H. F., G. Cliff, H. L. Pratt Jr., and J. D. Stevens.
2000. Reproductive biology of the female shortfin mako, *Isurus oxyrinchus*, Rafinesque, 1810 with comments on the embryonic development of lamnoids. Fish. Bull. 98:299–318.

Natanson, L. J., J. J. Mello, and S. E. Campana.
2002. Validated age and growth of the porbeagle shark, *Lamna nasus*, in the western North Atlantic Ocean. Fish. Bull. 100:266–278.

Parsons, G. R.
1983. The reproductive biology of the Atlantic sharpnose shark, *Rhizoprionodon terraenovae* (Richardson). Fish. Bull. 81:61–73.

Pratt, H. L., Jr.
1979. Reproduction in the blue shark, *Prionace glauca*. Fish. Bull. 77:445–470.
1993. The storage of spermatozoa in the oviducal glands of western North Atlantic sharks. Environ. Biol. Fish. 38: 139–149.
1996. Reproduction in the male white shark. *In* Great white sharks, the biology of *Carcharodon carcharias*. Proceedings of the symposium on the biology of the white shark, Bodega Marine Lab., Bodega, CA, 4 March, 1993 (A. P. Klimley and D. G. Ainley, eds.), p. 131–138). Acad. Press, San Diego, CA.

Schwartz, F. J.
1984. Occurrence, abundance, and biology of the blacknose shark, *Carcharhinus acronotus* in North Carolina. NE Gulf Sci. 7(1):29–47.

Shann, E. W.
1911. A description of the advanced embryonic stage of *Lamna cornubica*. Ann. Rep. Fish. Board Scotland 28(3): 73–79.
1923. The embryonic development of the porbeagle shark, *Lamna cornubica*. Proc. Zool. Soc. Lond. 11:161–171.

Stevens, J. D.
1974. The occurrence and significance of tooth cuts on the blue shark (*Prionace glauca* L.) from British waters. J. Mar. Biol. Assoc. U.K. 54:373–378.

Svetlov, M. F.
1978. The porbeagle, *Lamna nasus*, in Antarctic waters. J. Icthyol. 18(5):850–851.

Swenander, G.
1907. Über die Ernährung des Embryos der *Lamna cornubica*. Zool. Stud. Tullberg, Uppsala 1907:283–288.

Templeman, W.
1963. Distribution of sharks in the Canadian Atlantic (with special reference to Newfoundland waters). Bull. Fish. Res. Board Can. 140, 77 p.

Integration of submersible transect data and high-resolution multibeam sonar imagery for a habitat-based groundfish assessment of Heceta Bank, Oregon*

Nicole M. Nasby-Lucas
Pfleger Institute of Environmental Research
901-B Pier View Way
Oceanside, California 92054
E-mail address: nnasby@yahoo.com

Bob W. Embley
Pacific Marine Environmental Laboratory, NOAA
Hatfield Marine Science Center
Newport, Oregon 97365

Mark A. Hixon
Department of Zoology
Oregon State University
Corvallis, Oregon 97331

Susan G. Merle
Cooperative Institute for Marine Resources Studies
Hatfield Marine Science Center
Newport, Oregon 97365

Brian N. Tissot
Program in Environmental Science and Regional Planning
Washington State University
Vancouver, Washington 98686

Dawn J. Wright
Department of Geosciences
Oregon State University
Corvallis, OR 97331

Abstract—In the face of dramatic declines in groundfish populations and a lack of sufficient stock assessment information, a need has arisen for new methods of assessing groundfish populations. We describe the integration of seafloor transect data gathered by a manned submersible with high-resolution sonar imagery to produce a habitat-based stock assessment system for groundfish. The data sets used in this study were collected from Heceta Bank, Oregon, and were derived from 42 submersible dives (1988–90) and a multibeam sonar survey (1998). The submersible habitat survey investigated seafloor topography and groundfish abundance along 30-minute transects over six predetermined stations and found a statistical relationship between habitat variability and groundfish distribution and abundance. These transects were analyzed in a geographic information system (GIS) by using dynamic segmentation to display changes in habitat along the transects. We used the submersible data to extrapolate fish abundance within uniform habitat patches over broad areas of the bank by means of a habitat classification based on the sonar imagery. After applying a navigation correction to the submersible-based habitat segments, a good correlation with major boundaries on the backscatter and topographic boundaries on the imagery were apparent. Extrapolation of the extent of uniform habitats was made in the vicinity of the dive stations and a preliminary stock assessment of several species of demersal fish was calculated. Such a habitat-based approach will allow researchers to characterize marine communities over large areas of the seafloor.

Manuscript accepted 29 May 2002.
Fish. Bull. 100:739–751 (2002).

Dramatic declines in several groundfish populations have occurred along the U.S. West Coast during the last decade (Ralston, 1998; PFMC[1]; Sampson,[2] Bloeser[3]). One problem exacerbating these declines is that current stock assessments are not sufficiently precise or accurate to effect empirically based management. This is especially true for commercially important species of rockfish (Scorpaenidae, *Sebastes*), which comprise major groundfish fisheries along the Pacific Coast. Although evidence has accumulated for substantial declines in the abundance of several species of rockfish, the overall picture is unclear because 42 of 54 rockfish species (78%) have never been assessed (Ralston, 1998; NMFS, 1999; Bloeser[3]). Of the 12 species that have been assessed by the National Marine Fisheries Service, five were listed as "overfished" and one species was listed as "approaching overfished condition" (NMFS, 1999).

A possible alternative to single-species stock assessments of demersal fishes is a habitat-based community assessment, which serves to estimate groundfish population sizes by recognizing that species are not randomly distributed among varying habitats. It is known that the diversity, quality, and extent of bottom habitats are important in determining the distribution, abundance, and diversity of rockfishes (Carlson and Straty, 1981; Pearcy et al., 1989; Carr, 1991; Stein et al., 1992; O'Connell and Carlile, 1993). It has been previously demonstrated, within local study areas, that species richness and composition correlate with seafloor texture (Hallacher and Roberts, 1985; Richards, 1986; Love et al., 1991; Stein et al., 1992; Krieger, 1993; Yoklavich et

* Contribution 2477 of the Pacific Marine Laboratory, Newport, Oregon 97365.

[1] PFMC (Pacific Fishery Management Council). 1999. Status of the Pacific Coast groundfish gishery through 1999 and recommended acceptable biological catches for 2000: stock assessment and fishery evaluation, 75 p. Pacific Fishery Management Council, 7700 NE Ambassador Place, Suite 200, Portland, OR 97220.

[2] Sampson, D. B. 1997. Effective fishing effort in the Oregon groundfish trawl fishery. Final report to the Oregon Trawl Commission, 80 p. Oregon Trawl Commission, P.O. Box 569, Astoria, OR 97103.

[3] Bloeser, J. A 1999. Diminishing returns: the status of west coast rockfish. Pacific Marine Conservation Council, P.O. Box 59, Astoria, OR 97103.

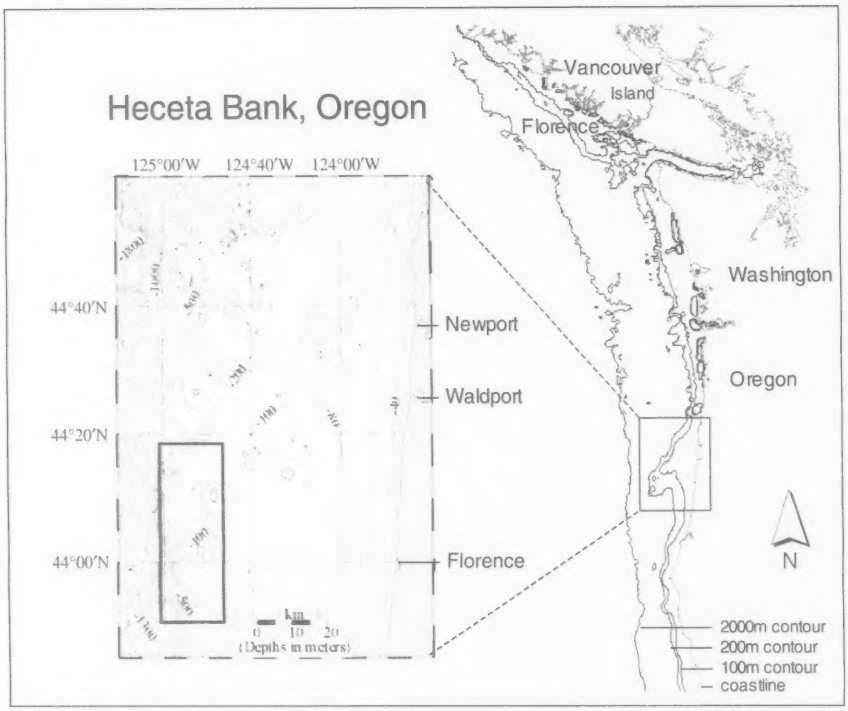

Figure 1

Location of Heceta Bank and the adjacent continental margin in relation to the Oregon coast. The survey area is outlined in bold lines.

al., 2000; Hixon et al.[4]; Hixon and Tissot[5]). Correlations over larger regions have been difficult to determine because of the limitations in the resolution and areal coverage of bathymetric charts, which are crucial in providing broad-scale habitat data. However, this difficulty no longer exists with the advent of differential GPS and high-resolution sonar systems (Hughes Clarke et al., 1996). When adequately groundtruthed, these new systems provide bathymetric and backscatter data with sufficient resolution to formulate habitat classifications over broad areas of the continental shelf and slope (Able et al., 1987; Yoklavich et al., 1995; Greene et al.[6]; Fox et al.[7]).

We developed this habitat-based groundfish assessment strategy by integrating a comprehensive submersible survey with new high-resolution sonar imagery of the seafloor. Sonar images produce habitat data by using acoustic signals to differentiate areas of hard substrata from surrounding soft sediments based on differences in the intensity of reflected sound. This technology has the distinct advantage of examining large regions of seafloor sediment and geological topographic features without relying on expensive direct underwater bottom sampling and observation techniques. Sonar data can be used in an assessment of seafloor habitat and fish density over large areas by extrapolating from direct observations of fish and seafloor morphology transects using manned submersibles or remotely operated vehicles.

The study site for this assessment was Heceta Bank, a 50-km long outcrop on the outer shelf of central Oregon (Fig. 1). Heceta Bank is the largest rocky reef of the Pacific Northwest and is characterized by high variability in bottom types and textures. The bank provides a diversity of habitat types for many species of groundfish and

[4] Hixon, M. A., B. N. Tissot, and W. G. Pearcy. 1991. Fish assemblages of rocky banks of the Pacific northwest. Final report, OCS Study MMS 91-0052, 410 p. USDI Minerals Management Service, 770 Pasea, Camarillo, CA 93010.

[5] Hixon, M. A., and B. N. Tissot. 1992. Fish assemblages of rocky banks of the Pacific northwest. Final report supplement, OCS Study MMS 92-0025, 128 p. USDI Mineral Management Service, 770 Pasea, Camarillo, CA 93010.

[6] Greene, H. G., M. M. Yoklavich, D. Sullivan, and G. Cailliet. 1995. A geophysical approach to classifying marine benthic habitats: Monterey Bay as a model. Alaska Department of Fish and Game Special Publ. 9, p. 15-30. Alaska Department of Fish and Game, P.O. Box 25526, Juneau, AK 99802.

[7] Fox, D., M. Amend, and A. Merems. 1999. Nearshore rocky reef assessment. Coastal Management Section 309 Grant. Contract No. 99-072. Oregon Department of Fish and Wildlife, 2040 SE Marine Science Drive, Newport, OR 97365

invertebrates. These characteristics have made Heceta Bank one of the largest and most important of the heavily fished rocky banks in the Pacific Northwest. Along with its commercial importance, the bank has been the subject of substantial scientific research, which has made it an ideal site for developing these methods.

Direct observations of Heceta Bank were first made in 1987 in a series of 16 submersible dives used to characterize fish populations and habitats on the bank (Pearcy et al., 1989). These initial dives were used to select representative transects which were repeated in 1988, 1989, and 1990 using the manned research submersible *Delta* (Hixon et al.[4]; Stein et al., 1992). The objective of these surveys was to investigate relationships between the abundance of groundfish and macroinvertebrates and the topography and texture of the seafloor, as well as to document interannual variation in these relationships. Fish observed during these surveys included 69 taxa, representing 24 families, dominated by 24 species of rockfish. Multivariate analysis detected statistical relationships between habitat characteristics and fish distribution and abundance by species and provided comprehensive data on fish-habitat associations, as well as a baseline for future comparisons.

Although invaluable, data from this set of submersible dives provided detailed "snapshots" of very limited areas of the Bank. To complement this study and to provide a broad view of the bank, a survey was performed in 1988 with hull-mounted, Simrad EM300 multibeam sonar, which provided high-resolution bathymetry and backscatter imagery of most of Heceta Bank (Merle et al.[8]).

Materials and methods

Submersible dives

Submersible observation data were collected by using the manned submersible *Delta* at six predetermined stations along Heceta Bank. Detailed descriptions of submersible operations used in our study can be found in Hixon et al.[4] and Stein et al. (1992), and a brief description follows. Surveys were conducted in the month of September and consisted of 18 dives in 1988, 12 in 1989, and 12 in 1990, for a total of 42 dives and 84 transects (Fig. 2). Each dive consisted of two 30-minute timed transects and a 10–15 minute "quiet period" between transects to assess the effects of the submersible's lights and motors on local fish distribution. The average length of each 30-minute transect was approximately 1015 m. Data on fish species, size, and abundance were collected by direct observations through the forward view port from approximately 2 m above the bottom, providing a bracketed transect width of about 2.3 m. During the transects, observations were verbally tape-recorded and visually recorded with a VHS

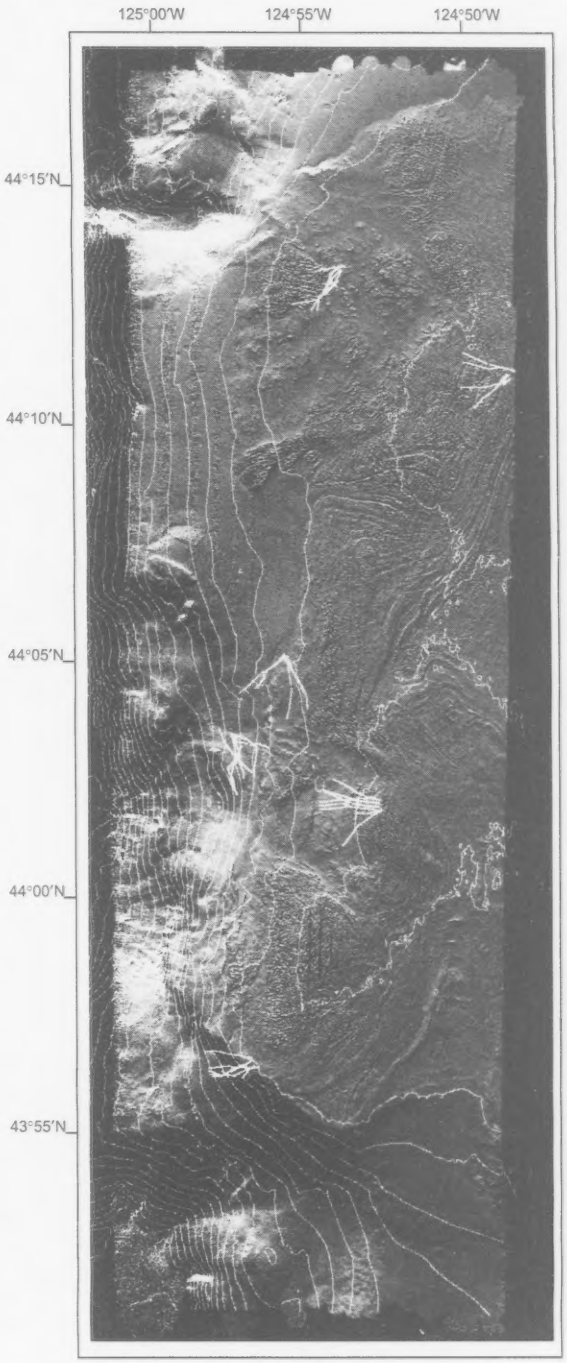

Figure 2

Simrad EM300 multibeam bathymetry illuminated from the northwest, which creates shadows to the southeast of the relief. The 1988, 1989, and 1990 *Delta* submersible transects (six clusters of white lines) have been overlaid on top of the bathymetric data. The isobathymetric contours are at 50-m intervals, beginning with 100 m on the east side of the bank.

[8] Merle, S., R. W. Embley, J. Reynolds, D. Clague, C. Goldfinger, and R. Yeats. 1998. A high-resolution image over the Heceta Bank off Central Oregon. Trans. Am. Geophys. Union 78, Fall Meeting Suppl., F818.

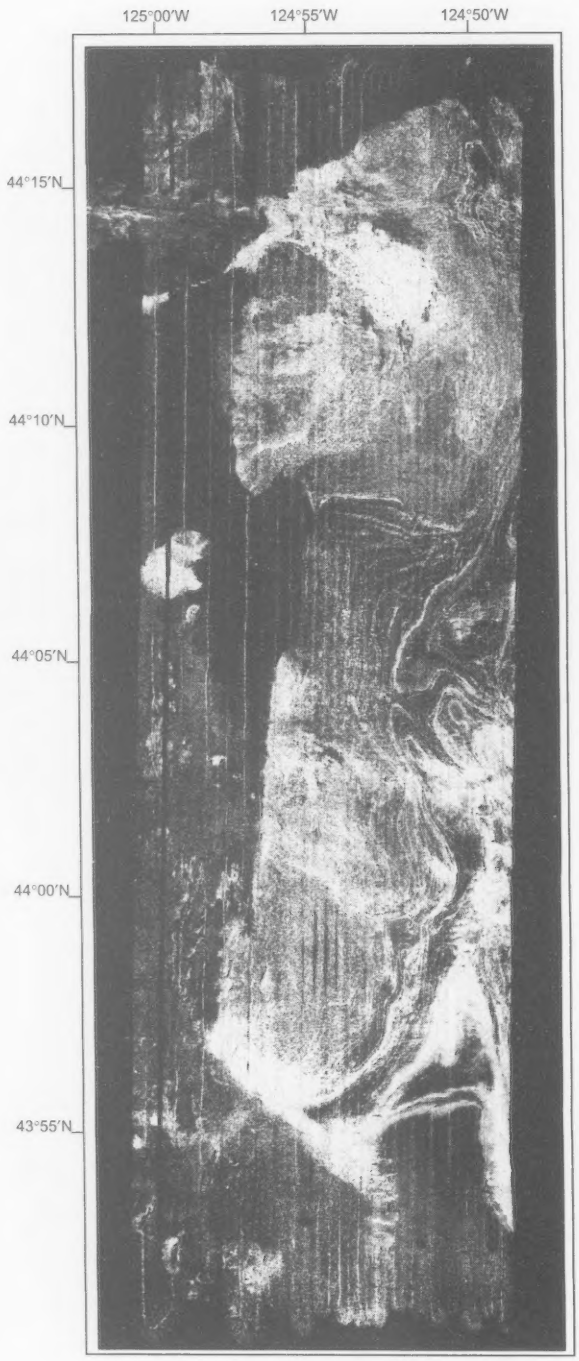

Figure 3

Backscatter imagery of Heceta Bank from Simrad EM300 multibeam survey. The lighter the shading the higher the reflectivity of the substratum.

videotape equipped with a timed data logger and audio track.

Direct and videotaped observations along the transects consisted of the number of species of fish and macroinvertebrates, and bottom-type characteristics. Fishes along the transects were identified, counted, and lengths were estimated to the nearest decimeter with a three-decimeter fiberglass rod suspended within the observer's view. Bottom type was categorized from videotapes by using a two-code combination, the first letter indicating the primary substratum (defined as covering at least 50% of the area viewed) and the second letter indicating the secondary substratum (defined as covering more than 20% of the area viewed). If the field of view was a single substratum, or the second most abundant substratum covered less than 20% of the field, the same letter was employed twice (e.g. MM for pure mud). The seven possible categories in order of increasing particle size or relief were mud (M), sand (S), pebble (P, diameter <6.5 cm), cobble (C, >6.5 and <25.5 cm), boulder (B, >25.5 cm), continuous flat rock (F, low vertical relief), and diagonal rock ridge (R, high vertical relief). The latitude and longitude positions of each transect were determined by using Loran-C with a Trackpoint II ultrashort baseline tracking system and by positioning the vessel directly above the submersible every 10 to 15 minutes. At least three position points were made per transect and the locations of bottom type and biological data were interpolated between these points. The absolute accuracy of the submersible's position, obtained by using Loran-C, was within about 150 to 500 m (Melton, 1986).

Multibeam sonar

The acoustic survey of Heceta Bank was conducted in May of 1998 with a Simrad EM300 (30 kHz) multibeam sonar system on the RV *Ocean Alert* (Merle et al.[8]). This survey provided a highly detailed, precisely navigated seafloor map of bathymetry and seafloor texture (Figs. 2 and 3). The data were processed with Swathed software (Hughes-Clarke et al., 1996). The data processing steps used in Swathed were the following: navigation and sounding editing, roll bias correction, tide correction, refraction correction, map sheet setup, gridding, and mosaicing which resulted in a composite map made up of acoustic backscatter imagery. The survey consisted of 47 overlapping north–south swaths up to 45 km long, which provided images of approximately 725 km^2 of the seafloor and nearly 100% coverage of high-resolution bathymetry and backscatter amplitude. These data were displayed in grids with a resolution of less than 5 meters on the shallowest portions of the bank from depths of 70 to 150 meters, and of about 5 to 10 meters at depths down to about 500 meters.

Data integration and habitat assessment

The sonar and submersible transect data were combined by using ArcView and ArcInfo geographic information system (GIS) software. The sonar data used were

bathymetry and backscatter and the submersible transect data included bottom type characteristics and fish density data. In order to represent the dive transects in GIS as linear features displaying changes in habitat and fish density, a dynamic segmentation data structure was used (ESRI, 1994).

Bottom type and fish density data to be displayed using dynamic segmentation were derived from transect observation data. Transects were divided into segments by uniform bottom type. Fish density was calculated along each segment of habitat type by using the data for the most common species observed, accounting for 90% of the total, plus a few rare species of commercial importance (i.e. lingcod, sablefish, Dover sole and rex sole). This complex of species consisted of a mixture of demersal and benthopelagic species. The following species were assessed: juvenile *Sebastes* sp. (unknown juvenile rockfish), *Sebastes chlorostictus* (greenstriped rockfish), *Sebastes wilsoni* (pygmy rockfish), *Sebastes helvomaculatus* (rosethorn rockfish), *Sebastes zacentrus* (sharpchin rockfish), *Sebastes flavidus* (yellowtail rockfish), *Ophiodon elongatus* (lingcod), *Sebastolobus alascanus* (shortspine thornyhead), *Anoplopoma fimbria* (sablefish), *Microstomus pacificus* (Dover sole), and *Errex zachirus* (rex sole). The density of fish (number per hectare) was calculated by taking the number of fish sighted in that habitat segment, dividing by the area of the habitat segment in meters, and multiplying by 10,000 square meters per hectare.

The use of dynamic segmentation data structure allowed for the display of changes in bottom type and fish density data within the transect lines. This was done by creating a "route" system in ArcInfo from the dive transect data and associating it with an "event table." The event table consisted of bottom type and fish density data, and their corresponding locations along the transect, and a route-identifier number to link the information to the corresponding transects in the route system. For visual display, bottom type segments were combined into three major habitat groups: 1) mud, which consisted of "MM" observations, 2) rock ridge, which consisted of "RR" observations, and 3) mixed substrate habitat, which consisted of combinations of all other bottom type observations.

In order to combine the sonar and submersible data sets, all segmented dive transect data were then reprojected with a 500-meter offset to the east. This was determined to be the best correction for discrepancies between the transect position data which were acquired by Loran-C and the sonar data which came from GPS positions. It was determined that this offset was necessary by comparing the two data sets and matching depth contours and borders of well-defined habitat, specifically interfaces between the mud and rock features of the bank. There did not appear to be a significant north–south offset, although this effect was more difficult to determine because the submersible transects did not cross any well-defined north–south boundaries. Transects segmented by both bottom type and fish density were overlaid on the sonar data in ArcView (Fig. 4, A–C).

Assessments of fish abundance within large habitat areas were performed by selecting patches of relative habitat homogeneity on the sonar map around the location of each submersible transect. These patches were chosen by examining both patterns in the backscatter values and topographic features indicated by the backscatter and bathymetric data. In areas of mud off the bank, borders were chosen by maintaining constant depth as well as equal distance from the bank. In selecting patches to represent areas of similar habitat, the boundaries were relatively well defined in areas of rock and mud, but for mixtures of sand, cobble, pebble, and boulder, it was more difficult to distinguish distinct boundaries and therefore these patch borders were drawn conservatively.

Using the observational data from the transects from all three years, we were able to characterize each habitat patch by percent bottom type, density of fish, and estimated abundance of fish as extrapolated from the dive transect data contained within that patch. The grand mean density and standard error for each species was determined by using a weighted density for each habitat segment based on a proportion of the length of that segment to the overall transect distance within that habitat patch. The grand mean density was calculated as

$$x = \sum_{i=1}^{n} d_i p_i, \tag{1}$$

where $x = \bar{x}$;
d = density of fish within a segment of continuous bottom type; and
p = bottom type segment length/total transect length within the patch.

This calculation used the associations of the fish species with substrate type and weighted its contribution to the overall density by the comparative length of that segment. Total fish abundance for each habitat patch was determined by multiplying the area of the patch and the grand mean density and standard error of each species. The total abundance for each species for all habitat patches was determined by adding the abundance for that species for all eight habitat patches. The standard error for the total abundance for each species was determined by calculating a grand mean standard error weighted by using the standard error of each habitat patch multiplied by the proportion of the abundance of that species for that habitat patch to the overall abundance for that species. Total abundance standard error was calculated by using Equation 1 where x = SE; d = standard error of fish abundance within a habitat patch; and p = abundance within that habitat patch/total abundance in all eight patches.

Results

Comparing the submersible data with the sonar data, we found that there was high correlation between the direct observations of bottom type and the habitat type indicated by the sonar data. Side-lit bathymetry revealed areas of outcropping substrata and the backscatter data

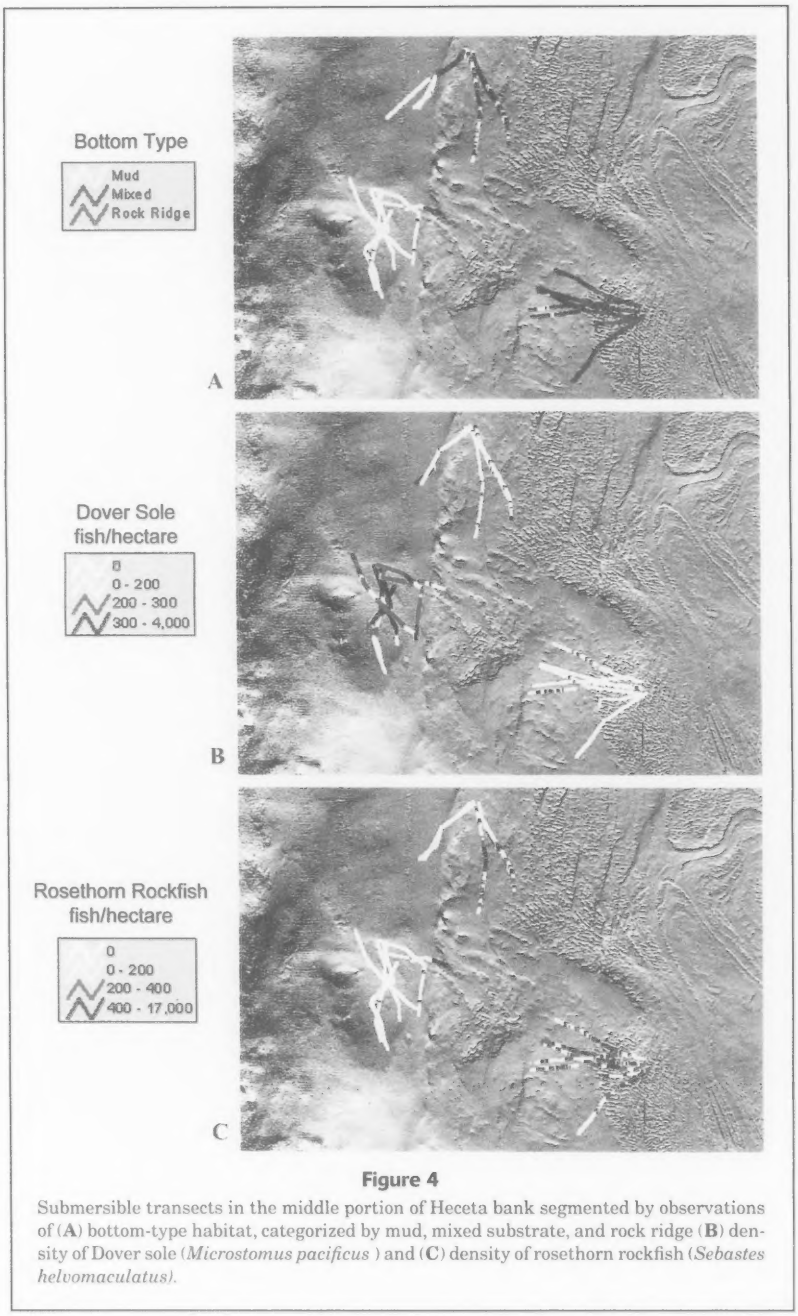

Figure 4

Submersible transects in the middle portion of Heceta bank segmented by observations of (**A**) bottom-type habitat, categorized by mud, mixed substrate, and rock ridge (**B**) density of Dover sole (*Microstomus pacificus*) and (**C**) density of rosethorn rockfish (*Sebastes helvomaculatus*).

showed changes in seafloor texture. Borders of rock ridge and mud observed in the submersible survey matched the bathymetric data, indicating areas of high relief for rocky patches and low relief for areas of mud (Figs. 4A and 5). Changes in backscatter also corresponded with changes observed in bottom type from the submersible data (Fig. 5). It was noted consistently that high-backscatter areas were associated with mixed substrate habitat, comprising a combination of pebble, cobble, and boulder, which due to their size and geologic composition have a relatively high reflectivity. Mid-backscatter values were found to be associated with rock ridge features. These are typically

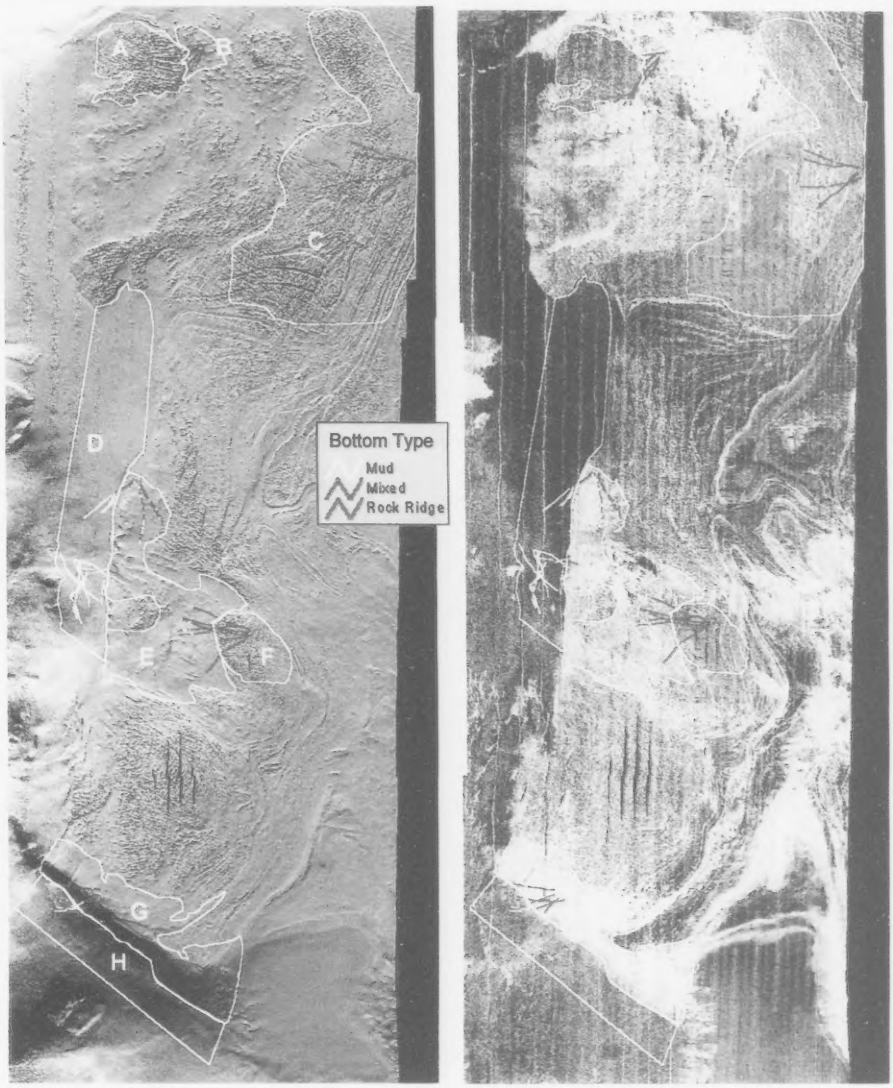

Figure 5

Habitat patch boundaries and transects segmented by bottom type overlaid on both bathymetric and backscatter sonar images. Habitat patches are labeled A–H. The bottom-type observations were grouped into three predominant habitats: mud, mixed substrate, and rock ridge.

large-scale rolling ridges with less small-scale relief. Low-backscatter values were associated with mud bottoms, which have characteristically low reflectivity.

Eight regional patch boundaries were drawn based on areas of relative homogeneous seafloor sonic characteristics around the six stations surveyed by submersible (Fig. 5). These patches (labeled A–H) ranged from 1.8 km^2 (patch B) to 38.9 km^2 (patch C) (Table 1). Patch boundaries for A, C, and F were drawn around areas of mid-backscatter reflectivity and high relief indicated by the bathymetric data, and were located in relatively shallow areas of the bank (75–125 m). Patch boundaries for D and H were drawn around mud areas located off the edge of the bank, which exhibited low-backscatter values, low relief on the bathymetric data, and were located in deeper waters (150–300 m). Patch boundaries for B, E, and G were drawn around areas of high backscatter and were present in intermediate depths (100–150 m).

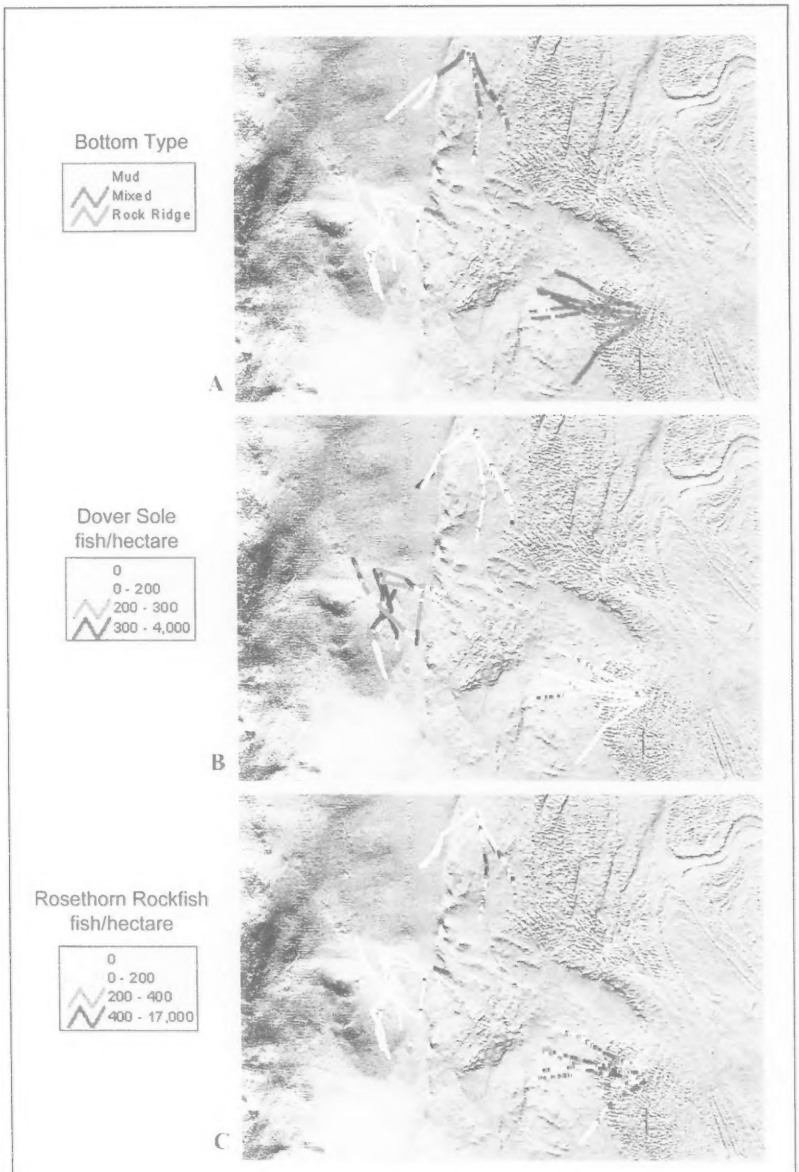

Figure 4

Submersible transects in the middle portion of Heceta bank segmented by observations of (**A**) bottom-type habitat, categorized by mud, mixed substrate, and rock ridge (**B**) density of Dover sole (*Microstomus pacificus*) and (**C**) density of rosethorn rockfish (*Sebastes helvomaculatus*).

showed changes in seafloor texture. Borders of rock ridge and mud observed in the submersible survey matched the bathymetric data, indicating areas of high relief for rocky patches and low relief for areas of mud (Figs. 4A and 5). Changes in backscatter also corresponded with changes observed in bottom type from the submersible data (Fig. 5).

It was noted consistently that high-backscatter areas were associated with mixed substrate habitat, comprising a combination of pebble, cobble, and boulder, which due to their size and geologic composition have a relatively high reflectivity. Mid-backscatter values were found to be associated with rock ridge features. These are typically

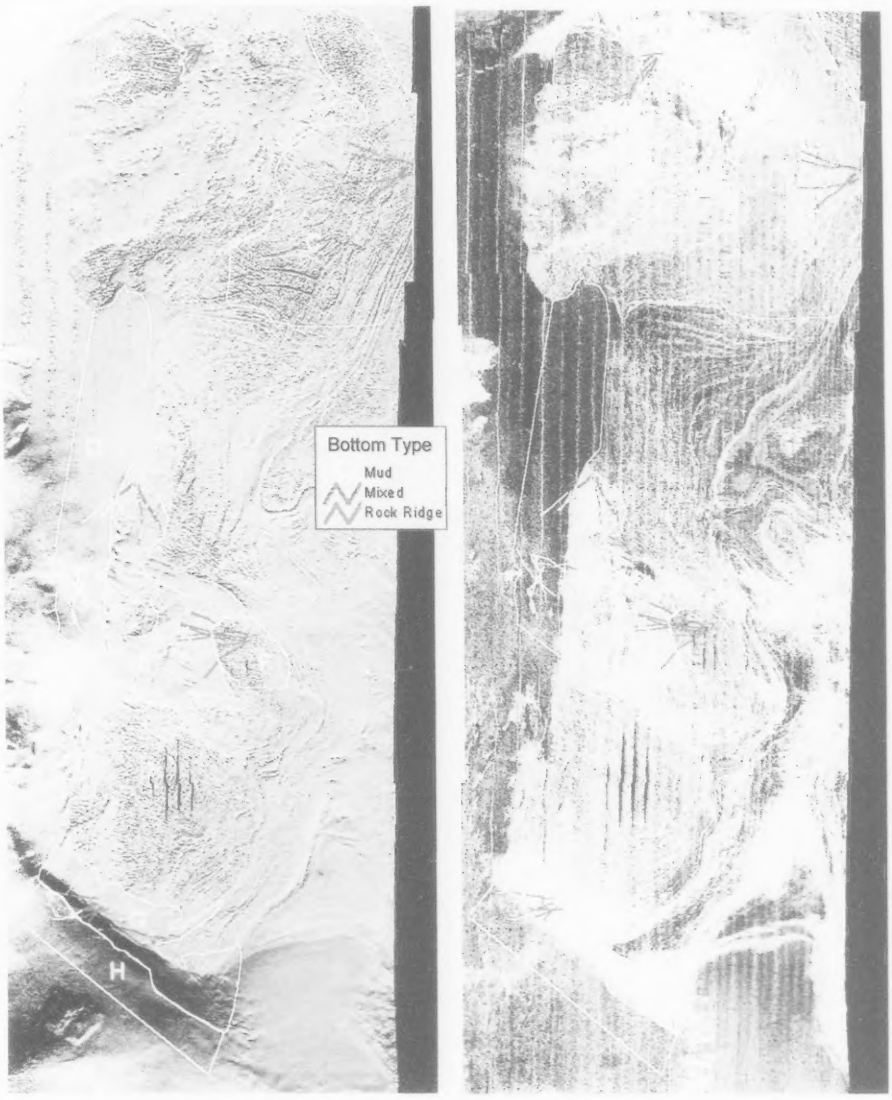

Figure 5

Habitat patch boundaries and transects segmented by bottom type overlaid on both bathymetric and backscatter sonar images. Habitat patches are labeled A–H. The bottom-type observations were grouped into three predominant habitats: mud, mixed substrate, and rock ridge.

large-scale rolling ridges with less small-scale relief. Low-backscatter values were associated with mud bottoms, which have characteristically low reflectivity.

Eight regional patch boundaries were drawn based on areas of relative homogeneous seafloor sonic characteristics around the six stations surveyed by submersible (Fig. 5). These patches (labeled A–H) ranged from 1.8 km^2 (patch B) to 38.9 km^2 (patch C) (Table 1). Patch boundaries for A, C, and F were drawn around areas of mid-backscatter reflectivity and high relief indicated by the bathymetric data, and were located in relatively shallow areas of the bank (75–125 m). Patch boundaries for D and H were drawn around mud areas located off the edge of the bank, which exhibited low-backscatter values, low relief on the bathymetric data, and were located in deeper waters (150–300 m). Patch boundaries for B, E, and G were drawn around areas of high backscatter and were present in intermediate depths (100–150 m).

Table 1

Estimated mean fish density and abundance (± standard error) by habitat patch (A–H) and species at Heceta Bank, Oregon. Density is in number of fish/hectare, abundance numbers are × 1000, and n = number of bottom type segments.

		Habitat patch								
		A	B	C	D	E	F	G	H	
	Habitat type	Rock ridge	Mixed	Rock ridge	Mud	Mixed	Rock ridge	Mixed	Mud	
	Area (km^2)	6.2	1.78	38.9	25.1	19.9	5.05	15.5	12.0	Total
Fish taxa	n	81	137	262	51	268	219	58	44	124
Juvenile rockfish	density	1140 ±536	1001 ±385	25,577 ±6521	2 ±1	95 ±217	4709 ±5309	30 ±12	0 ±0	
Sebastes sp.	abundance	711 ±335	178 ±69	99,595 ±25,394	6 ±3	190 ±433	2380 ±2683	46 ±18	0 ±0	103,110 ±24,593
Greenstriped rockfish	density	108 ±23	137 ±27	3 ±3	18 ± 13	232 ±23	10 ±4	65 ±23	0 ±0	
S. elongatus	abundance	68 ±15	24 ±5	13 ±10	46 ±32	463 ±46	5 ±2	101 ±35	0 ±0	759 ±37
Pygmy rockfish	density	2195 ±536	12,435 ±3392	3586 ±1264	0 ±0	2260 ±1139	12,119 ±3531	3236 ±581	0 ±0	
S. wilsoni	abundance	1370 ±335	2218 ±605	13,962 ±4922	0 ±0	4509 ±2273	6125 ±1785	5016 ±901	0 ±0	35,041 ±2746
Rosethorn rockfish	density	367 ±56	540 ±54	379 ±55	10 ± 24	238 ±21	473 ±121	595 ±88	5 ±2	
S. helvomaculatus	abundance	229 ±5	96 ±10	1478 ±213	24 ±61	475 ±43	239 ±61	922 ±137	6 ±2	3643 ±134
Sharpchin rockfish	density	265 ±71	1632 ±308	0 ±0	9 ±16	727 ±112	2 ±0.5	2916 ±505	0 ±0	
S. zacentrus	abundance	166 ±44	291 ±55	0 ±0	23 ±40	1450 ±224	1 ±0	4519 ±783	0 ±0	7552 ±515
Yellowtail rockfish	density	885 ±535	639 ±224	287 ±101	0 ±0	6 ±4	1578 ±421	0 ±0	0 ±0	
S. flavidus	abundance	552 ±334	114 ±40	1116 ±391	0 ±0	13 ±8	797 ±213	0 ±0	0 ±0	2747 ±289
Lingcod	density	2 ±5	4 ±5	27 ±5	0 ±0	3 ±2	23 ±70	9 ±3	0 ±0	
O. elongatus	abundance	1 ±3	1 ±1	103 ±19	0 ±0	6 ±3	12 ±35	14 ±4	0 ±0	143 ±17
Shortspine thornyhead	density	0 ±0	0 ±0	0 ±0	228 ±41	0 ±0	0 ±0	199 ±72	457 ±46	
S. alascanus	abundance	0 ±0	0 ±0	0 ±0	575 ±104	0 ±0	0 ±0	309 ±111	549 ±56	1433 ±87
Sablefish	density	0 ±0	0 ±0	0 ±0	52 ±10	0.7 ±0.6	0 ±0	23 ±25	96 ±35	
A. fimbria	abundance	0 ±0	0 ±0	0 ±0	131 ±25	1 ±1	0 ±0	36 ±39	116 ±42	284 ±34
Dover sole	density	28 ±20	41 ±17	0 ±0	312 ±33	79 ±14	8 ±5	137 ±71	217 ±29	
M. pacificus	abundance	17 ±12	7 ±3	0 ±0	786 ±82	158 ±29	4 ±3	212 ±110	260 ±35	1445 ±70
Rex sole	density	0 ±0	7 ±6	0 ±0	143 ±18	23 ±7	0 ±0	3 ±3	24 ±14	
E. zachirus	abundance	0 ±0	1 ±1	0 ±0	359 ±44	46 ±15	0 ±0	5 ±5	29 ±17	440 ±39
Total abundance		3115 ±288	2932 ±469	116,267 ±22,350	1949 ±28	7312 ±1464	9563 ±1830	11,181 ±738	960 ±47	156,598 ±16,854

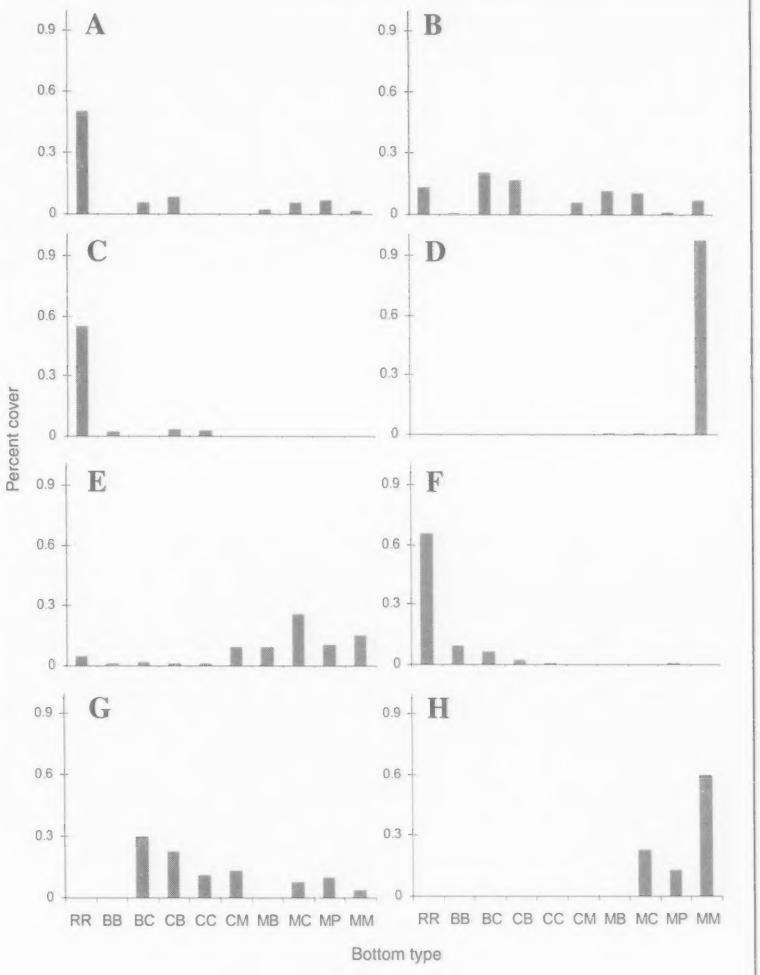

Figure 6

Percent cover of bottom types calculated from observations of all transects contained within each of the eight habitat patches labeled A–H. Bottom types are listed from left to right by decreasing relief and particle size, where the first letter is the dominant substratum and the second letter is the second most prevalent substratum. Substrate categories shown comprise only the 10 most dominant bottom types, consisting of combinations of R = rock ridge, B = boulder, C = cobble, M = mud, and P = pebble.

Combining the sonar-derived habitat patches and submersible observations gave an indication of bottom-type compositions for the defined patches. Of the eight habitat patches analyzed, three of the habitat patches were predominantly rock ridge (patch A—63% RR and 14% RC/RB; patch C—55% RR and 3% RB/RC; and patch F—66% RR), two were predominantly mud (patch D—98% MM; and patch H—60% MM and 36% MC/MP), and three were a mixture of boulder, cobble, pebble, and mud (patch B—75% BC/CB/MB/MC/MM/CM/MP/BM/BB; patch E—83% MC/MM/MP/CM/MB/CP/BM/BC/CB/PM/CC/BB/BP/PB; and patch G—100% BC/CB/CM/CC/MP/MC/MM/PM/BB) (Fig. 6).

There were differences in fish density within the patches between the three major habitat classification types, as well as differences among patches of similar bottom types (Fig. 7, Table 1). Species with the highest association with rock-ridge habitat patches were yellowtail rockfish, juvenile rockfish, and lingcod. Those primarily associated with mud habitats were Dover sole, rex sole, and shortspine thornyheads. Those associated with mixed substrate patches were sharpchin rockfish, rosethorn rockfish, green-

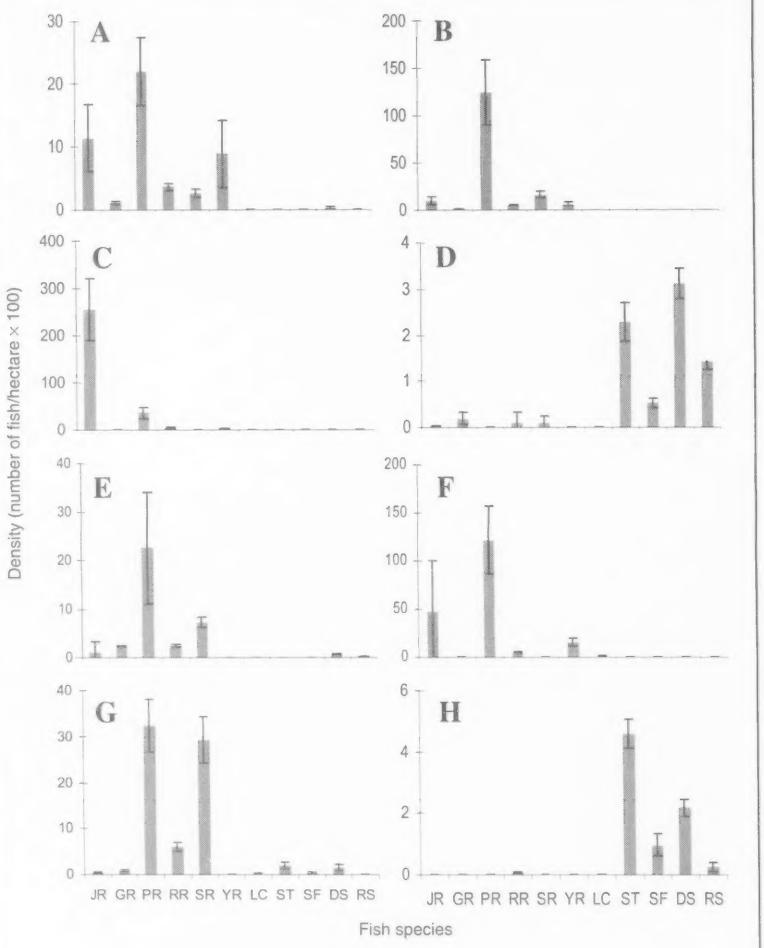

Figure 7

Fish densities (mean ±SE) for each habitat patch calculated from all transects contained within each patch. JR = juvenile rockfish (*Sebastes* species); GR = greenstriped rockfish (*Sebastes elongatus*); PR= pygmy rockfish (*Sebastes wilsoni*); RR = rosethorn rockfish (*Sebastes helvomaculatus*); SR = sharpchin rockfish (*Sebastes zacentrus*); YR = yellowtail rockfish (*Sebastes flavidus*); LC = lingcod (*Ophiodon elongatus*); ST = shortspine thornyhead (*Sebastolobus alascanus*); SB = sablefish (*Anoplopoma fimbria*); DS = Dover sole (*Microstomus pacificus*); and RS = rex sole (*E. zachirus*).

striped rockfish, and pygmy rockfish. Juvenile rockfish were found predominantly in rock-ridge habitats, and found in substantially high density (25,577 [±6521] fish/hectare) in patch C as compared with the other rock ridge patches (patch A 1140 [±536] fish/hectare and patch F 4709 [±5309] fish/hectare). Both Dover sole and rex sole were associated with mud habitat, and both were found in higher densities in patch D (Dover sole—312 [±33] fish/hectare, rex sole—143 [±18] fish/hectare) than patch H (Dover sol—217 [±29] fish/hectare, rex sole—24 [±14] fish/hectare). Pygmy rockfish were found in high density in mixed substrate patches B and F (12,435 [±3392] fish/hectare and 12,119 [±3531] fish/hectare) but at a substantially lower density in patch G (3236 [±81] fish/hectare).

Among all eight patches, the species found in the highest abundance overall were juvenile rockfish and pygmy rockfish, and those in the lowest abundance were lingcod and sablefish (Table 1). The total area of all habitats assessed was 124 km^2, which is approximately 17% of the total area of the sonar survey, and the total number of estimated fish and standard error for that area was 156,598,000 ±16,854,000. The coefficient of variation was relatively low

for greenstriped rockfish, rosethorn rockfish, sharpchin rockfish, shortspine thornyhead, and Dover sole (between 3.7% and 6%) and slightly higher for pygmy rockfish, yellowtail rockfish, lingcod, sablefish, and rex sole (between 7.8% and 11.9%).

Discussion

A primary finding of our study was that distinct bottom types found on Heceta Bank are distinguishable through the use of sonar data and that these interpreted habitats correlate with direct submersible observations of bottom type. The determination of habitat information from sonar data is significant in that it provides a broad-scale view of the seafloor habitat, previously unavailable, and allows a habitat-based groundfish assessment. Although seafloor imaging and GIS techniques have previously been used in the study of marine habitats (e.g. Meaden, 1999; McRea et al., 1999; Sherin, 1999; Yoklavich et al., 2000), ours is one of the first published studies where GIS technique was used to combine a detailed analysis of fish and habitat transect data with broad-area high-resolution sonar seafloor imagery and where total fish abundances were calculated for large areas of the seafloor (see also O'Connell et al.[9]).

Habitat type could not be determined by bathymetry or backscatter data alone, but the information provided by both data sets, in addition to groundtruthing by direct submersible observation, gives a clearer picture of the overall habitat environment. The use of the backscatter data combined with the bathymetric data has the advantage of providing an indication of substrate type, which is clearly important in fish-habitat associations. In general, however, backscatter provides a better indication of habitat for fish association purposes. Bathymetric data can provide geological structure on the resolution of five to ten meters, whereas backscatter data give an indication of structural variation on a smaller scale, which is of ecological importance in influencing the distribution of groundfish. For example, the physical properties of a substrate influence the types of invertebrates that colonize the seafloor, and local relief can provide microhabitats for some fish.

The extent to which a groundfish habitat can be effectively mapped by remote sensing is determined by the resolution of the system used. In general, sonars are optimized for specific operational depth ranges. A system designed for very shallow water can have sufficient resolution to provide contours of features or objects that deeper water (lower frequency and longer range) systems will only "see" as backscatter changes. As more sites are studied by combining visual seafloor transects, high-resolution sonar, and GIS techniques, it is likely the geologic indices most relevant to groundfish habitats will become apparent. These methods should lead to a more coherent approach to habitat-based stock assessments.

One of the limitations of this habitat-based approach to stock assessments has to do with strong reliance upon the fish-substratum association. The distribution and abundance of groundfish has been shown to be strongly correlated with substrate type (see introduction), but fish distributions and densities may vary with other factors as well, such as depth, currents, nutrients, and food availability. In this study there was an attempt to address this potential problem of over emphasizing the fish substratum relationship through the grouping of habitats into patches. The designation of habitat patches allowed the grouping of areas of potentially similar biotic and physical characteristics. Thus, the use of patches as areas for fish density estimates allowed for increased accuracy in forming abundance estimates from the habitat-groundfish association information. For example, this advantage was apparent by high variance in fish density estimates among patches of similar bottom type, such as the high density of juveniles in one of the three rock ridge patches. Variations in density in similar patch types of our study were also observed for Dover sole, rex sole, and pygmy rockfish. These patterns may be due to differences in depth, food availability or variations in percent composition of substrate type in separate areas of the bank. The other benefit of using habitat patches was that it allowed the testing of new groundfish assessment methods without making predictions for areas of high uncertainty where submersible transects were not performed.

Hixon et al.'s study[4] is one of only a few comprehensive habitat-groundfish studies available and has provided a foundation for testing this new approach. Hixon et al's dataset provided invaluable habitat information, but had several shortcomings. One problem was that of the inconsistency in positional data because of the use of Loran-C (GPS was not yet available). Another problem, characteristic of all submersible studies, was the overall limited spatial sampling provided by the survey. The stations for the study were chosen as representative habitats for Heceta Bank from exploratory submersible dives conducted by Pearcy et al. (1989) in 1987. However, not all of the representative habitat areas were sampled because maps of high-resolution bathymetry and backscatter were not available at that time. Lack of complete habitat data made it difficult to extrapolate bottom-type and fish-density data to the entire bank.

The use of observational data from submersibles for determination of fish density, and extrapolation from these data to total abundance within regional habitat patches, were based on several assumptions. First, we assumed that the areas sampled were representative of the entire regional patch to which each transect belonged. Whatever error was associated with this assumption, our approach is certainly more accurate that any method that ignores habitat variation. Second, we assumed that all fish within each submersible transect were accurately identified and counted. Identification of similar species of rockfish can be problematic, and counts clearly become estimates when dense schools are encountered. Third, we assumed

[9] O'Connell, V., and C. Carlile, and C. Brylinsky. 2001. Demersal shelf rockfish stock assessment and fishery evaluation report for 2002. Regional Information Report 1J01-35, 43 p. Southeast Region, Division of Commercial Fisheries, Alaska Department of Fish and Game, P.O. Box 25526, Juneau, AK 99802.

that avoidance or attraction of fish in response to the submersible was minimal, and thus did not affect counts substantially. This assumption was tested by Hixon et al.[4] by observing the local distribution and abundance of fish around the submersible just before and after the 10–15 minute "quiet periods" on the bottom, during which all motors and lights were turned-off. Quiet periods were conducted for all transect dives, and there was no indication that fish behavior was altered by the presence of the submersible. However, midwater schools of yellowtail rockfish sometimes circled the submersible during transects, which could have affected counts if fish were counted more than once. The final assumption was that transect width, which varied as a function of the altitude of the submersible above the seafloor, was constant. Certainly, there was some variation in altitude, yet the error introduced was presumably insubstantial except perhaps in areas of extremely heterogeneous vertical relief.

This study provides an expanded view of the groundfish habitat of Heceta Bank in areas adjacent to the historical *Delta* transects. In order to perform a full assessment of the bank it will be important to groundtruth habitat types for the entire extent of the bank. The new sonar data have indicated areas on the bank that contain unique habitats that have not been identified. The best study plan would have been to gather the sonar data first, then use the detailed imagery to define patches of uniform bottom type for planning subsequent stratified random sampling and groundtruthing using submersibles. The next phase of our project was initiated in June 2000 and involved operations with the manned submersible used in the original study and an advanced remotely operated vehicle (ROV) to conduct transects on unsurveyed areas, as well as to repeat the original historical transects. Not only will this approach optimize the techniques developed in our project but may also provide the opportunity to estimate changes in fish density on Heceta Bank over the past decade.

Conclusions

In this exploratory project we have demonstrated how sonar and submersible data can be combined to allow habitat-based stock assessments of multiple species of groundfish. Despite its limitations, this method provides the possibility for a detailed look at fish abundance using habitat associations. This approach could be used to address the problem of the high number of groundfish species that are currently unassessed. It offers the prospect of examining multiple species of fish and may provide a better indication of fish abundance estimates, particularly for multiple species, than is possible using current methods.

The method presented in our study provides an alternative for assessing these ten groundfish species and additional groundfish species that are currently unassessed, as well as for monitoring species that are considered to be overfished. Of the groundfish species examined in this study using the 1988–90 submersible observations, the status of all, but the pygmy, rockfish has been reported recently (NMFS, 1999). In the NMFS report on the status of fisheries in the United States, only the lingcod was reported as "overfished." Yellowtail rockfish, shortspine thornyhead, sablefish, and Dover sole were listed as "not approaching overfished," and the status of rex sole, greenstriped rockfish, rosethorn rockfish and sharpchin rockfish was reported as "unknown" (NMFS, 1999). In addition to the ten species that were examined here, the method described in our study would be important for assessing species of rockfish found on Heceta Bank that are considered overfished, such as the canary rockfish, Pacific ocean perch, and darkblotched rockfish. It should be stressed, however, that this method would be useful only for those species that are closely associated with seafloor habitats and spend most of their time near the bottom. For example, yellowtail rockfish are found as high as 25–35 m off the seafloor, so that transect data collected on the seafloor may not accurately reflect their true abundance (Pearcy, 1992).

The preliminary work in this study is a step toward creating a model approach for characterizing and quantifying groundfish and their habitat associations on a scale meaningful to the stock assessment of commercial species and the conservation of benthic communities. Traditional stock assessment methods for groundfish have been inadequate. Our study is the first step in the development of a new quantitative method of assessing groundfish stocks that is independent of traditional trawl surveys. Overall, this habitat-based approach to stock assessment has particular recommendation for defining and mapping essential fish habitat, as well as providing important data for designing and managing marine reserves and protected areas.

Acknowledgments

We would like to thank all who were involved in the collection and analysis of both the *Delta* submersible data and the Simrad EM300 multibeam sonar data. We especially thank D. Stein, B. Barss, R. Methot, B. Malouf, and J. Auyuong. W. Wakefield provided advice and support with this project. The high-resolution multibeam survey of Heceta Bank would not have been possible without the efforts of the captain and crew of the MV *Ocean Alert*, and the personnel from C&C Technologies. Also, D. Clague and Monterey Bay Aquarium Research Institute provided valuable support for the EM300 survey with both the onboard processing system and in allowing us to use some of their survey time to complete the Heceta Bank survey. J. Reynolds generously stayed on board *Ocean Alert* for the Heceta Bank survey and provided invaluable expertise in data collection and processing. We also thank N. Maher for valuable technical advice on EM300 processing. This research was funded by Oregon Sea Grant (NOAA), NOAA's National Undersea Research Program through NURP Headquarters and the West Coast and Polar Regions Undersea Research Center. The submersible and sonar portions of the work were funded through the U.S. Department of the Interior Minerals Manage-

ment Service, the National Undersea Research Program, Northwest Fisheries Science Center (NOAA/NMFS), and Oregon Sea Grant.

Literature cited

Able, K. W., D. C. Twitchell, C. G. Grimes, and R. S. Jones.
1987. Sidescan sonar as a tool for detecting demersal fish habitats. Fish. Bull. 85:725–744.

Carlson, H. R., and R. R. Straty.
1981. Habitat and nursery grounds of Pacific rockfish, *Sebastes* spp., in rocky coastal areas of Southeastern Alaska. Mar. Fish. Rev. 43:13–19.

Carr, M. H.
1991. Habitat selection and recruitment of an assemblage of temperate marine reef fishes. J. Exp. Mar. Biol. Ecol. 146:113–137.

ESRI
1994. Dynamic segmentation. *In* Network analysis, 263 p. Environmental Systems Research Institute, Inc., Redlands, CA.

Greene, H. G., M. M. Yoklavich, D. Sullivan, and G. Cailliet.
1995. A geophysical approach to classifying marine benthic habitats: Monterey Bay as a model. Alaska Dep. Fish and Game Special Publ. 9:15–30.

Hallacher, L. E ,and D. A. Roberts.
1985. Differential utilization of space and food by the inshore rockfishes (Scorpanidae: *Sebastes)* of Carmel Bay, California. Environ. Biol. Fish. 12:91–110.

Hughes Clarke, J. E., L. A. Mayer, and D. E. Wells.
1996. Shallow-water imaging multibeam sonars: a new tool for investigating seafloor processes in the coastal zone and on the continental shelf. Mar. Geophys. Res. 18:607–629.

Krieger, K. J.
1993. Distribution and abundance of rockfish determined from a submersible and by bottom trawling. Fish. Bull. 91:87–96.

Love, M. S., M. H. Carr, and L. J. Haldorson.
1991. The ecology of substrate-associated juveniles of the genus *Sebastes*. Environ. Biol. Fish. 30:225–243.

McRea, J. E., H. G. Greene, V. M. O'Connel, and W. W. Wakefield.
1999. Mapping marine habitats with high resolution sidescan sonar. Oceanol. Acta 22:679–686.

Meaden, G. J.
1999. Applications of GIS to fisheries management. *In* Marine and coastal geographical information systems (D. J. Wright and D. J. Bartlett, eds.), p. 205–226. Taylor & Francis, London.

Melton, L.
1986. The complete Loran-C handbook, 221 p. International Marine Publishing Company, Camden, ME.

NMFS (National Marine Fisheries Service).
1999. Report to Congress: status of fisheries of the United States, p. 35–39. NOAA Fisheries, 1315 East West Highway, SSMC3, Silver Spring, MD 20910.

O'Connell, V. M., and C. W. Carlile.
1993. Habitat-specific density of adult yelloweye rockfish *Sebastes ruberrimus* in the eastern Gulf of Alaska. Fish. Bull. 91:304–309.

Pearcy, W. G.
1992. Movements of acoustically-tagged yellowtail rockfish *Sebastes flavidus* on Heceta Bank, Oregon. Fish. Bull. 90: 726–735.

Pearcy, W. G., D .L. Stein, M.A. Hixon, E. K. Pikitch, W. H. Barss, R. M. Starr.
1989. Submersible observations of deep-reef fishes of Heceta Bank, Oregon. Fish. Bull. 87:955–965.

Ralston, S.
1998. The status of federally managed rockfish on the U.S. West Coast. *In* Marine harvest refugia for West Coast rockfish: a workshop (M. Yoklavich, ed.), p 6–16. U.S. Dep. Commer., NOAA Tech. Memo., NOAA-TMNMFS-SWFSC-255.

Richards, L .J.
1986. Depth and habitat distributions of three species of rockfish (*Sebastes*) in British Columbia: observations of deep-reef fishes of Heceta Bank, Oregon. Fish. Bull. 87:955–965.

Sherin, A. G.
1999. Linear reference data models and dynamic segmentation: application to coastal and marine data. *In* Marine and coastal geographical information systems (D. J. Wright and D. J. Bartlett, eds.), p. 95–116. Taylor & Francis, London.

Stein, D. L., B. N. Tissot, M. A. Hixon, and W. Barss.
1992. Fish-habitat associations on a deep reef at the edge of the Oregon continental shelf. Fish. Bull. 90:540–551.

Yoklavich, M. M., G. M. Cailliet, G. Greene, and D. Sullivan.
1995. Interpretation of sidescan sonar records for rockfish habitat analysis: examples from Monterey Bay. Alaska Dep. Fish and Game Special Publ. 9:11–14.

Yoklavich, M. M., H. G. Greene, G. M. Caillet, D. E. Sullivan, R. N. Lee, and M.S. Love.
2000. Habitat associations of deep-water rockfishes in a submarine canyon: an example of a natural refuge. Fish. Bull. 98 625–641.

An examination of spatial and temporal genetic variation in walleye pollock (*Theragra chalcogramma*) using allozyme, mitochondrial DNA, and microsatellite data*

Jeffrey B. Olsen
Susan E. Merkouris
James E. Seeb

Gene Conservation Laboratory
Alaska Department of Fish and Game
333 Raspberry Road
Anchorage Alaska 99518-1599

E-mail address (for James E. Seeb, contact author): jim_seeb@fishgame.state.ak.us

Abstract–We used allozyme, microsatellite, and mitochondrial DNA (mtDNA) data to test for spatial and interannual genetic diversity in walleye pollock (*Theragra chalcogramma*) from six spawning aggregations representing three geographic regions: Gulf of Alaska, eastern Bering Sea, and eastern Kamchatka. Interpopulation genetic diversity was evident primarily from the mtDNA and two allozyme loci (*SOD-2**, *MPI**). Permutation tests indicated that $\hat{F}_{ST}$ values for most allozyme and microsatellite loci were not significantly greater than zero. The microsatellite results suggested that high locus polymorphism may not be a reliable indicator of power for detecting population differentiation in walleye pollock. The fact that mtDNA revealed population structure and most nuclear loci did not suggests that the effective size of most walleye pollock populations is large (genetic drift is weak) and migration is a relatively strong homogenizing force. The allozymes and mtDNA provided mostly concordant estimates of patterns of spatial genetic variation. These data showed significant genetic variation between North American and Asian populations. In addition, two spawning aggregations in the Gulf of Alaska, in Prince William Sound, and off Middleton Island, appeared genetically distinct from walleye pollock spawning in the Shelikof Strait and may merit management as a distinct stock. Finally, we found evidence of interannual genetic variation in two of three North American spawning aggregations, similar in magnitude to the spatial variation among North American walleye pollock. We suggest that interannual genetic variation in walleye pollock may be indicative of one or more of the following factors: highly variable reproductive success, adult philopatry, source-sink metapopulation structure, and intraannual variation (days) in spawning timing among genetically distinct but spatially identical spawning aggregates.

Manuscript accepted 25 March 2002.
Fish. Bull. 100:752–764 (2002).

Detecting spatial structure in the genetic variation of some marine fishes is challenging because populations are often closely related due to high gene flow, and the relationships between populations may change over years (Hedgecock, 1994; Shaklee and Bentzen, 1998; Waples, 1998). For these species, independent population studies of genetic variation may result in conflicting evidence on the extent and complexity of population structure (McQuinn, 1997; Shaklee and Bentzen, 1998). Interpreting these results may be further complicated if the loci and classes of genetic markers differ by study and year. In addition, the discordant patterns of population structure may reflect complex population biology and ecology or merely differences in the resolving power of loci and marker classes to detect spatial structure. The walleye pollock (*Theragra chalcogramma*) is a marine fish that typifies this situation.

Walleye pollock inhabit basin, slope, and shelf waters of four major seas in the North Pacific Ocean: Sea of Japan, Sea of Okhotsk, Bering Sea, and Gulf of Alaska (Bailey et al., 1997). Their abundance is greatest in the eastern Bering Sea and the Sea of Okhotsk, but large aggregations are also found in the Sea of Japan, western Bering Sea, and the Gulf of Alaska. Smaller aggregations occur along coastal waters in bays and fjords such as in Prince William Sound, Alaska, and Puget Sound in Washington State. Population boundaries for walleye pollock may be correlated with the margins of spatially distinct spawning aggregates that occur throughout the species range in predictable locations during late winter and early spring (Bailey et al., 1999). Many of these spawning aggregates can be distinguished by spawning time and habitat, and by meristic and morphometric characters (e.g. Iwata, 1975b; Hinckley, 1987; Mulligan et al., 1989). Nevertheless, genetic support for discrete populations is equivocal, and the extent of population structuring in walleye pollock remains a controversial and unresolved issue for management and conservation in U.S. and international waters (Bailey et al., 1999).

Independent attempts to define genetic population structure in walleye pollock on a regional scale have shown mixed results. Some allozyme loci show genetic differentiation between walleye pollock from contiguous sea basins (e.g. eastern Bering Sea and Gulf of Alaska; Grant and Utter, 1980), and a single locus (*SOD*) appears to reveal a major east–west division between Asian and North American populations (Iwata, 1975a, 1975b; Grant and Utter, 1980). This major division is supported by a

* Contribution PP-217 of the Alaska Department of Fish and Game, Division of Commercial Fisheries, Juneau, AK 99802-5526.

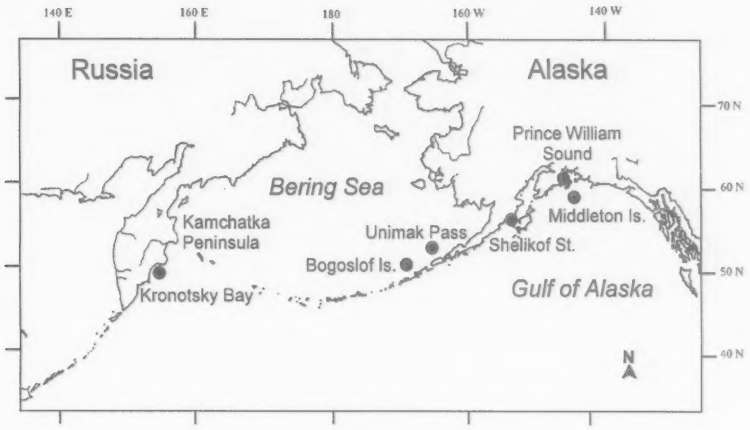

Figure 1

Map of the Gulf of Alaska and Bering Sea showing the location of walleye pollock spawning aggregations sampled for this study.

single study of mitochondrial DNA (mtDNA) sequence variation (Shields and Gust, 1995), but it is not evident in an unpublished study of microsatellite variation at two loci (reviewed in Bailey et al., 1999). Conversely, genetic differentiation among eastern Bering Sea and Gulf of Alaska populations is supported by the microsatellite study but is not supported by a study of mtDNA-RFLP (restriction fragment length polymorphism) variation (Mulligan et al., 1992). These discordant results may reflect attributes of walleye pollock population biology, the unique evolutionary properties of each marker class, or both. Nevertheless, an interpretation of the collective data is not possible because the studies were conducted as much as 22 years apart, and many samples were not from spawning aggregations.

Nonrepresentative sampling may bias attempts to define genetic population structure in walleye pollock, particularly on a fine spatial scale (within sea basins). For example, some studies using allozymes (Grant and Utter, 1980) and mtDNA (Shields and Gust, 1995) have included population samples taken during summer and fall, even though walleye pollock aggregate for spawning in late winter and early spring. These samples may obscure genetic differentiation because walleye pollock populations are believed to mingle in summer and fall during feeding migrations (Bailey et al., 1999). Also, the sample size used in some studies may be inadequate to detect population structure. The sample size in walleye pollock studies thus far has been typically less than 50, and the minimum sample size has been 22 (e.g. Grant and Utter, 1980; Mulligan et al., 1992). Sample sizes in this range (22–50) are generally insufficient to detect statistically significant differences in allele frequencies between populations that exhibit weak population structure (e.g. F_{ST} <0.02; Goudet et al., 1996; Ruzzante, 1998; Waples, 1998). These studies suggest that a sample size of 50 should be considered an absolute minimum for high gene flow species and that sample sizes of 100 or greater may be necessary when allele frequencies differ by 5% or less.

In our empirical study, we accounted for the sources of sample bias described above and addressed two important questions: 1) Do allozymes, mtDNA, and microsatellites provide concordant estimates of inter- and intraregional population structure in walleye pollock? 2) Is the genetic variation in walleye pollock populations stable from year to year? We tested for spatial patterns of genetic variation among six population samples from three regions: Gulf of Alaska, eastern Bering Sea, and eastern Kamchatka. We also tested for interannual stability of the genetic signal in replicate samples from three of the North American populations. Our results showed that two of 24 polymorphic allozyme loci (*SOD-2**, *MPI**) reveal significant spatial heterogeneity at the inter- and intraregional level. In general, the mtDNA data were concordant with these two allozymes, revealing significant genetic variation between North American and Asian (eastern Kamchatka) populations, as well as evidence of intraregional genetic variation, particularly among the Gulf of Alaska populations. The microsatellites, although highly polymorphic, showed little spatial variation. The allozyme and mtDNA data provided evidence of interannual genetic variation in two North American populations. $\hat{F}_{ST}$ values showed this interannual variation is of similar magnitude to the spatial variation in these populations.

Materials and methods

Sample collection

Tissue samples for allozyme and DNA analysis were obtained from six spawning aggregations of walleye pollock representing three major geographic regions: Gulf of Alaska, eastern Bering Sea, eastern Kamchatka (Fig. 1, Table 1).

Table 1
Location, sample data, and spawning habitat of walleye pollock examined in this study.

Major region and population	Spawning habitat	Date	*n*	N Lat.	W Long.
North America–Gulf of Alaska					
Shelikof Strait	shelf	1 Mar 97	100	57°55′	154°35′
		19 Mar 98	100	57°55′	154°40′
Prince William Sound	fjord	6 Feb 97	100	60°05′	148°20′
		6 Feb 98	100	60°05′	148°19′
Middleton Island	shelf	5 Mar 98	100	59°26′	145°45′
North America–Bering Sea					
Bogoslof Island	basin	1 Mar 97	100	53°15′	169°00′
		7 Mar 98	100	53°08′	169°11′
Unimak Pass	shelf	11 Apr 98	40	54°33′	165°38′
Asia–eastern Kamchatka					
Kronotsky Bay	shelf	1 Feb 99	96	52°00′	161°00′E

In total, nine samples were collected from 1977 through 1999: six from each of the major spawning aggregations shown in Figure 1, and three samples that were interannual replicates from Prince William Sound (PWS), Shelikof Strait (SHEL), and Bogoslof Island (BOG). Other samples included Unimak Pass (UNI) and Middleton Island (MID) in 1998 and Kronotsky Bay (KRON) in 1999. Tissue samples from heart, liver, muscle, and eye were taken from 100 individuals per population with the exception of Unimak Pass (n=40) and Kronotsky Bay (n=96). Only muscle tissue was sampled from Bogoslof Island walleye pollock in 1997. Samples were stored at –80°C until analyzed.

Allozyme analysis

Allozyme alleles were resolved by using horizontal starch-gel electrophoresis and enzyme-specific histochemical staining procedures described by Aebersold et al. (1987). Thirty six loci were screened for polymorphism (Table 2): *sAAT-1**, *sAAT-2**, *mAAT-1**, *ADA-1**, *ADA-2**, *AH-1**, *AH-2**, *ALAT**, *CK-A**, *FH**, *GAPDH-1**, *G3PDH-1**, *G3PDH-2**, *G3PDH-3**, *G3PDH-4**, *GPI-1**, *GPI-2**, *IDHP-1**, *IDHP-2**, *IDHP-3**, *LDH-2**, *LDH-3**, *MDH-A**, *MEP-1**, *MEP-2**, *MPI**, *PEPA**, *PEPB**, *PEPD**, *PEPLT**, *PGDH**, *PGM-1**, *PGM-2**, *SOD-1**, *SOD-2**, and *TPI**. Twenty-four loci were polymorphic in at least one of nine populations, and these loci were used in the tests of spatial and temporal genetic variation (Table 3).

DNA analysis

Total genomic DNA was isolated from 20–30 mg of heart tissue by using a Gentra Systems™ (Minneapolis, MN) Puregene DNA isolation kit. Precipitated DNA was hydrated in 50–100 µL tris-ethylenediaminetetraacetic acid (EDTA) buffer (10 mM Tris, 0.1 mM EDTA, pH 8.0) and heated at 55°C for approximately 12 h. Approximately 1 µL of hydrated DNA was used from each sample for polymerase chain reaction (PCR) amplification of mtDNA and microsatellite fragments.

mtDNA For an initial screen, six segments of the walleye pollock mitochondrial genome were examined for restriction fragment length polymorphism in a sample of 12 walleye pollock. The mtDNA segments examined were ND5/6 (~2400 base pairs /bp/; Cronin et al., 1993), cytochrome *b* (~1200 bp and~800 bp; Bickham et al., 1995), cytochrome oxidase I (~700 bp; Powers[1]), D-loop (~1400 bp; Cronin et al., 1993), and 16S (~600 bp; Palumbi et al., 1991). We used the following restriction enzymes: *Alu* I, *Apa* I, *Ase* I, *Ava* I, *Ava* II, *BamH* I, *Bcl* I, *Bgl* I, *Bgl* II, *BstE* II, *BstU* I, *Dpn* II, *EcoR* I, *EcoR* V, *Hae* II, *Hae* III, *Hha* I, *Hinf* I, *Hind* III, *Kpn* I, *Mse* I, *Msp* I, *Nci* I, *Pst* I, *Rsa* I, *Sac* I, *Sac* II, *Sau96* I, *Sca* I, *Stu* I, *Taq* I, *Xba* I, and Xho I.

PCRs were performed in 25–100 µL volumes containing 10 mM Tris-HCl (pH 8.3), 50 mM KCl, 2.0–3.5 mM $MgCl_2$, 0.8 mM dNTPs, 0.05 units/µL *Taq* polymerase, 0.3–1.2 µM primer, and about 250 ng DNA template. The PCR profile was 92°C (2 min) + 30–40 cycles of (92°C (30 sec) + X°C (30 sec) + 72°C (140 sec)) + 72°C (5 min), where the annealing temperature X varied among primer pairs. Restriction digests followed manufacturer's specifications (New England Biolabs, Beverly, Maine).

The mtDNA fragment and enzyme combinations ND5/6 (~2400 bp)—*Ase* I, *Ava* I, *Msp* I, *Rsa* I; cytochrome *b* (~1200 bp)—*Alu* I, *Hae* III, *Mse* I; and cytochrome oxidase (~700 bp)—*Alu* I revealed polymorphism and were used to test for spatial and temporal genetic variation. The PCR annealing temperatures for these fragments were the following: (for ND5/6) 50°C; (for cytochrome *b*) 54°C; and (for cytochrome oxidase) 50°C. Restriction fragments

[1] Powers, D. A. 1997. The use of molecular techniques to dissect the genetic architecture of pollock populations. Unpubl. rep. to the National Marine Fisheries Service, 11 p. Hopkins Marine Station, Stanford University, Pacific Grove, CA, 93950.

Table 2

Buffers and tissues used to resolve enzyme-coding loci in walleye pollock. Enzyme nomenclature and Enzyme Commission (EC) number follow IUBNC (1984); locus nomenclature follows Shaklee et al., (1990).

Enzyme or protein	EC number	Locus	Tissue[1] (buffer[2])
Aspartate aminotransferase	2.6.1.1	*sAAT-1**	L(AC6.5)
		*sAAT-2**	H(AC6.1), M(AC6.1)
		*mAAT-1**	M(AC6.1)
Adenosine deaminase	3.5.4.4	*ADA-1**	L(AC6.5)
		*ADA-2**	L(AC6.5)
Aconitate hydratase	4.2.1.3	*AH-1**	L(AC6.5)
		*AH-2**	H(AC6.5), M(AC6.1, AC6.5), L(AC6.5)
Alanine aminotransferase	2.6.1.2	*ALAT**	M(TBE)
Creatine kinase	2.7.3.2	*CK-A**	M(TBE)
Fumarate hydratase	4.2.1.2	*FH**	M(ACEN7.0)
Glyceraldehyde-3-phosphate dehydrogenase	1.2.1.12	*GAPDH-1**	M(AC6.9)
Glycerol-3-phosphate dehydrogenase	1.1.1.8	*G3PDH-1**	L(AC6.5)
		*G3PDH-2**	M(AC6.5), L(AC6.5)
		*G3PDH-3**	H(AC6.5), L(AC6.5)
		*G3PDH-4**	L(AC6.5)
Glucose-6-phosphate isomerase	5.3.1.9	*GPI-1**	H(TBCL)
		*GPI-2**	H(TBCL)
Isocitrate dehydrogenase (NADP+)	1.1.1.42	*IDHP-1**	L(ACE7.0), L(TC7.0)
		*IDHP-2**	M(ACEN7.0)
		*IDHP-3**	L(ACE7.0)
L-Lactate dehydrogenase	1.1.1.27	*LDH-2**	H(TBCL), M(TBE)
		*LDH-3**	H(TBCL), M(TBE)
Malate dehydrogenase	1.1.1.37	*MDH-A**	H(AC6.1), M(AC6.1, AC6.9)
Malic enzyme (NADP+)	1.1.1.40	*MEP-1**	M(AC6.5, AC6.9, ACEN7.0)
		*MEP-2**	M(AC6.5, AC6.9, ACEN7.0)
Mannose-6-phosphate isomerase	5.3.1.8	*MPI**	H(TBCL), M(TBE)
Dipeptidase	3.4.-.-	*PEPA**	H(AC6.5)
Tripeptide aminopeptidase	3.4.-.-	*PEPB**	M(AC6.9)
Proline dipeptidase	3.4.13.9	*PEPD**	M(AC6.1)
Peptidase-LT	3.4.-.-	*PEPLT**	H(AC6.1)
Phosphogluconate dehydrogenase	1.1.1.44	*PGDH**	M(AC6.9, ACEN7.0)
Phosphoglucomutase	5.4.2.2	*PGM-1**	H(TBCL), M(TBE), L(ACE7.0)
		*PGM-2**	M(TBE)
Superoxide dismutase	1.15.1.1	*SOD-1**	M(ACEN7.0, TBE)
		*SOD-2**	H(ACEN7.0)
Triose-phosphate isomerase	5.3.1.1	*TPI**	H(AC6.1), M(AC6.1)

[1] H = heart; E = eye; M = muscle; L = liver.

[2] Buffers: AC, ACN, ACE, ACEN: amine-citric acid buffer (Clayton and Tretiak, 1972) modified with EDTA (E), NAD (N), or both (Aebersold et al., 1987), values indicate pH; TBCL: tris-citric acid gel, pH 8.7 and lithium hydroxide-boric acid electrode buffer, pH 8.0 (Ridgway et al., 1970); TBE: tris-boric acid-EDTA buffer, pH 8.7 (Boyer et al., 1963).

were size fractionated on 3% agarose gels, stained with ethidium bromide, and visualized and photographed under ultraviolet light (312 nm). Fragment sizes as small as 50 bp were estimated by comparison with 100 bp and 250 bp ladders on each gel. A composite haplotype was generated for each individual by recording the presence or absence of restriction sites for all restriction enzymes and mtDNA segments (Lansman et al., 1981). The length of

Table 3

Single locus statistics: number of individuals (n); number of alleles (A); frequency of the most common allele over all populations (P_a); total heterozygosity ($\hat{H}_T$); analogs of Wright's F-statistics F_{IS}, F_{ST}, and F_{IT} ($\hat{f}$, $\hat{\theta}$, $\hat{F}$). Note: The analog of F_{ST} for haplotype data, $\hat{\Phi}_{ST}$, is computed for mtDNA. Values in bold type with an asterisk are statistically significant. The α-level (0.05) was adjusted (α/k) for k tests, where k is the number of loci (allozymes, 24; microsatellites, 3).

Locus	n	A	P_a	$\hat{H}_T$	$\hat{f}$	$\hat{\theta}$	$\hat{F}$
Allozyme							
*sAAT-1**	692	3	0.996	0.008	–0.001	–0.001	–0.003
*sAAT-2**	793	4	0.992	0.016	–0.011	0.006	–0.005
*mAAT-1**	803	2	0.998	0.004	0.001	–0.002	–0.001
*AH-1**	657	4	0.958	0.081	0.060	0.001	0.061
*ALAT**	811	3	0.898	0.188	–0.019	0.002	–0.017
*FH**	814	2	0.999	0.002	0.001	–0.001	–0.001
*G3PDH-2**	811	4	0.994	0.012	–0.002	–0.002	–0.004
*G3PDH-3**	715	4	0.992	0.016	–0.004	–0.002	–0.007
*GPI-1**	815	3	0.992	0.016	–0.008	0.002	–0.006
*GPI-2**	815	4	0.990	0.020	–0.010	0.003	–0.007
*IDHP-1**	714	4	0.976	0.047	–0.018	–0.001	–0.020
*IDHP-2**	814	3	0.996	0.008	–0.002	–0.001	–0.003
*LDH-2**	815	2	0.999	0.002	0.001	–0.001	–0.001
*LDH-3**	814	2	0.999	0.002	0.000	0.000	0.000
*MDH-A**	815	3	0.996	0.008	–0.002	0.000	–0.002
*MEP-1**	815	4	0.994	0.012	–0.004	–0.001	–0.004
*MPI**	810	5	0.788	0.337	0.016	**0.017***	0.032
*PEPB**	802	4	0.962	0.074	–0.001	0.003	0.003
*PEPD**	815	3	0.985	0.030	**0.158***	–0.001	0.157
*PGDH**	814	9	0.544	0.590	0.043	–0.002	0.041
*PGM-1**	815	4	0.993	0.014	–0.004	0.000	–0.004
*SOD-1**	815	2	0.999	0.002	0.000	–0.001	0.000
*SOD-2**	711	3	0.916	0.154	–0.014	**0.088***	0.075
*TPI**	815	3	0.997	0.006	–0.002	0.000	–0.002
Mean	788	4	0.956	0.069	0.024	**0.010***	0.033
SE		1	0.100	0.136	0.014	0.011	0.010
Microsatellite							
Tch10	741	32	0.395	0.811	0.069	0.001	0.070
Tch12	671	12	0.305	0.782	0.035	0.000	0.035
Tch22	637	15	0.367	0.713	0.039	**0.005***	0.043
Mean	683	20	0.356	0.769	**0.048***	**0.002***	0.050
SE		11	0.046	0.050	0.011	0.001	0.011
mtDNA							
ND5/6-CB-CO	684	66	0.371	0.837		**0.022***	

the recognition sequence (bp) and the number of recognition sites identified by each enzyme were the following: for ND5/6—*Ase* I (6, 5), *Ava* I (6, 4), *Msp* I (4, 4), *Rsa* I (4, 5); for cytochrome *b*—*Alu* I (4, 2), *Hae* III (4, 2), *Mse* I (4, 7); and for cytochrome oxidase—*Alu* I (4, 4). A total of 150 nucleotides were surveyed for polymorphism or approximately 3.5% of the combined 4300-bp region.

Microsatellites Thirteen microsatellite loci were screened for polymorphism, amplification quality, and null alleles in walleye pollock by using primer pairs derived from Atlantic cod, *Gadus morhua*, (*Gmo1*, *Gmo2*, *Gmo9*, *Gmo10*, *Gmo123*, *Gmo132*, and *Gmo145*; Brooker et al., 1994) and walleye pollock (*Tch5*, *Tch10*, *Tch11*, *Tch12*, *Tch18*, and *Tch22*; O'Reilly et al., 2000). PCRs were performed in 10 µL volumes containing 10 mM Tris-HCl (pH 8.3), 50 mM KCl, 1.5 mM $MgCl_2$, 0.8 mM dNTPs, 0.05 units/µL Taq polymerase, 0.3–1.2 µM primer, and about 250 ng DNA template. The following PCR profile was used: 92°C (2 min) + 30 cycles of (92°C (30 sec) + X°C (30 sec) + 72°C (140 sec)) + 72°C (5 min) where the annealing temperature X varied among microsatellites.

Microsatellites were size fractionated by using an Applied Biosystems Inc. (ABI, Foster City, CA) 377-96 automated DNA sequencer operated in GeneScan™ mode (ABI, 1996a). Data were analyzed by using the internal

lane sizing standard and local Southern sizing algorithm in the GeneScan 672 software vers. 1.1 (ABI, 1996a). Alleles for each locus were scored and data were tabulated for importing into statistical software with Genotyper software, vers. 2.0 (ABI, 1996b).

Of the thirteen loci screened, *Tch10*, *Tch12*, and *Tch22* were used to test for spatial and temporal genetic variation. The PCR annealing temperatures for these loci were the following: (for *Tch10*) 54°C; (for *Tch12*) 47°C; and (for *Tch22*) 52°C. The loci *Gmo10*, *Gmo123*, *Gmo145*, *Tch5*, and *Tch18* did not amplify consistently by the methods above, and *Gmo1*, *Gmo2*, *Gmo9*, *Gmo132*, and *Tch11* appeared to possess null alleles as revealed by significant heterozygote deficits (data not shown).

Statistical analyses

Estimates of allele and haplotype frequency were calculated for each locus and population sample. Heterozygosity estimates ($\hat{H}$) were calculated by using Equation 8.4 of Nei (1987) and haplotype diversity estimates ($\hat{h}$) were computed by using the program ARLEQUIN vers. 1.1 (Schneider et al., 2000). A permutation test of the statistic $\hat{f}$ (Weir and Cockerham, 1984) was used to assess conformity to Hardy-Weinberg equilibrium (HWE) for each locus and over all loci for each population with the computer program FSTAT vers. 2.8 (Goudet 2000). The data set was permuted 1000 times (alleles were permuted among individuals, within population samples), and the threshold for statistical significance (α=0.05) was corrected for simultaneous tests by using the sequential Bonferroni method (Rice, 1989).

Spatial and temporal genetic variation were quantified by estimating analogs of Wright's F_{ST} for each marker class: θ (allozymes and microsatellites, Weir and Cockerham, 1984), R_{ST} (microsatellites, Slatkin, 1995), Φ_{ST} (mtDNA, Excoffier et al., 1992). Estimates of θ, R_{ST}, and Φ_{ST} ($\hat{\theta}$, $\hat{R}_{ST}$, and $\hat{\Phi}_{ST}$) were computed for all nine population samples, for all contemporaneous population samples (1997, 1998), and for the temporal replicates. The haplotype frequency estimates were used to compute $\hat{\Phi}_{ST}$. A hierarchical approach was used to determine if more detailed assessment of spatial variation was necessary. That is, only those statistics ($\hat{\theta}$, $\hat{R}_{ST}$, $\hat{\Phi}_{ST}$) that were significant over all samples from a given year were then calculated for populations pooled by region, and for populations within regions. Statistics significant at the regional level were calculated for each population pair. This hierarchical approach was applied over all loci for allozymes and microsatellites as well as for individual loci because in some instances statistically significant spatial variation was evident for a single locus but not for the marker class. The computer programs FSTAT, version 2.8 (Goudet, 2000), RST Calc, version 2.2 (Goodman, 1997), and ARLEQUIN, version 1.1 (Schneider et al., 2000) were used to compute $\hat{\theta}$, $\hat{R}_{ST}$, and $\hat{\Phi}_{ST}$.

The statistical significance of spatial and temporal variation in genetic diversity of walleye pollock was estimated by using F_{ST} estimator tests and allelic (haplotypic) goodness-of-fit tests (Goudet et al., 1996). First, the statistical significance of estimates for each F_{ST} analog ($\hat{\theta}$, $\hat{R}_{ST}$, and $\hat{\Phi}_{ST}$) was determined by using a permutation test option in the respective computer programs. In each case the data set was permuted 1000 times (alleles or haplotypes among population samples). Second, allele and haplotype frequency homogeneity was tested for the same population comparisons by using a *G*-test (allozymes and microsatellites) and probability test (mtDNA). The threshold for statistical significance (α=0.05) for multiple comparisons was determined by using the sequential Bonferroni method (Rice, 1989).

Results

Single-locus statistics and a comparison of marker classes

The degree of polymorphism indicated by the number of alleles per locus, allele frequency, and total heterozygosity ($\hat{H}_T$) varied across loci and marker classes and was generally lower for allozymes than for microsatellites (Table 3). The number of alleles per allozyme locus ranged from two to nine (mean=four) and the frequency of the common allele in the pooled population sample was greater than 0.950 for all but four loci (*ALAT**, *MPI**, *PGDH**, and *SOD-2**, Table 3). In contrast, the number of alleles per locus was higher for microsatellites (range=12–32, mean=20), and the maximum allele frequency did not exceed 0.400 (Table 3). Relatively high polymorphism was also detected from restriction digests of ND5/6, cytochrome *b*, and cytochrome oxidase I regions of mtDNA (66 composite haplotypes, maximum haplotype frequency 0.371, Table 3). Values of mean $\hat{H}_T$ were an order of magnitude greater for microsatellites (0.769) than for allozymes (0.069); however, some overlap in range was evident because of the large variation in $\hat{H}_T$ among loci (Table 3). The estimate of haplotype diversity (h=0.837) was slightly greater than the H_T for microsatellites (Table 3).

Values for $\hat{\theta}$ and $\hat{\Phi}_{ST}$ varied among loci and failed to expose a single marker class, regardless of overall variability, as most informative for detecting population structure in walleye pollock (Table 3). Permutation tests revealed two allozyme loci (*MPI**, *SOD-2**) and one microsatellite (*Tch22*) with $\hat{\theta}$ values significantly greater than zero over all population samples (Table 3, Fig. 2). The $\hat{\theta}$ of 0.088, for *SOD-2** was exceptionally high. The $\hat{\Phi}_{ST}$ for mtDNA was within the range of $\hat{\theta}$ for allozymes and microsatellites and was significantly greater than zero (P<0.001).

Intrapopulation genetic variation and Hardy-Weinberg equilibrium

Estimators of intrapopulation diversity (alleles per locus, $\hat{H}_E$ and $\hat{h}$) differed among marker types within populations but generally showed little variation between populations (Table 4). As expected, the values for the diversity estimators were usually lowest in the population with the smallest sample sizes (e.g. UNI, n=40). This was most notable in haplotype number (range 12–27) because most

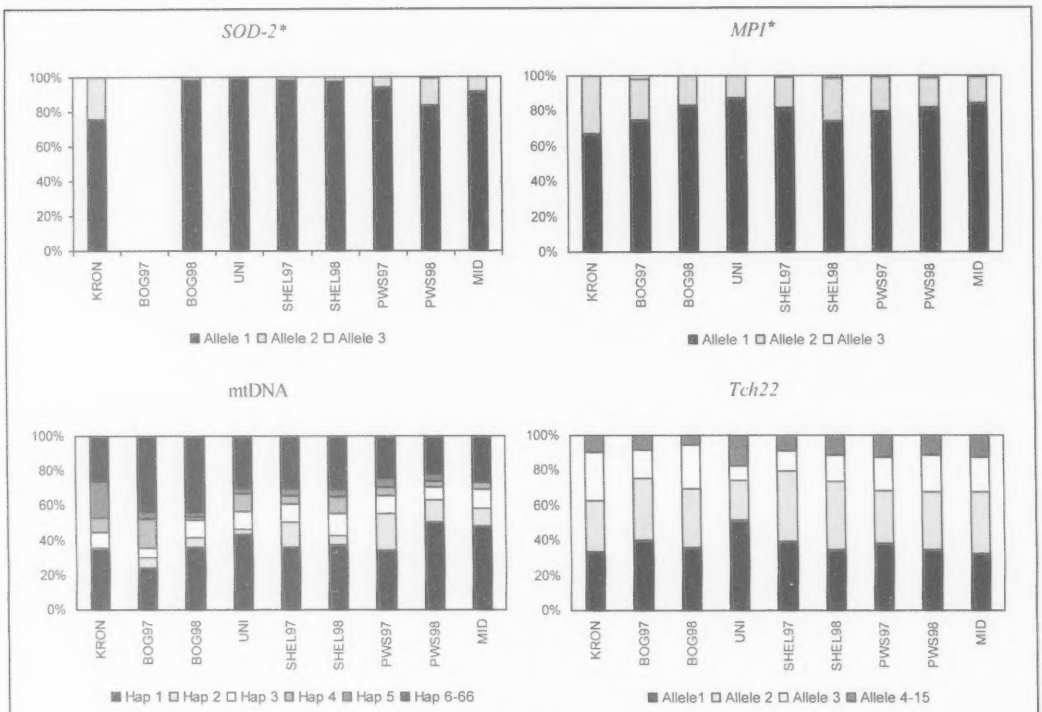

Figure 2

Frequency histograms for *SOD-2**, *MPI**, and *Tch22* alleles, and mtDNA haplotypes. Abbreviations: Kronotsky Bay (KRON); Bogoslof Island, 1997 (BOG97); Bogoslof Island, 1998 (BOG98); Unimak Pass (UNI); Shelikof Strait, 1997 (SHEL97); Shelikof Strait, 1998 (SHEL98); Prince William Sound, 1997 (PWS97); Prince William Sound, 1998 (PWS98); Middleton Island (MID). *SOD-2** data were not available for BOG97.

Table 4

Population statistics: mean number of individuals (n); mean number of alleles (A); expected heterozygosity ($\hat{H}_E$); analog of Wright's F_{IS} ($\hat{f}$); haplotype diversity ($\hat{h}$). Values in bold type with an asterisk are statistically significant. The α-level (0.05) was adjusted (α/k) for k tests, where k is the number of populations (9). SHEL = Shelikof Strait: PWS = Prince William Sound; MID = Middleton Island; BOG = Bogoslof Island; UNI = Unimak Pass; and KRON = Kronotsky Bay.

		Allozyme				Microsatellite				mtDNA		
Population	Year	n	A	$\hat{H}_E$	$\hat{f}$	n	A	$\hat{H}_E$	$\hat{f}$	n	A	$\hat{h}$
North America–Gulf of Alaska												
SHEL	1997	79.7	2.0	0.061	–0.002	80.0	12.0	0.762	0.037	99	27	0.832
	1998	99.7	2.1	0.064	0.023	84.3	12.3	0.774	0.021	72	22	0.828
PWS	1997	99.4	2.2	0.065	0.012	75.0	14.7	0.757	0.002	99	20	0.820
	1998	99.8	2.2	0.069	0.020	95.3	14.0	0.778	0.066	65	16	0.718
MID	1998	99.6	2.3	0.064	0.033	91.7	13.7	0.735	0.018	75	19	0.743
North America–Bering Sea												
BOG	1997	99.5	2.3	0.079	0.015	44.3	11.0	0.777	0.100	99	25	0.885
	1998	99.1	2.2	0.068	0.073	91.7	13.3	0.773	**0.094***	75	21	0.838
UNI	1998	39.8	1.5	0.062	0.007	40.0	10.3	0.746	**0.159***	30	12	0.786
Asia–eastern Kamchatka												
KRON	1999	92.0	2.0	0.080	–0.011	81.7	14.0	0.766	0.008	70	19	0.822
Mean		89.8	2.1	0.068	0.020	76.0	12.8	0.763	0.048	76.0	20.1	0.808

of the rare haplotypes were found in large samples. For example, 52 of 66 composite haplotypes had frequencies of 1% or less and only three of these haplotypes were present in the UNI sample, but 8, 14, and 15 rare haplotypes were present in the three largest samples (PWS 1997, BOG 1997, SHEL 1997; Table 4).

Population genotypic frequencies generally did not deviate from Hardy-Weinberg expectations. Permutation tests for the statistic $\hat{f}$, conducted independently for allozymes and microsatellites, were concordant for all but two populations (BOG 1998; UNI 1998). The observed value of $\hat{f}$ for microsatellites in these two populations was significantly greater than zero ($P<0.005$) when $\alpha=0.05$ was adjusted for nine simultaneous tests (Table 4).

Spatial structure in genetic variation

1997 Gulf of Alaska and Bering Sea Population structure among the three North America samples was evident from mtDNA (overall $\hat{\Phi}_{ST}=0.017$, $P=0.002$; Table 5). The hierarchical analysis indicated that the two Gulf of Alaska populations were genetically different from the Bering Sea population ($\hat{\Phi}_{ST}=0.028$, $P<0.001$) but were not distinguishable from each other (Table 5). These results were confirmed by goodness-of-fit tests of haplotype homogeneity. Spatial genetic structure among the 1997 samples was not evident from values of $\hat{\theta}$ over all allozymes and microsatellites (Table 5).

1998 Gulf of Alaska and Bering Sea, and 1999 eastern Kamchatka Indices of population structure for allozymes ($\hat{\theta}=0.017$, $P<0.001$) and mtDNA ($\hat{\Phi}_{ST}=0.021$, $P<0.001$) were similar over all population samples and larger than for microsatellites ($\hat{\theta}=0.002$, $P>0.050$; $\hat{R}_{ST}=0.001$, $P>0.050$; Table 5). Because the values of $\hat{\theta}$ and $\hat{R}_{ST}$ over all microsatellites and pop-ulations were not significant, analyses of population structure were conducted with only the allozyme and mtDNA data. Significant genetic differences were revealed between pooled samples from North America and Asia with allozymes ($\hat{\theta}=0.030$, $P<0.001$) and mtDNA ($\hat{\Phi}_{ST}=0.035$, $P<0.001$; Table 5), between samples from the Gulf of Alaska and Bering Sea with allozymes ($\hat{\theta}=0.005$, $P=0.006$), and within the Gulf of Alaska with allozymes ($\hat{\theta}=0.009$, $P<0.001$) and mtDNA ($\hat{\Phi}_{ST}=0.018$, $P=0.009$).

Values for $\hat{\theta}$ were considerably larger for *SOD-2** than for the two other informative markers *MPI**, and mtDNA (Table 6, Fig. 2). Estimates of F_{ST} from mtDNA and *MPI** for each of the regional comparisons were similar but the most informative microsatellite locus, *Tch22*, did not vary significantly among regions.

Based on permutation test results from the hierarchical analyses, estimates of genetic differentiation were computed for all population pairs by using both allozyme and mtDNA data, except for Gulf of Alaska versus Bering Sea populations (allozyme data only). Values of $\hat{\theta}$ (allozymes) and $\hat{\Phi}_{ST}$ for most pairwise comparisons from North America and Asia were relatively large and highly significant (Table 5). In contrast, values of $\hat{\theta}$ (allozymes) for most population pairs from the Gulf of Alaska and Bering Sea were relatively small, and only the UNI × SHEL and UNI × PWS pairs were significant ($\hat{\theta}=0.021$, $P<0.003$; $\hat{\theta}=0.017$, $P<0.006$). Pairwise comparisons within the Gulf of Alaska were significant for SHEL × PWS (allozymes, $\hat{\theta}=0.017$, $P<0.002$) and for SHEL × MID (mtDNA, $\hat{\Phi}_{ST}=0.025$, $P<0.007$; Table 5).

In goodness-of-fit tests, allele and haplotype frequency homogeneity were concordant with the statistically significant values of $\hat{\theta}$ (allozymes) and $\hat{\Phi}_{ST}$ for all populations and pooled samples within and between regions (Table 5). However, results from the two types of tests conflicted for some population pairs. For example, *G*-tests of allozyme data revealed significant genetic variation for two population pairs (BOG × PWS; BOG × MID; Table 5) for which $\hat{\theta}$ was not significant. In contrast, $\hat{\theta}$ was significant for two population pairs, KRON × PWS and UNI × SHEL, which were not genetically different based on *G*-test results. One population pair, PWS × MID, was genetically different in the probability test of mtDNA data, but $\hat{\Phi}_{ST}$ for this pair was not significant (Table 5).

Temporal change in genetic variation: Bogoslof Island, Shelikof Strait, and Prince William Sound

Significant temporal change in mtDNA variation was detected in one population, BOG, by using the probability test of haplotype homogeneity ($P<0.001$) and $\hat{\Phi}_{ST}$ ($P=0.003$, Table 5). The Φ_{ST} was within the range of values described for spatial variation and indicated a significant interannual change in haplotype frequency. Interestingly, this interannual shift in genetic variation was not evident from allozymes and microsatellites. However, the single most-informative locus *SOD-2** was not analyzed in the BOG 1997 sample because heart tissue was not available. Also, variation at the locus *MPI**, although not statistically significant, suggested that the BOG replicates were genetically different ($\hat{\theta}=0.011$, $P=0.066$; Table 6). A similar indication of temporal genetic variation was detected in the PWS population for all allozymes ($\hat{\theta}=0.005$, $P=0.046$), but $\hat{\theta}$ was not significant when α was adjusted for three simultaneous tests (initial $\alpha=0.016$, Table 5). In this case *SOD-2** was resolved and exhibited significant genetic variation ($\hat{\theta}=0.047$, $P=0.004$; Table 6). The mtDNA data, although not significant, also provided an indication of temporal variation in the PWS population ($\hat{\Phi}_{ST}=0.012$, $P=0.055$; Table 6).

Discussion

Comparison of marker classes

Our empirical results support two tentative conclusions regarding the usefulness of these marker classes for detecting population structure in walleye pollock. First, high overall heterozygosity such as that observed in some microsatellites may not be a reliable indicator of power for detecting population differences in walleye pollock, regardless of spatial scale. This conclusion contrasts with some simulation studies that have shown a positive relationship between locus polymorphism and the power to

Table 5

Tests for spatial and interannual genetic variation in walleye pollock. Abbreviations are as follows: number of populations (N); Gulf of Alaska (GOA); Bering Sea (BS); North America (NA); Bogoslof Island (BOG); Shelikof Strait (SHEL); Prince William Sound (PWS); Kronotsky Bay (KRON); Unimak Pass (UNI); Middleton Island (MID). Values in bold type with an asterisk are statistically significant. The α-level (0.05) for pairwise comparisons was adjusted (α/k) for k tests, where k is the number of population pairs per grouping strategy. Allo = allozyme; msat = microsatellite. Pr - P = the P-value for the probability test.

		F_{ST} analog tests				Goodness-of-fit tests		
						G-test P		Pr - P
Grouping strategy	N	$\hat{\theta}$ allo	$\hat{\theta}$ msat	$\hat{R}_{ST}$ msat	$\hat{\Phi}_{ST}$ mtDNA	allo	msat	mtDNA
1997 populations	3	0.000	0.000	–0.005	**0.017***	0.711	0.585	**<0.001**
Between GOA and BS	3				**0.028***			**<0.001**
BOG × SHEL					**0.024***			**<0.001**
BOG × PWS					**0.029***			**<0.001**
Within GOA	2							
SHEL × PWS					–0.004			0.876
1998 populations, Asia	6	**0.017***	0.002	0.001	**0.021***	**<0.001**	0.106	**<0.001**
Between NA and Asia	6	**0.030***			**0.035***	**<0.001**		**<0.001**
KRON × BOG		**0.039***			**0.035***	**<0.001**		**<0.001**
KRON × UNI		**0.057***			0.024	**<0.001**		0.028
KRON × SHEL		**0.028***			**0.026***	**<0.001**		**<0.001**
KRON × PWS		**0.014***			**0.051***	0.016		**<0.001**
KRON × MID		**0.029***			**0.048***	**<0.001**		**<0.001**
Between GOA and BS	5	**0.005***			0.004	**<0.001**		0.070
BOG × SHEL		0.004				0.216		
BOG × PWS		0.010				**<0.001**		
BOG × MID		0.001				**0.007**		
UNI × SHEL		**0.021***				0.017		
UNI × PWS		**0.017***				**<0.001**		
UNI × MID		0.011				0.011		
Within BS	2							
BOG × UNI		0.000			–0.008	0.454		0.754
Within GOA	3	**0.009***			**0.018***	**0.040**		**<0.001**
SHEL × PWS		**0.017***			0.007	**0.006**		0.504
SHEL × MID		0.006			**0.025***	0.109		**<0.001**
PWS × MID		0.002			0.019	0.722		**<0.001**
Interannual (1997–98)								
Bogoslof Island	2	0.001	–0.002	–0.007	**0.023***	0.162	0.479	**<0.001**
Prince William Sound	2	0.005	0.002	0.003	0.012	0.212	0.363	0.641
Shelikof Strait	2	0.001	0.001	0.000	–0.003	0.618	0.030	0.804

resolve population differentiation (e.g. Rousset and Raymond, 1995; Goudet et al., 1996). Nevertheless, empirical support for this relationship is mixed (e.g. Pogson et al., 1995; Estoup et al., 1998; Scribner et al., 1998). We believe our results suggest that mutation, which varies among these marker classes, has relatively little bearing on detecting genetic variation among walleye pollock populations. Instead, spatial differentiation may be limited because populations are large (i.e. genetic drift is weak) and gene flow among populations is high. The fact that only one private allele was found at the most variable microsatellite locus (Middleton Island, locus *Tch10*, allele 147) is an argument for high gene flow. Further, the index of population structure $\hat{R}_{ST}$ (Slatkin, 1995) developed to reflect the high mutation rate and mutation process of microsatellites is no larger than $\hat{\theta}$. The similarity of these values suggests that gene flow is relatively high and that mutation has relatively little influence on population differentiation (Slatkin, 1995).

Our second conclusion is that balancing selection may influence some but certainly not all allozymes in walleye pollock, as posited for marine species exhibiting low variation in allozyme allele frequencies (Pogson et al., 1995). Our conclusion is supported by two observations. First, microsatellites and mtDNA provide no greater resolution of overall population structure than allozymes (Tables 5

Table 6

F_{ST} estimates for *SOD-2**, *MPI**, and mtDNA. Abbreviations are as follows: number of populations (*N*); Gulf of Alaska (GOA); Bering Sea (BS); North America (NA). Values in bold type with an asterisk are statistically significant.

		F_{ST} analog tests		
Grouping strategy	*N*	$\hat{\theta}$ *SOD-2**	$\hat{\theta}$ *MPI**	$\hat{\Phi}_{ST}$ mtDNA
1997 populations	3	N/A	0.001	**0.017***
1998 populations, Asia	6	**0.095***	**0.028***	**0.021***
Between NA and Asia	6	**0.155***	**0.059***	**0.035***
Between GOA and BS	5	**0.043***	0.002	0.004
Within BS	2	0.001	0.000	0.000
Within GOA	3	**0.051***	**0.013***	**0.018***
Interannual (1997–98)				
Bogoslof Island	2	N/A	0.011	**0.023***
Prince William Sound	2	**0.047***	0.000	0.012
Shelikof Strait	2	0.000	0.011	–0.003

and 6). Second, two allozyme loci (*SOD-2**; *MPI**) provided the strongest evidence of regional genetic variation among the 1998 samples (Table 6). In fact, the locus *SOD-2** had exceptionally high values of $\hat{\theta}$ for most regional comparisons in contrast to the other nuclear loci and mtDNA. Diversifying selection may be acting on this locus (e.g. Hudson et al., 1997); however, the general concordance between *SOD-2**, *MPI**, and mtDNA data suggests that the values of $\hat{\theta}$ most likely reflect the influence of genetic drift (Table 6, Fig. 2).

Spatial structure in genetic variation

North America to Asia The signature of a major east–west division between Asian and North American walleye pollock was evident in our allozyme and mtDNA data but not in our microsatellite data. The results of our F_{ST} analog tests and goodness-of-fit tests confirm the findings of earlier studies (e.g. Iwata, 1975a, 1975b; Grant and Utter, 1980; Shields and Gust, 1995, Bailey et al., 1999) and add some new insight regarding genetic heterogeneity in walleye pollock from different geographic regions. For example, we confirm the significant *SOD-2** variation observed in the past but we also reveal that a second allozyme locus, *MPI**, exhibits substantial spatial variation at this geographic scale (Table 6, Fig. 2). Nevertheless, only these two loci and the mtDNA reveal genetic variation between these two regional groups although some of the other 25 nuclear loci screened were equally or more polymorphic (e.g. *ALAT**, *PGDH**, *Tch10*, *Tch11*, and *Tch22*). These results suggest that, despite broad spatial separation, Asian and North American walleye pollock populations are remarkably genetically similar. This outcome supports the notion that the effective population size in walleye pollock is large, the rate of genetic drift is very low, and migration despite physical distance is a strong homogenizing force.

North America–Bering Sea and Gulf of Alaska The allozyme and mtDNA provided discordant results with respect to inter- and intraregional population structure within North American walleye pollock. The most noteworthy instance was the contradictory evidence of genetic variation between populations from the Bering Sea and the Gulf of Alaska. That is, significant genetic differentiation between populations from these two regions was evident from both the allozymes and mtDNA, but in different years (Table 5). We believe that the intraannual differences between marker classes is an artifact due primarily to the lack of *SOD-2** data for the Bogoslof Island sample in 1997. The values of $\hat{\theta}$ and $\hat{\Phi}_{ST}$ were similar in magnitude for the 1998 Bering Sea and Gulf of Alaska comparison, but only $\hat{\theta}$ was statistically significant (Table 5). This result appears to be due to the influence of *SOD-2** for which $\hat{\theta}$ was 0.043 and highly significant ($P<0.002$, Table 6). The value of $\hat{\theta}$ over all allozymes for the 1997 Bering Sea and Gulf of Alaska comparison might have been similar to or larger than the $\hat{\Phi}_{ST}$ for mtDNA if the *SOD-2** data had been available for the 1997 Bogoslof Island sample.

The 1998 samples provided the first indication of statistically significant genetic variation among populations in the Gulf of Alaska with both allozymes and mtDNA. Populations from Prince William Sound and Middleton Island were genetically distinguishable from the Shelikof Strait population, but they were not distinguishable from each other. These results are important for two reasons. First, this is the first indication of limited gene flow between a fjord spawning population (Prince William Sound) in the Gulf of Alaska and the numerically dominant Shelikof Strait population which spawns over the ocean shelf. Obvious factors that may limit gene flow between these two populations are the differences in spawning habitat preference and the counterclockwise flow of the Gulf of Alaska gyre which prevents larval drift from Shelikof Strait to the Prince William Sound (Bailey et al., 1999).

Second, the Prince William Sound and Middleton Island populations may warrant consideration as a distinct stock, which should be managed independently of the Shelikof Strait population.

The significant genetic differences between population pairs in the Gulf of Alaska are alternately supported by allozymes and mtDNA. That is, the Shelikof Strait and Prince William Sound populations differ significantly according to the allozyme data but not the mtDNA data, and the Shelikof Strait and Middleton Island populations differ significantly according to the mtDNA data but not the allozyme data (Table 5). We believe that the significant variation observed for each population pair is, in fact, real but is not supported by both marker types because these populations differ at only three loci (*SOD-2**, *MPI**, mtDNA). Thus, it is reasonable to expect differences between the populations at one locus (in this case, the marker class) and not the others based solely on the random effects of genetic drift.

Temporal change in genetic variation: Bogoslof Island, Prince William Sound

In addition to evidence of spatial structure within the Gulf of Alaska, we found evidence of interannual variation in genetic diversity among replicate samples from Bogoslof Island (mtDNA) and Prince William Sound (allozyme *SOD-2**). In each case the statistically significant variation was evident at only one marker, although in each case a second marker showed noticeable, but not statistically significant, variation between years (e.g. Bogoslof Island, *MPI**—$\hat{\theta}$=0.011, P=0.066; Prince William Sound, mtDNA—$\hat{\Phi}_{ST}$=0.012, P=0.055). We believe there are four likely sources for this apparent temporal shift.

First, walleye pollock may experience high variability in reproductive success among spawning adults as has been shown, for example, in oysters (Hedgecock, 1994). Walleye pollock have many life history traits such as semiplanktonic larvae, high fecundity, and external fertilization in a variable environment (Hedgecock, 1994), that may result in highly variable reproductive success and may contribute to temporal instability, particularly in small census populations such as that in Prince William Sound.

Second, walleye pollock may have varying degrees and types of philopatry. For example, juvenile walleye pollock may recruit to any one of a number of spawning aggregations and then exhibit repeat spawning behavior as an adult (adult philopatry). Adult philopatry has been used to explain the temporal instability observed in Atlantic herring (*Clupea harengus*, [McQuinn, 1997]) and could explain the apparent heterozygote deficit at microsatellites in the Bogoslof Island 1998 and Unimak Pass 1998. Alternatively, the degree of philopatry in walleye pollock may be extremely low despite the spatial and temporal predictability of spawning aggregations.

Third, a source-sink type metapopulation relationship may exist between some walleye pollock populations (e.g., Shelikof Strait and Prince William Sound; Unimak Pass and Bogoslof Island). Bailey et al., (1999) suggested that a metapopulation theory may explain existing data on population structure and dynamics of walleye pollock. The temporal genetic variation we observed in Prince William Sound and Bogoslof Island is consistent with this theory. Other circumstantial evidence supporting a source-sink relationship among some walleye pollock populations includes the discovery of walleye pollock in Prince William Sound (sink) concurrent with the increase in biomass of walleye pollock in the neighboring Shelikof Strait (source).

Finally, our supposed temporal replicates may actually represent samples from different spawning aggregates that spawn in the same location but at different times of the year. This finding suggests that fine-scale, intra-annual, genetic variation exists among walleye Pollock that spawn in the same area but perhaps days or weeks apart.

Summary

Our results show that the genetic variation, as measured by F_{ST}, among spatially distinct spawning aggregations of walleye pollock is generally low and is similar to the spatial genetic variation observed in other gadids such as Atlantic cod and European hake, *Merluccius merluccius* (e.g. Ruzzante et al., 1998; Lundy et al., 2000). In contrast, evidence of temporal genetic variation in gadid fishes is equivocal. Although some populations of European hake exhibit interannual variation in gene frequencies (Lundy et al., 2000), Ruzzante et al. (1997) found no evidence of temporal instability in Atlantic cod. For walleye pollock more detailed studies are needed to determine the extent to which all or some of the factors described above explain the temporal variability observed within some spawning aggregations. A priority of future genetic studies of walleye pollock should be to examine both fine-scale temporal variation (days and weeks within a year) and the genetic relationship among age cohorts from spatially distinct spawning aggregations. Because these studies will require extensive sampling, we recommend detailed examination of one or two spawning aggregations, such as those at Prince William Sound and Shelikof Strait. To further evaluate the metapopulation theory, candidate samples should include potential source populations (e.g. Shelikof Strait and Unimak Pass) and sink populations (e.g. Bogoslof Island and Prince William Sound). Future studies should also include a statistical examination of single locus $\hat{\theta}$ values to assess if *SOD-2** exceeds expectation and is perhaps influenced by a locus-specific force such as diversifying selection (e.g. Beaumont and Nichols, 1996).

Acknowledgments

Funding for this study was provided by the Alaska Department of Fish and Game general funds and test fish funds, and by the *Exxon Valdez* Oil Spill Trustee Council (Restoration Study 99252). Genetic data were collected by Judy Berger, Barbara Debevec, and Eric Kretschmer of the Alaska Department of Fish and Game. Substantial assistance in organizing sample collections was provided

by Denise McKelvey (National Oceanic and Atmospheric Administration), Bill Bechtol (Alaska Department of Fish and Game), and Nataly Varnavskaya (Kamchatka Research Institute of Fisheries Oceanography). The genetic data used in this study are available from the corresponding author by e-mail or on floppy disk.

Literature cited

ABI (Applied Biosystems Inc.).
1996a. GeneScan 672 software users manual, rev. A, 337 p. Perkin-Elmer Corp., Foster City, CA.
1996b. Genotyper 2.0 users manual, 75 p. Perkin-Elmer Corp., Foster City, CA.

Aebersold, P. B., G. A. Winans, D. J. Teel, G. B. Milner, and F. M. Utter.
1987. Manual for starch gel electrophoresis: a method for the detection of genetic variation. U.S. Dep. Commer., NOAA Technical Report NMFS 61, 19 p.

Bailey, K. M., T. J. Quinn II, P. Bentzen, and W. S. Grant.
1999. Population structure and dynamics of walleye pollock, *Theragra chalcogramma*. Adv. Mar. Biol. 37: 179–255.

Bailey, K. M., P. J. Stabeno, and D. A. Powers.
1997. The role of larval retention and transport features in mortality and potential gene flow of walleye pollock. J. Fish Biol. 51:135–155.

Beaumont, M. A., and R. A. Nichols.
1996. Evaluating loci for use in the analysis of population structure. Proc. R. Soc. Lond., ser. B. 263:1619–1626.

Bickham, J. W., C. C. Wood, and J. C. Patton.
1995. Biogeographic implications of Cytochrome b sequences and allozymes in sockeye (*Oncorhynchus nerka*). J. Hered. 86:140–144.

Boyer, S. H., D. C. Fainer, and M. A. Naughton.
1963. Myoglobin: inherited structural variation in man. Science 140:1228–1231.

Brooker, A. L., D. Cook, P. Bentzen, J. M. Wright, and R. W. Doyle.
1994. Organization of microsatellites differs between mammals and cold-water teleost fishes. Can. J. Fish. Aquat. Sci. 51:1959–1966.

Clayton, J. W., and D. N. Tretiak.
1972. Amine-citrate buffers for pH control in starch gel electrophoresis. J. Fish. Res. Board Can. 29:1169–1172.

Cronin, M. A., W. J. Spearman, R. L. Wilmont, J. C. Patton, and J. W. Bickham.
1993. Mitochondrial DNA variation in chinook salmon (*Oncorhynchus tshawytscha*) and chum salmon (*O. keta*) detected by restriction enzyme analysis of polymerase chain reaction (PCR) products. Can. J. Fish. Aquat. Sci. 50:708–715.

Estoup, A., F. Rousset, Y. Michalakis, J.-M. Cornuet, M. Adriamanga, and R. Guyomard.
1998. Comparative analysis of microsatellite and allozyme markers: a case study investigating microgeographic differentiation in brown trout (*Salmo trutta*). Mol. Ecol. 7: 339–353.

Excoffier, L., P. E. Smouse, and J. M. Quattro.
1992. Analysis of molecular variance inferred from metric distances among DNA haplotypes: application to human mitochondrial DNA restriction data. Genetics. 131:479–491.

Goodman, S. J.
1997. RST Calc: a collection of computer programs for calculating estimates of genetic differentiation from microsatellite data and determining their significance. Mol. Ecol. 6:881–886 .

Goudet, J.
2000. FSTAT (version 1.2): a computer program to calculate *F*-statistics. J. Hered. 86(6):485–486.

Goudet, J., M. Raymond, T. de Meeus, and F. Rousset.
1996. Testing differentiation in diploid populations. Genetics 144:1933–1940.

Grant, W. S., and F. M. Utter.
1980. Biochemical genetic variation in walleye pollock, *Theragra chalcogramma*: population structure in the Southeastern Bering Sea and the Gulf of Alaska. Can. J. Fish. Aquat. Sci. 37:1093–1100.

Hedgecock, D.
1994. Does variance in reproductive success limit effective population sizes of marine organisms? *In* Genetics and evolution of aquatic organisms (A. R. Beaumont, ed.), p. 122–134. Chapman and Hall, London.

Hinckley, S.
1987. The reproductive biology of walleye pollock, *Theragra chalcogramma*, in the Bering Sea, with reference to spawning stock structure. Fish. Bull. 85:481–498.

Hudson, R. R., A. G. Sáez, and F. J. Ayala.
1997. DNA variation at the *Sod* locus of *Drosophila melanogaster*: an unfolding story of natural selection. Proc. Natl. Acad. Sci. 94:7725–7729.

IUBNC (International Union of Biochemistry, Nomenclature Committee).
1984. Enzyme nomenclature, 646 p. Academic Press, Orlando, Florida.

Iwata, M.
1975a. Genetic identification of walleye pollock, *Theragra chalcogramma* (Pallas), populations on the basis of tetrazolium oxidase polymorphism. Comp. Biochem. Physiol. 50(B):197–201.
1975b. Population identification of walleye pollock, *Theragra chalcogramma* (Pallas), in the vicinity of Japan. Memoirs of the Faculty of Fisheries, Hokkaido University 22: 193–258.

Lansman, R. A., R. O. Shade, J. F. Shapiro, and J. C. Avise.
1981. The use of restriction endonucleases to measure mitochondrial DNA sequence relatedness in natural populations. III. Techniques and potential applications. J. Mol. Evol. 17:214–226.

Lundy, C. J., C. Rico, and G. M. Hewitt.
2000. Temporal and spatial genetic variation in spawning grounds of European hake (*Merluccius merluccius*) in the Bay of Biscay. Mol. Ecol. 9:2067–2079

McQuinn, I. H.
1997. Metapopulations and the Atlantic herring. Rev. Fish Biol. Fish. 7:297–329.

Mulligan, T. J., K. M. Bailey, and S. Hinckley.
1989. The occurrence of larval and juvenile walleye pollock, *Theragra chalcogramma*, in the eastern Bering Sea with implications for stock structure. *In* Proceedings of the international symposium on the biology and management of walleye pollock, p. 471–490. Alaska Sea Grant Report 89-1. Univ. Alaska, Fairbanks, AK.

Mulligan, T. J., R. W. Chapman, and B. L. Brown.
1992. Mitochondrial DNA analysis of walleye pollock, *Theragra chalcogramma*, from the eastern Bering Sea and Shelikof Strait, Gulf of Alaska. Can. J. Fish. Aquat. Sci. 49:319–326.

Nei, M.
1987. Molecular evolutionary genetics, 512 p. Columbia Univ. Press, New York, NY

O'Reilly, P. T., M. F. Canino, K. M. Bailey, and P. Bentzen.
2000. Isolation of twenty low stutter di- and tetranucleotide microsatellites for population analyses of walleye pollock and other gadoids. J. Fish Biol. 56(5):1074–1086.

Palumbi, S. R., A. Martin, S. Romano, W. O. McMillan, L. Stice, and G. Grabowski.
1991. The simple fool's guide to PCR, version 2, 46 p. Zoology Dep., Univ. Hawaii, Honolulu, HI.

Pogson, G. H., K. A. Mesa, and R.G. Boutilier.
1995. Genetic population structure and gene flow in the Atlantic cod *Gadus morhua*: a comparison of allozyme and nuclear RFLP loci. Genetics 139:375–385.

Rice, W. R.
1989. Analyzing tables of statistical tests. Evolution 43(1): 223–225.

Ridgway, G. J., S. W. Sherburne, and R. D. Lewis.
1970. Polymorphism in the esterases of Atlantic herring. Trans. Am. Fish. Soc. 99:147–151.

Rousset, F., and M. Raymond.
1995. Testing heterozygote excess and deficiency. Genetics 140:1413–1419.

Ruzzante, D. E.
1998. A comparison of several measures of genetic distance and population structure with microsatellite data: bias and sampling variance. Can. J. Fish. Aquat. Sci. 55:1–14.

Ruzzante, D. E., C. T. Taggart, and D. Cook.
1998. A nuclear DNA basis for shelf- and bank-scale population structure in northwest Atlantic cod (*Gadus morhua*): Labrador to Georges Bank. Mol. Ecol. 7:1663–1680.

Ruzzante, D. E., C. T. Taggart, D. Cook, and S. V. Goddard.
1997. Genetic differentiation between inshore and offshore Atlantic cod (*Gadus morhua*) off Newfoundland: a test and evidence of temporal stability. Can. J. Fish. Aquat. Sci. 54: 2700–2708.

Scribner, K. T., P. A. Crane, W. J. Spearman, and L. W. Seeb.
1998. DNA and allozyme markers provide concordant estimates of population differentiation: analyses of U.S. and Canadian populations of Yukon River fall-run chum salmon (*Oncorhynchus keta*). Can. J. Fish. Aquat. Sci. 55:1748–1758.

Schneider, S., D. Roessli, and L. Excoffier.
2000. ARLEQUIN version 2.000: a software for population genetics data analysis. Genetics and Biometry Laboratory, Dept. of Anthropology and Ecology. Univ. Geneva, CP 511, 1211 Geneva 24, Switzerland.

Shaklee, J. B., and P. Bentzen.
1998. Genetic identification of stocks of marine fish and shellfish. Bull. Mar. Sci. 62(2):589–621.

Shaklee, J. B., F. W. Allendorf, D. C. Morizot, and G. S. Whitt.
1990. Gene nomenclature for protein-coding loci in fish. Trans. Am. Fish. Soc. 119(1):2–15

Shields, G. F., and J. R. Gust.
1995. Lack of geographic structure in mitochondrial DNA sequences of Bering Sea walleye pollock, *Theragra chalcogramma*. Mol. Mar. Biol. Biotechnol. 4(1):69–82.

Slatkin, M.
1995. A measure of population subdivision based on microsatellite allele frequencies. Genetics 139:457–462.

Waples, R. S.
1998. Separating the wheat from the chaff: patterns of genetic differentiation in high gene flow species. J. Hered. 89(5):438–450.

Weir, B. S., and C. C. Cockerham.
1984. Estimating *F*-statistics for the analysis of population structure. Evolution 38(6):1358–1370.

Movements, behavior, and habitat selection of bigeye tuna (*Thunnus obesus*) in the eastern equatorial Pacific, ascertained through archival tags

Kurt M. Schaefer
Daniel W. Fuller
Inter-American Tropical Tuna Commission
8604 La Jolla Shores Drive
La Jolla, California 92037-1508
E-mail address (for K. M. Schaefer): kschaefer@iattc.org

Abstract–Ninety-six bigeye tuna (88–134 cm fork length) were caught and released with implanted archival (electronic data storage) tags near fish-aggregating devices (FADs) in the equatorial eastern Pacific Ocean (EPO) during April 2000. Twenty-nine fish were recaptured, and the data from twenty-seven tags were successfully downloaded and processed. Time at liberty ranged from 8 to 446 days, and data for 23 fish at liberty for 30 days or more are presented. The accuracy in geolocation estimates, derived from the light level data, is about 2 degrees in latitude and 0.5 degrees in longitude in this region. The movement paths derived from the filtered geolocation estimates indicated that none of the fish traveled west of 110°W during the period between release and recapture. The null hypothesis that the movement path is random was rejected in 17 of the 22 statistical tests of the observed movement paths. The estimated mean velocity was 117 km/d. The fish exhibited occasional deep-diving behavior, and some dives exceeded 1000 m where temperatures were less than 3°C. Evaluations of timed depth records, resulted in the discrimination of three distinct behaviors: 54.3% of all days were classified as unassociated (with a floating object) type-1 behavior, 27.7% as unassociated type-2 behavior, and 18.7% as behavior associated with a floating object. The mean residence time at floating objects was 3.1 d. Data sets separated into day and night were used to evaluate diel differences in behavior and habitat selection. When the fish were exhibiting unassociated type-1 behavior (diel vertical migrations), they were mostly at depths of less than 50 m (within the mixed layer) throughout the night, and during the day between 200 and 300 m and 13° and 14°C. They shifted their average depths in conjunction with dawn and dusk events, presumably tracking the deep-scattering layer as a foraging strategy. There were also observed changes in the average nighttime depth distributions of the fish in relation to moon phase.

Manuscript accepted 24 May 2002.
Fish. Bull. 100:765–788 (2002).

Bigeye tuna (*Thunnus obesus*) occur in subtropical and tropical oceanic waters throughout the world, except in the Mediterranean Sea (Collette and Nauen, 1983; Collette et al., 2001). They are captured by longliners operating in the eastern Pacific Ocean (EPO) from about 40°N to 40°S and by purse seiners from about 5°N to 10°S (Miyabe and Bayliff, 1998; Bayliff, 2000). They are economically the most important species of tuna harvested by longline fisheries in the EPO. The estimated average catch of bigeye tuna by the longline fleets of Japan, Taiwan, and the Republic of Korea in the EPO has declined from an average of about 79 thousand metric tons (t) during 1985–94 to about 40 thousand t during 1995–98 (Bayliff, 2000). The longline fishery targets medium to large bigeye tuna. There is a growing purse-seine fishery that catches primarily small to medium bigeye tuna, most of which are associated with drifting fish-aggregating devices (FADs). The purse-seine catch in the EPO has dramatically increased from an estimated annual average of about 5 thousand t during 1964–93, to about 45 thousand t during 1994–98 (Bayliff, 2000; Lennert-Cody and Hall, 2000). There is concern that the longline fishery is being adversely affected by the purse-seine fishery and that current catch rates are not sustainable (Watters and Maunder, 2001).

Elucidating the environmental variables that define bigeye tuna habitat can be used to adjust gear vulnerability, to standardize catch and effort data, and thus improve bigeye tuna stock assessments (Brill, 1994; Hinton and Nakano, 1996; Brill and Lutcavage, 2001; Hampton et al.[1]). It is also necessary to understand the affinity of bigeye tuna to drifting FADs, now a common feature of their habitat in the equatorial EPO, and to quantify the effect of FAD densities on vulnerability to capture. Sonic tracking studies (Holland et al., 1990; Holland et al., 1992; Daggorn et al., 2000), along with studies of catches per unit of effort (CPUEs) by longlines (Suzuki and Kume, 1982; Hanamoto, 1987; Boggs, 1992; Nakano et al., 1997) have provided information on differences in depth and temperature distributions for bigeye tuna by size and time of day.

Studies of fine-scale movements and short-term behavior, based on data from acoustic tags, have been reported for bigeye tuna associated with anchored FADs (Holland et al., 1990) and in the open ocean (Dagorn et al., 2000), but not for fish associated with drifting FADs. Bigeye tuna tend to stay within close proximity of anchored FADs during the day, move away at night, and return the next morning (Holland et al., 1990). When not associated with FADs, they swim within the mixed layer above the thermocline at night and well below the thermocline during

[1] Hampton, J., K. Bigelow, and M. Labelle. 1998b. Effect of longline fishing depth, water temperature and dissolved oxygen on bigeye tuna (*Thunnus obesus*) abundance indices. Working Paper 17, 18 p. Eleventh meeting of the standing committee on tuna and billfish, Sec. Pac. Comm., Noumea, New Caledonia. Oceanic Fisheries Programme, SPC, B.P. D5, 98848 Noumea Cedex, New Caledonia.

the day (Holland et al., 1990; Dagorn et al., 2000). They are capable of exploiting cold, deep waters below the thermocline because of their unique anatomy (Graham and Dickson, 2001), which enables them to physiologically and behaviorally thermoregulate by making vertical forays into the warm mixed layer throughout the day to increase their body temperatures (Holland et al., 1992, Holland and Sibert, 1994). Apparent differences in behavioral patterns of tunas around anchored FADs versus drifting FADs have been discussed, but almost no empirical results have been reported (Holland et al., 1990; Dagorn et al., 2000).

Although conventional and sonic tagging studies, and those on depth, temperature, and time of capture with longline gear, have provided valuable information on bigeye tuna biology and ecology, the present generation of archival (electronic data storage) tags can further our understanding of bigeye tuna movement, behavior, and habitat selection. Archival tags record swimming depth, internal and external temperatures, and ambient light levels. The light data can be processed to provide daily estimates of latitudes and longitudes (Hill, 1994; NMFS, 1994; Welch and Eveson, 1999; Hill and Braun, 2001).

This study presents results from analyses of data recorded by archival tags recovered from bigeye tuna that were released in the equatorial EPO during April 2000. An evaluation of the accuracy and precision of the geolocation estimates derived from the archival tag data is provided. Descriptions of movement and behavioral patterns, and also habitat characteristics of bigeye, are presented.

Materials and methods

Tag releases

Bigeye tuna were captured, tagged, and released at three FADs in the equatorial EPO between 0°52′ and 2°01′N and between 95°24′ and 97°06′W, during the period of 15–22 April 2000. Tagging was conducted on the chartered FV *Her Grace*, a 17.7-m, 99 gross-t, United States west-coast-style live-bait pole-and-line vessel. The FADs were taken out of the water before the vessel left the tagging area in order to minimize the probability of short-term recaptures, and to permit the fish to disperse.

The archival tags used in this study were model Mk7 manufactured by Wildlife Computers (Redmond, WA) (Wildlife Computers, 2002). The total weight of a tag in air is about 32 g. The Mk7 tag is designed for implantation into the peritoneal cavity of the fish so that the sensor stalk protrudes outside the fish through an incision in the abdominal wall. A label, printed in Spanish, with information about reporting the recovery of the tag and the associated reward (US$500) was encased in the epoxy of the main body of the instrument.

The depth, internal and ambient temperatures, and light level were stored in the memory of the tag every 4 minutes. At this sampling rate, the memory of each tag (2 MB) was capable of storing 3.8 years of data. The pressure sensors measured over a range of –40 to 1000 m with 0.5-m resolution. The temperature sensors measured over a range of –40° to 60°C with 0.05°C resolution. The light sensors had a logarithmic range from 3×10^{-10} W.cm^{-2} to 1×0^{-2} W.cm^{-2}. Bright sunshine is approximately 2×10^{-3} W.cm^{-2}. Light-level readings of about 200 and 50 are observed in bright sunshine and in complete darkness, respectively. Exploratory analyses of our data indicated that the light sensor is able to identify dawn and dusk events at 300 m.

Each tag was rigorously tested and evaluated at sea before deployment in bigeye tuna. Tags were programmed to collect data from all four sensors at one-second intervals, placed in a nylon mesh bag with a Sea-Bird SBE-39 temperature-depth probe, and sent down to approximately 300 m. After retrieval, the data were downloaded from each tag and their performance was evaluated in relation to the temperature-at-depth data collected by the Sea-Bird SBE-39.

Bigeye tuna specimens were captured by using handline gear during the day and night. Each fish was brailed with a heavy-gauge aluminum rigid-framed net of knotless webbing and landed on a wet foam pad covered with smooth vinyl. The eyes of the fish were immediately covered with a wet synthetic chamois, the hook was removed, and the condition of the fish was determined. If the fish was in excellent condition (i.e. no damage to the eyes or gills and no significant bleeding), the surgery required for implanting the archival tag was initiated. An incision about 2 cm long was made in the abdominal wall about 10 cm anterior of the anus and about 2 cm to the left of the centerline of the fish. Special care was taken to cut through the dermis only and partially through the muscle, but not into the peritoneal cavity. A gloved finger was inserted into the incision and forced through the muscle into the peritoneal cavity. The tag, sterilized by soaking it in Betadine solution, was inserted, pointed end first, through the incision into the peritoneal cavity. The tag was then manipulated to the caudal end of the incision, and two sutures were placed rostral of where the stalk protruded to close the incision by using a sterile needle and suture material (Ethicon (PDS II) size 0, cutting cp-1, 70 cm).

Fish were also tagged with two serially numbered 12.5-cm green plastic dart tags (Hallprint, Pty., Holden Hill, Australia) by using tubular stainless steel applicators. Tags were inserted into the dorsal musculature with the barbed heads passing between the pterygiophores below the base of the second dorsal fin, from both sides of the fish. Information for reporting the recovery of the fish and for receiving the reward (US$500) for the return of the fish was printed in Spanish on these tags. Lastly, five to ten mL of 100-mg/mL oxytetracycline hydrochloride solution were injected into the dorsal musculature with a disposable automatic vaccinator.

The 96 bigeye tuna released with archival tags were measured to the nearest centimeter with a caliper (mean=109.2 cm FL, 95% CI=1.9 cm, range=88–134 cm). The fish were then picked up by hand and released back into the sea by one or more individuals standing in a rack at the stern of the vessel. The total time most of the fish were out of the water was recorded to the nearest second (mean=2:17, 95% CI=0:06, range=1:27–4:19, n=86). All

Table 1

Release and recapture information for 28 bigeye tuna from which archival tags were recovered. The fish lengths are those measured at release. The locations are given in decimal degrees (dd).

Tag no.	Fish length (cm)	Release			Recapture			Days at liberty
		Location (dd)		Date	Location (dd)		Date	
99-787	115	0.87 N	97.10 W	15 Apr 00	1.72 N	83.08 W	22 Aug 00	128.7
99-792	126	0.87 N	97.10 W	15 Apr 00	1.35 N	95.82 W	15 Oct 00	182.7
99-793	114	0.87 N	97.10 W	15 Apr 00	2.25 N	97.25 W	21 Mar 01	339.7
99-801	112	1.47 N	96.97 W	17 Apr 00	1.47 N	90.72 W	06 Jul 00	79.8
99-803	113	2.02 N	95.40 W	22 Apr 00	2.20 N	102.72 W	26 Jul 00	94.1
99-804	104	1.47 N	96.97 W	17 Apr 00	4.80 N	105.42 W	23 Dec 00	249.6
99-810	120	2.02 N	95.40 W	22 Apr 00	1.65 S	93.17 W	18 Jun 00	56.0
99-812	116	2.02 N	95.40 W	22 Apr 00	0.55 N	109.00 W	29 Sep 00	159.1
99-814	120	2.02 N	95.40 W	22 Apr 00	1.42 N	88.93 W	13 Jul 01	446.1
99-816	122	2.02 N	95.40 W	22 Apr 00	1.78 N	97.60 W	30 May 00	37.1
99-817	106	1.47 N	96.97 W	17 Apr 00	1.12 S	95.87 W	18 Jun 00	61.7
99-826	119	1.47 N	96.97 W	17 Apr 00	0.50 N	101.52 W	14 Jan 01	271.8
99-835	109	2.02 N	95.40 W	22 Apr 00	1.20 N	99.68 W	18 Jun 00	56.1
99-839	109	1.47 N	96.97 W	17 Apr 00	2.33 S	95.75 W	12 Jun 00	55.8
99-847	102	1.47 N	96.97 W	17 Apr 00	1.77 N	97.23 W	29 May 00	41.7
99-853	103	2.02 N	95.40 W	22 Apr 00	1.20 N	99.68 W	18 Jun 00	56.1
99-860	104	1.47 N	96.97 W	17 Apr 00	2.18 S	97.87 W	10 Jun 00	53.7
99-861	110	1.47 N	96.97 W	17 Apr 00	2.23 S	96.67 W	04 May 00	16.8
99-862	93	1.72 N	96.80 W	18 Apr 00	1.77 S	94.80 W	21 Jun 00	63.7
99-864	110	2.02 N	95.40 W	22 Apr 00	2.70 N	97.87 W	17 May 00	24.1
99-865	101	1.47 N	96.97 W	17 Apr 00	2.67 S	99.05 W	15 Jun 00	58.6
99-869	113	1.08 N	97.08 W	16 Apr 00	4.85 N	103.18 W	07 Aug 00	112.4
99-874	108	1.47 N	96.97 W	17 Apr 00	2.70 N	97.87 W	17 May 00	29.8
99-877	88	1.08 N	97.08 W	16 Apr 00	2.77 S	99.20 W	08 May 00	21.4
99-883	116	1.93 N	96.55 W	19 Apr 00	1.60 S	95.55 W	18 Jun 00	59.7
99-884	102	0.87 N	97.10 W	15 Apr 00	1.12 N	86.18 W	01 Jul 01	441.7
99-889	112	1.08 N	97.08 W	16 Apr 00	0.37 N	98.58 W	02 Jul 00	76.4
99-891	124	2.02 N	95.40 W	22 Apr 00	0.25 S	92.88 W	01 May 00	8.1

fish released with archival tags were observed to swim rapidly down and away from the vessel after release, and all appeared to be in excellent condition.

Tag recoveries

Twenty-nine of the 96 bigeye released with archival tags were recaptured by 4 October 2001. Twenty-eight archival tags were recovered, and the data from twenty-seven were successfully downloaded and processed. The fish lengths, release and recapture positions, and number of days at liberty of the twenty-eight fish from which archival tags were recovered are given in Table 1. Twenty-five of the tags were recovered from fish caught by purse-seine vessels during sets on FADs. Scientific observers were aboard these purse-seine vessels, thus providing verification of recapture information. Three fish, from which archival tags (99-793, 99-812, and 99-865) were recovered, were recaptured by longline vessels without scientific observers aboard.

Data processing

Data were downloaded, decoded, and processed by using software provided by the tag manufacturer (Wildlife Computers, 2002). Light-level data were used to obtain daily position estimates for each fish and ranges of uncertainty about those estimates (Hill, 1994; Hill and Braun, 2001). The accuracy and precision of the position estimates were evaluated by calculating the differences between the known recapture locations for 21 bigeye tuna, determined by global-positioning systems (GPS) aboard the fishing vessels, and the corresponding geolocation estimates.

Two criteria were used for filtering (accepting or rejecting) daily geolocation estimates. The first was based on the uncertainty associated with estimates of latitude for the days of recapture, and the second was based on the distance between geolocation estimates for consecutive days. Those daily estimates in which the range between the north and south errors was greater than 6° or the location was farther than 4° in latitude from that for the

previous day were considered improbable and excluded from further analyses. For the 22 bigeye tuna at liberty for at least 30 days, this filtering procedure retained an average of 48.8% (95%CI=7.8%, range=15.3% to 76.5%) of the daily geolocation estimates. This procedure provided data sets of geolocation estimates throughout the period of time at liberty for each fish, about which we have a high level of confidence based on the expected accuracy and precision of these data (accuracy being the closeness of geolocation estimates to the actual position and precision the closeness or dispersion of repeated estimates [Kendall and Buckland, 1982]).

Each set of filtered geolocation estimates for individual bigeye tuna was integrated into a Geographic Information System (GIS). The animal movement analyst extension (AMAE) (Hooge and Eichenlaub, 1997; Hooge, et al.[2]) and the ArcView (Environmental Systems Research Institute, Inc., Redlands, CA) GIS program were used for mapping movement paths and for performing various spatial analyses of the data. The site-fidelity test in AMAE, employing 1000 random walks, was used to test the null hypothesis of random movement. The test is a modified Monte Carlo random walk, starting at the location of release, constrained by the coastline, and uses the actual sequence of distances between geolocation estimates to determine walk points. The fixed kernel home range model in the AMAE, which incorporates a least-squares cross-validation smoothing function, was used to assess probabilistic home ranges of fish for which the null hypothesis was rejected in the site-fidelity test. The 95% and 50% utilization distributions (probability contours) were chosen to describe the areas probably used (95%) and the probable core areas (50%) of activity, respectively, of individual fish.

For fish at liberty for 30 d or more, the behavior for each day at liberty was classified as unassociated (with a floating object) type-1, unassociated type-2, or associated with a floating object. Type-1 behavior is defined as that in which the fish primarily occupies the mixed layer during the night, descends at dawn below the thermocline to depths greater than 100 m and remains below 100 m throughout the day (aside from vertical forays into the mixed layer with a frequency of no more than 12 per day) and then ascends back into the mixed layer at dusk. This basic pattern has been described by Holland et al. (1990) and Dagorn et al. (2000), based on sonic tracking studies of bigeye tuna. Data from periods immediately after release at FADs until the time the FADs were removed and the data immediately preceding recapture at FADs were evaluated to determine criteria for classifying behavior of fish associated with floating objects. The percentages of time that 19 bigeye tuna spent at depths greater than 50 m, within 24-h intervals, for a total of 74 days, ranged from 0.0% to 29.1%. Sixty-nine percent of the 24-h intervals indicated that 16% or less time was spent below 50 m. The days when the fish were below 50 m for 16% of the time or less were classified as behavior associated with a floating object, and the days in which that time was greater than 16% were classified as unassociated type-2 behavior. For each fish, the numbers and durations of each behavioral event were determined throughout the period at liberty. A statistical test for a difference between the spatial distributions of the geolocation estimates for unassociated and associated behavior was conducted (Syrjala, 1996).

Dives in excess of 500 m were classified as deep dives, and the time, duration, and maximum depth of each event was determined for each bigeye tuna throughout periods at liberty. For those dives in which the pressure sensor reached its limit, at approximately 1000 m, depth was estimated from the ambient temperature value recorded by the tags by using historical annual mean temperatures at depths for the area of the deep diving event (Levitus and Boyer, 1994). The light level and ambient temperature data recorded by tags from bigeye tuna making dives in excess of 500 m indicated that light was essentially nonexistent below 500 m and that the ambient temperature was less than 8.5°C.

The archival tag data sets (for each recaptured bigeye tuna at liberty for at least 30 d) were separated into periods of nighttime and daytime by using light-level records. Nighttime was classified as the period between the time of the first record after dusk when there was no recognizable light from the sun until the time of the last record (before dawn) of no recognizable light from the sun. The individual data sets for night and day were used in evaluations of diel differences in behavior and habitat selection. The data for each night were classified by the moon phase (U. S. Naval Observatory, 2001). The classification scale used was 1 through 29 for the entire moon phase cycle. We analyzed changes in average daytime and nighttime depths for 20 individual bigeye tuna in relation to the visible disk area of the moon.

Results

Behavior

Evaluation of the depth and temperature records for bigeye tuna carrying archival tags resulted in the discrimination of four distinct behaviors: 1) unassociated type-1, 2) unassociated type-2, 3) associated with a floating object, and 4) deep diving. For the 23 fish at liberty for 30 or more days, behavior was classified for each day at liberty, and the duration of each behavior was determined (Table 2).

The behaviors of fish released or recaptured at FADs were distinct and discernible from the behaviors after the FAD was removed until the fish associated with the FAD at which it was recaptured (Fig. 1). Fish released at FADs showed a consistent swimming depth, predominantly less than 50 m during the night and day. When the FAD was removed fish showed an erratic up-and-down swimming behavior, followed by a consistent pattern of shallow (less

[2] Hooge, P. N., W. Eichenlaub, and E. K. Solomon. 2001. Using GIS to analyze animal movements in the marine environment. *In* 2001, spatial processes and management of marine populations (G. H. Kruse, N. Bez, A. Booth, M. W. Dorn, S. Hills, R. N. Lipcius, D. Pelletier, C. Roy, S. J. Smith, and D. Witherell, eds.), 20 p. Univ. Alaska Sea Grant, P.O. Box 755040, Fairbanks, AK 99775-5040.

Table 2

Summary statistics for the classification of daily behavior of 23 bigeye tuna at liberty for 30 days or more. The definitions for the four behavioral types and the classification criteria used are given in the text. The percentage of the total days at liberty for which an individual was classified as exhibiting a behavioral type is given as % days. The total number of events observed and classified in each dataset for a behavioral type and the mean duration for those events are given. Durations are given in days, except for deep diving events, which are given in hours.

	Unassociated type-1			Unassociated type-2			Associated			Deep diving	
Tag no.	% days	events	$\bar{x}$ duration	% days	events	$\bar{x}$ duration	% days	events	$\bar{x}$ duration	events	$\bar{x}$ duration
99-787	64.7	8	10.4	22.5	8	3.6	12.8	5	3.3	1	0.9
99-792	37.6	16	4.3	41.9	15	5.1	37.5	5	7.5	14	1.5
99-793	41.0	19	7.0	49.9	24	6.5	9.2	7	4.1	4	2.2
99-801	64.5	5	10.3	13.5	3	3.6	22.0	4	4.4	5	1.2
99-803	59.2	7	8.0	15.9	6	2.5	24.9	7	3.4	2	1.1
99-804	41.9	13	5.7	45.7	14	5.7	12.3	6	3.6	5	0.5
99-810	79.0	5	8.9	2.6	2	0.7	18.4	6	1.7	6	0.7
99-812	49.9	20	4.0	34.6	19	2.9	15.4	10	2.5	10	1.7
99-814	48.5	41	4.3	43.9	43	3.7	7.6	12	2.3	22	1.7
99-816	68.1	3	8.5	30.6	3	3.8	1.3	1	0.5	5	1.1
99-817	43.4	5	5.4	33.3	6	3.4	23.3	4	3.6	1	0.7
99-826	59.5	18	9.0	33.0	18	5.0	7.5	6	3.4	10	1.0
99-835	79.5	4	11.2	1.5	2	0.4	19.0	4	2.7	0	—
99-839	70.3	5	7.9	8.9	3	1.7	20.8	3	3.9	3	1.7
99-847	35.3	6	2.5	38.0	6	2.7	26.7	3	3.7	0	—
99-860	45.4	7	3.5	40.4	5	4.4	14.2	5	1.5	0	—
99-862	50.2	5	6.4	10.8	5	1.4	39.0	7	3.6	3	0.6
99-865	52.0	5	6.1	22.3	8	1.6	25.7	5	3.0	7	1.0
99-869	42.2	8	6.0	38.6	6	7.3	19.2	5	4.3	0	—
99-874	36.0	2	5.4	35.5	4	2.7	28.5	4	2.1	1	0.3
99-883	69.6	7	6.0	14.4	7	1.2	16.0	5	1.9	5	1.0
99-884	41.4	25	5.3	40.0	31	4.1	18.6	23	2.6	10	1.0
99-889	69.6	6	8.9	20.4	7	2.2	10.0	3	2.6	3	2.3
Mean	54.3	10.4	6.7	27.7	10.7	3.3	18.7	6.1	3.1	5.1	1.2
95%CI	6.1	4.0	1.0	6.2	4.5	0.8	4.0	1.9	0.6	2.3	0.3

than about 50 m) depths at nighttime and depths of about 200 to 300 m during the daytime (during the latter period vertical forays were made toward the surface [Fig. 1A]). Fish at FADs prior to recapture consistently swam at less than 50 m during the day and night, but made excursions to depths of 200 to 300 m for about 2 hours in the late afternoon. It was almost always apparent when a fish associated with a FAD because there was a change in swimming depths and behavior, specifically during the daytime (Fig. 1B).

Unassociated type-1 behavior

Type-1 behavior of bigeye tuna in the equatorial EPO was exhibited by fish not associated with FADs or other floating objects. The fish remained at 10 to 50 m at night and at 200 to 350 m during the day but undertook brief vertical forays into the mixed layer throughout the day (Fig. 2). The percentage of total days classified as type-1 behavior for individual fish ranged from 35.3% to 79.5% (mean=54.3%, 95% CI=6.1%). The mean duration of type-1 behavior ranged from 2.5 to 11.2 d (grand mean=6.7 d, 95% CI=1.0 d) (Table 2). The distribution of the durations of the 240 type-1 behaviors is shown in Figure 3A.

The differences in behavior between a 93-cm (tag 99-862) and 116-cm (tag 99-883) bigeye tuna within one week after release at the same FAD, both exhibiting type-1 behavior, are illustrated in Figure 4. Both fish showed the characteristic diel shifts in depth distribution at dawn and dusk. However, the 116-cm fish showed a shallower and less variable swimming depth at night and undertook fewer vertical forays during the daytime than did the 93-cm fish (Fig. 4A). The difference in the number of vertical forays by these two fish is explained by the more rapid rate of heat loss by the smaller individual, as indicated by the differences between the peritoneal cavity temperatures and the ambient temperatures (Fig. 4B). The 116-cm fish was able to maintain its internal temperature for longer periods of time. Thus, although these two fish were at similar maximum depth during the day, the average depth during the day for the 93-cm fish was less because of the increased time spent undergoing vertical forays.

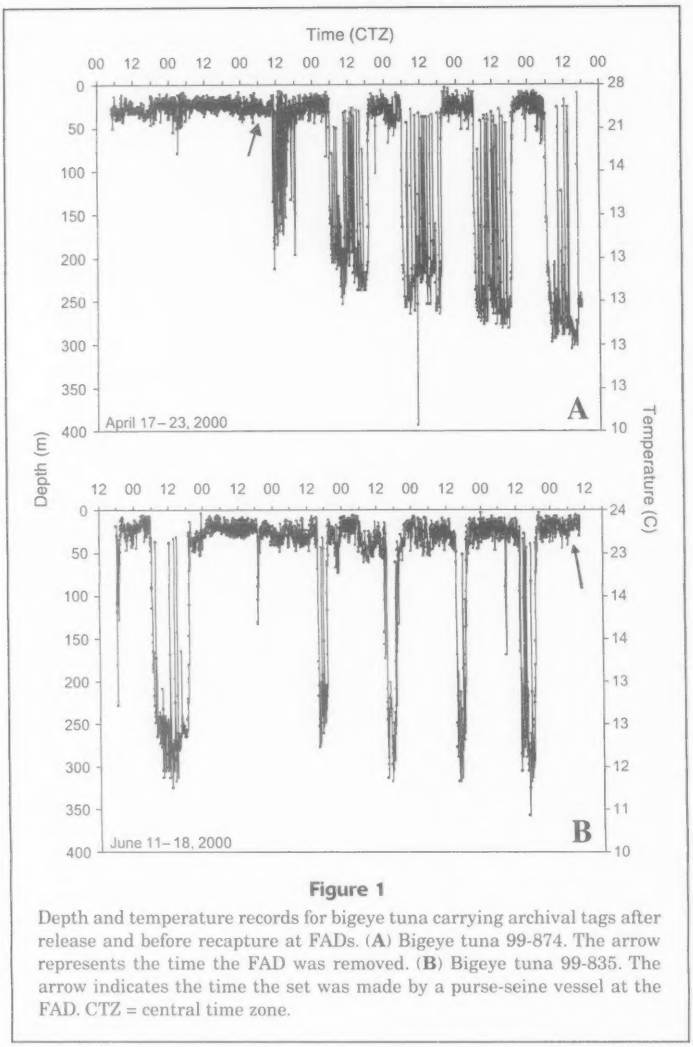

Figure 1

Depth and temperature records for bigeye tuna carrying archival tags after release and before recapture at FADs. (**A**) Bigeye tuna 99-874. The arrow represents the time the FAD was removed. (**B**) Bigeye tuna 99-835. The arrow indicates the time the set was made by a purse-seine vessel at the FAD. CTZ = central time zone.

Unassociated type-2 behavior

Type-2 behavior was defined as the behavior of fish that did not undergo the diel shifts in swimming depths at dawn and dusk but remained at depths in excess of 50 m for more than 16% of the time during a 24-h period (Fig. 5). The percentage of total days classified as type-2 behavior for individual fish ranged from 1.5% to 49.9% (mean=27.7%, 95% CI=6.2%). The mean duration of type-2 behavior for individual fish ranged from 0.4 to 7.3 d (grand mean=3.3 d, 95% CI=0.8 d) (Table 2). The distribution of the durations for each of the 245 type-2 behaviors is shown in Figure 3B.

Behavior associated with floating objects

Behavior associated with floating objects was defined as the behavior of fish that remained below 50 m for no more than 16% of the time throughout a 24-h period (Fig. 6). Although bigeye tuna mostly remained in the mixed layer while associated with floating objects, there was, nevertheless, a prominent diel cycle in the average depth distribution—from shallower at night to slightly deeper during the day (Fig. 6). The mean swimming depths for the data illustrated in Figure 6 are 27.7 m at night and 33.5 m during the day. The percentage of total days classified as associated behavior for individual fish ranged from 1.3% to 39.0% (mean=18.7%, 95% CI=4.0%). The mean duration of associated behaviors for individual fish ranged from 0.5 to 7.5 d (grand mean=3.1 d, 95% CI=0.6 d) (Table 2). The distribution of the durations of the 140 associated behaviors is shown in Figure 3C.

An examination of the classification of daily behavioral types by individual fish sorted by lengths (Table 2) indicated that a greater percentage of time was spent at FADs by bigeye tuna less than 110 cm in length (mean=23.3%,

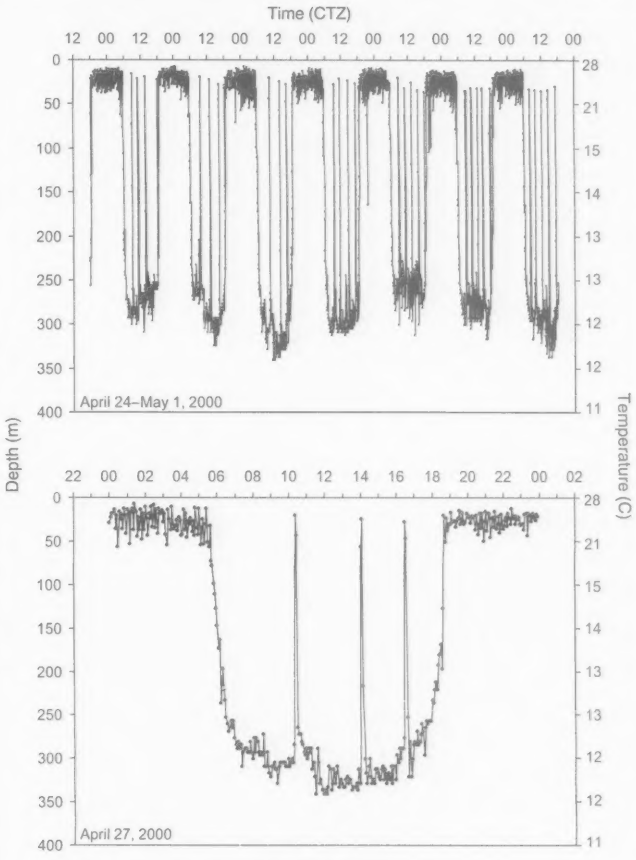

Figure 2

Depth and temperature records for a bigeye tuna carrying an archival tag (tag 99-889), exhibiting unassociated type-1 behavior. Approximate area, 1°N 97°W, is based on geolocation estimates from the archival tag. CTZ = central time zone.

n=9), even though the larger fish (mean=16.2%, n=12) still had an obvious affinity for floating objects.

Deep-diving behavior

Deep-diving behavior was defined as dives in excess of 500 m (Fig. 7). The mean duration of deep-diving behaviors for individual fish ranged from 0.3 to 2.3 h (grand mean=1.2 h, 95% CI=0.3 h) (Table 2). The distributions of the time of day, duration, and maximum depth of the 115 deep-diving events are shown in Figure 8. The majority of the deep dives occurred during daylight hours (mean=11:56 central time zone [CTZ]), although some deep dives were made at night. The prominent mode in the maximum depth distribution was about 650 to 850 m. The estimated maximum depth and minimum temperature reached by three bigeye tuna (99-801, 99-803, and 99-889) were 1500 m and 3°C, respectively.

Reliability of the geolocation estimates

The estimated mean accuracy and precision in the geolocation estimates of latitude were 2.04 and 0.79 degrees, respectively (Table 3). The associated uncertainty in those estimates averaged 2.57 degrees (95% CI=0.85) for the south error and 3.40 degrees (95% CI=1.00) for the north error. The estimated mean accuracy and precision of the geolocation estimates for longitude was 0.46 and 0.26 degrees, respectively (Table 3). The associated uncertainty in those estimates averaged 0.33 degrees (95% CI=0.13) for the west error and 0.17 degrees (95% CI=0.13) for the east error.

Additional information on the accuracy and precision of the estimates from the processed archival tag light-level data was obtained by comparing the differences between estimates and actual latitudes and longitudes of recapture for tags 99-864 and 99-874 (Table 3). The two bigeye tuna

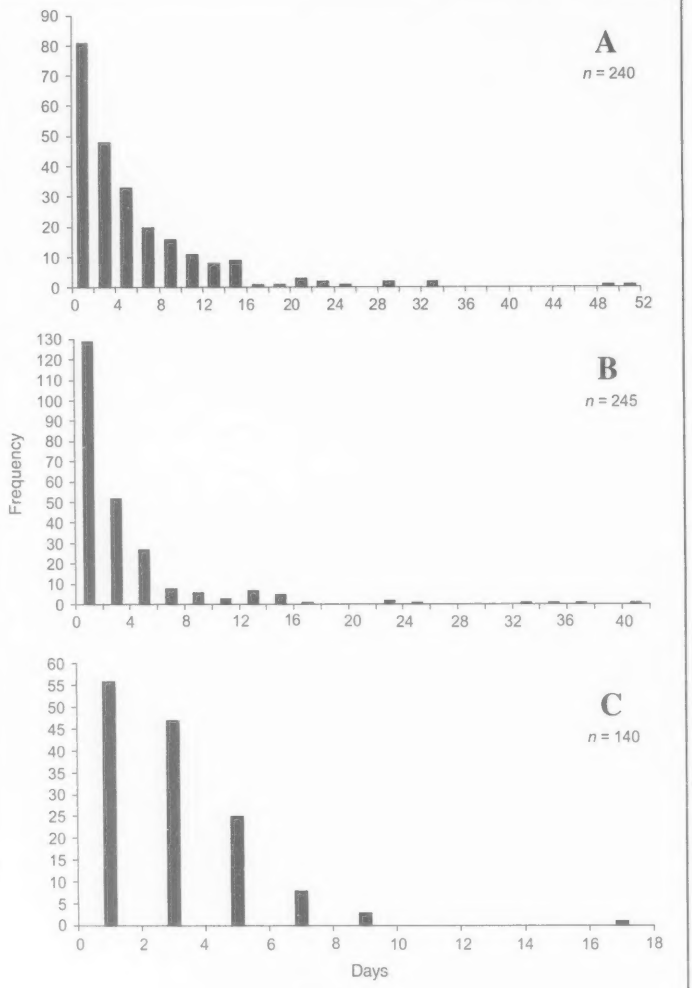

Figure 3

Distributions of the durations of all unassociated type-1 (**A**) and unassociated type-2 (**B**) events and events associated with floating objects (**C**) observed and classified for bigeye tuna listed in Table 2. The total number of events are given in the upper right corner of each panel.

carrying these tags were recaptured at the same location in the same purse-seine set. The respective differences between estimates and actual values were 0.20 and 0.30 for latitude and 0.23 and 0.06 for longitude. We also noted that the differences between estimated and actual latitudes and longitudes were 1.95 and 0.29, respectively, for the fish with tag 99-812, and 2.67 and 0.28, respectively, for the fish with tag 99-865 (Table 3). These two fish carrying these tags were recaptured by longline vessels, and scientific observers were not aboard to verify recapture positions.

Aside from the large differences between the estimates and actual recapture latitudes in Table 3 for tag numbers 99-801, 99-847, and 99-891, the majority of the estimates were within 2 degrees of the actual latitudes. Tags 99-792, 99-835, 99-861, and 99-877 were the only tags that provided differences more than 1 degree between the estimates and actual recapture longitudes.

Fish with tags 99-792, 99-793, 99-804, and 99-826 were at liberty during the autumn equinox. The geolocation estimates for longitude were unaffected by this event, but the estimates for latitude were unreliable for a few weeks

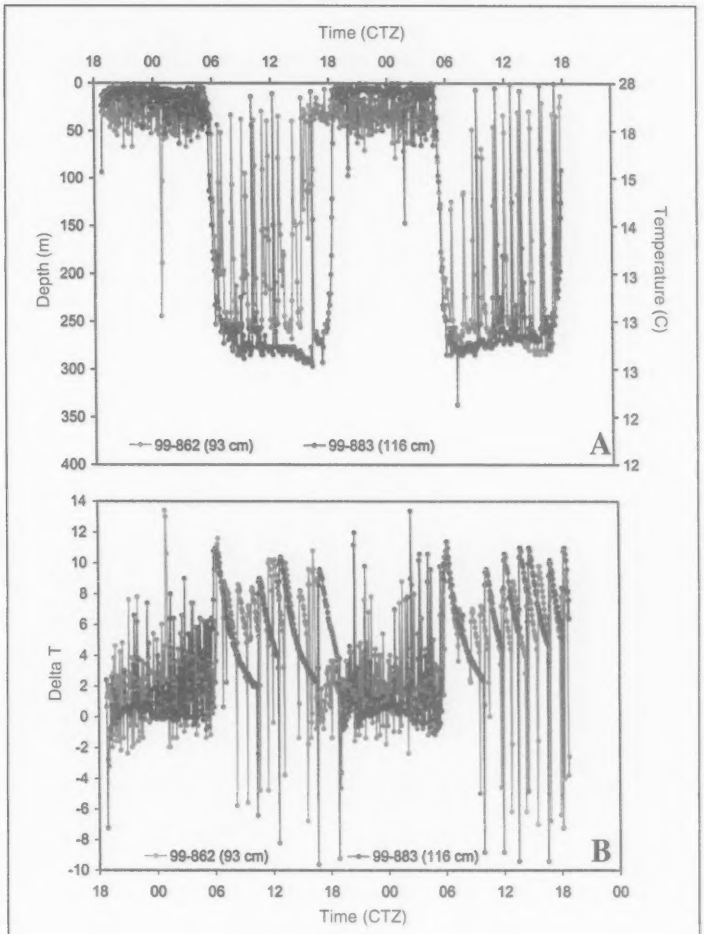

Figure 4

Simultaneous depth and temperature records for two bigeye tuna carrying archival tags, exhibiting unassociated type-1 behavior, 23–25 April 2000. Approximate area, 0°N 96°W, is based on geolocation estimates from the archival tags. (**A**) Depth and ambient temperature records (**B**) delta T's (differences between peritoneal cavity and ambient temperature) for the same time period as in A above. CTZ = central time zone.

surrounding the autumn equinox because there was very little variation in day length near the spring and autumn equinoxes (Hill and Braun, 2001).

Movements

The movements of 8 bigeye tuna at liberty for 76 to 340 days are plotted in Figure 9, A–D. No bigeye tuna went farther west than about 110°W and most spent the majority of time between 90°W to 105°W and 5°N to 5°S. Data for the estimated movement paths of 22 fish, derived from the filtered geolocation estimates, are given in Table 4. The estimated mean speeds ranged from 76 to 165 km/d (grand mean=116.6 km/d, 95% CI=10.0 km/d). The hypothesis that the observed movement path is random was rejected for 17 of the 22 fish (Table 4). A significant positive correlation (r=0.61, P<0.05) was found between the number of days at liberty and their corresponding 95% utilization distributions (Tables 1 and 4).

The areas encompassed by the 95% probability ellipses for the geolocation estimates of unassociated behavior and behavior associated with floating objects (Fig. 10), for the 22 bigeye tuna at liberty for 30 d or more (Table 4), were 3.9 and 3.1×10^6 km^2, respectively. The difference between

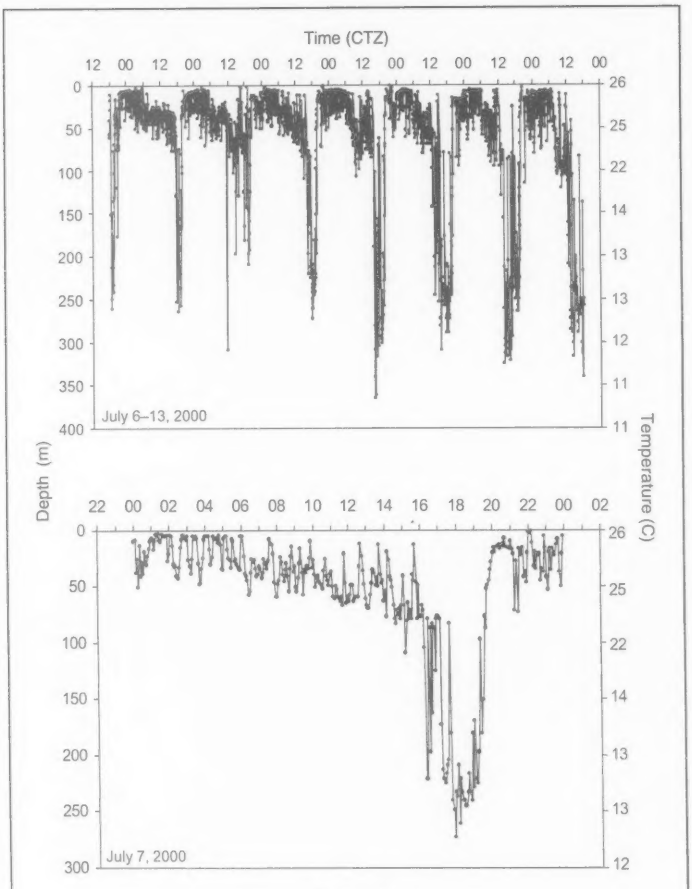

Figure 5

Depth and temperature records for a bigeye tuna carrying an archival tag (99-869), exhibiting unassociated type-2 behavior. Approximate area, 2°N 107°W, is based on geolocation estimates from the archival tag. CTZ = central time zone.

the two spatial distributions was not statistically significant (Ψ=0.313, P=0.524).

The fish with tag 99-793 was at liberty 340 d and exhibited behavior associated with floating objects for 9.2% of those days. It traveled initially to the east, remained for a considerable period in a relatively restricted area north of the Galapagos Islands, displayed some range in latitudinal movements between about 5°N and 5°S, and was recaptured only 83 nmi north of its release location (Fig. 9A, Tables 1, 2, and 4). The fish with tag 99-812 was released at a different FAD and was at liberty for a shorter period (159 d). It exhibited behavior associated with floating objects for 15.4% of the days at liberty. In contrast to the fish with tag 99-793, the fish with tag 99-812 traveled westward, displaying a fairly directed movement path, and was subsequently recaptured 821 nmi west of its release location (Fig. 9A, Tables 1, 2, and 4).

The fish with tag 99-826 was at liberty 272 d and exhibited behavior associated with floating objects for 7.5% of those days. It traveled the greatest total distance, displaying extensive longitudinal and latitudinal movements, and yet was recaptured only 279 nmi west of its release location (Fig. 9B, Tables 1, 2, and 4). The fish with tag 99-804 was released at the same FAD as the fish with tag 99-826 and was at liberty for a comparable period (250 d). It exhibited behavior associatede with floating objects for 12.4% of the days at liberty. In contrast to the fish with tag 99-826, the fish with tag 99-804 displayed a much more constrained movement path. This fish started moving to the northwest during its last few months at liberty and was subsequently recaptured 544 nmi west of its release location (Fig. 9B, Tables 1, 2, and 4).

The fish with tag 99-792 was at liberty for 183 d and exhibited behavior associated with floating objects for 37.5%

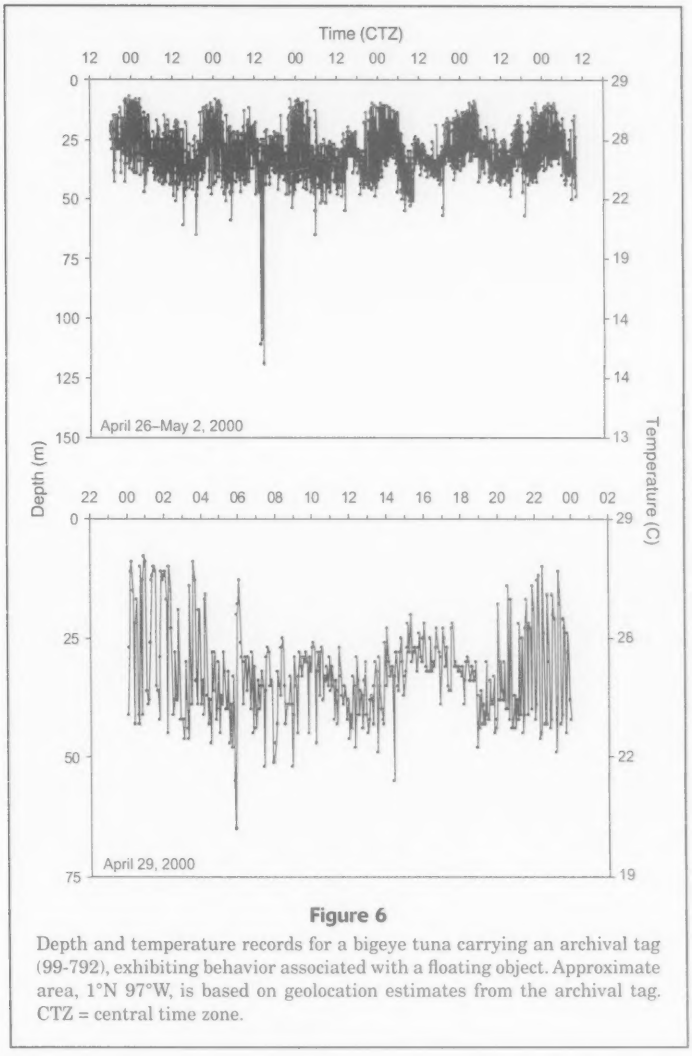

Figure 6

Depth and temperature records for a bigeye tuna carrying an archival tag (99-792), exhibiting behavior associated with a floating object. Approximate area, 1°N 97°W, is based on geolocation estimates from the archival tag. CTZ = central time zone.

of time at liberty. The fish traveled a considerable distance west and southwest to about 5°S and 110°W, before moving back toward the east. It was recaptured only 82 nmi east of its release location (Fig. 9C, Tables 1, 2, and 4). The fish with tag 99-787 was released at the same FAD where the fish with tag 99-792 was also released. It was at liberty for 129 d and exhibited behavior associated with floating objects for 12.8% of time at liberty. In contrast to the fish with tag 99-792, the fish with tag 99-787 traveled in the opposite direction, toward the east, moving fairly rapidly to around 82°W, and then moving north and south between about 3°N and 3°S. This fish was recaptured 843 nmi east of its release location (Fig. 9C, Tables 1, 2, and 4).

The fish with tag 99-889 was at liberty 76 d and exhibited behavior associated with floating objects for 10.0% of time at liberty. This fish traveled a considerable distance south to about 7°S, before moving back northward, and was subsequently recaptured only 100 nmi southwest of its release location (Fig. 9D, Tables 1, 2, and 4). The fish with tag 99-869 that was released at the same FAD where fish 99-889 was released, was at liberty 112 d and exhibited behavior associated with floating objects for 19.2% of time at liberty. The fish initially traveled in a similar direction as that of fish 99-889 before moving westward. It showed extensive latitudinal movements from about 5°S to 5°N, and was recaptured 430 nmi northwest of its release location (Fig. 9D, Tables 1, 2, and 4).

Habitat selection

The habitat selected by bigeye tuna is presented by month in Figure 11, for days with unassociated type-1 behavior only. The nighttime and daytime depth distributions were very similar for April, May, and June. Most of the time

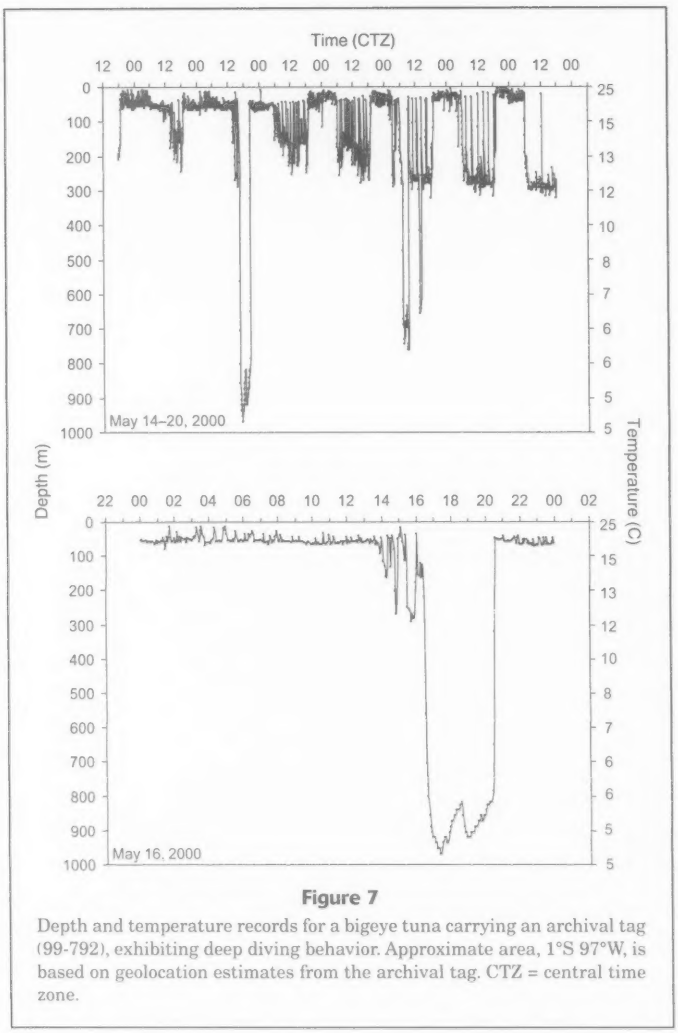

Figure 7

Depth and temperature records for a bigeye tuna carrying an archival tag (99-792), exhibiting deep diving behavior. Approximate area, 1°S 97°W, is based on geolocation estimates from the archival tag. CTZ = central time zone.

was spent above 50 m at night and between 250 to 300 m during the day. From April to June, the average depths of the 20°C and 15°C isotherms were 50 and 100 m, respectively. The habitat selected by the fish during July, August, and September was different and more variable during the day than that for the previous three months. Most of the time was spent above 50 m during the night. During the day the primary mode in depth in July was similar to the previous three months, but in August the primary mode shifted to about 200–275 m. In July the average depths of the 20°C and 15°C isotherms were 17 and 90 m, respectively, whereas in August and September the average depths of the 20°C and 15°C isotherms were 10 and 75 m, respectively. In September the depth distribution during the day was more uniform from about 100–350 m, with a slight mode between 175 and 250 m. The daily vertical behavior of the fish during September was highly unusual and erratic in relation to previous months and to October; 78% of the days for five fish were classified as unassociated type-2 behavior. The habitat selected by the fish during October, November, and December was different during the night, than that for the previous six months. Most of the time was spent above 25 m during the night. During the day the primary modes in depth during October, November, and December were not as distinct as in previous months, excluding September, but were primarily between 150 and 275 m. The average depths of the 20°C and 15°C isotherms for October and December were 15 and 75 m respectively, whereas in November the average depths of the 20°C and 15°C isotherms were 25 and 50 meters, respectively. The habitat selected by the fish during the day in January, February, and March was similar, with a distinct mode in depth between about 200 and 300 m. During the night, there was a transition

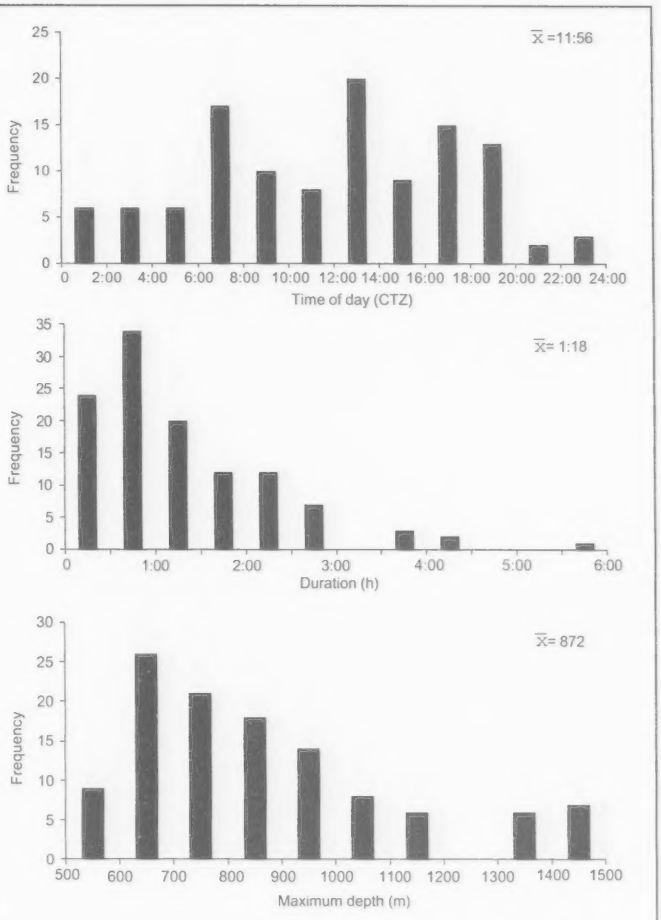

Figure 8

Distributions of the time of day, duration, and maximum depth for 115 deep-diving events observed and classified for bigeye tuna listed in Table 2. The average value is given in the upper right corner of each panel. CTZ = central time zone.

during these three months from most of the time being spent above 25 m in January to a greater amount of time spent between 25 to 50 m at night in March. This transition corresponded with a downward shift in the depths of the 20°C and 15°C isotherms from an average of 30 and 80 m in January and February to 50 and 100 m in March, respectively.

The percentages of time that 13 bigeye tuna (112–126 cm in length at release) spent within 25-m depth intervals from the surface to 400 m, during each hour of each day at liberty, while exhibiting unassociated type-1 behavior, are given in Table 5. The average daytime temperatures and depths for these fish throughout their times at liberty, when exhibiting type-1 behavior, indicated that the highest concentration (about 50%) were between 13° and 14°C and 200 and 300 m depth. About 85% of the data were distributed between 13° and 16°C and 150 and 300 m in depth.

Twelve of the twenty-two bigeye tuna showed significant correlations (r=0.61 to 0.75, P<0.05) between the visible disk area of the moon and their average nighttime depth distributions. There was a significant correlation (r=0.81, P<0.05) between the average nighttime depth for all 22 fish and the visible disk area of the moon (Fig. 12A). Fish occupied significantly greater depths for the 7-day period surrounding the full moon (29.0 m), in contrast to the other 22 days of the lunar cycle (21.2 m) (Fig. 12A). The average nighttime light levels indicated that the change in depth did not totally compensate for the greater light intensity during the full moon phase (Fig. 12A). Eight of the twenty-two fish showed significant correlations (r=0.54 to 0.75, P<0.05) between average daytime depth

Table 3

The accuracy, precision, and uncertainty in estimated latitudes and longitudes derived from archival tag light-level data from 21 bigeye tuna, processed with the geolocation programs of Wildlife Computers (Hill and Braun, 2001). The latitudes and longitudes are given as decimal degrees (dd). The error estimates are the uncertainty about the individual estimates of latitude or longitude. The differences are those between the actual latitude and longitude of recapture and the corresponding geolocation estimates.

	Recapture latitude (dd)					Recapture longitude (dd)				
Tag no.	Actual	Estimate	South error	North error	Difference	Actual	Estimate	West error	East error	Difference
99-787	1.72 N	1.0 N	2.5	2.5	0.72	83.08 W	82.97 W	0.5	0.0	0.11
99-792	1.35 N	3.0 N	3.0	4.0	1.65	95.82 W	93.93 W	0.5	0.0	1.89
99-801	1.47 N	5.0 S	1.5	4.5	6.47	90.72 W	90.62 W	0.5	0.0	0.10
99-803	2.20 N	1.0 N	2.5	2.0	1.20	102.72 W	102.12 W	0.5	0.0	0.60
99-810	1.65 S	2.5 S	1.5	2.0	0.85	93.17 W	93.21 W	0.0	0.5	0.04
99-812	0.55 N	2.5 N	0.0	2.0	1.95	109.00 W	109.29 W	0.0	0.5	0.29
99-816	1.78 N	1.5 N	3.0	3.5	0.28	97.60 W	97.40 W	0.0	0.5	0.20
99-817	1.12 S	2.0 S	3.5	5.5	0.88	95.87 W	95.47 W	1.0	0.0	0.40
99-835	1.20 N	5.0 N	2.5	2.5	3.80	99.68 W	98.48 W	0.5	0.0	1.20
99-839	2.33 S	0.0 N	6.5	0.5	2.33	95.75 W	95.54 W	0.5	0.0	0.21
99-847	1.77 N	3.0 S	2.5	5.0	4.77	97.23 W	97.17 W	0.0	0.5	0.06
99-860	2.18 S	2.0 S	3.0	2.0	0.18	97.87 W	97.20 W	0.5	0.0	0.67
99-861	2.23 S	1.5 N	6.0	6.5	3.73	96.67 W	95.56 W	0.0	0.0	1.11
99-864	2.70 N	2.5 N	1.0	3.0	0.20	97.87 W	98.10 W	0.5	0.5	0.23
99-865	2.67 S	0.0 N	1.5	6.5	2.67	99.05 W	99.33 W	0.5	0.0	0.28
99-869	4.85 N	4.0 N	2.5	2.0	0.85	103.18 W	103.35 W	0.5	0.0	0.17
99-874	2.70 N	3.0 N	1.0	2.0	0.30	97.87 W	97.81 W	0.5	0.0	0.06
99-877	2.77 S	2.0 S	7.0	3.0	0.77	99.20 W	97.37 W	0.0	1.0	1.83
99-883	1.60 S	0.5 N	0.5	0.5	2.10	95.55 W	95.67 W	0.0	0.0	0.12
99-889	0.37 N	2.5 S	1.5	2.5	2.87	98.58 W	98.57 W	0.0	0.0	0.01
99-891	0.25 S	4.5 S	1.0	9.5	4.25	92.88 W	92.74 W	0.5	0.0	0.14
Mean			2.57	3.40	2.04			0.33	0.17	0.46
95% CI			0.85	1.00	0.79			0.13	0.13	0.26

distributions and visible disk area of the moon. The patterns in average daytime depths for 5 of the 8 fish showed a significantly shallower depth distribution for a 3-day period surrounding the full moon (190 m) compared to the other 26 days of the lunar cycle (221 m). There was no apparent pattern, and the correlation coefficient (r=0.15, P>0.05) was not significant for the average daytime depth for all 22 bigeye tuna in relation to the visible disk area of the moon (Fig. 12B).

Discussion

The results obtained in our study are useful for evaluating fine- to large-scale horizontal and vertical movements, behavioral patterns, and habitat characteristics on spatial and temporal scales previously undocumented for bigeye tuna. Movement paths, residence times at FADs, and habitat selection are essential for understanding the ecology of this species, and should be incorporated into stock assessment models to evaluate its vulnerability to various modes of fishing.

In addition to the 96 bigeye tuna released with archival tags, we released 101 bigeye tuna, in the same area and time period, with conventional plastic dart tags only. To date, 29 (30%) of the fish with archival tags and 22 (23%) of these with conventional tags have been confirmed as recaptured. The difference between these percentages was not significant (P>0.05), indicating that tagging mortality was probably no greater for the fish with archival tags than the fish with conventional tags.

Several of the archival tags were removed from recaptured bigeye tuna by members of the scientific staff of the Inter-American Tropical Tuna Commission (IATTC). All but two of the tags were situated in the peritoneal cavity, in the general area where they were implanted, and were apparently encapsulated by fibrous connective tissue. Of the two other tags, one had apparently been invaginated into the lumen of the stomach and the other into the lumen of the intestine. Apparently the fish were attempting to expel these foreign bodies from their peritoneal cavities. Transintestinal expulsion of surgically implanted transmitters by fish was previously considered an exceptional phenomenon, except in the case of catfish (Marty and

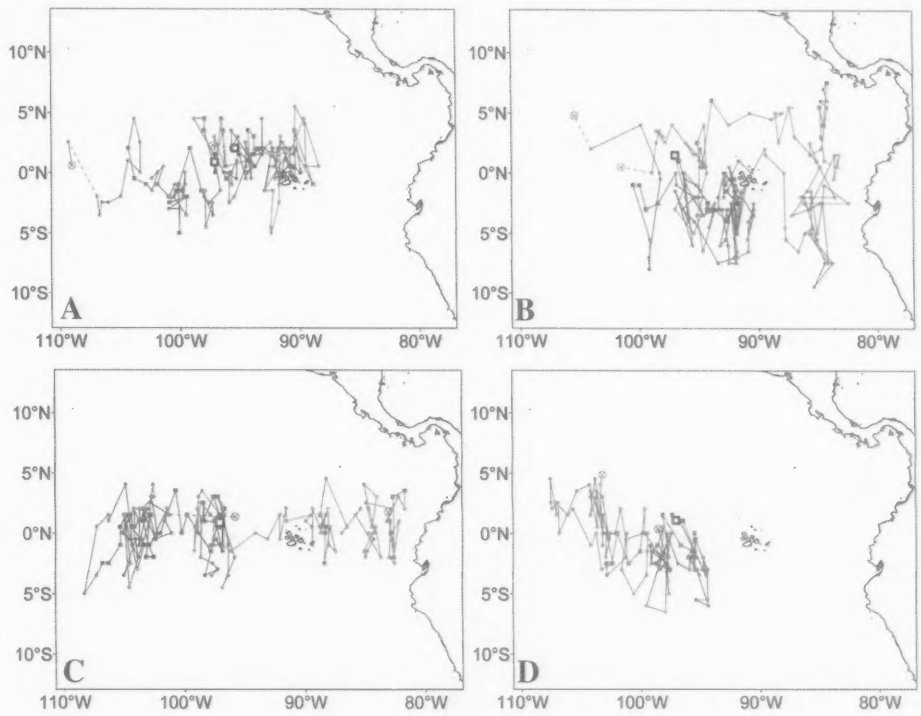

Figure 9

Movement paths of bigeye tuna derived from filtered geolocation estimates. The open squares are the release positions at FADs. The open circles and solid squares are geolocation estimates for unassociated behavior and behavior associated with a floating object, respectively, and the crosshairs are the recapture positions. The color code for each fish, in each map, corresponds with the following tag number. (**A**) blue: 99-812. The dashed line, between two geolocation estimates on 16 August and 27 September 2000, represents our inability to obtain reliable estimates of latitude from light level data near the equinox. red: 99-793. The dashed line, preceding the recapture position, represents our inability to obtain reliable estimates of latitude from light level data near the equinox and the failure of the tag to log data on 3 October 2000. (**B**) blue: 99-804. The dashed line, preceding the recapture position, represents the failure of the tag to log data on 9 October 2000. red: 99-826. The dashed line, between two geolocation estimates on 20 August and 4 October 2000, represents our inability to obtain reliable estimates of latitude from light level data near the equinox. The dashed line, preceding the recapture position, reflects the failure of the tag to log data on 25 December 2000 (**C**) blue: 99-792. The dashed line, beginning on 31 August 2000 preceding the recapture position, represents our inability to obtain reliable estimates of latitude from light level data near the equinox. red: 99-787. (**D**) blue: 99-889. red: 99-869.

Summerfelt, 1986; Baras and Westerloppe, 1999). In most specimens, the ventral region of the body wall, where the stalk protruded, did not appear to be completely healed. A small, dark, circular crater was seen at the base of the stalk—obviously a mark of irritation from the movement of the stalk even after the tag body had been encapsulated by flesh. Unless it is necessary to collect internal temperature data, the dorsal musculature is a potentially better location for implanting archival tags, of appropriate size and shape, for long-term deployment (Brill et al.[3]).

The long-term performance of the archival tags used in our experiment was questionable. The bigeye tuna that we studied pushed these tags to the limits of their design specifications by undergoing regular daily vertical forays with fairly dramatic temperature and pressure fluctuations, in addition to making the unexpected deep diving events exceeding 1000 m.

Of the 27 archival tags recovered to date, four of them failed to collect light data because of apparent problems

[3] Brill, R. W., K. Cousins, and P. Kleiber. 1997. Test of the feasibility and effects of long-term intramuscular implantation of archival tags in pelagic fishes using scale model tags and captive juvenile yellowfin tuna (*Thunnus albacares*). NMFS Admin. Rep. H-97-11,12 p. Southwest Fisheries Center Honolulu Laboratory, National Marine Fisheries Service, NOAA, Honolulu, HI 96822-2396.

Table 4

Spatial statistics for 22 bigeye tuna at liberty for 30 days or longer, based on filtered estimates of the geographic locations derived from the archival tag light level data. n is the total number of geographic locations in the data set. Distance is the total distance traveled per data set. Linearity is the ratio of the distance between the data set endpoints and the total distance traveled. MSD is the mean squared distance from the center of activity. p is the proportion of MSD values, from a Monte Carlo simulation, higher than the MSD value from the observed data. UD is the utilization distribution, for the 95% and 50% probability levels, reported as area in km^2. NA stands for non applicable because those estimates are only valid if the movement path indicates site fidelity.

Tag no.	n	Distance (km)	$\bar{x}$ bearing	$\bar{x}$ speed (km/d)	Linearity	MSD (km 10^9)	Site fidelity (p)	95% UD (km^2)	50% UD (km^2)
99-787	75	13596	11	105	0.12	408.017	59.6	NA	NA
99-792	94	20017	217	142	0.01	195.310	99.7	1,182,310	131,437
99-793	52	11996	30	86	0.06	111.726	99.9	793,555	103,429
99-801	32	7513	171	94	0.09	227.857	78.9	NA	NA
99-803	72	11721	186	123	0.08	134.198	95.3	802,037	100,354
99-804	75	17044	219	115	0.06	218.924	98.4	1,169,153	104,391
99-810	33	6975	51	122	0.05	79.566	99.9	430,586	83,410
99-812	78	14603	182	92	0.11	262.036	84.2	NA	NA
99-814	70	17671	138	143	0.02	109.497	99.9	836,649	158,936
99-816	27	4752	309	128	0.08	62.609	96.7	393,121	49,882
99-817	36	7970	158	129	0.03	83.159	99.9	478,858	50,205
99-826	108	23,085	219	113	0.03	494.010	78.9	NA	NA
99-835	37	6785	183	119	0.09	111.445	91.9	NA	NA
99-839	24	6143	267	110	0.03	90.090	99.4	501,057	107,094
99-847	11	3188	126	76	0.04	113.948	96.3	516,561	145,177
99-860	38	8893	324	165	0.02	65.013	99.9	389,426	51,713
99-865	29	6572	258	111	0.06	69.959	99.8	508,706	94,889
99-869	81	15811	335	140	0.05	221.813	95.5	1,295,394	205,956
99-874	17	4395	96	146	0.03	123.812	95.4	526,085	84,107
99-883	29	7282	58	121	0.03	83.922	99.9	564,556	103,384
99-884	149	32501	115	98	0.04	174.997	99.9	1,164,992	341,468
99-889	31	6694	252	87	0.03	85.269	99.3	609,874	154,383

with their stalks. The batteries in four of the six tags, which were in fish at liberty for 175 days or more, failed and these tags stopped collecting data. Fortunately, however, previously collected data were preserved in the nonvolatile memories of the tags. Perhaps the most important feature of archival tags is their ability to collect data on the movement of tagged fish at frequent intervals from release until recapture (Hunter et al., 1986; Gunn and Block, 2001). There are, however, several factors that can affect the accuracy of the geoposition estimates. These include, but are not limited to, latitude, equinoxes, resolution of the light sensor, light attenuation, and behavior of the fish (Gunn and Block, 2001; Musyl et al., in press).

Gunn et al.[4] previously reported the accuracy of geolocation estimates from the light data from archival tags attached to southern bluefin tuna (*Thunnus maccoyii*) held in cages in the Indian Ocean to be about 0.5° in longitude and 1.5° in latitude. Welch and Eveson (1999) and Musyl et al. (2001) estimated the accuracy of geolocation estimates from the light-level data recorded by archival tags by comparing the known and estimated locations of tags that were attached to oceanographic buoys in the north Pacific. The reported accuracy by Welch and Eveson (1999) was ±0.9° in longitude and ±1.2° in latitude. The reported accuracy by Musyl et al. (2001) ranged from 0.2° to 0.3° in longitude and from 1.5° to 4.4° in latitude. In our study, we estimated the accuracy of geolocation estimates (longitude: 0.5°, latitude: 2.0°) by comparing the known and estimated locations of 21 bigeye tuna on their days of recapture (Table 3).

We used our estimates of accuracy and precision as criteria for filtering the daily geolocation estimates. In other studies where archival tags were used to provide estimated movement paths, geolocation estimates derived from light data have been verified or adjusted by comparing recorded temperatures from archival tags with maps of estimated sea-surface temperatures from satellite data (Gunn and Block, 2001). In the equatorial EPO, sea-sur-

[4] Gunn, J. S., T. W. Polacheck, T. L. O. Davis, M. Sherlock, and A. Betlehem. 1994. The development and use of archival tags for studying the migration, behavior and physiology of southern bluefin tuna, with an assessment of the potential for transfer of the technology to groundfish research. *In* Proceedings of ICES mini-symposium on fish migration, 23 p. International Council for the Exploration of the Sea, Palaegade 2-4, DK-1261 Copenhagen K, Denmark.

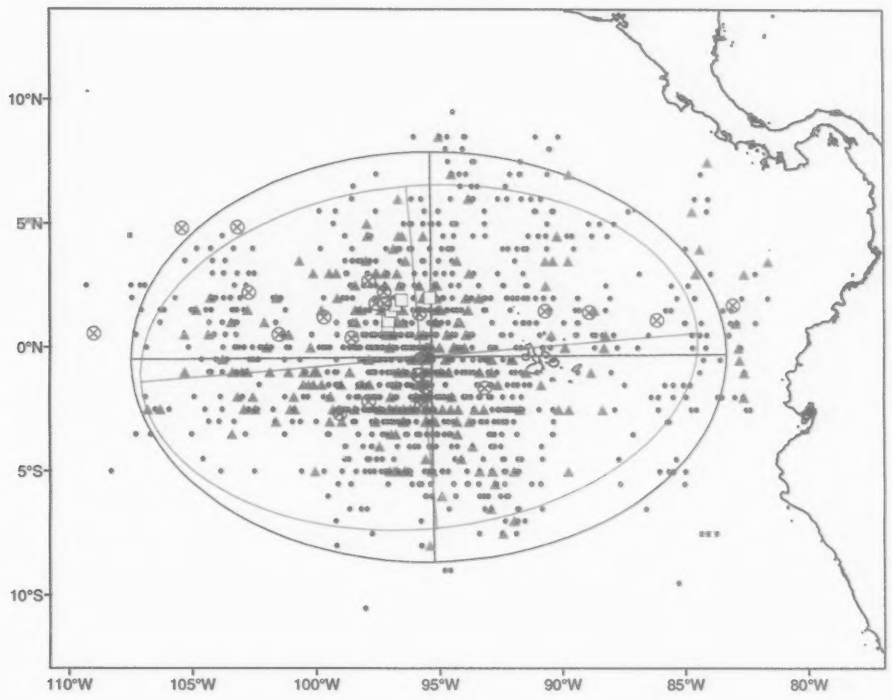

Figure 10

Geolocation estimates for 22 bigeye tuna at liberty for 30 d or longer (Table 4) classified as unassociated (blue dots) or associated with floating objects (red triangles). The yellow solid squares are the release locations and the green crosshairs are the recapture locations. The larger blue and red dots, axes, and elipses are the arithmetic means, major and minor axes, and 95% probability ellipses, respectively, for the spatial distributions of the geolocation estimates for unassociated behavior and behavior associated with floating objects.

face temperatures vary little over extremely large areas (Fiedler, 1992); therefore this technique is much less useful than in temperate regions.

The movement paths shown for bigeye tuna in our study (Figs. 9 and 10) derived from the filtered archival tag light data indicated that the area was restricted to the equatorial EPO. No fish traveled further west than about 110°W, and most movements were constrained between about 95° and 100°W and 3°N and 5°S. However, the value of the archival tags in providing fisheries-independent information on dispersion and movement paths is apparent, especially considering the fact that 16 of the fish were recaptured within 300 nmi of where they were released. Furthermore, the minimum convex polygon for the filtered archival tag data is approximately four times the area of the minimum convex polygon surrounding the release and recapture positions. Movements of bigeye tuna inferred from large-scale conventional tagging programs in the western Pacific (Hampton and Gunn, 1998; Hampton et al.[5]; Kaltongga[6]) and Hawaii (Itano and Holland, 2000) indicate that, although there are some long-distance movements, most recoveries are near their points of release. Those data appear to indicate, as do those of the present study, regional fidelity for bigeye tuna, and that the expected degree of mixing is quite low between the EPO and the central and western Pacific Ocean (CWPO).

The estimated mean velocity of 117 km/d or 2.6 knots (Table 4) is comparable to the estimate of 130 km/d for Pacific bluefin tuna (*Thunnus orientalis*) from archival tag data (Tsuji et al., 1999). Although this estimate should not be interpreted as actual swimming speed through the water, considering the imprecision of the movement paths and the fact that daily vertical movements were not

[5] Hampton, J., K. Bigelow, and M. Labelle. 1998. A summary of current information on the biology, fisheries and stock assessment of bigeye tuna (*Thunnus obesus*) in the Pacific Ocean, with recommendations for data requirements and future research. Secretariat of the Pacific Community, Oceanic Fisheries Programme, Technical Report 36,46 p. Oceanic Fisheries Programme, SPC, B.P. D5, 98848 Noumea Cedex, New Caledonia.

[6] Kaltongga, B. 1998. Regional tuna tagging project: data summary. Oceanic Fish. Prog. Tech. Rept. 35, 70 p. Secretariat of the Pacific Community. Noumea, New Caledonia. Oceanic Fisheries Programme, SPC, B.P. D5, 98848 Noumea Cedex, New Caledonia.

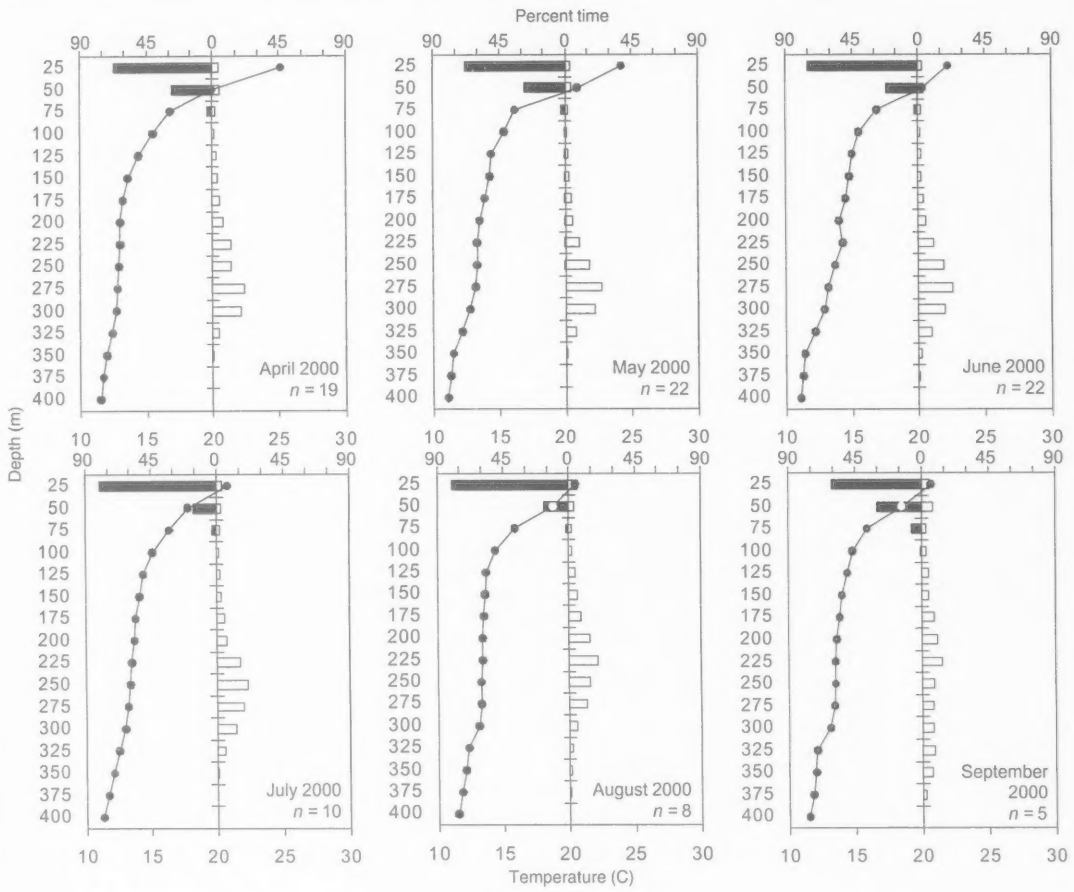

Figure 11

Depth frequencies of bigeye tuna during the night (solid bars) and day (open bars), along with the vertical thermal profiles by month and year (unassociated type-1 behavior days only). Data from depths greater than 400 m are excluded. The number of fish represented in each month is given.

included in the calculations of velocity. Nevertheless, this estimate should be useful for incorporation into a spatially stratified movement model that is designed to evaluate dispersion and mixing rates between large regions (see Sibert and Fournier, 2001).

Sonic tracking studies have shown that the diel vertical migrations of bigeye tuna are closely associated with vertical movements of organisms of the deep scattering layer (DSL). Bigeye tuna probably forage on squids and other mesopelagic organisms within the DSL throughout the day and night (Josse et al., 1998; Dagorn et al., 2000). As reported by Blunt (1960), squid are very important in the diet of subsurface bigeye tuna, in the eastern tropical Pacific (ETP)—70% of the stomachs examined contained squid equivalent to 60% of the total food volume. Fiedler et al. (1998) reported the depths of the DSL in the ETP as 300–400 m during the day and 0–100 m at night. Other studies have documented that bigeye tuna have evolved anatomical and physiological adaptations to enable them to exploit organisms of the DSL during the daytime in a dark, cold, and oxygen-poor environment (Kawamura et al., 1981; Holland et al., 1992; Brill, 1994; Holland and Sibert, 1994; Schaefer, 1999; Lowe et al., 2000; Graham and Dickson, 2001).

The depth distributions of bigeye tuna not associated with FADs near Hawaii and in the Coral Sea are significantly greater than those for bigeye tuna in the equatorial EPO. It seems possible that the greater daytime depths exhibited by bigeye tuna in the CWPO are related to the greater daytime DSL depths (≥400 m) in that region (Maynard et al., 1975; Tont, 1976; Davies, 1977; Kuznetsov et al., 1982; Fiedler et al., 1998; Josse et al., 1998). For a 112-cm

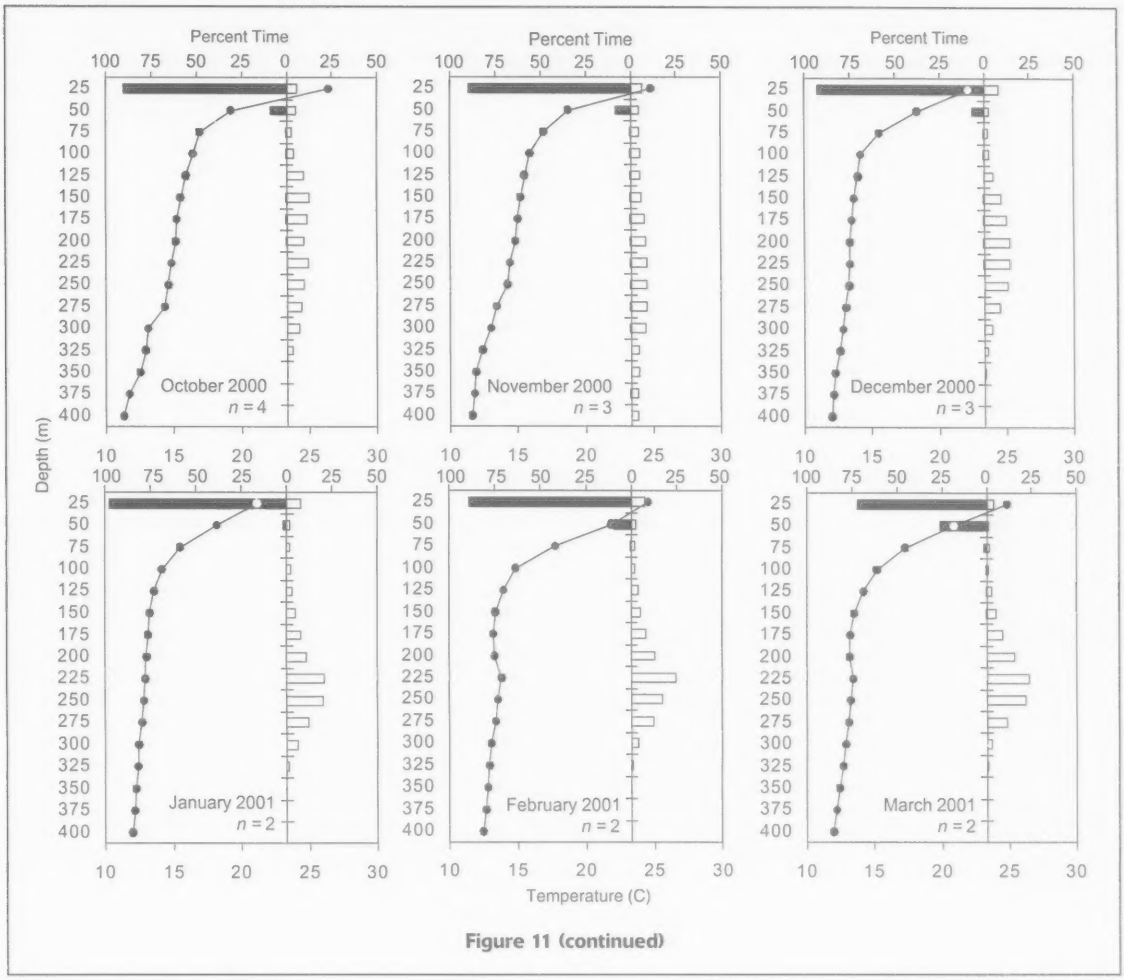

Figure 11 (continued)

bigeye tuna in the equatorial EPO not associated with a FAD (Fig. 2), the baseline daytime depth was 250 to 300 m at temperatures of 12° to 13°C. For a 131-cm bigeye tuna exhibiting similar behavior in Hawaiian waters, the baseline daytime depth was 400 to 500 m at temperatures of 7° to 10°C (Musyl et al., in press). Gunn and Block (2001) reported that bigeye tuna with archival tags in the Coral Sea showed that the mean depth of the fish at night was 50 m and that during the day they were at depths of 450 to 500 m and at temperatures of 7° to 9°C.

The average light level experienced by bigeye tuna at night (77 Wildlife Computer's light level [wcl] at 24 m), is below that experienced during the day (126 wcl at 242 m). Therefore, bigeye tuna do not occupy an isolume as has been suggested for other vertically migrating organisms (Widder and Frank, 2001). Bigeye tuna are also able to adapt to much higher light levels (195 wcl) for prolonged periods when remaining at shallow depths during daylight hours when they are associated with FADs.

Unassociated type-2 behavior observed in bigeye tuna (Fig. 5 and Table 2) may be attributed to a shift in the vertical distribution of prey items. Monospecific 100- to 200-ton schools of bigeye tuna (>100 cm length) were observed feeding at the surface on the mesopelagic fish *Vinciguerria lucetia* during daylight hours on 15 December 1978 in the equatorial EPO (K. Schaefer, unpubl. data). *Vinciguerria lucetia* is normally distributed at depths of 500 m or more during the day and is common in the 0–90 m layer at night (Blackburn, 1968). During the 1971–91 period, previous to the development of the drifting FAD fishery in the EPO, many purse-seine sets made during daylight hours were successful in capturing bigeye tuna schools not associated with drifting objects (Calkins et al., 1993). Atypical behavior of large schools of *Vinciguerria nimbari*, present in large concentrations within the mixed layer during the day, has also been observed in the equatorial Atlantic Ocean (Marchal and Lebourges, 1996). This type of behavior has also been observed in the Coral Sea, where bigeye

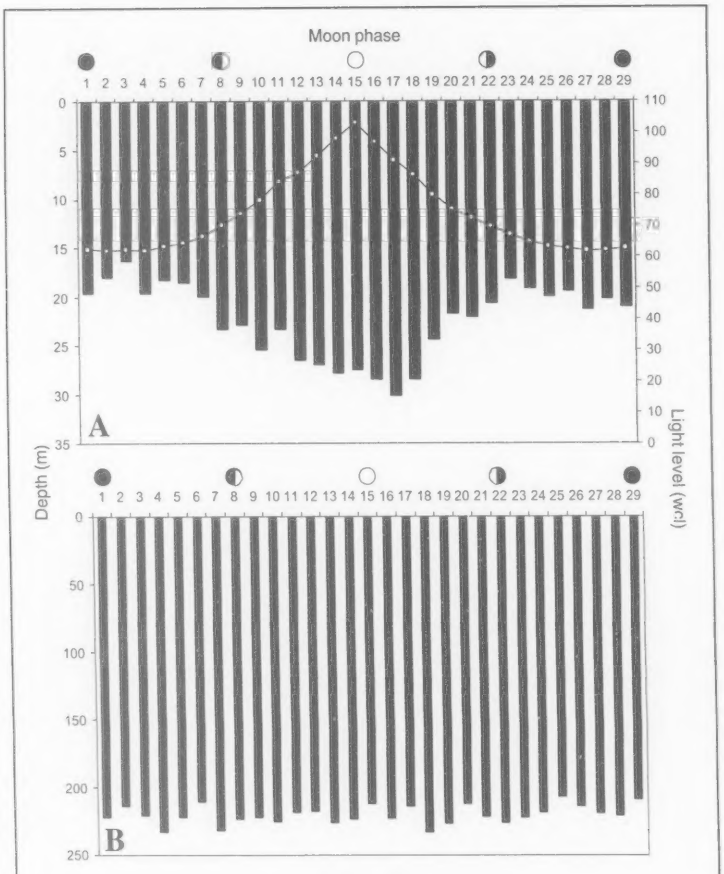

Figure 12

Average (**A**) nighttime and (**B**) daytime depths (solid bars) and light levels (open circles) for 22 bigeye tuna, by moon phase (unassociated type-1 behavior days only).

tuna are caught throughout the day near the surface by both handline and longline fisheries between October and December (Hisada, 1973). A second explanation for some of the unassociated type-2 behavior is that the fish were still possibly associated with a FAD but were making afternoon excursions into the DSL, foraging for food.

Occasionally bigeye tuna make dives in excess of 500 m (Fig. 7 and Table 2). The durations of the deep diving events are not correlated (r=0.0008, P>0.05) with body size. Moreover, there appear to be two types of deep dives (Table 2). One may be for predator avoidance. The fish descend and then ascend rapidly back to the depth at which it had been previous to the dive. The second type may be a foraging behavior, where prolonged time is spent at greater depths, up to 1000 m. Deep dives to 1000 m or more have also been reported from archival tag data for bigeye tuna in the Coral Sea (Gunn and Block, 2001) and for Atlantic bluefin tuna (Block et al., 2001a; Block et al., 2001b).

Bigeye tuna exhibiting behavior associated with floating objects (Fig. 6 and Table 2) generally remain above the thermocline, but they still show a diel shift in depth distribution. They remain at about 6 m, on average, deeper during the day than at night (Fig. 6). Stomach content analysis of FAD-associated bigeye tuna in the eastern Atlantic Ocean by Ménard et al. (2000) showed that 82.7% of the stomachs were empty, where as only 25% of the stomachs of bigeye tuna unassociated with floating objects were empty. They concluded that FADs do not have a trophic function. However, the observed excursions to depths of about 300 m for a few hours at about 1800 h for four consecutive days by a FAD-associated bigeye tuna (Fig. 1B) may be related to foraging for prey in association with the DSL.

Parin and Fedoryako (1999) stated that tunas associate with floating objects only temporarily because there are insufficient food resources in the vicinity of these devices. We found that residence times and total times spent at FADs are limited (Table 2). Our observations do not support the

hypothesis of Marsac et al. (2000) that association with FADs causes bigeye tuna to be retained within areas or transported to new areas, thus creating an ecological trap. An alternative hypothesis, suggested by Hunter and Mitchell (1966), is that FADs function by simply providing a visual stimulus in an optically void environment. An extension of their hypothesis should include the fact that FADs provide a general sensory stimulus, including sound produced by the FAD and associated fauna, which may be the mechanism by which tunas locate FADs. In addition to a general sensory stimulus, FADs may also function as reference points (Freon and Dagorn, 2000).

Archival tags have provided data on the type of habitat selected (light levels, depths, and temperatures) that should be useful for standardizing the catch per unit of effort (CPUE) of bigeye tuna by surface and longline fisheries in the EPO. The data in Table 5 indicate that bigeye tuna greater than 110 cm spend 87% or more of their time above 50 m, in the mixed layer at night and 53% or more of their time between 200 and 300 m during the day. Habitat-based stock assessment models (Hinton and Nikano, 1996; Hinton and Deriso, 1998; Hampton et al.[1]) have been developed for the integration of data, such as those provided in Table 5, to adjust effort based on estimated fishing depth of longline gear (Mizuno et al., 1999) in relation to the vertical distribution of target species by time of day. The fishing depth of longline gear has been shown to be an important source of variation in the CPUE for bigeye tuna (Hanamoto, 1987; Boggs, 1992); higher catch rates of bigeye tuna have been associated with greater fishing depths of the longline gear. This has been interpreted previously as a preference of bigeye tuna for 10° to 15°C water during daylight hours (Hanamoto, 1987; Holland et al., 1990; Boggs, 1992; Brill, 1994).

We suggest that bigeye tuna are most likely not selecting their daytime and nighttime habitats based on temperature, depth, or light preferences, but on the distributions of their preferred prey. Cephalopods and mesopelagic fishes also show diel vertical migrations (as do other organisms) associated with the DSL. We suggest that the depths and temperatures preferred by bigeye tuna during daylight hours when exhibiting unassociated type-1 behavior are the environmental variables associated with their preferred prey.

The greater depths and lower temperatures at which bigeye tuna are caught during the daytime in the CWPO (Hampton et al.[5]; Miyabe[7]) may be a function of the greater daytime depths of the DSL

Table 5

The percentages of time 13 bigeye tuna (greater than 110 cm) spent within depth intervals by time of day (unassociated type-1 behavior days only). CTZ = central time zone.

Depth (m)	Hour (CTZ)																								
	0000	0100	0200	0300	0400	0500	0600	0700	0800	0900	1000	1100	1200	1300	1400	1500	1600	1700	1800	1900	2000	2100	2200	2300
0–25	73.4	73.0	73.0	73.9	72.6	44.0	3.6	2.2	2.5	2.8	3.1	2.9	3.2	3.0	3.0	2.9	2.8	2.3	17.3	63.2	72.6	72.0	71.7	72.6
26–50	21.9	22.0	22.2	21.9	23.4	26.7	5.7	2.4	2.9	3.0	2.9	3.1	2.7	2.8	2.8	2.7	2.5	2.1	12.0	25.2	23.7	23.5	23.4	22.7
51–75	3.1	3.1	3.3	2.7	2.9	8.3	3.4	1.0	1.0	1.1	1.2	0.9	1.1	0.9	0.9	1.1	1.0	1.1	6.6	4.5	2.7	3.3	3.8	3.3
76–100	0.5	0.4	0.5	0.5	0.4	4.5	2.8	0.8	0.9	0.8	0.7	0.7	0.7	0.8	0.7	0.6	0.8	1.2	3.6	1.2	0.4	0.3	0.4	0.6
101–125	0.2	0.3	0.3	0.2	0.2	4.2	5.1	2.6	1.9	1.3	1.6	1.2	1.3	1.3	1.5	1.6	1.7	2.1	4.9	1.1	0.2	0.2	0.1	0.1
126–150	0.2	0.3	0.2	0.2	0.2	3.3	6.3	3.9	3.1	2.4	2.5	2.3	2.3	2.7	2.5	2.9	3.1	3.5	5.7	1.0	0.2	0.2	0.1	0.2
151–175	0.2	0.2	0.1	0.2	0.2	2.7	8.8	5.4	5.1	4.7	4.7	4.6	4.0	4.8	5.3	5.0	4.6	5.0	6.7	1.1	0.1	0.1	0.2	0.1
176–200	0.2	0.1	0.1	0.1	0.1	2.1	10.8	7.1	7.6	7.4	7.1	7.1	7.1	6.5	6.4	6.8	6.5	7.1	8.0	1.0	0.1	0.2	0.1	0.1
201–225	0.2	0.2	0.1	0.1	0.1	1.9	16.9	11.7	12.1	12.9	12.7	12.9	13.4	13.0	13.3	12.0	11.9	12.1	12.9	0.8	0.1	0.1	0.1	0.1
226–250	0.1	0.1	0.1	0.1	0.1	1.1	17.2	17.3	13.9	14.5	15.0	15.8	16.7	15.7	15.4	15.0	14.8	19.0	12.1	0.4		0.1	0.1	0.1
251–275		0.2	0.1	0.1		0.8	12.5	24.5	21.2	19.6	19.6	19.3	18.4	19.1	19.0	19.4	22.3	26.1	7.0	0.2			0.1	
276–300				0.1		0.4	5.1	16.3	19.5	18.8	17.9	17.8	17.7	18.1	18.5	19.7	19.8	14.0	2.4	0.1				
301–325						0.1	1.7	3.9	7.1	8.6	8.5	8.3	8.5	8.8	8.4	8.7	6.8	3.9	0.7	0.1				
326–350							0.2	0.9	1.2	1.5	2.0	2.3	2.5	2.0	1.8	1.4	1.2	0.5	0.1					
351–375								0.1	0.1	0.3	0.4	0.6	0.4	0.5	0.4	0.3	0.1							
376–400											0.1	0.1		0.1	0.1									

[7] Miyabe, N. 1995. Follow-up study on the stock status of bigeye tuna in the Pacific ocean. Western Pacific Yellowfin Research Group 5, working paper 12; 21–23 August 1995, 15 p. Oceanic Fisheries Programme, SPC, B.P. D5, 98848 Noumea Cedex, New Caledonia.

in those regions, compared to the daytime depths of the equatorial EPO (Maynard et al., 1975; Tont, 1976; Davies, 1977; Kuznetsov et al., 1982; Fiedler et al., 1998; Josse et al., 1998). Farr and Best (1998) reported that DSL distributions are related to mesoscale oceanographic features, defined by flow and temperature variability, and are most commonly observed at the pycnocline.

Geographic variation in DSL depths throughout the Pacific are possibly related to isolumes of the associated micronekton, and can potentially be estimated from the light level data recorded by the archival tags attached to bigeye tuna. Variation in daytime DSL depths is probably a function of light penetration (which is regulated by biological production) and absorption of light by chlorophyll and phaeopigments (Tont, 1976).

The behavior of bigeye tuna is strongly influenced by the presence of drifting FADs within their habitat. Because of this behavior associated with FADs, even though it is for relatively short periods, bigeye tuna are highly vulnerable to capture by purse-seine vessels. Estimates of bigeye tuna residence times and percentages of total time associated with drifting FADs, along with estimates of FAD densities, could be used to evaluate vulnerability to capture by the surface fishery. There is a critical need for conducting a large-scale tagging program in the EPO focused on bigeye tuna—a program where conventional tags are used for estimating size-specific mortality and mixing rates and archival tags are used for evaluating fine-scale movements, behavior, and habitat selection.

Acknowledgments

We are grateful for invaluable advice and assistance provided by B. Block, T. Booth, M. Braun, R. Brill, J. Gunn, R. Hill, P. Hooge, and T. Williams. We are thankful to B. Blocker and the crew of *Her Grace* for their performance in fishing and tagging operations. We are indebted to vessel owners, captains, fishermen, unloaders, and industry representatives for returning recovered archival tags. We thank Juan Gracia for his assistance with tagging and the IATTC field office personnel for recovering archival tags. We also wish to thank B. Bayliff, R. Brill, R. Deriso, G. Watters, and two anonymous reviewers for constructive comments on drafts of the manuscript.

Literature cited

Baras, E., and L. Westerloppe.
1999. Transintestinal expulson of surgically implanted tags by African catfish *Heterobranchus longifilis* of variable size and age. Trans. Am. Fish. Soc. 128(4):737–746.

Bayliff, W. H. (editor).
2000. Inter-Am. Trop. Tuna Comm., Ann. Rep. for 1998, 358 p. IATTC, La Jolla, CA.

Blackburn, M.
1968. Micronekton of the eastern tropical Pacific Ocean: family composition, distribution, abundance and relations to tuna. Fish. Bull. 67:71–115.

Block, B. A., H. Dewar, S. B. Blackwell, T. Williams, E. D. Prince, C. J. Farwell, A. Boustany, S. L. H. Teo, A. Seitz, A. Walli, and D. Fudge.
2001a. Migratory movements, depth preferences and thermal biology of Atlantic bluefin tuna. Science 293:1310–1314.

Block, B.A., H. Dewar, S. B. Blackwell, T. Williams, E. Prince, A. M. Boustany, C. Farwell, D. J. Dau, and A. Seitz.
2001b. Archival and pop-up satellite tagging of Atlantic bluefin tuna. *In* Electronic tagging and tracking in marine fisheries (J. Sibert and J. Nielsen, eds.), p. 65–88. Kluwer Academic Publs., Dordrecht.

Blunt, C. E., Jr.
1960. Observations on the food habits of longline caught bigeye and yellowfin tuna from the tropical eastern Pacific 1955–1956. Calif. Fish Game 46(1):69–80.

Boggs, C. H.
1992. Depth, capture time, and hooked longevity of longline-caught pelagic fish: timing bites of fish with chips. Fish. Bull. 90:642–658.

Brill, R.W.
1994. A review of temperature and oxygen tolerance studies of tunas pertinent to fisheries oceanography, movement models and stock assesements. Fisheries Oceanogr. 3(3): 204–216.

Brill, R. W., and M. E. Lutcavage.
2001. Understanding environmental influences on movements and depth distributions of tunas and billfishes can significantly improve population assessments. Am. Fish. Soc. Symp. 25:179–198.

Calkins, T. P., M. Yamaguchi, and N. Miyabe.
1993. Some observations on bigeye tuna (*Thunnus obesus*) caught by the surface and longline fisheries for tunas in the eastern Pacific Ocean. Inter-Am. Trop. Tuna Comm., Bull. 20(8):443–499.

Collette, B. B., and C. E. Nauen.
1983. FAO species catalogue. Scombrids of the world. An annotated and illustrated catalogue of tunas, mackerels, bonitos and related species known to date. FAO Fish. Synop. 125, vol. 2, 137 p. FAO, Rome.

Collette, B. B., C. Reeb, and B. A. Block.
2001. Systematics of the tunas and mackerels (Scombridae). *In* Tunas: ecological physiology and evolution. (B. A. Block, and E. D. Stevens, eds.), p. 1–33. Academic Press, San Diego, CA.

Dagorn, L., P. Bach, and E. Josse.
2000. Movement patterns of large bigeye tuna (*Thunnus obesus*) in the open ocean, determined using ultrasonic telemetry. Mar. Biol. 136(2):361–371.

Davies, I. E.
1977. Acoustic volume reverberation in the eastern tropical Pacific Ocean and its relationship to oceanographic features. Deep-Sea Res. 24:1049–1053.

Farr, R., and T. Best.
1998. Relating high frequency volume scattering distributions to mesoscale oceanographic features. http://www.nnic.noaa.gov/SOCC/TVRS_paper.html. [Access date: 9 August 2001.]

Fiedler, P. C.
1992. Seasonal climatologies and variability of eastern tropical Pacific surface waters. U.S. Dep. Commer., U.S., NOAA Tech. Rep. NMFS 109:1–65.

Fiedler, P. C., J. Barlow, and T. Gerrodette.
1998. Dolphin prey abundance determined from acoustic backscatter data in eastern Pacific surveys. Fish. Bull. 96: 237–247.

Freon, P., and L. Dagorn.
2000. Associative behaviour of pelagic fish: facts and hypotheses. *In* Pêche thonière et dispositifs de concentration de poissons, colloque Caraïbe-Martinique; Trois-Îlets, 15–19 Octobre 1999 (J.-Y. Le Gall, P. Cayré, and M. Taquet, eds.), p. 483–491. Inst. Fran. Recherche Exploitation Mer (IFREMER)28.

Graham, J. B., and K. A. Dickson.
2001. Morphological and physiological specializations for endothermy. *In* Tunas: ecological physiology and evolution (B. A. Block and E. D. Stevens, eds.), p. 121–165. Academic Press, San Diego, CA.

Gunn, J., and B. A. Block.
2001. Advances in acoustic, archival and pop-up satellite tagging of tunas. *In* Tunas: ecological physiology and evolution (B. A. Block and E. D. Stevens, eds.), p. 167–224. Academic Press, San Diego, CA.

Hampton, J., and J. Gunn.
1998. Exploitation and movements of yellowfin tuna (*Thunnus albacares*) and bigeye tuna (*T. obesus*) tagged in the north-western Coral Sea. Mar. Freshwater Res. 49(6): 475–489.

Hanamoto, E.
1987. Effect of oceanographic environment on bigeye tuna distribution. Bull. Jap. Soc. Fish. Oceanogr., 51(3):203–216.

Hill, R. D.
1994. Theory of geolocation by light levels. *In* Elephant seals: population ecology, behavior, and physiology (B. J. LeBouef and R. M. Laws, eds.), p. 227–236. Univ. California Press, Berkeley, CA.

Hill, R. D., and M. J. Braun.
2001. Geolocation by light levels—the next step: latitude. *In* Electronic tagging and tracking in marine fisheries (J. Sibert and J. Nielsen, eds.), p. 315–330. Kluwer Academic Publs., Dordrecht.

Hinton, M. G., and R. D. Deriso.
1998. Distribution and stock assessment of swordfish, *Xiphias gladius*, in the eastern Pacific Ocean from catch and effort data standardized on biological and environmental parameters. *In* Biology and fisheries of swordfish, *Xiphias gladius* (I. Barrett, O. Sosa-Nishizaki, and N. Bartoo, eds.), p. 161–179. U.S. Dep. Commer., NOAA Tech. Rep. NMFS 142.

Hinton, M. G., and H. Nikano.
1996. Standardizing catch and effort statistics using physiological, ecological, or behavioral constraints and environmental data, with an application to blue marlin (*Makaira nigrans*) catch and effort data from Japanese longline fisheries in the Pacific. Inter-Am. Trop. Tuna Comm., Bull. 21(4):69–200.

Hisada, K.
1973. Investigation on tuna hand-line fishing ground and some biological observations on yellowfin and bigeye tunas in the northwestern Coral Sea. Bull. Far Seas Fish. Res. Lab. 8:35–69.

Holland, K. N., R. W. Brill, and R. K. C. Chang.
1990. Horizontal and vertical movements of yellowfin and bigeye tuna associated with fish aggregating devices. Fish. Bull. 88:493–507.

Holland, K. N., R. W. Brill, J. R. Sibert, and D. A. Fournier.
1992. Physiological and behavioral thermoregulation in bigeye tuna *Thunnus obesus*. Nature 358(6385):410–412.

Holland K. N., and J. R. Sibert.
1994. Physiological thermoregulation in bigeye tuna, *Thunnus obesus*. Environ. Biol. Fish. 40(3):319–327.

Hooge, P. N., and B. Eichenlaub.
1997. Animal movement extension to arcview, version 2.04. Alaska Biological Science Center, U.S. Geological Survey, Anchorage, AK. http://www.absc.usgs.gov/glba/gistools/ [Access date: 28 November 2000.]

Hunter, J. R., A.W. Argue, W. H. Bayliff, A. E. Dizon, A. Fonteneau, D. Goodman, and G. R. Seckel.
1986. The dynamics of tuna movements: an evaluation of past and future research. FAO Fish. Tech. Pap., 277, 78 p. FAO, Rome.

Hunter, J. R., and C. T. Mitchell.
1966. Association of fishes with flotsam in the offshore waters of central America. Fish. Bull. 66:13–29.

Itano, D. G., and K. N. Holland.
2000. Movement and vulnerability of bigeye (*Thunnus obesus*) and yellowfin tuna (*Thunnus albacares*) in relation to FADs and natural aggregation points. Aquat. Living Res. 13(4):213–223.

Josse, E., P. Bach, and L. Dagorn.
1998. Simultaneous observations of tuna movements and their prey by sonic tracking and acoustic surveys. Hydrobiologia 371/372(1-3):61–69.

Kawamura, G., W. Nishimura, S. Ueda, and T. Nishi.
1981. Vision in tunas and marlins. Mem. Kagoshima Univ. Res. Cent. South Pac. 2(1):3–47.

Kendall, M. G., and W. R. Buckland.
1982. A dictionary of statistical terms, 213 p. Longman Inc., New York, NY.

Kuznetsov, I. L., S. R. Stefanov, and V. I. Savagov.
1982. A migrating sound scattering layer in the equatorial Pacific Ocean. Oceanology 22(6):702–703.

Lennert-Cody, C. E., and M. A. Hall.
2000. The development of the purse seine fishery on drifting fish aggregating devices in the eastern Pacific Ocean: 1992–1998. *In* Pêche thonière et dispositifs de concentration de poissons, colloque Caraïbe-Martinique; Trois-Îlets, 15–19 Octobre 1999 (J.-Y. Le Gall, P. Cayré, and M. Taquet, eds.), p. 78–107. Inst. Fran. Recherche Exploitation Mer (IFREMER) 28.

Levitus, S., and T. Boyer.
1994. World ocean atlas 1994, vol. 4., Temperature. NOAA Atlas, NESDIS 4, 117 p. NOAA, Washington, D.C.

Lowe, T. E., R. W. Brill, and K. L. Cousins.
2000. Blood oxygen-binding characteristics of bigeye tuna (*Thunnus obesus*), a high-energy-demand teleost that is tolerant of low ambient oxygen. Mar. Biol. 136(6):1087–1098.

Marchal, E., and A. Lebourges.
1996. Acoustic evidence for unusual diel behaviour of a mesopelagic fish (*Vinciguerria nimbaria*) exploited by tuna. ICES J. Mar. Sci. 53(2):443–447.

Marsac, F., A. Fonteneau, and F. Ménard.
2000. Drifting FADs used in tuna fisheries: an ecological trap? *In* Pêche thonière et dispositifs de concentration de poissons, colloque Caraïbe-Martinique; Trois-Îlets, 15–19 Octobre 1999 (J.-Y. Le Gall, P. Cayré, and M. Taquet, eds.), p. 537–552. Inst. Fran. Recherche Exploitation Mer(IFREMER) 28.

Marty, G. D., and R. C. Summerfelt.
1986. Pathways and mechanisms for expulsion of surgically implanted dummy transmitters from channel catfish. Trans. Am. Fish. Soc. 115(4):577–589.

Maynard, S. D., F. V. Riggs, and J. F. Walters.
1975. Mesopelagic micronekton in Hawaiian waters: faunal composition, standing stock, and diel vertical migration. Fish. Bull.73:726–736.

Ménard, F., B. Stequert, A. Rubin, M. Herrera, and E. Marchal.
2000. Food consumption of tuna in the equatorial Atlantic Ocean: FAD-associated versus unassociated schools. Aquat. Living Res. 13(4):233–240.

Miyabe, N., and W. H. Bayliff.
1998. A review of information on the biology, fisheries, and stock assessment of bigeye tuna, *Thunnus obsesus*, in the Pacific Ocean. Inter-Am. Trop. Tuna Comm., Spec. Rept. 9:129–170.

Mizuno, K., M. Okazaki, H. Nakano, and H. Okamura.
1999. Estimating the underwater shape of tuna longlines with micro-bathythermographs. Inter-Am. Trop. Tuna Comm., Spec. Rep. 10:1–35.

Musyl, M. K., R. W. Brill, D. S. Curran, J. S. Gunn, J. R. Hartog, R. D. Hill, D. W. Welch, J. P. Eveson, C. H. Boggs, and R. E. Brainard.
2001. Ability of electronic archival tags to provide estimates of geographical position based on light intensity. *In* Electronic tagging and tracking in marine fisheries (J. Sibert and J. Nielsen, eds.), p. 343–367. Kluwer Academic Publs., Dordrecht.

Musyl, M. K., R. W. Brill, C. H. Boggs, D. S. Curran, T. K. Kazama, and M. P. Seki.
In press. Vertical movements of bigeye tuna *(Thunnus obesus)* associated with islands, buoys, and sea mounts of the Hawaiian Archipelago from archival tagging data. Fish. Ocean.

Nakano, H., M. Okazaki, and H. Okamoto.
1997. Analysis of catch depth by species for tuna longline fishery based on catch by branch lines. Bull. Nat. Res. Inst. Far Seas Fish. 34:43–62.

NMFS (National Marine Fisheries Service).
1994. Archival tags 1994: present and future. Archival tag working group, 45th annual tuna conference, Lake Arrowhead, CA, May 23–26, 1994. U.S. Dep. Commer., NOAA Tech. Memo. NMFS-SEFSC-357, 42 p.

Parin, N., and B. Fedoryako.
1999. Pelagic fish communities around floating objects in the open ocean. Inter-Am. Trop. Tuna Comm., Spec. Rep. 11:447–458.

Schaefer, K. M.
1999. Comparative study of some morphological features of yellowfin (*Thunnus albacares*) and bigeye (*Thunnus obesus*) tunas. Inter-Am. Trop. Tuna Comm., Bull. 21 (7): 489–526.

Sibert, J. R., and D. A. Fournier.
2001. Possible models for combining tracking data with conventional tagging data. *In* Electronic tagging and tracking in marine fisheries (J. Sibert and J. Nielsen, eds.), p. 443–456. Kluwer Academic Publs., Dordrecht.

Suzuki, Z., and S. Kume.
1982. Fishing efficiency of deep longline for bigeye tuna in the Atlantic as inferred from the operations in the Pacific and Indian Oceans. Int. Comm. Conser. Atlan. Tunas, Coll. Vol. Sci. Papers, 17(2):471–486.

Syrjala, S. E.
1996. A statistical test for a difference between the spatial distributions of two populations. Ecology 77(1):75–80.

Tont, S. A.
1976. Deep scattering layers: patterns in the Pacific. Rep. Calif. Coop. Ocean. Fish. Invest. 18:112–117.

Tsuji, S., T. Itoh, A. Nitta, and S. Kume.
1999. The trans-Pacific migration of a young bluefin tuna, *Thunnus thynnus*, recorded by an archival tag. Working Paper ISC2/99/15, Interim Scientific Committee for Tuna and Tuna-like Species in the North Pacific Ocean, January 15–23, 1999, Honolulu.

U. S. Naval Observatory, Astronomical Applications Department.
2001. Fraction of the moon illuminated, 2000 at midnight, Central Standard Time. http://mach.usno.navy.mil/cgi-bin/aa_moonill.pl. [Access date: 5 April 2001.]

Watters, G., and M. Maunder.
2001. Status of bigeye tuna in the eastern Pacific Ocean. Stock assessment report of the Inter-Am. Trop. Tuna Comm. 1:109–210.

Welch, D. W., and J. P. Eveson.
1999. An assessment of light-based geoposition estimates from archival tags. Can. J. Fish. Aquat. Sci. 56(7):1317–1327.

Widder, E. A., and T. M. Frank.
2001. The speed of an isolume: a shrimp's eye view. Mar. Biol. 138(4):669–677.

Wildlife Computers.
2002. Mk9 archival tag. http://www.wildlifecomputers.com/Archival%20Tags/Mk9.htm. [Access date: 6 August 2001.]

An evaluation of back-calculation methodology using simulated otolith data

Michael J. Schirripa
Hatfield Marine Science Center
Northwest Fisheries Science Center
2030 SE Marine Science Drive
Newport, Oregon 97365-5296
E-mail address: Michael.Schirripa@noaa.gov

Abstract–I simulated somatic growth and accompanying otolith growth using an individual-based bioenergetics model in order to examine the performance of several back-calculation methods. Four shapes of otolith radius-total length relations (OR-TL) were simulated. Ten different back-calculation equations, two different regression models of radius-length, and two schemes of annulus selection were examined for a total of 20 different methods to estimate size at age from simulated data sets of length and annulus measurements. The accuracy of each of the twenty methods was evaluated by comparing the back-calculated length-at-age and the true length-at-age. The best back-calculation technique was directly related to how well the OR-TL model fitted. When the OR-TL was sigmoid shaped and all annuli were used, employing a least-squares linear regression coupled with a log-transformed Lee back-calculation equation (*y*-intercept corrected) resulted in the least error; when only the last annulus was used, employing a direct proportionality back-calculation equation resulted in the least error. When the OR-TL was linear, employing a functional regression coupled with the Lee back-calculation equation resulted in the least error when all annuli were used, and also when only the last annulus was used. If the OR-TL was exponentially shaped, direct substitution into the fitted quadratic equation resulted in the least error when all annuli were used, and when only the last annulus was used. Finally, an asymptotically shaped OR-TL was best modeled by the individually corrected Weibull cumulative distribution function when all annuli were used, and when only the last annulus was used.

Manuscript accepted 29 May 2002.
Fish. Bull. 100:789–799 (2002).

The average rate of growth of an individual fish in a population is critical to age-based stock assessments. The average rate at which the fish within the stock increases in weight ultimately determines the level of effort required to extract a desired yield from the stock as a whole (Ricker, 1975). Furthermore, current conservation standards (Gulland and Boerema, 1973; Goodyear, 1993) are dependent upon the rate of individual growth. Thus, errors in the estimation of growth can lead to erroneous advice to fishery managers concerning the present and possible future status of a population.

By far the most common method of estimating fish growth rate is by estimating the age of individual fish from calcified structures (scales, otoliths, spines, etc.; but for this study, however, otoliths were considered the representative hard structure) and with the subsequent assumption that these fish are an unbiased representation of size at that age. Growth is then described as the change in weight or length over some unit of time. To standardize age at which size is estimated, or to obtain length-at-age data on ages not included in the sample, back-calculation techniques are often employed to estimate a fish's size at a previous age (Bagenal, 1978). The process of back calculation can be broken down into three steps: verification of the periodicity of annulus formation, establishment of an otolith radius-total body length (OR-TL) relation, and the estimation of size at the time of annulus formation. In this study, I used simulations to examine how the establishment of the OR-TL relation and the form of the back-calculation equation used may influence growth rate estimates made from otoliths.

The back-calculation process assumes that somatic growth is directly related to otolith growth (Bagenal, 1978). This assumption is usually validated through the demonstration of a relationship between the otolith radius and body length by a least-squares regression of body length on otolith radius. A variation of this technique uses a functional (model II) regression, based on the assertion that neither body length nor otolith radius are truly independent (i.e. measured without error) (Ricker, 1973, Laws and Archie, 1981). Uncertainties can enter this process from several sources. For example, incomplete data can make it difficult to discern if this relationship is linear. Furthermore, using regression to estimate beyond the range of the data is not recommended. Estimating beyond the range of the data can become a problem when back-calculating to very early ages that are not represented in the sample. Furthermore, several studies have found that otolith growth and somatic growth can be uncoupled (Mosegaard et al., 1988; Reznick et al., 1989; Secor and Dean, 1989; Wright et al., 1990; Milicich and Choat, 1992; Secor and Dean, 1992). Hales and Able (1995) found that changes in somatic growth accounted for only half of the variation in otolith growth. This uncoupling of somatic and otolith growth rates challenges the assumption that back-calculation is based on.

The question of what is the proper back-calculation equation to use is a question that has received considerable attention. Bagenal (1978) discussed three separate methods and suggested that a combination of methods might be helpful in some cases. Francis (1990) presented an in-depth review of

six different back-calculation equations and their use. Ricker (1992) later commented on the conclusions of Francis (1990) to suggest yet another variation on the method. Further variation exists on exactly which combination of annuli to use. Standard method suggests the use of all available annuli within the otolith to increase sample size. However, recent literature (Vaughan and Burton, 1994), as well as older reports (Ricker, 1973), have suggested that only the most recently formed annuli should be used. A review of the literature on age and growth shows that a variety of techniques are in use today and that there is no real agreement on a definitive method. The purpose of this study was to examine how well the various back-calculation techniques accurately estimate lengths at previous ages and to examine the biases associated with each technique.

Methods

Model structure

I simulated somatic and otolith growth using a bioenergetics model. A detailed description of the model is presented in Schirripa and Goodyear (1997). The life history and growth parameters were calibrated to fit, as closely as possible, to reported estimates of striped bass growth (Bason[1]); however the model is not intended to be a striped bass model *per se*. Because of the commercial and recreational importance of striped bass, a great body of literature from the field and laboratory work is available. One of the most studied populations of striped bass is that of the Chesapeake Bay system (Cohen et al., 1983; Coutant et al., 1984; Goodyear, 1984, 1985; Tuncer, 1988; Coutant and Benson, 1990; Secor, 1992; Brandt and Kirsch, 1993; Rose and Cowan, 1993; Rutherford and Houde, 1995; Secor and Houde, 1995). Biological and environmental parameters reported for the populations of this system were used whenever possible. The growth model used an individually based framework, but rather than following every fish of the cohort singly, "cells" of fish with identical attributes were followed instead (Rose et al., 1993). A total of 250 cells, each with eleven attributes, were modeled. Attributes examined included age, length, biomass, daily food ration, food conversion efficiency, otolith weight, otolith radius, maximum length attained, maximum biomass attained, brain weight, condition factor, and number of fish that the cell represented.

The term "population" is used to define those fish that remained alive for the entire simulation, unaffected by either natural or fishing mortality. The term "catch" refers to the entire group of fish that were susceptible and killed due to fishing mortality, and "sample" refers to a subsample of individuals from the catch, selected on the basis of length and frequency within the catch. Frequency in the catch was a function of the selectivity of the gear under consideration and frequency in the population. For the purposes of this study, gear was considered nonselective. Annulus formation within the otolith was assumed to occur at the end of every growth year and to be measured without error.

The specific somatic growth rate of an individual fish was calculated by a balanced energy equation. Equations for rates of consumption, respiration, egestion, and excretion generally followed those given by Hewett and Johnson.[2] The otolith growth model used was a modification of the equations presented by Mosegaard.[3] Fish formed an otolith when they reached 90 mm in length. Daily change in otolith weight (O_w) was modeled as a function of daily change in either brain weight (B_w) or brain length (B_l). In the case of brain weight, weight specific brain growth rate was modeled as a function of the somatic growth rate as follows

$$Growth.Brain = Growth.Somatic \times a_2, \quad (1)$$

where a_2 = less than 1, denoting that brain growth rate is slower than somatic growth rate.

The change in B_W then was calculated as

$$dB_w/dt = Growth.Brain \times B_W. \quad (2)$$

The daily change in otolith weight was then calculated as

$$dO_W/dt = a_4 \times Brain.weight \times temp^{a_1}, \quad (3)$$

where a_4 = the conversion factor from brain weight to otolith weight (see below);
$temp$ = the average temperature for the day in degrees centigrade; and
a_1 = 0.77, which is used to determine the overall size of the otolith.

Otolith radius, O_r, was then calculated from O_w assuming a spherical shape as

$$O_r = \frac{O_W}{SpD} \times (3/4\pi)^{0.333}, \quad (4)$$

where SpD = 2.5 and is the specific density of the otolith.

Assuming a spherical shape resulted in a unique radius for a given weight (i.e. a sphere made it unnecessary to consider otolith length).

When brain length was used to model otolith radius, B_w was calculated as in Equation 2 and B_l was calculated as the cube root of B_w:

[1] Bason, W. H., S. E. Allison, L. O. Horseman, W. H. Keirsey, P. E. LaCivita, R. D. Sander, and C. A. Shirey. 1976. Ecological studies in the vicinity of the proposed Summit Power Station January through December 1975. Vol. 1, Fishes, 392 p. Ichthyological Associates, Ithaca, NY.

[2] Hewett, S. W., and B. L. Johnson. 1992. Fish bioenergetics model 2. Sea Grant Institute, Technical Report WIS-SG-92-250, 79 p. University of Wisconsin, Madison, WI.

[3] Mosegaard, H. 1994. A model of otolith and larval fish growth. *In* ICES, Report of the working group on recruitment processes, C.M. 1994/L:12, p. 34–38.

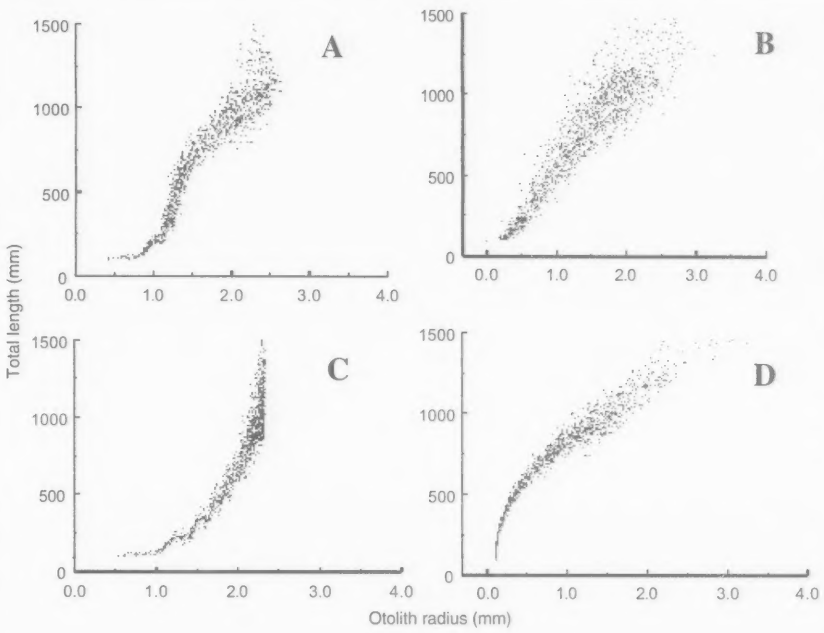

Figure 1

Scatter plot of the four simulated otolith radius-total length relations (OR-TLs). (**A**) OR-TL/SIG = sigmoid shaped; (**B**) OR-TL/LIN = linear shaped; (**C**) OR-TL/EXP = exponentially shaped; (**D**) OR-TL/ASYM = asymptotically shaped.

$$B_1 = B_W{}^{0.333}. \quad (5)$$

O_r was then calculated as

$$O_r = B_1 \times 0.5. \quad (6)$$

Otolith radius-total length relation

The OR-TL relation was fitted as closely as possible to that reported for striped bass by Heidinger and Clodfelter (1987). Modeling the conversion factor a_4 (Eq. 3) as a function enabled me to generate four different OR-TL relations typically found in nature. A sigmoid shaped OR-TL (OR-TL/SIG) relation (Fig. 1A) relation was achieved by setting the parameter $a_2 = 0.08$ and modeling the parameter a_4 as a function of body length:

$$a_4 = 9 + (-7 \times \mathrm{Sin}(0.006 \times Length) + 5). \quad (7)$$

A linear shaped OR-TL (OR-TL/LIN) relation (Fig. 1B), as found in striped bass (Heidinger and Clodfelter, 1987) was achieved by setting the parameter a_2 (from Eq. 1) to 0.85 and modeling otolith radius as a function of brain length (the parameter a_4 was not necessary for this relation). An exponential OR-TL(OR-TL/EXP) relation (Fig. 1C), similar to that found for vermilion snapper, *Rhomboplites aurorubens*, (Grimes, 1978) was achieved by again setting the parameter a_2 to 0.08 and modeling the parameter a_4 as a linear function of otolith weight:

$$a_4 = 25 - (1.75 \times O_W). \quad (8)$$

An asymptotic OR-TL (OR-TL/ASYM) relation (Fig. 1D), similar to that found for walleye, *Stizostedion vitreum*, (Heidinger and Clodfelter, 1987), was achieved by keeping the parameter $a_2 = 0.08$ and modeling the parameter a_4 as a function of total length:

$$a_4 = 8.717E - 12 \times Length^4. \quad (9)$$

Mortality

Mortality could occur from three sources: direct starvation, random natural mortality based on length, and fishing mortality. If a fish lost more than a specified percentage of its maximum attained body weight (35% for larvae and 50% for juveniles), it died from starvation. Fishing mortality was described first as an overall value (F=0.4) and then divided by 365 to calculate a daily value. In order to ensure that there would be no sampling bias due to gear selectivity, fishing mortality was assumed to be nonselective (random).

The four simulated OR-TL relations were described by using four different functions: 1) ordinary least squares (OLS) linear regression (model I)

Table 1

The ten back-calculation and OR-TL regression equations evaluated in this study. Method number refers to all annulus/last annulus only. L_n is the estimated length at formation of annulus R_n; L_c and R_c is total length of fish and otolith radius at capture, respectively. OLS = ordinary least squares.

Method	Back-calculation equation	OR-TL fitting method
1/11	$L_n = (R_n/R_c)\,L_c$	none
2/12	$L_n = a + (bR_n)$	OLS linear regression
3/13	$L_n = a + (R_n/R_c)\,(L_c - a)$	OLS linear regression
4/14	$L_n = a + (bR_n)$	functional linear regression
5/15	$L_n = a + (R_n/R_c)\,(L_c - a)$	functional linear regression
6/16	$\log_e(L_n) = \log_e(a) + b(\log_e(R_n))$	OLS linear regression with log transformation
7/17	$\log_e(L_n) = \log_e(L_c) + b(\log_e(R_n) - \log_e(R_c))$	OLS linear regression with log transformation
8/18	$L_n = K(1 - \exp(-(R_n/\alpha)^{\beta}))$	Weibull cumulative function
9/19	$L_n = c + (dR_n) + (eR_n^2) + (fR_n^3)$	quadratic equation
10/20	$L_n = (K(L_c/L_p))\,(1 - \exp(-(R_n/\alpha)^{\beta}))$	Weibull cumulative function

$$L_c = a + R_c b, \tag{10}$$

where L = the total length; and R = the otolith radius and represents the independent variable (assumed to be measured with out error); 2) functional regression (model II), which has the identical formula as Equation 10 but does not assume an independent variable (i.e. both L and R are measured with error); 3) Weibull cumulative function (Weibull, 1951),

$$L_c = K\left(1 - \exp\left[-\left(\frac{R_c}{\alpha}\right)^{\beta}\right]\right), \tag{11}$$

and 4) a third order quadratic equation

$$L_c = c + (d_1 R_c) + (e_2 R_c^2) + (f_3 R_c^3). \tag{12}$$

These four functions were fitted with the SAS NLIN procedure (SAS, 1988).

Ten combinations of the back-calculation formula and OR-TL fitting procedures were used (Table 1). Methods 1 through 9 were simple derivations from a standard regression equation and required only a fitting of the parameters and substitution into the equation (Bagenal, 1978). Method 10 however used a derivation of the Weibull distribution function. In this method, the parameter defining the asymptotic limit of the function (K) was modified by L_c/L_p as

$$L_n = \left(K(L_c / L_p)\right)\left(1 - \exp\left[-\left(\frac{R_c}{\alpha}\right)\right]^{\beta}\right), \tag{13}$$

where L_p = the theoretical length of the fish according to its otolith radius as predicted by the fitted OR-TL Weibull function; and
L_c = the actual length at capture.

If, for instance, the actual length of the fish was less than the theoretical length (L_c/L_p is less than 1), the parameter K was corrected downward and subsequent back-calculations for that fish were made according to its own individual trajectory (Fig. 2). In this way, L_c/L_p was calculated for each individual fish in the same way that the slope of the Fraser-Lee back-calculation equation was estimated for each fish. These ten combinations were used for all available annuli and then repeated by using the last annulus only, for a total of twenty different methods.

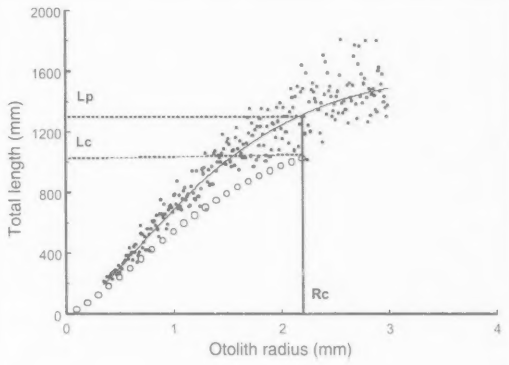

Figure 2

Demonstration of the individually corrected Weibull cumulative distribution function. The curve is the fitted equation to all data, *Rc* = otolith radius at capture, *Lc* = total length at capture, and *Lp* = total length predicted from *Rc* and the fitted curve. The asymptote parameter of the fitted equation (*K*) is multiplied by *Lc*/*Lp* to arrive at that fish's particular trajectory, denoted by the large empty circles.

As a measure of bias, the back-calculated length at age 2 was regressed on the age of the fish from which the estimate came (source age). In this way, for instance, a strong "Lee's phenomenon" (the phenomenon that back-calculated lengths for a given age group become smaller as

Table 2

Age (yr)	1	2	3	4	5	6	7	8	9	10	11	12	13	14	*n*
Age and calculated true mean length-at-age (mm) for a typical simulated population.															
1	102	—	—	—	—	—	—	—	—	—	—	—	—	—	250
2	108	208	—	—	—	—	—	—	—	—	—	—	—	—	250
3	108	208	330	—	—	—	—	—	—	—	—	—	—	—	250
4	108	208	329	457	—	—	—	—	—	—	—	—	—	—	250
5	107	207	329	457	573	—	—	—	—	—	—	—	—	—	250
6	107	207	329	457	572	674	—	—	—	—	—	—	—	—	250
7	107	207	329	457	572	674	763	—	—	—	—	—	—	—	250
8	108	207	329	457	574	676	766	845	—	—	—	—	—	—	250
9	108	208	330	459	576	679	769	849	917	—	—	—	—	—	250
10	108	208	330	460	578	681	772	853	921	980	—	—	—	—	250
11	108	208	331	460	577	680	771	852	920	981	1032	—	—	—	250
12	108	208	331	460	577	680	771	851	920	980	1031	1077	—	—	250
13	109	208	331	460	578	681	772	853	920	980	1031	1076	1115	—	250
14	109	208	331	459	577	678	769	849	916	974	1025	1070	1108	1139	250
Mean	104	208	330	458	575	677	768	850	918	978	1029	1073	1110	1138	
Age and calculated true mean length-at-age (mm) for a typical simulated catch.															
1	102	—	—	—	—	—	—	—	—	—	—	—	—	—	117
2	109	207	—	—	—	—	—	—	—	—	—	—	—	—	105
3	108	207	323	—	—	—	—	—	—	—	—	—	—	—	101
4	108	208	323	448	—	—	—	—	—	—	—	—	—	—	86
5	108	205	321	449	572	—	—	—	—	—	—	—	—	—	93
6	107	205	319	445	567	673	—	—	—	—	—	—	—	—	95
7	108	206	323	448	569	676	765	—	—	—	—	—	—	—	98
8	107	206	322	450	572	680	771	853	—	—	—	—	—	—	104
9	108	207	323	449	571	679	771	853	918	—	—	—	—	—	115
10	108	205	318	443	562	665	755	834	901	962	—	—	—	—	105
11	109	206	320	442	561	667	757	836	903	964	1016	—	—	—	106
12	107	204	316	438	557	661	751	831	901	964	1017	1060	—	—	102
13	107	204	315	439	559	664	756	838	908	973	1027	1071	1107	—	101
14	108	203	316	442	563	670	763	844	910	970	1021	1061	1096	1127	88
Mean	106	206	321	446	567	672	763	843	908	966	1020	1064	1102	1127	

the fish from which they are calculated become older) or a similar effect would result in a negative slope. If there is no bias caused by this approach, the expected value of this slope is zero when randomly sampled from an unfished population.

The accuracy of each of the twenty methods of back-calculation was evaluated by plotting the percent error of the estimated length-at-age in relation to the true value. As an overall evaluation of the method, a sum-of-squares (SS) was calculated by squaring the percent error between the estimated length-at-age and the true length-at-age and summing across all ages.

Results

The true underlying mean length-at-age of both the surviving population and the catch (Table 2) was calculated and tabulated in standard back-calculation type tables. There was no apparent trend in the estimates as a function of the age used in the back-calculation. This lack of trend, and the high degree of similarity between the mean length-at-age of the population and catch suggested that the catch was a random and representative sample of the population.

Methods 2, 4, 6, 8, and 9 resulted in the least bias and method 1 the most bias when the slopes were examined across the various shapes of the OR-TL relation (Fig. 3). The linear shaped OR-TL (OR-TL/LIN) relation resulted in the least amount of bias, and the exponential shaped OR-TL (OR-TL/EXP) relation resulted in the most when the various relations were examined across methods.

Sigmoid-shaped OR-TL relation

Of the four functions fitted to the OR-TL/SIG relation (Table 3), the Weibull cumulative function resulted in the highest coefficient of determination (r^2=0.914); however the coefficient of determination of the quadratic fit was very similar (r^2=0.913).

Table 3

Summary of the combination of OR-TL and back-calculation models that resulted in the best lack-of-fit (lowest sum of squares [SS]) for each of the four shapes of OR-TL examined

	Best lack-of-fit result	
OR-TL shape	OR-TL model	Back-calculation model
Sigmoid		
All annuli	linear regression, model I	$\log_e(L_n) = \log_e(L_c) + b(\log_e(R_n) - \log_e(R_c))$
Last annulus only	none	$L_n = (R_n / R_c) L_c$
Linear		
All annuli	linear regression, model II	$L_n = a + (R_n / R_c)(L_c - a)$
Last annulus only	linear regression, model II	$L_n = a + (R_n / R_c)(L_c - a)$
Exponential		
All annuli	quadratic equation	$L_n = c + (dR_n) + (eR_n^2) + (fR_n^3)$
Last annulus only	quadratic equation	$L_n = c + (dR_n) + (eR_n^2) + (fR_n^3)$
Asymptotic		
All annuli	Weibull cumulative function	$L_n = (K(L_c / L_p))(1 - \exp(-(R_n / \alpha)^\beta))$
Last annulus only	Weibull cumulative function	$L_n = (K(L_c / L_p))(1 - \exp(-(R_n / \alpha)^\beta))$

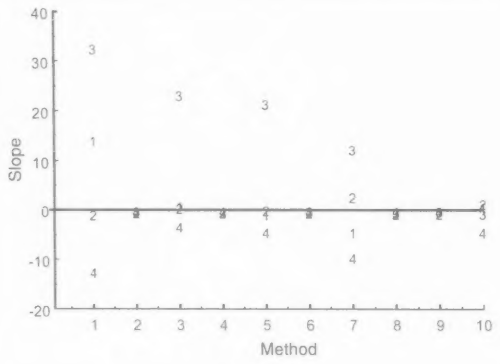

Figure 3

Scatterplot of the slopes of the regression of back-calculated length at age 2 versus age at capture for the ten back-calculation methods that used all annuli. The numbers plotted indicate the shape of the OR-TL relation examined (1=OR-TL/SIG [sigmoid], 2=OR-TL/LIN [linear], 3=OR-TL/EXP [exponential], 4=OR-TL/ASYM [asymptotic]).

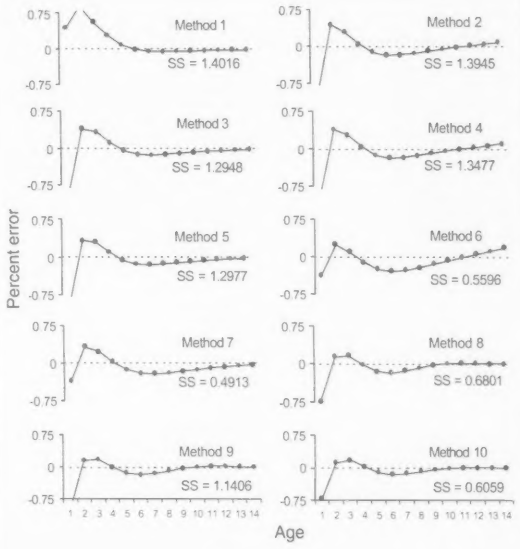

Figure 4

Error in mean length at age estimates using all annuli and the ten back-calculation methods outlined in Table 1 for the sigmoid-shaped OR-TL relation. SS = sum of squares.

The sigmoid shape of the OR-TL relation was evident in the shape of the percent error plots for methods 1 through 10 (Fig. 4). When the OR-TL relation was sigmoid-shaped and all annuli were used, the least error resulted from employing a ordinary least-squares regression coupled with the log-transformed Fraser-Lee back-calculation equation (method 7, SS=0.4913). The greatest error appeared when using the direct proportion equation (Fig. 4, method 1, SS=1.4016). Using the *y*-intercept of the OR-TL relation in the back-calculation equation (methods 3/13 and 5/14 in Table 1) had little effect on the total sum of squares when comparing method 2 with method 3; in addition, correcting for different limits of the Weibull function in methods 8 versus 10 had little effect. However, the log transformation of methods 6 and 7 reduced the sum of squares considerably.

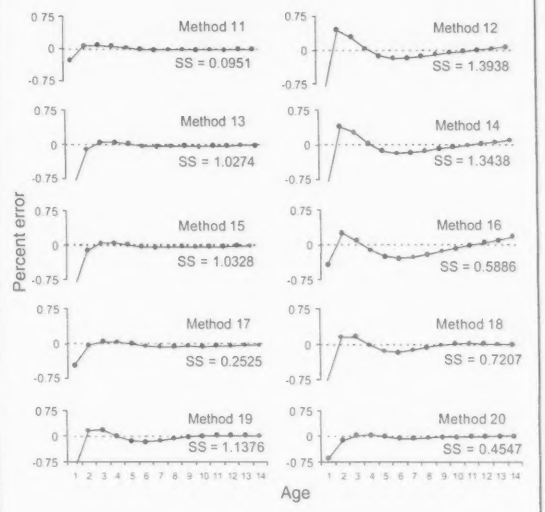

Figure 5

Error in mean length at age estimates using the last annulus only and the ten back-calculation methods outlined in Table 1 for the sigmoid-shaped OR-TL relation. SS = sum of squares.

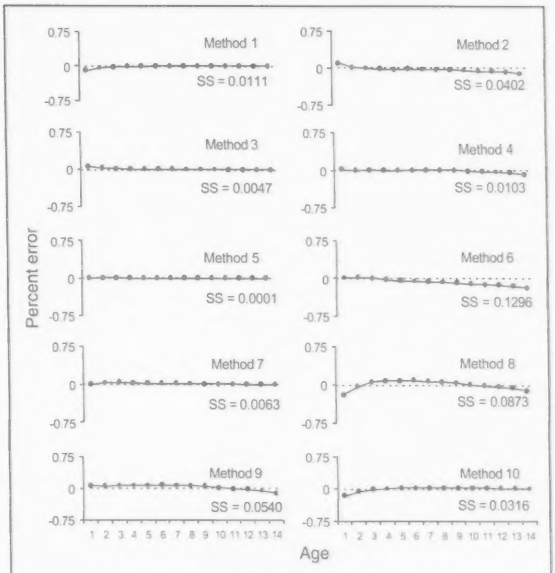

Figure 6

Error in mean length at age estimates using all annuli and the ten back-calculation methods outlined in Table 1 for the linear-shaped OR-TL relation. SS = sum of squares.

The sigmoid shape of the OR-TL relation was not as evident in the shape of the percent error plots for methods 11 through 20 (Fig. 5). When only the last annulus was used, the least error resulted from employing a direct proportionality back-calculation equation (Fig. 5, method 11, SS=0.0951), and the greatest error from using direct substitution into the OLS regression equation (Fig. 5, method 12, SS=1.3938). When only the last annulus was used with comparable back-calculation equations, as in methods 12 versus 13 and 18 versus 20, both the sum of squares and bias were reduced considerably.

Linear-shaped OR-TL relation

Of the four functions fitted to OR-TL/LIN, the ordinary least squares and functional linear regressions resulted in the highest coefficient of determination value (r^2=0.916). The curvature of the Weibull and quadratic fits showed that the relation deviated slightly from a straight line.

There was a high degree of similarity between the percent error plots for all twenty methods (Figs. 6 and 7), suggesting that the estimation of length-at-age is not as sensitive to the method of back-calculation when the OR-TL relation is linear as when it is curved. When the OR-TL relation was linear, the least error resulted from employing a functional regression coupled with the Fraser-Lee back-calculation equation when all annuli were used (Fig. 6, method 5, SS=0.0001) and when only the last annulus was used (Fig. 7, method 15, SS=0.0013). The greatest error resulted from direct substitution into the OLS regression following a natural log transformation of all parameters, both when all annuli were used (Fig. 6, method 6, SS=0.1296) and when only the last annulus (Fig. 7, method 16, SS=0.1245).

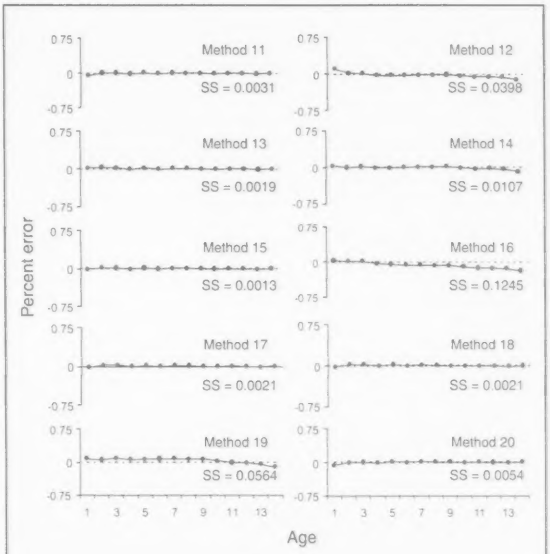

Figure 7

Error in mean length at age estimates using the last annulus only and the ten back-calculation methods outlined in Table 1 for the linear-shaped OR-TL relation. SS = sum of squares.

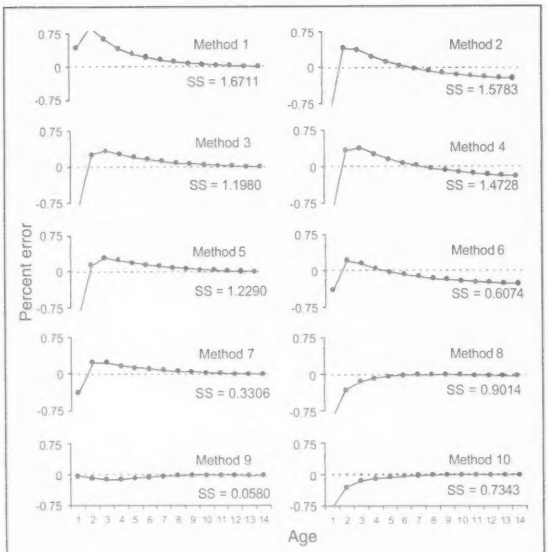

Figure 8

Error in mean length at age estimates using all annuli and the ten back-calculation methods outlined in Table 1 for the exponentially shaped OR-TL relation. SS = sum of squares.

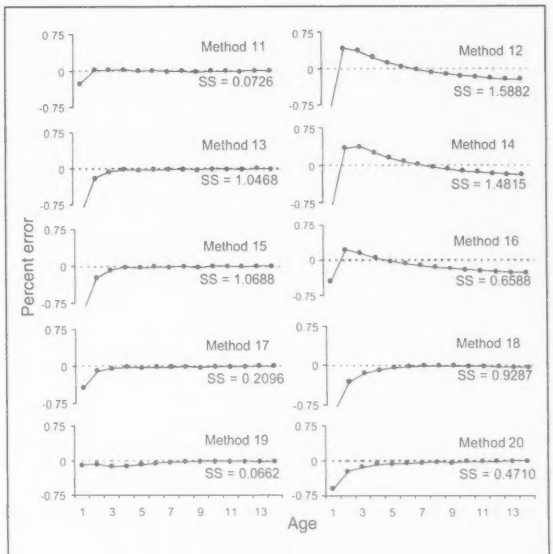

Figure 9

Error in mean length at age estimates using the last annulus only and the ten back-calculation methods outlined in Table 1 for the exponentially shaped OR-TL relation. SS = sum of squares.

Exponentially shaped OR-TL relation

Of the four functions fitted to OR-TL/EXP, the quadratic function resulted in the highest coefficient of determination (r^2=0.883); however the coefficient of determination of the Weibull function fit was nearly as high (r^2=0.878). The percent errors, when using all annuli and linear regression, followed a pattern similar to the residuals of the OR-TL relation (Fig. 8). This trend was also evident, although not as strong, when only the last annulus was used (Fig. 9). Using the quadratic function rather than the linear regression to fit the OR-TL relation did the most at removing this bias (Fig. 8 method 9, and Fig. 9 method 19).

When the OR-TL relation was exponentially shaped and all annuli were used, the least error resulted from direct substitution into the fitted quadratic equation (Fig. 8, method 9, SS=0.0580), and the greatest error from using the direct proportionality equation (Fig. 8, method 1, SS=1.6711). When only the last annulus was used, the least error resulted from direct substitution into the fitted quadratic equation (Fig. 9, method 19, SS=0.0662), and the greatest error from using direct substitution into the OLS regression equation (Fig. 9, method 12, SS=1.5882).

Asymptotically shaped OR-TL relation

Of the four functions fitted to OR-TL/ASYM, the quadratic equation resulted in the highest coefficient of determination (r^2=0.963); however the coefficient of determination of the Weibull function fit was nearly as high (r^2=0.958). As with the exponentially shaped OR-TL relation, when linear regression was used to model the OR-TL relation, the percent error by age followed the trend of residuals for the residuals for the regression (Fig. 10). Using the last annulus only resulted in generally lower sums-of-squares, especially when the y-intercept was corrected for log transformation of the OR-TL relation used (Fig. 11).

When the OR-TL relation was asymptotically shaped and all annuli were used, the least error resulted from using the individually corrected Weibull cumulative distribution function (Fig. 10, method 10, SS=0.7388), and the greatest error from using direct substitution in to the OLS regression equation (Fig. 10, method 2, SS=1.9319). When only the last annulus was used, the least error again resulted from using the individually corrected Weibull cumulative distribution function (Fig. 11, method 20, SS=0.0516), and the greatest error from using direct substitution in to the OLS regression equation (Fig. 11, method 12, SS=1.9261).

Discussion

The most accurate estimates of length-at-age resulted from the best model fits of the OR-TL relation. Even though sampling was random, poorly fitted OR-TL regressions resulted in back-calculation tables with obvious "Lee's phenomenon" effects. Ricker (1969) pointed out that the use of an incorrect otolith radius-total length relationship can result in this effect. Smale and Taylor (1987) also

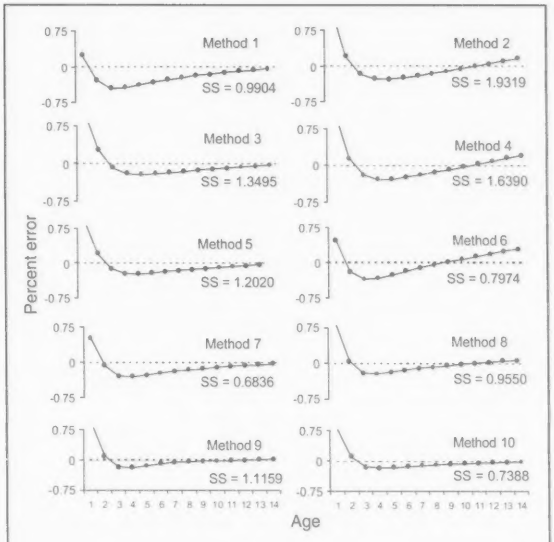

Figure 10

Error in mean length at age estimates using all annuli and the ten back-calculation methods outlined in Table 1 for the asymptotically shaped OR-TL relation. SS = sum of squares.

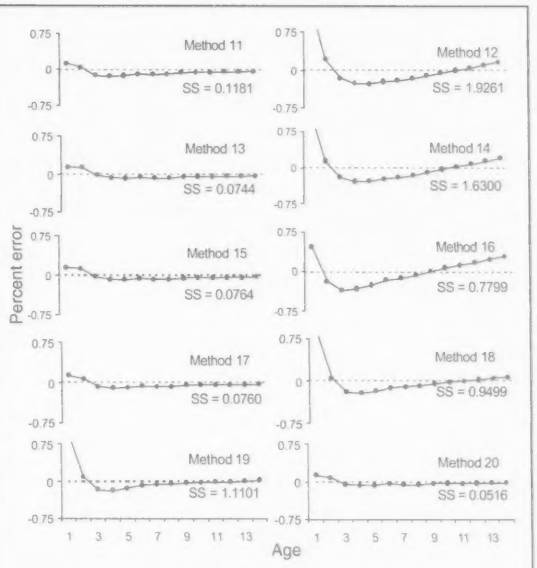

Figure 11

Error in mean length at age estimates by using the last annulus only and the ten back-calculation methods outlined in Table 1 for the asymptotically shaped OR-TL relation. SS = sum of squares.

showed that using the improper back-calculation method can result in a false "Lee's phenomenon" effect. Using only the last annulus reduced this effect with some back-calculation methods in this study, but not all of them. In general, the accuracy of the estimated length-at-age was directly related to how well the particular model fitted the OR-TLrelation, suggesting that the OR-TL model is just as, if not more, important as selecting the appropriate back-calculation model.

Based on the importance of the fit of the OR-TL model, it follows that the methods used to sample the catch are of equal importance. Nonrandom samples of the catch, or length-based regulations that cause the catch to misrepresent the population, will affect the OR-TL regression. For instance, a minimum legal size will artificially truncate the OR-TL relation in samples of the catch and selectively sample faster-growing small fish. This could eliminate the youngest ages from the regression and could necessitate extrapolation of the regression beyond the range of the data. Furthermore, a truncation of the OR-TL regression would positively bias the y-intercept and lead to an overestimation of length-at-age, especially for the younger ages.

It has been pointed out that univariate statistical models, which assume independence of observations, are generally inappropriate for analysis of otolith increment data (Chambers and Miller, 1995). These authors have suggested that because otolith data constitute multiple measures, perhaps examination of the covariance is more appropriate than the comparison of individual means. In this study, however, I did not seek to emphasize the existence of (or lack of) a statistical difference between the true and estimated means sizes. Given the large sample sizes made available through simulation, conclusions of significant differences resulting from any statistical tests can be misleading. More useful, I believe, is the shape, direction, and magnitude of the biases that emerged from each back-calculation method. Consequently, I chose to emphasize the percent error between the true and estimated mean size-at-age. Using percent error allows more freedom of interpretation and is not subject to the problems associated with excessively large degrees of freedom of simulated data sets.

The individually corrected Weibull cumulative distribution function presented here proved to be very flexible and capable of accounting for the individual otolith radius-total length trajectories. This function is very similar to the linear y-intercept corrected back-calculation equation of Fraser-Lee but can accommodate a wide varieties of curvatures. The Weibull equation I reported (Eq. 13) has an origin at x and y of 0; however, a y-intercept term can easily be added to accommodate an OR-TL relation with a nonzero intercept.

Much of the cohort's diversity in biological attributes was lost within the first few months of the life because of mortalities. By the time the cohort had completed one year of growth, the diversity in biological attributes of the individuals that would ultimately represent the cohort were established. Based on the observations of Secor and Houde (1995), the establishment of the biological attributes of a

cohort occurring after one year is a realistic representation of what occurs in the early life history of striped bass. Although the number of fish that a cell represented could be less than one, this number was used as a relative weighting to all other cells; thus, proportionally, the value was valid. Consequently, the actual starting number of fish of the cohort was irrelevant for this study but could be used to calibrate the model to a particular population of interest.

I was able to simulate a number of dissimilarly shaped OR-TL relationships by modifying the parameter used to convert brain weight to otolith weight from a constant to a function. However, trial runs showed that when this parameter was held constant, the resulting OR-TL relation was not linear. I later determined that because both soma and otolith growth were modeled as functions of weight and because the exponent of the weight-length equation (0.31) did not exactly equal the exponent of the equation that calculates the radius of a sphere (0.333), two rates must at some point diverge from linearity. For the purposes of this study, it was not necessary that the equations precisely depict the actual bioenergetics processes, only that true length of fish at annulus formation be known with certainty.

This study yields several conclusions important to studies of growth estimates from otolith back-calculations. The best back-calculation technique was directly related to how well the OR-TL model fitted. The percent error of any given method was rarely consistent across ages, although estimates of older ages were more accurate than those of younger ones. Younger ages were generally best estimated by using direct proportionality on the last annulus only. Thus, it may be necessary to use multiple methods to accurately estimate a growth curve. However, it would be difficult to select which combination of methods would be most accurate without prior knowledge of the true length-at-age.

Acknowledgments

I would like to acknowledge the following people for their contributions to this work: J. A. Bohsack, C. P. Goodyear, P. Johnson, S. Quackenbush, and J. C. Trexler. And I would like to thank the manuscript reviewers for their editorial comments.

Literature cited

Bagenal, T.
1978. Methods for assessment of fish production in fresh waters. IBP (International Biological Programme) Handbook 3, 3rd ed., 365 p. Blackwell Sci. Publ., Oxford.

Brandt, S. B., and J. Kirsch.
1993. Spatially explicit models of striped bass growth potential in Chesapeake Bay. Trans. Am. Fish. Soc. 122: 845–869.

Chambers, R. C. and T. J. Miller.
1995. Evaluating fish growth by means if otolith increment analysis: special properties if individual-level longitudinal data. *In* Recent developments in fish otolith research (D. H. Secor, J. M. Dean, S. E. Campana, eds.), p. 155–175. Univ. South Carolina Press, Columbia, SC.

Cohen, J. E., S. W. Christensen, and C. P. Goodyear.
1983. A stochastic age-structured population model of striped bass (*Morone saxatilis*) in the Potomac River. Can. J. Fish. Aquat. Sci. 40:2170–2183.

Coutant, C. C., and D. L. Benson.
1990. Summer habitat suitability for striped bass in Chesapeake Bay: reflections on a population decline. Trans. Am. Fish. Soc. 119:757–778.

Coutant, C. C., K. L. Zachman, D. K. Cox, and B. L. Pearman.
1984. Temperature selection by juvenile striped bass in laboratory and field. Trans. Am. Fish. Soc. 113:666–671.

Francis, R. I. C. C.
1990. Back-calculation of fish lengths: a critical review. J. Fish Biol. 36:883–902.

Goodyear, C. P.
1984. Analysis of potential yield per recruit for striped bass produced in Chesapeake Bay. North Am. J. Fish. Manage. 4:488–496.
1985. Relation between reported commercial landings and abundance of young striped bass in Chesapeake Bay, Maryland. Trans. Am. Fish. Soc. 114:92–96.
1993. Spawning stock biomass per recruit in fisheries management: foundation and current use. *In* Risk evaluation and biological reference points for fisheries management (S. J. Smith, J. J. Hunt, and D. Rivard, eds.), p. 76–81. Can. Spec. Publ. Fish. Aqat. Sci. 120.

Gulland, J. A., and L. K. Borerema.
1973. Scientific advice on catch levels. Fish. Bull. 71:325–335.

Grimes, C. B.
1978. Age, growth, and length-weight relationship of vermilion snapper, *Rhomboplites aurorubens*, from North Carolina and South Carolina. Fish. Bull. 78:137–146.

Hales, L. S., Jr., and K. W. Able.
1995. Effects of oxygen concentration on somatic and otolith growth rates of juvenile black sea bass, *Centropristis striata*. *In* Recent developments in fish otolith research (D. H. Secor, J. M. Dean, and S. E. Campana eds.), p. 135–153. Univ. South Carolina Press. Columbia, SC.

Heidinger, R. C., and K. Clodfelter.
1987. Validity of the otolith for determining age and growth of walleye, striped bass, and smallmouth bass in power plant cooling ponds. *In* Age and growth of fish (R. C. Summerfelt and G. E. Hall, eds.), p. 241–251. Iowa State University Press, Ames, IA.

Laws, L. A., and J. W. Archie.
1981. Appropriate use of regression analysis in marine biology. Mar. Biol. 65:13–16.

Milicich, M. J., and J.H. Choat.
1992. Do otoliths record changes in somatic growth rates? Conflicting evidence from a laboratory and field study of a temperate reef fish, *Parika scaber*. Aust. J. Mar. Freshwater Res. 43:1203–1214.

Mosegaard, H., H. Svedang, and K. Taberman.
1988. Uncoupling of somatic and otolith growth rates in Arctic char (*Salvelinus alpinus*) as an effect of difference in temperature response. Can. J. Fish. Aquat Sci. 45:1514–1524.

Reznick D., E. Lindbeck, and H. Bryga.
1989. Slower growth results in larger otoliths: an experimental test with guppies (*Poecilia reticulata*). Can. J. Fish. Aquat. Sci. 46:108–112.

Ricker, W. E.
1969. Effects of size-selective mortality and sampling bias on estimates of growth, mortality, production and yield. J. Fish. Res. Board Can. 26:479–541.

1973. Linear regressions in fishery research. J. Fish. Res. Board Canada 30:343–409.
1975. Computation and interpretation of biological statistics of fish populations. Bull. Fish. Res. Board Can. 191, 382 p.
1992. Back-calculation of fish lengths based on proportionality between scale and length increments. Can. J. Fish. Aquat. Sci. 49:1018–1026.

Rose K. A., S. W. Christensen, and D. L. DeAngelis.
1993. Individual-based modeling for populations with high mortality: a new method based on following a fixed number of model individuals. Ecol. Modeling 68:273–292.

Rose K. A., and J. C. Cowan.
1993. Individual-based model of young-of-the-year striped bass population dynamics. I. Model description and baseline simulations. Trans. Am. Fish. Soc. 122:415–438.

Rutherford, E. S., and E. D. Houde.
1995. The influence of temperature on cohort-specific growth, survival, and recruitment of striped bass, *Morone saxatilis*, larvae in Chesapeake Bay. Fish. Bull. 93:315–332.

SAS (SAS Institute, Inc.).
1988. SAS/STAT user's guide, release 6.03 ed., 1028 p. SAS Institute, Inc., Cary, NC.

Schirripa, M. J., and C. P. Goodyear.
1997. Simulation of alternative assumptions of fish otolith-somatic growth with a bioenergetics model. Ecol. Modeling 102:209–223.

Secor, D. H.
1992. Application of otolith microchemistry analysis to investigate anadromy in Chesapeake Bay striped bass, *Morone saxatilis*. Fish. Bull. 90:798–806.

Secor D. H., and J. M. Dean.
1989. Somatic growth effects on the otolith—fish size relationship in young pond-reared striped bass, *Morone saxatilis*. Can. J. Fish. Aquat. Sci. 46:113–121.
1992. Comparison of otolith-based back-calculation methods to determine individual growth histories of larval striped bass, *Morone saxatilis*. Can. J. Fish. Aquat. Sci. 49:1439–1454.

Secor D. H., and E. D. Houde.
1995. Temperature effects on the timing of striped bass egg production, larval viability, and recruitment potential in the Patuxent River (Chesapeake Bay). Estuaries 18(3): 527–544.

Smale, M. A., and W. W. Taylor.
1987. Sources of back-calculation error in estimating growth of lake whitefish. *In* Age and growth of fish (R. C. Summerfelt and G. E. Hall, eds.), p. 189–202. Iowa State Univ. Press, Ames, IA.

Tuncer, H.
1988. Growth, survival, and energetics of larval and juvenile striped bass (*Morone saxatilis*) and its white bass hybrid (*M. saxatilis* × *M. chrysops*). M.S. thesis, 136 p. Univ. Maryland, College Park, MD.

Weibull, W.
1951. A statistical distribution function of wide applicability. J. Appl. Mechanics 18:293–297.

Wright, P. J , N. B. Metcalfe, and J.E. Thorpe.
1990. Otolith and somatic growth rates in Atlantic salmon parr, *Salmo salar* L: evidence against coupling. J. Fish. Biol. 36:241–249.

Vaughan, D. S., and M. L. Burton.
1994. Estimation of von Bertalanffy growth parameters in the presence of size-selective mortality: a simulated example with red grouper. Trans. Am. Fish. Soc. 123:1–8.

Sustainability of elasmobranchs caught as bycatch in a tropical prawn (shrimp) trawl fishery

Ilona C. Stobutzki
Margaret J. Miller
Don S. Heales
David T. Brewer
CSIRO Marine Research
PO Box 120
Cleveland
Queensland 4163, Australia
E-mail address: ilona.stobutzki@csiro.au

Abstract–The bycatch of Australia's northern prawn fishery (NPF) comprises 56 elasmobranch species (16 families). The impact of this fishery on the sustainability of these species has not been addressed. We obtained estimates of catch rates and the within-net survival of elasmobranchs. *Carcharhinus tilstoni, C. dussumieri, Rhynchobatus djiddensis,* and *Himantura toshi* represented 65% of the bycatch. For most species, >50% of individuals in the bycatch were immature, and some species recruited to the fishery at birth. For all species combined, 66% of individuals in the bycatch died in the trawl net.

The relative sustainability of elasmobranchs caught as bycatch was examined by ranking species with respect to their susceptibility to capture and mortality due to prawn trawling and with respect to their capacity to recover once the population was depleted. The species that were least likely to be sustainable were four species of pristids, *Dasyatis brevicaudata,* and *Himantura jenkinsii*. These are bottom-associated batoids that feed on benthic organisms and are highly susceptible to capture in prawn trawls. The recovery capacity of these species was also low according to our criteria. Our results provide a valuable first step towards ensuring the sustainability of elasmobranchs that are caught as bycatch by highlighting species for management and research. The effectiveness of turtle excluder devices (TEDs) in reducing elasmobranch bycatch varied greatly among species but was generally not very effective because most of the captured species were small.

Manuscript accepted 29 May 2002.
Fish. Bull. 100:800–821 (2002).

Worldwide, there is increasing concern over the capture of elasmobranchs (sharks and rays) as bycatch. The global landings of elasmobranchs are currently 760,000 metric tons (t) but a similar amount is part of unreported bycatch (Stevens et al., 2000). This bycatch is unmanaged in most fisheries and elasmobranchs are less able to sustain their populations under fishing regimes designed to sustain the target teleosts or invertebrates (Heuter, 1998). Some species have declined significantly because they are captured as bycatch, e.g. the common (*Dipturus batis*) and barndoor (*D. laevis*) skates (Brander, 1981; Casey and Myers, 1998). Despite these prevailing fishery practices, there have been few evaluations of the ability of elasmobranch species to sustain population levels (Walker and Hislop, 1998).

In general, an evaluation of the sustainability of any bycatch species is hampered by a lack of information. This is particularly so for elasmobranchs. Elasmobranch bycatch is often not recorded (Bonfil, 1994), or when it is recorded, the species composition is unknown. There is also limited biological information on most bycatch species, such as age at maturity, growth rate, and fecundity. This lack of information hampers the use of conventional stock assessment methods to determine the population status of these species.

Australia has a highly diverse elasmobranch fauna; almost half of the species are endemic (Last and Stevens, 1994). In northern Australian waters, elasmobranchs are impacted by a range of fisheries. Gillnet, longline, and dropline fisheries target shark species. Sharks, rays, and sawfish are also caught as bycatch in dropline and gillnet fisheries that target teleosts and in trawl fisheries that target teleosts or prawns. The current levels of elasmobranch bycatch are unknown for most of these fisheries. However, we know that the retained elasmobranch bycatch has increased because of the rising value of elasmobranch products, such as fins.

The largest fishery in northern Australia is the northern prawn fishery (NPF), which covers an area over 1,000,000 km^2 of ocean (Fig. 1) (McLoughlin et al., 1997). In the NPF, elasmobranchs contribute about 4% of the total bycatch weight (Stobutzki et al., 2001b). Prior to 2001, NPF trawlers were allowed to retain shark products but were restricted with respect to the amount on board at any one time. Management required fishermen to record retained bycatch in trawler logbooks, but the records were not validated. In 1999, 4177 kg of fillet, trunk, and whole shark and 1531 fins were recorded (Sharp et al.[1]). The compulsory use of turtle excluder devices (TEDs) in NPF trawls, beginning with the year 2000, have excluded some elasmobranchs from the bycatch (Brewer et al., 1998). However species-specific exclusion has not been examined.

[1] Sharp, A., J. Malcolm, and J. Bishop. 2000. Northern prawn fishery and Kimberley prawn fishery data summary 1999. Final report to Australian Fisheries Management Authority, Canberra, Australia. AFMA, PO Box 7051, Canberra BC ACT 2610, Australia.

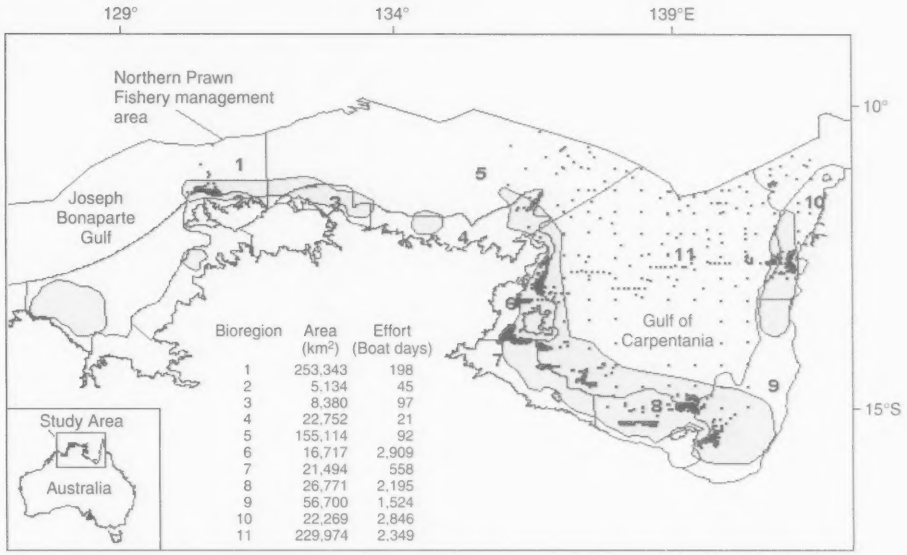

Bioregion	Area (km^2)	Effort (Boat days)
1	253,343	198
2	5,134	45
3	8,380	97
4	22,752	21
5	155,114	92
6	16,717	2,909
7	21,494	558
8	26,771	2,195
9	56,700	1,524
10	22,269	2,846
11	229,974	2,349

Figure 1

The management area of the northern prawn fishery (NPF) and the bioregions defined through the interim marine and coastal rationalization (IMCR) process (Thackway and Cresswell, 1998). The shaded area represents the regions fished by commercial prawn trawlers. The dots mark the positions of the trawls that were sampled to estimate the removal rates and total biomass of bycatch species (Table 1). The numbers refer to the bioregions (1=Oceanic Shoals, 2=Tiwi, 3=Cobourg, 4=Arnhem Wessel, 5=Arafura, 6=Groote, 7=Pellew, 8=Wellesley, 9=Karumba-Nassau, 10=West Cape York, 11=Carpentaria).

This study is one of several (Milton, 2001; Stobutzki et al., 2001a) that broadly examine the sustainability of bycatch species groups in the NPF. The aim of this study was to assess the relative sustainability of elasmobranch species taken as bycatch in the NPF. We use a broadbrush method developed by Stobutzki et al (2001a) to encompass the high diversity of and limited amount of information. This semiquantitative technique assesses the sustainability of species according to two overriding characteristics: 1) their susceptibility to capture and mortality due to trawling; and 2) the ability of a population to recover after depletion. Traditional population assessment methods have attempted to measure or model these factors. The broadbrush method uses biological and ecological criteria to rank species with respect to these two characteristics, maximizing the use of the limited information available. The method identifies species that are least likely to be sustainable in the bycatch, so that these can be the focus of further research and management.

Methods

Species present in the NPF and those captured as bycatch

A list of the elasmobranchs species recorded in the area of the NPF was compiled from Last and Stevens (1994). A list of species taken as NPF bycatch has been collated from two sources: 1) fishery research surveys undertaken within the NPF fishing grounds (Crocos and Coman, 1997; Stobutzki et al., 2001b; Blaber et al.[2]; Crocos et al.[3]); and 2) records of elasmobranch bycatch by observers on commercial vessels (these observers were either scientific staff or trained crew-members) (Stobutzki, 2001b; Pender et al.[4]; Stobutzki et al.[5]).

[2] Blaber, S., D. Brewer, C. Burridge, M. Farmer, D. Milton, J. Salini, Y-G. Wang, T. Wassenberg, C. Buxton, I. Cartwright, S. Eayrs, N. Rawlinson, R. Buckworth, N. Gill, J. MacCartie, R. Mounsey, and D. Ramm. 1997. Effects of trawl design on bycatch and benthos in prawn and finfish fisheries. Final report to Fisheries Research and Development Corporation (FRDC), Project 93/179, 190 p. FRDC, PO Box 222, Deakin West ACT 2600, Australia.

[3] Crocos, P. J., D. M. Smith, and G. Marsden. 1997. Factors affecting the reproductive performance of captive and wild broodstock prawns. Final report to the Fisheries Research and Development Corporation (FRDC), Project 92/51, 87 p. FRDC, PO Box 222, Deakin West ACT 2600, Australia.

[4] Pender, P. J., R. S. Willing, and D. C. Ramm. 1992. Northern prawn fishery bycatch study: distribution, abundance, size and use of bycatch from the mixed species fishery. Northern Territory Department of Primary Industry and Fisheries (NT DPIF), fishery report 26, 97 p. NT DPIF, GPO Box 3000, Darwin NT 0801, Australia.

[5] See next page for footnote 5.

Estimates of current bycatch rates and size frequency of species

Current bycatch rates were obtained from research and observer surveys. The research surveys and gear are described in detail in Stobutzki et al. (2001b) and Stobutzki et al.[5] Briefly, the research surveys sampled the nine major NPF fishing regions (1997 and 1998) to describe the bycatch. A scientific observer conducted three trips (of one-month duration) on commercial vessels in the NPF during 1996–97. A crew member of the commercial fleet was trained in elasmobranch identification and recorded the elasmobranch catch on commercial vessels during 1997. All elasmobranchs caught were identified, most to species, and their total number and weight were recorded. Where possible, each individual's sex, weight, and length were recorded. Total length (TL) was recorded for sharks, rhynchobatids, and pristids, and disc width (DW) was recorded for the remaining rays. Trawls during the research survey were of 0.5-h duration and a single trawl net was used. The observer data were collected from commercial trawls, 3–4 h in duration and where two nets were towed.

The overall catch rate for each species was calculated from the three sources. Catch rates were corrected for duration of the trawl and the length of the headrope. The catch rates of species in each trawl were converted into catch per swept area of the trawl as the numbers of individuals per square kilometer swept (no./km^2). We used the trawl speed recorded during the trawls and assumed that the prawn trawls had a spread of 0.66 of the headrope length (Bishop and Sterling, 1999). Individuals of the species *Carcharhinus tilstoni* and *C. limbatus* are difficult to distinguish. Genetic studies in this region have indicated that *C. limbatus* is very rare (Lavery and Shaklee, 1991); therefore all specimens were recorded as *C. tilstoni*.

Size at first maturity and fecundity

Because there is limited biological information on dasyatidids and gymnurids (Last and Stevens, 1994), we retained specimens from the scientific surveys to obtain preliminary estimates of size at maturity and fecundity. For females, gonad weight, diameter of the largest ovum in the ovary, and their fecundity status (whether they were pregnant of not, and whether there were *in utero* embryos present) were recorded. For pregnant individuals, the number of embryos was recorded. For males, we recorded gonad weight, clasper length, and the calcification state of the clasper (uncalcified, partially calcified, or totally calcified). Size at sexual maturity for females was estimated as the length of the smallest pregnant individual; for males it was determined from clasper size and calcification (Bass et al., 1973).

Within-net survival

Currently there is no information on the survival rate of elasmobranchs caught as bycatch in prawn trawlers. The October 1998 research survey and crew-member observer (Table 1) recorded whether individuals were dead or alive when landed on the deck. This record provided an estimate of the within-net mortality, which was no doubt lower than the total mortality because some individuals recorded as alive would subsequently die as a result of capture. Logistic regressions (PROC LOGISTIC, SAS 1997) were used to determine whether there was a relationship between the likelihood of survival and the length or sex of an individual. The species were analyzed in two groups: sharks (species where TL was recorded) and rays (species where DW was recorded).

Assessment of the sustainability of elasmobranch species

The assessment was based on the method developed by Stobutzki et al. (2001a) which was designed to accommodate a high diversity of and a limited amount of information. The sustainability of the species was assumed to be dependent on two overriding features: 1) the susceptibility of the species to capture and mortality caused by trawling and 2) the capacity of the population to recover after depletion. Biological and ecological information was collated from the literature (Compagno, 1984a; 1984b; Last and Stevens, 1994; Froese and Pauly[6]). This information was used to rank the species along two axes describing the overriding features:

Axis 1: The susceptibility of a species to capture and mortality due to a prawn trawl (susceptibility),
Axis 2: The capacity of a species to recover once the population is depleted (recovery).

Each feature (or axis) was derived from several criteria (listed below) that summarized aspects of the biology of the species (six criteria for axis 1 and five criteria for axis 2). Each species was given a ranking from 1 to 3 for each criterion (the definitions of the ranks for the criteria are provided in Table 2). A rank of 1 suggested that the species was highly susceptible to capture or had little capacity to recover; a rank of 3 suggested that the species had a low susceptibility to capture or a high capacity to recover. Depending on the criterion, these ranks were based on categorical or continuous data (Table 2). Where continuous data were used, because no information was available to assign divisions between the ranks, the range of the data was divided into thirds to create the categories.

[5] Stobutzki, I., S. Blaber, D. Brewer, G. Fry, D. Heales, P. Jones, M. Miller, D. Milton, J. Salini, T. Van der Velde, Y-G. Wang, T. Wassenberg, M. Dredge, A. Courtney, K. Chilcott, and S. Eayrs. 2000. Ecological sustainability of bycatch and biodiversity in prawn trawl fisheries. Final report to the Fisheries Research and Development Corporation (FRDC), Project 96/257, 512 p. FRDC, PO Box 222, Deakin West ACT 2600, Australia.

[6] Froese, R., and D. Pauly, eds. 1999. Fishbase 99. URL htpp://www.fishbase.org. [Date accessed: November 1999.]

Table 1

The surveys that contributed to the estimate of the removal rate (*), total biomass, and within-net survival for elasmobranch species in the Northern Prawn Fishery, Australia. # indicates the surveys whose data contributed to the list of bycatch species.

Year	Month	Type	Gear	No. of trawls	No of nets used	Reference
1998*#	Sep–Oct	research survey	Florida flyer	366	1	Stobutzki et al.[5]
1997*#	Oct	research survey	Florida flyer	424	1	Stobutzki et al. (2001b)
1997*#	Sep–Oct	scientific observer	Florida flyer	60	2	Stobutzki et al. (2001b)
1997*#	Aug–Oct	crew member observer	Florida flyer	141	2	Stobutzki et al.[5]
1997*#	May–Jun	scientific observer	Florida flyer	76	2	Stobutzki et al. (2001b)
1997*#	Feb–Mar	research survey	Florida flyer, Engels	248	1	Stobutzki et al. (2001b)
1996*#	Sep	scientific observer	Florida flyer	83	2	Stobutzki et al. (2001b)
1995#	Jun	research survey	Florida flyer	38	1	Blaber et al.[2]
1995#	Oct–Nov	research survey	Florida flyer	39	1	Blaber et al.[2]
1995#	Feb–Mar	research survey	Florida Flyer	39	1	Blaber et al.[2]
1994#	Nov	research survey	Florida flyer	7	2	Crocos and Coman (1997); Crocos et al.[3]
1994#	Jul	research survey	Florida flyer	7	2	Crocos and Coman (1997); Crocos et al.[3]
1994#	Ma	research survey	Florida flyer	4	2	Crocos and Coman (1997); Crocos et al.[3]
1994#	Mar	research survey	Florida flyer	5	2	Crocos and Coman 1997; Crocos et al.[3]
1993#	Nov	research survey	Florida flyer	81	1	Crocos and Coman 1997; Crocos et al.[3]
1993#	Oct	research survey	Florida Flyer	5	2	Blaber et al.[2]
1993#	Aug	research survey	Florida Flyer	9	2	Crocos and Coman (1997; Crocos et al.[3]
1993	Jan–Feb	research survey	Engels, Frank and Bryce	71	1	Milton et al. (1995)
1991	Nov	research survey	Frank and Bryce	62	1	Milton et al. (1995)
1990	Nov–Dec	research survey	Frank and Bryce	128	1	Blaber et al. (1994); Milton et al. (1995)

Where species-specific information was not available, a species was given the same rank as other species within its family for the criteria water column position, diet, and day and night catchability. For the other criteria, where it was not necessarily logical that family members would be similar, or where family information was not available, a rank of 1 was assigned as a precautionary approach.

Axis 1: Susceptibility of a species to capture and mortality induced by the prawn trawl

There were six criteria (water column position, survival, range, day and night catchability, diet, and depth range) on axis 1.

Water column position Because prawn trawls fish close to the sea floor, demersal species are more likely to be captured than pelagic species.

Survival This estimate was based on the survival-in-the-net data outlined previously. The possible survival range of 0–100% was divided into thirds for the divisions between the ranks.

Range This criterion reflects the geographic spread of a species within the NPF and was determined from the research, scientific, and crew-member observer surveys undertaken by Stobutzki et al.[5] and Stobutzki et al. (2001b). Commercial fishing is highly aggregated within the managed area of the fishery. The nine regions of highest effort were surveyed in 1997 (Table 1) and the presence or absence of each species was recorded in each region. We assumed that species with a restricted range could be impacted more heavily by trawling than those with a broader range.

Day and night catchability The tiger prawn fishery is predominantly a nighttime fishery (McLoughlin et al., 1997). Species with a higher catchability at night are more susceptible to capture as bycatch. The relative catch rate of species during night and daytime trawling was compared during research surveys in October 1997 (Table 1).

Diet This criterion reflects whether the diet of the species may attract them to trawl grounds and whether they feed within the area of the water column swept by a prawn trawl. Species that feed on commercial prawns may be attracted to the commercial fishing grounds, increasing their susceptibility to capture. Species that feed on demersal organisms are assumed to be more susceptible to prawn trawls than species that feed higher in the water column.

Depth range Commercial trawls in the NPF are made mainly between 15 m and 40 m (Somers, 1994). An overlap between the depth range of trawling and the preferred

Table 2

The criteria used to assess 1) the relative susceptibility of bycatch species to capture and mortality due to prawn trawls and 2) their recovery capacity after depletion due to trawling. These combine to provide the ranks for the axes in Figure 2. For each criterion the definition of the three ranks is given, as well as the weighting score and the percentage of species for which species-specific information was used to rank them.

Criteria	Weight	Species-specific information (%)	Rank 1	Rank 2	Rank 3
Susceptibility					
Water column position	3	100	Demersal or benthic	Not applicable	Benthopelagic or pelagic
Survival	3	18	Probability of survival <33%	Probability of survival between 33% and 66%, inclusive	Probability of survival >66%
Range	2	71	Species range ≤3 fishery regions	3 fishery regions < species range ≤6 fishery regions	Species range >6 fishery regions
Day and night catchability	2	32	Higher catch rate at night	No difference between night and day	Higher catch rate at day
Diet	2	55	Known to, or capable of, feeding on commercial prawns or benthic organisms	Not applicable	Feed on pelagic organisms
Depth range	1	100	Less than 60 m	Not applicable	Deeper than 60 m
Recovery					
Probability of breeding	3	42	Probability of breeding before capture <50%	Probability of breeding before capture not significantly different from 50%	Probability of breeding before capture >50%
Maximum size	3	100	Maximum disc width >1755 mm	853 mm < maximum disc width ≤1755 mm	Maximum disc width ≤853 mm
			Maximum total length >4781 mm	1861 mm < maximum total length ≤4781 mm	Maximum total length ≤1861 mm
Removal rate	3	79	Removal rate >66%	33% < removal rate ≤66%	33% ≤ removal rate
Annual fecundity	1	52	Annual fecundity ≤5 young per year	5 young per year < annual fecundity ≤19 young per year	Annual fecundity >19 young per year
Mortality index	1	64	mortality index >3.47	0.92 < mortality index ≤3.47	mortality index ≤0.92

depth range of species will influence their susceptibility to capture: a higher proportion of a species' population is likely to be taken if there is an overlap. Species with a broader depth range may have a spatial refuge from trawling, making them less susceptible. The depth range of species was determined from previous research surveys in the NPF and from the literature.

Axis 2: The capacity of a species to recover once the population is depleted

There were five criteria (probability of breeding, maximum size, removal rate, annual fecundity, mortality index) on this axis.

Probability of breeding We assumed that a species is likely to have a greater capacity to recover from a decrease in population due to trawling if most individuals are captured after they have bred. The probability that an individual of a species had bred before capture was determined from the mean length at capture in relation to the species' recorded size at maturity. The mean length at capture of a species was recorded in the research and observer surveys 1996–98 (Table 1). Size at maturity was determined from the available literature and from our estimates outlined previously.

A *t*-test (Sokal and Rohlf, 1996) was used to determine whether the mean length at capture was significantly different from the size at maturity for each species.

Table 3

The elasmobranch species that are known to occur in the region of the northern prawn fishery (NPF), Australia, and of these species, those that have been recorded in NPF bycatch (Table 1). The labels in parentheses refer to the species abbreviations in Figure 2.

	Recorded in bycatch		
Family	Yes		No
Carcharhinidae	*Carcharhinus albimarginatus*	(Cal)	*Carcharhinus amblyrhynchoides*
	Carcharhinus amboinensis	(Cam)	*Carcharhinus amblyrhynchos*
	Carcharhinus brevipinna	(Cb)	*Carcharhinus cautus*
	Carcharhinus dussumieri	(Cd)	*Carcharhinus obscurus*
	Carcharhinus fitztroyensis	(Cf)	*Carcharhinus plumbeus*
	Carcharhinus leucas	(Cle)	*Carcharias taurus*
	Carcharhinus limbatus	(Cli)	*Carcharinus falciformis*
	Carcharhinus macloti	(Cm)	*Carcharinus melanopterus*
	Carcharhinus sorrah	(Cs)	*Loxodon macrorhinus*
	Carcharhinus tilstoni	(Ct)	*Rhizoprionodon oligolinx*
	Galeocerdo cuvier	(Gc)	*Triaenodon obesus*
	Negaprion acutidens	(Na)	
	Prionace glauca	(Pg)	
	Rhizoprionodon acutus	(Rac)	
	Rhizoprionodon taylori	(Rta)	
Dasyatidae	*Amphotistius annotata*	(Aa)	*Dasyatis fluviorum*
	Dasyatis brevicaudatus	(Db)	*Taeniura lymma*
	Dasyatis leylandi	(Dl)	
	Dasyatis kuhlii	(Dk)	
	Dasyatis sp. A	(Dsa)	
	Dasyatis thetidis	(Dt)	
	Himantura fai	(Hf)	
	Himantura granulata	(Hg)	
	Himantura jenkinsii	(Hj)	
	Himantura sp. A	(Hsa)	
	Himantura toshi	(Ht)	
	Himantura uarnak	(Hua)	
	Himantura undulata	(Hun)	

continued

Maximum size The maximum size of a species was used as an indicator of the species' relative recovery rate. In general, larger species tend to live longer and their populations recover more slowly (Roberts and Hawkins, 1999). Size appears to be a good predictor of vulnerability for marine fishes (Jennings et al., 1999), and in particular skates (Walker and Hislop, 1998; Dulvy et al., 2000). Estimates of maximum size came from the literature. Species were grouped according to whether DW or TL was measured. The range of the maximum sizes of species was calculated and divided into thirds for the divisions between the ranks.

Removal rate We assumed that species with a higher proportion of their biomass removed as bycatch would have a lower capacity to recover. The estimate of removal rate was based on the catch rates from research surveys and scientific observer collections undertaken between 1996 and 1998 (Table 1). We assumed that these catch rates were representative of the overall catch rates in the commercial fishery.

The catch rates of bycatch species vary spatially within the NPF (Stobutzki et al., 2001b). Therefore, the fishery was stratified before we estimated the mean catch rate, using the bioregions identified in the Interim Marine and Coastal Regionalization for Australia (IMCRA) process (Thackway and Cresswell, 1998) (Fig. 1). A mean catch rate for each species was calculated for each bioregion where commercial tiger prawn trawling occurs.

The biomass (in numbers of individuals per year) of bycatch removed by the commercial fishery was estimated by multiplying the mean catch rate calculated above by the 1997 commercial tiger prawn fishery effort in each bioregion (Table 3). Commercial fishing effort is recorded in log books in boat days (held by the Australian Fisheries Management Authority). One boat day was assumed to be the

Table 3 (continued)

Family	Recorded in bycatch: Yes		Recorded in bycatch: No
Dasyatidae (continued)	*Pastinachus sephen*	(Ps)	
	Taeniura meyeni	(Tm)	
	Urogymnus asperrimus	(Ua)	
Ginglymostomatidae	*Nebrius ferrugineus*	(Nf)	
Gymnuridae	*Gymnura australis*	(Ga)	
Hemigaleidae	*Hemigaleus microstoma*	(Hm)	*Hemiscyllium ocellatum*
	Hemipristis elongatus	(He)	*Hemiscyllium trispeculare*
Hemiscylliidae	*Chiloscyllium punctatum*	(Cp)	
Mobulidae			*Manta birostris*
			Mobula eregoodootenkee
Myliobatidae	*Aetobatus narinari*	(Ana)	
	Aetomylaeus vespertilio	(Av)	
	Aetomyleus nichofii	(Ani)	
Narcinidae	*Narcine westraliensis*	(Nw)	*Narcine* sp. A
Orectolobidae	*Orectolobus ornatus*	(Oo)	*Eucrossorhinus dasypogon*
			Orectolobus wardi
Pristidae	Anoxypristis cuspidata	(Ac)	
	Pristis clavata	(Pc)	
	Pristis microdon	(Pm)	
	Pristis pectinata	(Pp)	
	Pristis zijsron	(Pz)	
Scyliorhinidae	*Atelomycterus fasciatus*	(Af)	*Atelomycterus macleayi*
	Galeus sp. A	(Gsa)	
Sphyrnidae	*Eusphyra blochii*	(Eb)	
	Sphyrna lewini	(Sl)	
	Sphyrna mokarran	(Sm)	
Squatinidae	*Squatina* sp. A	(Ssa)	
Stegostomatidae	*Stegostoma fasciatum*	(Sf)	
Rhincodontidae			*Rhiniodon typus*
Rhinobatidae	*Rhinobatos typus*	(Rty)	*Aptychotrema* sp. A
Rhynchobatidae	*Rhynchobatus djiddensis*	(Rd)	
	Rhina ancylostoma	(Ran)	

equivalent of 14 hours of trawling with two nets and with 14-fathom (25.48 m) headropes at a speed of 3.2 knots (5.9 km/h) (Bishop and Sterling, 1999).

The estimate of the total amount removed for a species within the whole fishery was calculated by summing the removal estimates for the bioregions. This estimate was then converted to a proportion of the estimated total biomass of the species.

An estimate of the total biomass of each species in the bioregions where tiger prawn trawling occurs was generated from all research and scientific observer surveys conducted in the NPF during the 1990s (Fig. 1, Table 1). The gears used were prawn trawls (Florida flyer nets) and two types of fish trawls (Frank and Bryce trawls and Engel trawls). Both night and daytime trawling were undertaken. Both prawn-trawl and fish-trawl surveys were analyzed in order to cover the management area of the fishery.

The catch rates of species in each trawl were converted to the catch per swept area of the trawl as described previously. The fish trawls were assumed to have a spread of 0.6 of the headrope length (Blaber et al., 1994). A mean catch rate for each gear at each time (day or night) was calculated in each bioregion, resulting in up to six catch rate estimates for a species in a bioregion. The highest of these means was used for each species in that bioregion. This catch rate was then multiplied by the area of the bioregion to give an estimate of total numbers of individuals in the bioregion. Currently there are no robust estimates of the catchability coefficients for the various trawl gears and therefore a catchability coefficient of one was assumed for

all species. Such a high catchability coefficient is unlikely to be valid for most species and results in an underestimate of the total biomass. For the two bioregions where commercial tiger prawn trawlers operate, there was no survey data from which to estimate catch rates (bioregions 4 and 5, Fig. 1). Therefore, the mean catch rate of the other bioregions was used to allow an estimate of catch rate. The total biomass of each species was calculated by summing the estimates for the bioregions. The removal rate would range between 0% and 100%; this range was divided into thirds for the division between the ranks.

Annual fecundity The annual fecundity of species was estimated from data in the literature and the biological samples collected during our study. The annual fecundity of a species was estimated as the average number of pups per female multiplied by the number of times the females bred per year. Where the frequency of breeding was not known, it was assumed to be annual, unless the known gestation period was longer than 12 months. The range of fecundities was calculated and divided into thirds for the divisions between the ranks.

Mortality index The recovery capacity of a population is likely to be related to its fishing mortality rate (Sparre and Venema, 1992). A measure of this rate can be derived from the length-frequency of a species and the von Bertlanffy growth parameters (Sparre and Venema, 1992). However, for most species von Bertalanffy parameters were not available and therefore an index of mortality was calculated as follows:

$$Mortality\ index = (L_{max} - L_{ave})/(L_{ave} - L_{min}), \quad (1)$$

where L_{max} = the maximum length;
L_{ave} = the mean length at capture in the fishery; and
L_{min} = the smallest length caught.

The closer the mean length of captured individuals (L_{ave}) to the maximum length (L_{max}) the lower the mortality the population is subject to. As mortality due to fishing increases, the mean length of species in a population approaches the minimum length (L_{min}). For our analysis, we assumed constant catchability and mortality across the whole length range caught. The L_{ave} and L_{min} were calculated from length data collected during our study.

The range of mortality estimates was calculated and divided into thirds for the divisions between the ranks.

Analysis of criteria

Partial correlations (Sokal and Rohlf, 1996) were used to determine whether there was any redundancy in the criteria. Strong correlations would suggest that two or more criteria explained the same factors, which would lead to overemphasis of their effect. One of the correlated criteria was, therefore, removed.

The total susceptibility, or removal ranking, of a species was determined by the following equation:

$$S_i = \frac{\sum_{j=1}^{n} w_j R_i}{\sum_{j=1}^{n} w_j}, \quad (2)$$

where S_i = the total susceptibility or recovery ranks for species i;
w_j = the weighting for criterion j;
R_i = the rank of species i for criterion j; and
n = the number of criteria on each axes.

The criteria were weighted to reflect the relative importance of each criterion in determining the overall characteristic and the robustness and quality of the data (Table 2), the latter in terms of the amount of species-specific information and the scale of the information available. The criteria that were seen as major determinants of susceptibility or recovery and for which there were more robust data were weighted highest. This weighting was done in collaboration with the NPF Fishery Assessment Group.

The total susceptibility and recovery ranks for the species were graphed to determine the relative sustainability of the species caught as bycatch by prawn trawlers. The species least likely to be sustainable would be identified as the species with the lowest ranks on both axes.

Contour lines were drawn on the graph to group species that would be similar with respect to their sustainablity. Because neither susceptibility, nor recovery alone, provide a complete index to the sustainability of species, the index is a combination of these two features. Recovery is likely to be conditionally important on susceptibility, and therefore, a multiplicative relationship between the two axes is appropriate. We assumed that this relationship is symmetrical and given this assumption, the contour lines followed the equation

$$16(y - 0.75)(x - 0.75) = 4, 9, 16, 25, 36, 49. \quad (3)$$

The impact of turtle excluder devices on elasmobranch bycatch

Data on the size of species captured in nets fitted with TEDs and with nets with standard codends were available from two sources. The crew-member observer recorded seven pairs of trawls in which one net was fitted with a TED and one had a standard codend. The TED was a Seymour TED with 110-mm bar spacing. Previous research surveys from one area of the NPF also recorded information on elasmobranchs captured in nets with and without TEDs. The TEDs were AusTEDs, NørdMore Grids, and SuperShooters; the design of these nets is detailed in Brewer et al. (1998).

The length frequency of elasmobranchs caught in nets with TEDs was compared to the length frequency of elasmobranchs caught in nets without a TED. First, species were grouped into sharks (TL measured) and rays (DW measured) for analysis. The mean length of individuals captured in nets fitted with a TED was compared with that of elasmobranchs caught in nets with a standard codend by using a one-way ANOVA. The lengths were

transformed (log (*length* + 1)) prior to analysis to normalize the data. There were sufficient data for three species of shark (*Rhizoprionodon acutus, Hemigaleus microstoma,* and *Carcharhinus dussumieri*), two stingrays (*Dasyatis leylandi* and *Himantura toshi*) and a shovel-nosed ray (*Rhynchobatus djiddensis*) to examine them separately with one-way ANOVAs.

Results

Species captured as bycatch in prawn trawls of the NPF

At least 79 species of elasmobranchs from 18 families, inhabit the NPF region (Table 3). Of these, 56 species (16 families) have been recorded in the prawn-trawl fishery bycatch (Table 3). The Carcharhinidae and Dasyatidae, the most species-rich families in the region, are the also the families for which the highest number of species are recorded in bycatch (Table 3). There are 9 families in which all species found in this region have been recorded in bycatch (Table 3).

Current catch rates

In the research and observer surveys (1996 and 1998) 44 species of elasmobranchs were recorded. The highest overall catch rates were for *Carcharhinus tilstoni, C. dussumieri, R. djiddensis,* and *H. toshi* (Table 4). These four species contributed almost 65% of the observed elasmobranch bycatch. *Carcharhinus dussumieri* and *C. tilstoni* were recorded in 20% of all trawls, *R. dijiddensis* in 14%, and *H. toshi* in 17%.

Size at first maturity and fecundity

Specimens of five species of ray were examined to assess size at first maturity and to provide estimates of fecundity (Table 5). None of the species showed a change in gonadosomatic index (GSI) or diameter of the largest egg, both of which would clearly indicate maturity. The average number of embryos was low (Table 5); most species had one or two, with the exception of *Gymnurus australis,* which had up to five embryos present.

Males of most species showed an increase in GSI with calcification of the claspers. The estimates of size at maturity for the males were lower than the estimates for females for four of the five species (Table 5). However, this finding might have been influenced by the low numbers of pregnant females sampled (Table 5). The size at maturity of the males appeared to be between 44% and 79% of the maximum size for the species.

The mean size of rays caught in bycatch ranged from 182 mm for *D. leylandi* to 1117 mm for *H. toshi* (Table 6). The mean size of sharks ranged from 541 mm for *Carcharhinus sorrah* to 1643 mm for *Rhina ancylostoma* (Table 6). For 30 species, a size at birth was available from the literature and, of these, eight species were caught in bycatch at this size (Table 6).

Where an estimate of the size at first maturity (L_m) was available for a species, an estimate could be made of the percentage of individuals captured that were mature. In species with sufficient samples sizes, the percentage of mature individuals caught ranged from <1% for *S. lewini,* to 54% for *R. acutus* (Table 6). Species such as *D. leylandi* had an average size at capture not significantly different from L_m, indicating that, on average, half the individuals caught had reached maturity before capture. Species such as *R. acutus*, with an average size less than L_m, were those for which the majority were unlikely to have bred before capture. At the other extreme were species such as *G. australis*, for which it was likely that the majority had reached maturity before capture (Table 6).

The female-to-male ratio of individuals caught was close to 1:1 for the two common species, *D. leylandi* and *C. dussumieri* (Table 6). However, other species had a range from predominantly male (e.g. *R. acutus*) to predominantly female (e.g. *H. toshi*) (Table 6).

Within-net survival

Whether an individual was alive or dead when landed on the deck was recorded for 847 animals. Overall 56% were dead after capture in the trawl and 44% were alive. Both sharks and rays showed that the probability of survival was lower for males than for females (sharks χ^2=19.7, P<0.001, rays χ^2=10.5, P=0.0012) and that survival increased with length of the individual (sharks χ^2=4.8, P=0.029, rays χ^2=11.08, P=0.0009). Two-thirds of male sharks and rays were recorded as dead after capture in the trawl (Table 7). The mean size of rays and sharks that died (sharks 684 (±10 SE) mm, rays 424 (±41 SE) mm) was smaller than the mean size of those that survived (sharks 797 (±17 SE) mm, rays 546 (±33 SE) mm). The overall percentage of individuals of a species that died varied from 10% (*R. djiddensis*) to 82% (*C. dussumieri* and *R. acutus*) (Table 7).

Assessment of the sustainability of elasmobranch species

The 56 species of elasmobranchs recorded as bycatch in the NPF were ranked on each of the criteria on the two axes (Appendices 1 and 2). The extent to which species-specific information was available varied among the criteria (Table 2). Water column position, depth range, and maximum size had species-specific information for all species. Survival and day and night catchability had little species-specific information.

Most of the criteria were not correlated (Table 8). On the susceptibility axis the strongest correlation was between diet and water column position (Table 8). However, both criteria were retained because we believed there was sufficient difference between them; the correlation coefficient (r) was only 0.67. On the recovery axis no correlations were significant (Table 8).

On the susceptibility axis (Appendix 1) the four species of Pristidae, *Atelomycterus fasciatus, Himantura jenkinsi,* and *Stegostoma fasciatum* had a rank of 1, the lowest possible rank, suggesting they were the most susceptible to capture

Table 4

The percentage of trawls in which species were caught, mean catch rate (SE=standard error), and the percentage of catch contributed by each species.

			No./km^2		
Family	Species	% of trawls	Mean	SE	% of catch
Carcharhinidae	*Carcharhinus albimarginatus*	0.10	0.58	0.41	0.26
	Carcharhinus amboinensis	0.20	0.04	0.04	0.02
	Carcharhinus dussumieri	20.57	38.80	4.89	17.54
	Carcharhinus fitztroyensis	0.20	0.80	0.40	0.35
	Carcharhinus macloti	0.20	0.98	0.50	0.43
	Carcharhinus sorrah	1.67	1.47	0.57	0.65
	Carcharhinus tilstoni	19.49	44.20	5.98	20.07
	Galeocerdo cuvier	0.20	0.01	0.00	<0.01
	Negaprion acutides	0.10	0.00	0.00	<0.01
	Rhizoprionodon acutus	9.15	10.61	1.63	4.83
	Rhizoprionodon taylori	0.10	0.00	0.00	<0.01
Dasyatidae	*Amphotistius annotata*	1.97	1.56	0.41	0.74
	Dasyatis kuhlii	2.56	1.48	0.56	0.69
	Dasyatis leylandi	15.35	9.44	1.18	4.48
	Dasyatis sp. A	0.10	0.00	0.00	<0.01
	Dasyatis thetidis	0.49	0.03	0.01	0.01
	Himantura fai	0.10	0.01	0.00	<0.01
	Himantura granulata	0.20	0.01	0.01	<0.01
	Himantura jenkinsii	0.59	2.11	0.77	0.95
	Himantura sp. A	2.17	0.11	0.04	0.05
	Himantura toshi	17.72	27.85	3.10	12.84
	Himantura uarnak	0.98	1.44	0.58	0.70
	Himantura undulata	0.89	0.96	0.40	0.43
	Pastinachus sephen	3.44	0.69	0.31	0.31
	Taeniura meyeni	0.10	0.40	0.28	0.18
	Urogymnus asperrimus	0.39	0.40	0.28	0.18
Ginglymostomatidae	*Nebrius ferrugineus*	0.10	0.58	0.41	0.26
Gymnuridae	*Gymnura australis*	5.91	8.02	1.64	3.82
Hemiscylliidae	*Chiloscyllium punctatum*	5.41	11.83	1.96	5.42
	Hemigaleus microstoma	9.84	9.64	1.55	4.56
	Hemipristis elongatus	0.20	0.02	0.02	0.01
Myliobatidae	*Aetobatus narinari*	0.30	0.60	0.41	0.27
	Aetomylaeus nichofii	1.08	1.57	0.61	0.74
Orectolobidae	*Orectolobus ornatus*	0.10	0.52	0.52	0.27
Pristidae	*Anoxypristis cuspidata*	0.98	0.71	0.42	0.32
	Pristis zijsron	0.10	0.02	0.02	0.01
Rhinobatidae	*Rhinobatos typus*	0.39	0.02	0.01	0.01
Rhynchobatidae	*Rhina ancylostoma*	0.89	0.10	0.04	0.05
	Rhynchobatus djiddensis	14.27	30.87	3.39	14.26
Scyliorhinidae	*Atelomycterus fasciatus*	0.49	0.18	0.08	0.08
Sphyrnidae	*Eusphyra blochii*	0.20	0.04	0.04	0.02
	Sphyrna lewini	2.95	6.91	1.52	3.07
	Sphyrna mokarran	0.39	0.02	0.02	0.01
Stegostomatidae	*Stegostoma fasciatum*	2.17	2.17	1.02	1.10

Table 5

The estimated size (disc width) at first maturity and mean number of pups for ray species (sample size is shown in parentheses; SE=standard error).

Species	Size at maturity (mm)		Number of pups	
	Male	Female	Mean	SE
Amphotistius annotata	200 (9)	233 (8)	1.5	0.7 (2)
Dasyatis kuhlii	300 (10)	378 (6)	2	— (1)
Dasyatis leylandi	185 (103)	180 (110)	1.1	0.3 (17)
Gymnura australis	350 (29)	610 (16)	3.2	1.2 (6)
Himantura toshi	400 (31)	660 (21)	1.5	0.7 (2)

and mortality. The next 19 species had a rank of 1.15, also low. *Carcharhinus tilstoni, C. macloti, Sphyrna lewini, Prionace glauca, C. brevipinna,* and *Aetomyleus nichofii* had the highest ranks on this axis (>1.92), indicating that they were the least susceptible to capture and mortality.

On the recovery axis (Appendix 2) *Aetomyleus vespertilio, Dasyatis brevicaudatus, Pristis clavate,* and *P. pectinata* had the lowest ranks, indicating that they had the lowest capacity to recover. *Gymnura australis, H. toshi, Hemigaleus microstoma,* and *R. taylori* had the highest ranks on this axis and therefore the highest capacity to recover.

When the ranks of the species on the two axes were plotted (Fig. 2), *Dasyatis brevicaudatus, P. pectina, P. clavata, P. microdon, P. zijsron,* and *Himantura jenkinsii* ranked the lowest on the combination of the two axes, indicating that they were the least likely to be able to survive capture as bycatch. The species *Eusphyrna blochii, H. toshi, C. macloti,* and *C. tilstoni* ranked the highest on the two axes, indicating that they were the most likely to be able to survive capture as bycatch.

The impact of turtle exclusion devices on elasmobranch bycatch

Both sharks and rays taken as bycatch were significantly smaller in nets with a codend fitted with a TED (Table 9). The length frequency of the sharks and rays caught in the nets with TEDs showed a lower proportion of the larger individuals (Fig. 3). Where individual species were examined, there was a decrease in the size of *C. dussumieri* and *R. djiddensis* caught in the net with a TED (Table 9). There was no significant difference in size for *H. microstoma, A. annotata,* and *H. toshi* (Table 9). However, significantly larger individuals of *Rhizoprionodon acutus* were caught in the net with a TED (Table 9).

Discussion

Of the elasmobranch species known to inhabit this region, 71% were taken as bycatch in the NPF. The highly diverse bycatch is characteristic of tropical prawn trawl fisheries (Hall, 1999). Two critical pieces of information for assessing the impact of trawling in this region on elasmobranchs are the catch rates and survival of species.

Current catch rates

Although the bycatch was highly diverse, four species dominated the catch of the present study (*C. tilstoni, C. dussumieri, R. djiddensis,* and *H. toshi,* Table 4), occurring in 14–20% of trawls, so that one individual was seen at least every seven trawls. However, most species (75%) contributed <1% of the catch and had low catch rates (Table 4). However, even low catch rates can result in a large overall take of individuals. The fishery recorded 18,314 days of fishing in 1999 (Sharp et al.[1]) and if each day consisted of four trawls (Bishop and Sterling, 1999), 73,256 trawls (with two nets) would have been undertaken in the year. Hence for a species occurring in 1% of trawls, 733 individuals would have been caught in the year.

There are no long-term catch data available that can be examined for changes in catch rates of elasmobranch species. Although shark byproducts are recorded in NPF logbooks, the data are of limited value because they are not validated and not species-specific. Pender et al.[4] surveyed the bycatch in Northern Territory waters of the NPF during the 1980s. Rhynchobatids (71% of the elasmobranch catch), carcharhinids (12%) and dasyatids (11%) dominated the catch (Pender et al.[4]). All species recorded by Pender et al.[4] were recorded in our study. Direct comparisons of the catch rates of Pender et al.[4] with those of our study were not possible because of differences in gear, season, and region.

Most elasmobranchs caught in bycatch are small (<1000 mm). For some species, this means that most individuals have not bred before capture (Table 6) and therefore the fishery will have a greater adverse impact on the species. At least eight species were caught at sizes close to their known birth size (Table 6). This finding suggests that pupping may occur in the area of the fishery. Whether these species have restricted pupping grounds is unknown.

Within-net survival

Our estimates of within-net survival are the first for elasmobranchs in prawn trawls. The results suggest that most

Table 6

The mean, minimum (min), and maximum (max) size (TL or DW) of elasmobranch species caught in nighttime prawn trawling. The size at maturity (L_m) and at birth (pup size) are shown based on Last and Stevens (1994) or Table 5. The percentage of individuals caught that were mature (% mature) and the sex ratio are also shown. SE = standard error; n = sample size; P is the probability that the mean length at capture is different from L_m.

		Size (mm)					Sex ratio					
Family	Species	Mean	SE	Min.	Max.	n	F:M	n	L_m	P	% mature	Pup size (mm)
Carcharhinidae	*Carcharhinus albimarginatus*	850	—	—	—	1	—	—	1700	—	100	550
	Carcharhinus amboinensis	1700	—	—	—	1	—	—	2100	—	0	600
	Carcharhinus dussumieri	636	6	270	850	377	1.08	139	700	<0.001	41	350
	Carcharhinus fitzroyensis	1045	225	820	1270	2	—	—	800	>0.5	50	500
	Carcharhinus macloti	745	75	670	820	2	—	—	690	>0.5	20	450
	Carcharhinus sorrah	542	43	300	950	25	3.03	16	900	<0.001	8	500
	Carcharhinus tilstoni	794.3	9	100	1950	344	0.95	84	1200	<0.001	0.6	600
	Galeocerdo cuvier	1175	285	890	1460	2	all M	1	3000	>0.1	0	500
	Negaprion acutidens	2600	—	—	—	1	—	—	2200	—	—	500
	Rhizoprionodon acutus	689	14	280	960	140	0.56	81	750	<0.001	54	—
	Rhizoprionodon taylori	546	—	—	—	1	all F	1	400	—	100	250
Dasyatidae	*Amphotistius annotata*	211.4	12	140	452	25	1.43	3	200	>0.5	24	—
	Dasyatis kuhlii	297.3	12	190	400	24	4.00	10	300	>0.5	8	160
	Dasyatis leylandi	182.2	3	110	400	206	1.05	162	180	>0.2	46	110
	Dasyatis sp. A	350	—	—	—	1	—	—	360	—	0	—
	Dasyatis thetidis	1162	129	800	1420	5	all M	1	—	—	—	350
	Himantura fai	1900	—	—	—	1	—	—	—	—	—	550
	Himantura granulata	960	—	—	—	1	—	—	—	—	—	280
	Himantura jenkinsii	890	150	300	1140	5	all M	1	—	—	—	—
	Himantura sp. A	350	65	80	1800	57	all F	12	—	—	—	—
	Himantura toshi	456	11	150	1330	235	4.17	52	400	<0.001	12	200
	Himantura uarnak	1055	132	290	1600	12	all F	2	—	—	—	280
	Himantura undulata	1117	131	400	1500	7	all F	1	—	—	—	200
	Pastinachus sephen	1076	53	450	2000	43	3.03	12	—	—	—	180
	Taeniura meyeni	1300	—	—	—	1	—	—	—	—	—	350
	Urogymnus asperrimus	850	106	530	1150	5	all M	2	—	—	—	—
Ginglymostomatidae	*Nebrius ferrugineus*	2400	—	—	—	1	—	—	2250	—	100	400
Gymnuridae	*Gymnura australis*	462	19	120	860	87	2.00	42	350	<0.001	24	—
Hemigaleidae	*Hemigaleus microstoma*	609	19	250	950	152	0.68	91	600	>0.5	47	300
	Hemipristis elongata	1340	190	1150	1530	2	all F	1	1100	>0.5	50	520
Hemiscylliidae	*Chiloscyllium punctatum*	668	23	230	1000	63	2.50	7	700	<0.001	52	170
Myliobatidae	*Aetobatus narinari*	625	125	500	750	2	all F	1	—	—	—	260
	Aetomylaeus nichofii	437	42	240	720	11	all F	3	—	—	—	170
Pristidae	*Anoxypristis cuspidata*	1930	193	1240	2550	8	all F	1	—	—	—	—
Rhinobatidae	*Rhinobatos typus*	1953	188	1500	2340	4	—	—	—	—	—	—
Rhynchobatidae	*Rhina ancylostoma*	1643	112	1010	2090	9	0.33	3	—	—	—	—
	Rhynchobatus djiddensis	869	36	230	2650	187	4.76	35	1100	<0.001	8	—
Scyliorhinidae	*Atelomycterus fasciatus*	300	0	300	300	2	—	—	320	—	0	—
Sphyrnidae	*Eusphyra blochii*	990	320	670	1310	2	—	—	1080	>0.5	50	450
	Sphyrna lewini	832	54	400	2400	37	all F	3	1400	<0.001	3	450
	Sphyrna mokarran	1780	457	400	2400	3	1.00	2	2100	>0.5	33	650
Stegostomatidae	*Stegostoma fasciatum*	1305	82	400	2000	26	0.80	3	1700	<0.001	23	200

Table 7

The percentage of elasmobranchs that died within the trawl net, recorded on research and crew-member observer surveys. "Combined sharks" refers to all species where total length was recorded; "combined rays" refers to all species where disc width was recorded; n = number of specimens measured.

		% dead					
Family	Taxa	Female	n	Male	n	Overall	n
	combined sharks	23	149	66	59	61	639
	combined rays	56	360	67	279	40	208
Carcharhinidae	*Carcharhinus dussumieri*	48	207	58	114	52	321
	Carcharhinus sorrah	73	15	50	8	65	23
	Carcharhinus tilstoni	78	40	85	33	82	73
	Rhizoprionodon acutus	75	44	86	72	82	116
Dasyatidae	*Dasyatis leylandi*	27	22	95	19	59	41
	Himantura toshi	43	40	78	18	53	58
Gymnuridae	*Gymnura australis*	31	26	75	8	41	34
Hemigaleidae	*Hemigaleus microstoma*	44	29	64	39	62	68
Rhynchobatidae	*Rhynchobatus djiddensis*	21	24	20	5	10	59

Table 8

The correlations between the criteria on 1) the susceptibility axis and 2) the recovery axis. * indicates significance at $P < 0.05$.

Susceptibility	Survival	Range	Day and night catchability	Diet	Depth range
Water column position	0.07	–0.18	0.13	0.67*	0.07
Survival		0.48*	0.07	–0.11	–0.00
Range			0.25	0.06	0.09
Day and night catchability				–0.15	0.04
Diet					0.05

Recovery	Maximum size	Removal rate	Annual fecundity	Mortality index
Probability of breeding	0.07	0.25	0.16	0.08
Maximum size		–0.22	–0.25	0.17
Removal rate			–0.27	0.21
Annual fecundity				0.12

sharks and rays, particularly the smaller individuals, die within the trawl net (56%). The lower survival rates of male individuals is possibly because the males of most elasmobranch species are smaller than the females. The rhynchobatid *R. djiddensis* had a higher survival rate (90%) than most other species, whereas the lowest survival rate was seen in *C. tilstoni* and *R. acutus* (18%). Although the larger elasmobranchs appeared to have a higher within-net survival, in the commercial fishery these were the very individuals killed for their fins and therefore their mortality was ultimately higher than that predicted by their size alone. In 2001 the NPF introduced an industry-initiated ban on all shark products, so that the only mortality these species are subject to is that caused by the capture process. Differences between species in survival rates may influence changes in the relative abundance of species.

Assessment of the sustainability of elasmobranch species

Elasmobranchs, in general, are more susceptible to overfishing than are bony fishes, but there is likely to be a range of sensitivities among the species (Walker, 1998; Stevens et al., 2000). The process we applied in our study allowed us to examine these different sensitivities and to highlight those species whose populations were most likely to be affected by the NPF. The process was designed to deal with the high diversity of the bycatch and the

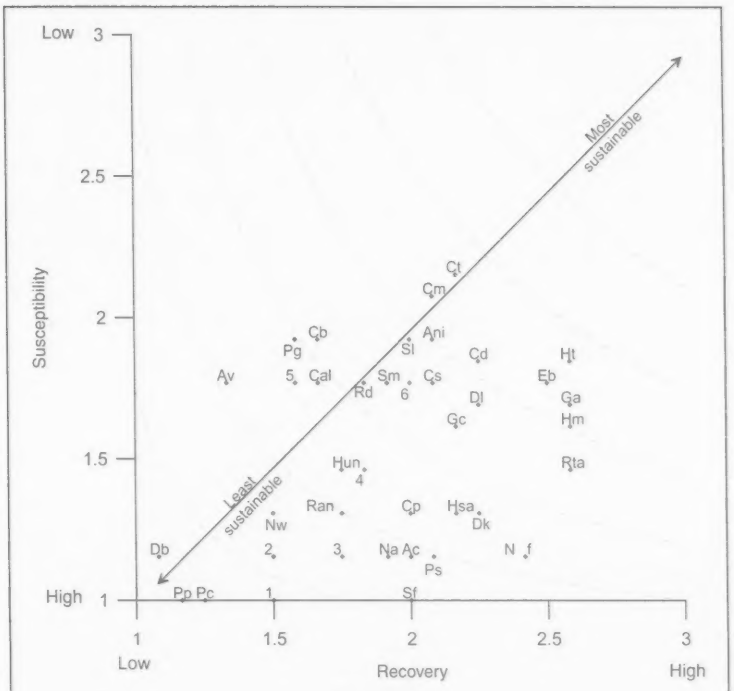

Figure 2

The ranking of elasmobranch species with respect to criteria that reflect their susceptibility to capture and mortality due to prawn trawling and their capacity to recover after depletion by trawling. These factors combine to reflect the relative ability of species to sustain capture as prawn trawl bycatch in the northern prawn fishery and therefore their relative priority with respect to research and management. Numbers refer to species combinations that fall together on the graph. (1=Hj, Pm, Pz; 2=Ca, Cle, Dt, Gsa, Ssa, Tm; 3=Af, Dsa, Hf, Hg Hua, Oo, Rty, Ua; 4=Cf, Aa; 5=Ana, Cli; 6=Rac, He). Explanations of the abbreviations for species are given in Table 3.

paucity of information available for most species. Our process was similar to that used by the International Union for the Conservation of Nature and Natural Resources (IUCN) red lists (IUCN, 1995) that categorize species with respect to the threat of extinction worldwide. The IUCN uses criteria on the extent of population decrease, area of occurrence, percentage of population that is mature, and the probability of extinction (IUCN, 1995). The IUCN criteria have been modified for application to marine fishes and to smaller geographic scales (Musick, 1998). With respect to elasmobranchs, several authors have examined the variable resilience of species to fishing pressure. These approaches have focused on life history characteristics that influence the recovery of populations, including reproductive and growth parameters (reviewed by Stevens et al., 2000). Our process is similar to these but focuses at the level of an individual fishery, incorporating fishery-specific information on the susceptibility of species to the fishery. Of significant importance with all methods is the ability to calculate the range of parameters required for a large number of species (Stevens et al., 2000). The semi-quantitative method used in our study maximizes what can be determined from the data available and enables consistency across the species. The criteria include characteristics that influence the probability of extinction of a species and its sensitivity to overfishing (McKinney, 1997; Carlton et al., 1999; Roberts and Hawkins, 1999; Stevens et al., 2000). Our analysis provides a process for highlighting gaps in information and for prioritizing species for future management and research. This process does not replace traditional methods of population assessment but provides a rapid assessment of the species, so that traditional methods can be focused on the high-risk species.

The species that were least likely to be sustainable in the bycatch of the NPF were *D. brevicaudatus, P. pectinata, P. clavata, P. microdon, P. zijsron,* and *Himantura jenkinsii* (Fig. 3). The pristids and *H. jenkinsii* had ranks of 1 on the susceptibility axis, the lowest possible rank, and *D. brevicaudatus* ranked 1.15 (Appendix 1). These species are demersal, are rare in the bycatch, and at least for the pristids (which have restricted depth distributions) are likely to be rare. Nothing is known about their sur-

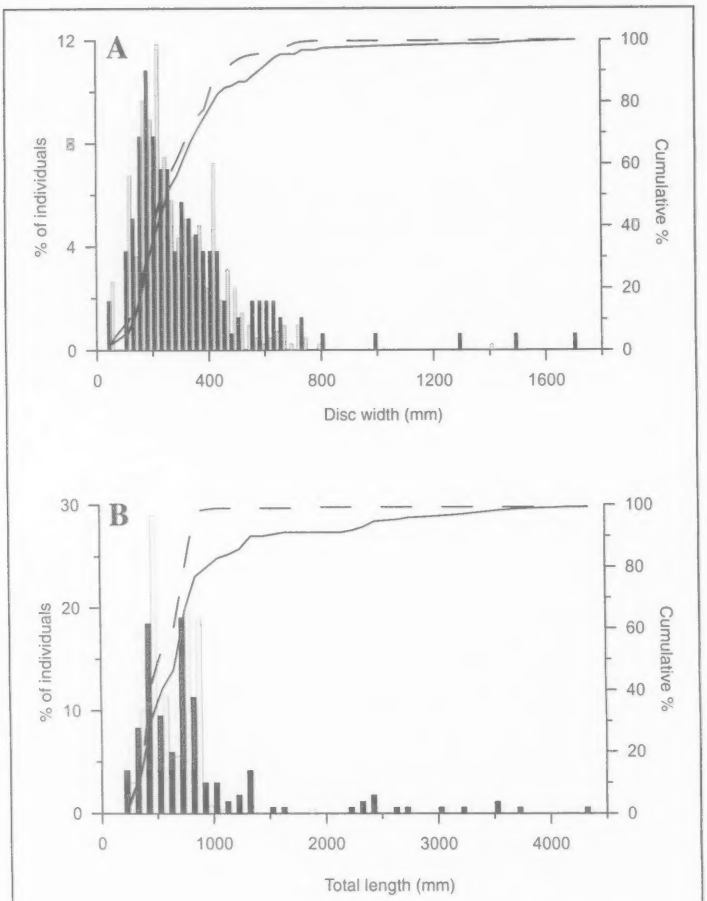

Figure 3

The length frequency and cumulative length frequency of rays (**A**) and sharks (**B**) caught in nets with a standard codend (black columns and solid line) and nets with a TED (grey columns and broken line).

vival. Their diets include benthic organisms and are likely to include commercial prawns; their range and day and night catchability is unknown. The combination of these factors means that these species are likely to occur in trawl grounds and that they are highly susceptible to capture and mortality due to trawlers. The recovery capacity of populations of these species is also low (Appendix 2). The rarity of the species in the bycatch means that no data are available to estimate the probability of breeding before capture, removal rate, total biomass, or the mortality index for most of these species, and they therefore received ranks of 1 for these criteria. In general these are large animals and are therefore likely to have slower recovery rates for their population than those of smaller species. The annual fecundity was low for all species.

The pristids are the focus of increasing international concern because their populations are declining worldwide (Stevens et al. 2000). They are rarely seen today in areas where they were previously abundant (Simpfendorfer, 2000). This decrease in pristid populations has resulted in four species being listed on the IUCN 1996 red list (Bailie and Groombridge, 1996). Of the species studied in our study, *P. pectinata* and *P. microdon* are listed as endangered. Recent demographic analysis of pristid populations has indicated that their recovery will take several decades even if they are given effective conservation (Simpfendorfer, 2000).

In comparison, the species that were most likely to be able to sustain capture in the bycatch of the NPF were *H. toshi, E. blockii, C. macloti,* and *C. tilstoni.* These species had a lower susceptibility to capture and mortality due to trawling (Appendix 1). With the exception of *H. toshi*, these are pelagic species and there is little likelihood of their capture in prawn trawls. For the species for which

Table 9

The mean size of elasmobranch species caught in nets with codends fitted with TEDs and with standard codends, and the ANOVA results from the comparison of these nets. "Combined sharks" refers to all species where total length was recorded; "combined rays" refers to all species where disc width was recorded. SE = standard error; n = number of trawls.

		Size (mm)			ANOVA results		
Species	Codend	mean	SE	n	F	df	P
Combined sharks	standard	887	59	168	4.25	1,569	0.0398
	TED	596	36	269			
Combined rays	standard	330	19	157	26.77	1,435	<0.0001
	TED	286	7	414			
Carcharhinus dussumieri	standard	844.4	96.4	60	26.88	1,139	<0.0001
	TED	489.1	13.8	81			
Rhizoprionodon acutus	standard	636.9	34.2	45	7.15	1,134	0.0084
	TED	724.2	17.4	91			
Hemigaleus microstoma	standard	708.9	148.5	23	2.77	1,79	0.0988
	TED	508.0	19.9	58			
Amphotistius annotata	standard	206.4	31.1	50	2.97	1,200	0.4395
	TED	169.8	3.4	156			
Himantura toshi	standard	371.0	19.4	51	0.60	1,200	0.4395
	TED	351.6	9.7	151			
Rhynchobatus djiddensis	standard	1076.9	125.6	19	20.81	1,41	<0.0001
	TED	611.6	32.3	24			

data were available, their survival was higher in trawls. The depth range of the species was wide and their catch rates during the day were the same as or higher than at night. This range provides partial refuge from the nighttime commercial trawling. The data available suggest that their recovery capacity is higher than that of most elasmobranch species (Appendix 2). Individuals of most of these species are likely to have bred before capture and they are smaller. These species were common in the bycatch, and estimates of their removal rate (which was low) and their mortality index (average) were therefore easy to determine. However, all species had low annual fecundities.

This assessment of the elasmobranch bycatch is an important first step in ensuring their sustainability because it provides a focus for future research and management. The current ranking is constrained, however, by the available data and by the assumptions outlined in the "Methods" section. The effect of the lack of species-specific information on the ranks should be taken into account because it may reduce the rank of some species. The application of our assessment has highlighted important information gaps, which should be the focus of research, particularly for the species that are least likely to be sustainable.

It is also important that the assessment of the sustainability of elasmobranch species is extended to include the impact of other fisheries in the region. There are, for instance, fisheries targeting sharks, as well as other fisheries that capture elasmobranchs as bycatch. Because elasmobranch species may have a wide distribution range, their populations could be impacted by several fisheries, which might create an unsustainable status for the population overall. For example, the pristids are likely to be impacted by the inshore and estuarine gillnet fisheries in this region.

The results of our analysis, it is to be hoped, will help in the management of elasmobranch species and in earmarking the least sustainable of these species. Future management may include the use of exclusion devices (TEDs and BRDs), closures, or further limits on retaining shark products. The compulsory introduction of TEDs and BRDs into the NPF in 2000 is likely to affect catch rates of elasmobranchs. The TEDs have the potential to exclude large individuals. However, the majority of elasmobranchs caught are <1000 mm (Fig. 3) and may escape through TEDs. The effectiveness of TEDs will depend on their configuration (particularly the width between the bars) and the size and shape of the bycatch species. *Rhynchobatus djiddensis*, a large, broad species, appeared to be excluded well by TEDs (Table 9). In comparison, the smaller rays and small, slim sharks were not excluded well (Fig. 3, Table 9). With the introduction of TEDs to the fishery, species-specific exclusion rates should be monitored so that these can be taken into account in assessing the sustainability of a species. Juveniles of many elasmobranch species are still likely to be captured and their capture could potentially have a large impact on their respective populations. The TEDs may also be ineffective for species, such as the pristids, that may tangle their saw in the net or the TED. Species and the life stages of species, for which exclusion devices are not effective, may require different management strategies, such as marine protected areas.

This research is the first large-scale assessment of its kind on elasmobranch bycatch. The results highlight the diversity of elasmobranch bycatch in the NPF and the species that are least likely to be sustainable. We have also highlighted the limited information available for making this assessment. However, our method was designed to maximize the use of the limited information. The process we have used is applicable to other fisheries and also across fisheries, particularly where bycatch diversity is high.

Acknowledgments

We thank the commercial fishermen who took the time to record their catch in logbooks and support this project. The skippers and crews of the boats on which our scientific observer sampled are also thanked for their cooperation and patience. We also thank the Northern Prawn Fishery Management Advisory Committee for its support; the Northern Prawn Fishery, Fishery Assessment Group for their participation in this process and feedback; C. Rose for collection of the crew-member observer data; and T. Walker for valuable comments on the manuscript. CSIRO Marine Research colleagues helped in many ways, M. Haywood, F. Manson and J. Bishop for assistance with the bioregion data and commercial effort data, C. Burridge and W. Venables for assistance with the statistical analysis; S. Blaber, G. Fry, D. Milton, J. Salini, J. Stevens and T. Wassenberg for constructive comments on the manuscript. We also thank the fishing, scientific, and electronics crew of the RV *Southern Surveyor* who made the research surveys possible. This project was funded by the Australian Fisheries Research and Development Corporation (Project no. 96/257) and CSIRO Marine Research.

Literature cited

Bailie, J., and B. Groombridge.
1996. IUCN red list of threatened animals, 448 p. IUCN (International Union for the Conservation of Nature and Natural Resources), Gland, Switzerland.

Bass, A. J., J. D. D'Aubrey, and N. Kistnasamy.
1973. Sharks of the east coast of southern Africa. I. The genus *Carcharhinus* (Carcharhinidae). Oceanographic Research Institute Investigation Report 33.

Bishop J., and D. Sterling.
1999. Survey of technology utilised in the northern prawn fishery, 48 p. AFMA (Australian Fisheries Management Authority), Canberra.

Blaber, S. J. M., D. T. Brewer, and A. N. Harris.
1994. Distribution, biomass and community structure of demersal fishes of the Gulf of Carpentaria, Australia. J. Mar. Freshwater Res. 45:375–396.

Bonfil, R.
1994. Overview of world elasmobranch fisheries. FAO Fisheries Tech. Paper 341, 119 p. FAO, Rome.

Brander, K.
1981. Disappearance of common skate *Raia batis* from Irish Sea. Nature 290:48–49.

Brewer, D. T., N. Rawlinson, S. Eayrs, and C. Burridge.
1998. An assessment of bycatch reduction devices in a tropical Australian prawn trawl fishery. Fish. Res. 36:195–215.

Carlton, J. T., J. B. Geller, M. L. Reaka-Kudla, and E. A. Norse.
1999. Historical extinctions in the sea. Annu. Rev. Ecol. Syst. 30:515–538.

Casey, J. M., and R. A. Myers.
1998. Near extinction of a large, widely distributed fish. Science 281:690–691.

Compagno, L. J. V.
1984a. FAO species catalogue. Vol. 4. Sharks of the world. An annotated and illustrated catalogue of shark species known to date. Part 1. Hexanchiformes to Lamniformes, 249 p. FAO, Rome.
1984b. FAO species catalogue. Vol. 4. Sharks of the world. An annotated and illustrated catalogue of shark species known to date. Part 1. Carcharhiniformes, 405 p. FAO, Rome.

Crocos, P. J., and G. J. Coman.
1997. Seasonal and age variability in the reproductive performance of *Penaeus semisulcatus* broodstock, optimising broodstock selection. Aquaculture 155:57–69.

Dulvy, N. K., J. D. Metcalfe, J. Glanville, M. G. Pawson, and J. D. Reynolds.
2000. Fishery stability, local extinctions and shifts in community structure in skates. Cons. Biol. 14:283–293.

Hall, S. J.
1999. The effects of fishing on marine ecosystems and communities, 274 p. Blackwell Science, Oxford.

Hueter, R. E.
1998. Science and management of shark fisheries—introduction. Fish. Res. 39:105.

IUCN (International Union for the Conservation of Nature and Natural Resources).
1995. IUCN red list categories, 21 p. IUCN, Gland, Switzerland.

Jennings S., J. D. Reynolds, and N. V. C. Polunin.
1999. Predicting the vulnerability of tropical reef fishes to exploitation: an approach based on phylogenies and life histories. Cons. Biol. 13:1466–1475.

Last, P. R., and J. D. Stevens.
1994. Sharks and rays of Australia, 513 p. CSIRO Publishing, Australia.

Lavery, S., and J. B. Shaklee.
1991. Genetic evidence for separation of two sharks, *Carcharhinus limbatus* and *C. tilstoni*, from Northern Australia. Mar. Biol. 108:1–4.

McKinney, M. L.
1997. Extinction vulnerability and selectivity: combining ecological and paleontolgical views. Annu. Rev. Ecol. Syst. 28:495–516.

McLoughlin, K., B. Wallner, and D. Staples.
1997. Fishery status reports 1996, 144 p. Bureau of Resource Sciences, Kingston, Australia.

Milton, D. A., S. A. Short, M. F. O'Neill, and S. J. M. Blaber.
1995. Ageing of three species of tropical snapper (Lutjanidae) from the Gulf of Carpentaria, Australia, using radiometry and otolith ring counts. Fish. Bull. 93:103–115.

Milton, D. A.
2001. Assessing the susceptibility to fishing of populations of rare trawl bycatch: sea snakes caught by Australia's Northern Prawn Fishery. Biol. Cons. 101:281–290

Musick, J. A.
1998. Endangered marine fishes: criteria and identification of north American stocks at risk. Fish. 23:28–31.

Roberts, C. M., and J. P. Hawkins.
1999. Extinction risk in the sea. Trends Envir. Ecol. 14: 241–246.

SAS.
2001. Logistic regression examples using the SAS system, version 6, first ed., 176 p. SAS Institute Inc., Cary, NC.
Simpfendorfer, C. A.
2000. Predicting population recovery rates for endangered western Atlantic sawfishes using demographic analysis. Environ. Biol. Fish. 58:371–377.
Sokal, R. R., and R. J. Rohlf.
1996. Introduction to biostatistics, 2nd edition, 363 p. Freeman and Company, New York, NY.
Somers, I.
1994. No resources, no fishery, prawns and their habitat. *In* Australia's northern prawn fishery (P. C. Pownall, ed.), p. 49–65. NPF 25, Cleveland, Australia.
Sparre, P., and S. C. Venema.
1992. Introduction to tropical fish stock assessment, part 1. FAO Fisheries Technical Paper 306/1, 376 p. FAO Rome.
Stevens, J. D., R. Bonfil, N. K. Dulvy, and P. A. Walker.
2000. The effects of fishing on sharks, rays and chimaeras (chondrichthyans), and the implications for marine ecosystems. ICES J. Mar. Sci. 57:476–494.
Stobutzki, I. C., M.J . Miller, and D. T. Brewer.
2001a. Sustainability of fishery bycatch: a process for dealing with highly diverse and numerous bycatch. Environ. Cons. 28:167–181.
Stobutzki, I. C., M. J. Miller, J. P. Jones, and J. P. Salini.
2001b. Bycatch diversity and variation in penaeid fisheries; the implications for monitoring. Fish. Res. 53:283–301.
Thackway, R., and I. D. Cresswell.
1998. Interim marine and coastal rationalization for Australia; an ecosystem-based classification for marine and coastal environments, version 3.3, 120 p. Environment Australia, Commonwealth Department of the Environment, Canberra.
Walker, T. I.
1998. Can shark resources be harvested sustainably? A question revisited with a review of shark fisheries. Mar. Freshwater Res. 49:553–572.
Walker, P.A., and J. R. G. Hislop.
1998. Sensitive skates or resilient rays? Spatial and temporal shifts in ray species composition in the central and north-western North Sea between 1930 and the present day. ICES J. Mar. Sci. 55:392–402.

Appendix 1

The ranking of elasmobranch species that occurred in the bycatch of the northern prawn fishery with respect to criteria that influence their susceptibility to capture and mortality due to prawn trawls. The weights of the criteria are shown in parentheses; * indicates where species-specific information was not available. The information was obtained from Compagno (19984a; 1984b), Last and Stevens (1994), and Froese and Pauly[6].

		Criteria						
Family	Species	Water column position (3)	Survival (3)	Range (2)	Day and night catchability (2)	Diet (2)	Depth range (1)	Susceptibility ranking
Dasyatidae	*Himantura jenkinsii*	1	1*	1	1*	1*	1	1.00
Pristidae	*Pristis clavata*	1	1*	1*	1*	1*	1	1.00
Pristidae	*Pristis microdon*	1	1*	1*	1*	1*	1	1.00
Pristidae	*Pristis pectinata*	1	1*	1*	1*	1*	1	1.00
Pristidae	*Pristis zijsron*	1	1*	1	1*	1*	1	1.00
Stegostomatidae	*Stegostoma fasciatum*	1	1*	1*	1	1	1	1.00
Scyliorhinidae	*Atelomycterus fasciatus*	1	1*	1	1*	1*	3	1.15
Carcharhinidae	*Carcharhinus amboinensis*	1	1*	1	1*	1	3	1.15
Carcharhinidae	*Carcharhinus leucas*	1	1*	1*	1*	1	3	1.15
Dasyatidae	*Dasyatis brevicaudatus*	1	1*	1*	1*	1*	3	1.15
Dasyatidae	*Dasyatis* sp. A	1	1*	1	1*	1*	3	1.15
Dasyatidae	*Dasyatis thetidis*	1	1*	1	1*	1*	3	1.15
Scyliorhinidae	*Galeus* sp. A	1	1*	1*	1*	1*	3	1.15
Dasyatidae	*Himantura fai*	1	1*	1	1*	1*	3	1.15
Dasyatidae	*Himantura granulata*	1	1*	1	1*	1	3	1.15
Dasyatidae	*Himantura uarnak*	1	1*	1*	1*	1*	3	1.15
Ginglymostomatidae	*Nebrius ferrugineus*	1	1*	1	1*	1	3	1.15
Carcharhinidae	*Negaprion acutidens*	1	1*	1	1*	1	3	1.15
Orectolobidae	*Orectolobus ornatus*	1	1*	1	1	1	3	1.15
Rhinobatidae	*Rhinobatos typus*	1	1*	1	1*	1*	3	1.15
Squatinidae	Squatina *sp. A*	1	1*	1*	1*	1*	3	1.15
Dasyatidae	*Taeniura meyeni*	1	1*	1	1*	1*	3	1.15
Dasyatidae	*Urogymnus asperrimus*	1	1*	1	1*	1*	3	1.15
Pristidae	*Anoxypristis cuspidata*	1	1*	1*	2	1*	1	1.15
Dasyatidae	*Pastinachus sephen*	1	1*	2	1*	1	1	1.15
Hemiscylliidae	*Chiloscyllium punctatum*	1	1*	2	1	1	3	1.31
Dasyatidae	*Dasyatis kuhlii*	1	1*	2	1	1*	3	1.31
Dasyatidae	*Himantura* sp. A	1	1*	2	1*	1*	3	1.31
Narcinidae	*Narcine westraliensis*	1	1*	1*	1*	2	3	1.31
Rhynchobatidae	*Rhina ancylostoma*	1	1*	2	1	1	3	1.31
Carcharhinidae	*Carcharhinus fitztroyensis*	3	1*	1	1*	1	1	1.46
Dasyatidae	*Amphotistius annotata*	1	1*	2	2	1*	3	1.46
Dasyatidae	*Himantura undulata*	1	1*	2	2	1*	3	1.46
Carcharhinidae	*Rhizoprionodon taylori*	1	1*	1	3	1	3	1.46
Carcharhinidae	*Galeocerdo cuvier*	3	1*	1	1*	1	3	1.62
Hemiscylliidae	*Hemigaleus microstoma*	1	1	3	1*	2	3	1.62
Dasyatidae	*Dasyatis leylandi*	1	2	3	1	1	3	1.69
Gymnuridae	*Gymnura australis*	1	2	3	2	1*	1	1.69
Carcharhinidae	*Carcharhinus sorrah*	3	1	2	1*	1	3	1.77
Carcharhinidae	*Rhizoprionodon acutus*	1	1	3	3	1	3	1.77
Rhynchobatidae	*Rhynchobatus djiddensis*	1	3	2	1*	1*	3	1.77

continued

Appendix 1 (continued)

		Criteria						
Family	Species	Water column position (3)	Survival (3)	Range (2)	Day and night catchability (2)	Diet (2)	Depth range (1)	Susceptibility ranking
Myliobatidae	*Aetobatus narinari*	3	1*	1	1*	2	3	1.77
Myliobatidae	*Aetomylaeus vespertilio*	3	1*	1*	1*	2*	3	1.77
Carcharhinidae	*Carcharhinus albimarginatus*	3	1*	1	1*	2	3	1.77
Hemiscylliidae	*Hemipristis elongatus*	3	1*	1	1*	2	3	1.77
Sphyrnidae	*Sphyrna mokarran*	3	1*	1	1*	2	3	1.77
Carcharhinidae	*Carcharhinus limbatus*	3	1	1*	1*	3	1	1.77
Sphyrnidae	*Eusphyra blochii*	3	1*	1	2	1	3	1.77
Carcharhinidae	*Carcharhinus dussumieri*	1	2	2	3	1	3	1.85
Dasyatidae	*Himantura toshi*	1	2	3	2	1	3	1.85
Myliobatidae	*Aetomyleus nichofii*	3	1*	2	1	2*	3	1.92
Carcharhinidae	*Carcharhinus brevipinna*	3	1*	1*	1*	3	3	1.92
Carcharhinidae	*Prionace glauca*	3	1*	1*	1*	3	3	1.92
Sphyrnidae	*Sphyrna lewini*	3	1*	1*	1*	3	3	1.92
Carcharhinidae	*Carcharhinus macloti*	3	1*	1	3	2	3	2.08
Carcharhinidae	*Carcharhinus tilstoni*	3	2	2	2	1	3	2.15

Appendix 2

The ranking of elasmobranch species that occurrred in the bycatch of the northern prawn fishery with respect to criteria that reflect their capacity to recover after depletion by trawling. The weights of the criteria are shown in parentheses; * indicates where species-specific information was not available. The information was obtained from Compagno (1984a; 1984b), Last and Stevens (1994), and Froese and Pauly[6].

		Criteria					
Family	Species	Probability of breeding (3)	Maximum size (3)	Removal rate (3)	Annual fecundity (2)	Mortality index (1)	Recovery ranking
Dasyatidae	*Dasyatis brevicaudatus*	1	1	1*	1	2	1.08
Pristidae	*Pristis pectinata*	1*	1	1*	2	1*	1.17
Pristidae	*Pristis clavata*	1*	2	1*	1*	1*	1.25
Myliobatidae	*Aetomylaeus vespertilio*	1*	2	1*	1*	2	1.33
Dasyatidae	*Taeniura meyeni*	1	1	3	1	1	1.50
Dasyatidae	*Himantura jenkinsii*	1*	2	2	1*	1	1.50
Carcharhinidae	*Carcharhinus amboinensis*	1	2	1	2	2	1.50
Carcharhinidae	*Carcharhinus leucas*	1	3	1*	1	1	1.50
Scyliorhinidae	*Galeus* sp. A	1*	3	1*	1*	1*	1.50
Narcinidae	*Narcine westraliensis*	1*	3	1*	1*	1*	1.50
Pristidae	*Pristis microdon*	1*	3	1*	1*	1*	1.50
Squatinidae	*Squatina* sp. A	1*	3	1*	1*	1*	1.50
Carcharhinidae	*Prionace glauca*	1*	2	1*	3	1*	1.58
Myliobatidae	*Aetobatus narinari*	1*	1	3	1	2	1.58
Carcharhinidae	*Carcharhinus limbatus*	1*	3	1*	1	2	1.58
Carcharhinidae	*Carcharhinus albimarginatus*	1*	2	2	2	1*	1.67
Carcharhinidae	*Carcharhinus brevipinna*	1*	3	1*	2	1*	1.67
Dasyatidae	*Dasyatis thetidis*	1*	2	3	1*	1	1.75
Pristidae	*Pristis zijsron*	1*	2	3	1*	1*	1.75
Dasyatidae	*Himantura fai*	1*	2	3	1*	1*	1.75
Dasyatidae	*Himantura granulata*	1*	2	3	1*	1*	1.75
Dasyatidae	*Himantura uarnak*	1*	2	3	1*	1	1.75
Dasyatidae	*Himantura undulata*	1*	2	3	1*	1	1.75
Orectolobidae	*Orectolobus ornatus*	1*	2	3	1*	1*	1.75
Dasyatidae	*Urogymnus asperrimus*	1	2	3	1	1	1.75
Scyliorhinidae	*Atelomycterus fasciatus*	2	2	2	1	1	1.75
Dasyatidae	*Dasyatis* sp. A	2	3	1	1*	1*	1.75
Dasyatidae	*Amphotistius annotata*	2*	1	3	1*	2	1.83
Rhynchobatidae	*Rhynchobatus djiddensis*	1	2	3	1*	2	1.83
Carcharhinidae	*Carcharhinus fitztroyensis*	2	2	2	1	2	1.83
Sphyrnidae	*Sphyrna mokarran*	2	1	3	2*	1	1.92
Carcharhinidae	*Negaprion acutidens*	3	2	1	2	1*	1.92
Rhynchobatidae	*Rhina ancylostoma*	1*	3	3	1*	1	2.00
Rhinobatidae	*Rhinobatos typus*	1*	3	3	1*	1	2.00
Pristidae	*Anoxypristis cuspidata*	1	3	3	1	1*	2.00
Hemiscylliidae	*Chiloscyllium punctatum*	1*	3	3	1*	1	2.00
Hemiscylliidae	*Hemipristis elongatus*	2	2	3	1	1	2.00
Carcharhinidae	*Rhizoprionodon acutus*	1	3	3	1	1	2.00
Stegostomatidae	*Stegostoma fasciatum*	2*	2	3	1*	1	2.00
Sphyrnidae	*Sphyrna lewini*	1*	2	3	2*	2*	2.00
Myliobatidae	*Aetomyleus nichofii*	1*	3	3	1	2	2.08
Carcharhinidae	*Carcharhinus macloti*	2	2	3	1	2	2.08

continued

Appendix 2 (continued)

Family	Species	Criteria					
		Probability of breeding (3)	Maximum size (3)	Removal rate (3)	Annual fecundity (2)	Mortality index (1)	Recovery ranking
Carcharhinidae	*Carcharhinus sorrah*	1	3	3	1*	2	2.08
Dasyatidae	*Pastinachus sephen*	3	1	3	1*	2	2.08
Carcharhinidae	*Galeocerdo cuvier*	2	1	3	3	2	2.17
Dasyatidae	*Himantura* sp. A	1*	3	3	1*	3	2.17
Carcharhinidae	*Carcharhinus tilstoni*	1	3	3	1	3	2.17
Carcharhinidae	*Carcharhinus dussumieri*	3	2	3	1	1	2.25
Dasyatidae	*Dasyatis kuhlii*	2	3	3	1	1*	2.25
Dasyatidae	*Dasyatis leylandi*	2	3	3	1*	1*	2.25
Ginglymostomatidae	*Nebrius ferrugineus*	3	2	3	2	1*	2.42
Sphyrnidae	*Eusphyra blochii*	2	3	3	2	2	2.50
Gymnuridae	*Gymnura australis*	3	3	3	1	2	2.58
Dasyatidae	*Himantura toshi*	3	3	3	1	2	2.58
Carcharhinidae	*Rhizoprionodon taylori*	3	3	3	1	2	2.58
Hemiscylliidae	*Hemigaleus microstoma*	2	3	3	2	3	2.58

Age and growth of the swordfish (*Xiphias gladius* L.) in the waters around Taiwan determined from anal-fin rays

Chi-Lu Sun
Sheng-Ping Wang
Su-Zan Yeh

Institute of Oceanography
National Taiwan University
No. 1, Sec. 4, Roosevelt Road
Taipei, Taiwan 106
E-mail address (for C. L. Sun): chilu@ccms.ntu.edu.tw

Abstract–Age and growth of the swordfish (*Xiphias gladius*) in Taiwan waters was studied from counts of growth bands on cross sections of the second ray of the first anal fin. Data on lower jaw fork length and weight, and samples of the anal fin of male and female swordfish were collected from three offshore and coastal tuna longline fishing ports on a monthly basis between September 1997 and March 1999. In total, 685 anal fins were collected and 627 of them (293 males and 334 females) were aged successfully. The lower jaw fork lengths of the aged individuals ranged from 83.4 to 246.6 cm for the females and from 83.3 to 206 cm for the males.

The radii of the fin rays and growth bands on the cross sections were measured under a dissecting microscope equipped with an image analysis system. Trends in the monthly marginal increment ratio indicated that growth bands formed once a year. Thus, the age of each fish was determined from the number of visible growth bands. Two methods were used to estimate and compare the standard and the generalized von Bertalanffy growth parameters for both males and females. The nonlinear least square estimates of the generalized von Bertalanffy growth parameters in method II, in which a power function was used to describe the relationship between ray radius and LJFL, were recommended as most acceptable. There were significant differences in growth parameters between males and females. The growth parameters estimated for females were the following: asymptotic length (L_∞) = 300.66 cm, growth coefficient (K) = 0.040/yr, age at zero length (t_0) = –0.75 yr, and the fitted fourth parameter (m) = –0.785. The growth parameters estimated for males were the following: asymptotic length (L_∞) = 213.05 cm, growth coefficient (K) = 0.086/yr, age at zero length (t_0) = –0.626 yr, and the fitted fourth parameter (m) = –0.768.

Manuscript accepted 21 February 2002.
Fish. Bull. 100:822–835 (2002).

The swordfish (*Xiphias gladius* L.) is a cosmopolitan species found in the tropical, subtropical, and temperate waters of the world's oceans and adjacent seas (Sakagawa, 1989). In the Pacific Ocean, swordfish is generally distributed from Asia to the Americas between 50°N and 50°S (Bartoo and Coan, 1989). In the waters of Taiwan, the swordfish is an incidental bycatch of the offshore tuna longline and harpoon fisheries. Both fisheries contributed an estimated 1528 metric tons (99%) to the total swordfish landings from Taiwan waters in 1999.

Information on age and growth of fishes is a central element in fishery management (Brothers, 1983). Measurement of the age of the fish provides the key variable of time needed to estimate life history and biology factors, such as mortality and growth. Mortality and growth-rate models provide quantitative information on the status of fish stocks and at the same time may be used in more sophisticated models, such as yield-per-recruit analyses and cohort analyses (Powers, 1983), which will directly contribute to the rational exploitation of fish resources, as well as to the development of proper management plans.

Most age determination studies of swordfish have dealt with Atlantic populations and have used different hard parts, such as anal-fin rays (Berkeley and Houde, 1983; Wilson and Dean 1983; Prince et al., 1988; Ehrhardt, 1992; Esteves et al., 1995; Ehrhardt et al., 1996), otolith (Radtke and Hurley, 1983; Wilson and Dean, 1983; Esteves et al., 1995), and vertebrae (Esteves et al., 1995). In contrast, only a few attempts have been made to determine the age of swordfish in the Pacific Ocean. Yabe et al. (1959) estimated the growth of swordfish caught in the western North Pacific (140°–160°E) by longline during the period from 1948 to 1956 using the modal analysis of length frequencies. Castro-Longoria and Sosa-Nishizaki (1998) compared the age estimates of swordfish caught by drift gillnet vessels off Baja California from 1992 to 1993 based on otolith microstructure and cross sections of the second ray from the first anal fin, and highly recommended the use of cross sections of the second ray to determine the ages of swordfish in the Pacific Ocean. Uchiyama et al. (1998) evaluated various hard parts (including rays of the first dorsal and first anal fins, vertebrae, and sagittae) for aging swordfish in the central North Pacific by Hawaii longline fishery from 1991 to 1993, and provided preliminary estimates of length-at-age.

The objectives of our study were to estimate the age and growth of swordfish by counting the growth rings on the cross sections of the second ray of the first anal fin and to compare the generalized growth function proposed by Richards (1959) with the standard von Bertalanffy model for representing the best growth model of swordfish around Taiwan waters. The information is crucial because it will allow the age composition of the catch to be determined, which in turn will allow the status of the swordfish stock in the

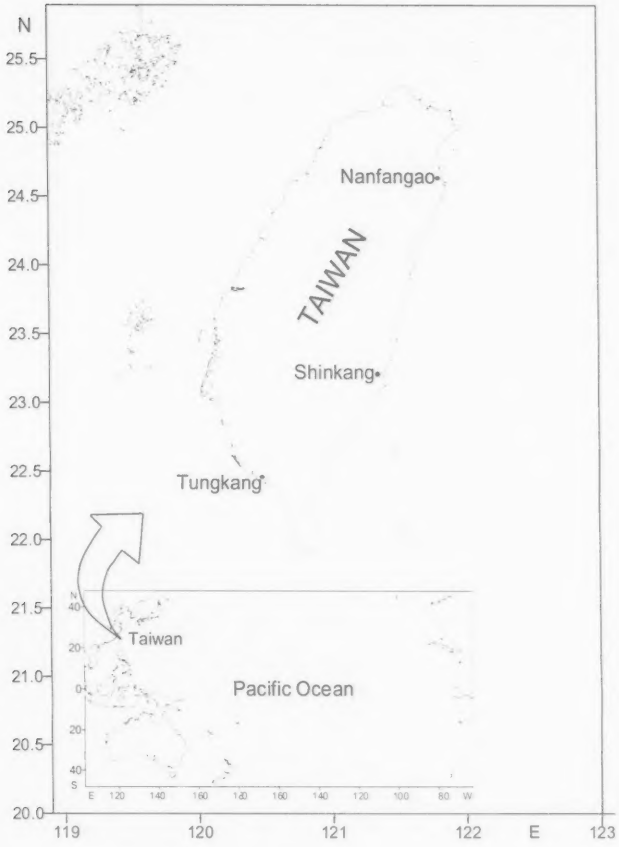

Figure 1

Three fishing ports in Taiwan where the swordfish anal-fin ray samples were collected in this study.

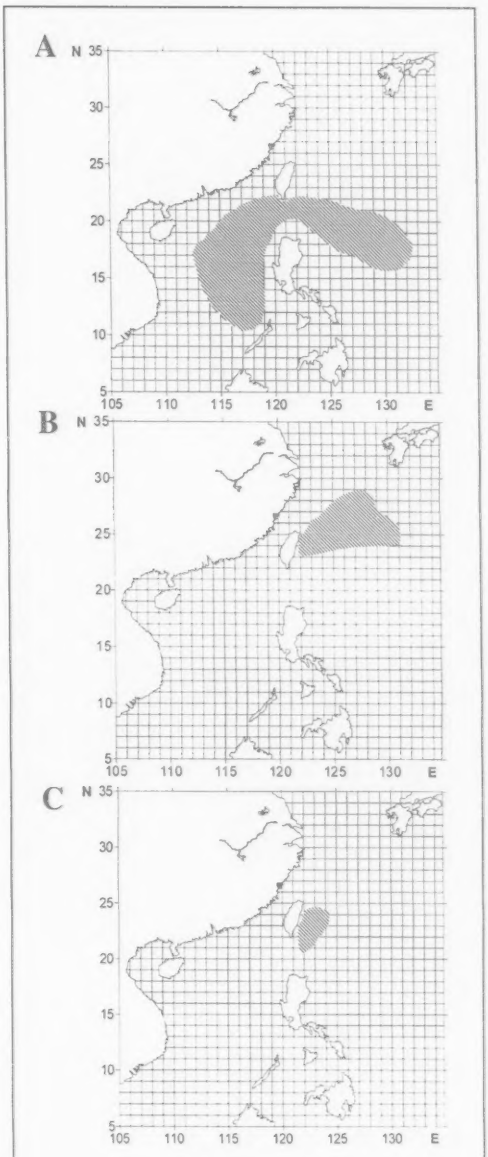

Figure 2

The fishing grounds (oblique dot lines) of the longline and harpoon fishing boats based in Tungkang (**A**), Nanfangao (**B**), and Shinkang (**C**) fishing ports.

waters around Taiwan to be assessed by using yield-per-recruit and sequential population analyses.

Material and methods

Data on lower jaw fork length (LJFL) and weight, and samples of the first anal fin of male and female swordfish were collected from three offshore tuna longline and harpoon fishing ports (Fig. 1) on a monthly basis between September 1997 and March 1999. The fishing grounds for those vessels are shown in Figure 2. In total, 769 LJFLs and 685 anal fins were collected. The anal fins were frozen for approximately one month before being thawed and boiled to remove the tissue and to separate the second rays. Three cross sections ranging in thickness from 0.5 to 0.75 to 1.0 mm were taken successively along the length of each ray with a low-speed "ISOMET" saw (model no. 11-1280) and diamond wafering blades, at a location equivalent to 1/2 of the maximum width of the condyle base measured above the line of maximum condyle width (Fig. 3) (Ehrhardt, 1992; Ehrhardt et al., 1996). The sections were immersed in 95% ethanol for several minutes, placed in a labeled (with sampling date and a number) small plastic case to air dry, and then stored for later reading. Anal-fin ray sections were then taken from the small cases randomly and examined under a dissecting microscope (model: Leica MZ 6) with transmitted light at various

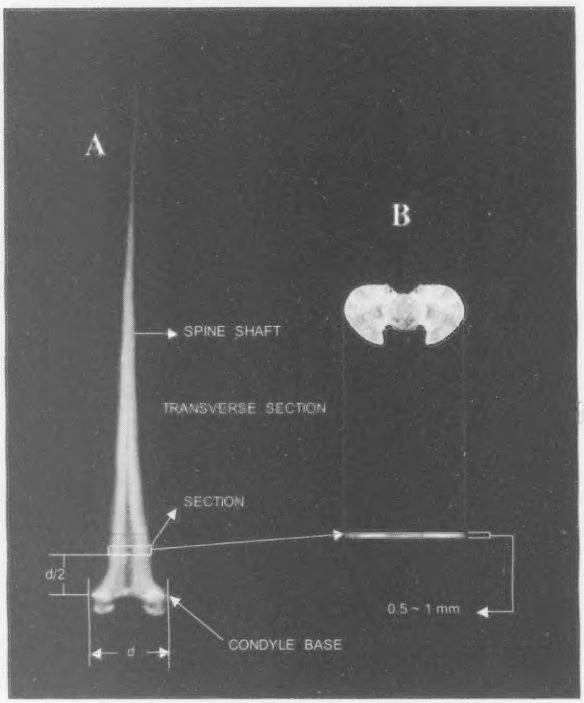

Figure 3

The second ray of the first anal fin showing the location of the cross section at a distance equal to a half of the width of the condyle base above the base (**A**), and a section of the second ray of the first anal fin (**B**).

magnifications from 8× to 16× depending on the size of the section. The clearest one of the three sections from each fin ray was read three times by one reader about one to three months apart with no knowledge of fish length. The precision of readings was evaluated as the average percent error (APE, Beamish and Fournier, 1981) and coefficient of variation (CV, Campana et al., 1995, 2001). For those sections resulting in three different readings, each section was reread by two to three readers simultaneously. Specimens whose age estimates still disagreed were omitted from further analyses.

The images of the anal-fin ray sections were captured by using an Image Analysis Software package (Media Cybernetics, 1997) in combination with a dissecting microscope equipped with a charged coupled device (CCD) camera (model: Toshiba IK-630) and a Pentium II computer equipped with a 640 × 480 pixel frame grab card and a 800 × 600 pixel monitor. The images were measured in microns after distance calibrations were incorporated. The distances from the focus to the distal edge of the section (ray radius) and from the focus to the distal edge of each growth band (annulus) were measured and recorded (Fig. 4). The focus, the growth band, and the false growth band (multiple bands) were defined according to Berkeley and Houde (1983), Tserpes and Tsimenides (1995), and Ehrhardt et al. (1996).

The marginal increment ratio (MIR), which was used to validate the reading of annuli, was estimated for each specimen by the following formula (Prince et al., 1988; Esteves et al., 1995):

$$MIR = (S - S_n)/(S_n - S_{n-1}),$$

where S = ray radius; and
S_n and S_{n-1} = the distance from ray focus to bands n and $n-1$, respectively.

The mean MIR and the standard deviation were computed for each month by sex for all ages combined and also for each age separately.

Growth was analyzed by using the back-calculation of length-at-age for each sex. For this purpose, a relationship was determined between the ray radius and the LJFL. This relationship and the distance from the focus

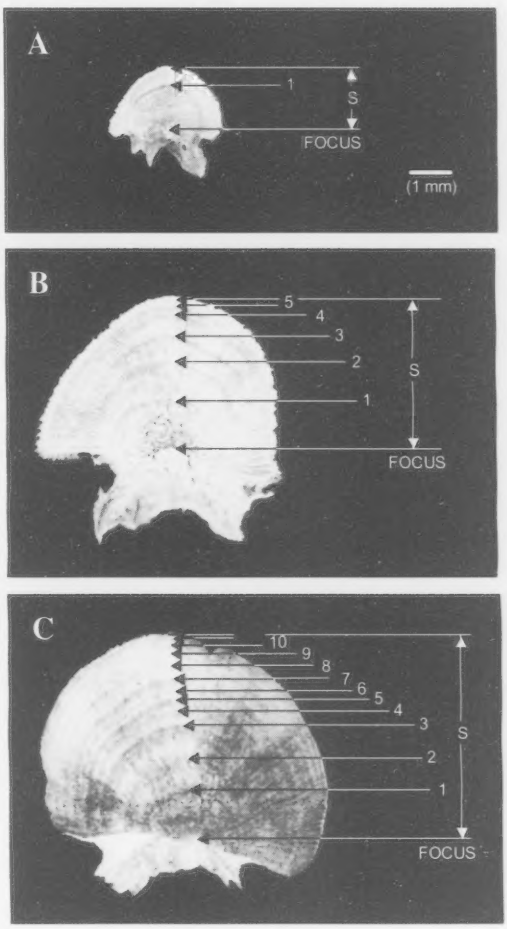

Figure 4

The section of three typical second anal fin rays of swordfish. Ray radius (S) measured from focus to edge; annuli for estimated age 1+ (**A**), age 5+ (**B**) and age 11+ (**C**).

to successive rings were used to back-calculate lengths at presumed previous ages (Ehrhardt, et al., 1996). For the relationship between ray radius and LJFL and the back-calculation of lengths-at-age, the following two methods were used.

Method I

The relationship between ray radius (S) and LJFL (L) was determined by using the standard linear regression procedure, $L = a + bS$ (Berkeley and Houde, 1983). This relationship and the distance from focus to successive growth bands, which we assumed to be based on annual growth events, were used to back-calculate the lengths at presumed ages by the following formula (Fraser, 1916):

$$L_n - a = \frac{S_n}{S}(L - a),$$

where L = LJFL at time of capture;
L_n = LJFL when band n was formed;
a = the intercept on the length axis from the regression line of length (L) on ray radius (S), e.g. $L = a + bS$; and
S_n = the distance from ray focus to band n.

Method II

The relationship between ray radius and LJFL was determined by using a power function procedure, $L = aS^b$ (Ehrhardt, 1992; Ehrhardt et. al., 1996). Parameters of this function were estimated by nonlinear least square fits to the observed data. This relationship and the distance from focus to successive growth bands were used to back-calculate the lengths at presumed ages by the following formula (Tserpes and Tsimenides, 1995; Ehrhardt et al., 1996):

$$L_n = \left(\frac{S_n}{S}\right)^b L,$$

where b = the exponent of the regression of length (L) on ray radius (S) which is assumed to be a power function of the form $L = a\,S^{\,b}$.

The data of the back-calculated length-at-age from method I and method II were then applied to the following standard von Bertalanffy growth equation (standard VB) and to the generalized growth function (generalized VB) (Richards, 1959):

Standard VB:

$$L_t = L_\infty\left(1 - e^{-k(t-t_0)}\right);$$

Generalized VB:

$$L_t = L_\infty\left(1 - e^{-K(1-m)(t-t_0)}\right)^{\frac{1}{1-m}},$$

where L_t = the mean LJFL at age t;
L_∞ = the asymptotic length;
t_0 = the hypothetical age at length zero;
k and K = the growth coefficients; and
m = the fitted fourth growth-function parameter.

Parameters of the above two equations for male and female were estimated, respectively, by fitting a curve to the observed back-calculated LJFL-at-age by using a nonlinear least square procedure (Gauss-Newton method, NLIN of SAS Institute, 1990). The measure of goodness-of-fit chosen was r^2. A multivariate statistical procedure (Hotelling's T^2) was used to test for differences in growth between males and females (Bernard, 1981) for the two growth models and two methods. The r^2 values were ranked between the two different growth functions with the smaller as 1. A non-parametric test (Friedman 1937, 1940) was then employed

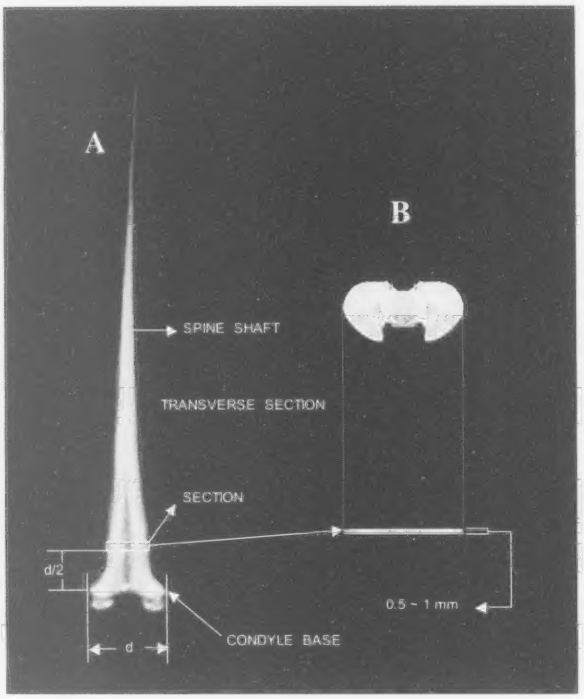

Figure 3

The second ray of the first anal fin showing the location of the cross section at a distance equal to a half of the width of the condyle base above the base (**A**), and a section of the second ray of the first anal fin (**B**).

magnifications from 8× to 16× depending on the size of the section. The clearest one of the three sections from each fin ray was read three times by one reader about one to three months apart with no knowledge of fish length. The precision of readings was evaluated as the average percent error (APE, Beamish and Fournier, 1981) and coefficient of variation (CV, Campana et al., 1995, 2001). For those sections resulting in three different readings, each section was reread by two to three readers simultaneously. Specimens whose age estimates still disagreed were omitted from further analyses.

The images of the anal-fin ray sections were captured by using an Image Analysis Software package (Media Cybernetics, 1997) in combination with a dissecting microscope equipped with a charged coupled device (CCD) camera (model: Toshiba IK-630) and a Pentium II computer equipped with a 640 × 480 pixel frame grab card and a 800 × 600 pixel monitor. The images were measured in microns after distance calibrations were incorporated. The distances from the focus to the distal edge of the section (ray radius) and from the focus to the distal edge of each growth band (annulus) were measured and recorded (Fig. 4). The focus, the growth band, and the false growth band (multiple bands) were defined according to Berkeley and Houde (1983), Tserpes and Tsimenides (1995), and Ehrhardt et al. (1996).

The marginal increment ratio (MIR), which was used to validate the reading of annuli, was estimated for each specimen by the following formula (Prince et al., 1988; Esteves et al., 1995):

$$MIR = (S - S_n)/(S_n - S_{n-1}),$$

where S = ray radius; and
S_n and S_{n-1} = the distance from ray focus to bands n and $n-1$, respectively.

The mean MIR and the standard deviation were computed for each month by sex for all ages combined and also for each age separately.

Growth was analyzed by using the back-calculation of length-at-age for each sex. For this purpose, a relationship was determined between the ray radius and the LJFL. This relationship and the distance from the focus

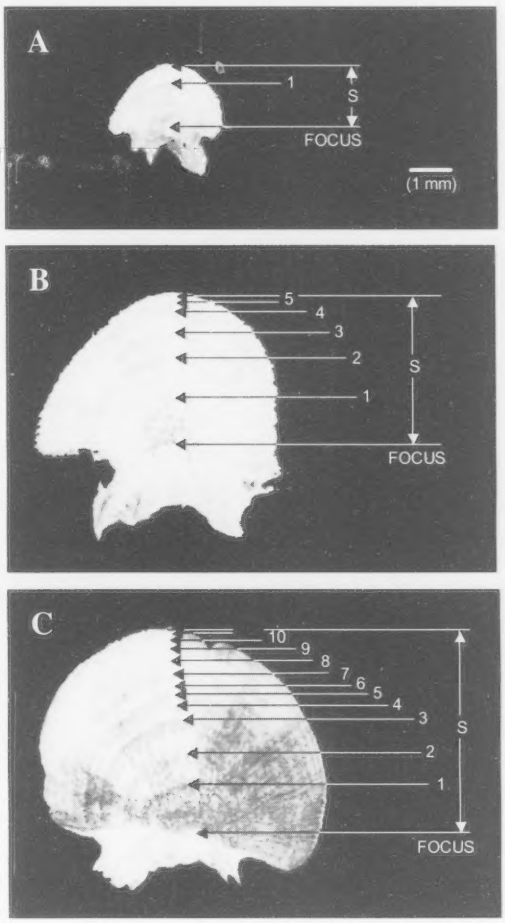

Figure 4

The section of three typical second anal fin rays of swordfish. Ray radius (S) measured from focus to edge; annuli for estimated age 1+ (**A**), age 5+ (**B**) and age 11+ (**C**).

to successive rings were used to back-calculate lengths at presumed previous ages (Ehrhardt, et al., 1996). For the relationship between ray radius and LJFL and the back-calculation of lengths-at-age, the following two methods were used.

Method I

The relationship between ray radius (S) and LJFL (L) was determined by using the standard linear regression procedure, $L = a + bS$ (Berkeley and Houde, 1983). This relationship and the distance from focus to successive growth bands, which we assumed to be based on annual growth events, were used to back-calculate the lengths at presumed ages by the following formula (Fraser, 1916):

$$L_n - a = \frac{S_n}{S}(L - a),$$

where L = LJFL at time of capture;
L_n = LJFL when band n was formed;
a = the intercept on the length axis from the regression line of length (L) on ray radius (S), e.g. $L = a + bS$; and
S_n = the distance from ray focus to band n.

Method II

The relationship between ray radius and LJFL was determined by using a power function procedure, $L = aS^b$ (Ehrhardt, 1992; Ehrhardt et. al., 1996). Parameters of this function were estimated by nonlinear least square fits to the observed data. This relationship and the distance from focus to successive growth bands were used to back-calculate the lengths at presumed ages by the following formula (Tserpes and Tsimenides, 1995; Ehrhardt et al., 1996):

$$L_n = \left(\frac{S_n}{S}\right)^b L,$$

where b = the exponent of the regression of length (L) on ray radius (S) which is assumed to be a power function of the form $L = a\,S^b$.

The data of the back-calculated length-at-age from method I and method II were then applied to the following standard von Bertalanffy growth equation (standard VB) and to the generalized growth function (generalized VB) (Richards, 1959):

Standard VB:

$$L_t = L_\infty\left(1 - e^{-k(t-t_0)}\right);$$

Generalized VB:

$$L_t = L_\infty\left(1 - e^{-K(1-m)(t-t_0)}\right)^{\frac{1}{1-m}},$$

where L_t = the mean LJFL at age t;
L_∞ = the asymptotic length;
t_0 = the hypothetical age at length zero;
k and K = the growth coefficients; and
m = the fitted fourth growth-function parameter.

Parameters of the above two equations for male and female were estimated, respectively, by fitting a curve to the observed back-calculated LJFL-at-age by using a nonlinear least square procedure (Gauss-Newton method, NLIN of SAS Institute, 1990). The measure of goodness-of-fit chosen was r^2. A multivariate statistical procedure (Hotelling's T^2) was used to test for differences in growth between males and females (Bernard, 1981) for the two growth models and two methods. The r^2 values were ranked between the two different growth functions with the smaller as 1. A non-parametric test (Friedman 1937, 1940) was then employed

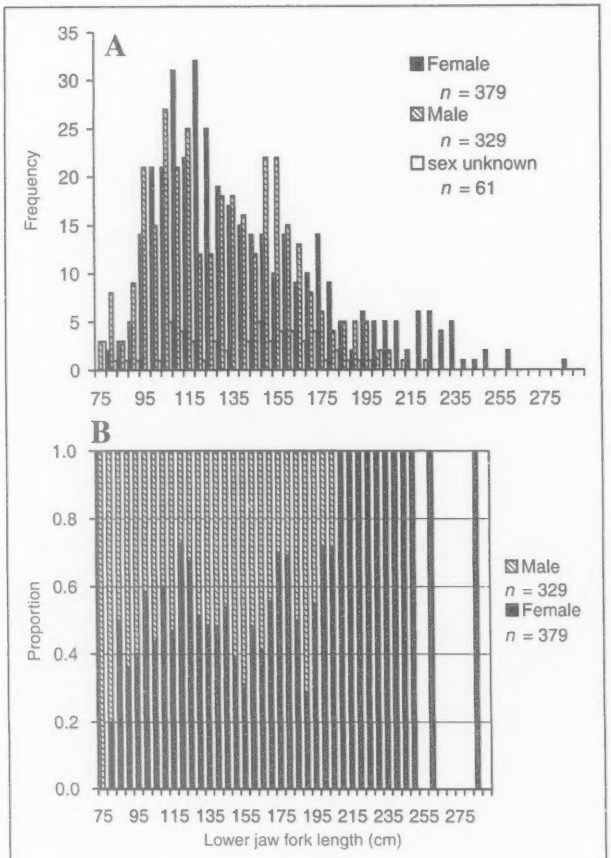

Figure 5

The size-frequency distribution by 5-cm intervals (**A**) and the proportions (**B**) of female and male swordfish collected from Tungkang, Nanfangao, and Shinkang fish markets, September 1997 to March 1999.

on the ranked results of r^2 to test the significance of the goodness-of-fit comparisons between the two growth functions (Chen et al., 1992). Friedman's test statistic χ^2_r was calculated with a correction for tied ranks (Zar, 1999). The association of rank ordering of r^2 values between the two growth functions was measured nonparametrically by using the Kendall coefficient of concordance (Kendall, 1962).

Results

Of the 685 anal fin rays sampled, 627 (334 females and 293 males) were aged successfully. The average percent error (APE) was 5.18% (5.09% for females and 5.29% for males) and the coefficient of variation (CV) was 8.50% (8.28% for female and 8.76% for males). The LJFL of the aged fish ranged from 83.4 to 246.6 cm for the females and from 83.3 to 206 cm for the males. The remaining 58 fin rays were considered unreadable mostly because the opaque-translution zonation was so unclear that annuli could not be defined (32 specimens); 7 specimens were unreadable because of the existence of multiple bands, which made the identification of annuli difficult or resulted in aging discrepancies between readings and readers; and 19 specimens were unreadable because of both the above factors.

For all the 769 swordfish with LJFL measured, individuals ranged from 83.4 to 290 cm for females and 78 to 206.6 cm for males (Fig. 5A). The proportion of the females (Fig. 5B) varied at sizes less than 195 cm, then increased to 100% at 210 cm and thereafter.

The relationship between LJFL and round weight for 227 specimens (sexes pooled) is shown in Figure 6; ANCOVA revealed no differences between males and females (P>0.05). The LJFL-EFL (eye fork length) conversion equation is $LJFL = 1.0647EFL + 7.7911$, with df = 563 and r^2=0.99.

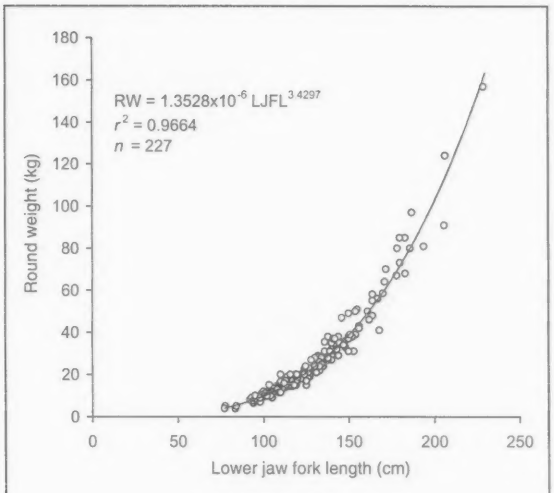

Figure 6

Relationship between round weight and lower jaw fork length for the swordfish collected from Shinkang fish market regardless of sex.

The monthly means of marginal increment ratio, MIR, for females with all ages combined, dropped drastically from the maximum of 0.86 in June to the minimum of 0.32 in July and August (Fig. 7). Similarly, the monthly means of MIR value for males declined sharply from the maximum of 0.65 in June to 0.37 and 0.35 in July and August. For both females and males, the monthly means of MIR during the period from September to March were not different (ANOVA, P_{δ}=0.95, P_{φ}=0.48), but the monthly means of MIR in April, May, and June were significantly higher than that in July or August, respectively (two sample t-tests, P<0.001). Also, the mean MIR in August was significantly lower than that in September (t-tests, P_{δ}<0.001, P_{φ}<0.01). The trends exhibited by monthly means of MIR for females and males for ages 2 to 5, respectively, were the same as those just described for all ages combined (Fig. 8). These patterns indicated the formation of one ring per year during the period from July to August. The MIR analysis by age was not performed for age 1 and ages greater than 5 because the formula used to determine MIR does not apply to samples less than or equal to age 1 and there was a lack of a sufficient number of samples for ages greater than 5.

The mean band radii, by band group for female and male, are shown in Table 1. The observed LJFLs of female and male swordfish were plotted against their corresponding ray radii for method I and method II, respectively (Fig. 9). The relationships between LJFL and ray radius are described as follows:

Method I Female: $LJFL = 21.137S + 65.091$ [r^2=0.8894, n=334];

Male: $LJFL = 19.966S + 68.160$ [r^2=0.8737, n=293].

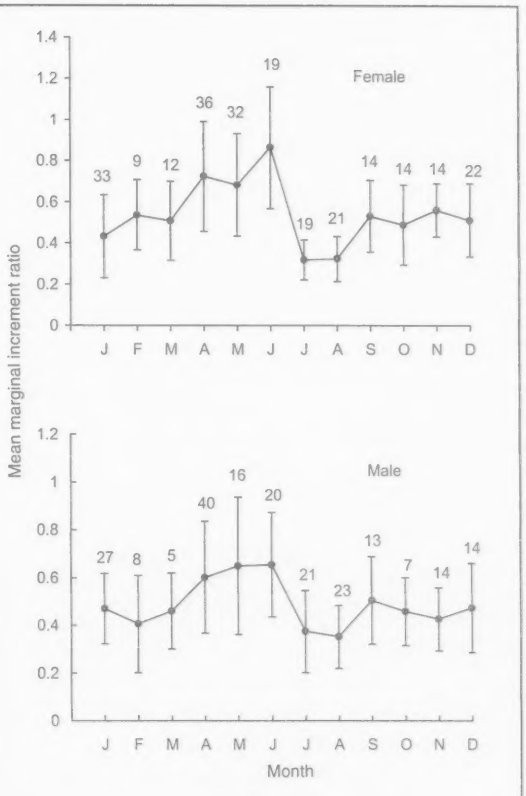

Figure 7

Monthly means of marginal increment ratio of female and male swordfish in the waters around Taiwan for all ages combined. Vertical bars are 1 SE, numbers on the top of vertical bars are sample sizes.

Method II Female: $LJFL = 73.754S^{0.5193}$ [r^2 = 0.8753, n=334];

Male: $LJFL = 77.075S^{0.4772}$ [r^2=0.8742, n=293].

ANCOVA revealed significant differences in the relationship between the males and females for both methods (for method I, $F_{333, 292}$=8.36, P<0.001; for method II, $F_{333, 292}$ =15.59, P=0.004). The average back-calculated lengths-at-age obtained using method I and method II are shown in Table 2. Growth rates were higher during the first year of age (mean 95.2 cm and 96.1 cm LJFL for males and females, respectively, for method I, compared to 88.6 cm and 90.4 cm LJFL for males and females, respectively, for method II). After the first year of age, the growth rates of both sexes slowed appreciably. Growth rates of females were always higher than those of males, especially after the age of three. Also, the growth rates were always higher for method II than for method I except for the first year of age. Fitted standard VB and generalized VB growth

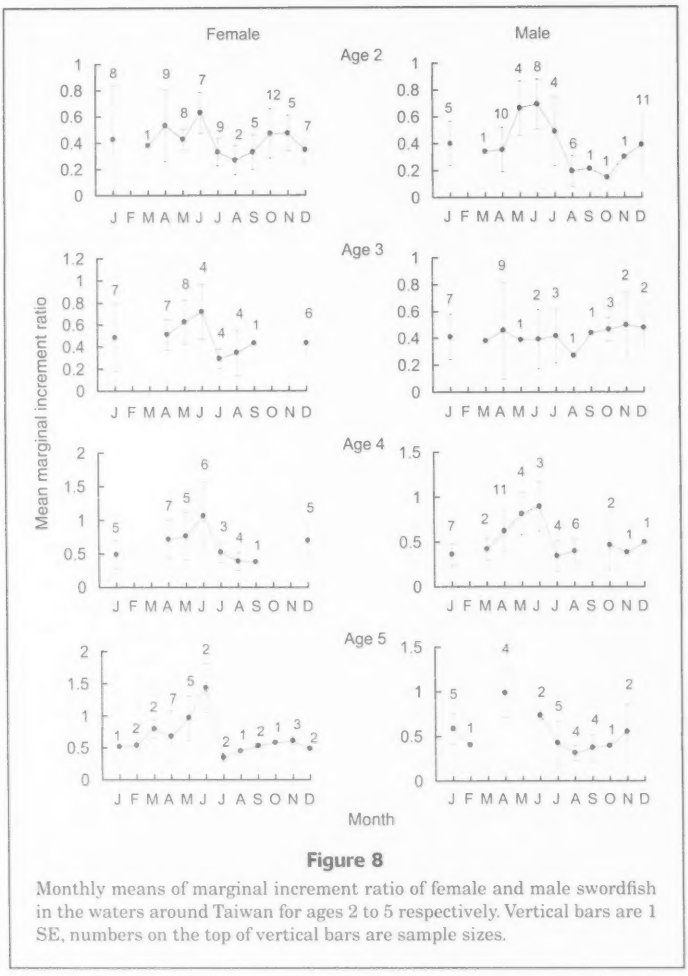

Figure 8

Monthly means of marginal increment ratio of female and male swordfish in the waters around Taiwan for ages 2 to 5 respectively. Vertical bars are 1 SE, numbers on the top of vertical bars are sample sizes.

curves for males and females with method I and method II back-calculation are shown in Figure 9, and the estimated parameters corresponding to each curve are shown in Table 3.

Hotelling's T^2 test results showed significant difference in growth parameters between female and male swordfish for either standard or generalized VB with either method I or method II back-calculation (Table 4). The calculated T^2 is considerably higher than the tabulated value in Table 4 for each case, and all the parameters, except for m of the generalized VB, significantly affect the differences in growth between male and female swordfish (The Roy-Bose simultaneous confidence intervals around differences between parameter values fail to include zero). The results of goodness-of-fit comparison showed that the generalized VB had larger r^2 ranks for method II, but had equal ranks with the standard VB for method I. Considering the tie rank groups in each sex-by-method, Friedman's χ^2_r statistics is 2 (n=4). This was not significant at the 5% level (i.e. χ^2=3.841, df=1), which indicated no significant difference in the r^2 rank ordering of the values between the two growth functions. Kendall's coefficient of concordance was 0.5 (n=4), which did not indicate a good agreement in the r^2 ranks for all sexes-by-method.

Discussion

Just as reported by Berkeley and Houde (1983), Radtke and Hurley (1983), Wilson and Dean (1983), Tsimenides and Tserpes (1989), Ehrhardt (1992), Tserpes and Tsimenides (1995), and Stone and Porter (1997), females in our study were typically larger than males although the length-weight relationship between the sexes did not differ significantly. The overall sex ratio for the sampling period in our study did not deviate significantly from 1:1 (P<0.01) but differed substantially from the ratios of 2.3 females to 1 male and 2.7 females to 1 male reported respectively by Stone and Porter (1997) and Caton et al. (1998). This discrepancy may have been caused by the dif-

Table 1

Mean radius from focus to distal edge of each band of female (**A**) and male (**B**) swordfish in the waters around Taiwan. Roman numerals indicate the number of bands.

A		Mean radius (mm) from focus to each band											
Band class	Sample size	I	II	III	IV	V	VI	VII	VIII	IX	X	XI	XII
0	2												
1	86	1.44											
2	76	1.44	2.38										
3	42	1.44	2.43	3.09									
4	39	1.51	2.34	3.08	3.52								
5	26	1.43	2.39	3.26	3.84	4.23							
6	20	1.51	2.35	3.14	3.77	4.24	4.75						
7	13	1.43	2.40	3.33	3.90	4.40	4.80	5.20					
8	13	1.58	2.60	3.47	4.10	4.52	4.95	5.39	5.84				
9	7	1.60	2.36	3.18	3.81	4.35	4.86	5.39	5.80	6.26			
10	2	1.49	2.37	3.35	3.96	4.46	4.84	5.33	5.64	6.21	6.66		
11	3	1.55	2.43	3.23	3.81	4.18	4.67	5.23	5.76	6.25	6.65	6.80	
12	5	1.50	2.44	3.30	3.88	4.41	5.02	5.39	5.94	6.29	6.69	6.98	7.24
Mean		1.49	2.41	3.24	3.84	4.35	4.84	5.32	5.80	6.25	6.66	6.89	7.24
SD		0.18	0.23	0.34	0.40	0.40	0.49	0.40	0.42	0.33	0.46	0.57	0.40
Growth increase			0.91	0.84	0.60	0.50	0.49	0.48	0.47	0.46	0.41	0.22	0.35

B		Mean radius (mm) from focus to each band									
Band class	Sample size	I	II	III	IV	V	VI	VII	VIII	IX	X
0	2										
1	84	1.47									
2	57	1.32	2.16								
3	32	1.28	2.36	3.06							
4	43	1.31	2.32	3.04	3.51						
5	27	1.32	2.32	3.11	3.65	4.05					
6	22	1.32	2.44	3.21	3.71	4.11	4.47				
7	9	1.39	2.41	3.21	3.75	4.28	4.62	4.98			
8	8	1.33	2.52	3.24	3.82	4.26	4.66	5.02	5.37		
9	4	1.25	2.25	3.35	3.92	4.29	4.70	5.05	5.37	5.74	
10	5	1.40	2.36	3.16	3.93	4.41	4.80	5.11	5.47	5.76	6.06
Mean		1.34	2.35	3.17	3.76	4.23	4.65	5.04	5.40	5.75	6.06
SD		0.17	0.22	0.26	0.30	0.31	0.33	0.32	0.35	0.39	0.38
Growth increase			1.01	0.82	0.58	0.48	0.41	0.39	0.36	0.35	0.20

ference in size ranges of LJFL sampled for studying the sex ratio (Mejuto, et al., 1995). Most of the LJFL in our sample ranged between 100 and 185 cm, close to Arocha and Lee's (1995) middle size range within which the sex ratio was also almost 1:1 (Arocha and Lee, 1995). Besides the size range difference, the differences in geographical areas and seasons can also affect the sex ratio (Hoey, 1991; Mejuto et al., 1991). The proportion of females in our study, which increased to 100% at 210 cm and thereafter, was similar to those described by Turner et al. (1996), Stone and Porter (1997), and DeMartini et al. (2000).

Several genetic studies (Grijalva-Chon et al., 1994; Rosel and Block, 1996; Chow et al., 1997; Chow, 1998) have been unable to reject the hypothesis that swordfish comprise a single, homogenous population in the Pacific. However, from recent analyses of mtDNA, Reeb et al. (2000) concluded that swordfish are not homogenous in the Pacific. They found significantly different northern and southern populations in the western Pacific and several overlapping swordfish populations may occur in the eastern Pacific, making swordfish genetically continuous there. Gene flow between the populations occurs through

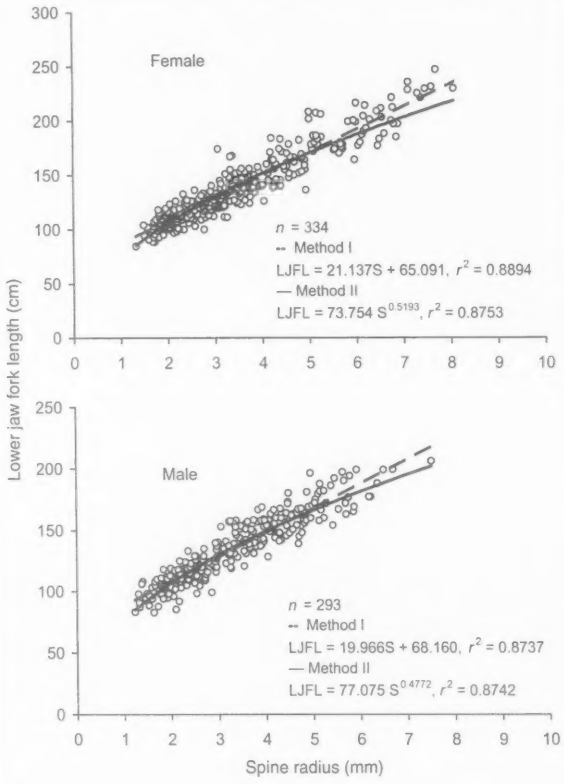
Female
n = 334
-- Method I
LJFL = 21.137S + 65.091, r² = 0.8894
— Method II
LJFL = 73.754 S^0.5193, r² = 0.8753
Male
n = 293
-- Method I
LJFL = 19.966S + 68.160, r² = 0.8737
— Method II
LJFL = 77.075 S^0.4772, r² = 0.8742
Lower jaw fork length (cm)
Spine radius (mm)

Figure 9

Relationship between LJFL and anal ray radius for female and male swordfish in the waters around Taiwan.

a horseshoe-shaped corridor, running between the northwestern Pacific, across to the eastern Pacific and back to the southwestern Pacific (Ward and Elscot, 2000). According to Reed's studies, the swordfish in our samples can be considered a part of the northern population in the western Pacific Ocean.

We found that anal-fin rays are useful for aging swordfish; they are easily sampled without reducing the economic value of the fish and can be read easily (the growth rings stand out clearly). This aging tool is especially important because swordfish lack scales and their very small otoliths are not amenable to traditional aging techniques (Ovchinnikov, 1971; Beckett, 1974; Tserpes and Tsimenides, 1995). Moreover, fin rays can be easily stored for future reexamination (Compeán-Jimenez and Bard, 1983). One problem associated with the fin-ray method used in our study, also indicated by Berkeley and Houde (1983) and Tserpes and Tsimenides (1995), was the possible existence of multiple bands and the missing first annulus in larger fish. However, González-Garcés and Fariña-Perez (1983) and Tserpes and Tsimenides (1995) noted that experienced readers could overcome the prob-

Table 2

Mean back-calculated lower jaw fork lengths at age for swordfish in the waters around Taiwan.

	Back-calculated length (cm)			
	Method I		Method II	
Age (yr)	Male	Female	Male	Female
1	95.19	96.07	88.60	90.35
2	114.86	115.70	114.96	116.18
3	131.88	133.41	133.80	136.47
4	143.12	146.30	145.22	150.35
5	152.14	157.99	154.40	162.91
6	159.15	169.95	161.36	175.34
7	165.60	180.48	167.84	186.40
8	174.76	190.14	176.87	195.83
9	184.00	198.40	185.23	204.62
10	190.89	207.79	191.58	214.15
11		215.06		220.58
12		222.15		226.62

Table 3

Parameter estimates for the standard von Bertalanffy and the generalized von Bertalanffy growth models for swordfish in the waters around Taiwan. Numbers in parentheses are standard errors.

	Standard von Bertalanffy growth model				Generalized von Bertalanffy growth model			
	Method I		Method II		Method I		Method II	
Parameter	Male	Female	Male	Female	Male	Female	Male	Female
L_∞	224.170 (12.802)	281.809 (6.805)	207.520 (8.465)	267.441 (6.517)	231.772 (26.937)	301.877 (11.068)	213.052 (19.153)	300.656 (38.869)
k	0.140 (0.025)	0.101 (0.006)	0.198 (0.031)	0.130 (0.009)				
K					0.066 (0.103)	0.060 (0.055)	0.086 (0.035)	0.040 (0.116)
t_0	−3.089 (0.523)	−3.204 (0.171)	−1.955 (0.406)	−2.302 (0.190)	−1.556 (2.942)	−2.036 (1.263)	−0.626 (1.196)	−0.750 (2.272)
m					−0.625 (2.388)	−0.409 (0.943)	−0.768 (1.730)	−0.785 (1.324)

Table 4

Results of the multivariate (Hotelling's T^2) tests for difference between the estimated von Bertalanffy growth parameters of female and male swordfish in the waters around Taiwan.

	Standard von Bertalanffy growth model		Generalized von Bertalanffy growth model	
	Method I	Method II	Method I	Method II
T^2	20715.1	56005.2	1614630	6782.34
df	3, 623	3, 623	4, 623	4,623
$T^2_{0.01,df}$	11.48	11.48	13.46	13.46
99% CI for[1]				
$L_{\infty ♀}-L_{\infty ♂}$	53.842 ~ 61.436**	56.452 ~ 63.390**	68.845 ~ 71.365**	85.621 ~ 89.587**
$k_♀-k_♂$	−0.044 ~ −0.034**	−0.071 ~ −0.065**		
$K_♀-K_♂$			−0.008 ~ −0.004**	−0.050 ~ −0.042**
$t_{0♀}-t_{0♂}$	−0.216 ~ −0.014**	−0.406 ~ −0.288**	−0.542 ~ −0.418**	−0.163 ~ −0.085**
$m_♀-m_♂$			0.205 ~ 0.227**	−0.062 ~ 0.028

[1] Roy-Bose simultaneous confidence intervals around differences between parameter values.

** Indicates the parameter tested that significantly affects differences in growth between the females and the males at a significant level of 0.01.

lem of multiple bands by determining whether the bands were continuous around the circumference of the entire ray section and by judging their distance from preceding and following bands. In our study, 91 out of the 627 readable specimens had "multiple bands" that were read without a problem by using these criteria. Of the 26 discarded specimens that had multiple unreadable bands, most were found in swordfish larger than 200 cm in size. The missing first band in larger fish can be estimated from observations of its position on young specimens where the first band is visible. Similar approaches for solving the problem of missing band have also been used for Atlantic swordfish (Berkeley and Houde, 1983) and eastern Mediterranean swordfish (Tserpes and Tsimenides, 1995).

Results of marginal increment ratio analysis (Figs. 7 and 8) suggest one growth ring (annulus) is formed each year from July to August, which is toward the end of the spawning period for the swordfish in the north Pacific (Yabe et al., 1959). Although the timing of annulus deposition coincides with the swordfish's spawning season in the north Pacific, it may also be related to swordfish migration, as suggested by Berkeley and Houde (1983) for Atlantic

swordfish and by Tserpe and Tsimenides (1995) for eastern Mediterranean swordfish. The relationship between annulus formation and migration for the western Pacific swordfish should be investigated. Others (Nelson and Manooch, 1982; Beckman et al., 1990; Sturm and Salter, 1990; Ferreira and Russ, 1994; Franks et al., 1999) have commented on the physiological nature of annulus formation and the importance of environmental factors, suggesting that reproduction may not be the sole determining factor in annulus deposition. Our results only partially validated age. Validation of ages requires either a mark-recapture study or the identification of known-age fish in the population (Beamish and McFarlane, 1983; Prince et al., 1995; Tserpes and Tsimenides, 1995; Sun et al., 2001).

According to Hotelling's T^2 analysis, the female and male swordfish in either method I or method II of both standard VB and generalized VB grew differently. Those of the generalized VB had a little larger r^2 ranks than those of the standard VB, although the goodness-of-fit of nonparametric analysis of r^2 ranks did not show a significant difference between two growth equations (P=0.22). In addition, the generalized VB appeared to fit the data well over the range of ages and it provided more realistic growth patterns for juveniles less than one year. However, the standard VB, commonly used to describe fish asymptotic growth, did not fit these data well, and generated grossly overestimated values for individuals less than one year (Table 3 and Fig. 10) (Ehrhardt, 1992; Ehrhardt et al., 1996).

In Table 3, the t_0 values estimated for the generalized VB with method II (i.e. a power function was used to describe the relationship between ray radius and LJFL) were much closer to zero than those estimated for the generalized VB with method I (i.e. a simple linear function was used to describe the relationship between ray radius and LJFL). Also, Ehrhardt (1992), Ehrhardt et al. (1996), and Tserpes and Tsimenides (1995) favored the power function (method II) because they believed its description to be more biologically realistic. Therefore, the parameter estimates for the generalized VB model with method II shown in Table 3 are recommended as the most acceptable for determining the age composition of swordfish in the waters around Taiwan.

Age-length relationships of swordfish (Fig. 11) are mostly based on Atlantic specimens (Berkeley and Houde, 1983; Radtke and Hurley, 1983; Wilson and Dean, 1983; Ehrhardt, 1992; Ehrhardt et al., 1996), and a few on Pacific samples (Yabe et al., 1959; Castro-Longoria and Sosa-Nishizaki, 1998; Uchiyama et al., 1998; Castro-Longoria[1]; Uchiyama[2]). Differences in estimates of growth parameters for males and females arise from the use of different hard parts, e.g. anal-fin rays (our study) versus otoliths (Radtke and Hurley, 1983; Wilson and Dean, 1983) or vertebrae (Esteves et al., 1995), artifacts of preparation, or interpretation. Even though we used the same method as Ehrhardt (1992), Tserpes and Tsimenides (1995), and Ehrhardt et al. (1996), observed difference could be related to geographical coverage of the studies. Our results were in the mid-range of previous estimates, well within the range of variation that might be expected due to the somewhat subjective nature of the processing, measuring, and interpreting of growth rings on fin rays. Therefore, we believe our growth parameter estimates are appropriate for use in assessment studies of the northern swordfish population in the western Pacific Ocean.

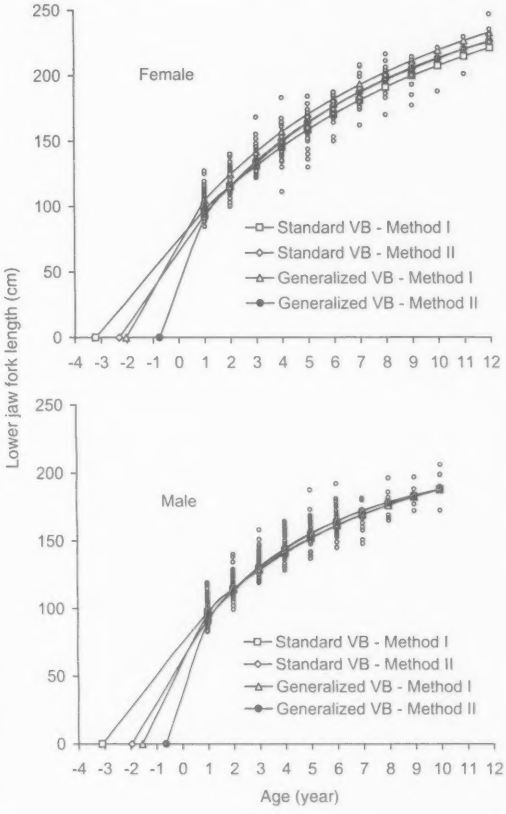

Figure 10

Standard and generalized von Bertalanffy growth curves for female and male swordfish in the waters around Taiwan.

Acknowledgments

The authors express sincere gratitude to Nancy Lo and David Au, Southwest Fisheries Science Center of the

[1] Castro-Longoria, R. 2000. Personal communication of the length-at-age estimates mentioned in Castro-Longoria and Sosa-Nishizaki, 1998. Departmento de Investigaciones Científicas y Tecnológicas de la Universidad de Sonora, Rosales y Niños Héroes S/N, Hermosillo, Sonora, 83000 Mexico.

[2] Uchiyama, J. H. 2000. Personal communication of the length-at-age estimates mentioned in Uchiyama et al., 1998. Honolulu Laboratory, Southwest Fisheries Service Center, NOAA, 2570 Dole Street, Honolulu, Hawaii 96822-2396.

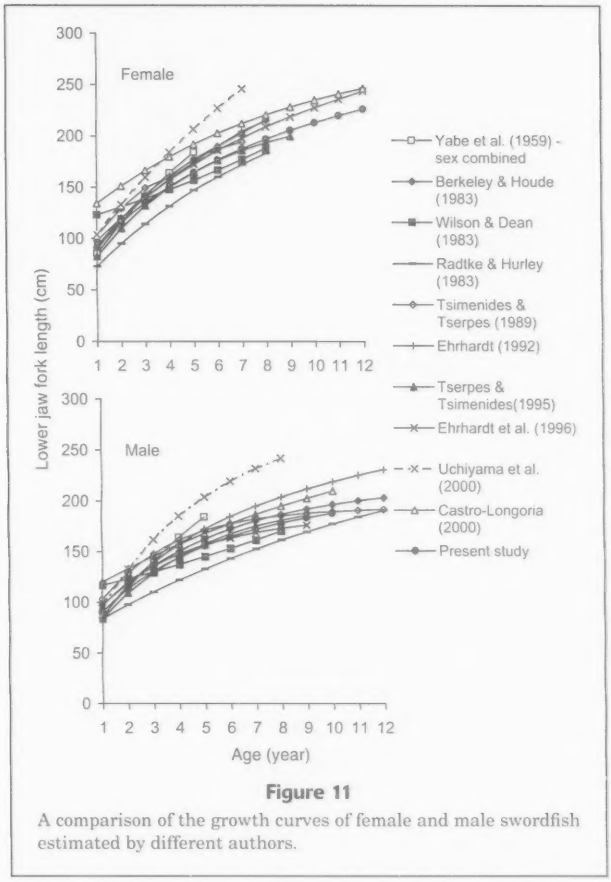

Figure 11

A comparison of the growth curves of female and male swordfish estimated by different authors.

National Marine Fisheries Services, NOAA, for their comments on the initial draft of this paper. Our many thanks are also given to four anonymous referees for their valuable comments. This study was in part supported financially by the "Fisheries Administration, Council of Agriculture, Taiwan," through grant 88-AST-1.4-FID-04 (04) to Chi-Lu Sun.

Literature cited

Arocha, F., and D. Lee.
1995. The spawning of swordfish from the Northwest Atlantic. ICCAT (International Commission for the Conservation of Tunas) Coll. Vol. Sci. Pap. 44(3):179–186.

Bartoo, N. W., and A. L.Coan.
1989. An assessment of the Pacific swordfish resource. *In* Proceedings of the second international billfish symposium; Hawaii, August 1–5, 1988 (R. H. Stroud, ed.), p. 137–151. National Coalition for Marine Conservation, Inc., Savannah, GE.

Beamish, R. J., and D. A. Fournier.
1981. A method for comparing the precision of a set of age determinations. Can. J. Fish. Aquat. Sci. 38:982–983.

Beamish, R. J., and G. A. McFarlane.
1983. Validation of age determination estimates: the forgotten requirement. U.S. Dep. Commer., NOAA Tech. Rep. NMFS 8:29–33.

Beckett, J. S.
1974. Biology of swordfish, *Xiphias gladius* L., in the Northwest Atlantic Ocean. U. S. Dep. Commer., NOAA Tech. Rep. NMFS SSRF-675:103–106.

Beckman, D. W., A. L. Stanley, J. H. Render, and C. A. Wilson,
1990. Age and growth of black drum in Louisiana waters of the Gulf of Mexico. Trans. Am. Fish. Soc. 119:537–544.

Berkeley, S. A., and E. D. Houde.
1983. Age determination of broadbill swordfish, *Xiphias gladius*, from the Straits of Florida, using anal fin spine sections. U. S. Dep. Commer., NOAA Tech. Rep. NMFS 8: 137–143.

Bernard, D. R.
1981. Multivariate analysis as a means of comparing growth in fish. Can. J. Fish. Aquat. Sci. 38:233–236.

Brothers, E. B.
1983. Summary of round table discussions on age validation. U. S. Dep. Commer., NOAA Tech. Rep. NMFS 8:35–44.

Campana, S. E.
2001. Accuracy, precision and quality control in age deter-

mination, including a review of the use and abuse of age validation methods. J. Fish. Biol. 59:197–242.

Campana, S. E., M. C. Annand, and J. I. McMillan.
1995. Graphical and statistical methods for determining the consistency of age determinations. Tran. Am. Fish. Soc. 124:131–138.

Castro-Longoria, R., and O. Sosa-Nishizaki.
1998. Age determination of swordfish, *Xiphias gladius* L., from waters off Baja California, Mexico, using anal fin rays and otoliths. U. S. Dep. Commer., NOAA Tech. Rep. NMFS 142:231–257.

Caton, A., K. Colgan, P. Sahlqvist, P. Ward, C. Ramirez, and M. Scott.
1998. Swordfish, *Xiphias gladius,* and the fisheries for tunas and billfishes in the Australian fishing zone. U. S. Dep. Commer., NOAA Tech. Rep. NMFS 142:11–35.

Chen, Y., D. A. Jackson, and H. H. Harvey.
1992. A comparison of von Bertalanffy and polynomial functions in modelling fish growth data. Can. J. Fish. Aquat. Sci. 49:1228–1235.

Chow, S.
1998. Genetic comparison of Pacific and Mediterranean swordfish, *Xiphias gladius,* by RFLP analysis of the mitochondrial D-loop region. U. S. Dep. Commer., NOAA Tech. Rep. NMFS 142:239–244.

Chow, S., H. Okamoto, Y. Uozumi, Y. Takeuchi, and H. Takeyama.
1997. Genetic stock structure of the swordfish (*Xiphias gladius*) inferred by PCR-RFLP analysis of the mitochondrial DNA control region. Mar. Biol. 127:359–367.

Compeán-Jimenez, G., and F. X. Bard.
1983. Growth increments on dorsal spines of eastern Atlantic bluefin tuna, *Thunnus thynnus*, and their possible relation to migration patterns. U. S. Dep. Commer., NOAA Tech. Rep. NMFS 8:77–86.

DeMartini, E. E., J. H. Uchiyama, and H. A. Williams.
2000. Sexual maturity, sex ratio, and size composition of swordfish, *Xiphias gladius*, caught by the Hawaii-based pelagic longline fishery. Fish. Bull. 98:489–506.

Ehrhardt, N. M.
1992. Age and growth of swordfish, *Xiphias gladius*, in the northwestern Atlantic. Bull. Mar. Sci. 50(2): 292–301.

Ehrhardt, N. M., R. J. Robbins, and F. Arocha.
1996. Age validation and growth of swordfish, *Xiphias gladius*, in the northwest Atlantic. ICCAT (International Commission for the Conservation of Tunas) Col. Vol. Sci. Pap. 45(2):358–367.

Esteves, E., P. Simões, H. M. Da Silva, and J. P. Andrade.
1995. Ageing of swordfish, *Xiphias gladius* Linnaeus, 1758, from the Azores, using sagittae, anal-fin spine and vertebrae. Bull. Univ. Azores, Life and Marine Sciences 13A:39–51.

Ferreira, B. P., and G. R. Russ.
1994. Age validation and estimation of growth rates of the coral trout, *Plectropomus leopardus* (Lacepede 1802), from Lizard Island, Northern Great Barrier Reef. Fish Bull. 92:46–57.

Franks, J. S., J. R. Warren, and M. V. Buchanan.
1999. Age and growth of cobia, *Rachycentron canadum*, from the northeastern Gulf of Mexico. Fish. Bull. 97:459–471.

Fraser, C. Mcl.
1916. Growth of the spring salmon. Trans. Pacific Fish. Soc. 1915, p. 29–39.

Friedman, M.
1937. The use of ranks to avoid the assumption of normality implicit in the analysis of variance. J. Am. Stat. Assoc. 32: 675–701.
1940. A comparison of alternate tests of significance for the problems of *m* rankings. Ann. Math. Stat. 11: 86–92.

González-Garcés, A., and A.C. Fariña-Perez.
1983. Determining age of young albacore, *Thunnus alalunga*, using dorsal spines. U. S. Dep. Commer., NOAA Tech. Rep. NMFS 8:117–122.

Grijalva-Chon, J.M., K. Numachi, O. Sosa-Nishizaki, and J. de la Rosa-Velez.
1994. Mitochondrial DNA analysis of North Pacific swordfish (*Xiphias gladius*) population structure. Mar. Ecol. Prog. Ser. 115:15–19.

Hoey, J.
1991. Sex ratio data for western North Atlantic swordfish. ICCAT Coll. Vol. Sci. Pap. 34(2):429–436.

Kendall, M. G.
1962. Rank correlation methods, 3rd ed, 199 p. Charles Griffin, Condon.

Media Cybernetics.
1997. Image-Pro Plus, version 3.0 for Windows, 480 p. Media Cybernetics, Silver Spring, MD.

Mejuto, J., B. Garcia, and M. Quintans.
1991. A preliminary analysis of the sex-ratio of the swordfish (*Xiphias gladius*) in the north Atlantic by size class using space-time strata. ICCAT Coll. Vol. Sci. Pap. 35(2): 473–481.

Mejuto, J., J. M. de la Serna, and B. Garcia.
1995. An overview of the sex-ratio at size of the swordfish (*Xiphias gladius L.*) around the world: similarity between different strata. ICCAT Coll. Vol. Sci. Pap. 44(3):197–205.

Nelson, R. S., and C. S. Manooch.
1982. Growth and mortality of red snappers in the west-central Atlantic Ocean and northern Gulf of Mexico. Trans. Am. Fish. Soc. 111:465–475.

Ovchinnikov, V. V.
1971. Swordfishes and billfishes in the Atlantic Ocean, ecology and functional morphology, 77 p. Israel Program for Scientific Translations. U.S. Dep. Commer., NOAA NMFS TT 71-50011.

Powers, J. E.
1983. Some statistical characteristics of ageing data and their ramifications in population analysis of oceanic pelagic fishes. U. S. Dep. Commer., NOAA Tech. Rep. NMFS 8:19–24.

Prince, E. D., D. W. Lee, and S. A. Berkeley.
1988. Use of marginal increment analysis to validate the anal spine method for ageing Atlantic swordfish and other alternatives for age determination. ICCAT Coll. Vol. Sci. Pap. 27:194–201.

Prince, E. D., D. W. Lee, J. L. Cort, G. A. McFarlane, and A.Wild.
1995. Age validation evidence for two tag-recaptured Atlantic albacore, *Thunnus alalunga,* based on dorsal, anal, and pectoral finrays, vertebrae, and otoliths. *In* Recent developments in fish otolith research (D. H. Secor, J. M. Dean, and S. E. Campana (eds.), p. 375–396. Univ. of South Carolina Press, Columbia, SC.

Radtke, R. L., and P. C. F. Hurley.
1983. Age estimation and growth of broadbill swordfish, *Xiphias gladius*, from the northwest Atlantic based on external features of otoliths. U. S. Dep. Commer., NOAA Tech. Rep. NMFS 8:145–150.

Reeb, C. A., L. Arcangeli, and B. A. Block.
2000. Structure and migration corridors in Pacific populations of the swordfish *Xiphias gladius*, as inferred through analyses of mitochondrial DNA. Mar. Biol. 136: 123–1131.

Richards, F. J.
1959. A flexible growth function for empirical use. J. Exp. Bot. 10:290–300.
Rosel, P. E., and B. A. Block.
1996. Mitochondrial control region variability and global population structure in the swordfish, *Xiphias gladius*. Mar. Biol. 125:11–22.
SAS Institute.
1990. SAS/STAT user's guide, version 6, fourth ed., p. 1135–1194. SAS Institute Inc., Cary, NC.
Sakagawa, G. T.
1989. Trends in fisheries for swordfish in the Pacific Ocean. *In* Proceedings of the second international billfish symposium; Hawaii, August 15, 1988 (R. H. Stroud, ed.), p. 61–79. National Coalition for Marine Conservation, Inc., Savannah, GE.
Stone, H. H., and J. M. Porter.
1997. Development of a swordfish sex-ratio-at-size relationship for catches from the Canadian fishery. ICCAT Col. Vol. Sci. Pap. 46(3):311–314.
Sturm, M. G. de L., and P. Salter.
1990. Age, growth, and reproduction of the king mackerel, *Scomberomorus cavalla* (Cuvier) in Trinidad waters. Fish. Bull. 88:361–370.
Sun, C. L., C. L. Huang, and S. Z. Yeh.
2001. Age and growth of the bigeye tuna *Thunnus obesus* in the western Pacific Ocean. Fish. Bull. 99: 502–509.
Tserpes, G., and N. Tsimenides.
1995. Determination of age and growth of swordfish, *Xiphias gladius* L., 1758, in the eastern Mediterranean using anal-fin spines. Fish. Bull. 93:594–602.
Tsimenides, N., and G. Tserpes.
1989. Age determination and growth of swordfish, *Xiphias gladius* L., 1758, in the Aegean Sea. Fish. Res. 8:159–168.
Turner, S. C., P. Arocha, and G. P. Score.
1996. U.S. swordfish catch at age by sex. ICCAT Col. Vol. Sci. Pap. 45(2):373–378.
Uchiyama, J. H., R. A. Skillman, J.D. Sampaga, and E. E DeMartini.
1998. A preliminary assessment of the use of hard parts to age central Pacific swordfish, *Xiphias gladius*. U. S. Dep. Commer., NOAA Tech. Rep. NMFS 142:261–273.
Ward, P., and S. Elscot.
2000. Broadbill swordfish: status of world fisheries, 208 p. Bureau of Rural Sciences, Canberra.
Wilson, C. A., and J. M. Dean.
1983. The potential use of sagittae for estimating age of Atlantic swordfish, *Xiphias gladius*. U. S. Dep. Commer., NOAA Tech. Rep. NMFS 8:151–156.
Yabe, H., S. Ueyanagi, S. Kikawa, and H. Watanabe.
1959. Study on the life-history of the swordfish, *Xiphias gladius* Linnaeus. Rep. Nankai Reg. Fish. Res. Lab. 10:107–150
Zar, J. H.
1999. Biostatistical analysis. 4th ed., 929 p. Prentice-Hall Inc., Englewood Cliffs, NJ.

Abstract–The rockfishes of the sebastid genus *Sebastes* are a very important fishery resource off the coasts of California and southern Oregon. However, many of the 54 managed stocks of west coast rockfish have recently reached historically low population levels, leading fishery managers to reexamine current management practices. Management of rockfish stocks as multispecies aggregates, as opposed to independent stocks within the groundfish fishery, can be more desirable when nontargeted bycatch, discard, and management complexity are considered. Rockfish assemblage structure and species co-occurrences were determined by using data from the Alaska Fisheries Science Center triennial continental shelf bottom trawl survey. The weight of rockfish species in trawl catches was expressed as a catch-per-unit-of-effort (CPUE) statistic, from which species spatial distributions, overlaps, diversity, and richness were analyzed. Multidimensional scaling of transformed CPUE data was employed in indirect gradient and multivariate partitioning analyses to quantify assemblage relationships. Results indicated that rockfish distributions closely match the bathymetry of coastal waters. Indirect gradient analysis suggested that depth and latitude are the principal factors in structuring the spatial distributions of rockfish on trawlable habitat. In addition, four assemblages were identified through the joint evaluation of species' distributions and multivariate partitioning analyses: 1) deep-water slope; 2) northern shelf; 3) southern shelf; and 4) nearshore. The slope, shelf, and nearshore groups are found in depth ranges of 200–500 m, 100–250 m, and 50–150 m, respectively. The division of northern and southern shelf assemblages occurs over a broad area between Cape Mendocino and Monterey Canyon. The results of this analysis are likely to have direct application in the management of rockfish stocks off the coasts of southern Oregon and California.

Manuscript accepted 6 June 2002.
Fish. Bull. 100:836–855 (2002).

Distribution and co-occurrence of rockfishes (family: Sebastidae) over trawlable shelf and slope habitats of California and southern Oregon

Erik H. Williams
Stephen Ralston

Southwest Fisheries Science Center
National Marine Fisheries Service
110 Shaffer Road
Santa Cruz, California 95060
Present address (for E H. Williams): Southeast Fisheries Science Center
National Marine Fisheries Service
101 Pivers Island Road
Beaufort, North Carolina 28516-9722
E-mail address (for E. H. Williams): Erik.Williams@noaa.gov

Rockfishes (family Sebastidae according to recent work by Eschmeyer (1998) and Kendall (2000), genera *Sebastes* and *Sebastolobus*) are a very important part of the groundfish fishery off the United States west coast, representing a relatively high value in the market. In 1997, rockfish species accounted for 17% of total west coast groundfish landings, but 33% of total exvessel value (Herrick et al.[1]). Rockfishes on the U. S. west coast are managed under the groundfish Fishery Management Plan (FMP) by the Pacific Fishery Management Council. Some of the 52 *Sebastes* and 2 *Sebastolobus* species that are included in the FMP are managed as single-species stocks, and other, generally less well-known species, are managed as part of larger multispecies aggregations. Moreover, the 54 "rockfishes" listed in the FMP do not include all of the *Sebastes* spp. found in the region. More than 70 species are known from the northeast Pacific Ocean (Eschmeyer et al., 1983; Chen, 1986).

The current status of the principal west coast rockfish stocks is that many have reached historically low levels and the population sizes of many of the minor species remain virtually unknown. Moreover, seven rockfishes (bocaccio (*S. paucispinis*), cowcod (*S. levis*), canary (*S. pinniger*) darkblotched (*S. crameri*), widow (*S. entomelas*), and yelloweye (*S. ruberrimus*) rockfishes, and Pacific ocean perch (*S. alutus*) have recently been declared overfished by the National Marine Fisheries Service. The continuing declines in rockfish populations and other groundfish stocks off the U. S. west coast have prompted changes in harvest policy and other management practices (Ralston, 1998, 2002).

Management of exploited fish stocks on an individual basis often results in discarded bycatch of nontargeted species, which is wasteful. In contrast, management of species as aggregates or complexes can be more practical and desirable (Ralston and Polovina, 1982; Leaman and Nagtegaal, 1986; Fujita et al., 1998). However, the multispecies management approach is only as good as the assemblage or group definitions used, which depend on the availability and accuracy of species-specific distributional information. Most fisheries managers rely on fishery-independent surveys or at-sea observations of fishery catches recorded in vessel logbooks or noted by observers to provide spatial information on fish abundance patterns. Data collection for groundfish population assessments off the coast

[1] Herrick, S. F., J. Hastie, and W. Jacobson. 1998. Economic status of the Washington, Oregon, and California groundfish fisheries. *In* Pacific Fishery Management Council, Status of the Pacific Coast groundfish fishery through 1998 and recommended biological catches for 1999: stock assessment and fishery evaluation. Pacific Fishery Management Council, 2130 SW Fifth Ave., Suite 224, Portland, Oregon 97201.

of California consists primarily of sampling commercial and recreational landings at ports, and for these landings there is little information on catch location (Pearson and Erwin, 1997; Sampson and Crone, 1997). The National Marine Fisheries Service, Alaska Fisheries Science Center (AFSC) westcoast triennial continental shelf bottom-trawl survey, which enters into California waters, has yielded useful spatial information for determining groundfish distributions and co-occurrences. This survey began in 1977 as a rockfish survey but changed focus in subsequent years, depending on the particular information needs at the time (Dark and Wilkins, 1994; Wilkins et al., 1998). For the eight surveys conducted from 1977 to 1998, the shelf trawl survey covered the area from central Vancouver Island, British Columbia, to Point Conception, California, at depths ranging from 50 to 500 m (Wilkins et al., 1998).

Along the U.S. west coast, 60–65% of the groundfish catch (exclusive of Pacific whiting) is taken off the coasts of Washington and Oregon (PFMC[2]). This area has been the focus of past studies examining groundfish population distributions and assemblages (e.g. Gabriel and Tyler, 1980; Leaman and Nagtegaal, 1986; Rickey and Lai, 1990; Rogers and Pikitch, 1992; Weinberg, 1994; Jay, 1996; Gunderson, 1997). In these previous studies of rockfish distributions and groupings, rockfish could be broken into shelf and slope assemblages (e.g. Rogers and Pikitch, 1992; Weinberg, 1994). These studies have all indicated that along the Oregon–Washington coast a "slope" or deep-water rockfish assemblage exists, consisting of darkblotched rockfish, Pacific ocean perch, splitnose rockfish (*S. diploproa*), yellowmouth rockfish (*S. reedi*), and shortspine thornyhead (*Sebastolobus alascanus*). In addition, a "shelf" or bottom rockfish assemblage consists of yellowtail rockfish (*S. flavidus*), canary rockfish (*S. pinniger*), sharpchin rockfish (*S. zacentrus*), greenstriped rockfish (*S. elongatus*), rosethorn rockfish (*S. helvomaculatus*), and redstripe rockfish (*S. proriger*). Weinberg (1994) also examined patterns in abundance and number of rockfish species with respect to depth gradients. Both abundance and the number of species increased with depth to a maximum in the range of 151–250 m but both quantities decreased at depths greater than 250 m.

Groundfish assemblages off California have not been studied, primarily because of the absence of detailed at-sea fishery data collection programs and because of smaller landings. Although California landings account for only 35% of the nonwhiting groundfish total (PFMC[2]), nearly 43% of west coast rockfish landings are taken in California waters (Herrick et al.[1]). Thus, an understanding of the distribution and co-occurrence of rockfishes off the California coast would help with efforts to implement effective fishery management actions leading to a sustainable California rockfish fishery. In particular, an understanding of rockfish distributions and co-occurrences could lead to improved definitions of species complexes. Weinberg (1994) analyzed rockfish assemblages of the "Columbia" and U.S. portion of the "Vancouver" fishery management areas, as specified by the International North Pacific Fisheries Commission (INPFC) (Fig. 1). In part to complement Weinberg's (1994) analysis, we analyzed the AFSC continental shelf trawl survey data from the more southerly waters of the Eureka, Monterey, and Conception INPFC areas, i.e. all sampling conducted south of lat. 43°N (Fig. 1).

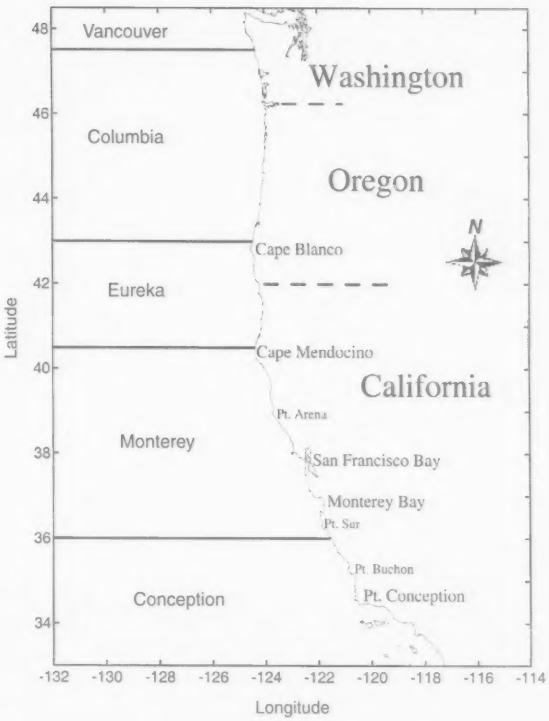

Figure 1

Map of the west coast of the United States, including names of important coastal features and International North Pacific Fisheries Commission management areas.

Materials and methods

Rockfish likely form aggregations or complexes as a response to oceanographic and bathymetric features. For this reason the bathymetry of the region encompassed by the limits of the survey area in the Eureka, Monterey, and Conception INPFC areas was characterized. The study area is the area of marine waters located from lat. 34° to 43°N within a depth range of 50–500 m. Bathymetric data for this region were obtained from the National Ocean Service Hydrographic Data Base (NOSHDB). The

[2] PFMC (Pacific Fishery Management Council). 2000. Status of the Pacific Coast groundfish fishery through 2000 and recommended acceptable biological catches for 2001—stock assessment and fishery evaluation. Pacific Fishery Management Council, 2130 SW Fifth Ave., Suite 224, Portland, Oregon 97201.

NOSHDB contains data digitized from hydrographic surveys completed from 1930 to 1965 and from survey data acquired digitally on NOS survey vessels since 1965. The total amount of habitat by depth and latitude, as well as the location of the shelf break, was determined by analysis of the NOSHDB.

Because the NOSHDB contains a vast amount of data, we computed depth profiles only at each 0.5 interval of latitude. Profiles were obtained by contouring a narrow (0.05°=5.56 km) swath of depth soundings by using inverse distance to a power for interpolations (Surfer, 1995). After correcting for latitudinal differences in the relationship between longitude and distance, the resulting depth profiles were used to estimate the total amount of habitat [km] in 50-m depth intervals. In addition, the distance offshore and the depth of the continental shelf break were estimated. The location of the shelf break was estimated by using a three-parameter segmented linear model that minimized the sums of squared differences between a contoured depth profile and points along two linear sections of a segmented line. The fitted join point of the two segments was then used to estimate the location of the shelf break. In the estimation procedure, the offshore end of the offshore segment was fixed at the exact 500 m depth value obtained from the computed profiles.

Information on rockfish abundance was obtained from trawl survey data collected by the Resource Assessment and Conservation Engineering division of the AFSC. Trawl samples were generally collected by using a sampling design that was stratified by depth and latitude, and where allocation of sample sizes was based on prior fishery catches (Wilkins et al., 1998). From 1977 to 1998, trawl samples in the Eureka, Monterey, and Conception INPFC areas (Fig. 1) were typically taken between 50 and 500 m from June to August with a standardized Nor'eastern high-opening rockfish bottom trawl rigged with roller gear. Measurements recorded for each trawl sample were the following: trawl net width and height; time of the tow; distance traveled; and the number and weight of species in the catch (Wilkins et al., 1998).

The fundamental objective of the AFSC triennial continental shelf trawl survey is to estimate the distribution and abundance of fishes vulnerable to capture by bottom trawl along the U. S. west coast. This basic goal has not changed since the first year of the survey in 1977, although specific objectives have changed over time, which has resulted in alterations in the distribution of sampling effort. For example, sampling effort in 1977 was stratified by depth and latitude according to rockfish fishery information. Sampling efforts in 1980, 1983, and 1986 were shifted to improve biomass estimates of canary and yellowtail rockfish. However, the lack of any significant improvement in the precision of the rockfish biomass estimates prompted a shift in the 1989 and 1992 surveys to include all demersal groundfish and to improve estimates of Pacific hake (*Merluccius productus*) and juvenile sablefish (*Anoplopoma fimbria*) abundance. More recently in 1995 and 1998 the survey was expanded to include slope rockfish found in deeper waters (to 500 m) with an emphasis on obtaining a uniform sampling density. These changes in the goals and objectives of the AFSC shelf survey significantly altered the data on the spatial distribution of samples over time, which, in turn, confounded interannual comparisons of the spatial distributions of rockfish species.

Due to changes in survey design detailed above, all years of the survey were simply pooled into a single composite data set, from which the starting position of each haul, depth of haul [m], net width (m), distance towed (km), numbers of species collected, and species weights (kg) were extracted for analysis. The distribution of all hauls was analyzed by depth and latitude to reveal any patterns that might affect inferences about rockfish distributions or co-occurrences. Because management is primarily concerned with biomass estimates of abundance, only species weights were used in our analysis. All trawl-specific species weight measurements were converted to a catch-per-unit-of-effort (CPUE) statistic by dividing species catch weight by the product of the distance towed and net width, i.e. the area swept (ha). An analysis of the frequency of occurrence of each species in trawls was conducted to obtain a subset of the most ubiquitous rockfishes for use in all subsequent analyses. These species were selected based on their occurrence in at least six of the eight survey years, with the exception of halfbanded rockfish (*S. semicinctus*), which was included because it yielded moderately frequent catches in five of eight years (Table 1).

The data representing the selected subset of species were plotted by depth and latitude to display distributional patterns of CPUE. Next, interspecific distributional overlaps were computed by calculating the percentage of joint occurrences with other species based on presence or absence (Krebs, 1989). Joint occurrences were determined both on a trawl-specific basis and after catches had been aggregated into 50-m depth and 0.5°-latitude intervals. In addition, *Sebastes* diversity and species richness were computed for each haul to summarize the overall distribution of rockfishes captured in the survey. For our analysis, diversity was computed by using the Shannon-Wiener index, and the number of species was used to scale richness (Krebs, 1989). Diversity and richness measures were then spatially contoured over depth and latitude dimensions to display spatial structure (Surfer, 1995).

Distributional patterns and groupings of rockfish based on the CPUE data were analyzed by indirect gradient analysis by using multivariate ordination and partitioning methods. Multivariate analyses are often strongly influenced by the choice of distance or (dis)similarity measure. Members of the set of Minkowski distance measures (e.g. Manhattan, Euclidean, maximum, etc.) tend to be strongly affected by extreme values. Moreover, species composition data from trawl surveys have a high proportion of zero catches and a distance measure that is little affected by this property is desirable. The Bray-Curtis index, also known as Czekanowski's quantitative index, is a commonly used statistic in other similar applications and is robust to the presence of zero values (see Bloom, 1981; Field et al., 1982; Krebs, 1989; Rogers and Pikitch, 1992; Weinberg, 1994; Meuter, 1999). A fourth-root transformation of the data was conducted before calculation of the Bray-Curtis index, as suggested by Field et al. (1982) and as implemented by

Table 1

Frequency of trawl samples with rockfish (family: Sebastidae) present in the Eureka, Monterey, and Conception areas from 1296 AFSC triennial shelf bottom trawl survey samples. The first 26 species (in bold) were included in the detailed analyses; the remaining 23 were not.

		Survey year								
Common name	Scientific name	1977	1980	1983	1986	1989	1992	1995	1998	Total
Stripetail rockfish	*Sebastes saxicola*	155	47	53	55	60	78	114	96	658
Chilipepper	*Sebastes goodei*	119	35	39	48	53	80	87	81	542
Splitnose rockfish	*Sebastes diploproa*	211	31	46	16	20	34	88	95	541
Shortspine thorneyhead	*Sebastolobus alascancus*	149	22	46	19	21	28	83	95	463
Greenstriped rockfish	*Sebastes elongatus*	58	23	56	57	44	57	72	75	442
Bocaccio	*Sebastes paucispinis*	127	65	46	53	40	30	41	26	428
Shortbelly rockfish	*Sebastes jordani*	101	38	20	56	45	59	62	42	423
Darkblotched rockfish	*Sebastes crameri*	122	31	56	28	36	38	56	51	418
Aurora rockfish	*Sebastes aurora*	83	1	2	1			56	60	203
Widow rockfish	*Sebastes entomelas*	42	23	26	10	14	28	30	28	201
Canary rockfish	*Sebastes pinniger*	31	21	39	22	17	17	17	34	198
Redbanded rockfish	*Sebastes babcocki*	51	12	20	8	12	17	37	21	178
Sharpchin rockfish	*Sebastes zacentrus*	8	13	15	14	16	32	22	23	143
Bank rockfish	*Sebastes rufus*	57	9	8	3	3	7	32	8	127
Yellowtail rockfish	*Sebastes flavidus*	17	10	26	14	8	18	19	10	122
Pacific ocean perch	*Sebastes alutus*	24	13	22	5	5	14	17	20	120
Blackgill rockfish	*Sebastes melanostomus*	49	1	3			1	30	35	119
Halfbanded rockfish	*Sebastes semicinctus*	6				13	40	31	27	117
Greenspotted rockfish	*Sebastes chlorostictus*	23	8	6	16	14	6	24	15	112
Cowcod	*Sebastes levis*	11	2	4	0	14	2	22	12	67
Rosethorn rockfish	*Sebastes helvomaculatus*	14	3	7	4	4	7	11	12	62
Brown rockfish	*Sebastes auriculatus*		3	5	7	6	3	4	1	29
Copper rockfish	*Sebastes caurinus*	2	1	5	2	6	4	5	4	29
Vermilion rockfish	*Sebastes miniatus*	2		1		6	7	3	1	20
Redstripe rockfish	*Sebastes proriger*			3	3	2	2	2	7	19
Yelloweye rockfish	*Sebastes ruberrimus*		2	2	3	5	3	1	1	17
Longspine thorneyhead	*Sebastolobus altivelis*	1						19	24	44
Rougheye rockfish	*Sebastes aleutianus*	7				1	1	7	12	28
Unidentified rockfish	*Sebastes* sp.	3		5	1	2	4	5	3	23
Flag rockfish	*Sebastes rubrivinctis*	20			1	1		1		23
Tiger rockfish	*Sebastes nigrocinctus*		2		10					12
Pygmy rockfish	*Sebastes wilsoni*			2	3	1	2	1	3	12
Squarespot rockfish	*Sebastes hopkinsi*					1	5	4	1	11
Greenblotched rockfish	*Sebastes rosenblatti*			1		2	4	1	3	11
Speckled rockfish	*Sebastes ovalis*	2	1		1	1	1		1	7
Shortraker rockfish	*Sebastes borealis*	2	1				1	1	2	7
Blue rockfish	*Sebastes mystinus*					1	1	2	1	5
Pink rockfish	*Sebastes eos*	2					1	1		4
Black rockfish	*Sebastes melanops*		1	1	1		1			4
Olive rockfish	*Sebastes serranoides*	1					2			3
Silvergray rockfish	*Sebastes brevispinis*				2					2
Yellowmouth rockfish	*Sebastes reedi*				2					2
California scorpionfish	*Scorpaena guttata*	1				1				2
Starry rockfish	*Sebastes constellatus*					1				1
Calico rockfish	*Sebastes dalli*					1				1
Freckled rockfish	*Sebastes lentiginosus*					1				1
Rosy rockfish	*Sebastes rosaceus*						1			1
Harlequin rockfish	*Sebastes variegatus*	1								1
Chameleon rockfish	*Sebastes phillipsi*	1								

Meuter (1999). A different measure of similarity, based on converting the data to presence-absence binary form and computing the proportion of nonzero values held in common, has also been used (Krebs, 1989). However, preliminary analyses indicated very little difference between the Bray-Curtis and binary similarity measures (r=0.973). Therefore, the Bray-Curtis similarity measure was used in all subsequent multivariate analyses.

Ordination techniques used in indirect gradient analysis were principal components, detrended correspondence analysis, and multidimensional scaling (Rogers and Pikitch, 1992; Mahon et al., 1998; Meuter, 1999). Multidimensional scaling (MDS) has the advantage of not requiring an assumption about the underlying response model and has been shown to be robust to different relationships of species abundances and environmental gradients (Minchin, 1987; Meuter, 1999). In our study we used MDS in conjunction with the Bray-Curtis similarity measure, similar to previous analyses (Field et al., 1982; Meuter, 1999). The first three dimensions from the MDS were extracted, plotted, and correlated with suspected gradients, which were then used to numerically define assemblage groupings in the data.

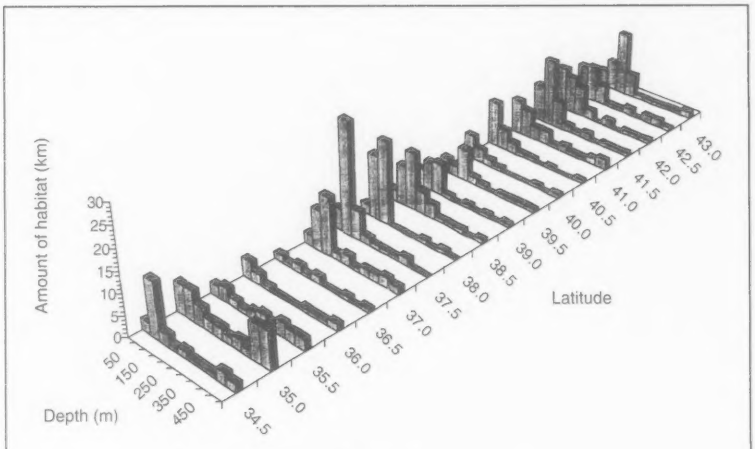

Figure 2

Estimated amount of habitat (km) at half degree latitude intervals and depths of 50–500 m.

Species groupings or assemblages were also determined by partitioning cluster analysis, rather than using other commonly employed hierarchical cluster analyses (e.g. Rogers and Pikitch, 1992; Weinberg, 1994; Mahon et al., 1998). Hierarchical cluster techniques result in dendrogram trees whose shape and structure depend largely on the division and linking methods used, frequently resulting in little similarity among the many methods (Johnson and Wichern, 1992; Ripley, 1996). Results from this type of analysis are often reported for a single method, indicating results consistent with the analyst's expectations, while neglecting to report the range of variability produced by the other alternative hierarchical methods. A more objective method of determining groupings is to use a partitioning technique such as the classical k-means algorithm (Hartigan and Wong, 1979), where the number of groups (k) is specified *a priori* and a single solution to the grouping structure is determined.

For our partitioning analysis we used a more robust variant of the k-means method, which is termed k-medians (Kaufman and Rousseeuw, 1990). The k-means and k-medians methods rely on the minimization of the (dis)similarity between cluster centers and their members. Specifically, the k-means algorithm minimizes the squared (dis)similarities, and k-medians minimizes the untransformed (dis)similarities, resulting in a measure that is less sensitive to extreme values (Kaufman and Rousseeuw, 1990; Ripley, 1996). In our study a range of k's or cluster numbers was evaluated and the best grouping structure for the data was determined according to the highest average silhouette measure (Rousseeuw, 1987). To detect misclassifications, the final rockfish assemblage structure was compared to the several dimensions obtained from the MDS ordination analysis and to our mapped CPUE distributions.

Results

There are a number of large-scale bathymetric features in the Eureka, Monterey, and Conception INPFC areas that may influence the distribution and abundance of shelf and slope rockfish species. For example, the Mendocino Escarpment is a large fracture zone that forms a huge submarine ridge near Cape Mendocino that extends nearly 2500 km westward into the Pacific Ocean and that measures 100 km across at its widest point. Well to the south of the escarpment are a number of large submarine canyons in the region of Monterey Bay and Point Sur. These submarine features, including Monterey and Sur Canyons, result in a coastal bathymetry characterized by limited shelf area and rapidly increasing depth. Farther south, in the vicinity of Point Buchon, is a large offshore area that rises to 430 m depth, i.e. the Santa Lucia Bank. Lastly, Point Conception divides zoogeographic provinces and forms the southern boundary of the area of this study.

Our restricted analysis of the bathymetry at 0.5°-latitude intervals indicates that variability in depth profiles reflects some of the important features described above. The amount of habitat in each 50-m depth interval seems to peak in the 100 to 150-m depth range for latitudes greater than 37.0°N (Fig. 2). The observed decrease in the total amount of habitat at 40.0°N, especially in waters shallower than 200 m, is due primarily to the Mendocino

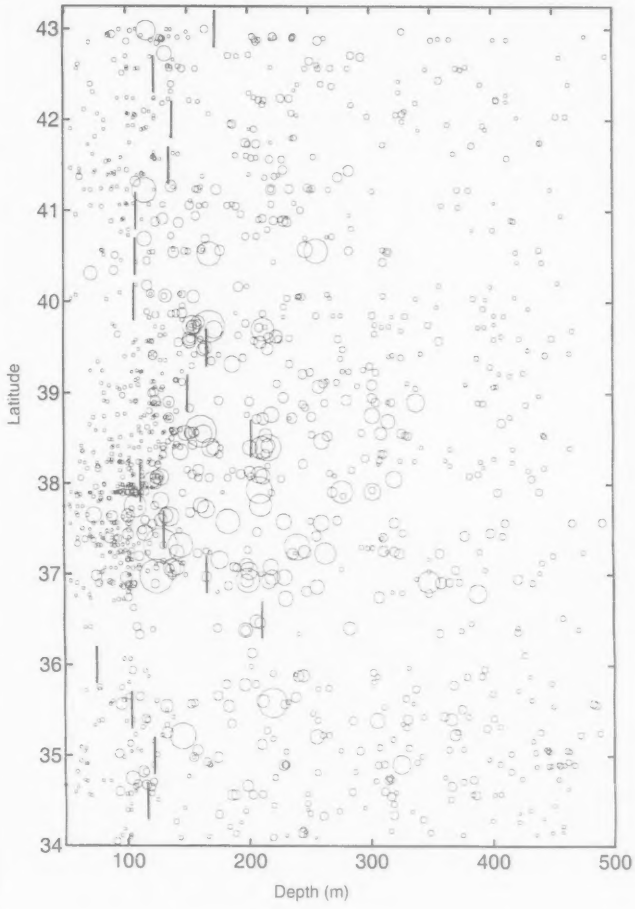

Figure 3

Plot of total rockfish CPUE estimates by depth and latitude from the AFSC triennial bottom trawl survey. Circle diameters are proportional to the square root of total rockfish CPUE. Vertical bold lines represent an estimate of the shelf break (see text).

Escarpment. Likewise, the abrupt decrease in the amount of shallow depth habitat from 35.5° to 36.5°N is directly attributable to the occurrence of submarine canyons, and the increase in habitat from 450 to 500 m at 35.0°N is due to the Santa Lucia Bank (Fig. 2). The depth at which the shelf break occurs seems to be fairly constant, generally ranging from 100 to 175 m (Fig. 3). The relatively deep (210 m) estimated shelf break at 36.5 N is due to the presence of Monterey Canyon (Fig. 3).

For the combined Eureka, Monterey, and Conception INPFC areas, the shelf trawl survey database pooled over the 1977–98 period totaled 1296 hauls that together captured 49 rockfish species, including an unidentified category (Table 1). Based on the frequency of positive trawl samples for each of the rockfish species, 26 were selected for detailed analysis (Table 1). In Table 1, the effect of changing survey sampling objectives is evident in the interannual variation in frequency of occurrence for some of the species. Perhaps most noticeable is the abrupt decline in samples of aurora (*S. aurora*) and blackgill (*S. melanostomus*) rockfish in the years 1980–92 (Table 1). Both are deep-water species and, clearly, the relatively high frequencies of occurrence in 1977, 1995, and 1998 were due to increased sampling at deeper depths that resulted from the altered objectives of the sampling design discussed earlier.

The distribution of trawl sampling locations and CPUE by depth and latitude indicated that the sampling pattern followed some of the bathymetric features mentioned above (Fig. 3). One notable feature was the paucity of samples in the 36.5°N latitude region, which was partly

Table 2

Percentage overlap of rockfish species captured in the AFSC triennial shelf bottom trawl survey by smoothed depth (50–500 m) and taken in trawls containing the species listed in the columns. POP = Pacific ocean perch.

	stripetail	chili-pepper	split-nose	short-spine	green-striped	bocaccio	short-belly	dark-blotched	aurora	widow	canary
stripetail	100	52	37	4	3	30	39	9	2	7	4
chilipepper	57	100	25	3	3	29	33	7	0	7	5
splitnose	19	12	100	7	1	8	14	12	4	1	1
shortspine	17	11	61	100	3	11	7	35	47	6	3
greenstriped	94	85	39	24	100	79	68	52	2	57	60
bocaccio	78	69	41	6	6	100	41	13	1	16	8
shortbelly	50	39	36	2	3	20	100	7	0	5	4
darkblotched	36	25	89	30	6	20	21	100	7	11	6
aurora	9	2	42	53	0	1	1	10	100	1	0
widow	84	88	36	15	23	80	49	35	1	100	36
canary	51	60	18	9	25	42	43	21	1	38	100
redbanded	52	36	99	89	14	42	32	92	30	23	15
sharpchin	88	80	52	17	18	76	57	48	1	41	25
bank	31	30	76	21	3	27	26	56	8	8	5
yellowtail	20	21	5	4	17	21	10	8	0	17	41
POP	44	11	91	64	13	28	6	98	8	17	8
blackgill	18	8	75	63	1	7	5	20	83	3	2
halfbanded	50	99	31	1	11	51	97	1	0	4	7
greenspotted	98	97	65	30	75	96	84	55	3	72	64
cowcod	100	96	97	30	20	95	93	56	7	37	21
rosethorn	81	80	95	60	40	93	61	94	12	60	36
brown	14	57	18	3	20	91	12	2	0	35	54
copper	24	19	16	5	13	33	15	2	0	15	72
vermilion	71	83	47	23	21	79	65	21	7	28	36
redstripe	21	17	18	15	21	17	21	16	1	19	24
yelloweye	97	96	80	37	52	89	72	76	2	91	57

due to the precipitous Big Sur coastline, with its marked reduction in the amount of trawlable habitat in the 50–500 m depth range. Morever, the 1980, 1983, and 1986 surveys did not sample south of Monterey Bay. Similarly, the increase in the number of samples in the 37.0–39.0°N area (Fig. 3) was attributable to an increase in the total amount of shelf habitat in that region (Fig. 2). Starting at the shallowest depths, there was a tendency for the size of the total rockfish catch to increase to a maximum in deeper waters just beyond the shelf break (~200 m), followed by a slight decrease in catch in the deepest waters (Fig. 3). Not apparent to the eye in Figure 3 is a slight, but significant trend in the distribution of sample locations towards deeper waters at more southerly sites (linear slope=–0.26, P-value=0.0041). This was probably due to the decreasing amount of shelf habitat and the increasing quantity of slope habitat as one moves south along the California coast (Fig. 2).

The amount of interspecific overlap in spatial distributions among the subset of 26 species differed, depending on whether co-occurrence was assessed from a categorization of the catches into depth-latitude intervals or by specific trawl locations (Tables 2 and 3). As expected, depth-latitude overlaps were greater than the site-specific trawl catch overlaps, due to the effect of spatial smoothing. Inspection of the depth-latitude species overlaps (Table 2) indicated that stripetail (*S. saxicola*), splitnose, chilipepper (*S. goodei*), bocaccio, and shortbelly (*S. jordani*) rockfish were most widespread with respect to co-occurrence with other rockfishes. Similarly, overlaps measured from actual trawl catches indicated that bocaccio, chilipepper, stripetail, canary, and widow rockfish have relatively high likelihoods of co-occurring with other rockfish species (Table 3).

The spatial distribution of rockfish over the continental shelf and slope generally indicated a ridge of increased diversity at approximately 250 m depth, at least for samples taken at northern latitudes (38.0–43.0°N) (Fig. 4). In contrast, for southern latitudes (34.0–38.0°N), the ridge of high diversity veered well offshore to a depth of 450

Table 2

latitude (34.0–43.0°N) locations. Individual table elements represent the percentage of occurrence of a species (reading across the row)

red-banded	sharp-chin	bank	yellow-tail	POP	black-gill	half-banded	green-spotted	cow-cod	rose-thorn	brown	copper	vermilion	red-stripe	yellow-eye
1	7	5	2	2	1	1	1	2	1	0	0	0	0	0
1	7	5	2	0	1	2	1	2	1	0	0	0	0	0
1	2	6	0	2	3	0	0	1	0	0	0	0	0	0
12	6	16	2	11	23	0	1	2	2	0	0	1	1	1
13	47	14	45	15	3	6	12	11	9	0	2	3	7	8
3	16	11	4	3	1	2	1	4	2	0	0	1	0	1
1	6	5	1	0	1	2	1	2	1	0	0	0	0	0
10	15	35	2	14	6	0	1	4	3	0	0	0	1	1
4	0	7	0	2	33	0	0	1	0	0	0	0	0	0
8	42	17	17	8	2	1	5	8	5	0	1	2	2	6
5	27	10	44	4	2	1	4	5	3	0	4	2	3	4
100	23	47	5	28	33	1	5	8	12	0	0	4	3	3
8	100	26	8	13	1	0	3	8	7	0	0	1	4	5
8	13	100	0	4	10	0	1	6	3	0	0	1	0	2
2	8	1	100	3	0	1	2	1	1	1	2	1	6	2
21	28	16	6	100	2	0	1	0	4	0	0	0	3	4
12	2	21	0	1	100	0	1	2	2	0	0	1	0	0
2	2	2	6	0	0	100	4	4	0	0	3	14	0	0
26	54	43	33	6	11	13	100	44	21	0	4	16	3	18
14	38	57	3	1	11	4	14	100	20	0	1	4	0	2
49	80	61	15	19	17	1	16	48	100	0	0	3	9	12
5	3	1	76	0	0	7	1	6	0	100	64	34	0	0
1	2	3	36	0	0	13	5	2	1	10	100	22	0	0
22	12	26	24	3	20	44	17	15	4	5	18	100	1	1
7	29	7	46	12	1	0	2	1	6	0	0	0	100	13
19	91	68	27	30	3	1	20	8	17	0	0	1	29	100

m, and there was some indication of a secondary increase in diversity at 150 m for the most southerly latitudes 34.0–36.0°N (Fig. 4). The distribution of species richness indicated that the existence of a distinct ridge at depths of 200–250 m—the highest portion of the ridge occurring between 36.0 and 39.0°N latitude (Fig. 5). In that region, in excess of eight distinct species co-occurred in individual trawl samples. A solitary peak in richness occurred at a depth of 500 m near 37.5°N latitude (Fig. 5). Inspection of the raw data revealed that this peak was heavily influenced by a single trawl sample, but there was no indication of a data recording error in this sample.

The spatial distribution of CPUE for each of the rockfish species is shown in Figures 6–10. The particular sequence of species in these figures corresponded to clustering results that are presented below. Careful examination of these 26 distributions revealed that the depth distributions of almost all species were not related to latitude. The sole exception to this generalization was the depth distribution for shortspine thornyhead, which showed a significant interaction between depth of capture and latitude, based on results from a two-way factorial ANOVA. For that species, depth distribution shifts into deep water at more southerly latitudes (Fig. 6).

Latitudinal boundaries of rockfish distributions appeared to be influenced by two of the main bathymetric features on the U.S. west coast. In particular, the Mendocino Escarpment (ME), located at approximately 40.4°N latitude, and Monterey Canyon (MC), located near 36.8°N latitude, appear to form distributional impediments for some of the species, and other species appeared to be distributed more uniformly across the entire latitudinal range of the study (Figs. 1, 6–10). Examples of species whose distributional boundaries appeared to be influenced by the ME were blackgill rockfish (*S. melanostomus*), Pacific ocean perch, chilipepper (*S. goodei*), shortbelly rockfish (*S. jordani*), bocaccio, and greenspotted rockfish. Species whose distributions appeared to border on MC were dark-blotched, greenstriped, canary, yellowtail, widow, sharpchin, and rosethorn rockfish (Figs. 6–10).

Table 3

Percentage overlap of rockfish species captured in the AFSC triennial shelf bottom trawl survey. Individual table elements represent Pacific ocean perch.

	stripetail	chili-pepper	split-nose	short-spine	green-striped	bocaccio	short-belly	dark-blotched	aurora	widow	canary
stripetail	100	35	11	1	3	9	12	5	0	3	1
chilipepper	29	100	4	1	3	10	8	2	0	6	2
splitnose	10	4	100	4	0	3	3	9	1	1	0
shortspine	12	8	50	100	3	7	3	30	27	3	2
greenstriped	48	57	7	4	100	26	27	9	0	18	15
bocaccio	23	31	8	2	4	100	8	7	0	8	6
shortbelly	9	7	3	0	1	2	100	1	0	1	1
darkblotched	27	15	57	14	3	15	6	100	1	3	2
aurora	3	0	24	38	0	0	0	4	100	0	0
widow	14	29	3	1	5	14	6	3	0	100	6
canary	9	22	2	1	7	19	7	3	0	11	100
redbanded	37	21	61	53	5	33	13	51	8	7	3
sharpchin	38	47	14	4	9	46	24	10	0	20	7
bank	11	11	48	7	1	9	3	39	1	3	1
yellowtail	4	16	0	0	6	12	1	1	0	20	18
POP	25	2	44	28	6	25	4	72	1	9	2
blackgill	3	2	41	32	1	2	2	9	45	0	0
halfbanded	2	34	0	0	3	5	18	0	0	1	3
greenspot	41	72	20	6	55	52	35	5	0	32	44
cowcod	64	39	73	8	10	93	21	10	2	10	8
rosethorn	26	41	37	32	37	56	29	36	2	32	20
brown	0	2	0	0	0	47	1	0	0	56	36
copper	1	4	0	0	3	23	2	0	0	11	73
vermilion	6	14	3	1	1	31	6	2	1	11	19
redstripe	4	8	0	0	4	8	15	0	0	8	4
yelloweye	16	72	10	2	34	63	18	12	0	63	75

A general comparison of interspecific relationships, based on depth-latitude distributions, can be gathered by inspection of a plot of CPUE-weighted depth-latitude centroids (Fig. 11). From results presented in Figure 11, some species (e.g. copper [*S. caurinus*] and brown [*S. auriculatus*] rockfish) appear to have very similar depth-latitude distributions. Aurora and blackgill rockfish are clearly deep-water southern species, whereas halfbanded (*S. semicinctus*) and vermilion (*S. miniatus*) rockfish are southern species found principally in shallow water. Although this plot is useful for identifying related species by their average distribution in space, it does not fully represent actual joint co-occurrences and assemblage relationships, as does a complete multivariate community analysis.

The results of the multidimensional scaling of the fourth-root transformed CPUE data, with the Bray-Curtis similarity measure, revealed highly significant correlations of the first three dimensions with mean depth (r=0.90, P<0.0001), total CPUE$^{0.25}$ (r=–0.82, P<0.0001), and mean latitude (r=–0.74, P<0.0001), respectively. However, these first three dimensions accounted for only 39% of the total variance in the data.

The k-medians partitioning analysis was used to examine a range of k's or cluster numbers, effectively predefining the number of distinct assemblages. The best fits were determined by the highest average silhouette measures of 0.143 and 0.140 for k = 8 and k = 4, respectively (Table 4). According to Kaufman and Rouseeuw (1990) an average silhouette measure less than 0.25 does not indicate any substantial structure in the data. Despite the low average silhouette measurements, the suggested groupings of four and eight clusters were used as an initial guideline in determining distinct species assemblages. The species groups defined in Table 4 by a division into four clusters (A, B, C, and D), and further delineated in Figure 11, show that these assemblages generally follow depth and the latitude distributions of their member species.

The first three dimensions from the multidimensional scaling analysis, along with the k = 8 cluster divisions, are shown in Figure 12. The eight clusters comprising the 26

Table 3

the percentage of occurrence of a species (reading across the row) taken in trawls containing the species listed in the columns. POP =

red-banded	sharp-chin	bank	yellow-tail	POP	black-gill	half-banded	green-spotted	cow-cod	rose-thorn	brown	copper	vermilion	red-stripe	yellow-eye
1	3	1	1	1	0	0	0	1	0	0	0	0	0	0
0	4	1	2	0	0	1	1	0	0	0	0	0	0	0
1	1	4	0	1	1	0	0	1	0	0	0	0	0	0
11	4	7	1	9	10	0	1	1	2	0	0	0	0	0
1	13	1	15	3	0	1	9	2	4	0	0	0	3	2
1	10	2	5	2	0	0	1	2	1	1	0	1	1	1
0	2	0	0	0	0	0	0	0	0	0	0	0	0	0
5	5	19	1	11	1	0	0	1	1	0	0	0	0	0
2	0	2	0	1	21	0	0	0	0	0	0	0	0	0
1	8	1	14	1	0	0	2	0	1	2	0	1	1	1
0	5	1	21	0	0	0	4	1	1	2	4	2	1	3
100	12	15	0	17	5	0	3	2	6	0	0	1	0	0
2	100	9	1	3	0	0	2	1	3	0	0	0	9	3
3	10	100	0	2	2	0	1	2	1	0	0	0	0	0
0	0	0	100	0	0	0	2	0	0	3	1	1	0	0
10	9	8	3	100	1	0	0	0	1	0	0	0	1	0
3	0	6	0	1	100	0	0	0	1	0	0	0	0	0
0	0	0	1	0	0	100	4	1	0	0	1	3	0	0
5	21	11	29	1	1	7	100	7	4	0	1	2	2	10
3	10	22	0	0	1	1	8	100	11	0	0	1	0	2
17	47	14	9	6	3	0	8	18	100	1	1	1	23	15
0	0	0	71	0	0	0	0	0	1	100	13	12	0	0
0	0	0	24	0	0	2	1	0	1	11	100	25	0	0
1	1	2	13	0	0	6	2	1	1	8	19	100	0	0
0	20	0	0	0	0	0	1	0	3	0	0	0	100	5
0	68	0	13	2	0	0	24	5	20	0	0	1	42	100

species and listed in Table 4 closely follow the ordination plots. In particular, dimensions one and three in combination showed clear segregation of the eight distinct clusters (lower panel in Fig. 12). Clearly, the A-1 group in Table 4 stands out as a distinct assemblage in the MDS ordinations (Fig. 12). Because dimensions one and three were highly correlated with depth and latitude, respectively, we concluded that the species groups are defined by depth and latitude. However, the low amount of variance explained by the dimensions, the small sample sizes for some species, and the relatively low average silhouette measures in the partitioning analysis, would indicate that some caution should be exercised when using these results. In fact, there appeared to be some discrepancies in depth-latitude distributions and partitioning groups for the rockfish species (Table 4, Fig. 11).

Group A-1 in Table 4 represents the deep-water slope species of rockfish, and the species in groups B-2 and B-3 represent the nearshore species of rockfish. The separation of halfbanded rockfish from the nearshore group suggested by the k = 8 clustering was likely the result of a more southerly distribution for this species than that for the other members of the group (Fig. 7). The remaining C and D groups in Table 4 represent shelf species, group C being a southern shelf group and D representing a northern shelf group. A likely misclassification in the clustering results was the inclusion of greenspotted rockfish in the northern shelf assemblage, which was not warranted by the distribution of catches shown in Figure 9. Within the C group, the separation of cowcod as an isolate in the k = 8 analysis was due to this species' relatively deep distribution (Fig. 8). The separation of canary and yellowtail rockfish as a distinct cluster was the result of their relatively northern distribution and their inclusion in the southern shelf species group by the partitioning analysis was probably the result of a boundary effect (Fig. 9). Lastly, the division of the northern shelf group into D-7 and D-8 subgroups, suggested by the k = 8 partitioning, was likely the result of differences in the survey's total catch of rockfish (MDS dimension 2), which is not evident in distributional patterns (Table 4).

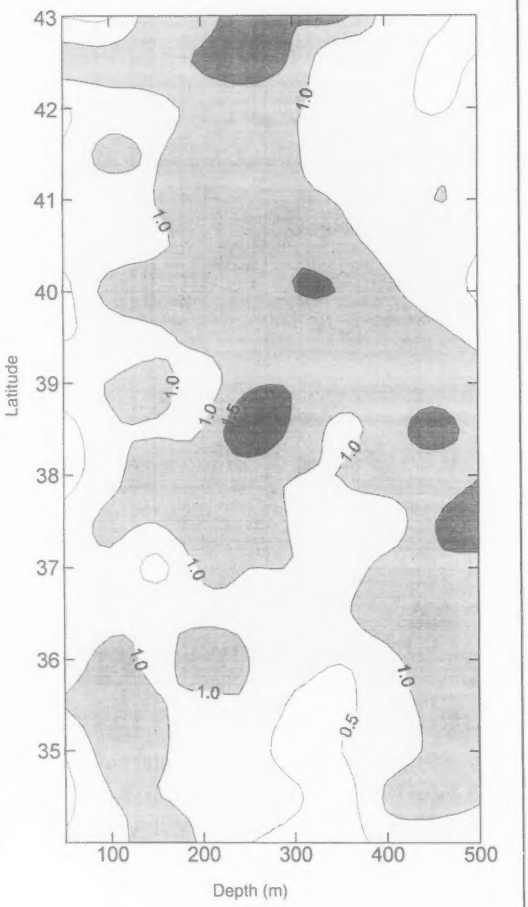

Figure 4

Contour map of Shannon-Weiner diversity indices from the AFSC triennial bottom trawl survey for all samples containing rockfish species (abundance is measured by biomass).

Table 4

Separation of rockfish species into four and eight groups, labeled by letters and numbers, respectively, based on *k*-medians analysis of AFSC triennial bottom trawl surveys from 1977 to 1998.

Group	Species	Group	Species
A-1	blackgill rockfish, aurora rockfish, shortspine thornyhead, bank rockfish, darkblotched rockfish, Pacific ocean perch, redbanded rockfish, splitnose rockfish	C-4	chilipepper, shortbelly rockfish, bocaccio, stripetail rockfish, greenstriped rockfish
		C-5	cowcod
		C-6	canary rockfish, yellowtail rockfish
B-2	copper rockfish, vermilion rockfish, brown rockfish	D-7	greenspotted rockfish, widow rockfish, sharpchin rockfish, rosethorn rockfish
B-3	halfbanded rockfish	D-8	yelloweye rockfish, redstripe rockfish

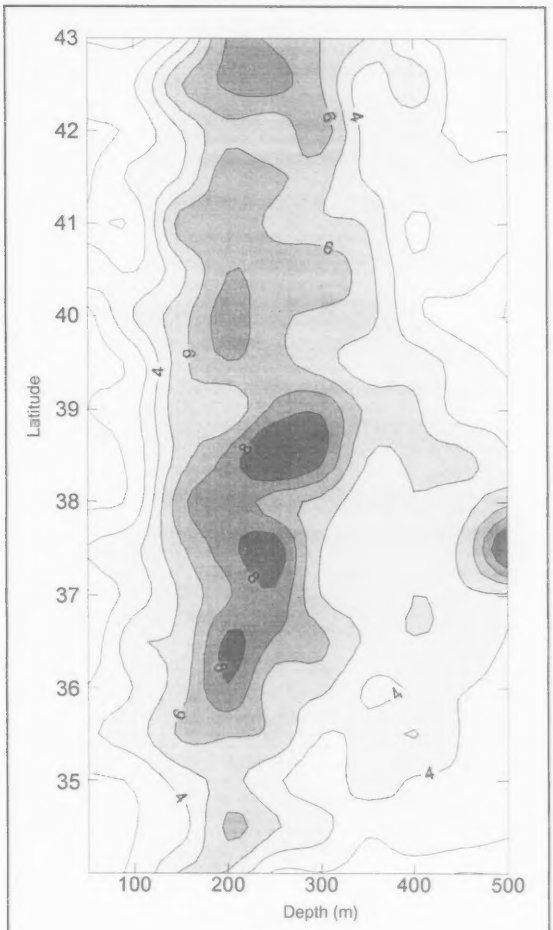

Figure 5

Contour map of species richness (number of species) from the AFSC triennial bottom trawl survey for all samples containing rockfish species.

Discussion

Our data were the result of pooling samples collected during AFSC triennial continental shelf trawl surveys conducted from 1977 to 1998. Because this interval represents a period of substantial fishery removals (Ralston, 1998), one might expect that rockfish assemblage structure changed over time as commercially important species were serially removed (e.g. bocaccio and canary rockfish). Although we did not perform year-specific analyses that would allow us to address this possibility, results from Weinberg (1994) showed that, over a comparable period of time (1977–92), the trawlable assemblages of rockfishes off Oregon and Washington were reasonably stable in composition. In particular, his year-specific recurrent group analyses revealed good agreement among surveys, from which he inferred the existence of three groups representing a deep-water assemblage (shortspine thornyhead, Pacific ocean perch, darkblotched, and redbanded (*S. babcocki*) rockfish), a mid-shelf assemblage (canary, yellowtail, and greenstriped rockfish), and a shelf-break assemblage (sharpchin, rosethorn, and redstriped rockfish). Notably, there was substantial overlap between the latter two groups, which is consistent with our findings.

It is no surprise that rockfish distributions are related to bathymetric features, particularly when viewed through bottom trawl survey samples, as we did in our study. It is noteworthy that physical barriers, particularly the Mendocino Escarpment and Monterey Canyon, seem to affect the latitudinal distribution of certain rockfishes. The former may act as a barrier to dispersal because converging currents at Cape Mendocino create conditions

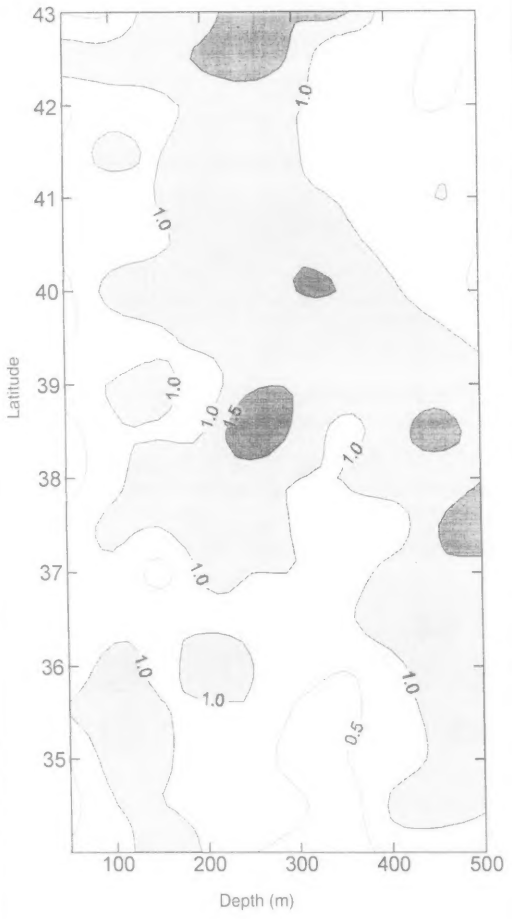

Figure 4

Contour map of Shannon-Weiner diversity indices from the AFSC triennial bottom trawl survey for all samples containing rockfish species (abundance is measured by biomass).

Table 4

Separation of rockfish species into four and eight groups, labeled by letters and numbers, respectively, based on *k*-medians analysis of AFSC triennial bottom trawl surveys from 1977 to 1998.

Group	Species	Group	Species
A-1	blackgill rockfish, aurora rockfish, shortspine thornyhead, bank rockfish, darkblotched rockfish, Pacific ocean perch, redbanded rockfish, splitnose rockfish	C-4	chilipepper, shortbelly rockfish, bocaccio, stripetail rockfish, greenstriped rockfish
		C-5	cowcod
		C-6	canary rockfish, yellowtail rockfish
B-2	copper rockfish, vermilion rockfish, brown rockfish	D-7	greenspotted rockfish, widow rockfish, sharpchin rockfish, rosethorn rockfish
B-3	halfbanded rockfish	D-8	yelloweye rockfish, redstripe rockfish

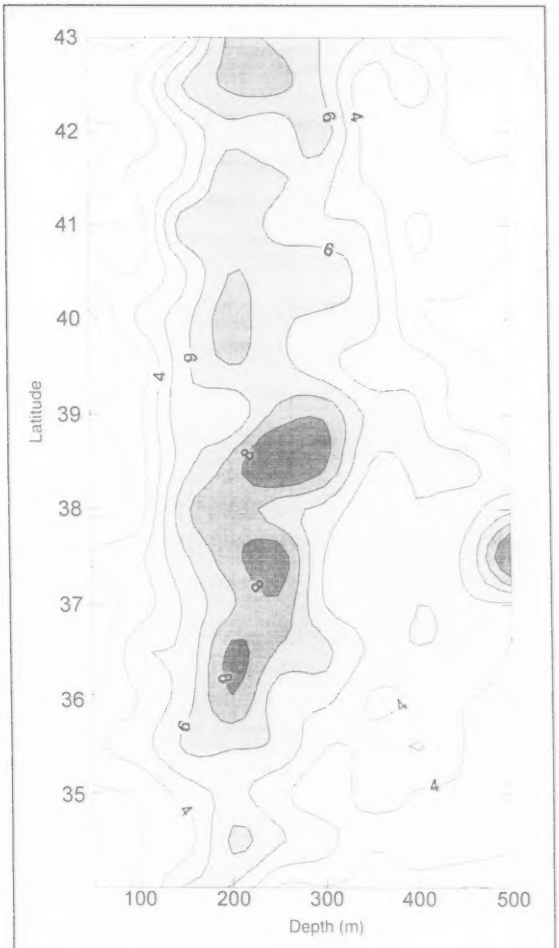

Figure 5

Contour map of species richness (number of species) from the AFSC triennial bottom trawl survey for all samples containing rockfish species.

Discussion

Our data were the result of pooling samples collected during AFSC triennial continental shelf trawl surveys conducted from 1977 to 1998. Because this interval represents a period of substantial fishery removals (Ralston, 1998), one might expect that rockfish assemblage structure changed over time as commercially important species were serially removed (e.g. bocaccio and canary rockfish). Although we did not perform year-specific analyses that would allow us to address this possibility, results from Weinberg (1994) showed that, over a comparable period of time (1977–92), the trawlable assemblages of rockfishes off Oregon and Washington were reasonably stable in composition. In particular, his year-specific recurrent group analyses revealed good agreement among surveys, from which he inferred the existence of three groups representing a deep-water assemblage (shortspine thornyhead, Pacific ocean perch, darkblotched, and redbanded (*S. babcocki*) rockfish), a mid-shelf assemblage (canary, yellowtail, and greenstriped rockfish), and a shelf-break assemblage (sharpchin, rosethorn, and redstriped rockfish). Notably, there was substantial overlap between the latter two groups, which is consistent with our findings.

It is no surprise that rockfish distributions are related to bathymetric features, particularly when viewed through bottom trawl survey samples, as we did in our study. It is noteworthy that physical barriers, particularly the Mendocino Escarpment and Monterey Canyon, seem to affect the latitudinal distribution of certain rockfishes. The former may act as a barrier to dispersal because converging currents at Cape Mendocino create conditions

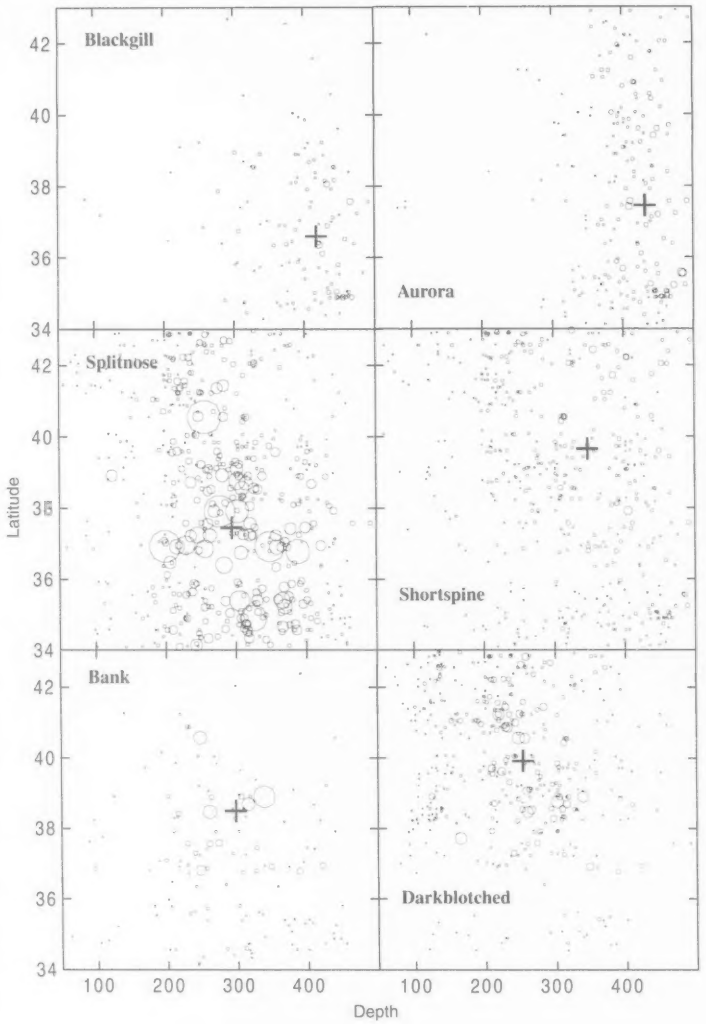

Figure 6

Plot of rockfish CPUE estimates by depth and latitude from the AFSC triennial bottom trawl survey. Circle diameters are proportional to the square root of rockfish CPUE and the bold plus symbol represents the centroid of the CPUE estimates.

that result in offshore transport (Magnell et al., 1990). Likewise, Monterey Canyon may act as a distributional barrier because continental shelf habitats constrict severely, creating a potential bottleneck to dispersion. Some support for this hypothesis is evident in the rockfish distributional maps (Figs. 6–10), which show that shallow water species are more likely to have Monterey Canyon as a distributional boundary when compared to the deeper dwelling species, for which there apparently exists ample habitat.

Overall, depth appears to be the single most important determinant of rockfish distributions. Most of the abundance patterns we observed followed the distribution of habitats by depth. Species diversity in the study area also seemed to follow the pattern of depth habitat distribution. However, species richness did not follow this pattern, but instead followed the region of overlap between shelf and slope rockfish assemblages. In fact, the contoured ridge of highest richness may be useful in spatially delineating the shelf and slope assemblages. This ridge appeared to

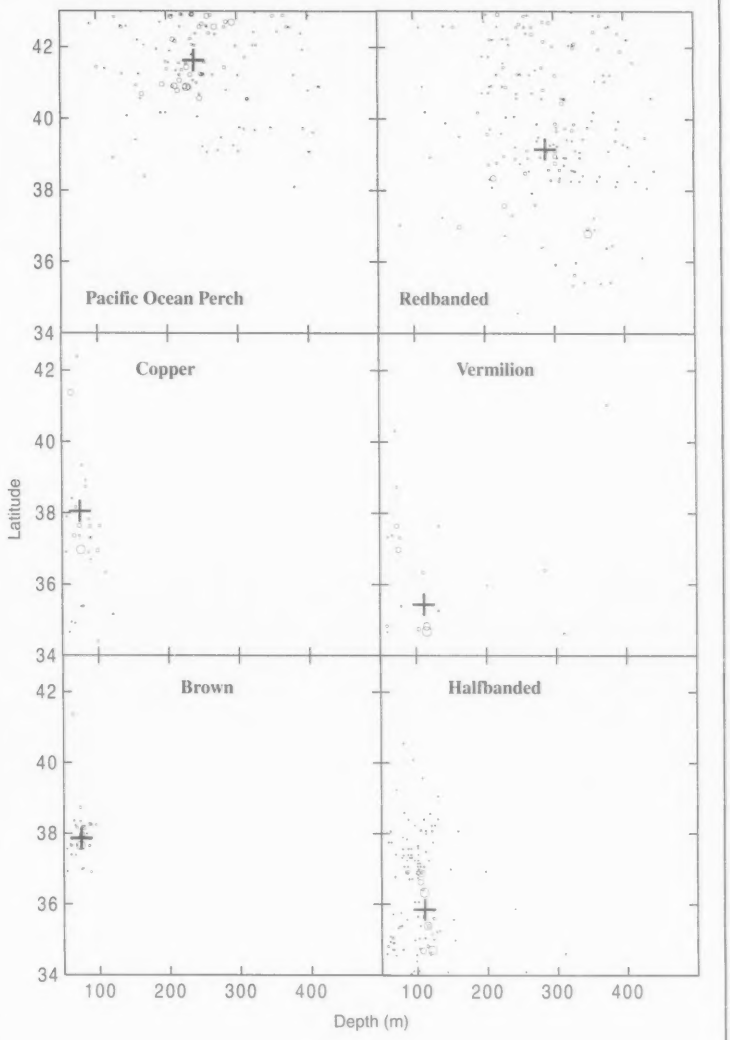

Figure 7

Plot of rockfish CPUE estimates by depth and latitude from the AFSC triennial bottom trawl survey. Circle diameters are proportional to the square root of rockfish CPUE and the bold plus symbol represents the centroid of the CPUE estimates.

be fairly constant at ~200–250 m across all latitudes included in our study.

The ridge of increased species richness indicated that there is substantial overlap in rockfish distributions. The analysis of rockfish overlap in our study was computed in two ways, i.e. by smoothed depth-latitude abundance and by raw trawl catches. The smoothed species-specific abundance estimates for all depth-latitude combinations could not be presented here because of space limitations. However, such data could be useful for detailed spatial analyses of rockfish co-occurrences in future analyses. The trawl-catch overlap data represent the best estimate of bottom trawl co-occurrence probabilities for the study area. A potential limitation of the overlap estimates presented in our study is that they came from only one survey, which employed a single sampling gear. However, the bottom trawl gear used in the AFSC triennial survey is generally similar to the fishing gear used by commercial fishermen, and previous studies have shown that catch rates from the continental shelf bottom trawl survey closely match commercial catch rates (Fox and Starr,

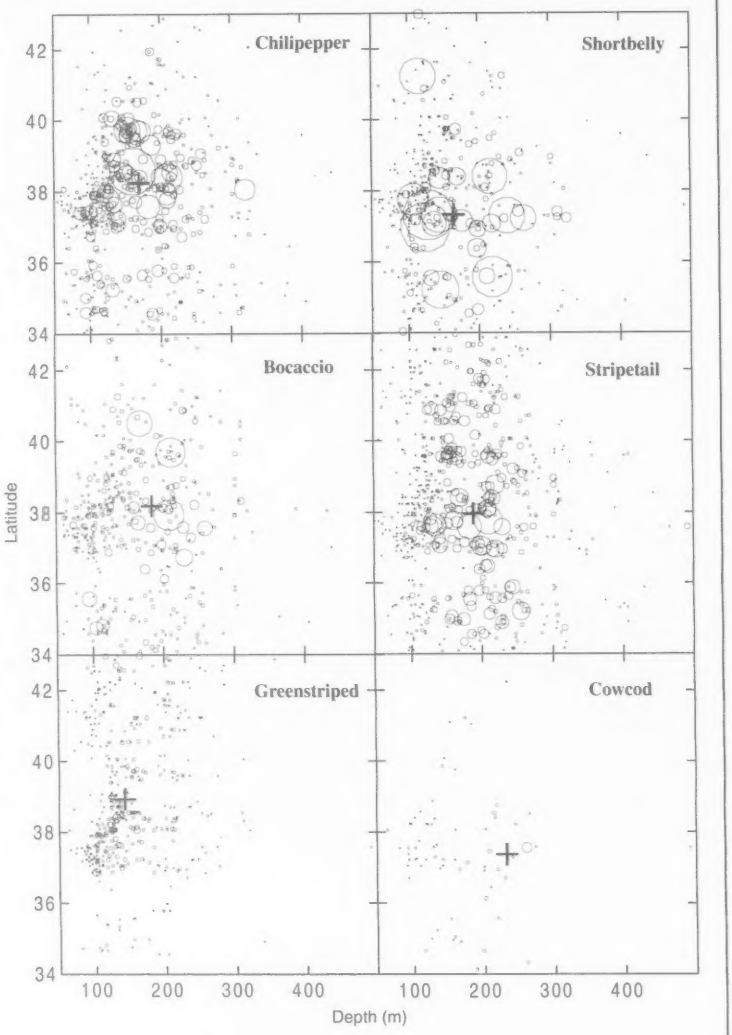

Figure 8

Plot of rockfish CPUE estimates by depth and latitude from the AFSC triennial bottom trawl survey. Circle diameters are proportional to the square root of rockfish CPUE and the bold plus symbol represents the centroid of the CPUE estimates.

1996). Another potential criticism of bottom trawl gear is its selectivity for capturing demersal fishes. Of the rockfishes included in our analysis, shortbelly and widow rockfish are two species that are known to be distributed in the water column (Lenarz, 1980; Wilkins, 1986; Chess et al., 1988). Despite their occurrence off the bottom, however, both species were captured with regularity in the bottom trawl survey (Table 1). We conclude that, at least for the trawl sector of the groundfish fishery, the results of our study should prove useful in defining assemblages for rockfish management.

As previously discussed, the assemblage descriptions given in Table 4 contain some inconsistencies with respect to the spatial distributions of the species. These apparent misclassifications may be the result of temporal variability in total rockfish abundance, as was captured by the second dimension of the MDS analysis. Because the estimated abundance of a species in our analysis was influenced by population levels of the stock at the time of each survey, which can change over time, our pooled analysis may not provide the best indication of historical assemblage asso-

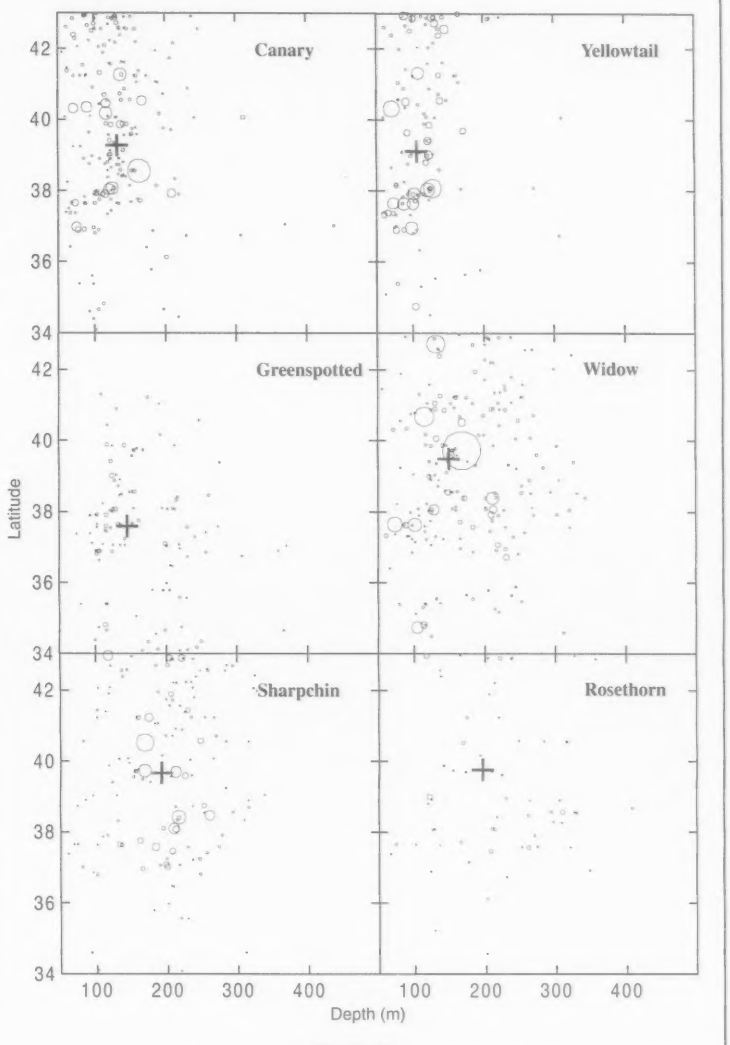

Figure 9

Plot of rockfish CPUE estimates by depth and latitude from the AFSC triennial bottom trawl survey. Circle diameters are proportional to the square root of rockfish CPUE and the bold plus symbol represents the centroid of the CPUE estimates.

ciations (see Weinberg, 1994). Furthermore, overfishing of rockfish stocks may alter spatial distributions. A good example is cowcod, which has shown a dramatic decline in abundance in recent years within the southern California Bight; most of the remaining population resides in relatively deep water (Butler et al.[3]).

Because the total abundance of each species of rockfish may have affected the results of the assemblage analysis, the species distributions were carefully re-examined and a final assemblage structure determined (Table 5). The changes from Table 4 for the k=4 groups include the placement of greenspotted rockfish into the southern shelf assemblage and canary and yellowtail rockfish into the

[3] Butler, J. L., L. D. Jacobson, J. T. Barnes, H. G. Moser, and R. Collins. 1999. Stock assessment of cowcod. *In* Pacific Fishery Management Council, Status of the Pacific Coast groundfish fishery through 1999 and recommended biological catches for 2000: stock assessment and fishery evaluation. Pacific Fishery Management Council, 2130 SW Fifth Ave., Suite 224, Portland, Oregon 97201.

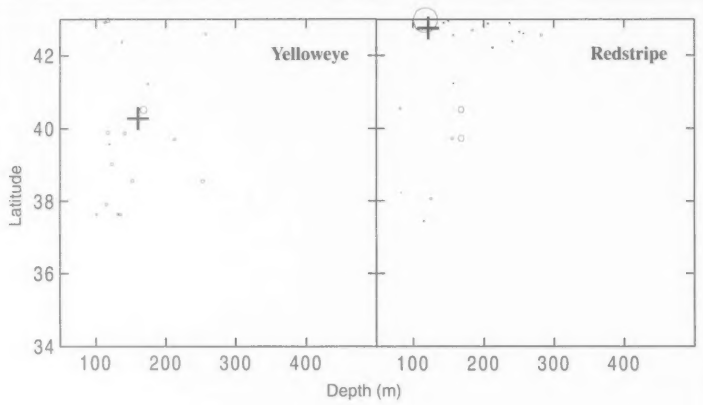

Figure 10

Plot of rockfish CPUE estimates by depth and latitude from the AFSC triennial bottom trawl survey. Circle diameters are proportional to the square root of rockfish CPUE and the bold plus symbol represents the centroid of the CPUE estimates.

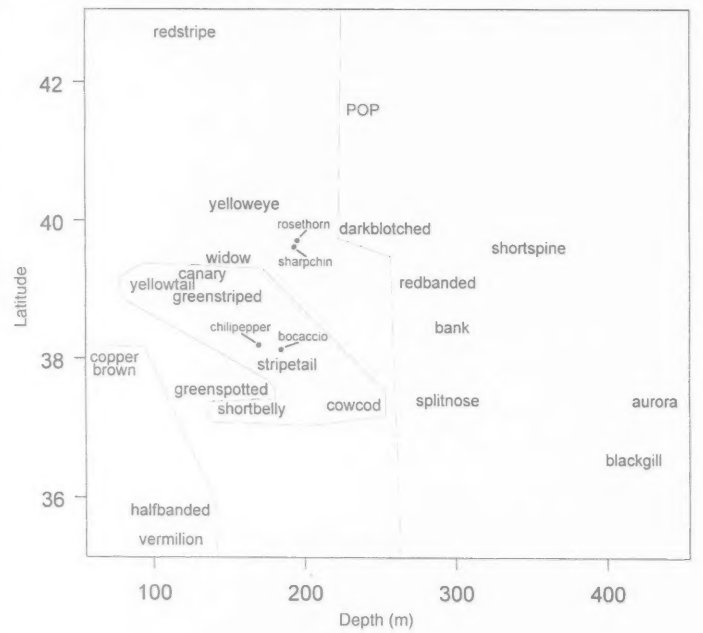

Figure 11

Plot of CPUE weighted mean depth and latitude for 26 rockfish species (center of names correspond to point estimates except for labeled points) from the AFSC triennial bottom trawl survey. Lines indicate divisions of species into clusters based on a k-medians (with k=4) partitioning analysis (see text).

northern shelf assemblage. Greenspotted rockfish has a distribution that clearly warrants its inclusion in the southern shelf assemblage. Canary and yellowtail rockfish were placed into the northern shelf assemblage because of their known abundance in northern waters outside the area of our study (see Weinberg, 1994).

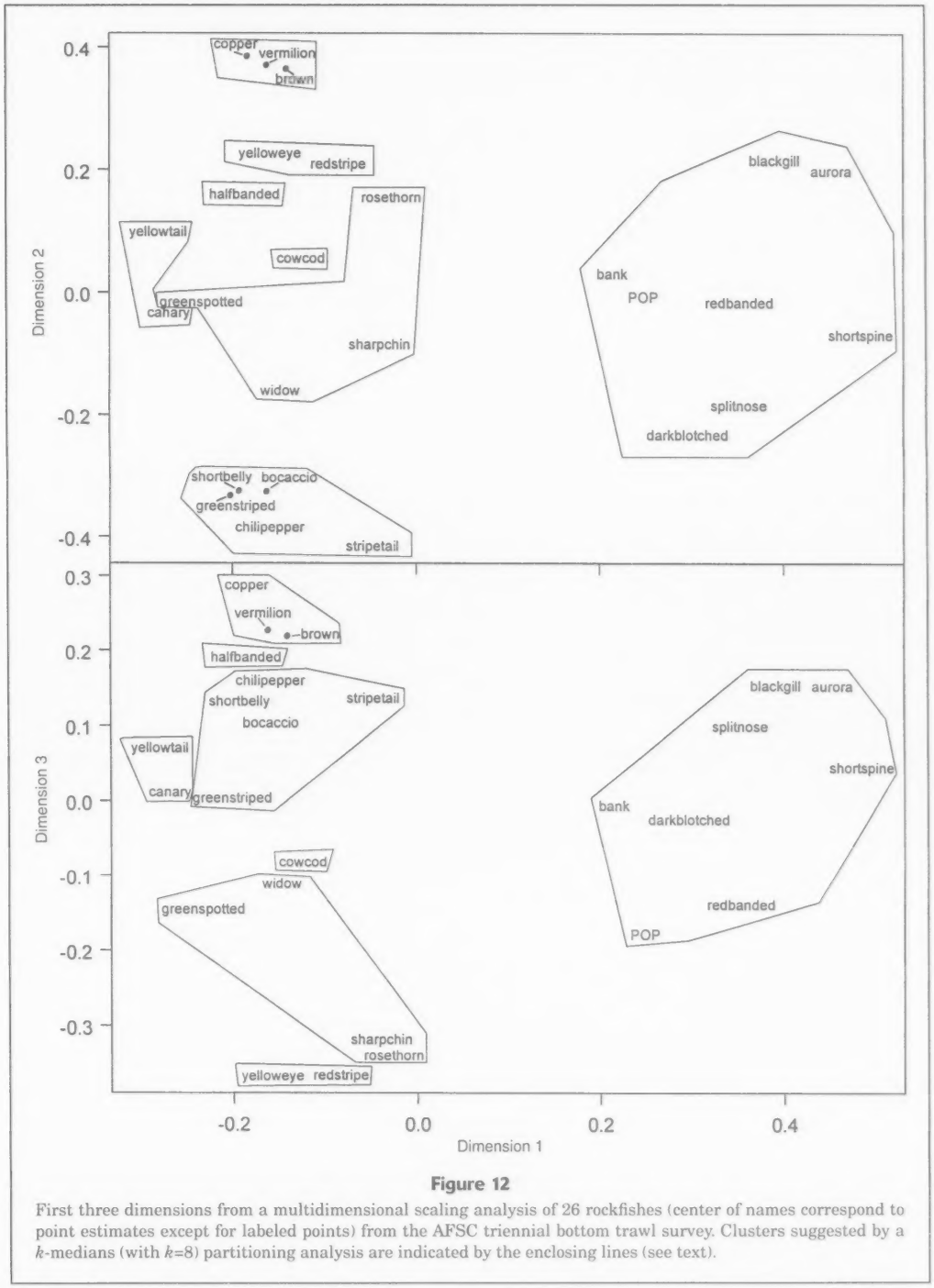

Figure 12

First three dimensions from a multidimensional scaling analysis of 26 rockfishes (center of names correspond to point estimates except for labeled points) from the AFSC triennial bottom trawl survey. Clusters suggested by a k-medians (with k=8) partitioning analysis are indicated by the enclosing lines (see text).

The dividing line between the assemblages based on depth and latitude was determined by visual examination of the distributions in Figures 6–10. The separation between shelf and slope species is roughly at 200–250 m; very few slope species were captured at depths less than 200 m. Most of the shelf species did not occur below 250 m,

Table 5

Suggested species assemblages based on distribution, ordination, and partitioning analyses completed in this study.

Habitat	Species
Deepwater slope	blackgill rockfish, aurora rockfish, shortspine thornyhead, bank rockfish, darkblotched rockfish, Pacific ocean perch, redbanded rockfish, splitnose rockfish
Nearshore	copper rockfish, vermilion rockfish, brown rockfish, halfbanded rockfish
Southern shelf	chilipepper, shortbelly rockfish, bocaccio, stripetail rockfish, greenstriped rockfish, greenspotted rockfish, cowcod
Northern shelf	canary rockfish, yellowtail rockfish, widow rockfish, sharpchin rockfish, rosethorn rockfish, yelloweye rockfish, redstripe rockfish

leaving the 200–250 m zone as an area of overlap for the two assemblages, which is exactly where the peak in richness occurred. The species in the nearshore assemblage seem to reside in waters less than 150 m depth. Perhaps the 100–150 m zone represents an area of overlap between the shelf and nearshore species.

Latitudinal divisions between species in the northern and southern shelf assemblages are not as well defined as those based on depth. It appears that most of the southern shelf group are uncommon above the Mendocino Escarpment (40.8°N latitude), with the exception of stripetail and greenspotted rockfish. The northern shelf species tend to range as far south as Monterey Canyon, leaving the area between Monterey Canyon and the Mendocino Escarpment as an area of overlap for these assemblages. This overlap is confirmed in the species richness contour plot which indicates the areas where the highest number of species were found in that latitude zone (Fig. 5). The only questionable assemblage assignment was the placement of greenstriped rockfish, which does not range south of the Monterey Canyon region but whose center of its distribution was observed in the 38.0°N latitude area.

Overall, the results of our study indicate that rockfish can be classified into fairly distinct assemblages based on their depth and latitude distributions. This study also provides estimates of the co-occurrence in the form of overlap measures for the important rockfish species off the coast of California. Both the assemblage and co-occurrence information should prove useful to fishery managers for modeling fishery dynamics, solving bycatch issues, establishing area closures, and determining effective marine reserves. Although our study highlights some uses of spatial information, the limited amount of data that is now available prevents a more thorough analysis of interannual variability in the distribution of species. We would therefore like to stress the importance of collecting more information describing the spatial distribution and co-occurrence of catches and the usefulness of those data in developing new strategies for managing west coast rockfish fisheries.

Acknowledgments

We gratefully acknowledge the assistance of Mark Wilkins, who instructed us on how to properly access and interpret RACEBASE, the Alaska Fisheries Science Center's relational data base in which the triennial continental shelf trawl survey data are stored. We also wish to thank Alec MacCall, Rick Methot, Ken Weinberg, and Mark Wilkins for their reviews of an early version of this manuscript.

Literature cited

Bloom, S. A.
1981. Similarity indices in community studies: potential pitfalls. Mar. Ecol. Prog. Ser. 5:125–U128.

Chen, L. C.
1986. Meristic variation in *Sebastes* (Scorpaenidae), with an analysis of character association and bilateral pattern and their significance in species separation. U.S. Dep. Commer., NOAA Tech. Rep. NMFS 45, 17 p.

Chess, J. R., S. E. Smith, and P. C. Fischer.
1988. Trophic relationships of the shortbelly rockfish, *Sebastes jordani*, off central California. CalCOFI Rep. 29:129–136.

Dark, T. A., and M. E. Wilkins.
1994. Distribution, abundance, and biological characteristics of groundfish off Washington, Oregon, and California, 1977–1986. U.S. Dep. Commer., NOAA Tech. Rep. NMFS 117, 73 p.

Eschmeyer, W. N. (ed.).
1998. Catalog of fishes, 2905 p. California Academy of Sciences, San Francisco, CA.

Eschmeyer, W. N., E. S. Herald, and H. Hammann.
1983. A field guide to Pacific coast fishes, 336 p. Houghton Mifflin Company, Boston, MA.

Field, J. G., K. R. Clarke, and R. M. Warwick.
1982. A practical strategy for analyzing multispecies distribution patterns. Mar. Ecol. Prog. Ser. 8:37–52.

Fox, D. S., and R. M. Starr.
1996. Comparison of commercial fishery and research catch data. Can. J. Fish. Aquat. Sci. 53:2681–2694.

Fujita, R. M., T. Foran, and I. Zevos.
1998. Innovative approaches for fostering conservation in marine fisheries. Ecol. Appl. 8(1):S139–S150.

Gabriel, W. L., and A. V. Tyler.
1980. Preliminary analysis of Pacific coast demersal fish assemblages. Mar. Fish. Rev. 42(3-4):83–88.

Gunderson, D. R.
1997. Spatial patterns in the dynamics of slope rockfish stocks and their implications for management. Fish. Bull. 95:219–230.

Hartigan, J. A., and M. A. Wong.
1979. A *k*-means clustering algorithm. Appl. Stat. 28:100–108.

Jay, C. V.
1996. Distribution of bottom-trawl fish assemblages over the

continental shelf and upper slope of the U. S. west coast, 1977–1992. Can. J. Fish. Aquat. Sci. 53:1203–1225.

Johnson, R. A., and D. W. Wichern.
1992. Applied multivariate statistical analysis, 645 p. Prentice Hall, Englewood Cliffs, NJ.

Kaufman, L., and P. J. Rousseeuw.
1990. Finding groups in data: an introduction to cluster analysis, 319 p. John Wiley & Sons, Inc., New York, NY.

Kendall, A. W., Jr.
2000. An historical review of Sebastes taxonomy and systematics. Mar. Fish. Rev. 62(2):1–23.

Krebs, C. J.
1989. Ecological methodology, 654 p. Harper Collins Publishers, Inc., New York, NY.

Leaman, B. M., and D. A. Nagtegaal.
1986. Identification of species assemblages and results of management applications for shelf and slope rockfishes off British Columbia. *In* Proceedings of the international rockfish symposium, p. 309–328. Alaska Sea Grant Report No. 87-2, University of Alaska, Anchorage, AK.

Lenarz, W. H.
1980. Shortbelly rockfish, *Sebastes jordani*: a large unfished resource in waters off California. Mar. Fish. Rev. 1980: 34–40.

Magnell, B. A., N. A. Bray, C. D. Winant, C. L. Greengrove, J. Largier, J. F. Borchardt, R. L. Bernstein, and C. E. Dorman.
1990. Convergent shelf flow at Cape Mendocino. Oceanography 3(1):4–11.

Mahon, R., S. K. Brown, K. C. T. Zwaneburg, D. B. Atkinson, K. R. Buja, L. Claflin, G. D. Howell, M. E. Monaco, R. N. O'Boyle, and M. Sinclair.
1998. Assemblages and biogeography of demersal fishes of the east coast of North America. Can. J. Fish. Aquat. Sci. 55:1704–1738.

Meuter, F-J.
1999. Spatial and temporal patterns in the Gulf of Alaska groundfish community in relation to the environment. Ph.D. diss., 199 p. Univ. Alaska Fairbanks, Fairbanks, AK.

Minchin, P.R.
1987. An evaluation of the robustness of techniques for ecological ordination. Vegetatio 69:89–107.

Pearson, D. E., and B. Erwin.
1997. Documentation of California's commercial market sampling data entry and expansion programs. U.S. Dep. Commer., NOAA Tech. Memo. NMFS 240, 65 p.

Ralston, S.
1998. The status of federally managed rockfish on the U.S. West Coast. *In* Marine harvest refugia for West Coast rockfish: a workshop (M. Yoklavich, ed.), p. 6–16. U.S. Dep. Commer., NOAA Tech. Memo. NMFS 255.
2002. West coast groundfish harvest policy. N. Am. J. Fish. Manage. 22:249–250.

Ralston, S., and J. J. Polovina.
1982. A multispecies analysis of the commercial deep-sea handline fishery in Hawaii. Fish. Bull. 80:435–448.

Rickey, M. H., and H-L. Lai.
1990. The deep water complex species mix in the Washington and Oregon trawl fishery. Wash. Dep. Fish. Tech. Rep. No. 111, 40 p.

Ripley, B. D.
1996. Pattern recognition and neural networks, 403 p. Cambridge Univ. Press, Cambridge.

Rogers, J. B., and E. K. Pikitch.
1992. Numerical definition of groundfish assemblages caught off the coasts of Oregon and Washington using commercial fishing strategies. Can. J. Fish. Aquat. Sci. 48:1264–1272.

Rousseeuw, P. J.
1987. Silhouettes: a graphical aid to the interpretation and validation of cluster analysis. J. Comp. Appl. Math. 20: 53–65.

Sampson, D. P., and P. R. Crone.
1997. Commercial fisheries data collection procedures for U.S. Pacific coast groundfish. U.S. Dep. Commer., NOAA Tech. Memo. NMFS 31, 140 p.

Surfer.
1995. Surfer for Windows user's guide, version 6, 538 p. Golden Software, Inc., Golden, CO.

Weinberg, K. L.
1994. Rockfish assemblages of the middle shelf and upper slope off Oregon and Washington. Fish. Bull. 92:620–632.

Wilkins, M. E.
1986. Development and evaluation of methodologies for assessing and monitoring the abundance of widow rockfish, *Sebastes entomelas*. Fish. Bull. 84:287–310.

Wilkins, M. E., M. Zimmermann, and K. L. Weinberg.
1998. The 1995 Pacific Coast bottom trawl survey of groundfish resources: estimates of distribution, abundance, and length and age composition. U.S. Dep. Commer., NOAA Tech. Memo. NMFS 89, 138 p.

Properties of the residuals from two tag-recovery models*

Robert J. Latour
John M. Hoenig
Department of Fisheries Science
Virginia Institute of Marine Science
College of William and Mary
Gloucester Point, Virginia 23062
E-mail address (for R. J. Latour): latour@vims.edu

Kenneth H. Pollock
Biomathematics Graduate Program
Department of Statistics
North Carolina State University
Raleigh, North Carolina 27695

Researchers often use multiyear tag-recovery studies to assess fish populations; yet deriving useful stock assessment parameter estimates from the resulting data can be difficult. The reliability of those parameter estimates generally depends on data quality and meeting the assumptions inherent to the models used for analysis. As a result, practical application of multiyear tag-recovery models generally requires that a large portion of the data analysis involve investigation and evaluation of biases due to potential assumption violation.

Brownie et al. (1985) developed a class of models that has become widely used for the analysis of multiyear tag-recovery data. These models constitute a generalization of the class of models developed by Seber (1970), which have recently been resurrected as an important tool for the analysis of multiyear tag-recovery data by the development of the software program MARK (White and Burnham, 1999). Although these models are fairly simple and robust, in practical situations at least one of the assumptions is often not supported by the data.

Approaches that are commonly used to assess the fit of multiyear tag-recovery models include the formal goodness-of-fit test, Akaike's information criterion (AIC) (Akaike, 1973; Burnham and Anderson, 1992; Burnham et al., 1995) and other related measures such as quasilikelihood AIC (Akaike, 1985). Although these measures are informative about overall model fit, they do not provide any information about why a model fit is poor or which assumption(s) is (are) possibly in violation. To remedy this problem, Latour et al. (2001a) conducted a series of simulations and demonstrated that distinct patterns in model residuals will be evident if particular assumptions are violated. They discussed in detail the residuals associated with the time-specific parameterizations of the Seber (1970) and Brownie et al. (1985) models, as well as the time-specific instantaneous rates model developed by Hoenig et al. (1998).

The genesis of the work by Latour et al. (2001a) can be traced to two particular applications of multiyear tag-recovery models. Specifically, Latour et al. (2001b) analyzed tag-recovery data of red drum (*Sciaenops ocellatus*) in South Carolina and found systematic patterns along the diagonals in the upper right corner of the residuals matrix. Frusher and Hoenig (2001) applied a series of tag-recovery models to Australian rock lobster (*Jasus edwardsii*) data and found consistent patterns in the columns of the residuals matrix. In both instances, the researchers could only speculate as to the cause of these patterns in residuals. Although the simulations conducted by Latour et al. (2001a) have since provided reasonable explanations for the observed patterns, the development of those diagnostic procedures led to the discovery that the residuals associated with the time-specific Seber (1970) and Brownie et al. (1985) models are subject to several constraints.

This note contains a series of simple mathematical arguments that verify the assertions made by Latour et al. (2001a) about the residuals of the time-specific parameterizations of the Seber (1970) and Brownie et al. (1985) models. Unfortunately, the constraints inherent to the residuals of those models partially cloud a researcher's ability to assess the existence of a pattern. As such, knowledge of the inherent properties of the residuals of these models is of particular importance, especially because the time-specific parameterizations are commonly used for the analysis of tag-recovery data.

Materials and methods

Multiyear tag-recovery models

Multiyear tagging data are generally represented by an upper triangular matrix of tag recoveries. For example, the matrix for a study with I years of tagging and J years of tag-recovery would be, when $I = J$,

$$r = \begin{bmatrix} r_{11} & r_{12} & \cdots & r_{1J} \\ - & r_{22} & \cdots & r_{2J} \\ \vdots & \vdots & \ddots & \vdots \\ - & - & - & r_{IJ} \end{bmatrix}, \qquad (1)$$

where r_{ij} = the number of tags recovered in year j that were released in year i (note, $i = 1, \ldots, I; j=i, \ldots, J$).

Application of multiyear tag-recovery models generally involves constructing a matrix of expected values and comparing them to the observed

* Contribution 2490 of the Virginia Institute of Marine Science, Gloucester Point, VA 23062.

Manuscript accepted 10 July 2002.
Fish. Bull. 100:856–860 (2002).

data. The matrix of expected values corresponding to the time-specific parameterization of Brownie et al. (1985), which is referred to as model 1, takes the form

$$E_r = \begin{bmatrix} N_1 f_1 & N_1 S_1 f_2 & \cdots & N_1(S_1 \cdots S_{J-1}) f_J \\ - & N_2 f_2 & \cdots & N_2(S_2 \cdots S_{J-1}) f_J \\ \vdots & \vdots & \ddots & \vdots \\ - & - & - & N_I f_J \end{bmatrix}, \quad (2)$$

where N_i = the number tagged in year i;
f_i = the tag recovery rate in year i; and
S_i = the survival rate in year i.

As stated above, the Brownie et al. (1985) models constitute a generalization of those developed by Seber (1970). The only difference lies in the definition of the tag recovery rate. Specifically, Seber (1970) modeled the tag recovery rate in year i as $f_i = (1 - S_i)r_i$, where r_i is the rate at which tags are reported from killed fish in year i regardless of the source of mortality. The matrix of expected values associated with time-specific parameterization of the Seber (1970) models, which we will refer to as model 1*, takes the form (when $I = J$)

$$E_r = \begin{bmatrix} N_1(1-S_1)r_1 & N_1 S_1(1-S_2)r_2 & \cdots & N_1(S_1 \cdots S_{J-1})(1-S_J)r_J \\ - & N_2(1-S_2)r_2 & \cdots & N_2(S_2 \cdots S_{J-1})(1-S_J)r_J \\ \vdots & \vdots & \ddots & \vdots \\ - & - & - & N_1(1-S_J)r_J \end{bmatrix}. \quad (3)$$

The data in each row of Equation 1 follow a multinomial distribution and maximum likelihood estimation can be used to derive parameter estimates from either model 1 or model 1*. Program MARK has emerged as the leading software package for deriving these estimates (White and Burnham, 1999).

Patterns in residuals

Latour et al. (2001a) manipulated a hypothetical perfect data set (i.e. the observed number of tag recoveries was equal to the expected number of tag recoveries) to simulate four specific forms of assumption violation for multiyear tag-recovery models. For each scenario, they analyzed the modified data with model 1, model 1*, and a time-specific parameterization of the instantaneous rates (IR) models (Hoenig et al., 1998) and noted any patterns in the residuals matrix that resulted from each particular assumption violation. Specifically, they found the following: 1) the presence of nonmixing (which violates the assumption that the tagged population is representative of the target population) leads to consistent patterns on the main and super diagonals of the residuals matrix (the main diagonal contains the (1,1),(2,2),...,(I,I) cells and the first super diagonal contains the (1,2),(2,3),...(I–1,I) cells in a square matrix); 2) permanent emigration from the study area of individuals within a tagged cohort (which violates the assumption that all tagged fish within a cohort are subject to the same annual survival and tag-recovery rates) leads to a pattern of negative residuals along the diagonals of the upper right corner of the residuals matrix; 3) tag-induced mortality or immediate loss of tags due to poor tagging (which violates the assumptions that tags are not lost and survival rates are not affected by tagging) leads to row patterns in the residuals matrix (note that these patterns are detectable only in the residuals matrix of the IR model); and 4) a change in the natural mortality rate (which violates the frequently imposed assumption that natural mortality is constant over time) leads to column patterns in the residuals matrix (again, this only applies to the IR model).

Constraints on residuals of model 1 and model 1*

Latour et al. (2001a) asserted without proof that the residuals associated with model 1 and model 1* are subject to several constraints. Specifically, they stated that the relationship $E_{II} = r_{II}$ always holds, regardless of the number of years of tagging and tag-recovery (note that E_{ij} is the expected number of tags recovered in year j that were released in year i). This implies that the observed data and the expected value associated with the (1,1) cell are always identical and that the residual for that cell is always equal to zero. They also stated that the residuals associated with the implicit "never seen again" category are also always equal to zero (recall that under a multinomial formulation, one of the possible outcomes is to never recapture a tagged fish). Collectively, these constraints imply that the residuals matrix derived from using model 1 or model 1* to analyze data from a study with I years of tagging and J years of tag-recovery takes the form

$$resid = \begin{bmatrix} 0.00 & (r_{12} - E_{12}) & \cdots & (r_{1,J} - E_{1,J}) & 0.00 \\ - & (r_{22} - E_{22}) & \cdots & (r_{2,J} - E_{2,J}) & 0.00 \\ \vdots & \vdots & \ddots & \vdots & 0.00 \\ - & - & \cdots & (r_{I,J} - E_{I,J}) & 0.00 \end{bmatrix}, \quad (4)$$

where r_{ij} and E_{ij} are as defined previously and the last column of the matrix represents the residuals associated with the "never seen again" category.

In addition to the aforementioned zero residuals, Latour et al. (2001a) stated that the sum of each row and each column of the residuals matrix must equal zero and that for the case when $I = J$ (i.e. the recovery matrix is square), the constraint that $E_{II} = r_{II}$ is also present (i.e. the residual associated with the (I, I) cell is always equal to zero).

In the context of searching for patterns in residuals, these constraints have the following implications. First, the presence of residuals that are constrained to be zero essentially reduces the total number of values that are available for inspection and ultimately forces conclusions about the existence of a pattern to be based on the signs of fewer residuals. For short-term tagging studies (e.g. 3–4 years), the loss of residuals for inspection makes it extremely difficult to evaluate model performance because each row, column, and diagonal of the residuals matrix already contains only a few values. Second, because the sum of each row of the residuals matrix must total zero, and

because the residuals corresponding to the "never seen again" cells are zero, it is not possible for a row pattern to be expressed in the residuals matrices of either model 1 or model 1*. This constraint renders it very difficult to detect assumption violations that are cohort-specific—the most common being tag-induced and handling mortality and short-term tag loss.

Results

To verify that the aforementioned constraints about the structure of the residuals matrices associated with model 1 and model 1* are true, we offer the following mathematical arguments. The proofs simply involve algebraic manipulation of equations involving the analytical formulae for the maximum likelihood parameter estimates (MLE) of model 1. The formulae for the MLEs were originally developed by Seber (1970) and can be applied to both to model 1 and model 1* (because r_i can be expressed as a function of S_i and f_i, the invariance property of MLEs implies that an MLE of r_i can be obtained by the transform). Hence, the proofs are developed for model 1, and we note that similar arguments could be constructed for the residuals of model 1*.

Recall that the analytical solutions for the maximum likelihood estimates of f_i and S_i from Seber (1970) and Brownie et al. (1985) are given by

$$\hat{f}_i = \frac{R_i C_i}{N_i T_i} \quad \text{and} \quad \hat{S}_i = \frac{R_i}{N_i}\frac{(T_i - C_i)}{T_i}\frac{N_{i+1}}{R_{i+1}},$$

where R_i and C_i are the row and column totals of the observed data in year i; and

$$\begin{aligned} T_1 &= R_1 \\ T_i &= R_i + T_{i-1} - C_{i-1} \qquad i = 2, \ldots, I \\ T_{I+j} &= T_{I+j-1} - C_{I+j-1} \qquad j = 1, \ldots, J-I \text{ if } J > I. \end{aligned}$$

The (1,1) cell

To show that the residual associated with the (1,1) cell is always zero, we must demonstrate that the difference between the observed and estimated expected value in the first cell is always zero. Hence, we have

$$\begin{aligned} r_{11} - \hat{E}_{11} &= r_{11} - N_1\hat{f}_1 \\ &= r_{11} - N_1\left(\frac{R_1 C_1}{N_1 T_1}\right) \text{(substituting for } \hat{f}_1) \\ &= r_{11} - C_1 \text{ (since } T_1 = R_1) \\ &= r_{11} - r_{11} = 0 \text{ (because the column total} \\ &\qquad \text{in the first recovery year is } r_{11}). \end{aligned}$$

The (*I*,*I*) cell when *I* = *J*

To show that the residual associated with the (I,I) cell is always zero when $I = J$, again we must demonstrate that the difference between the observed and estimated expected values in that cell is always zero. Hence, we have

$$\begin{aligned} r_{II} - \hat{E}_{II} &= r_{II} - N_I\hat{f}_I \\ &= r_{II} - N_I\left(\frac{R_I C_I}{N_I T_I}\right) \text{(substituting for } \hat{f}_I) \\ &= r_{II} - R_I \text{ (because } T_I = C_I) \\ &= r_{II} - r_{II} = 0 \text{ (because the row total in the} \\ &\qquad \text{final recovery year is } r_{II}). \end{aligned}$$

Column sums when *I* = *J*

To show that the column sums of the residuals matrix equal zero, we must demonstrate the column sum of the observed data equals that of the expected values. Consider the sum of the expected values associated with the I^{th} column of the recovery matrix, that is

$$Q = E_{1I} + E_{2I} + \cdots + E_{II} = N_1(\hat{S}_1 \cdots \hat{S}_{I-1})\hat{f}_I + N_2(\hat{S}_2 \cdots \hat{S}_{I-1})\hat{f}_I + \cdots + N_{I-1}\hat{S}_{I-1}\hat{f}_I + N_I\hat{f}_I.$$

Now substitute for $\hat{f}_i$ and $\hat{S}_i$ on the right hand side:

$$Q = N_1\left(\left(\frac{R_1}{N_1}\frac{(T_1 - C_1)}{T_1}\frac{N_2}{R_2}\right)\cdots\left(\frac{R_{I-1}}{N_{I-1}}\frac{(T_{I-1} - C_{I-1})}{T_{I-1}}\frac{N_I}{R_I}\right)\right)\left(\frac{R_I C_I}{N_I T_I}\right) + N_2\left(\left(\frac{R_2}{N_2}\frac{(T_2 - C_2)}{T_2}\frac{N_3}{R_3}\right)\cdots\left(\frac{R_{I-1}}{N_{I-1}}\frac{(T_{I-1} - C_{I-1})}{T_{I-1}}\frac{N_I}{R_I}\right)\right)\left(\frac{R_I C_I}{N_I T_I}\right) + \cdots + N_{I-1}\left(\frac{R_{I-1}}{N_{I-1}}\frac{(T_{I-1} - C_{I-1})}{T_{I-1}}\frac{R_I}{N_I}\right)\left(\frac{R_I C_I}{N_I T_I}\right) + N_I\left(\frac{R_I C_I}{N_I T_I}\right).$$

Cancel terms and factor out the term $\frac{C_I}{T_I}$:

$$Q = \left(\frac{C_I}{T_I}\right)\left[\left(\frac{R_1(T_1 - C_1)}{T_1}\right)\left(\frac{T_2 - C_2}{T_2}\right)\cdots\left(\frac{T_{I-1} - C_{I-1}}{T_{I-1}}\right) + \left(\frac{R_2(T_2 - C_2)}{T_2}\right)\left(\frac{T_3 - C_3}{T_3}\right)\cdots\left(\frac{T_{I-1} - C_{I-1}}{T_{I-1}}\right)\right] + \cdots + \left(\frac{C_I}{T_I}\right)\left[\left(\frac{R_{I-1}(T_{I-1} - C_{I-1})}{T_{I-1}}\right) + R_I\right].$$

Systematically factor out terms of the form $\frac{(T_i - C_i)}{T_i}$ (recall that $T_1 = R_1$):

$$Q = \left(\frac{C_I}{T_I}\right)\left[\left(\frac{T_{I-1}-C_{I-1}}{T_{I-1}}\right)\left[\left(\frac{T_{I-2}-C_{I-2}}{T_{I-2}}\right)\right.\right.$$

$$\left.\left.\left[\cdots\left[\left(\frac{T_2-C_2}{T_2}\right)(R_1-C_1+R_2)+R_3\right]+R_4\right]+\cdots+R_{I-1}\right]+R_I\right].$$

Utilize the definition of $T_i = R_i + T_{i-1} - C_{i-1}$ to systematically simplify and cancel starting with the innermost parenthetic expression:

$$Q = \left(\frac{C_I}{T_I}\right)\left[\left(\frac{T_{I-1}-C_{I-1}}{T_{I-1}}\right)T_{I-1}+R_I\right]$$

$$= \left(\frac{C_I}{T_I}\right)[T_{I-1}-C_{I-1}+R_I]$$

$$= \left(\frac{C_I}{T_I}\right)T_I = C_I = r_{1I}+r_{2I}+\cdots+r_{IJ},$$

which demonstrates that the column sum of expected values equals the column sum of observed recoveries, as desired for the I^{th} column. Similar arguments hold for the other columns.

Column sums when $I > J$

The proof that the column sums of the residuals matrix equal zero when the recovery matrix is nonsquare is similar to the proof above except for making use of the definition $T_{I+j} = T_{I+j-1} - C_{I+j-1}$.

Row sums when $I = J$

To show that the row sums (excluding the "never seen again" cell) of the residuals matrix equal zero, we must demonstrate the sum of the observed data equals that of the expected values. Consider the sum of the expected values associated with the first row of the recovery matrix:

$$Q = E_{11}+E_{12}+\cdots+E_{1I} = N_1\hat{f}_1 + N_1\hat{S}_1\hat{f}_2+\cdots+N_1(\hat{S}_1\cdots\hat{S}_{I-1})\hat{f}_I.$$

Now substitute for $\hat{f}_i$ and $\hat{S}_i$ on the right hand side:

$$Q = N_1\left(\frac{R_1C_1}{N_1T_1}\right)+N_1\left(\frac{R_1}{N_1}\frac{(T_1-C_1)}{T_1}\frac{N_2}{R_2}\right)\left(\frac{R_2C_2}{N_2T_2}\right)+$$

$$\cdots+N_1\left(\left(\frac{R_1}{N_1}\frac{(T_1-C_1)}{T_1}\frac{N_2}{R_2}\right)\cdots\right.$$

$$\left.\left(\frac{R_{I-1}}{N_{I-1}}\frac{(T_{I-1}-C_{I-1})}{T_{I-1}}\frac{N_I}{R_I}\right)\right)\left(\frac{R_IC_I}{N_IT_I}\right).$$

Cancel and factor out the term $T_1 - C_1$ (recall that $T_1 - R_1$):

$$Q = \left(\frac{R_1C_1}{T_1}\right)+(T_1-C_1)\left[\frac{C_2}{T_2}+\left(\frac{T_2-C_2}{T_2}\right)+\right.$$

$$\left.\cdots+\left(\frac{T_2-C_2}{T_2}\right)\left(\frac{T_3C_3}{T_3}\right)\cdots\left(\frac{T_{I-1}-C_{I-1}}{T_{I-1}}\right)\left(\frac{C_I}{T_I}\right)\right].$$

Systematically factor out terms of the form $\frac{(T_i - C_i)}{T_i}$:

$$Q = \left(\frac{R_1C_1}{T_1}\right)+(T_1-C_1)$$

$$\left[\frac{C_2}{T_2}\left(\frac{T_2-C_2}{T_2}\right)\left[\frac{C_3}{T_3}+\cdots+\left[\frac{C_{I-1}}{T_{I-1}}+\left(\frac{T_{I-1}-C_{I-1}}{T_{I-1}}\right)\right]\left[\frac{C_I}{T_I}\right]\cdots\right]\right].$$

The expression inside the innermost square brackets is equal to 1 (recall $T_I = C_I$). Hence, we have

$$Q = \left(\frac{R_1C_1}{T_1}\right)+(T_1-C_1) = \frac{R_1C_1+R_1T_1-R_1C_1}{T_1} = R_1$$

$$= r_{11}+r_{12}+\cdots+r_{1I},$$

which shows the sum of the expected values in row 1 is equal to the sum of the observed data. Similar arguments hold for the other rows.

Row sums when $I > J$

As with the proof of the column sums when $I > J$, the defintion $T_{I+j} = T_{I+j-1} - C_{I+j-1}$ is needed to show the row sum of a nonsquare matrix (excluding the "never seen again" cells) are zero.

"Never seen again" cells

The likelihood function for the Brownie-type model is a product multinomial and the parameters for each row are constrained to sum to one. Therefore, the expected values in a row are simply an apportionment of the number tagged to the years of recovery and the "never seen again" category. Hence, the sum of the estimated expected values has to equal the row sum (including the "never seen again" cell), which implies the residuals of the "never seen again" cells are always equal to zero.

Discussion

The residuals of multiyear tag-recovery models can be very helpful for evaluating model performance. Unfortunately, examining the residuals matrix for patterns is not a commonly employed procedure for assessing model fit in practical situations. The work by Latour et al. (2001a) was intended

to demonstrate the insight a researcher can acquire by using residuals as a diagnostic probe to gauge the possibility of assumption violation. Similarly, the work presented here is intended to further guide researchers by explicitly delineating the properties of the residuals associated with two commonly applied multiyear tag-recovery models.

Model 1 and model 1* represent parameterizations of only two classes of tag-recovery models. Properties of the residuals associated with other classes of models (e.g. movement models, age-structured tag-recovery models, capture-recapture models) have not been studied. We feel strongly that similar types of insight about model performance and model fit can be acquired by examining the residuals for patterns. As such, we recommend that the residuals from other classes of models be more thoroughly investigated.

Literature cited

Akaike, H.
1973. Information theory as an extension of the maximum likelihood principle. *In* Second international symposium on information theory (B. N. Petrov and F. Csaki. eds.), p. 267–281. Akademiai Kiado, Budapest.

Akaike, H.
1985. Prediction and entropy. *In* A celebration of statistics (A. C. Atkinson and S. E. Fienberg, eds.), p. 1–24. Springer, New York, NY.

Brownie, C., D. R. Anderson, K. P. Burhnam, and D. S. Robson.
1985. Statistical inference from band recovery data: a handbook, 2nd ed., 305 p. U.S. Fish and Wildl. Serv. Resour. Publ. 156.

Burnham, K. P., and D. R. Anderson.
1992. Data-based selection of an appropriate biological model: the key to modern data analysis. *In* Wildlife 2001: populations (D. R. McCullough and R. H. Barrett, eds.), p. 16–30. Elsevier Science Publishers, London.

Burnham, K. P., G. C. White, and D. R. Anderson.
1995. Model selection strategy in the analysis of capture-recapture data. Biometrics 51:888–898.

Frusher, S. D., and J. M. Hoenig.
2001. Estimating natural and fishing mortality and tag reporting rate of rock lobster from a multiyear tagging model. Can. J. Fish. Aquat. Sci. 58:2490–2501.

Hoenig, J. M., N. J. Barrowman, W. S. Hearn, and K. H. Pollock.
1998. Multiyear tagging studies incorporating fishing effort data. Can. J. Fish. Aquat. Sci. 55:1466–1476.

Latour, R. J., J. M. Hoenig, J. E. Olney, and K. H. Pollock.
2001a. Diagnostics for multiyear tagging models with application to Atlantic striped bass (*Morone saxatilis*). Can. J. Fish. Aquat. Sci. 58:1717–1726.

Latour, R. J., K. H. Pollock, C. A. Wenner, and J. M. Hoenig.
2001b. Estimates of fishing and natural mortality for red drum *Sciaenops ocellatus* in South Carolina waters. N. Am. J. Fish. Manage. 21:733–744.

Seber, G. A. F.
1970. Estimating time-specific survival and reporting rates for adult birds from band returns. Biometrika 57:313–318.

White, G. C., and K. P. Burnham.
1999. Program MARK–survival estimation from populations of marked animals. Bird Study 46:120–138.

Preliminary study on the use of neural arches in the age determination of bluntnose sixgill sharks (*Hexanchus griseus*)

Gordon A. McFarlane
Jacquelynne R. King
Mark W. Saunders

Pacific Biological Station
Fisheries and Oceans Canada
Nanaimo
British ColumbiaV9R 5K6, Canada
E-mail address (for G. A. McFarlane): McFarlaneS@pac.dfo-mpo.gc.ca

Conventional structures used for age determinations of teleost fishes (e.g. fin rays, otoliths, scales) cannot be used for elasmobranchs in which these structures are cartilaginous. However, vertebral centra with systematic deposits of calcium phosphate, have been used for age estimation in a number of elasmobranch species such as the tiger shark (*Galeocerdo cuvier*), scalloped hammerhead (*Sphyrna lewini*), and several smoothhound sharks (*Mustelus* spp.) (Cailliet, 1990). Cailliet et al. (1983) provided preparation techniques for enhancing and examining vertebral bands in these elasmobranchs. Unfortunately, the vertebral centra of a number of sharks, including bluntnose sixgill sharks (*Hexanchus griseus*), are too poorly calcified to provide age information (Cailliet, 1990). Previous attempts to age sixgill sharks by using vertebral centra have been unsuccessful (Ebert, 1986). Sharks with poorly calcified vertebral centra tend to be either deep-water species or from relatively primitive families (Cailliet, 1990). However, systematic deposits of calcium phosphate have also been found in chondrocranium, jaws, visceral arches, fin cartilage, claspers, neural and haemal arches (Clement, 1992).

Bluntnose sixgill sharks (hereafter referred to as simply "sixgill sharks") are one of the largest and most primitive species of elasmobranchs. They have a world-wide distribution and in the north-east Pacific Ocean range from the Aleutian Islands to Baja, California (Hart, 1973). Because they are deep-water inhabitants occupying depths up to 2500 m along the outer continental shelf and upper slope waters (Compagno, 1984; Ebert, 1994), little is known about their biology. Sixgill sharks are about 65–70 cm at birth and the maximum length recorded is 482 cm (Castro, 1983). They are ovoviviparous and have reported litter sizes ranging from 22 to 108 (Compagno, 1984; Ebert, 1992). The estimated size-at-maturity for females is 396 cm (Ebert, 1992), although capture of mature sixgill sharks is rare. It is likely that the young inhabit inshore waters (Compagno, 1984).

Off the west coast of Canada, an experimental fishery for sixgill sharks was initiated in the early 1990s but was terminated because of conservation concerns. Recently, there has been a renewed interest in a fishery, both commercial and sport, for the species. Incomplete knowledge regarding the biology and life history of sixgill sharks remains a concern. Given the continuing interest in a fishery (commercial and sport) and potential conservation concerns, we investigated the use of neural arches as an alternate body structure to use for the age determination of sixgill sharks. We describe the staining technique used and the bands (annuli) observed. We suggest that our technique represents a possible avenue for developing an aging technique for various elasmobranchs, particularly those with poorly calcified vertebral centra.

Methods

From May through September 1994, as part of a co-operative industry–government sixgill shark tagging program, 259 sixgill sharks were captured with hook and line gear off the west coast of Vancouver Island, British Columbia, Canada. Fishing occurred within five main areas: Kyoquot Sound (50°00′N and 127°20′W), Esperanza Inlet (49° 45′N 127°00′W), Nootka Sound (49° 25′N and 126°40′W), Tofino Inlet (49° 05′N and 125°40′W), and Barkley Sound (48°50′N and 125°20′W). A sample of ten sharks was obtained for age determination research. Total length (TL, cm) and sex were recorded for each shark.

A portion of the vertebral column containing 15–20 vertebrae, including the neural and haemal arches, was removed just posterior to the head and immediately frozen. In the laboratory the vertebral column section was thawed. The connective tissue and the outer layer of cartilage were removed from each vertebra and neural arch (Fig. 1A) by soaking them in bleach for 15 minutes and rinsing in distilled water. Some teasing away of tissue was required. For each set of vertebrae, five neural arches were separated from the vertebral centra (Fig. 1B). A single dorsoventral cut was made in each neural arch to expose the inner portions (Fig. 1B). The silver nitrate staining technique for revealing calcium deposits in vertebral centra of other shark species (Cailliet et al., 1983) was modified and applied to the neural arches. Each arch was soaked in 150 mL of 1% silver nitrate while exposed to wide spectrum light (320–400 nm). Soak times in silver nitrate varied according to the size of the arch, but all soak times lasted at least one hour. The degree of staining was assessed on an initial arch for each shark. If required, subsequent arches were restained in the silver nitrate solution and removed at 15–30 minute intervals after removal of the first arch.

Manuscript accepted 27 May 2002.
Fish. Bull. 100:861–864 (2002).

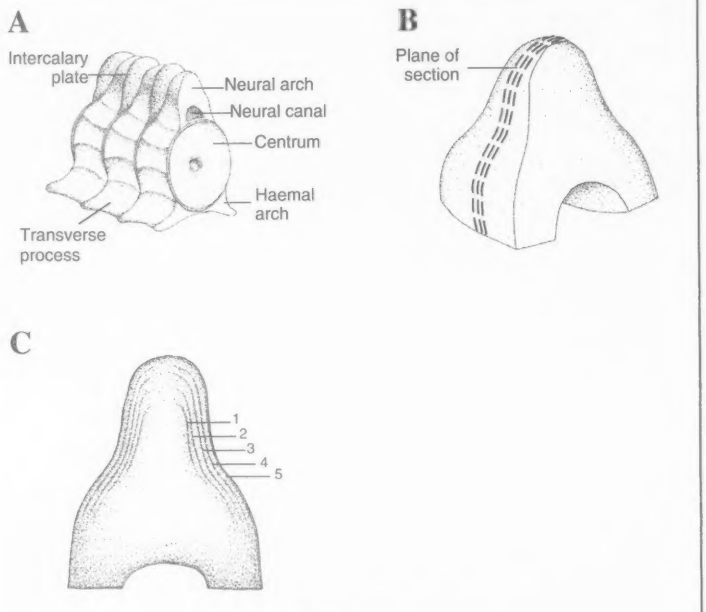

Figure 1

(**A**) Schematic diagram of the section of vertebral column with attached neural and haemal arches from a bluntnose sixgill shark. (**B**) Neural arch; an initial dorsoventral cut was made perpendicular to the arch face prior to saturation with silver nitrate solution. Subsequent sections (dotted lines) were made to reveal banding patterns. (**C**) Sectioned neural arch showing band patterns.

After soaking in silver nitrate, each neural arch was rinsed with distilled water to remove any excess solution. A scalpel was used to cut sections approximately 2–3 mm thick, parallel to the initial cut (Fig. 1B). Sections were placed under the white light (400–700 nm) of a dissecting microscope for a few minutes to allow bands to appear (Fig. 1C). A 2–3 minute soak in 5% sodium thiosulphate (Cailliet et al., 1983) was unsuccessful in halting the development process and fixing the chemical substitution of calcium salts for silver nitrate. However, a 3–5 minute soak in Kodak Stop Bath SB-1a® (1.0 L water; 125 mL 28% acetic acid) did halt the development process. The stained neural arch sections were mounted on a microscope slide with an acrylic toluene mounting medium.

Results

Of the ten sharks sampled, eight of the sharks were female (130–349 cm TL), and two were male (140 and 242 cm TL). All sharks were immature. The soak time required for the silver nitrate to penetrate the whole neural arch varied between arches of similarly sized sharks and even between arches from the same shark. Generally arches from sharks less than 200 cm TL, 200–250 cm TL, 250–300 cm TL, and greater than 300 cm TL were removed after 1, 2, 3, and 4 hours respectively. It was necessary to use several neural arches per shark in order to differentiate a clear set of bands (annuli).

The staining occurred only near the outer portion of each arch, and this left the central portion unstained (Figs. 2 and 3). Distinct, thin, dark bands were discernible in nine of the 10 sets of neural arches examined (e.g. Fig. 2). Bands in the neural arches from the 349 cm female were not all clearly defined even after soaking in the silver nitrate solution for eight hours. In general, bands appeared at regular intervals (Fig. 2). The widths between bands were asymmetrical along the whole edge of the neural arch. These widths were greater along the top edge compared to widths at the side edges (Fig. 3). In some neural arches, the bands were not continuous (Figs. 3 and 4), which made examination of different portions of the arch necessary in order to count the number of bands formed. In some arches, bands were identifiable but fainter towards the inner portions (Fig. 4). These bands appeared granular, but patterns were still detectable (Fig. 4). The number of bands increased linearly with the total length of the shark (Fig. 5). By using 67.5 cm as the median length at birth (Castro, 1983), the mean estimated growth rate was 25 cm/band (SD=4, n=9). Because all of the specimens in our study were immature, a change in the growth rate was not observed, as would be expected when size at maturity was reached.

Figure 2
A stained neural arch from a 207-cm (total length) female bluntnose sixgill shark. Note that the staining occurs along the outer third portion of the arch. Five bands are indicated by dots.

Figure 3
A stained neural arch from a 242-cm (total length) male bluntnose sixgill shark. Seven bands are indicated by dots. Note that the widths between bands are asymmetrical and the bands are discontinuous along the whole perimeter.

Discussion

The nature of the staining observed on the neural arches suggests that these structures have a potential use in the age determination of elasmobranchs. In sixgill sharks, the bands were distinct and appeared at regular intervals. The number of bands per neural arch increased with total length of the shark, suggesting their potential for age determination. The banding occurred only on the outer portions, indicating that the calcium was deposited after the proximal portion of the arches developed, probably after birth. The methodology used in our study for the staining of calcium deposits in neural arches offers some promise for age determination of sixgill sharks. Future research is required to refine the method by determining sectioning methods and thickness, optimum staining times, or perhaps alternative solution concentrations. For example, it might be more effective to cut neural arches into thin sections prior to soaking in silver nitrate rather than to soak larger portions and then section them.

Calcium deposits have been observed in the neural arches of several elasmobranchs (Cailliet, 1990). For example, Peignoux-Deville et al. (1982) provided an extensive description of these deposits for dogfish (*Scyliorhinus canicula*). However, age determination research for elasmobranchs has focused on the calcium deposits in the vertebral centra. Use of the neural arches as aging structures may provide an alternative age determination method for species in which the vertebral centra are poorly calcified

Valid age and growth information is fundamental to stock assessment and management. However, Cailliet (1990) lists only 39 species of elasmobranchs for which there are published or ongoing age verification studies. As interest and concern in commercial and recreational fishing of elasmobranchs increases, the need for age determination techniques becomes more pressing. Researchers need to investigate alternative methods for aging elasmobranchs, and we suggest that neural arches may prove to be useful. It is important to note that our observations on calcium banding in sixgill shark neural arches are preliminary and are for immature sixgill sharks only. We stress that fundamental to all aging determination studies is the validation of the method (Beamish and McFarlane, 1983), and future work is required to determine if the bands observed in our study are formed on annual, or regular, intervals.

Acknowledgments

Bill Andrews and Grady O'Neill provided technical assistance in producing the photographs. Maria Surry produced the schematic diagrams of the vertebral columns and neural arches.

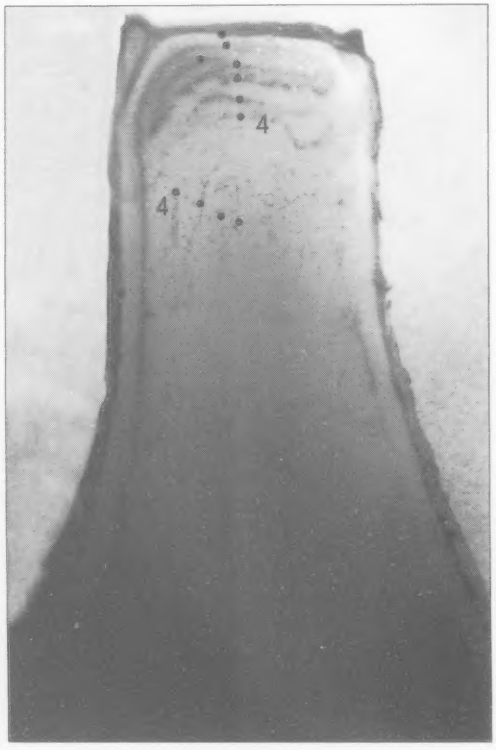

Figure 4

A stained neural arch from a 330 cm (total length) female bluntnose sixgill shark. The arch was soaked in 1% silver nitrate for 7.25 hours, but the inner portions of the arch were barely stained. Ten bands are indicated by dots, but the first four are difficult to determine. The fourth band is labelled with the number four.

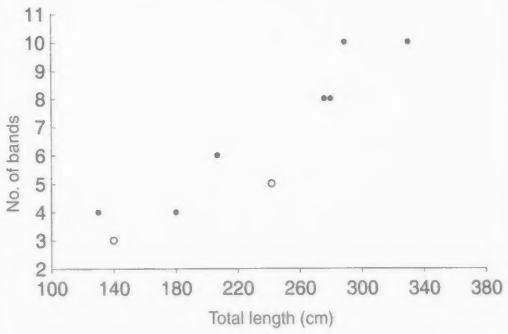

Figure 5

Number of bands observed in neural arches by total length (cm) of sixgill shark. Dots represent females; open circles represent males. As the total length of the shark increases, the number of annuli observed increases.

Literature cited

Beamish, R. J., and G. A. McFarlane.
1983. The forgotten requirement for age validation in fisheries biology. Trans. Am. Fish. Soc. 112(6):735–743.

Cailliet, G. M.
1990. Elasmobranch age determination and verification an updated review. *In* Elasmobranchs as living resources: advances in the biology, ecology, systematics, and the status of the fisheries, (H. L. Pratt Jr., S. H. Gruber, and T. Taniuchi, eds.), p. 157–165. U. S. Dep. Commer., NOAA Tech. Rep. NMFS 90.

Cailliet, G. M., L. K. Martin, D. Kusher, P. Wolf, and B. A. Welden.
1983. Techniques for enhancing vertebral bands in age estimation of California elasmobranchs. *In* Proceedings of the international workshop on age eetermination of oceanic pelagic fishes: tunas, billfishes, and sharks (E. D. Prince and L. M. Pulos, eds.), p. 157–165. U.S. Dep. Commer., NOAA Tech. Rep. NMFS 8.

Castro, J. I.
1983. The sharks of North American waters, 180 p. Texas A&M Univ. Press, College Station.

Clement, J. G.
1992. Re-examination of the fine structure of endoskeletal mineralization in chondrichthyans: implications for growth, ageing and calcium homeostasis. Aust. J. Mar. Freshwater Res. 43:157–181.

Compagno, L. J. V.
1984. FAO species catalogue. Volume 4. Sharks of the world. An annotated and illustrated catalogue of shark species known to date. Part 1. Hexanchiformes to Lamniformes. FAO Fish. Synop. 125 (vol. 4, part 1): 249 p. FAO, Rome.

Ebert, D. A.
1986. Biological aspects of the sixgill shark, *Hexanchus griseus*. Copeia 1986(1):131–135.
1992. Cowsharks. *In* California's living marine resources and their utilization, (W. S. Leet, C. M. Dewees, and C. W. Haugen, eds.), p. 54–55. Sea Grant Extension Publication UCSGEP-92-12.
1994. Diet of the sixgill shark *Hexanchus griseus* off southern Africa. Afr. J. Mar. Sci. 14:213–218.

Hart, J. L.
1973. Pacific fishes of Canada. Bull. Fish. Res. Board, Canada 180, 740 p.

Peignoux-Deville, J., F. Lallier, and B. Vidal.
1982. Evidence for the presence of osseous tissue in dogfish vertebrae. Cell and Tissue Research 222:605–614.

Re-identification of a lamnid shark embryo

Henry F. Mollet
Moss Landing Marine Laboratories
Moss Landing, California 95039-9647
E-mail address: mollet@pacbell.net

Antonio D. Testi
Italian Shark Research Project
Via A. Solari 43/2
20144 Milan, Italy

Leonard J. V. Compagno
Shark Research Centre
P.O. Box 61
8000 Cape Town, South Africa

Malcolm P. Francis
National Institute of Water and Atmospheric Research
P.O. Box 14-901
Wellington, New Zealand

In August 1903, a 400–500 kg pregnant female lamnid shark was caught in the Strait of Messina, Mediterranean Sea. She was reported to contain 25–30 embryos, one of which was saved and taken to the local Marine Institute, where it was subsequently examined by Sanzo (1912). The male embryo measured 36.1 cm total length (TL), weighed 800 g, and had a greatly distended abdomen, as is typical of embryos of oophagous lamnoid sharks (Gilmore, 1993). The mother and the remaining embryos were not saved. Because Sanzo was not able to examine the adult female from which the embryo was taken, the embryo was identified by a process of elimination, based mostly on morphometrics of postnatal specimens. Sanzo (1912) concluded that the embryo was a white shark, *Carcharodon carcharias* (Linnaeus, 1758). According to Sanzo (1912), the embryo was requested in 1909 by E. Giglioli and was then (in 1912) conserved at the Vertebrate Museum of the Superior Institute of Studies in Florence.

Sanzo's (1912) identification was questioned by many (Tortonese, 1950, 1956; Bass et al., 1975; Pratt[1]) but was assumed to be correct by Gilmore (1993). Tortonese (1950) suggested that the morphometric arguments used by Sanzo (1912) did not rule out the shortfin mako (*Isurus oxyrinchus* Rafinesque, 1810) but that the high fecundity of 25–30 was more consistent with *C. carcharias* than with *I. oxyrinchus* or a *Lamna species*. A lack of information on lamnid reproduction and the misidentification of a likely *Galeorhinus galeus* (Stevens[2]) with a litter of 30 as *Lamna* by Neill (1811), may have led Sanzo (1912) to consider the porbeagle *Lamna nasus* (Bonnaterre, 1788) instead of the shortfin mako as the most likely alternative to the white shark. Shann (1911) had questioned Neill's identification but this was not available to Sanzo (1912). Bass et al. (1975) incorrectly quoted Tortonese (1956) as saying that the embryo could have been a porbeagle. Tortonese (1950) pointed out that Sanzo (1912) mistook the large yolk-filled stomach (due to oophagy) for a yolk sac. Gilmore (1993) reviewed the reproductive biology of lamnoid sharks and included a redrawn sketch of the Sanzo (1912) embryo, still identified as a white shark, and also incorrectly stated that Sanzo (1912) had documented oophagy for the white shark. Francis (1996) reviewed lamnid fecundity data and showed that the shortfin mako has the highest known fecundity (18 embryos; Branstetter, 1981) in the order Lamniformes, which suggested to us that the embryo was more likely a shortfin mako.

Sanzo's (1912) embryo, well preserved in 75% ethanol, was photographed by Storai[3] in the Species Museum "La Specola" (MZUF 5911) in Florence in 1992 (Mojetta et al., 1997). The photograph—in color—suggested to us that the lost embryo had been found. This presented an opportunity for re-examining the embryo and checking Sanzo's identification.

The correct identification of the Sanzo embryo is important to our understanding of lamnid reproduction and possibly white shark conservation. Few pregnant female white sharks or embryos have been reported, and little is known about litter size, gestation period, or the timing and duration of the reproductive cycle (Uchida et al., 1987, 1996; Francis, 1996; Mollet et al., 2000). Such information is vital for understanding the population dynamics of the white shark, which is now regarded as a threatened species (Compagno et al., 1997). If the Sanzo embryo were a white shark, then it would be the smallest white shark embryo ever reported. Most have been greater than 100 cm TL (Francis, 1996; Uchida et al., 1996), although Bigelow and Schroeder (1948) reported white shark embryos in the range 20–61.6 cm TL, without giving any details. A white shark litter with embryos of 61 cm TL (5.4 kg each, Ellis and McCosker, 1991) was caught in the Mediterranean Sea (Norman and Fraser, 1938). No description of the embryos was given; however, the mass of the embryo suggested that it had a

[1] Pratt, H. L. 1996. Personal commun. Narragansett Laboratory, National Marine Fisheries Service, 28 Tarzwell Drive, Narragansett RI 02882.

[2] Stevens, J. D. 1998. Personal commun. CSIRO Marine Research, P. O. Box 1538, Hobart, Tasmania 7001, Australia.

[3] Storai, T. 1992. Personal commun. Museum of Natural Science of Valdinievole. Piazza L. da Vinci 1, Pescia PT Italy.

Manuscript accepted 24 May 2002.
Fish. Bull. 100:865–875 (2002).

substantial yolk-stomach as expected for a mid-term embryo (Mollet et al., 2000). Reports of pregnant females and small juveniles have indicated that white sharks breed in the Mediterranean (Fergusson, 1996). The reported litter size of the Sanzo shark (25–30) is the largest yet recorded for any lamnid shark. Therefore, correct identification of the embryo will also increase our knowledge of maximum fecundity in whichever species is involved. In this note, we report the results of our investigation into the identity of the Sanzo embryo. We first attempted to use morphometrics, dentition, and vertebral count and then, for unambiguous identification, we used skeletal anatomy—namely, the chondro-neurocranium, palatoquadrate, and pectoral girdle.

Materials and methods

Materials

Sanzo embryo (MZUF 5911) The preserved embryo in the "La Specola" Museum of the University of Florence, rediscovered and photographed by Storai[3] in 1992, was undoubtedly the embryo described by Sanzo (1912). Vanni,[4] curator of fishes at La Specola, provided us with the following account: "The current collection number 5911 MZUF (= Museo Zoologico Università di Firenze) corresponds to precedent n.3052 of the "Collezione Centrale dei Vertebrati Italiani" (Italian Central Vertebrate Collection), established by Giglioli in 1877 and now merged with the general collection. In the original catalogue ("libro di magazzino"), E. H. Giglioli himself wrote: "Carcharon Rondeleti ?? feto. VIII. 1903 Messina. La femmina dal quale fu tolto pesava da 400 a 500 kg e oltre a questo aveva nell'utero 25-30 altri feti nelle medesime condizioni. Avuto dal dr. Luigi Sanzo" ("Carcharadon Rondeletii ?? foetus VIII.1903 Messina.") (The female from which the embryo was taken had a weight between 400 to 500 kg and in addition to this specimen, had 25–30 other fetuses in the same condition. Presented by Luigi Sanzo" ("Carcharadon Rondeletii ?? foetus VIII.1903 Messina.")). The "Vertebrate Museum of the Superior Institute of Studies in Florence" corresponds exactly to the present "Museo Zoologico 'La Specola' dell'Università di Firenze." The "Vertebrate Museum" is actually the "Museo Zoologico 'La Specola'"; the "Superior Institute of the Studies in Florence" in 1926 became "Università degli Studi di Firenze" ("University of the Studies of Florence"). If in his paper Sanzo (1912) reported that the embryo was collected in 1903 near Messina, then undoubtedly the specimen in question is that preserved at present in the "La Specola" Museum."

Uchida embryo (SAM-35742) A 35.8-cm-TL female shortfin mako embryo was shipped to the South African Museum in Cape Town in November 2000 (SAM-35742). It came from a female (TL=3.37 m, 380 kg) that was caught near Okinawa, Japan, on 15 November 1984 (Uchida et al., 1987; Mollet et al., 2000). The litter comprised 16 embryos (11 females) with mean TL = 39.4 cm and mean mass = 1.456 kg and was preserved in formalin. A 38.4-cm-TL female embryo of this litter weighed 1.400 kg and the yolk-stomach content weighed 0.937 kg or 66.9% of the total mass (Uchida et al., 1987).

Morphometrics

Morphometric measurements of the Sanzo embryo were taken by author ADT using the methods and abbreviations of Compagno (1984). Total length (TOT) was measured with the caudal fin in the extended position. In an embryo of this size, TOT is very close to total length (TL) measured with the caudal fin in the natural position. A flexible aluminum tape was used for measurements exceeding 140 mm and rounded to the nearest millimeter. Measurements less than 140 mm were made with calipers at 0.2 mm precision. The Uchida embryo was measured six years later by authors LJVC and HFM.

We compared both our and Sanzo's (1912) measurements with the morphometrics of white sharks less than 4 m TL reported by Mollet et al. (1996) and with those of the shortfin makos summarized in Table 1. No morphometrics of white sharks of less than 1.26 m TL were available; therefore we had to use larger specimens for comparison, including two nearterm embryos reported by Francis (1996). This approach is reasonable for isometric characters, but it is inappropriate for allometric characters. The shortfin mako data included a shortfin mako litter of similar size to the Sanzo embryo (mean TL=36.2 cm, range 29.5–39.5 cm; Putz and Gilmore litter in Table 1). Morón[5] provided additional eye length data from 51 shortfin makos in Moreno and Morón (1992). We focused attention on the four morphometrics used by Sanzo (1912) to distinguish between white and shortfin mako sharks: snout shape; eye shape (EYL/EYH); ratio of mouth width to length (MOW/MOL); distance between the origins of the second dorsal and anal fins (PAL–PD2)). Our preliminary analysis indicated that eye size (EYL) and the distance between the origin of the first dorsal fin and the pectoral fin free rear tip (PD1–PRT) might be more suitable for identification and they were also included. We tested these variables graphically for their ability to distinguish between the two species (Mollet and Cailliet, 1996). The statistical program SYSTAT-SYGRAPH (Wilkinson, 1986) was used for analysis and graph production.

For specimens in which the relative positions of dorsal and anal fin origins were not measured directly, we calculated them from the difference between snout to anal fin and snout to second dorsal fin measurements (DAO=PAL–PD2). For the evaluation of the relative positions of the first dorsal and pectoral fins, we calculated the distance

[4] Vanni S. 2000. Personal commun. Sezione di Zoologia "La Specola," Museo di Storia Naturale dell'Universit, Via Romana, 17-50125 Firenze, Italy.

[5] Morón, J. 1994. Personal commun. Departamento doe Biología Animal I, Universidad Complutense de Madrid, Madrid E-28040, Spain.

Table 1

Summary of *Isurus oxyrinchus* specimens used for comparison of morphometrics with Sanzo embryo.

TL (m)	Comments	Reference
0.295	Smallest of 15 embryos [1]	Putz, Gilmore [2]
0.360	Strait of Messina, male embryo	This study [3]
0.361	Strait of Messina, male embryo	Sanzo (1912)
0.362	Mean of 15 embryos[1]	Putz, Gilmore [2]
0.395	Largest of 15 embryos [1]	Putz, Gilmore [2]
0.615	Nearterm female embryo	Stevens (1983)
0.641	Nearterm male embryo	Stevens (1983)
0.705	California, UMMZ 94726	Garrick (1967)
0.710	Smallest of 10 males and 8 females	Bass et al. (1975)
0.847	Japan, MCA 35071	Garrick (1967)
1.130	Algoa Bay, male	Smith (1953)
1.251	Smallest of 11 males and 2 females	Strasburg (1958)
1.438	New Zealand, NMNZ P.3014	Garrick (1967)
1.598	Ocean City MD, HMCZ 35899, male	Bigelow and Schroeder (1948)
1.659	Mean of 53 males and females	Moreno and Morón (1992)
1.920	South Africa, USNM 197686	Garrick (1967)
2.000	W. of Azores USNM 197706	Garrick (1967)
2.057	Mean of 11 males and 2 females	Strasburg (1958)
2.169	Mean of 13 with range 2–3 m TL	Gubanov (1974)
2.337	Bahamas, HMCZ 35367, male	Bigelow and Schroeder (1948)
2.400	Algoa Bay, male	Smith (1958)
2.579	Largest of 11 males and 2 females	Strasburg (1958)
2.692	Provincetown MA, female	Atwood (1869)
3.130	Largest of 10 males, 8 females	Bass et al. (1975)
3.210	Carmel Bay CA, female	Lea, Cailliet [4]
3.366	Santa Catalina Island Ca, female	Applegate (1966)
3.480	Redondo Beach CA, female	Seigel [5]
3.507	Anacapa Island CA, female	Applegate (1977)
3.800	Indian Ocean, female	Gubanov (1974)

[1] 15 embryos from same litter, Putz and Gilmore litter.

[2] Putz, O. 1995. Personal commun. Grolmanstrasse 48, 10634 Berlin, Germany. Gilmore, R. G. 1995. Personal commun. Dynamic Corp., Kennedy Space Center, FL 32899.

[3] Specimen identical to Sanzo (1912) embryo.

[4] Lea, R. N. 1995. Personal commun. California Fish & Game, Monterey CA 93940. Cailliet G. M. 1996. Personal commun. MLML, 8272 Moss Landing Road, Moss Landing CA 95039.

[5] Seigel, J. A. 1996. Personal commun. LACM, Los Angeles CA 90007.

between the first dorsal fin origin and the pectoral fin free rear tip (PD1–PRT = PD1 – (PP1 + P1B + P1I)). If P1B or P1I were not available for shortfin makos, we estimated (P1B + P1I) as 11% of TL (or TOT).

Tissue samples for DNA sequencing

Tissue samples were taken from the gill slits, the oral cavity, and the caudal peduncle. The samples were stored at room temperature in Wheaton polypropylene vials in 95% ethanol. DNA was extracted from the samples and polymerase chain reaction (PCR) amplification and sequencing were attempted but did not yield useful results (Bernardi[6]). This was likely due to initial fixing of the specimen in formalin (which destroys DNA) before transferal to ethanol.

X-ray analysis

For vertebral counts, we used radiographs taken initially with a Siemens Triselenix 750 (in Milan) and later with a Shimadzu R20 computerized x-ray machine for high-

[6] Bernardi, G. 1996. Personal commun. Dept. of Biology, University of California, Santa Cruz, CA 95064.

resolution radiography (in Cape Town). A pin was inserted perpendicular to the upper origin of the caudal fin to count the precaudal vertebrae. Distinct shortening of the centra was used to distinguish between monospondylic and diplospondylic vertebrae.

Dentition and mucous denticle examination

We used the term "embryonic teeth" for teeth in an embryo, which do not resemble teeth in the adult (Gilmore, 1993). We used "row" for teeth at the same developmental stage in the mesial-distal direction and "file" for teeth at different developmental stages in the labiolingual direction derived from a single locus (tooth germ) (Zangerl, 1981). We followed Applegate (1965) for the terminology anterior, intermediate, lateral, and posterior teeth and for the definition of the dental formula. This terminology and definition apply to fully formed dentition in postnatal sharks but they appeared to be applicable to the embryo under investigation. If a tooth was missing in the first row, the one behind it was counted. We used the term "mucous denticles" for dermal denticles in the oral cavity (Yano et al., 1997). We examined the mucous denticles with a Leitz DMRB microscope at 25× and 45× magnification.

The jaws could not be removed; therefore a nondestructive examination was carried out with close attention to the positions of teeth in the functional and replacement rows in the upper jaw. The functional tooth and the first replacement tooth in the fifth file (counted from the symphysis) of the upper left jaw were extracted and examined through a Leitz DMRB microscope at 25× and 45× magnification. The examination of replacement teeth required lifting the tissue that covered the developing teeth. The lower jaw was not examined as closely because only one tooth was visible to the naked eye.

We measured enameloid height (E2), if possible, for all teeth in the upper jaw (Mollet et al., 1996). We estimated the total vertical height (H) of the largest tooth, from a 25× photograph showing the outline of the root, for comparison with the likely total heights reported by Sanzo (1912). We calculated the enameloid height of each tooth in relation to the third tooth. For comparison, we estimated tooth sizes in relation to the third tooth of postnatal shortfin makos from photographs or drawings (Bigelow and Schroeder, 1948; Bass et al., 1975; Compagno, 1984).

Dissection

The Sanzo and the Uchida embryos were dissected conservatively in order to examine the internal structure of the head, jaws, and pectoral fins. The chondroneurocranium was exposed dorsally and on the left side by dissecting away flaps of skin, muscle, and connective tissue. We examined the structure of the ethmoid region, epiphysial area, orbital process, and otic capsule. Dissection of the left lateral surface of the embryo's head exposed the palatoquadrate and allowed observation of the proportions of the palatine process. Dorsal dissection of the pectoral fin allowed examination of the basal metapterygium's skeletal structure. No white shark embryo of suitable size was available for dissection and direct comparison. The white shark embryo (TL=55 cm) described by Parker (1887) was a misidentified *Carcharhinus* (Francis, 1996).

Results

General condition and morphometrics

After more than 90 years of storage in a glass container in 75% ethanol, the 36.1-cm male Sanzo embryo (MZUF 5911) was curled up, and fins and other body parts were permanently bent (Fig. 1A). The jaws appeared protruded, possibly because of the strong retraction and shrinkage of the snout. The large yolk stomach was hardened. It was 13.4 cm long, 8.6 cm wide, and 6.9 cm high and had an estimated volume of 416 cm^3. The embryo weighed 0.548 kg (condition factor, CF=11.7 kg/m^3) compared with 0.800 kg (CF=17.1 kg/m^3) reported by Sanzo (1912). The 31.5% mass loss was likely due to dehydration and dissolving and leaching of lipids from the yolk and liver into the ethanol. Despite this, the embryo did not appear to have shrunk in length because it still measured 36.0 cm TOT, 30.0 cm fork length (FOR), 27.4 cm precaudal length (PRC).

After 16 years in formalin, the female Uchida embryo (SAM-35742) looked shriveled (Fig. 1B). The embryo measured TOT = 35.8 cm, FOR = 28.8 cm, PRC = 26.6 cm, mass = 1.227 kg on 6 June 2001. The condition factor of 26.7 kg/m^3 of this embryo was similar to that calculated from the reported mean length and mass of all the embryos of the litter by Uchida et al. (1987) (CF=23.8 kg/m^3). TOT was almost the same as that of the Sanzo embryo, but this embryo weighed almost twice as much as the Sanzo embryo. Accordingly, the yolk stomach was considerably larger and was 18.5 cm long, 9.6 cm wide, and 11.5 cm high and had an estimated volume of 1069 cm^3.

Sanzo (1912) used the upturned snout, as one of four characters to distinguish his embryo from a shortfin mako, but this feature is probably an artifact of preservation (see "Skeletal anatomy" below). The three quantifiable morphometric characters used by Sanzo (1912) were also not suitable to distinguish between small white and shortfin mako sharks (Fig. 2). White sharks generally have a wider mouth, in relation to its length, than shortfin makos, but there is significant overlap (Fig. 2A). Furthermore, the ratio of mouth width to length (MOW/MOL) is allometric in small shortfin makos; mouth width becomes progressively larger than mouth length in smaller embryos. White and shortfin mako sharks both have slightly oval to round eyes and an eye length-to-height ratio between 0.9 and 1.3 (Fig. 2B). The origin of the anal fin is behind the origin of the second dorsal fin (PAL–PD2 > 0) in both white and shortfin mako sharks (Fig. 2C).

Two promising morphometrics not considered by Sanzo (1912) also proved unsuitable for identification. The first dorsal fin origin (PD1) of the Sanzo embryo was 2.3 cm (6.4% TOT) behind the pectoral fin rear tip (PRT), which suggested it might be a shortfin mako following Compagno (1984). However, the origin of the dorsal fin in both white and shortfin mako sharks varies from slightly-in-front-of

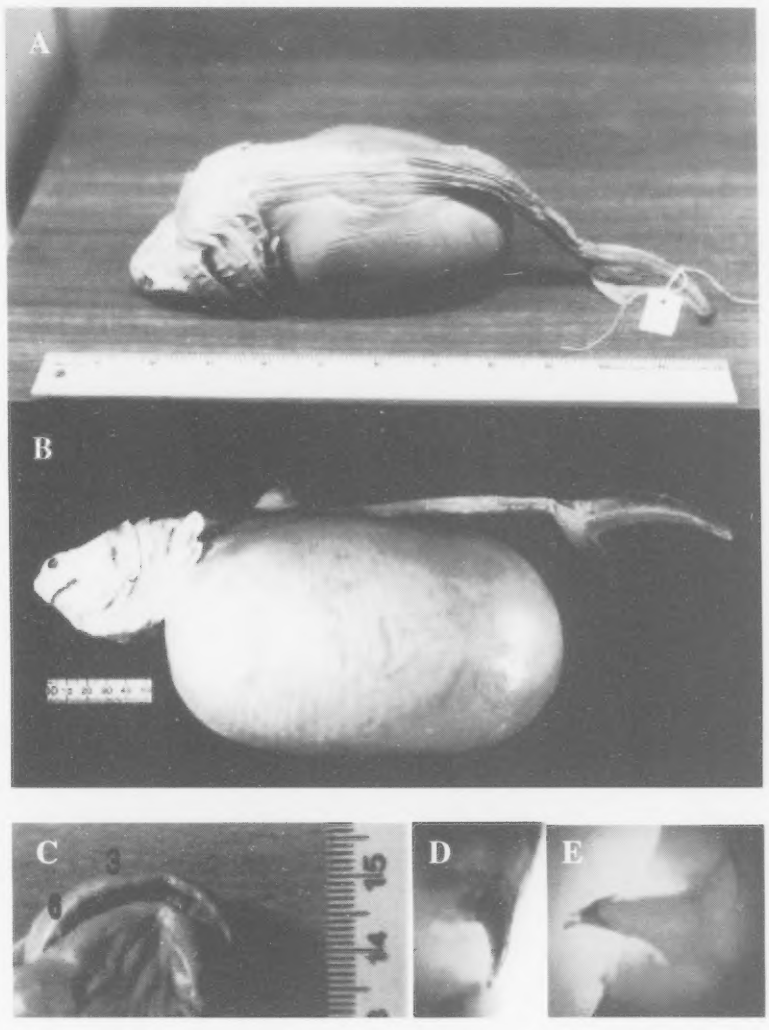

Figure 1

(**A**) Sanzo (1912) lamnid embryo (TOT 36.0 cm, MZUF 5911). Smallest scale intervals = 1/32". (**B**) Uchida (1989) shortfin mako embryo (TOT 35.8 cm, SAM 35742). Smallest scale interval = 1 mm. (**C**) Sanzo embryo ventral view of mouth focusing on upper right teeth in first row. Smallest scale intervals = 1 mm. (**D**) Sanzo embryo functional 5th upper left tooth (enameloid height E2 ~2 mm). (**E**) Sanzo embryo replacement 5th upper left tooth (E2 ~2.3 mm, total vertical height H ~2.9 mm). Thin layer of tissue is covering apex.

to slightly-behind the pectoral fin free rear tip (Fig. 2D, PD1–PRT). The eyes of the Sanzo embryo were unexpectedly small (EYL=1.4% and 1.8%, Sanzo's (1912) and our measurement, respectively) compared with those reported for nearterm shortfin mako embryos and neonates (e.g. EYL=2.7–2.9% TL; Stevens, 1983). On the other hand, they were similar in size to those of the Uchida embryo (1.7%) and the Putz and Gilmore litter (1.4–1.8%; Fig. 2E). Small shortfin mako embryos have small eyes; but relative eye length increases rapidly and reaches a maximum of about 3% in near-term embryos of 60–64 cm TL, before declining in postnatal fish.

No secondary caudal keel was observed in the Sanzo embryo by Sanzo (1912) or by us. Nevertheless, this does not allow the elimination of the porbeagle; secondary keels may be difficult to detect in preserved porbeagle embryos

because of wrinkling of the skin (Francis, personal observ.) Lohberger (1910) did not observe a secondary keel in preserved salmon shark (*Lamna ditropis*) embryos, although this keel is present in postnatal specimens (Compagno, 1984).

Dentition

The first observations by naked eye and magnifying lens suggested a tooth formula of 8-0-7 for the upper jaw. However, the functional tooth row (i.e. the outermost row containing erect, functional teeth) of the upper right jaw was not completely filled by teeth; it comprised eight visible teeth (in file positions 2–6 and 8–10) and six gaps (in file positions 1, 7 and 11–14 (Table 2). The gaps in the functional row were indicated by the presence of teeth in the replacement rows. The gap in file 1, the broken tooth in file 2 (the 2nd tooth on the left was not erect), and the teeth in files 3–6 (labeled) are in focus in Fig. 1C. The largest functional tooth in file 6 had an enameloid height of 2.4 mm. The tooth formula for Sanzo's embryo indicated that an embryo of this size and developmental stage has the full adult complement of replacement tooth files in the upper jaw: two anteriors, one intermediate, eight laterals, and three posteriors (Table 2). The first and second replacement rows contained teeth in all file positions, indicating an eventual tooth formula of 14-0-14.

The functional tooth extracted from the 5th file in the left upper jaw (E2 ~2 mm) was fanglike and was without any lateral flattening and we considered it to be an embryonic tooth (Fig. 1D). The replacement tooth behind it was slightly curved, had little lateral flattening, and a thin layer of tissue still covered the apex (E2 ~2.3 mm and H ~2.9 mm) (Fig. 1E). We suggest that this tooth is also an embryonic tooth. The relative position of these two teeth is as shown in Figs. 1D and E.

The relative heights of the embryonic teeth in the upper jaw differed considerably from those of postnatal shortfin makos (Table 2). The first two teeth in the Sanzo embryo were much smaller than the teeth in files 3–8; the largest tooth was in file 6. In postnatal shortfin makos, the first two teeth are the largest, followed by a much smaller third tooth and smaller ones in files 4–13 (Table 2).

The tooth formula for the lower jaw was less certain. Our initial observation with magnifying lens indicated 4-0-7. Sanzo (1912) reported 4-0-4 and we agree with Sanzo that the third lower tooth was the most prominent.

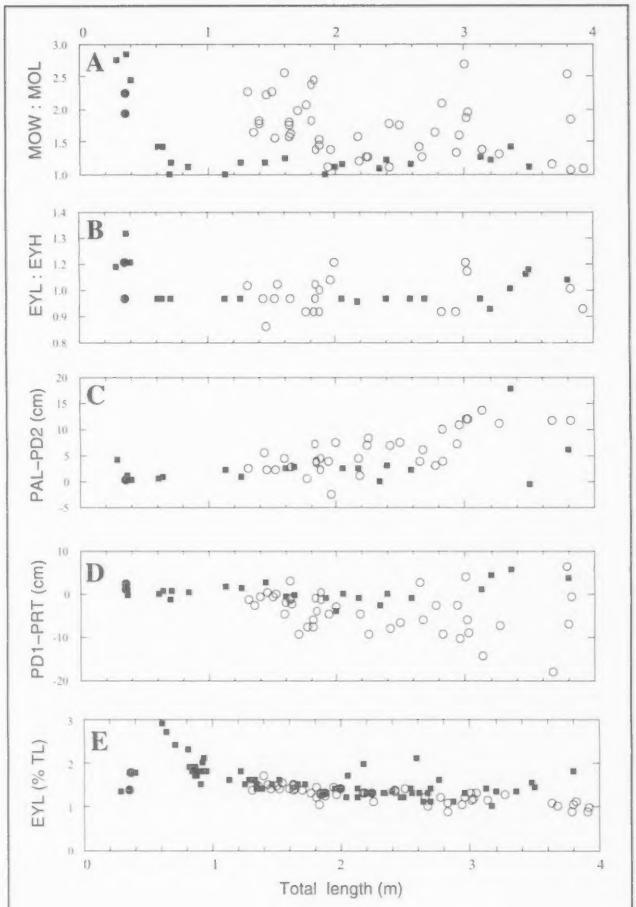

Figure 2

Relationships between selected morphometrics and total length of *Carcharodon carcharias* (open circle) and *Isurus oxyrinchus* (filled square). Sanzo embryo data (Sanzo, 1912 and our study) are indicated by dual symbols. (**A**) Ratio of mouth width to mouth length (MOW/MOL). (**B**) Ratio of eye length to eye height (EYL/EYH). (**C**) Relative position of the origins of anal and second dorsal fins (PAL–PD2). (**D**) Relative position of first dorsal fin origin and pectoral fin free rear tip (PD1–PRT). (**E**) Eye length (EYL as % TL).

Mucous denticles

Mucous denticles covered the palate and the tongue. Microscopic investigation revealed that the wartlike structures were round and had a circular, flat base and a small upward-pointing center cusp. No ridges were noted between the cusp and the base. The mucous denticles were small and far apart on the tongue, slightly larger and closer together on the palate, and largest (~0.4 mm diameter) and packed together in the region close to the cartilage of the upper jaw. There were few in the region close to the lower jaw and on the terminal part of the tongue.

Skeletal anatomy

The cranium of the Sanzo embryo differed notably from that of postnatal lamnids. The chondrocranium of the embryo was evidently damaged and foreshortened by the gen-

Table 2

Characterization of upper right dentition of Sanzo embryo (A and B) and comparison of relative tooth sizes with postnatal *Isurus oxyrinchus* (C). We report approximate enameloid height (E2) of teeth in mm. Sanzo (1912) probably reported total height. G = gap; P = present.

File number		1	2	3	4	5	6	7	8	9	10	11	12	13	14
Jaw position[1]		A2	A3	I	L1	L2	L3	L4	L5	L6	L7	L8	P1	P2	P3
A	Results of this study for Sanzo embryo														
	Functional row [2]	G	P[3]	1.5	1.2	2.2	2.4	G	1.4	P	P	G	G	G	G
	1st replacement row	0.7	P	P	P	2.3[4]	P	1.4	P	P	P	P	P	P	P
	2nd replacement row	P	P	P	P	P	P	P	P	P	P	P	P	P	P
B	Results of Sanzo (1912)														
	Functional row [5]	<<1	<1	<1	P	P	P	4	<1	<1	<1				
	1st replacement row								P	P					
C	Relative *Isurus oxyrinchus* teeth size in functional row														
	Sanzo (this study)	~0.4[6]	—	1.0	0.8	1.5	1.6	~0.9[6]	0.9	—[7]	—	—	—	—	—
	B&S [8], 1948	2.3	1.9	1.0	1.2	1.3	1.4	1.2	1.1	0.8	0.7	0.5	0.4	0.3	
	Bass et al., 1975	2.1	1.9	1.0	1.3	1.5	1.5	1.2	0.9	0.7	0.6	0.5	0.4		
	Compagno, 1984	2.1	1.9	1.0	1.1	1.2	1.4	1.3	1.1	0.9	0.7	0.4	0.35	0.3	

[1] A1 is missing in postnatal *Isurus oxyrinchus* (Applegate and Espinosa, 1996).

[2] Eight teeth present (P) and six gaps (G).

[3] Broken tooth, 2nd tooth on left not erect.

[4] Size estimate of upper left tooth from photograph of extracted tooth (Fig. 1D). Est. total height (H) = 2.9 mm.

[5] Tooth sizes preceded with < and << signs are estimates based on qualitative descriptions by Sanzo (1912): 1st tooth almost invisible, 2nd and 3rd tooth a little more developed than the 1st one and about equal in size, 3rd tooth almost half the size of the fourth tooth, teeth 4–7 much better developed, 7th tooth 4 mm.

[6] Based on enameloid height of first replacement tooth.

[7] Relative size could not be estimated.

[8] B&S, Bigelow and Schroeder.

eral compression of its snout. This presumably was a result of being fixed and preserved in a narrow jar, and the weight of the massive yolk stomach providing sufficient force to compress the snout. The cranium had an extremely short ethmoid region compared with that of postnatal lamnids, which was exaggerated by snout foreshortening. The rostral cartilages were only basally developed and partially crushed and had no well-developed rostral node. The protruding orbits were large but short and the otic capsules were more elongated than in postnatal lamnids.

In other features, the cranium agreed with that of the Uchida embryo and postnatal shortfin makos (Table 3). The bases of the lateral rostral cartilages were positioned on the nasal capsules, as in white and mako sharks, rather than on the preorbital processes as in *Lamna* (Compagno, 1990). The ethmoid region across the nasal capsules was relatively narrow, as in shortfin makos and porbeagles; white sharks, in contrast, have notably broad nasal capsules (Haswell, 1885; Parker, 1887; Compagno, 1990). The cranial roof of white sharks has an epiphysial bar and epiphysial fenestrum just behind the anterior fontanelle, but this is absent in postnatal crania of shortfin makos, porbeagles, and Sanzo's embryo (Compagno, 1990).

The upper jaw and the pectoral girdle of the Sanzo embryo agreed with those of the Uchida embryo and postnatal makos (Table 3). The palatine processes of the palatoquadrate were low, elongated, and ventrally bent or twisted as in shortfin makos. White sharks have higher, straight, and thicker palatine processes (Compagno, 1990). Porbeagles, postnatal shortfin makos, and Sanzo's embryo all have an unsegmented metapterygium in their pectoral fin skeletons, whereas white sharks have a transversely segmented basal metapterygium (Compagno and Gottfried, unpubl. data).

The precaudal vertebral count of Sanzo's embryo (110 centra in total, including 73 monospondylous and 37 diplospondylous centra) fell close to the average for shortfin makos, whereas white sharks and porbeagles have fewer precaudal vertebrae (Table 3). The caudal vertebrae count of Sanzo's embryo (77) falls in the range of both white sharks and shortfin makos and is slightly greater than caudal counts for porbeagles. Caudal vertebral counts from radiographs are often unreliable in newborn and late fetal sharks because of poor calcification of the posterior end of the vertebral column. The caudal vertebrae of the Sanzo embryo were difficult to count without dissection because they were small and are not expected to be fully formed until late in embryonic life (Springer and Garrick, 1964). The Uchida embryo is of similar length but is considerably heavier compared to the Sanzo embryo, but its vertebral column was insufficiently calcified and we were unable to obtain a precaudal vertebral count from the x-rays taken.

Table 3

Comparison of skeletal anatomy of the Sanzo (1912) embryo with that of the Uchida et al. (1987) *Isurus oxyrinchus* embryo, and postpartum *Isurus oxyrinchus*, *Carcharodon carcharias*, and *Lamna nasus*.

Description	Sanzo	Uchida	*Isurus oxyrinchus*	*Carcharodon carcharias*	*Lamna nasus*
Chondrocranium					
Epiphysial bar and epiphysial fenestrum just behind the anterior fontanelle	No	No	No	Yes	No
Ethmoid region narrow across nasal capsule	Yes	Yes	Yes	No	Yes
Bases of the lateral rostral cartilages positioned on the nasal capsule (not preorbital processes)	Yes	Yes	Yes	Yes	No
Upper jaw					
Palatine processes low, elongated, and ventrally bent or twisted	Yes	Yes	Yes	No	No
Pectoral girdle					
Unsegmented inner basals (metapterygium)	Yes	Yes	Yes	No	Yes
Vertebral counts					
Precaudal	110	[1]	104–114[2]	99–108[2]	83–91[2]
Caudal[3]	77	[1]	79–86	68–83	68–71[2]
Total	187	[1]	183–194[2]	172–187[2]	150–162[2]

[1] Vertebral column not sufficiently calcified.
[2] Combined ranges from Springer and Garrick (1964), Bass et al. (1975), and L. J. V. Compagno (unpublished precaudal data).
[3] Caudal vertebrae may not be fully formed in early stage embryos (Springer and Garrick, 1964).

Discussion

Skeletal anatomy and morphometrics

We had to use skeletal anatomy, including the chondroneurocranium, palatoquadrate, and pectoral girdle for unambiguous identification of the Sanzo (1912) embryo after capture data and the vertebral count suggested that the embryo might be a shortfin mako rather than a white shark. Our attempts to use morphometrics, dentition, and DNA analysis were not successful.

Sanzo (1912) correctly placed the embryo in the family Lamnidae using only morphometric criteria. Only three species of the family Lamnidae normally occur in the Strait of Messina of the Mediterranean Sea: porbeagle, white, and shortfin mako sharks (Compagno, 1984; Fergusson, 1996). However, the morphometric arguments used by Sanzo (1912) for identification to species were not characteristic, leading him to incorrectly eliminate the genus *Isurus*. The upturned snout was probably caused by distortion during preservation, and we have shown that the mouth width-to-length ratio, eye shape, and relative positions of the origins of second dorsal and anal fins are not suitable criteria for distinguishing between white and shortfin mako sharks. Other promising morphometrics also failed to distinguish between the two species. These conclusions are tentative—confirmation will depend on obtaining measurements of these characters from small embryonic white sharks, which were missing from our database.

Dentition

Tooth shape is species-specific in postnatal *Lamna*, *Isurus*, and *Carcharodon* (Compagno, 1984) but not in embryos. Lamnid embryos have specialized "embryonic" teeth that are adapted for grasping and tearing the membrane of the eggcases on which they feed (Gilmore, 1993; Francis and Stevens, 2000). We observed fanglike embryonic teeth in porbeagle embryos, which lacked the characteristic cusplets of adult specimens. We observed fanglike embryonic white shark teeth lacking serration in the intestine of a nearterm embryo similar to the embryonic teeth of the Sanzo embryo (Francis, 1996; Francis and Stevens, 2000). Embryonic teeth are similar in all lamnid embryos and do not appear to be suitable for identification. Shortfin mako embryos shed their embryonic dentition at about 45–50 cm TL and nearterm embryos have emerging adultlike teeth (Gilmore, 1993; Mollet et al., 2000).

It is difficult to describe a dentition completely without the benefit of prepared jaws, particularly in a relatively small embryo. In addition, the tooth formula of a small embryo may be different from that of a postnatal specimen. Sanzo (1912) reported an upper jaw tooth formula of 10-0-10; we observed 14-0-14, the full adult complement of replacement tooth files. That suggests that Sanzo (1912) had not observed the four replacement teeth in files 11–14. He reported two replacement teeth behind the functional teeth in files 7–8 and 8–9, whereas we observed replacement teeth in all position of two rows by pulling back the dental lamina (Table 2).

We could not resolve other discrepancies. Sanzo (1912) reported four relatively large teeth in files 4–7, the 4th one was more than twice the size of the 3rd one, and the 7th tooth was 4 mm (probably including the root). We concluded that the four largest teeth were in files 3–6 and we estimated the total height of the largest tooth in file 6 to be about 3 mm (based on E2=2.4 mm). It is possible that Sanzo's (1912) minute first tooth was a recessive parasymphysial tooth, which we overlooked or which had disappeared before we examined the embryo. Our description of the dentition of the Sanzo embryo agrees in general with that in similar-size salmon shark and porbeagle embryos (Lohberger, 1910; Mollet, personal observ.).

DNA sequencing and mucous denticles

DNA sequencing should have allowed identification of the Sanzo embryo but provided no useful results. This was likely due to initial fixing of the Sanzo embryo in formalin (which destroys DNA) before transferal to ethanol.

We did not have SEM at our disposal during the initial stage of the investigation but suggest that the mucous denticles might be suitable to identify lamnid embryos. Early development of mucous denticles is expected to occur in the oophagous lamnids (Reif, 1985; Raschi and Tabit, 1992). Reif (1985) suggested that dermal denticles are family, genus, and in some cases even species specific. Postnatal shortfin makos and white sharks have different mucous denticles (Reif, 1985; Peyer, 1968).

Capture information

The capture information provided by the fisherman who caught the Sanzo shark was more consistent with shortfin mako than with other lamnids, based on presently known lamnid reproductive biology (Francis and Stevens, 2000; Mollet et al., 2000). The litter size of 25–30 was estimated and may have been inaccurate, but it does indicate a large litter. The large litter size could be the reason that the Sanzo embryo weighed considerably less than the Uchida embryo although they had similar length. Litter size in porbeagles is nearly always four (maximum of five, Francis. 1996; Francis and Stevens, 2000). Maximum litter size in white sharks is at least ten; unconfirmed reports are as high as 14 (Francis, 1996). Shortfin makos have the largest litters yet reported in the Lamnidae, reaching at least 18 (Branstetter, 1981; Mollet et al., 2000).

The shark was estimated to weigh 400–500 kg, although this must be considered approximate. The TL of a female of this mass would be 3.58–3.85 m (Stevens, 1983; Mollet et al., 2000). A shortfin mako of this length would undoubtedly be mature (Mollet et al., 2000) and the maximum reported length is 4 m (Bigelow and Schroeder, 1948; Mollet[7]). Female white sharks do not mature until about 5.0 m (Mollet et al., 2000) with a corresponding mass of ~1200 kg (Mollet and Cailliet, 1996). A full-term litter of 25–30 shortfin makos would weigh ca. 75 kg, which would be reasonable for a female shortfin mako weighing around 500 kg (Mollet et al., 2000). A white shark litter of 25–30 would weigh about 500 kg at birth, i.e. the total mass of the female shark caught, which is not possible.

We conclude that the Sanzo embryo is *Isurus oxyrinchus*. This analysis corrects a long-standing error in the literature and should provide the incentive to procure and describe a white shark embryo of similar developmental stage to that of Sanzo's embryo. The smallest photo-documented white shark embryos were ca. 1.0–1.1 m TL (Uchida et al., 1996) and fully documented white shark embryos were all nearterm and had a TL between 1.35–1.51 m (Uchida et al., 1987, 1996; Francis, 1996). The definite identification of the Sanzo embryo suggests that the maximum litter size of the shortfin mako is likely larger than 18 (Branstetter, 1981; Mollet et al., 2000) and possibly as large as 25–30.

[7] Mollet, H.F. 1999. http://homepage.mac.com/mollet/Io/Io_large.html. [Access date: 9 August 2002.]

Acknowledgments

P. Stipa and A. Young translated Sanzo (1912) which gave this study momentum. A photograph taken by T. Storai led to our rediscovery of the Sanzo embryo. S. Vanni and M. Poggesi allowed a partially destructive examination of the embryo and we are grateful to S. Vanni for the historical identification of the specimen. E. Tavani and G. Sola helped with tooth histological sections and the first body radiographs. G. Bernardi spent much time attempting DNA sequencing. O. Putz, R. G. Gilmore, and J. Morón provided morphometrics of embryonic and postnatal shortfin mako embryos. G. Cailliet suggested the use of x-rays. We are grateful to Y. Kamei and S. Uchida for donating a shortfin mako embryo specimen and to A. Dainty and B. Human for help with the dissection. We also thank S. Branstetter, J. Bruner, J. Casey, G. Cliff, I. Fergusson, B. Habrich, R. Lea, G. Notarbartolo di Sciara, T. Otake, R. Phillips, R. Purdy, H. Pratt, O. Putz, J. Stevens, and S. Wintner for data and helpful suggestions and comments. HFM acknowledges computer support provided by the Monterey Bay Aquarium. The comments of three reviewers improved the manuscript.

Literature cited

Applegate, S. P.
1965. Tooth terminology and variation in sharks with special reference to the sand shark, *Carcharias taurus* Rafinesque. Contributions in Science (Los Angeles County Museum) 86:3–18.
1966. A possible record-sized bonito shark, *Isurus oxyrinchus* Rafinesque, from Southern California. Calif. Fish Game 52:204–207.
1977. A new record-sized bonito shark, *Isurus oxyrinchus* Rafinesque, from Southern California. Calif. Fish Game 63:126–129.

Applegate, S. P., and L. Espinosa-Arrubarrena.
1996. The fossil history of *Carcharodon* and its possible ancestor, *Cretolamna*: a study in tooth identification. *In* Great white shark: the biology of *Carcharodon carcharias*

(A. P. Klimley and D. G. Ainley, eds.), p. 19–36. Academic Press, San Diego, CA.

Atwood, N. E.
1869. Description of a shark, *Carcharias tigris* Atwood. Proceedings of the Boston Society of Natural History 12: 268–9.

Bass, A. J., J. D. D'Aubrey, and N. Kistnasamy.
1975. Sharks of the east coast of southern Africa. IV. The families Odontaspididae, Scapanorhynchidae, Isuridae, Cetorhinidae, Alopiidae, Orectolobidae and Rhiniodontidae. Oceanogr. Res. Inst. Invest. Rep. 39:1–102.

Bigelow, H. B., and W. C. Schroeder.
1948. Part 1. Sharks. *In* Fishes of the western North Atlantic, p. 59–546. Sears Foundation for Marine Research, Yale University.

Branstetter, S.
1981. Biological notes on the sharks of the north central Gulf of Mexico. Contrib. Mar. Sci. 24:13–34.

Compagno, L. J. V.
1984. FAO species catalogue. Sharks of the world. An annotated and illustrated catalogue of shark species known to date. FAO Fisheries Synopsis 125, vol. 4, part 1. Hexanchiformes to Lamniformes, p. 1–249. FAO, Rome.
1990. Relationship of the megamouth shark, *Megachasma pelagios* (Lamniformes: Megachasmidae), with comments on its feeding habits. *In* Elasmobranchs as living resources: advances in the biology, ecology, systematics, and the status of fisheries (H. L. Pratt, S. H. Gruber, and T. Taniuchi, eds.), p. 357–379. U.S. Dep. Commer., NOAA Technical Report NMFS 90.

Compagno, L. J. V., M. A. Marks, and I. K. Fergusson.
1997. Threatened fishes of the world: *Carcharodon carcharias* (Linnaeus, 1758) (Lamnidae). Environ. Biol. Fish. 50:61–62.

Ellis, R., and J. E. McCosker.
1991. Great white shark, 270 p. Harper Collins Publs., New York, NY.

Fergusson, I. K.
1996. Distribution and autoecology of the white shark in the eastern North Atlantic Ocean and the Mediterranean Sea. *In* Great white shark: the biology of *Carcharodon carcharias* (A. P. Klimley and D. G. Ainley, eds.), p. 321–345. Academic Press, San Diego CA.

Francis, M. P.
1996. Observations on a pregnant white shark with a review of reproductive biology. *In* Great white sharks: the biology of *Carcharodon carcharias* (A. P. Klimley and D. G. Ainley, eds.), p. 157–172. Academic Press, San Diego, CA.

Francis, M. P., and J. D. Stevens.
2000. Reproduction, embryonic development and growth of the porbeagle shark, *Lamna nasus*, in the Southwest Pacific Ocean. Fish. Bull. 98:41–63.

Garrick, J. A. F.
1967. Revision of sharks of genus *Isurus* with description of a new species (Galeoidea, Lamnidae). Proc. U. S. Nat. Mus. 118(3537):663–694.

Gilmore, R. G.
1993. Reproductive biology of lamnoid sharks. Env. Biol. Fish. 38:95–114.

Gubanov, Ye. P.
1974. The capture of a giant specimen of the mako shark (*Isurus glaucus*) in the Indian Ocean. J. Ichthyology 14: 589–591.

Haswell, W. A.
1885. Studies on the elasmobranch skeleton. Proc. Linn. Soc. N. S. Wales 9:71–119.

Lohberger, J.
1910. Über zwei riesige Embryonen von *Lamna*. Abh. K. Bayer. Akad. Wiss. IV, Suppl. Bd. 2:1–45.

Mojetta, A., T. Storay, and M. Zuffa.
1997. Notes on the presence and distribution of the white *shark (Carcharodon carcharias)* in Italian waters. Quad. Civ. Staz. Idrobiol. 22:125–128.

Mollet, H. F., and G. M. Cailliet.
1996. Using allometry to predict body mass from linear measurements of the white shark. *In* Great white sharks: the biology of *Carcharodon carcharias* (A. P. Klimley and D. G. Ainley, eds.), p. 81–89. Academic Press, San Diego CA.

Mollet, H. F., G. M. Cailliet, A. P. Klimley, D. A. Ebert, A. T. Testi, and L. J. V. Compagno.
1996. A review of length validation methods for large white sharks. *In* Great white shark: the biology of *Carcharodon carcharias* (A. P. Klimley and D. G. Ainley, eds.), p. 91–108. Academic Press, San Diego, CA.

Mollet, H. F., G. Cliff, H. L. Pratt Jr., and J. D. Stevens.
2000. Reproductive biology of the female shortfin mako *Isurus oxyrinchus* Rafinesque, 1810, with comments on the embryonic development of lamnoids. Fish. Bull. 98:299–318.

Moreno, J. A., and J. Morón.
1992. Comparative study of the genus *Isurus* (Rafinesque, 1810) and description of a form ('marrajo criollo') apparently endemic to the Azores. *In* Sharks: biology and fisheries (J. G. Pepperell, ed.), p. 109–22. Aust. J. Mar. Freshwater Res. 43.

Neill, P.
1811. A list of fishes found in the Firth of Forth, and rivers and lakes near Edinburgh, with remarks. Mem. Wernerian Nat. Hist. Soc. (Edinburgh). Vol. I (For the years 1808,-9,-10):526–555.

Norman, J. R., and F. C. Fraser.
1938. Giant fishes, whales and dolphins, 361 p. W. W. Norton and Company Inc., New York, NY.

Parker, T. J.
1887. Notes on *Carcharodon rondeletii*. Proc. Zool. Soc. London 1:27–40.

Peyer, B.
1968. Comparative odontology, 468 p. Translated and edited by R. Zangerl. Univ. Chicago Press, Chicago IL.

Raschi, W., and C. Tabit.
1992. Functional aspects of placoid scales: a review and update. *In* Sharks: biology and fisheries (J. P. Pepperell, ed.), p. 123–47. Aust. J. Mar. Freshwater Res. 43.

Reif, W. E.
1985. Squamation and ecology of sharks. Courier Forsch.-Inst. Senckenberg, Frankfurt am Main. 78:1–255.

Sanzo, L.
1912. Embrione di *Carcharodon Rondeletii* M. Hle. (?) con particolare disposizione del sacco vitellino. Regio Comitato Talassografico Italiano, Memoria XI:1–12.

Shann, E. W.
1911. A description of the advanced embryonic stage of *Lamna cornubica*. Fish. Board Scotland 28:73–79.

Smith, J. L. B.
1953. The shark, *Isurus oxyrinchus*, in South African waters. Nature 171:977.
1958. Sharks of the genus *Pterolaminops* Springer, 1951 with notes on isurid sharks. Rhodes Univ. Ichthyol. Bull. 10:131–134.

Springer, V. G., and J. A. F. Garrick.
1964. A survey of vertebral number in sharks. Proc. U. S. Nat. Mus. 116(3496):73–96.

Stevens, J. D.
1983. Observations on reproduction in the shortfin mako *Isurus oxyrinchus*. Copeia 1983:126–130.
Strasburg, D. W.
1958. Distribution, abundance, and habits of pelagic sharks in the Central Pacific Ocean. Fish. Bull. 58:335–361.
Tortonese, E.
1950. Studi sui plagiostomi. III. La viviparita: un fondamentale carattere biolico degli squali. Archivio Zoologico Italiano 35:101–155.
1956. Fauna d'Italia. Vol. II, Leptocardia ciclostomata selachii, 321 p. Edizioni Calderini, Bologna, Italy,
Uchida, S., M. Toda, K. Teshima, and K. Yano.
1996. Pregnant white sharks with near-term fetuses from Japan. *In* Great white sharks: the biology of *Carcharodon carcharias* (A. P. Klimley and D. G. Ainley, eds.), p. 139–155. Academic Press, San Diego, CA.
Uchida, S., F. Yasuzumi, M. Toda, and N. Okura.
1987. On the observation of reproduction in *Carcharodon carcharias* and *Isurus oxyrinchus*. Rep. of Japanese Group for Elasmobranch Studies 24:5–6.
Wilkinson, L.
1986. SYSTAT: the system for statistics. 18 chapters and 4 appendices without continuous page numbers. SYSTAT Inc., Evanston IL.
Yano K., M. Goto, and Y. Yabumoto.
1997. Dermal and mucous denticles of a female megamouth shark, *Megachasma pelagios*, from Hakata Bay, Japan. *In* Biology of the megamouth shark (K. Yano, J. F. Morrissey, Y. Yabumoto, and K. Nakaya, eds.), p. 77–91. Tokai University Press, Tokyo.
Zangerl, R.
1981. Chondrichthyes I Paleozoic Elasmobranchii. Volume 3A. *In* Handbook of paleoichthyology (H.-P. Schultze, ed.), p. 115 p. +116 figs. Gustav Fischer Verlag, Stuttgart, Germany, and New York, NY.

Necropsy findings in sea turtles taken as bycatch in the North Pacific longline fishery

Thierry M. Work

Hawaii Field Station
National Wildlife Health Center
U.S. Geological Survey
300 Ala Moana Blvd., Room 5-231
Honolulu, Hawaii 96850.
E-mail address: thierry_work@usgs.gov

George H. Balazs

Honolulu Laboratory
Southwest Fisheries Science Center
National Marine Fisheries Service, NOAA
2570 Dole St.
Honolulu, Hawaii 96822.

Concern about interactions between fisheries and marine turtles has increased in recent years, particularly since East Pacific leatherback turtles (*Dermochelys coriacea*) may become extinct (Spotila et al., 2000). However, relatively little published information exists on interactions between sea turtles and North Pacific longline fisheries. The most available literature on the topic focuses on modeling data from fisheries observers for estimating the probability of animals dying and fishery-induced mortality (McCracken[1]; Kleiber[2]). A more recent study was undertaken with satellite telemetry and remote sensing to evaluate the probability of interaction between longline fisheries and loggerhead sea turtles (*Caretta caretta*) and the effects of hooking (Polovina et al., 2000; Parker, in press).

Necropsies on turtles caught by longline fisheries may provide additional objective data on the causes of mortality and the health of pelagic turtles. Although ample literature exists on evaluating the health of benthic coastal-residing immature sea turtles in Hawaiian waters (Aguirre et al., 1994; Work and Balazs, 1999), nothing is known about the health status of pelagic sea turtles because of the difficulty in locating animals (Bolten and Balazs, 1983) and the unavailability of specimens for diagnosis. Most turtles caught in longline fisheries are released alive (McCracken[1]; Kleiber[2]). The few dead turtles that area recovered can be returned to shore legally only by observers (who are present in only ~5% of the Hawaii-based North Pacific fishing fleet) (Balazs et al., 1995). Nevertheless, examining freshly dead turtles caught in longline fisheries provides a unique opportunity to gain insight into the health status and diet of pelagic sea turtles. Our objective was to systematically evaluate all available carcasses of fresh-frozen sea turtles that had been caught in the Hawaii-based longline fishery for an evaluation of their health and to document their diet.

Methods

Free-ranging marine turtles accidentally taken as bycatch by the North Pacific longline fishery were landed on the fishing vessel and evaluated for signs of life by fishery observers employed by the National Marine Fisheries Service. Sea turtles that were judged to be dead by specific criteria (Balazs et al., 1995) were stored frozen and returned to Honolulu, Hawaii, where we recorded weight (kg) and body morphometrics (cm).

Gross necropsies entailed a complete external and internal exam of all organ systems. We also recorded any identifiable stomach contents. Body condition of turtles was subjectively classified as good, fair or poor if coelomic and mesenteric fat reserves appeared ample, moderate, or sparse, respectively. Postmortem condition was classified as good, fair, or poor depending on the gross appearance of organs during the necropsy. We classified turtles as lightly hooked if the longline fish hook was lodged in the mouth or externally, or as deeply hooked if the hook was present in the gastrointestinal tract caudal to the glottis. Hooks were classified as tuna (3.6 or 3.8 mm) or swordfish and mustad (offset 8/0 or 9/0).

Tissue samples (heart, lung, kidney, liver, spleen, brain, stomach, small intestines, skin, trachea, salt gland, gonad, thyroid, pancreas, and brain) were fixed in 10% buffered formalin, sectioned at 5 µm and stained with hematoxylin and eosin for microscopic examination. Representative tissues were stored frozen (–70°C) in sterile plastic bags. Where gross necropsy findings suggested infectious or inflammatory disease, swabs or tissues were processed for microbiology. For bacteriology, swabs were plated on McConkey and blood agar and incubated at 27°C and 37°C for 48 h. For virus isolation, frozen tissues were homogenized, the supernate filtered through a 0.22-µm filter, and plated on green sea turtle embryo fibroblasts (Moore et al., 1997).

[1] McCracken, M. L. 2000. Estimation of sea turtle take and mortality in the Hawaiian longline fisheries. Administrative Report H-00-06, 29 p. Southwest Fisheries Science Center, Nat. Mar. Fish. Service, NOAA, 2570 Dole St., Honolulu, HI 96822.

[2] Kleiber, P. 1998. Estimating annual takes and kills of sea turtles by the Hawaiian longline fishery, 1991–97, from observer program and logbook data. Administrative Report H-98-08, 21 p. Southwest Fisheries Science Center, Nat. Mar. Fish. Serv., NOAA, 2570 Dole St., Honolulu, HI 96822.

Manuscript accepted 28 May 2002.
Fish. Bull. 100:876–880 (2002).

Table 1

Vital necropsy statistics for turtles caught by the Hawaii-based pelagic longline fishery in the North Pacific. Age are immature (I), subadult (S), and adult (A). Body and post-mortem condition were classified as good (G) or fair (F). SCL, BC, PMC, and Set stand for smallest carapace length, body condition, postmortem condition, and hook set, respectively.

ID	Species	Wt (kg)	SCL	Age	Sex	BC	PMC	Hook	Set
1	*C. mydas*	25.4	55.6	I	M	G	F	tuna 3.6-mm	light
2	*C. mydas*	50	67.9	S	F	G	G	tuna 3.6-mm	light
3	*D. coriacea*	44.5	70.4	I	F	G	G	tuna 3.6mm	light
4	*D. coriacea*	74.1	85.3	I	F	G	G	tuna 3.6-mm	light
5	*L. olivacea*	13.2	43.7	I	F	G	F	tuna 3.6-mm	light
6	*L. olivacea*	15.3	46.6	I	F	F	G	offset 8/0	deep
7	*L. olivacea*	21	54	I	F	G	G	tuna 3.6-mm	light
8	*L. olivacea*	24.5	57.5	S	F	G	G	tuna 3.6-mm	light
9	*L. olivacea*	33.4	62.1	A	F	G	G	tuna 3.6-mm	light
10	*L. olivacea*	34.1	60.4	A	F	G	G	tuna 3.6-mm	deep
11	*L. olivacea*	37.7	62.9	A	F	G	G	tuna 3.6-mm	light

Results

We performed necropsies on seven olive ridley (*Lepidochelys olivacea*), two green (*Chelonia mydas*), and two leatherback sea turtles (Table 1). Turtles were caught between 5.4–18.0°N and 148.5–161.3°W in the North Pacific from February 1996 through June 2000.

One leatherback sea turtle (identification [ID] 3) had severe acute inflammation of the liver associated with clumps of fibrin (Fig. 1, A and B), mild acute inflammation of heart muscle, and mild diffuse pulmonary edema. No bacteria or viruses were isolated from the liver. The other leatherback sea turtle (ID 4) had severe diffuse fibrosis of the pancreas (Fig. 1C) and a large subcapsular hematoma of the liver. The lesions in both turtles were severe enough to cause significant impairment of organ function and probable morbidity. Incidental microscopic lesions in four of the seven olive ridley sea turtles included mild acute heart muscle inflammation (ID 6), mild focal necrosis in one lung (ID 7), parasite-induced necrosis in the stomach wall (ID 8), and foreign material (probable ingesta) in the bronchioles (ID 10). Microscopic lesions in the olive ridley sea turtles were not severe enough to cause morbidity, and no microscopic lesions were seen in the remaining turtles including the green sea turtles.

Cause of mortality for all sea turtles was drowning after hooking; however, in only one case (olive ridley ID 11) was there gross evidence of water in the lungs. Female (10/11) and lightly hooked (9/11) animals predominated. Most hooks were tuna 3.6-mm hooks (Table 1). In one deeply hooked olive ridley turtle (ID 10), the hook perforated the esophageal wall in two places at approximately half of the length of the wall. In the other olive ridley sea turtle, ID 6 (classified as deeply hooked by the observer), the hook perforated just caudal to the tongue. Both leatherback sea turtles had been entangled by the leader; one had the leader tightly wound around the right front flipper, the other had the leader around the neck, where it had caused lacerations .

Bait (sama; *Cololabias saira*) was seen in the esophagus of four olive ridley sea turtles; one turtle contained three fish, indicating ingestion from more than one hook. Other items in olive ridley stomachs included cowfish, pyrosomas, pelagic snails, bird feathers, and small fragments of plastic. Stomachs from both leatherback turtles and from one green turtle contained pyrosomas exclusively.

Discussion

Only two sea turtles were classified as deeply hooked; most turtles had no visible lesion indicative of hooking either to the observer present on board when the turtles were hauled into the boat, or to the observer and us at the time of necropsy. Turtles that scored as lightly hooked but that died later would suggest that deep or light hooking may not be satisfactory criteria for the probability of short-term survival in the species we studied. Similarly, Polovina et al. (2000) and Parker et al. (in press) observed that there was no significant difference in distance or speed of travel between deeply and lightly hooked loggerhead turtles that were caught by the North Pacific longline fishery and then marked with satellite tags, and followed for several months. Hence, deep versus light hooking may not be a useful indicator of long-term survival for these species.

The preponderance of females in our study was noticeable. Markedly skewed sex ratios in wild sea turtles are more commonly encountered among hatchlings (Gonzales et al., 2000), presumably due to incubation well below or above the pivotal temperature (Mrosovsky and Yntema, 1980). Studies of immature green sea turtles stranded with fibropapillomatosis in Hawaii revealed a sex ratio of close to 1:1 (Koga and Balazs, 1996). Ross (1984) in Oman reported sex ratios of adult green sea turtles to be closer to

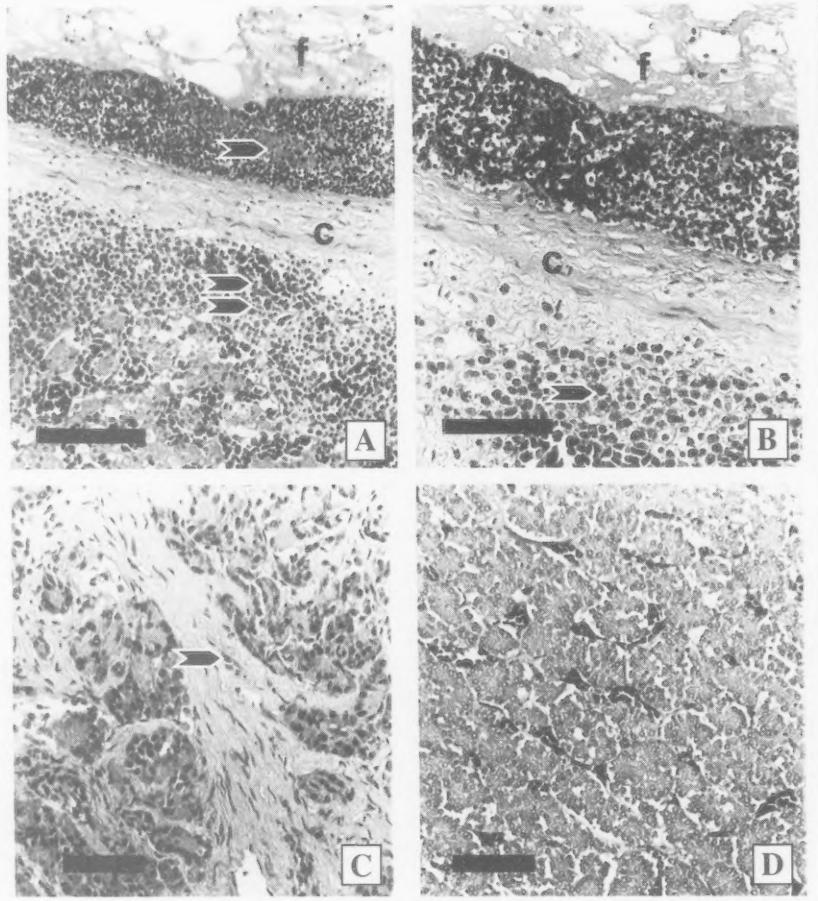

Figure 1

(**A**) Liver: Note fibrin (f), necrotic debris (large arrow), capsule (c), and inflammatory cells (double arrow), bar=100 µm; (**B**) Liver: note granulocytes (arrow), capsule (c), necrotic debris and fibrin (f), bar=50 µm; (**C**) Pancreas: Note large fibrous trabeculae coursing through pancreatic cells (arrow), bar=100 µm; (**D**) Normal pancreas from leatherback for comparison, bar=100 µm.

1:1 although slightly skewed towards females. Given the small sample size for each species, interpretation of the significance of the skewed sex ratio in our sample is problematic. Ross (1984) noted that bias in sampling, segregation of sexes in different areas, and small sample size could be responsible for deviations from the expected sex ratio of 1:1 in sea turtles.

Whether severe lesions of the digestive system occur commonly in leatherback sea turtles remains to be determined. Various factors can cause acute inflammation in the liver, including viruses, bacteria, protozoa, and poisons (Kelly, 1993); however, we saw no evidence of infectious agents in our histological examinations. Pancreatic fibrosis is a chronic lesion indicating earlier insult to the organ, secondary to infectious, toxic, or metabolic processes (Jubb, 1993). Necropsies of stranded leatherback sea turtles have revealed bacterial (Obendorf et al., 1987) and parasitic (Threlfall, 1979) infections, degenerative joint disease (Ogden et al., 1981), and struvite fecoliths (Davenport et al., 1993). The impact of these conditions to leatherback populations is unknown. Given the endangered status of East Pacific leatherback sea turtles, efforts to systematically evaluate health of these animals seem justified, including performing systematic necropsies on fresh carcasses recovered at sea or from nesting beaches, as well as performing health assessments of live animals on nesting beaches.

Lesions in the other species of sea turtles (olive ridley and green) were either mild, nonspecific, or absent al-

together. The absence of lesions in pelagic green turtles was in contrast to what is seen in immature and adult specimens caught in nearshore habitats. In those cases, most green turtles have systemic infections with vascular flukes or fibropapillomas (Aguirre et al., 1998). This would support the hypothesis that at least for immature turtles, these diseases, while absent pelagically, are acquired once the animals enter their near shore foraging pastures. It is possible that very mild subtle lesions could have been overlooked because many tissues had freeze-thaw artifacts. Should this be a major concern, future studies may focus on doing necropsies on freshly dead turtles caught on fishing boats; however, the logistics of doing this will be more complicated. For example, vessels of the Hawaii-based longline fishery are at sea for weeks at a time fishing many hundreds of km from port.

Stomach contents of olive ridley sea turtles in this study (pelagic snails, pyrosomas, foreign bodies) were similar to those seen by others (Parker et al., 2002; National Marine Fisheries Service and US Fish and Wildlife Service[3]). The presence of multiple baits in some olive ridley sea turtles suggests that animals may graze from longline hooks. Pyrosomas are found in stomachs of leatherback and green turtles (National Marine Fisheries Service and US Fish and Wildlife Service[4,5]), and leatherbacks are also attracted to hooks baited with sama (Grant[6]) and squid (Skillman and Balazs, 1992). Given that fisheries may play a significant role in the decline of leatherback sea turtles (National Marine Fisheries Service and US Fish and Wildlife Service[4]), determining whether bait attraction or entanglement pose the greater threat may be of management value. Similarly, evaluating the basis of bait attraction for olive ridley sea turtles caught in longline fisheries may provide clues that will help discourage interactions between this species and fisheries.

Acknowledgments

Thanks are due to Doug Docherty for virus isolation assays, and Robert Rameyer, Shawn K.K. Murakawa, Shandell Eames, and Denise M. Parker for technical assistance. This work was supported by a National Marine Fisheries Service Contract.40JJNF900126.

[3] National Marine Fisheries Service and U. S. Fish and Wildlife Service. 1998a. Recovery plan for U. S. Pacific populations of the olive ridley turtle (*Lepidochelys olivacea*), 63 p. National Marine Fisheries Service, Silver Springs, MD, 20814.

[4] National Marine Fisheries Service and U. S. Fish and Wildlife Service. 1998. Recovery plan for U.S. Pacific populations of the green turtle (*Chelonia mydas*), 84 p. National Marine Fisheries Service, Silver Springs, MD, 20814.

[5] National Marine Fisheries Service and U. S. Fish and Wildlife Service. 1998. Recovery plan for U.S. Pacific populations of the leatherback turtle (*Dermochelys coriacea*), 65 p. National Marine Fisheries Service, Silver Springs, MD, 20814.

[6] Grant, G. S. 1994. Juvenile leatherback turtle caught by long-line fishing in American Samoa. Marine Turtle Newsletter. 66:3–5.

Literature cited

Aguirre A. A., G. H. Balazs, B. Zimmerman, and T. R. Spraker.
1994. Evaluation of Hawaiian green turtles (*Chelonia mydas*) for potential pathogens associated with fibropapillomas. J. Wildl. Dis. 30:8–15.

Aguirre, A. A., T. R. Spraker, G. H. Balazs, and B. Zimmerman.
1998. Spirorchidiasis and fibropapillomatosis in green turtles from the Hawaiian islands. J. Widl. Dis. 34:91–98.

Balazs, G. H., S. G. Pooley, and S. K. K. Murakawa.
1995. Guidelines for handling marine turtles hooked or entangled in the Hawaii longline fishery: results of an expert workshop held in Honolulu, Hawaii, March 15–17, 1995. U.S. Dep. Commer., NOAA Tech. Memo-NMFS-SWFSC-222, 41 p.

Bolten, A. B. and G. H. Balazs.
1983. Biology of the early pelagic stage-the "lost year." *In* Biology and conservation of sea turtles (K. A. Bjorndal (ed.), p. 579–581. Smithsonian Institution Press, Washington, D.C.

Davenport, J., and G. H. Balazs.
1991. "Fiery bodies"-are pyrosomas an important component of the diet of leatherback turtles. British Herp. Soc. Bull. 37:33–38.

Davenport, J., G. H. Balazs, J. V. Faithfull, and D. A. Williamson.
1993. Struvite faecolith in the leatherback turtle *Dermochelys coriacea* vandelli: a means of packaging garbage? Herpetological Journal 3:81–83.

Gonzalez, C. V., F. de Asis Silva Batiz, and S. H. Vazquez
2000. Sex ratio of marine turtle (*Lepidochelys olivacea*) hatchlings in incubation corrals at La Gloria nesting beach, Jalisco, Mexico. Bol. Cent. Invest. Biol. (Maracaibo) 34: 305–313.

Jubb, K. F. V.
1993. The pancreas. *In* Pathology of domestic animals (K. F. V. Jubb, P. C. Kennedy, and N. Palmer (eds.), p. 407–424. Academic Press, Inc., San Diego, CA.

Kelly, W. R.
1993. The liver and biliary system. *In* Pathology of domestic animals (K. F. V. Jubb, P. C. Kennedy, and N. Palmer, eds.), p. 319–406. Academic Press, Inc., San Diego, CA.

Koga, S. K., and G. H. Balazs.
1996. Sex ratios of green turtles stranded in the Hawaiian Islands. *In* Proceedings of the fifteenth annual symposium on sea turtle biology and conservation, February 20–25, 1995, Hilton Head, South Carolina (J. A. Keinath, D. E. Barnard, J. A. Musick, and B. A. Bell, comps.), p. 148–152. U.S. Dep. Commer., NOAA-Tech Memo NMFS-SEFSC-387,

Moore, M. K., T. M. Work, G. H. Balazs, and D. E. Docherty.
1997. Preparation and cryopreservation, and growth of cells prepared from the green turtle (*Chelonia mydas*). Meth. Cell Sci. 19:161–168.

Mrosovsky, N., and C. L. Yntema.
1980. Temperature dependence of sexual differentiation in sea turtles: implications for conservation practices. Biol. Cons. 18:271–280.

Obendorf, D. L , J. Carson, and T. J. McManus.
1987. *Vibrio damsela* infection in a stranded leatherback turtle (*Dermochelys coriacea*). J. Wildl. Dis. 23:666–668.

Ogden, J. A., A. G. Rhodin, G. J. Conlogue, and T. R. Light.
1981. Pathobiology of septic arthritis and contiguous osteomyelitis in a leatherback turtle (*Dermochelys coriacea*). J. Wildl. Dis. 17:277–287.

Parker, D. M., G. H. Balazs, S. K. K. Murakawa, and J. J. Polvina.
In press. Post-hooking survival of sea turtles taken by

pelagic longline fishing in the North Pacific. *In* Proceedings of the twenty-first annual symposium on sea turtle biology and conservation, February 24–28, 2001, Philadelphia, PA. U.S. Dep. Commer., NOAA-Tech Memo, NMFS-SEFSC.

Parker D. M., W. Cooke, and G. H. Balazs.
2002. Dietary components of pelagic loggerhead turtles in the North Pacific Ocean. *In* Proceedings of the twentieth annual symposium on sea turtle biology and conservation, February 29–March 4, 2000, Orlando, Florida, p. 148–151. U.S. Dep. Commer., Memo, NMFS-SEFSC-477.

Polovina, J. J., D. R. Kobayashi, D. M. Parker, M. P. Seki, and G. H. Balazs.
2000. Turtles on the edge: movement of loggerhead turtles (*Caretta caretta*) along oceanic fronts, spanning longline fishing grounds in the central North Pacific, 1997–1998. Fish. Oceanog. 9:71–82.

Ross, J. P.
1984. Adult sex ratio in the green sea turtle. Copeia 1984: 774–776.

Skillman, R. A. and G. H. Balazs.
1992. Leatherback turtle captured by ingestion of squid bait on swordfish longline. Fish. Bull. 80:807–808.

Spotila J. R., R. D. Reina, A. C. Steyermark, P. T. Plotkin, and F. V. Paladino.
2000. Pacific leatherback turtles face extinction. Nature 405:529–30.

Threlfall, W.
1979. Three species of Digenea from the Atlantic leatherback turtle (*Dermochelys coriacea*). Can. J. Zool. 57:1825–1829.

Work, T. M. and G. H. Balazs.
1999. Relating tumor score to hematology in green turtles with fibropapillomatosis in Hawaii. J. Wildl. Dis. 35:804–807.

Acknowledgment of reviewers

The editorial staff of *Fishery Bulletin* would like to thank the following referees for their time and efforts in providing reviews of the manuscripts published in 2001–2002. Their contributions have helped ensure the publication of quality science.

Dr. Dean W. Ahrenholz
Dr. M. James Allen
Mr. Andrew J. Applegate
Ms. Larisa Avens

Mr. M. Scott Baker
Dr. M. Barange
Dr. Daniel D. Benetti
Dr. Dave Bengston
Dr. Steve Berkeley
Dr. Karen A. Bjorndal
Dr. Barbara Block
Dr. Philippe Borsa
Dr. S.A. Bortone
Dr. Louis W. Botsford
Dr. W. Alex Bradbury
Dr. Richard W. Brill
Dr. J.K.T. Brodziak
Mr. Michael Burton

Mr. Michael Canino
Dr. N. Caputi
Mr. John Carlson
Dr. John Carmichael
Dr. James Churchill
Dr. John E. Hughes Clarke
Dr. J. Stanley Cobb
Dr. A.C. Cockroft
Dr. Felicia Coleman
Dr. William Coles
Dr. Dean L. Courtney
Dr. Robert Cowen
Ms. Tara Cox
Dr. Roy E. Crabtree
Dr. Jean Cramer
Dr. Debbie Crouse

Dr. Laurent Dagorn
Dr. Edward E. DeMartini
Dr. M.C. DeVries
Dr. Heidi Dewar
Dr. Andrew Dizon
Dr. P.J. Doherty
Dr. M.L. Domeier
Dr. Richard L. O'Driscoll
Dr. Jakov Dulcic
Dr. Peter Dutton

Dr. D.A. Ebert
Dr. Thomas A. Edsall
Dr. Nelson M. Ehrhardt
Dr. Nick G. Elliot
Dr. Robert W. Elner
Mr. Robert L. Emmett
Dr. Charles E. Epifanio
Dr. Bruce T. Estrella
Dr. Alan R. Everson

Dr. Jeff Fargo
Dr. James D. Felley
Dr. Robert Foy
Dr. Malcolm P. Francis
Dr. Kevin Friedland

Dr. Sarah Gaichas
Dr. James Gelsleichter
Dr. Tony Gharrett
Dr. R. Grant Gilmore
Mr. C. Phillip Goodyear

Dr. Lewis J. Haldorson
Dr. Martin Hall
Dr. Michael Moller Hansen
Dr. Gareth Harding
Dr. Jon Hare
Dr. Patrick J. Harris
Mr. C.J. Harvey
Dr. Euan Harvey
Dr. James T. Harvey
Dr. Graeme Hays
Dr. Edward J. Heist
Dr. Thomas E. Helser
Dr. Frank J. Hernandez
Dr. Sarah Hinckley
Dr. John M. Hoenig
Dr. Aleta A. Hohn
Dr. Kim N. Holland
Dr. G.J. Holt
Mr. Peter B. Hood
Dr. Kevin Hovel
Dr. Robert Hueter

Dr. Tomoyuki Itoh

Dr. Elliot Jacobson
Dr. Chadwick V. Jay
Dr. Simon Jennings
Dr. A.L. Jensen
Mr. Brian M. Jessop
Dr. Susana Junquera
Dr. Michel J. Kaiser
Dr. Mario Katsuragawa
Dr. Gregory Todd Kellison
Dr. Daniel K. Kimura
Dr. Christopher C. Koenig
Dr. Syd Kraul

Dr. G. Lang

Ms. Anne M. Lange
Dr. Mark A. Lazzari
Dr. Rosangela Lessa
Dr. Kwang-Ming Liu
Dr. William F. Loftus
Dr. Thomas R. Loughlin
Dr. Flavia M Lucena

Dr. D.L. Mackas
Dr. William K. Macy
Dr. Charles S. Manooch III
Dr. Gary C. Matlock
Dr. James D. McCleave
Dr. Richard McGarvey
Dr. John C. McGovern
Dr. Robert J. Miller
Dr. David A. Milton
Dr. John Mitchell
Dr. N. Miyabe
Dr. Beatriz Morales-Nin
Dr. Franz-Josef Mueter
Dr. Robert G. Muller
Mr. David Munday
Dr. Bruce C. Mundy
Dr. Steven A. Murawski
Mr. Michael D. Murphy

Dr. K. Nagasawa
Dr. Hideki Nakano
Dr. John D. Neilson
Dr. R. John Nelson
Dr. K.T. Nilssen
Dr. CP Norman

Mr. Robert O'Gorman
Dr. T. Okutani
Dr. Kathryn A. Ono
Dr. Peter Ortner
Dr. Hazel A. Oxenford

Dr. Wayne Palsson
Dr. Y.C. Park
Dr. Richard O. Parker Jr.
Dr. Mark A. Pegg
Dr. Julian G. Pepperell
Mr. Peter C. Perkins
Dr. Michael Pennington
Dr. Marcelo A.A. Pinheiro
Dr. Margaret Platell
Dr. Dmitri Politov

Dr. Clay E. Porch
Dr. James H. Power
Dr. Eric D. Prince

Dr. John A. Quinlan

Dr. Paul Rago
Dr. William Raschi
Dr. W.J. Richards
Dr. Donna R. Rogers
Dr. Laura Rogers-Bennett
Mr. Bill Roumillat
Dr. Rodney A. Rountree
Dr. Michael R. Ross
Dr. Stephen T. Ross
Dr. Thomas L. Rutecki

Dr. Susan E. Safford
Dr. Robert E. Schmidt
Dr. Juan Jacobo Schmitter-Soto
Dr. David H. Secor
Dr. James B. Shaklee

Dr. Donna J. Shaver
Dr. Richard F. Shaw
Mr. Gary R. Shepard
Dr. Michiyo Shima
Dr. John Sibert
Dr. G.B. Skomal
Dr. Malcolm J. Smale
Dr. Barry D. Smith
Dr. David R. Smith
Dr. Stephen Smith
Dr. Susan A. Smith
Ms. Melissa Snover
Dr. Rick D. Stanley
Dr. Jay R. Stauffer
Dr. Garry B. Stenson
Dr. John D. Stevens

Dr. Dominic J. Tollit
Dr. Andrew W. Trites
Dr. Mark Tupper
Dr. W.N. Tzeng

Dr. Senzo Uchida
Dr. Glenn Ulrich
Dr. Fred M. Utter

Dr. David VanVorhees
Dr. Douglas S. Vaughan
Dr. Michael Vecchione
Dr. Eric Volk
Dr. Jon H. Vølstad

Dr. W. Waldo Wakefield
Dr. John Watson
Dr. Winsor Watson
Dr. Mark E. Wilkins
Dr. Graham Worthy

Dr. Mary M. Yoklavich

Dr. S. Zanuy
Dr. K.C.T. Zwanenburg

The index and/or table of contents has been removed and photographed separately within this volume year.

For roll film users, this information for the current volume year is at the beginning of the microfilm. For a prior year volume, this information is at the end of the microfilm.

For microfiche users, the index and/or contents is contained on a separate fiche.

Superintendent of Documents **Publications** Order Form

*5178

☐ YES, please send me the following publications:

____ Subscriptions to *Fishery Bulletin*
for $55.00 per year ($68.75 foreign)

The total cost of my order is $ _____ . Prices include regular domestic postage and handling and are subject to change.

_____
(Company or Personal Name) (Please type or print)

_____
(Additional address/attention line)

_____
(Street address)

_____
(City, State, ZIP Code)

_____
(Daytime phone including area code)

_____
(Purchase Order No.)

Charge your order. IT'S EASY!

VISA

MasterCard

Please Choose Method of Payment:

☐ Check Payable to the Superintendent of Documents
☐ GPO Deposit Account ☐☐☐☐☐☐–☐
☐ VISA or MasterCard Account
☐☐☐☐☐☐☐☐☐☐☐☐☐☐☐☐
☐☐☐☐ (Credit card expiration date)

To fax your orders (202) 512-2250

_____
(Authorizing Signature)

Mail To: Superintendent of Documents
P.O. Box 371954, Pittsburgh, PA 15250-7954

Thank you for your order!

This statement is required by the Act of August 12, 1970, Section 3685, Title 39, U.S. Code, showing ownership, management, and circulation of the *Fishery Bulletin*, publication number 366-370, and was filed on 14 September, 2002. The *Bulletin* is published quarterly (four issues annually) with an annual subscription price of $50.00 (sold by the Superintendent of Documents, U.S. Government Printing Office, Washington, DC 20402). The complete mailing address of the office of publication is NMFS Scientific Publications Office, NOAA, 7600 Sand Point Way NE, BIN C15700, Seattle, WA 98115. The complete mailing address of the headquarters of the publishing agency is National Marine Fisheries Service, NOAA, Department of Commerce, 1335 East-West Highway, Silver Spring, MD 20910. The name of the publisher is Willis Hobart and the managing editor is Sharyn Matriotti; their mailing address is: NMFS Scientific Publications Office, 7600 Sand Point Way NE, BIN 15700, Seattle, WA 98115. The owner is the U.S. Department of Commerce, 14th St. N.W., Washington, DC 20230; there are no bondholders, mortgages, or other security holders. The purpose, function, and nonprofit status of the organization (agency) and the exempt status for Federal income tax purposes has not changed during the preceding 12 months. The extent and nature of circulation is as follows: total number of copies (A) (average number of copies of each issue during the preceding 12 months) was 1918 and the actual number of copies of the single issue published nearest to the filing dates was 1906. Paid circulation (B) is handled by the U.S. Government Printing Office, Washington, DC 20402, and the total number printed for sales (mail subscriptions and individual sales) was 488 for both the average number of copies each issue during the preceding 12 months and 475 the actual number of copies of the single issue published nearest to the filing date (C). Free distribution (D) by mail; samples, complimentary and other free copies (average number of copies each issue during the preceding 12 months) was 1405 and the actual number of copies of the single issue published nearest to the filing date was 1418. Free distribution outside the mail (E) by carriers or other means was 0 for both average number of copies and actual number of copies. Total free distribution (F) was 0 for both average number of copies and actual number of copies of the single issue published nearest the filing date. The total distribution (G: sum of D and B) (average number of copies each issue during the preceding 12 months) was 1893 and the actual number of copies of the single issue published nearest to the filing date was 1881. There were 25 copies not distributed (H). The total (I: sum of G and H) is equal to the net press run figures shown in Item A: 1893 and 25 copies, respectively. I certify that the statements made by me above are correct and complete: (Signed) Willis Hobart, Publisher.

Fishery Bulletin

Guidelines for contributors

Content of papers

Articles

Articles are reports of 10 to 30 pages (double spaced) that describe original research in one or a combination of the following fields of marine science: taxonomy, biology, genetics, mathematics (including modeling), statistics, engineering, economics, and ecology.

Notes

Notes are reports of 5 to 10 pages without an abstract that describe methods and results not supported by a large body of data. Although all contributions are subject to peer review, responsibility for the contents of articles and notes rests upon the authors and not upon the editor or the publisher. It is therefore important that authors consider the contents of their manuscripts carefully. Submission of an article is un-derstood to imply that the article is original and is not being considered for publication elsewhere. Manuscripts must be written in English. Authors whose native language is not English are strongly advised to have their manuscripts checked for fluency by English-speaking colleagues prior to submission.

Preparation of papers

Text

Title page should include authors' full names and mailing addresses (street address required) and the senior author's telephone, fax number, e-mail address, as well as a list of key words to describe the contents of the manuscript. **Abstract** must be less than one typed page (double spaced) and must not contain any citations. It should state the main scope of the research but emphasize the author's conclusions and relevant findings. Because abstracts are circulated by abstracting agencies, it is important that they represent the research clearly and concisely. **General text** must be typed in double-spaced format. A brief introduction should state the broad significance of the paper; the remainder of the paper should be divided into the following sections: Materials and methods, Results, Discussion (or Conclusions), and Acknowledgments. Headings within each section must be short, reflect a logical sequence, and follow the rules of multiple subdivision (i.e. there can be no subdivision without at least two subheadings). The entire text should be intelligible to interdisciplinary readers; therefore, all acronyms and abbreviations should be written out and all lesser-known technical terms should be defined the first time they are mentioned. The scientific names of species must be written out the first time they are mentioned; subsequent mention of scientific names may be abbreviated. Follow *Scientific style and format: CBE manual for authors, editors, and publishers* (6th ed.) for editorial style and the most current issue of the *American Fisheries Society's common and scientific names of fishes from the United States and Canada* for fish nomenclature. Dates should be written as follows: 11 November 1991. Measurements should be expressed in metric units, e.g. metric tons (t). The numeral one (1) should be typed as a one, not as a lower-case el (l).

Footnotes

Use footnotes to add editorial comments regarding claims made in the text and to document unpublished works or works with local circulation. Footnotes should be numbered with Arabic numerals and inserted in 10-point font at the bottom of the first page on which they are cited. Footnotes should be formatted in the same manner as citations. If a manuscript is unpublished, in the process of review, or if the information provided in the footnote has been conveyed verbally, please state this information as "unpubl. data," "manuscript in review," and "personal commun.," respectively. Authors are advised wherever possible to avoid references to nonstandard literature (unpublished literature that is difficult to obtain, such as internal reports, processed reports, administrative reports, ICES council minutes, IWC minutes or working papers, any "research" or "working" documents, laboratory reports, contract reports, and manuscripts in review). If these references are used, please indicate whether they are available from NTIS (National Technical Information Service) or from some other public depository. Footnote format: author (last name, followed by first-name initials); year; title of report or manuscript; type of report and its administrative or serial number; name and address of agency or institution where the report is filed.

Literature cited

The literature cited section comprises works that have been published and those accepted for publication (works in press) in peer-reviewed journals and books. Follow the name and year system for citation format. In the text, write "Smith and Jones (1977) reported" but if the citation takes the form of parenthetical matter, write "(Smith and Jones, 1977)." In the literature cited section, list citations alphabetically by last name of senior author: For example, Alston, 1952; Mannly, 1988; Smith, 1932; Smith, 1947; Stalinsky and Jones, 1985. Abbreviations of journals should conform to the abbreviations given in the *Serial sources for the BIOSIS previews database*. Authors are responsible for the accuracy and completeness of all citations. Literature citation format: author (last name, followed by first-name initials); year; title of report or article; abbreviated title of the journal in which the article was published, volume number, page numbers. For books, please provide publisher, city, and state.

Tables

Tables should not be excessive in size and must be cited in numerical order in the text. Headings in tables should be short but ample enough to allow the table to be intelligible on its own. All unusual symbols must be explained in the table legend. Other incidental comments may be footnoted (use italic arabic numerals for footnote markers). Use asterisks only to indicate probability in statistical data. Place table legends on the same page as the table data. We accept tables saved in most spreadsheet software programs (e.g. Microsoft Excel). Please note the following:

- Use a comma in numbers of five digits or more (e.g. 13,000 but 3000).
- Use zeros before all decimal points for values less than one (e.g. 0.31).

Figures

Figures include line illustrations, computer-generated line graphs, and photographs (or slides). They must be cited in numerical order in the text. Line illustrations are best submitted as original drawings. Computer-generated line graphs should be printed on laser-quality paper. Photographs should be submitted on glossy paper with good contrast. All figures are to be labeled with senior author's name and the number of the figure (e.g. Smith, Fig. 4). Use Helvetica or Arial font to label anatomical parts (line drawings) or variables (graphs) within figures; use Times Roman bold font to label the different sections of a figure (e.g. **A**, **B**, **C**). Figure legends should explain all symbols and abbreviations seen within the figure and should be typed in double-spaced format on a separate page at the end of the manuscript. We advise authors to peruse a recent issue of *Fishery Bulletin* for standard formats. Please note the following:

- Capitalize the first letter of the first word of axis labels.
- Do not use overly large font sizes to label axes or parts within figures.
- Do not use boldface fonts within figures.
- Do not create outline rules around graphs.
- Do not use horizontal lines through graphs.
- Do not use large font sizes to label degrees of longitude and latitude on maps.
- Indicate direction of degrees longitude and latitude on maps (e.g. 170°E).
- Avoid placing labels on a vertical plane (except on *y* axis).
- Avoid odd (nonstandard) patterns to mark sections of bar graphs and pie charts.

Copyright law

Fishery Bulletin, a U.S. government publication, is not subject to copyright law. If an author wishes to reproduce any part of *Fishery Bulletin* in his or her work, he or she is obliged, however, to acknowledge the source of the extracted literature.

Submission of papers

Send four printed copies (one original plus three copies)—clipped, *not stapled*—to the Scientific Editor, at the address shown below. Send photocopies of figures with initial submission of manuscript. Original figures will be requested later when the manuscript has been accepted for publication. Do not send your manuscript on diskette until requested to do so.

Dr. Norman Bartoo
National Marine Fisheries Service, NOAA
8604 La Jolla Shores Drive
La Jolla, CA 92037

Once the manuscript has been accepted for publication, you will be asked to submit a software copy of your manuscript. The software copy should be submitted in WordPerfect or Word format (in Word, save as Rich Text Format). Please note that we do not accept ASCII text files.

Reprints

Copies of published articles and notes are available free of charge to the senior author (50 copies) and to his or her laboratory (50 copies). Additional copies may be purchased in lots of 100 when the author receives page proofs.

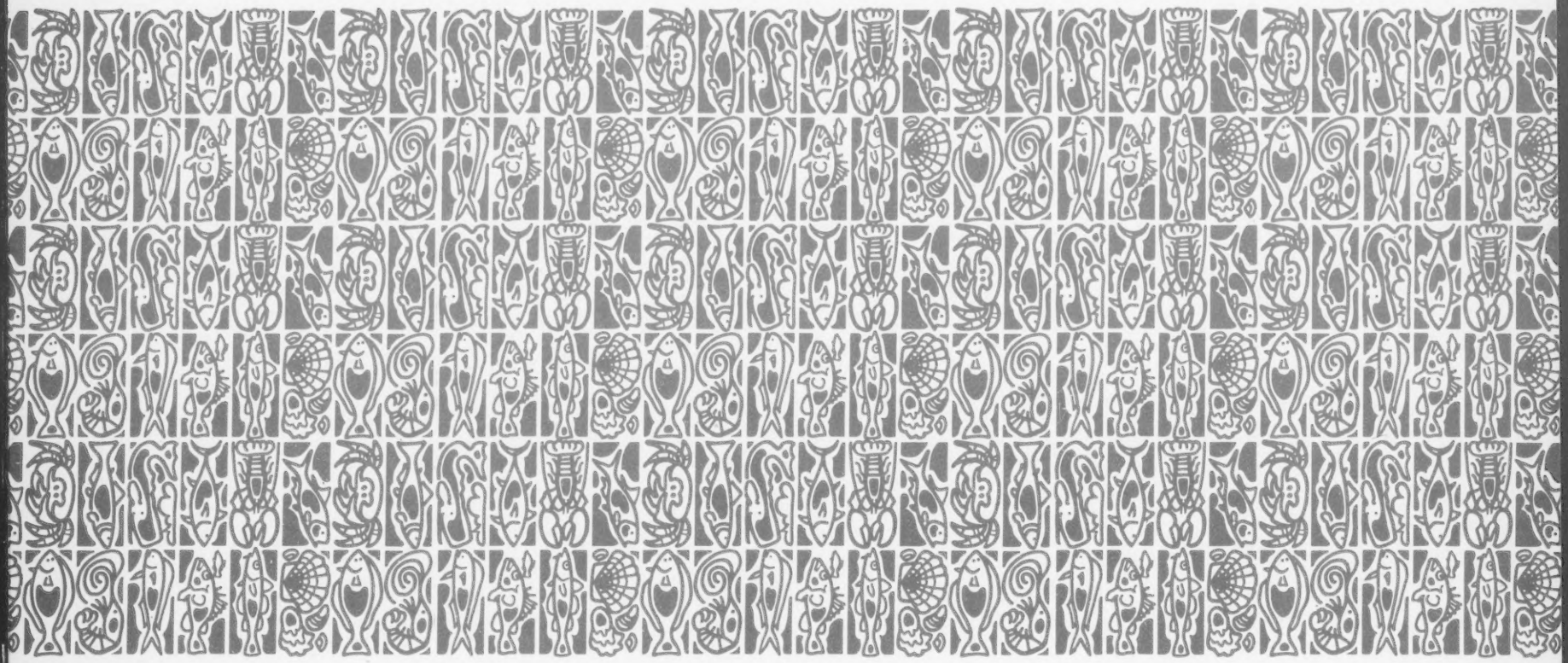

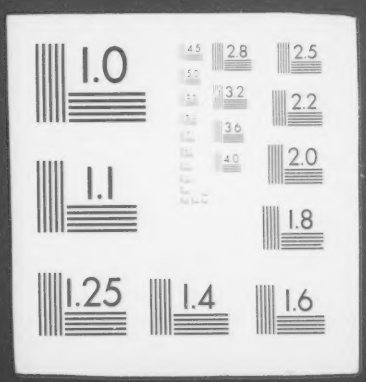
1.0
1.1
1.25
1.4
1.6
1.8
2.0
2.2
2.5
2.8
3.2
3.6
4.0
4.5
5.0